TOPICS IN CURRENT CHEMISTRY 290

Volume Editor B. Kirchner

Ionic Liquids

Springer

290

Topics in Current Chemistry

Topics in Current Chemistry

Recently Published and Forthcoming Volumes

Ionic Liquids
Volume Editor: Barbara Kirchner
Vol. 290, 2010

Orbitals in Chemistry
Volume Editor: Satoshi Inagaki
Vol. 289, 2009

Glycoscience and Microbial Adhesion
Volume Editors: Thisbe K. Lindhorst, Stefan Oscarson
Vol. 288, 2009

Templates in Chemistry III
Volume Editors: Broekmann, P., Dötz, K.-H., Schalley, C.A.
Vol. 287, 2009

Tubulin-Binding Agents: Synthetic, Structural and Mechanistic Insights
Volume Editor: Carlomagno, T.
Vol. 286, 2009

STM and AFM Studies on (Bio)molecular Systems: Unravelling the Nanoworld
Volume Editor: Samorì, P.
Vol. 285, 2008

Amplification of Chirality
Volume Editor: Soai, K.
Vol. 284, 2008

Anthracycline Chemistry and Biology II
Mode of Action, Clinical Aspects and New Drugs
Volume Editor: Krohn, K.
Vol. 283, 2008

Anthracycline Chemistry and Biology I
Biological Occurence and Biosynthesis, Synthesis and Chemistry
Volume Editor: Krohn, K.
Vol. 282, 2008

Photochemistry and Photophysics of Coordination Compounds II
Volume Editors: Balzani, V., Campagna, S.
Vol. 281, 2007

Photochemistry and Photophysics of Coordination Compounds I
Volume Editors: Balzani, V., Campagna, S.
Vol. 280, 2007

Metal Catalyzed Reductive C–C Bond Formation
A Departure from Preformed Organometallic Reagents
Volume Editor: Krische, M. J.
Vol. 279, 2007

Combinatorial Chemistry on Solid Supports
Volume Editor: Bräse, S.
Vol. 278, 2007

Creative Chemical Sensor Systems
Volume Editor: Schrader, T.
Vol. 277, 2007

In situ NMR Methods in Catalysis
Volume Editors: Bargon, J., Kuhn, L. T.
Vol. 276, 2007

Sulfur-Mediated Rearrangements II
Volume Editor: Schaumann, E.
Vol. 275, 2007

Sulfur-Mediated Rearrangements I
Volume Editor: Schaumann, E.
Vol. 274, 2007

Bioactive Conformation II
Volume Editor: Peters, T.
Vol. 273, 2007

Ionic Liquids

Volume Editor: Barbara Kirchner

With Contributions by
Bronya Clare · Ralf Giernoth · Margarida F. Costa Gomes · Barbara Kirchner · José N. Canongia Lopes · Douglas R. MacFarlane Anja-Verena Mudring · Agílio A. H. Padua · Mathieu Pucheault · Annegret Stark · Amal Sirwardana · Suzie Su Yin Tan · Andreas Taubert · Michel Vaultier

With a Foreword by Tom Welton

Springer

Editor
Prof. Barbara Kirchner
Universität Leipzig
Wilhelm-Oswald Institut für
Physikalische und Theoretische Chemie
Linnéstr. 2
04103 Leipzig, Germany
bkirchner@uni-leipzig.de

ISSN 0340-1022 e-ISSN 1436-5049
ISBN 978-3-642-01779-7 e-ISBN 978-3-642-01780-3
DOI 10.1007/978-3-642-01780-3
Springer Heidelberg Dordrecht London New York

Library of Congress Control Number: 2009940397

Cover design: WMXDesign GmbH, Heidelberg, Germany

Printed on acid-free paper

Springer is part of Springer Science+Business Media (www.springer.com)

Volume Editor

Prof. Barbara Kirchner

Universität Leipzig
Wilhelm-Oswald Institut für
Physikalische und Theoretische Chemie
Linnéstr. 2
04103 Leipzig, Germany
bkirchner@uni-leipzig.de

Editorial Board

Topics in Current Chemistry Also Available Electronically

Topics in Current Chemistry is included in Springer's eBook package *Chemistry and Materials Science*. If a library does not opt for the whole package the book series may be bought on a subscription basis. Also, all back volumes are available electronically.

For all customers who have a standing order to the print version of *Topics in Current Chemistry*, we offer the electronic version via SpringerLink free of charge.

If you do not have access, you can still view the table of contents of each volume and the abstract of each article by going to the SpringerLink homepage, clicking on "Chemistry and Materials Science," under Subject Collection, then "Book Series," under Content Type and finally by selecting *Topics in Current Chemistry.*

You will find information about the

- Editorial Board
- Aims and Scope
- Instructions for Authors
- Sample Contribution

at springer.com using the search function by typing in *Topics in Current Chemistry*.

Color figures are published in full color in the electronic version on SpringerLink.

Aims and Scope

The series *Topics in Current Chemistry* presents critical reviews of the present and future trends in modern chemical research. The scope includes all areas of chemical science, including the interfaces with related disciplines such as biology, medicine, and materials science.

The objective of each thematic volume is to give the non-specialist reader, whether at the university or in industry, a comprehensive overview of an area where new insights of interest to a larger scientific audience are emerging.

Thus each review within the volume critically surveys one aspect of that topic and places it within the context of the volume as a whole. The most significant developments of the last 5–10 years are presented, using selected examples to illustrate the principles discussed. A description of the laboratory procedures involved is often useful to the reader. The coverage is not exhaustive in data, but rather conceptual, concentrating on the methodological thinking that will allow the non-specialist reader to understand the information presented.

Discussion of possible future research directions in the area is welcome.

Review articles for the individual volumes are invited by the volume editors.

In references *Topics in Current Chemistry* is abbreviated *Top Curr Chem* and is cited as a journal.

Impact Factor 2008: 5.270; Section "Chemistry, Multidisciplinary": Rank 14 of 125

Foreword

"Ionic liquids will never find application in industry", "I don't understand this fad for ionic liquids" and "there is no widespread interest in these systems" are just three of quotes from the reports of referees for research proposals that I have received over the years. I wonder what these people think today. There are currently at least nine large-scale industrial uses of ionic liquids, including, we now recognise, the production of ε-Caprolactam (a monomer for the production of nylon-6) [1]. There has been a steady increase in the interest in ionic liquids for well over a decade and last year the number of papers and patents including ionic liquids was counted in the thousands. This remarkable achievement has been built on the hard work and enthusiasm, first of a small band of devotees, but now of huge numbers of scientists all over the world who do not see themselves as specialists in ionic liquids.

The ionic liquids field continues to develop at an incredible rate. No sooner do I think that I am on top of the literature than it turns out that a whole new area of work has emerged without me noticing. Things that were once supposedly impossible in ionic liquids, such as measuring the ^{1}H NMR of solutes, are now widely applicable (see Chapter 8). Hence, collected volumes such as this are very welcome. This volume complements some other excellent texts, notably: "Electrodeposition in ionic liquids", edited by Frank Endres, Andy Abbott and Doug MacFarlane; "Electrochemical Aspects of Ionic Liquids" edited by Hiro Ohno; "Ionic liquids in Synthesis", edited by Peter Wasserscheid and myself and a recent collected volume of Accounts of Chemical Research.

As one looks back over the last few decades it is possible to see trends emerging in the ionic liquids that are used and the main foci of interest. Early chloroaluminate systems with potential electrochemical applications gave way to ionic liquids with more air stable anions, with interest moving on to chemicals synthesis and catalysis. Then came new systems with specific properties to use as Task Specific Ionic Liquids (see Chapter 3), or for dissolving biomass polymers (Chapter 10), or as engineering fluids of various types. A small number of papers have now appeared on mixtures of ionic liquids. The exciting thing about ionic liquids is that as each development has occurred it has been in addition to the previous activities and not a replacement for these.

Now that the usefulness of ionic liquids has been established there is a return to the study of their structures and physicochemical properties, so that these can be

manipulated to maximise the benefits that ionic liquids can give. The importance of this need for greater understanding of and insight into the fundamental properties is the common thread that passes through the Chapters in this volume (particularly Chapters 2, 4, 5, 6 and 9). For me, it is a delight to see. Not because this makes for great academic research, even though it does, but because this is the only way to ensure that the full potential of ionic liquids can be realised. We are also fortunate nowadays that powerful modern theory and modelling tools are available to give us greater insight into the structures and properties of ionic liquids (Chapter 7) than the largely qualitative approaches that were available in the past. Of course, one can do nothing without reliable and reproducible syntheses for ionic liquids, which are admirably covered in Chapter 1.

What does this presage for the future of research in ionic liquids? Of course, one should always be aware that thing that you are most likely to see in any crystal ball is your own reflection. However, I do hope that the drive to understand how ionic liquids interact with solute materials to change their behaviour will continue. It would also be great to be able to truly realise the 'designer liquid' aspect of ionic liquids and to be able to produce an ionic liquid with any particular desired property by designing the ions *in silico* without having to make a library of variants. The work that is described in this volume is the first step on this path, but there is a very long way to go to this journey's end. My guess is that the most interesting developments will come from those who do not currently use ionic liquids, but will one day realise that they have a problem that an ionic liquid can solve. The truth about the future, as the proposal reviewers who produced the comments above should have known, is that nobody knows what is coming. That's what I like best about it.

London, Summer 2009

Professor Tom Welton
Imperial College London

Reference

Fábos, V.; Lantos, D.; Bodor, A.; Bálint, A.-M.; Mika, L. T.; Sielcken, O. E.; Cuiper, A.; Horváth, I. T. ChemSusChem, 2008, 1, 189

Preface

The discovery of ionic liquids can be dated back to the work of Paul Walden who was born in the Russian governorate of Livland on July 14th, 1863 and who worked out his thesis with Wilhelm Ostwald in Leipzig in 1891 under unusual circumstances. Among the many discoveries of Paul Walden, probably the most important ones are the Ostwald-Walden rule (1886: valency-conductivity relationship), the Walden inversion (1895: the inversion of the C-Atom for substitution reactions), Walden's viscosity rule (1906: constant product for viscosity and conductivity), Walden's rule (1909: molar volume at the boiling point) and the discovery of ionic liquids as reported in the article "Über die Molekulargrösse und elektrische Leitfähigkeit einiger geschmolzener Salze"("About the molecular size and electrical conductivity of some molten salts") [P. Walden, Bull. Acad. Imper. Sci. (St. Petersburg) 1914, 8, 405]. Walden was looking for salts that are liquid at small amounts of surrounding heat in order to conduct his low-temperature-studies: "…sie (BK: wasserfreie Salze) boten die Möglichkeit dar, mit Hilfe der für gewöhnliche Temperaturen gebräuchlichen Methoden und Apparate alle Messungen durchzuführen." ("…they (water-free salts) made it possible to take all relevant measurements with the aid of the methods and apparatus for usual temperatures.").

Since then, studies of "molten salts" have seldom been concerned with ionic liquids in particular, until a renaissance of the interest in these kinds of liquids began to be registered in literature. In 1982 John Wilkes introduced tetrachloroaluminate ionic liquids based on 1-alkyl-3-methyl-imidazolium as cation [Wilkes et al. Inorg. Chim. Acta 21, 1263 (1982)]. The water and air-sensitivity of these substances led to what can be termed the second generation of ionic liquids when in 1992 the groups of Seddon, Hussey, and Chauvin suggested air- and water-stable ionic liquids through the replacement of moisture-sensitive $AlCl_4^-$ anion by BF_4^- and other anions [e.g. Seddon, Kinetics and Catalysis 37, 693 (1996)]. From 1998, Jim Davis and others introduced the third generation which sometimes is featured in literature under the term "designer solvents" or "task-specific ionic liquids" [Davis Jr. JH, et al., Tetrahedron Lett. 39, 8955 (1998)]. That these liquids were new solvents which cannot be understood merely as cases of some kind of molten salts has been made clear in no uncertain terms by Ken Seddon: "To use the term molten salts to describe these novel systems (BK: ionic liquids) is as archaic as describing a car as a horseless carriage" [Seddon, J. Chem. Tech. Biotechnol. 68, 351 (1997)]

Although a new class of solvents has emerged in the form of these ionic liquids, a systematic classification of them seems almost impossible. Whenever a new characterisation was discussed or a rule was phrased, some counter-example appeared out of the blue. When ionic liquids were sold as green solvents, this ran into trouble when they were shown to be fairly toxic [Ranke et al., Chem. Rev., 107, 2183 (2007)] and non-digestable. And while their low vapour-pressure seemed to point in the general direction of green solvents, it remains demonstrably true that some ionic liquids can be distilled [Earle et al., Nature 439, 831 (2006)]. Judging from the components of these solvents, namely ions, one would expect a high polarity for ionic liquids; however, these have been found [Wakei et al., J. Phys. Chem. B 109, 17028 (2006)] to be rather moderate and comparable to alcohols. Even the presence of pure ionicitiy was, after a while, questioned by scientists [Tokuda et al., J. Phys. Chem. B 110, 19593 (2006)] who found a relaxing electrostatics and increasing dispersion for ionic liquids with increasing chain length at the side group. The quest for a common rule has also, among other things, looked into the question of the unity charge of the ions. Contrary to what many had believed, it was recently explained by my colleague Koen Binnemans [http://www.kuleuven.be/cv/u0007851e.htm] that higher charged species form ionic liquids as well.

The importance of ILs is elucidated by many existing scientific programmes and labs, for example the Japanese "Science of ionic liquids" [http://ionliq.chem.nagoya-u.ac.jp/english/index.html], the Power, Environmental & Energy Research Center PEER [http://www.peer.caltech.edu/ionic.htm], the Queen's University Ionic Liquid Laboratories QUILL [http://quill.qub.ac.uk/], or the German priority programme "Ionic liquids" [http://www.dfg-spp1191.de] to name but a few, and several conferences are being conducted on this topic. It is furthermore illustrated by the fact that many books on the topic exist.

This volume contains a selection of some pointers on the important topics that are now discussed regarding ionic liquids. The main focus is on fundamental problems. In that sense, it really is a "topics in current chemistry"- volume, because it covers a topic of broad current interest (ionic liquids) in a way that gives the non-specialist reader a comprehensive overview.

The volume begins with a chapter by Bronya Clare, Amal Sirwardana and Douglas R. MacFarlane on synthesis and purification of ionic liquids. A good starting point for a substance consists in understanding its synthesis. However, for the class of ionic liquids, large alterations of their properties were observed when impurities are present, which is why a special emphasis has to be given to this issue. In the next chapter, Annegret Stark evaluates induced effects on organic reactions when ionic liquids are chosen as a solvent. One of the most promising opportunities in the field of ionic liquids consists in the possibility to modify ionic liquids to obtain functionality. Mathieu Pucheault and Michel Vaultier elaborate on this topic of task specific ionic liquids, with special emphasis on onium salts. The solubility and other features of heavy elements in ionic liquids are discussed by Andreas Taubert. The author concludes that the many remaining open questions are due to the sometimes complex behaviour of the metal ions in an already complex liquid and an even more complex interplay between the two. This is a fact that applies to many more solutes in ionic liquids.

How useful a solute can be as a probe is presented in the chapter by Margarida F. Costa Gomes, José N. Canongia Lopes and Agílio A. H. Pádua. In this chapter the thermodynamics and microhetergeity are illuminated from the perspective of molecular dynamics simulations. The subsequent chapter by David Rooney, Johann Jacqemin and Ramesh Gardas discusses the thermophysical properties of ionic liquids from an experimental point of view and evaluates the application of models as predictive tools. The difficulties and inherent virtues of some theoretical methods are discussed by me in the next chapter. When applying NMR techniquies, some difficulties are faced. In the next chapter Ralf Giernoth devotes some thoughts to this and provides an overview of how NMR spectroscopy is applied to solve questions of ionic liquid structure and dynamics. An alternative to NMR is optical spectroscopy and consequently this topic is discussed in a separate chapter by Anja Mudring. Again the topic of purity is emphasized. This time, optical purity lies at the heart of the discussion. The final chapter by Suzie Su Yin Tan and Douglas R. MacFarlane highlights the recent progress of biomass processing in ionic liquids. Perspectives on how biomass reactions are related to green chemistry, economic viability and other biomass productions are given.

As editor of the volume, I hope that this collection of fine articles reflects the current status of this important field of ionic liquids in a timely fashion, while at the same time highlighting possible future trends of the field which started because of a practical advantage and grew to such an important field. I would like to thank Fritz Vögtle and Markus Reiher as well as Tom Welton for their support in compiling this volume. To all the contributing authors I am indebted for providing this volume with such excellent and detailed chapters.

Leipzig, Summer 2009 Barbara Kirchner

Contents

Top Curr Chem (2009) 290: 1–40
DOI: 10.1007/128_2008_31

Published online: 21 May 2009

Synthesis, Purification and Characterization of Ionic Liquids

Bronya Clare, Amal Sirwardana, and Douglas R. MacFarlane

Abstract The synthesis, purification and characterization of ionic liquids is reviewed. The major synthetic routes to low melting ionic salts are described in detail. The intrinsic properties of ionic liquids make purification difficult and therefore a special emphasis is placed on currently employed purification methodologies. Synthetic methods which are designed to avoid specific impurities are also discussed. For the same reasons highlighted above characterization of ionic liquids presents unique challenges; the available methods and some of the issues of their use are also reviewed.

Keywords Ionic Liquids • Synthesis • Purification • Characterization

Contents

B. Clare (✉), A. Sirwardana, and D.R. MacFarlane
School of Chemistry, Monash University,
Clayton, Victoria 3800, Australia
e-mail: Bronya.Clare@sci.monash.edu.au

1 Introduction

1.1 Overview

Ionic liquids (ILs) in principle are a diverse group of salts which are liquid at ambient temperatures. While early work in the field tended to presume that ionic liquids had very similar properties as a class, it is now widely recognized that, in fact, they offer a very wide range of properties and that one of the only properties that can be thought of as ubiquitous among ionic liquids is ion conductivity [1]. As the field has thus grown in recent years, producing a wide range of properties in an even wider range of salt structures, the synthetic methods applied to the preparation of these salts have become more sophisticated and capable of targeting more complex compounds. Our goal in this chapter is to provide a comprehensive overview of the synthetic approaches currently available, in such a way that a researcher beginning the synthesis of a new target compound can easily appreciate the synthetic methodology options that might be applied. We also discuss a number of the purification and characterization issues that arise and that are in some cases unique to the ionic liquids field, because of the very nature of the compounds involved.

We begin with a brief overview of the types of cations and anions that are known in the field, as of mid-2008. Part of our goal here is to provide a guide to some of the nomenclature that follows in the remainder of the chapter.

1.2 Cations

The ionic liquid cation is generally an organic structure of low symmetry. The cationic centre most often involves a positively charged nitrogen or phosphorus. Those described thus far are based on ammonium, sulphonium, phosphonium, imidazolium, pyridinium, picolinium, pyrrolidinium, thiazolium, oxazolium or pyrazolium cations, usually completely substituted. The more recent research has mainly focused on room temperature ionic liquids composed of asymmetric dialkylimidazolium cations associated with a variety of anions. Through modification of the cation, the properties of the liquid, notably the melting point and liquid range [2], viscosity [3] and miscibility with other solvents [4], can be altered. On the basis of the cation, ILs may be divided into six groups: (1) five-membered heterocyclic cations, (2) six-membered and benzo-fused heterocyclic cations, (3) ammonium, phosphonium and sulphonium based cations, (4) functionalized imidazolium cations and (5) chiral cations. The discussion below briefly overviews these different families of IL cations.

1.2.1 Five-Membered Heterocyclic Cations

Figure 1 shows some five-membered cations including imidazolium, pyrazolium, triazolium, thiazolium and oxazolium. While the halide salts are usually solids at room temperature there are many anions that lower the melting points of the salts

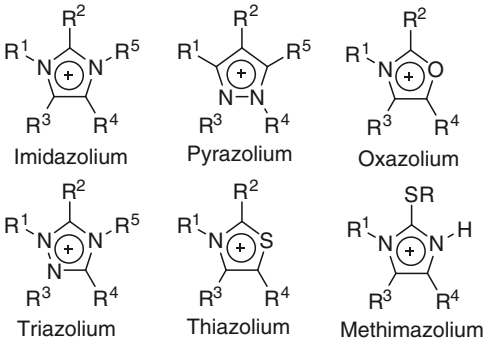

Fig. 1 Five-membered heterocyclic cations

below room temperature. It is generally assumed that non-symmetrical *N*,*N*'-alkylimidazolium cations yield salts having the lowest melting points; however, dibutyl, dioctyl, dinonyl and didecylimidazolium hexafluorophosphates are also liquid at room temperature [5], 1-Butyl-3-methyl and 1-ethyl-3-methylimidazolium cations are probably the most investigated structures of this class.

Similarly, the halide triazolium salts are solids at room temperature, but metathesis to salts, such as bis(trifluoromethanesulphonyl)amide, triflate or tetrafluoroborate, lowers the melting point to near or below room temperature.

1.2.2 Six-Membered and Benzo-Fused Heterocyclic Cations

Figure 2 shows some cations with aromatic character that have been investigated as ionic liquids, such as the pyridinium, viologen-type, benzotriazolium and isoquinolinium cations. Moving up one carbon from the five-membered heterocyclic cations, there is a second, though less explored, class of heterocyclic room-temperature ionic liquids – the pyridinium RTILs. These salts have been known for quite some time, but interest in them has been far less intense than that of the imidazolium family. This is likely due to their more limited stability in the presence of nucleophiles and the toxicity of pyridine. Gordon et al. [6] have reported a series of pyridinium hexafluorophosphate salts with long alkyl chains (C_{12}–C_{18}), some of which melt below 100 °C. A more recent area of focus is the viologen family of ionic liquids. While most viologens are very high melting solids, there is a handful that do exhibit much lower melting points, though not quite room temperature. Benzotriazolium based ILs are often good solvents for aromatic species [7].

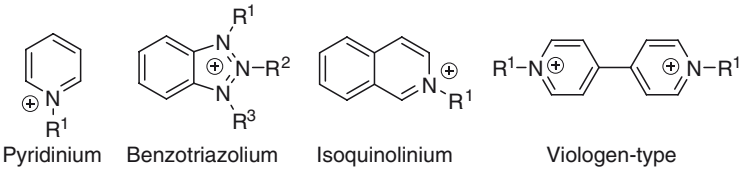

Fig. 2 Six-membered and benzo-fused heterocyclic cations

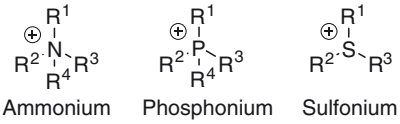

Fig. 3 Ammonium, phosphonium and sulphonium cations

1.2.3 Ammonium, Phosphonium and Sulphonium Based Cations

Tetraalkylammonium (Fig. 3) salts have been known for centuries. In terms of their use as RTILs, earlier studies led to the conclusion that longer alkyl chains were required to obtain room temperature melting points. These are typically prepared by alkylation of the parent amine. To obtain low melting points, typically at least two or three different alkyl groups are required to create crystal packing constraints; this usually requires several steps of alkylation. Although phosphonium RTILs are certainly known and finding growing applications in organic synthesis and other areas [8], there is surprisingly little in the way of published data regarding their physical properties [9]. The hydrogen sulphate salt of the tetrabutylphosphonium cation has a melting point of 122–124 °C, while the hydrogen sulphate salt of the tributyldecylphosphonium cation is a room temperature liquid [10]. In terms of other physical properties, the viscosity of these phosphonium RTILs are generally somewhat higher than their ammonium counterparts, but decrease very rapidly with increasing temperature. Phosphonium salts are generally more stable thermally than ammonium salts [9]. Phosphonium salts are typically made by alkylation of the parent phosphine [11]. As will be discussed further below, for the larger phosphonium cations this is straightforward, however the pyrophoric nature of the lighter alkyl phosphines makes this a more difficult matter. One of the least studied types of RTILs are those based on the trialkylsulphonium cation.

As might be expected, the melting point and density typically decrease as the size of the cation increases. The viscosity, however, reaches a minimum with the triethyl compound and then often increases significantly for the tributyl compound.

1.2.4 Functionalized Imidazolium Cations

Recent advances in ionic liquids research has provided routes for achieving functionalized ionic liquids (Fig. 4) in which a functional group is covalently tethered to the cation or anion of the ionic liquid, especially to the two N atoms of the

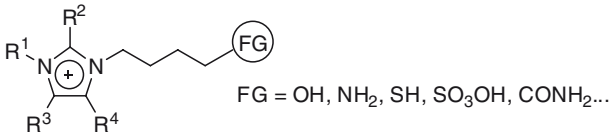

Fig. 4 Functionalized imidazolium cations

imidazole ring. It is expected that these functionalized ionic liquids may further enlarge the application scope of ionic liquids in chemistry.

1.2.5 Chiral Cations

There are growing numbers of reports indicating that chiral ionic liquids may be useful in many areas of science and technology, though synthesis and use of chiral ILs is in its infancy. For example, the use of ephedrinium-based chiral ILs (Fig. 5) as a gas chromatography stationary phase has been reported [12]. Chiral ILs can be prepared either from chiral starting materials (Scheme 1b) or using asymmetric synthesis (Scheme 1a) [13].

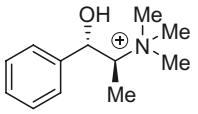

Fig. 5 (1*S*, 2*R*)-(+)-*N*,*N*-dimethylephedrinium ion

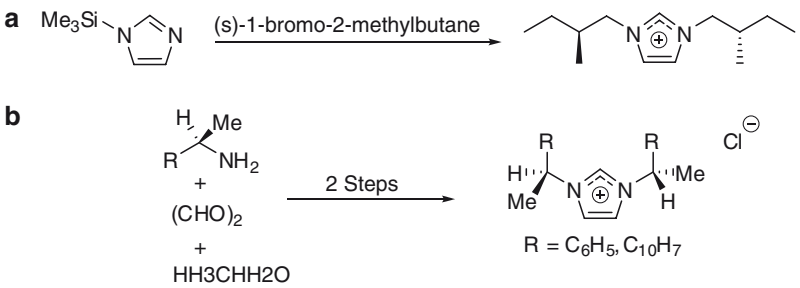

Scheme 1 Synthesis of chiral cations

1.3 Anions

Anions that form room temperature ionic liquids are usually weakly basic inorganic or organic compounds that have a diffuse or protected negative charge. On the basis of the anion, ILs may be divided into six groups: (1) ILs based on $AlCl_3$ and organic salts [14]; (2) ILs based on anions like PF_6^- [5, 15], BF_4^- [16, 17], and SbF_6^- [15];

(3) ILs based on anions like **a** [18, 19], **b** [19, 20], **c**[7] and **d**[19] in Fig. 6; (4) ILs based on anions like alkylsulphates [21], alkylsulphonates [22], alkylphosphates [9], alkylphosphinates [9] and alkylphosphonates [9] (Fig. 7); (5) ILs based on anions such as mesylate, [23, 24] tosylate ($CH_3PhSO_3^-$) [24], trifluoroacetate ($CF_3CO_2^-$) [3], acetate ($CH_3CO_2^-$) [7], SCN^- [25], triflate ($CF_3SO_3^-$) [15, 23, 26] and dicyanamide [$(N(CN)_2^-$] [27, 28]; (6) ILs based on anions such as the borates [29] and carboranes (Fig. 8) [30].

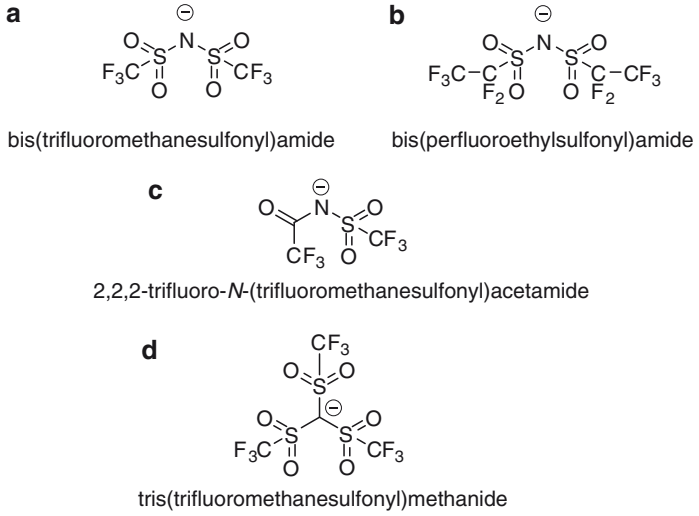

Fig. 6 Amide and methanide anions

Fig. 7 Phosphate, phosphonate, phosphinate, sulphate and sulphonate anions

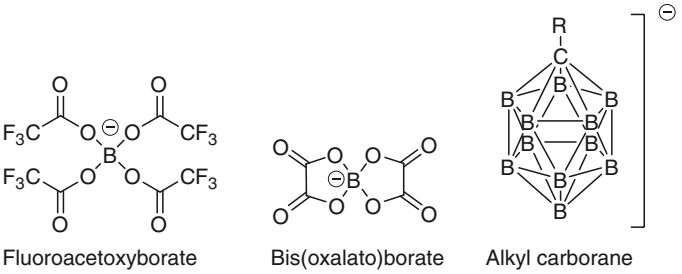

Fig. 8 Borate and borane anions

2 Synthesis

2.1 Metathesis

A great many ionic liquids are prepared by a metathesis reaction from a halide or similar salt of the desired cation. The general metathesis reaction can be divided into two categories (Scheme 2) depending on the water solubility of the target ionic liquid: metathesis via (1) Free acids or group 1 metals/ammonium salts, or (2) Ag salt metathesis.

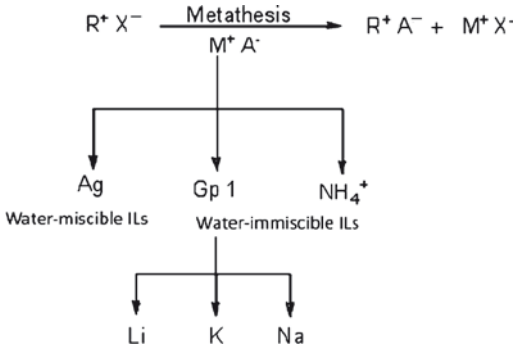

Scheme 2 General metathesis routes to ionic liquids

2.1.1 Metathesis Reactions Involving Free Acids, Group 1 Metals or Ammonium Salts

The most common approach to the preparation of *water immiscible* ionic liquids is the metathesis reaction of the corresponding halide salt, either with the free acid of the anion, or its metal or ammonium salt. Among these alternatives the free acid may be the favored approach as the hydrogen halide produced can easily be removed by washing with water. Here we explain the metathesis reactions based on metal salts, including ammonium salts. In 1996, Bonhote et al. [3] reported the synthesis of dialkylimidazolium bis(triflyl)amides and dialkylimidazolium nonafluorobutanesulphonate by reacting the corresponding halide or triflate with lithium bis(triflyl)amide, $LiNTf_2$, or potassium nonafluorobutanesulphonate in aqueous solution. The resulting ionic liquids were extracted from the aqueous solution into dichloromethane. $[C_2mim][BF_4]$ can be prepared by metathesis reaction of the corresponding chloride or bromide with sodium tetrafluoroborate in propanone; however this leaves appreciable amounts of chloride or bromide ions in the ionic liquid, as sodium halides are slightly soluble in propanone [16]. Therefore, Fuller et al. [31] reported the metathesis reaction of $[C_2mim]Cl$ with ammonium tetrafluoroborate in propanone in high purity.

The water solubility of ionic liquids is very dependent on both the cation and anion. Generally, water solubility decreases with increasing the alkyl chain length on the cation. Seddon et al. [16] have discussed the metathesis reaction of the halide salt

with HBF_4 or $NaBF_4$ in water, followed by extraction into dichloromethane yielding improved purity depending on the length of the alky chain (n) on the imidazolium cation. For example, for n = 6–10 the IL separates as a dense liquid, whereas for chain length $n > 10$ a solid separates from the aqueous reaction mixture. Chains lengths $n = 4$ and 5 can be extracted and purified from aqueous solution by partitioning into an organic solvent. For shorter chains the partition coefficient water:IL:organic solvent is too close to 1, hence the separation is not efficient. In that case metathesis via the alkyl halide with a silver salts is more useful.

Alternatively, the metathesis reaction can be carried out completely in an organic solvent such as CH_2Cl_2 [32] or acetone [31]. In both solvents the starting materials are not completely soluble; however the reaction can be carried out as a suspension. For example, in the case of CH_2Cl_2, the metathesis reaction of 1-alkyl-3-methylimidazole with metal salt can be carried out at room temperature for about 24 h and then the suspension filtered. However, the halide by-products have a limited solubility in CH_2Cl_2 and they can dissolve slightly in the IL/CH_2Cl_2 mixture. Therefore it is necessary that the organic layer be washed with water several times in order to remove the unwanted halides.

When the hydroxide salt is available (for example choline hydroxide is a readily available form of the choline cation), it is very straightforward to react the hydroxide with the acid of the desired anion in water. As long as the resultant ionic liquid can be separated into an organic phase, it is usually straightforward to remove the HX by-product by washing.

2.1.2 Ag Salt Metathesis

The preparation of water-miscible ionic liquids is an important but more difficult task since it requires separation of the by-products from the desired ionic liquid. This can be achieved via the simple metathesis reaction of the corresponding chloride or bromide with the silver salt of the anion. In 1992, Wilkes and Zaworotko [33] reported the first of the new generation of ionic liquids, $[C_2mim][BF_4]$, via metathesis of $[C_2mim]I$ with $AgBF_4$ in methanol. A range of other silver salts has been used for this reaction (such as $AgNO_3$, $AgNO_2$, $AgBF_4$, $Ag[CO_2CH_3]$ and Ag_2SO_4) in methanol or aqueous methanol. Additionally, we have described the use of $Ag[N(CN)_2]$ salts for metathesis reaction to produce dicyanamide ILs [27]. Ag(OH) is a useful approach to generating some of these silver salts where these are not otherwise readily available. Similarly, Reed et al. [30] obtained imidazolium carborane salts by metathesis reactions of silver carboranes with imidazolium chlorides or bromides in varying solvents.

Unfortunately, this route is expensive and forms a large amount of silver halide as by-product. Complete precipitation of silver halides from organic solvents can also be quite slow, leading to silver-contaminated products. The nature of the precipitate can also be troublesome; in some cases the silver halide forms as submicron particles which are difficult to filter. For these reasons, the preferred and most common metathesis approach is still to carry out the reaction in aqueous solution with either the free acid of the appropriate anion, or its ammonium or alkali metal salt as described in Sect. 2.1.1.

2.1.3 Ion Exchange Materials

Currently both natural and synthetic ion exchange materials are used extensively in industry and the laboratory for separation, purification and as convenient heterogeneous reagents for synthetic cation or anion exchange [34]. While ion exchange materials are commonly perceived to be appropriate for the industrial scale synthesis of ILs, very little information is openly available regarding their use in IL synthesis. Essentially ion exchange materials are salts where one of the ions is fixed in a stationary (solid/gel) phase and the counter ion (in solution) is exchangeable. As shown in (1) for anion exchange, when a solution is passed through a column of ion exchange material, the counter ion of the material $[A]^-$ will equilibrate with the corresponding ion of the solution $[B]^-$. Providing the column is of sufficient length and/or the equilibrium constant for (1) is sufficiently large, exchange will take place until complete exchange occurs and only species $[cation]^+ [A]^-$ is eluted as a pure solution:

$$[resin]^+[A]^- + [cation]^+[B]^- \Leftrightarrow [resin]^+[B]^- + [cation]^+[A]^-. \quad (1)$$

Ion exchange is almost always a reversible process and ion exchange materials usually show a preference for one ion over another. The most successful synthetic ion exchange occurs when the ion exchange material shows a strong preference for the counter ion of the starting material over the corresponding ion of the product, i.e. the reaction from left to right in (1) will be most successful if the ion exchange material prefers $[B]^-$ over $[A]^-$. The factors which determine this preference are complex, but in crude, well known terms ion exchange materials tend to have a higher affinity for ions:

- With a higher valence
- With a smaller (solvated) volume
- With greater polarizability
- Which interact more strongly with the exchange material

Commonly, target IL cations and anions are available as either the alkali metal salt or the halide salt and the above principles suggest many ion exchange materials will show a preference for these counter ions and therefore IL synthesis from these starting materials will be successful. The preference principles may hinder the initial loading of an ion exchange material with an IL ion; however there are additional techniques available to load a lower affinity ion onto an ion exchange material. For example, as long as the affinity difference is not too great, a high concentration and multiple passes of the loading solution will usually be effective. Acid/base neutralization can also be used to load a low affinity ion onto the ion exchange material, e.g. for a low affinity anion the ion exchange material can be preloaded with OH^- ions and then reacted with the acid of the of the low affinity anion.

Surprisingly, literature on the use of ion exchange materials for IL synthesis is scant; however two useful examples illustrate the process. Lall et al. described the use of an anion exchange material to synthesize polyammonium phosphate ILs from their parent halides [35] and Mizuta et al. have a patent on the use of an anion exchange material to produce $[C_2mim][DCA]$ from $[C_2mim][Br]$ on an industrial scale [36].

Determining the conditions required for successful ion exchange synthesis, including the choice of an optimum ion exchange material, can be a lengthy process and must be adjusted for each target product. This is considered a major hindrance to the use of ion exchange materials for the laboratory scale synthesis of ILs; however, many IL ions have similar chemical and physical properties and should therefore behave similarly in ion exchange. It is therefore the belief of the authors that the time investment required in determining suitable ion exchange conditions for the laboratory scale synthesis of ILs is in many cases justified, especially if > 100-g quantities and/or repeated preparations over an extended period of time are envisaged. Ion exchange also has the advantage of performing both synthesis and purification in one step.

2.2 *Halogen Free Synthesis*

The vast majority of ionic liquids are usually prepared by quaternisation of imidazoles, alkylamines or phosphines, often employing alkyl halides as alkylating agents, followed by anion metathesis (see Sect. 2.1 herein). Though the anion metathesis methods produce a large number of ionic liquids of good quality, production of high purity materials is a little problematic due to contamination by residual halide. The presence of halides in the resulting ionic liquids can drastically change the physical properties [37], and may result in catalyst poisoning and deactivation [38]. Therefore, various synthetic strategies have been devised to synthesize halide free ionic liquids. Dupont et al. [39] reported the direct synthesis of 1,3-disubstituted imidazolium tetrafluoroborate ionic liquids using a one step procedure (2). Reaction of formaldehyde with *n*-butylamine followed by addition of methylamine, aqueous HBF_4 solution and aqueous glyoxal solution affords, in 66% yield, a mixture of $[C_4mim][BF_4]$, $[BBIM][BF_4]$ and $[C_1mim][BF_4]$ in a molar ratio of 5:4:1:

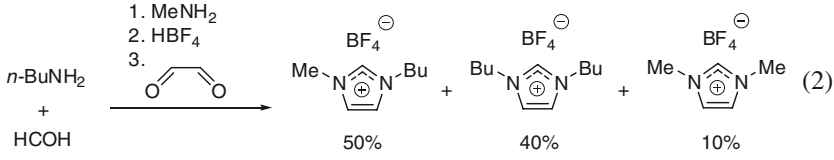

(2)

Other direct syntheses of halide free ionic liquids can be categorized into three groups: (1) synthesis via N-heterocyclic carbene intermediates, (2) phosphorus based direct reactions with imidazoles and (3) sulfur-based direct reactions with imidazoles as discussed further below.

2.2.1 Synthesis of Ionic Liquids via N-Heterocyclic Carbene (NHC) Intermediates

Carbenes are molecules which have a lone pair of electrons on a carbon atom; this in turn renders them highly reactive. As a result, carbenes are useful intermediates in the synthesis of chemical compounds. Generally they can only be isolated in

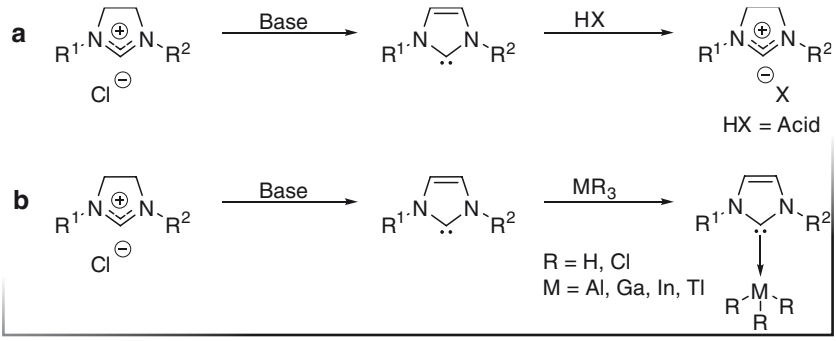

Scheme 3 Synthesis of ionic liquids via a carbene

the form of, for example, metal carbenoid species. The synthesis of ionic liquids via carbenes can be achieved either by the reaction of NHC adducts with acids (Scheme 3a), or reaction of NHC-organometallic intermediates with acids (Scheme 3b).

2.2.1.1 Preparation of NHCs and Reaction with Acids

Numerous methods for the generation of imidazole carbenes have been reported. For example, starting from an imidazolium halide, the use of systems such as sodium hydride in ammonia or dimethylsulphoxide (DMSO), sodium in ammonia, alkali metals in tetrahydrofuran (THF), metal *tert*-butoxides in THF or DMSO, etc. Recently, Seddon and Earle reported a simple procedure for the generation of the imidazolium carbene **2** in 90–95% yield from an imidazolium chloride **1** which does not require solvents, filtrations, or produce noxious waste products (Scheme 4) [40].

These carbenes can be used to produce the corresponding imidazolium salts by a simple reaction with the protonated form (**3**–**8** [41]) of the required anion (Scheme 4). The advantage of making these imidazolium salts by this process, i.e. by reaction of two neutral molecules, is that it generates ionic liquids which are not contaminated by unwanted halide ions or metal ions.

The 1,3-dialkylimidazolium-2-carboxylates **8** readily react with dry methanol, benzoylacetone and benzaldehyde in the presence of a stoichiometric amount of $NaBF_4$, KPF_6 or $NaBPh_4$ quantitatively affording the corresponding 1,3-dialkylamidazolium salt according to Scheme 5 [42].

Quite recently, Rogers et al. [43] reported the synthesis of intermediate **8a** (3) by the reaction of DMC with 1-methylimidazole **9** at 120–130 °C, in which the acidic C2-hydrogen of the resulting 1,3-dimethylimidazolium cation is abstracted by the methyl carbonate anion, leading to the heterocarbene and HOC(O)OMe which is unstable and gives rise to MeOH and CO_2. Nucleophilic attack on CO_2 by the carbene is the only favored process and leads to the observed zwitterion **8a**. Then 1,3-dimethylimidazolium-2-carboxylate **8a** can be reacted with any of the acidic components in Scheme 4:

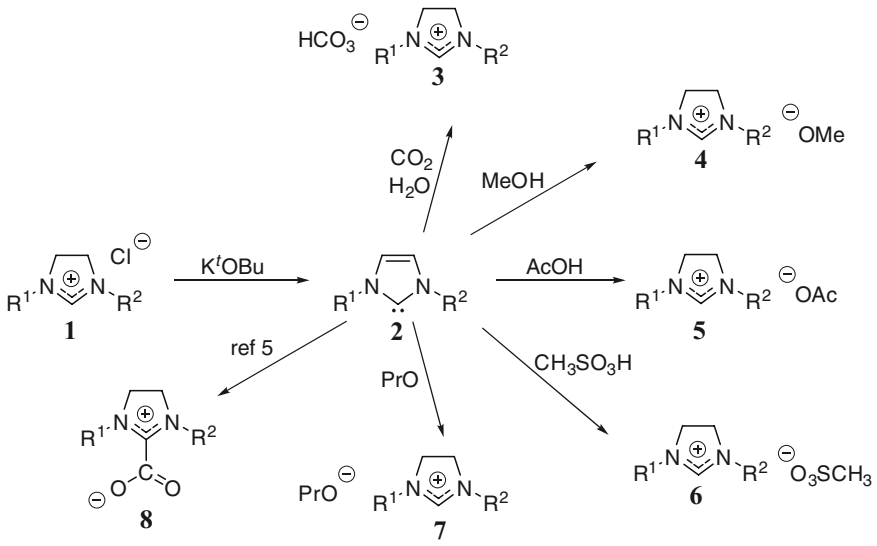

Scheme 4 Synthesis of various ionic liquids via a carbene intermediate

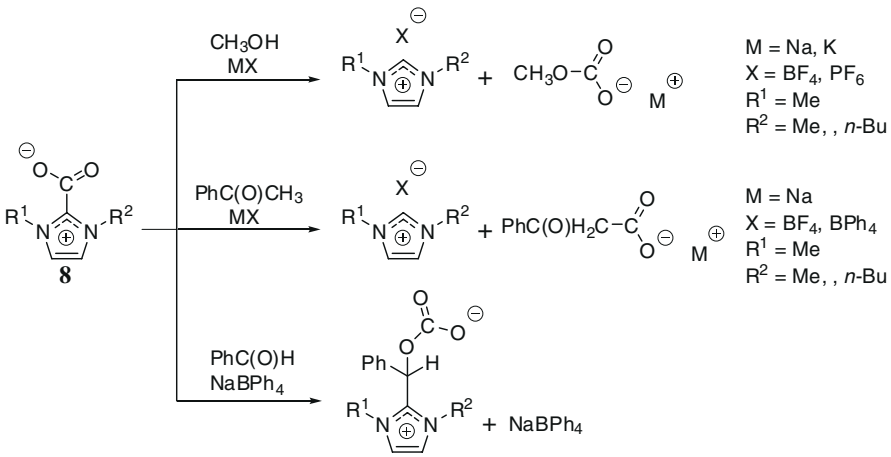

Scheme 5 Synthesis of 1,3-dialkylimidazolium salts from the dialkylimidazolium carboxylate

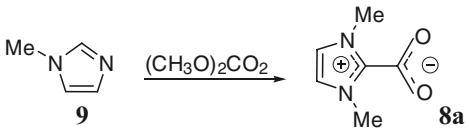

(3)

2.2.1.2 Reaction of NHC-Organometallic Intermediates with Acids

Recently, Cole et al. [44] have systematically studied the preparation, stability and synthetic utility of NHC adducted group 13 trihydrides and trihalides (Scheme 6). These

reactions suggest group-13 coordinated NHCs remain available for secondary acid–base reactions to synthesize ionic liquids. For example, the reaction of NHC stabilized aluminium trihydride species **10a** with three equivalents of phenol potentially offers a preferable path to **11** (route a). Meanwhile, the reaction of **10b** with 1,1,1,5,5,5,-hexafluoropentan-2,4-dione (F_6acacH) produced **12** (route b).

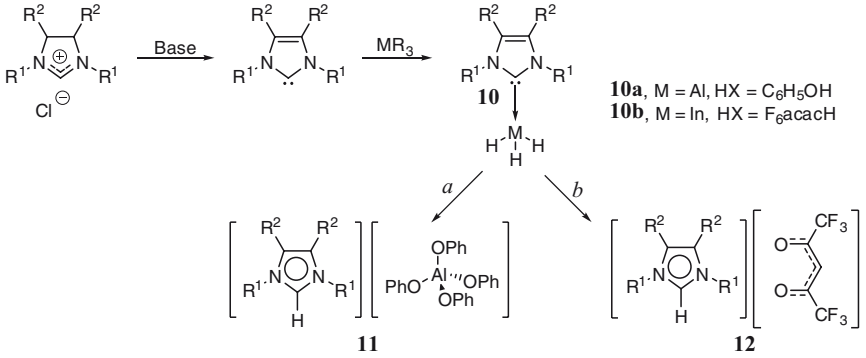

Scheme 6 Reaction of NHC-organometallic intermediates with acids

2.2.2 Phosphorus Based Ionic Liquids

Halogen-free phosphorus based ionic liquids can be produced by direct reaction of: (1) phosphines with sulphates; (2) tertiary phosphines or imidazoles with alkylating agents such as trialkylphosphates, dialkylphosphonates and monoalkylphosphinates; or (3) phosphines with acid (Scheme 7).

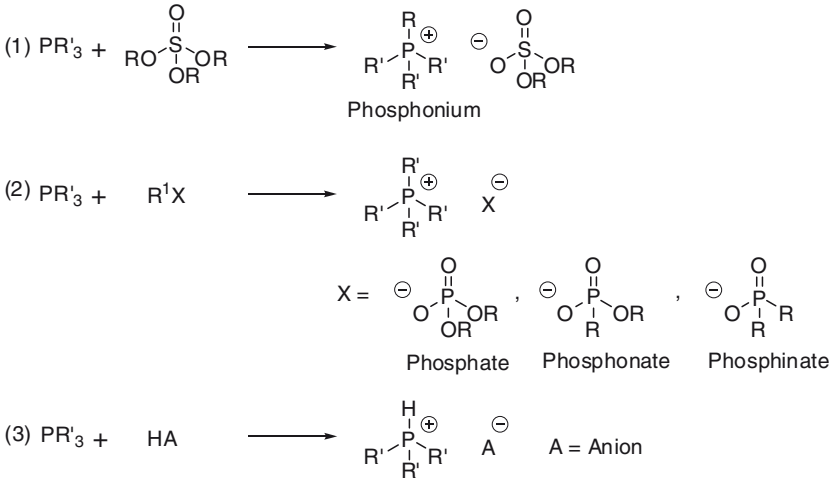

Scheme 7 Halogen free synthesis of phosphonium ionic liquids

Ammonium dialkylphosphates were first described in 1952 [45]. The alkylation products of pyridine and trialkylphosphates were described to be salts with very low melting points in 1989 [46]. Recently, Cytec filed patents on the synthesis of imidazolium based dialkylphosphate ionic liquids [9]. For example, they synthesized tetrabutylphosphonium dibutylphosphate, *N,N*-dimethylimidazolium dimethylphosphate, *N*-methyl-*N*-butylimidazolium dibutylphosphate, and *N*-methyl-*N*-ethylimidazolium ethylethanephosphonate. Downard and co-workers [9] reported synthesis of phosphonium, phosphates, phosphonates and phosphinates by direct reaction of phosphines or imidazoles with alkylating agents such as dialkylsulphate, trialkylphosphates and dialkylphosphonates and monoalkylphosphinates (Scheme 8).

Quite recently, to develop an optimized synthetic protocol for the alkylation of 1-alkylimidazole compounds with trimethylphosphate, the kinetics of the synthesis of 1,3-dimethylimidazolium dimethylphosphate were studied in detail [45]. The synthesis of the phosphonium salts derived from the reaction of phosphines with acids, has not been widely discussed. In 1991, Whitesides synthesized tris(2-carboxyethyl)phosphine hydrochloride [47]. Since then, air sensitive phosphonium salts have also been synthesized by the reaction of phosphine with a solution of aqueous HBF_4:

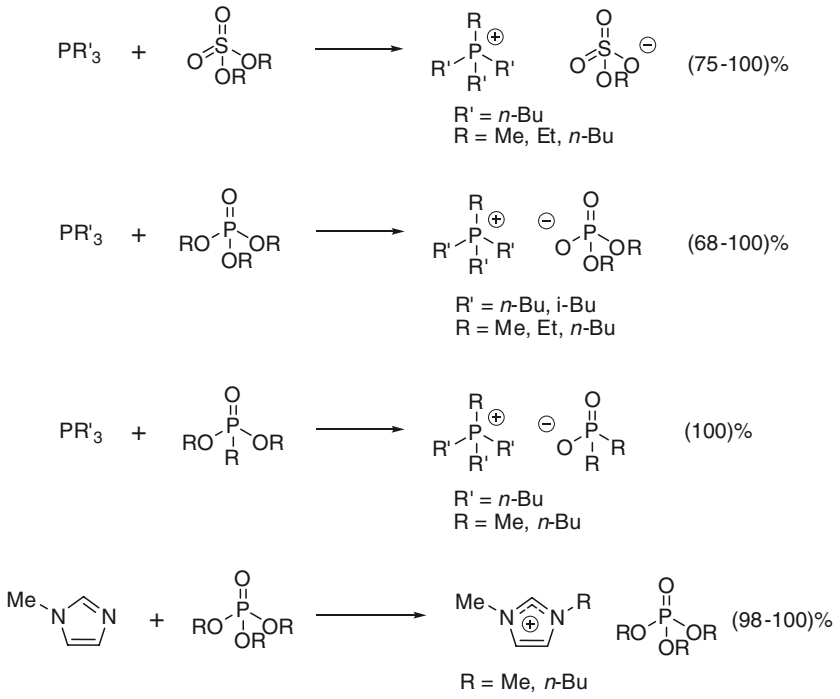

Scheme 8 Direct alkylation via sulphonates, phosphonates and phosphinates

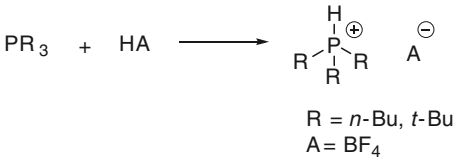

(4)

2.2.3 Sulfur Based Ionic Liquids

Direct synthesis of sulfur based ionic liquids has been developed as a useful synthetic method for halogen free ionic liquids. The synthesis of sulfur based ionic liquids can generally be split in to two sections: (1) sulphonate and (2) sulphate based ionic liquids (Scheme 9). The sulphate based salts are more common than the sulphonates.

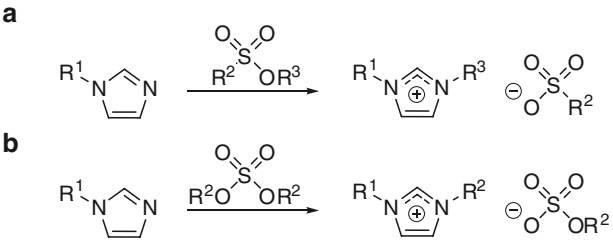

Scheme 9 Sulphate and sulphonate ionic liquids

2.2.3.1 Sulphonate Based Ionic Liquids

Direct addition of an alkylsulphonate into imidazole is useful, not only to synthesize the sulphonate anion, but also different anions via metathesis in the halogen free method. For example, the alkylation of *N*-alkylimidazoles such as *N*-methylimidazole with alkylsulphonate can be performed under solventless conditions at room temperature affording, after 48–72 h, the corresponding 1,3-dialkylimidazolium alkanesulphonate salts as crystalline solids in almost quantitative yields (5) [48]. The alkane sulphonate anions can easily be substituted by a series of other anions by metathesis:

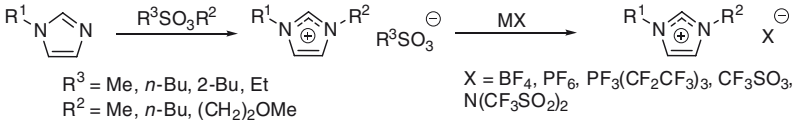

(5)

Jonathan and Mikami [49] reported a straightforward synthesis of new chiral ionic liquids bearing an imidazolium core, an easy and efficient method (6). Commercially available ethyl lactate was converted into its triflate derivative which upon reaction with 1-methylimidazole gave the triflate salt as a solid in excellent yield. Then anion metathesis was performed to obtain different anions with imidazole cation:

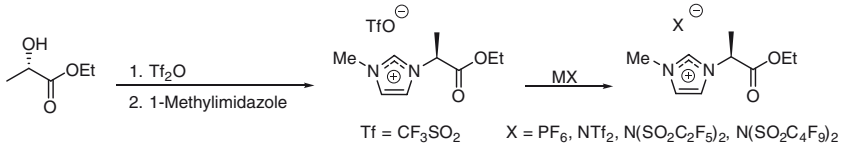

(6)

2.2.3.2 Sulphate Based Ionic Liquids

The hydrophilic ionic liquid [C_2mim][$EtSO_4$] has received great attention, becoming one of the first ionic liquids commercially available in bulk. Ionic liquids containing methyl- and ethyl-sulphate anions can be easily and efficiently prepared under ambient conditions by the reaction of 1-alkylimidazoles with dimethyl sulphate and diethylsulphate (7) [21]:

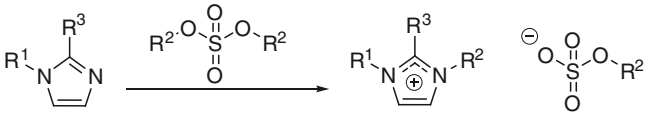

(7)

Quite recently, *trans*-esterification of 1-alkylimidazoliumsulphate was carried with functionalized and non-functionalized alcohols, to the corresponding new alkylsulphates (Scheme 10) [50].

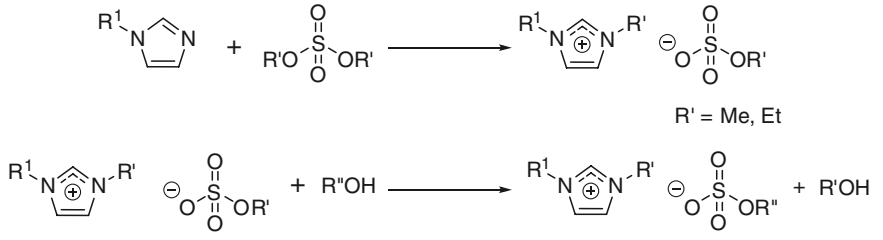

R"OH = *n*-Butanol, *n*-Hexanol, *n*-Octanol, Diethyleneglycolmonoethylether, 2-Mehtoxyethanol, 2-Ethoxyethanol, 2-Butoxyethanol, Diethyleneglycolmonomethylether

Scheme 10 Trans-esterification routes to alkylsulphates

2.3 Protic Ionic Liquids

Protic ionic liquids (PILs) are formed by proton transfer between an equimolar mixture of a Bronsted acid and a Bronsted base. The major difference between PILs and other ILs is the presence of this exchangeable proton. Among other things, this can produce hydrogen bonding between acid and base and in some cases an H-bonded extended network. Presuming that the parent acid and base are available in a highly pure state, the acid/base neutralisation process can directly produce a highly pure ionic liquid. Angell and co-workers [51] synthesized a variety of PILs including organic and inorganic anions. Based on the Walden rule, they pointed out that systems with either associated ions or weak proton transfer form only "poor" ionic liquids [52]. Ohno et al. [53] have also described the convenient synthesis of protic ionic liquids by neutralization of organic tertiary amines with organic acids or inorganic acids (Scheme 11).

Drummond et al. [54] synthesized protic ionic liquids by combining Bronsted acid/base pairs where the primary amine cations were of the form RNH_3 and R(OH) NH_3 combined with organic anions of the form RCOO, R(OH)COO or with an inorganic anion. They studied physicochemical properties of synthesized PILs at nominally equimolar ratio of anion and cation (1:1 stoichiometry) and in the presence

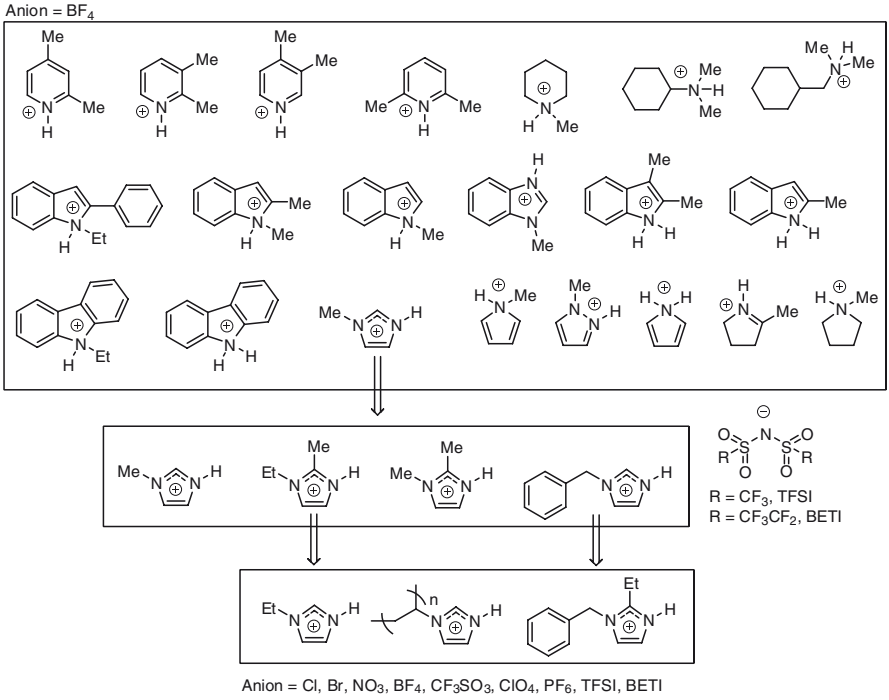

Scheme 11 Synthesis of a variety of protic ionic liquids

of either excess acid or excess base [55]. We have prepared (Scheme 12) PILs containing the methylpyrrolidinium cation and used NMR shifts as a function of the acid strength to establish an ionization curve and suggested that the aqueous p*K*a values for the acid and base may be useful in obtaining an indication of how ideal, in terms of ionicity, the PIL is likely to be [56]. It appears that a difference of aqueous p*K*a values > 10 is required for complete proton transfer to form the salt. This is a very significant issue [1] in that for acid/base pairs where this is not true, the liquid produced is in fact a complex mixture of ions dissolved in a mixture of acid and base.

Quite recently [57], we reported the synthesis of dimeric or oligomeric mixtures of *N*-methylpyrrolidine and acetic acid using a simple neutralization reaction by adding the stoichiometric amount of acid dropwise to the base. It appears that the highest degree of ionicity, corresponding to the strongest degree of proton transfer, occurs at compositions much richer in acid than the equimolar composition, suggesting that the dimer and oligomeric acids are much stronger acids in neat system than monomeric acid.

Protic imidazolium and alkoxyimidazolium based ionic liquids as both solvents and Bronsted catalysts for catalytic reactions have been synthesized (Fig. 9) [58].

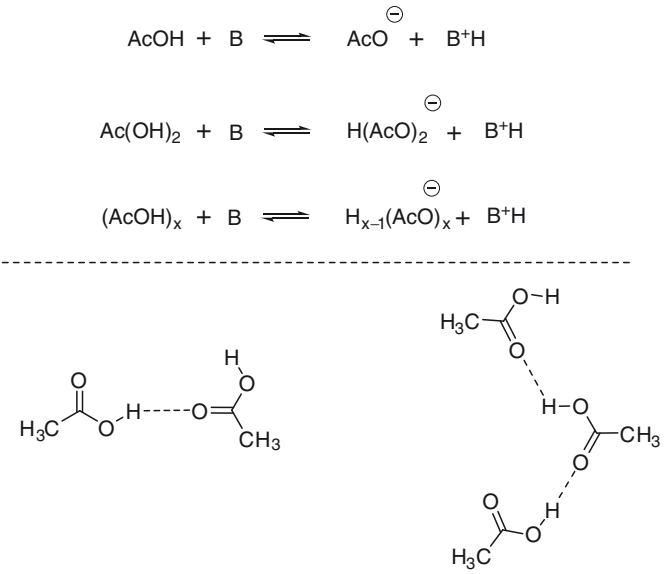

Scheme 12 Possible formation of dimeric and higher-order oligomeric acetic acid

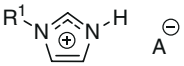

R^1 = Me, Butyl, Hexyl, Decyl, $CH_2OC_4H_9$, $CH_2OC_6H_{13}$, $CH_2OC_9H_{19}$, $CH_2OC_{10}H_{21}$
A = DL-Lactate, L-Lactate, Salicylate, BF_4, NTf_2

Fig. 9 Protoc imidazolium and alkoxyimidazolium based ionic liquids

There are two significant preparative issues that arise with protic ionic liquids:

1. As shown by Angell et al. [51] and MacFarlane et al. [59], ionic liquids can be distinctly volatile unless ΔpKa for the acid/base pair is high (>10). The volatility arises from the vapour pressure of the residual acid and base that exist in equilibrium with the ions. Since these will have different vapour pressures in principle, any evaporation from the ionic liquid will change its composition. Thus elevated temperature drying of these ILs must be treated with caution and the anion/cation stoichiometric balance proven by an appropriate method (NMR or microanalysis) after the drying is complete.
2. Primary and secondary amines can, in principle, form an amide rather than the salt when combined with certain acids. This is especially troublesome when elevated temperatures are involved in the process. Therefore, it is very important to prove the structure in those cases where amide formation is possible.

2.4 Special Cases

2.4.1 Metal Based Ionic Liquids

Ionic liquids with anions containing transition metal complexes were among the earliest developed room temperature ionic liquids [60]. Transition metal based ionic liquids have been synthesized either by reaction of phosphonium or imidazolium halides with the corresponding metal halides, or by metathesis with alkali salts of the metal-based anions. Among the metal containing ionic liquids, ionic liquid-crystals are excluded in this section as they were reviewed thoroughly in 2005 [61]. Synthesis of metal based salts can be divided in to three groups: (1) transition metal salts, (2) *p*-block metal salts and (3) *f*-block metal salts.

Co and Ni based ionic liquids [62] can be synthesized directly by mixing the corresponding metal chloride with $[C_2mim]Cl$ under an inert atmosphere. The metal chloride anions interact with the imidazolium ring hydrogens to form a hydrogen bonded network (Fig. 10).

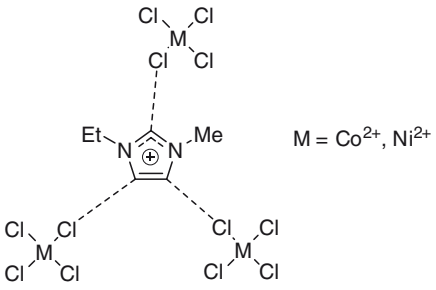

Fig. 10 Co- and Ni based ionic liquids

Vanadium-based salts [63] such as $[C_2mim]_2[VOCl_4]$ can be obtained from the reaction of $[C_2mim]Cl$ with $VOCl_2(CH_3CN)_x$. Addition of thionyl chloride to $[C_2mim]_2[VOCl_4]$ produces $[C_2mim]_2[VCl]_6$. Ferrocene containing room temperature ionic liquids [64] can be synthesized by the reaction of mono- or di-substituted (trimethylammonium) ferrocene iodide with imidazole or triazole (Scheme 13). These initially produce the ferrocene linked imidazole or triazole. Then quaternisation with methyliodide followed by metathesis with lithium bis(trifluoromethanesulphonyl) amide, $LiNTf_2$, produces the imidazolium or triazolium ionic liquids.

Several groups [65] have studied Fe^{2+} and Fe^{3+} based ionic liquids; $[C_4mim][FeCl]_4/[Fe_2Cl_7]$, $[C_4mim][FeCl_4]$, $[BDmim][Fe^{2+}Cl_4][Fe^{3+}Cl_4]_2$ have been reported. The formation of a Cu^+-based room temperature ionic liquid $[C_2mim]Cl$–$CuCl$ was reported in 1986. Very recently Sundermeyer's group [66] reported the Cu^{2+} containing ionic liquid $[C_4mim]_2[Cu_3Cl_8]$. The $[C_Rmim][ZnX_2Y_2]$ ionic liquid system (R = Me, Et, *n*-Bu, Benzyl; X = Y = Cl or Br or X = Cl, Y = Br) was synthesized by reacting ZnX_2 with (1-R-3-methylimidazolium)Y [67]. The single crystal X-ray structural analysis and elemental analysis of $[C_Rmim][ZnX_2Y_2]$ revealed that two imidazolium cations were paired with a dibromodichloro zincate dianion.

In 1998, Dupont et al. [68] reported the synthesis of $[C_4mim]_2[PdCl_4]$ (Fig. 11). Solid IL-coordinated Pd^{2+} complex **13** was synthesized by the reaction of a nitrile functionalized ionic liquid with $PdCl_2$ at room temperature. [69] Shreeve and co-workers [70] synthesized the IL-coordinated compound **14** (Fig. 11).

$[C_nmim][PtCl_n]$ (C_n = Et, Bu, n = 4, 6) was synthesized by the reaction of Pt^{2+} or Pt^{4+} chlorides with $[C_nmim]Cl/[AlCl_3]$ or $[C_nmim]Cl$ [71]. Several Pt metal based ionic liquids (**15**, **16** and **17**) have been reported (Fig. 12) [72].

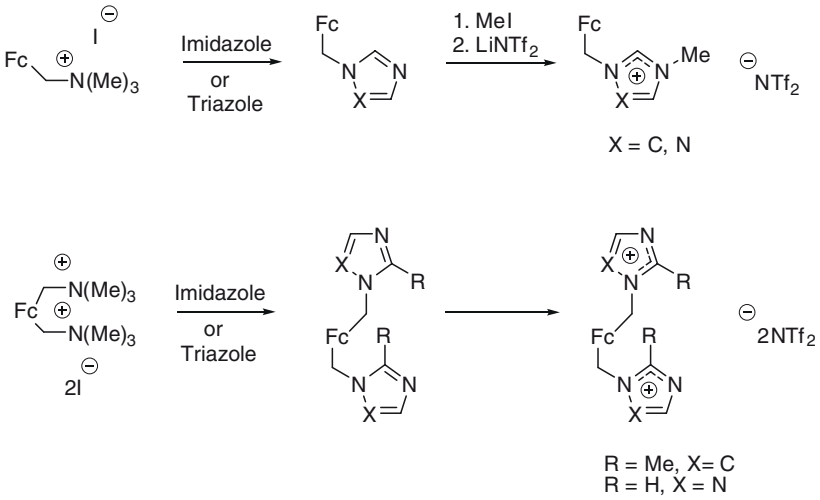

Scheme 13 Formation of imidazolium-based ionic liquids containing feurocenium

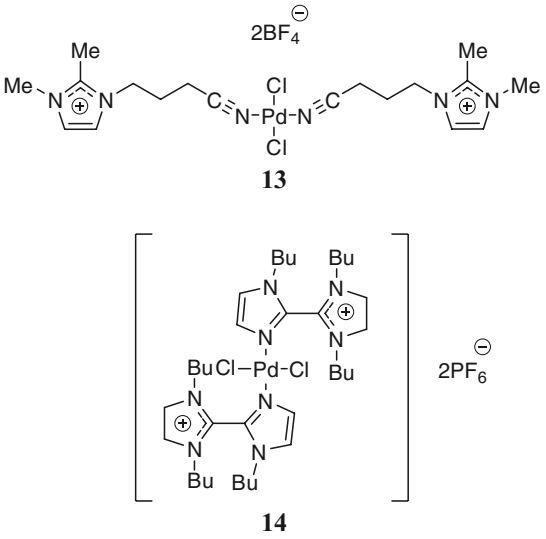

Fig. 11 Formation of imidazolium-based ionic liquids containing palladium

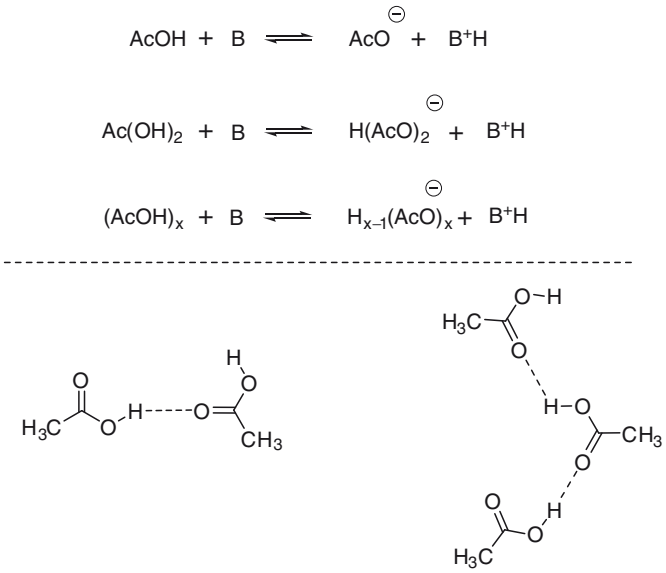

Fig. 12 Pt containing ionic liquids

Several transition metal based ionic liquids based on Nb [73], Ta [73], Ag [74], Au [75], Mn and Co [76], Rh [76] have been prepared by similar methods.

Other metal based ionic liquids have included *p*-block metal based ionic liquid systems based on Sn [77], In [78], Bi [76], Pb [79] have been prepared. In 1986,

Uranium-based salt of the type $[C_2mim]_2[UCl_6]$ was obtained from the reaction of $[C_2mim]Cl$ with UCl_4 [80]. Recently, synthesis of low-melting lanthanide-containing ionic liquids of the type $[C_4mim]_{x-3}[Ln(NCS)_x(H_2O)_y]$ (x = 6–8, y = 0–2, Ln = Y, La, Pr, Nd, Sm, Eu, Gd, Tb, Ho, Er, and Yb) have been reported [81].

2.4.2 Functionalized Ionic Liquids

During the last 8 years [82, 83], various types of functionalized ionic liquids (Fig. 13) expressly categorized as being "task-specific" ionic liquids have been designed and synthesized for specific purposes such as catalysis, organic synthesis, separation of specific materials, as well as for the construction of nanostructure materials and ion conductive materials, etc. The salts are defined as functionalized ionic liquids when they are ionic liquids in which a functional group is covalently tethered to (1) the cation, (2) the anion, or (3) a zwitterionic form of the salt. It is typically the cation that bears the reactive moiety. In fact, instances in which the anion comprises the active constituent are few.

Until recently, the method used to incorporate the functionality into the ionic liquid was almost always displacement of the halide from an organic halide containing the functional group by a parent imidazole, phosphine, etc.:

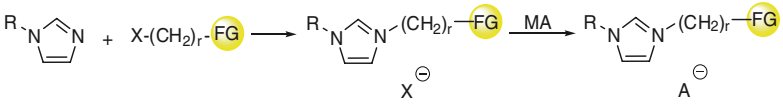

(8)

In their pioneering work Davis and Rogers [84, 85] have reported the synthesis of imidazolium salts with urea, thiourea and thioether groups in one of the *N*-alkyl substituents (Fig. 14).

Recently, novel sulphonyl-functionalized ionic liquids with SO_3H and SO_2Cl groups have been designed, synthesized and characterized. First reported were Bronsted-acidic functionalized ionic liquids bearing an alkane sulphonic acid group in an imidazole or triphenylphosphine cation (Fig. 15a) [86] or in a pyridinium cation (Fig. 15b) [87].

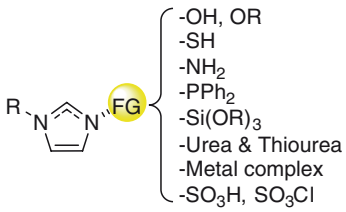

Fig. 13 Types of functionalised ionic liquids

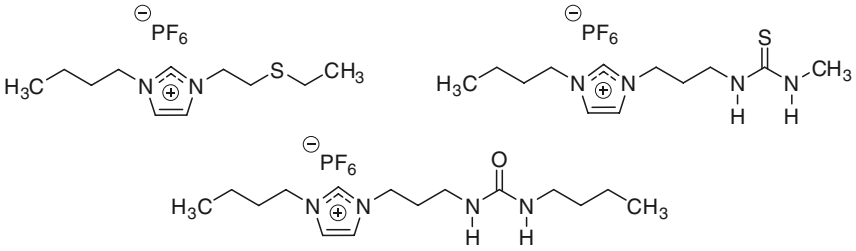

Fig. 14 Imidazolium salts with urea, thiourea and thioether groups

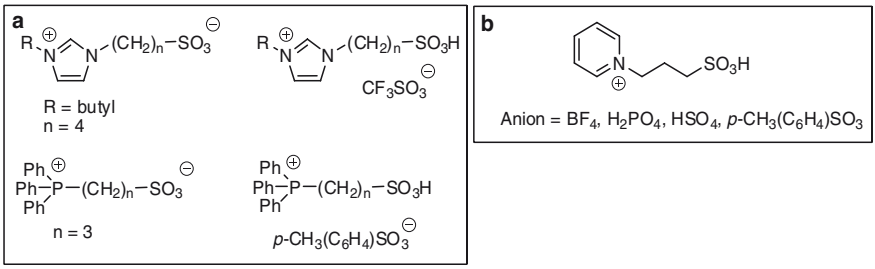

Fig. 15 Synthesis of sulphonate functionalized ionic liquids

Functionalized ionic liquids possessing two Bronsted acid sites with COOH, HSO_4 or H_2PO_4 groups were reported by Dan [40] in 2007:

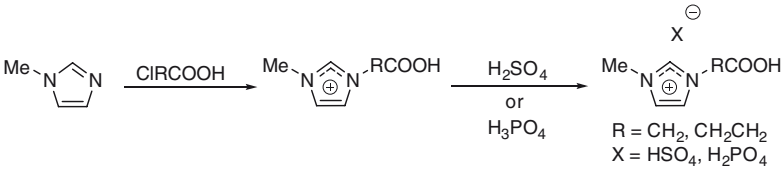

(9)

Recently, ionic liquids with amino acids as anions were synthesized by neutralization between $[C_2mim][OH]$ and amino acids [88]. Tetrabutylphosphonium amino acids $[P(C_4)_4][AA]$ were synthesized by the reaction of tetrabutylphosphonium hydroxide $[P(C_4)_4][OH]$ with amino acids, including glycine, L-alanine, L-β-alanine, L-serine and L-lysine [89]. The esters or amide derivatives of bromoacetic acid were either commercially available or formed in one step via the reaction of bromoacetyl bromide with the appropriate alcohol or amine [90–92]. An advantage of this route is that a wide range of ester and amide side chains can be prepared easily. For ionic liquids with anions other than bromide, a metathesis reaction was employed to introduce the counter ion of choice. Additionally, functionalized ionic liquids with electrophilic alkene-type appendages were synthesized.

Cations bearing nitrile functional groups which were used as ligands for organometallic chemistry, have been synthesized by several groups (Scheme 14) [90].

Phosphines bearing imidazolyl moieties have attracted substantial interest because of their potential to bind soft and hard transition metals via phosphorus or nitrogen. There are only a very few reports on phosphine functionalized ionic liquids (Fig. 16) – (1) Type 1: 2-imidazolium phosphines (D^+X^-) [91], (2) Type 2: guanidininium phosphines (C^+X^-) [92], and (3) Type 3: 3-imidazolium phosphines (B^+X^-) [91].

Afonso et al. [93] reported the synthesis of functionalized ionic liquids, based on imidazolium cations that contains ether or alcohol as functional groups. Alkylation of methylimidazole with the appropriate alkyl halide is followed by halogen exchange with slight excess KPF_6, $NaBF_4$ or $NaCF_3CO_2$ in order to reduce the amount of remaining halogen content.

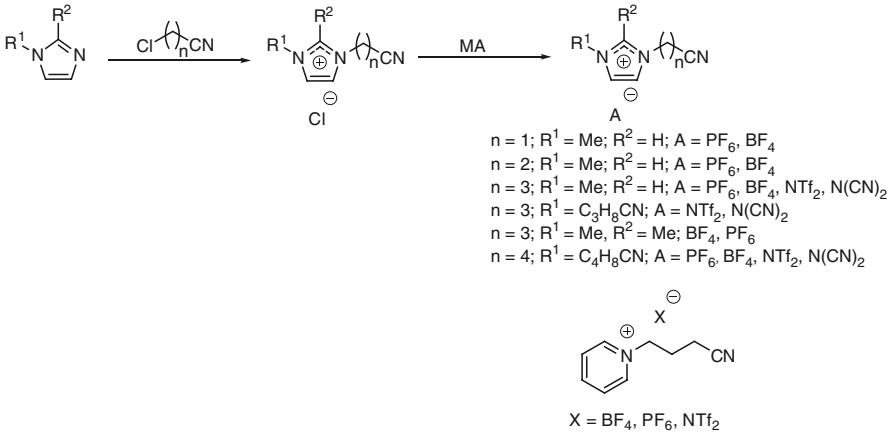

Scheme 14 Nitrile functionalized ionic liquids

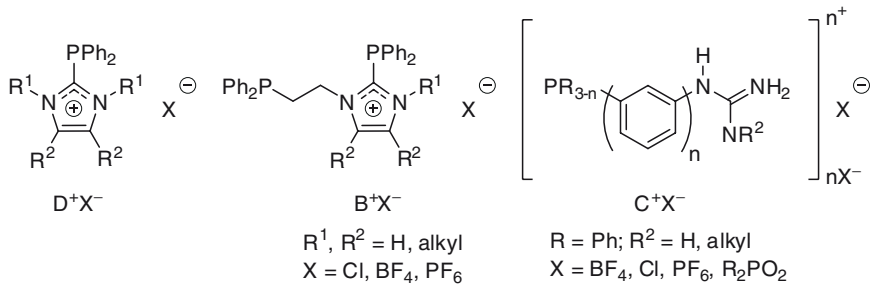

Fig. 16 Phosphine functionalized ionic liquids

2.4.2.1 Miscellaneous

Synthesis of functionalized hydrophobic ionic liquids bearing the 2-hydroxybenzylamine substructure, and their application in partitioning of metal ions from water have been described (Scheme 15) [94].

(*S*)-Proline-modified functionalized chiral ionic liquid is useful as a recoverable catalyst for direct asymmetric reactions [95]:

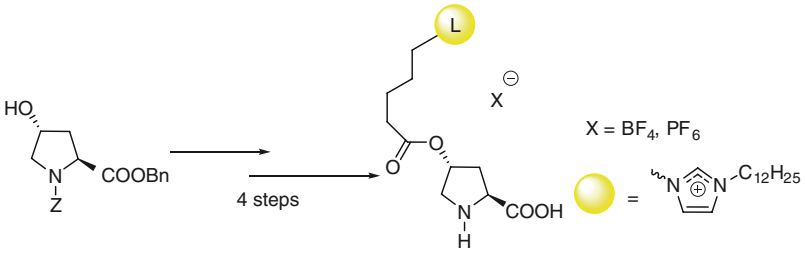

(10)

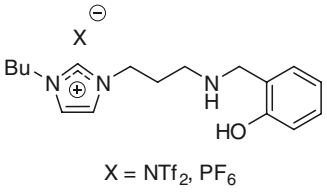

Scheme 15 Functionalized hydrophobic ionic liquids

Bazureau et al. reported the synthesis of novel ester and carbonyl groups appended functionalized grafted ionic liquid phases. Two synthetic strategies were developed for the preparation of the ionic liquid phases (Scheme 16) [96].

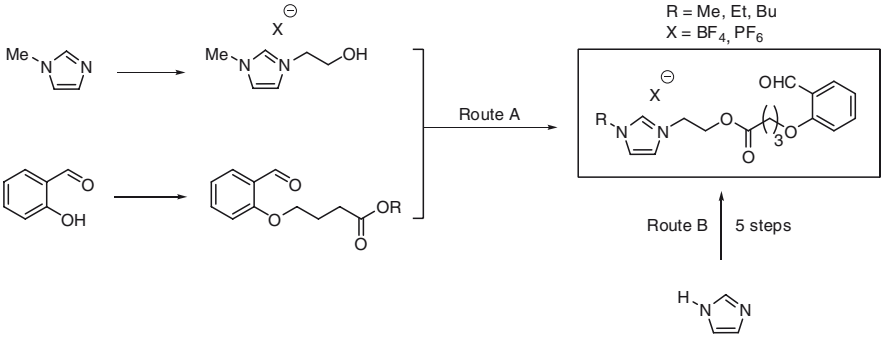

Scheme 16 Ester and carbonyl groups appended functionalized ionic liquid phases

Bazureau et al. reported the synthesis of poly(ethyleneglycol) functionalized -ionic liquid phases as functionalized ionic liquids which are promising tools for synthetic applications in ionic-phase combinatorial chemistry [97]. Moreover, several research groups have described ionic liquids with imidazolium cations carrying amino functionality. Davis et al. [98] reported for the first time a functionalized ionic liquid with NH_2 group, *n*-propylamine-3-butylimidazolium tetrafluoroborate **18**, for capturing CO_2 (Scheme 17).

2.4.2.2 Functional Group Covalently Tethered to the Anion

Electroactive, functionalized ionic liquid, tetraalkylphosphonium polyoxometalates were synthesized by the substitution of sodium tungstate with tetaralkylphosphoniumbromide $[(C_6H_{13})_3P(C_{14}H_{29})]_2W_6O_{19}$ [99].

2.4.2.3 Zwitterionic-Type

Ohno et al. [100] reported that the synthesis of zwitterionic-type molten salts and their polymers (Scheme 18). Since zwitterionic-type salts have both cation and anion in intramolecular form, these ions cannot migrate with the potential gradient.

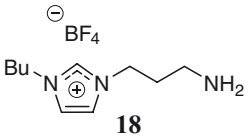

18

Scheme 17 Functionalized ionic liquids with NH_2 group

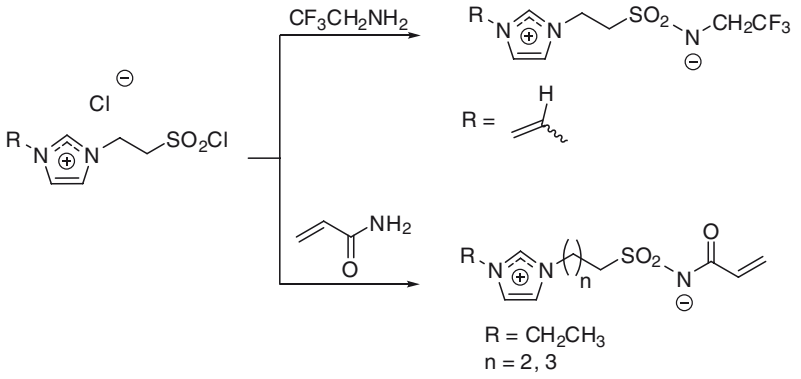

Scheme 18 Zwitterionic-type malten salts and their polymers

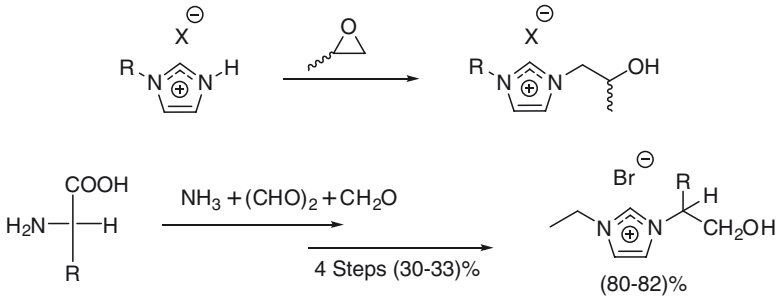

Scheme 19 Alcohol substituted ionic liquids

At least two alcohol-group specific synthetic approaches have recently been disclosed (Scheme 19). In the first, Holbrey and Rogers [101] describe a simple, high-yielding one pot method for the synthesis of alcohol-appended imidazolium functionalized ionic liquid. In the reaction, a pre-formed imidazolium-H salt of the functionalized ionic liquid anion is reacted with an epoxide, the latter ring opening to the alcohol without further alcohol-epoxide oligomerization. The second method built up the imidazolium ring up from a four-component condensation of amino acids, ammonia, formaldehyde and glyoxal [102]. The latter approach, while multi-step and lower yielding, produced functionalized ionic liquids that were also optically active.

Recently, Wasserscheid and co-workers [103] introduced a complementary method for functionalized ionic liquid synthesis (11). In a one-pot, two step synthesis, the protonation of an imidazolium or pyridinium cation followed by a Michael-type addition to methyl vinyl ketone was reported. The only drawback is the limited thermal stability of the cations, which at moderately elevated temperatures undergo a retro-Michael reaction:

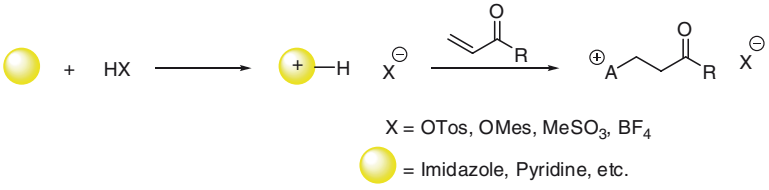

(11)

2.4.3 Microwave Synthesis

The preparation of 1,3-dialkylimidazolium halides via the classical heating method in refluxing solvents requires several hours to afford reasonable yields and also uses a large excess of alkylhalides/organic solvents as the reaction medium. The shortened reaction time, cleaner work-up procedure and unique transformations achieved

by microwave synthesis of ionic liquids can be impressive. Microwave synthesis can be classified into three groups: (1) the quaternisation step; (2) combined quaternisation and metathesis steps; (3) other routes.

2.4.3.1 The Quaternisation Step

The first report on the microwave-assisted synthesis of imidazolium-based ionic liquids appeared in 2000 [104]. Westman described a process of reacting *N*-methyl imidazole with an alkyl halide in ethyl acetate. Later Varma et al. [105, 106] reported a microwave assisted preparation of series of ambient temperature [$C_n$mim]-type ionic liquids by the reaction of 1-methylimidazole with alkyl halides/terminal dihalides under solvent-free conditions using a microwave oven as an irradiating source. The equipment used was a common household microwave oven equipped with inverter technology. The preparation of ionic liquids has also been carried out by irradiating equimolar amounts of *N*-methyl imidazole and an alkylating agent in open containers. In some cases the amount of alkylating agent had to be increased to two equivalents:

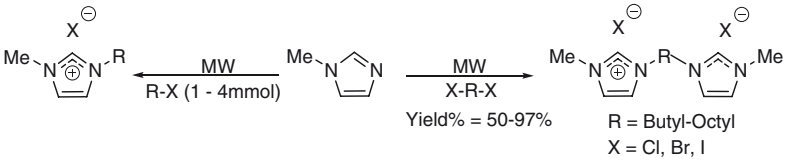

(12)

Thanh et al. [107] reported the synthesis of the chiral ionic liquids based on ephedrinium cation under solvent-free conditions and microwave activation (13). A series of different alkyl chain lengths was tested:

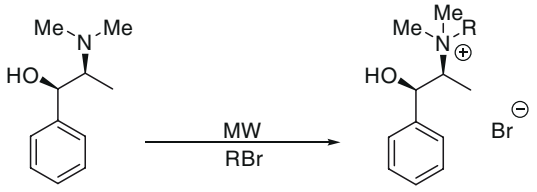

$R = C_4H_9, C_8H_{17}, C_{10}H_{21}, C_{16}H_{33}$ (13)

In an attempt to achieve solvent free preparation of ionic liquids, others have reported an improved approach whereby the reaction temperature was moderated by placement of the reaction vessel in a water bath. For example, Chan et al. [108] attempted to moderate the heat of the quaternisation reaction and thereby large scale preparation of imidazolium and pyridinium-based ionic liquids. Water moderation was successfully applied to avoid runaway reactions in the large-scale preparation of a number of ionic liquid precursors under solventless conditions using microwave irradiation:

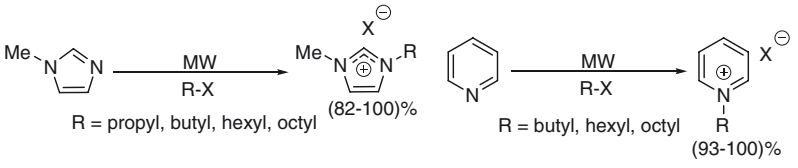

(14)

Rebeiro and later Seddon described an improved methodology to synthesize ionic liquids in an efficient way by carrying out the alkylation reaction in sealed vessels. Rebeiro et al. [109] reported a simple and quick method of preparation of alkyl pyridinium and 1-alkyl-3-methyl imidazolium salts on a large scale in a closed vessel under microwave irradiation in a microwave digestor:

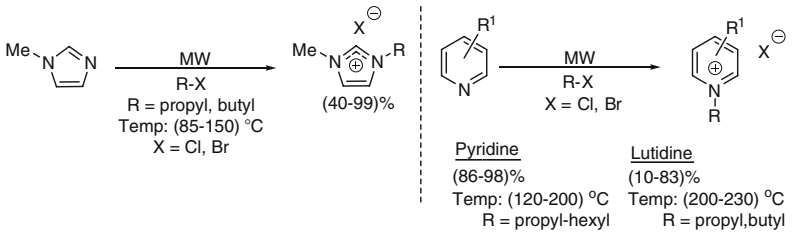

(15)

Seddon [110] described a process using a commercial multimode microwave reactor and apart from the classical [$C_n$mim]-derivatives his report also describes the preparation of *N*-alkylpyridinium-, *N*-alkyl-3-methylthiazolium- and *N*-alkyl-2-methyl-pyrazolium-based ionic liquids (Scheme 19).

2.4.3.2 Combined Quaternisation and Metathesis Steps

Recently, Cravotto and co-workers [111] demonstrated an efficient one-pot synthesis of second-generation ionic liquids, combining in one step the Menshutkin reaction and anion metathesis:

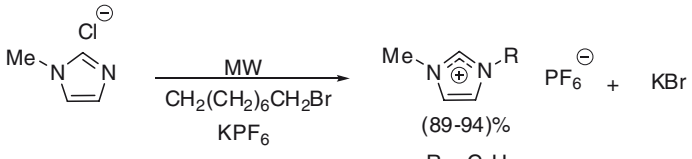

(16)

2.4.3.3 Other Routes

Microwave irradiation has also been used to speed up the synthesis of imidazolium-based ionic liquids bearing the tetrachloroaluminate counter ion [112]:

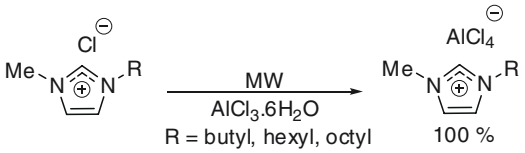

(17)

Equimolar amounts of $GaCl_3$ or $InCl_3$ were mixed with 1-butyl-3-methylimidazolium chloride, followed by MW irradiation for 30 s affording pure ionic liquid [113]:

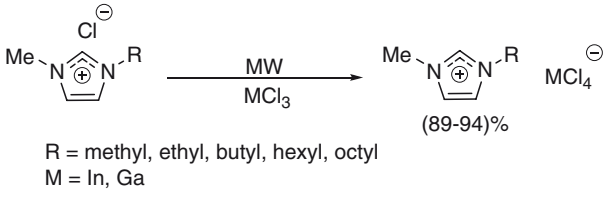

(18)

Quite recently [114], the amino acid ionic liquids were synthesized using the one-step microwave synthesis method by using 1-Glu (>99%), 42% HBF_4, 95–98% H_2SO_4, 65–68% HNO_3 acid and 37% HCl:

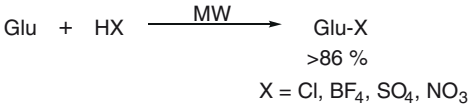

(19)

3 Purification

3.1 Common IL Impurities

The most abundant impurity found in ILs is water. Many IL applications are not affected (in fact they are sometimes enhanced) by the presence of water and so excessive drying is not always necessary. However, testing in water sensitive applications and fundamental characterization of new ILs should only be performed on very dry samples. The low volatility of most ILs allows for the removal of water by placing the wet IL under vacuum for several hours. Note however that this procedure is not appropriate for many protic ionic liquids since in those cases the conjugate acid and base species may also be volatile and loss of one of the species may occur. There can also be an issue with rigorous vacuum drying in those cases where the anion is a moderately strong base species (e.g. acetate) since small amounts of the conjugate acid can form from water and then be evaporated, leaving a hydroxide impurity. It is important to realize that vacuum drying involves mass transport of the water through the bulk of the material to the surface before it can be evaporated. Sample mass and surface area are therefore significant parameters; stirring may

also be required. It is strongly recommended that reporting of procedural details include information of sample volume and surface area in order that ensure reproducibility. It is also important to understand that during the process of evaporation of the water, or any other volatile material, the manifold pressure is often lower than the pressure at the material surface. In order to determine whether the sample has fully equilibrated with the applied vacuum one common technique involves isolating the manifold from the pump and monitoring the pressure in the manifold for approximately 20 min. When the sample is opened to the vacuum any pressure rise greater than the leak rate of the manifold indicates continued volatilisation from the sample. A typical procedure involves stirring the IL under vacuum on a standard Schlenk-line until a vacuum of approximately 0.4 mbar is maintained for 3 h. The time required for this process can be very short (a few hours) or very long (several weeks).

ILs can incorporate water very strongly and in some cases vacuum conditions alone do not reduce water to a suitable level within a suitable time-frame. The sample can be heated while under vacuum, but caution should be used as heat can accelerate IL decomposition. Alternatives include vacuum azeotropic distillation with solvents such as toluene or dissolving the IL in a low boiling solvent and placing over dry molecular sieves. Chemical drying agents (e.g. potassium metal, magnesium chloride, magnesium sulphate) can be very effective for the removal of water. However, consideration should be given to the impurities these additives will likely leave behind in the IL. If none of the above methods for drying ILs are appropriate, water should be avoided altogether, i.e. the IL can be synthesized in a dry atmosphere using dried reagents and reaction solvents.

Other common IL impurities are unreacted organic starting materials and residual organic reaction solvents. As with the removal of water, vacuum induced evaporation is usually very effective. If not, the IL can be washed with a low boiling, immiscible organic solvent such as diethyl ether, which can subsequently be removed under vacuum.

Suspended particles are a commonly overlooked impurity in ILs. They originate from many sources including:

- Metathesis byproducts (especially silver halide salts which often precipitate as very small particles)
- Sorbents
- Molecular sieves
- Chemical drying agents

Particles have been shown to affect several fundamental IL properties [115] and therefore their presence should be carefully considered. To the knowledge of these authors no methods have been shown to completely remove particulate contamination from ILs, but filtration through a 200 nm PTFE syringe filter can reduce their levels to <10 ppm [115].

Halide and alkali metal salts originating as metathesis by products can remain dissolved in ILs. For hydrophobic ILs simply washing with water until no salt is detected in the washings is very effective. With hydrophilic ILs removal of these salts can be more complex. The IL can be dissolved in a water immiscible solvent

such as dichloromethane and washed as above. However, this usually leads to a significant loss in IL yield (the loss in yield can be reduced by using very cold water). Passing the IL through silica gel has also been recommended as a method to reduce alkali metal halide salts [116]. If an IL is synthesized by precipitating an alkali metal halide salt from an organic solvent such as acetone, acetonitrile, methanol, etc. these solvents should be extensively dried. Even small traces of water can greatly increase the solubility of these salts in the IL.

3.2 Sorbents

The most common method for purifying ILs involves the use of sorbents such as activated carbon, silica and alumina. These sorbents are especially useful for the removal of coloured impurities. Many different methods for the use of sorbents have appeared in the literature, below are three popular examples:

- Passerini and co-workers purified $[C_4mpyr][NTF_2]$ by stirring over carbon at 70 °C, then stirring over alumna [117]
- Seddon and co-workers used a column filled with carbon and silica to remove coloured impurities from a range of ILs with $[NTf_2]^-$, $[BF_4]^-$, $[PF_6]^-$ and $[OTf]^-$ anions [118]
- Davis et al. recommend stirring over carbon then passing down a short alumina column [119]

To reduce viscosity, most ILs are diluted with an organic solvent before sorbent exposure.

It has always been assumed that sorbents are easily removed from the ILs after exposure. However recently evidence has arisen that these sorbents remain in the "purified" IL as nanoparticulate contamination [115, 120, 121]. Microfiltration (200 nm) can reduce the contamination to very low levels (<10 ppm) although even at this low level there is still an impact on the physicochemical properties of the IL. The crystallization kinetics [115], spectroscopic [115] and electrochemical [120] properties of the ILs have all shown changes after exposure to sorbents. There are many IL applications where sorbent contamination is not likely to be of concern. However, their presence or absence will affect how an IL behaves. It is therefore essential that all data presented on sorbent-exposed ILs is accompanied by a thorough explanation on the use and subsequent removal of the sorbents.

3.3 Distillation

Distillation is one of the most popular techniques employed for the purification and separation of molecular liquids. It had always been assumed that this technique was not available for the purification of ILs due to their apparent non-volatility. In 2005,

Kreher et al. drew attention to the potential of *N,N*-dialkyl-ammonium *N',N'*-dialkylcarbamates for use as distillable ionic media [122]. However, this class of ILs is generally considered to be a special case since the IL dissociates during distillation to give the respective amine and carbon dioxide. It is also widely recognized that many *protic* ionic liquids are distillable under easily accessible conditions [123].

Rebelo et al. reported on a method to predict the normal boiling points of ILs [124] and the results of these predictions suggested that many *aprotic* ILs may be distillable and attempts were made to distill $[C_{10}mim][NTf_2]$ and $[C_{12}mim][NTf_2]$. Small droplets of undecomposed IL formed on the upper walls of the distillation flask and were subsequently characterized as pure IL. More recently [125] many ILs have been distilled without significant decomposition of the residue or distillate. The range of successfully distilled ILs included salts of the $[C_nmim]^+$, $[C_nmpyr]^+$, $[C_ndbu]^+$, $[NTf_2]^-$, $[OTf]^-$ and $[PF_6]^-$ ions. It should be noted that many ILs decomposed under the distillation conditions used including salts of tetraalkylammonium, tetraalkylphosphonium, cholinium, halide, sulphate, carboxylate and triflate ions.

The ILs were typically distilled at pressures of 0.001–5.0 mbar and temperatures of 200–300 °C. Reduced pressure was found to be essential since distillations performed close to ambient pressure led to IL decomposition. Importantly, this work also showed the possibility for separation of ILs by distillation. Distillate from IL mixtures showed a higher concentration of one IL over the other.

The nature of the vaporized ILs was a topic of some controversy until a follow up study was published [126]. Fourier transform ion cyclotron resonance mass spectrometry (FTICR-MS) was used at distillation conditions (4.0×10^{-6}–1.3×10^{-5} mbar, > 200 °C). Aprotic IL vapors were found to be made up of neutral ion pairs, not free ions or clusters (neutral or ionic). It was also confirmed that protic IL vapors consisted of neutral molecules resulting from cation to anion proton transfer. Several studies have suggested that IL volatility is likely related to the extent of ion pairing present in the liquid phase [123, 127].

The studies described here show that distillation is a viable option for the ultrapurification of many ILs. However, this technique can be very time consuming and is not yet practical for the large-scale purification of ILs.

3.4 Zone Melting

Zone melting is a technique that has been used for the purification of many materials including metals [128], molecular liquids [129] and gases [130]. In 2005 Winterton and co-workers [131] reported the first use of this technique for the purification of ILs. Zone melting separates IL components from impurities by exploiting the differences in their molecular shape. The IL is cooled inside a sealed vessel to form a long column of frozen IL. A mobile energy source (e.g. an IR Laser) is then used to melt a small region of the solid and moved so that the liquid zone travels slowly along the frozen column. Because most impurities have a different molecular shape to the IL

they do not fit neatly into the crystal lattice of the solid IL (do not form solid solutions with the IL) and therefore tend to remain within the liquid zone. As the liquid zone is moved through the crystalline salt it picks up more impurities and leaves a wake of purified crystalline material. Usually several melting/crystallization scans are used to produce high purity ILs. Zone melting has been used within capillary tubes to grow good quality single crystals for diffraction, e.g.

- $[C_2mim][BF_4]$, $[C_4mim][PF_6]$, $[C_4mim][OTf]$, $[C_4mim][NTf_2]$, $[C_6mpyr][NTf_2]$ [131]
- $[C_2mim][OTf]$, $[C_2mim][NTf_2]$ [132]

or on larger scales for bulk IL purification achieving purities of ≥ 99.9%, e.g.

- $[C_2mim][Cl]$, $[C_2mim][Br]$ [133]

Special techniques must be used to avoid glass formation [131] and zone melting usually results in a sizable drop in yield. If reliable methods can be developed to produce a small, completely melted zone within the frozen IL, zone melting represents one of the most promising techniques being developed for the purification of ILs.

3.5 Clean Synthesis

The inherent properties of ILs can make their post-synthetic purification very difficult. For this reason many researchers [134] have adopted an approach whereby the ILs are synthesized as cleanly as possible, in order to minimise impurities from either starting materials or unwanted side reactions. For ILs containing a quaternary nitrogen many (especially coloured) impurities are thought to arise from by-products of the quaternisation process. Several simple precautions can be taken to minimize these impurities:

- Exposure to oxygen should be minimized and therefore it is often recommended [119] that starting materials are degassed and quaternisation is performed in a sealed vessel or under an inert atmosphere.
- The presence of trace acetone has been shown [119] to lead to more highly coloured quaternisation products and should therefore be completely excluded.
- The quaternisation reaction temperature should be kept at a minimum to reduce unwanted side reactions. For reactions using halide-based reagents the following temperatures are a general guide, chloride salts <80 °C, bromide salts <40 °C, and iodide salts <0 °C. It should be noted that these temperatures will not be appropriate for all reactions. It is the recommendation of these authors that novel quaternisation reactions are carried out in an ice bath and allowed to slowly warm while monitoring the reaction progress in order to determine the minimum temperature required. While reactions carried out at lower temperatures will require longer reaction times the products obtained should be of better quality.
- Quaternisation reactions are usually exothermic and it is therefore difficult to avoid local hotspots within the reaction mixture. For this reason if highly transparent/pure ILs are required, small scale (<0.3 mol) reactions are recommended [121].

If the above precautions are insufficient to produce the purity required, the starting materials required for the quaternisation reaction should be purified by distillation and/or the methods of purification outlined in "Purification of Laboratory Chemicals" by Armarego and Chai [135]. It should be noted that the starting materials often degrade over time and therefore these purification techniques should be employed immediately before the quaternisation reaction is undertaken.

For quaternisation products that are IL starting materials rather than ILs themselves, traditional purification techniques such as, distillation, recrystallisation, immiscible solvent washing and stirring over activated carbon can be used. These traditional techniques are often so effective that the previously mentioned precautions are not necessary.

While this section has focussed on quaternisation reactions, the basic principles of starting material purification and mild reaction conditions are applicable to all IL synthesis.

3.6 Phosphonium ILs

Phosphonium ILs are considered separately here as they often contain impurities not found in other ILs. These impurities are usually contained within the commercially available phosphonium chlorides which are used as ILs in their own right or as starting materials to produce subsequent ILs. Ramnial et al. [136] presented a study whereby these impurities were identified and a method for their removal was developed. Commercially available phosphonium chlorides were found to contain traces of:

- Phosphines
- Hydrochloric acid
- Water
- Phosphine oxides
- Isobutylnitrile

To remove these impurities the phosphonium chlorides were washed with aqueous sodium bicarbonate; care should be taken during this step as the sodium bicarbonate often caused excessive foaming. Next the ILs were thoroughly washed with water and extracted using hexanes. The hexanes solution was passed down a short silica column and dried by azeotropic distillation with toluene followed by treatment under vacuum.

3.7 Characterization

Because impurities can have a profound impact on subsequent IL applications [37], all data reported involving ILs should be accompanied by an analysis report on the presence (or absence) of common IL impurities. At least one technique should be used to

confirm the structure of the IL. Mass spectrometry, nuclear magnetic resonance (NMR) spectrometry, elemental analysis and X-ray crystallography can all be useful techniques for this purpose. However, many IL impurities cannot be directly quantified using these techniques and so it should be remembered that these techniques can only be used to confirm IL structure and should not be used as evidence of IL purity.

For example, in an IL contaminated with significant quantities of lithium chloride, neither lithium or chloride ions will appear in standard mass spectrometry because of their small masses, they may not significantly alter the C, H and N percentages in elemental analysis, and they are not detectable in standard ^{1}H and ^{13}C NMR. The presence of lithium chloride will likely prevent the growth of suitable crystals for diffraction; nonetheless, obtaining a single IL crystal suitable for analysis does not rule out the presence of lithium chloride in the bulk IL. Therefore a crystal structure should not be considered evidence of bulk purity. Thus the researcher must consider all possible sources of contamination and systematically determine specific impurities using techniques appropriate to the trace level involved.

There are four main categories of common IL impurities; water, organics (from unreacted starting materials or residual reaction solvents), halides and metals.

Water content can be crudely assessed using ^{1}H NMR or infra-red spectroscopy but at low levels (<1,000 ppm) must be accurately quantified using a Karl–Fischer titration.

Organic reaction solvents or unreacted starting materials can be detected by ^{1}H NMR for quantities greater than 1 mol%. Smaller quantities can be assessed by specific detection as described in texts such as "Vogel's textbook of quantitative chemical analysis" [137]. A useful example of specific detection involves detecting unreacted 1-methylimidazole (a common IL starting material that is difficult to remove by evaporation) [138]. Copper(II) chloride is added to the IL to form a coloured complex with 1-methylimidazole, which can be detected at high levels visually, or more accurately quantified using atomic absorption spectroscopy.

Halide impurities can be assessed using many techniques with varying degrees of accuracy. Techniques include:

- ^{19}F, ^{35}Cl NMR (>1 mol%)
- Titration with silver nitrate; monitored visually for qualitative analysis or using the Volhard procedure (>10 ppm)
- Ion selective electrodes (>100 ppm)
- Ion chromatography (>10 ppm)
- Inductively coupled plasma-mass spectrometry (>10 ppb)

In our own laboratories ion selective electrodes and ion chromatography are routinely used for halide analysis.

Metallic impurities are usually present as one of two forms; unreacted metallic starting material salts or as halide salts from metathesis by-products. Direct metal analysis is not always performed; instead the counterions from metathesis by-products or halide salts are analysed and if their levels are sufficiently low it is assumed the metal content is also sufficiently low. For metals present in other forms or where the counter ion is difficult to analyse, metal content can be assessed

directly using atomic absorption spectroscopy (available for most metals) or ion selective electrodes (available for Na^+, K^+, Ag^+, Ca^{2+}, Mg^{2+}, Cd^{2+}, Cu^{2+}, and Pb^{2+}).

It was not intended that this section exhaustively cover all possible IL impurities, instead methods for analysis of common IL impurities were suggested. As mentioned previously individual ILs should be assessed for all possible sources of contamination and texts such as "Vogel's Textbook of Quantitative Chemical Analysis" by Mendham et al. [137] should be consulted for methods to quantify impurities not covered here.

4 Conclusions

As has been stated by a number of workers the family of ionic liquids probably includes more than10^6 compounds. The synthetic strategies available developed to prepare these compounds will continue to expand as long as there are applications demanding greater structural variety.

Acknowledgments The authors are grateful to ARC for salary support for BC (Linkage Project with Degussa), AS (Linkage Project with Orica) and DRM (Federation Fellowship).

References

1. MacFarlane DR, Seddon KR (2007) Aust J Chem 60:3
2. Seddon KR (1996) Kinet Catal 37:693
3. Bonhote P, Dias AP, Papageorgiou N, Kalyanasundaram K, Gratzel M (1996) Inorg Chem 35:1168
4. Huddleston JG, Willauer HD, Swatloski RP, Visser AE, Rogers RD (1998) Chem Commun 1765
5. Dzyuba SV, Bartsch RA (2001) Chem Commun 1466
6. Gordon CM, Holbrey JD, Kennedy AR, Seddon KR (1998) *J Mater Chem* 8:2627
7. Forsyth SA, Pringle JM, MacFarlane DR (2004) *Aust J Chem* 57:113
8. Handy ST (2005) Curr Org Chem 9:959
9. Bradaric CJ, Downard A, Kennedy C, Robertson AJ, Zhou YH (2003) *Green Chem* 5:143
10. Degiorgi M, Landini D, Maia A, Penso M (1987) *Synth Commun* 17:521
11. Bradaric CJ, Downard A, Kennedy C, Robertson AJ, Zhou YH (2002) *Abstracts of Papers of the Am Chem Soc* 224:U611
12. Ding J, Welton T, Armstrong DW (2004) *Anal Chem* 76:6819
13. Ding J, Armstrong DW (2005) *Chirality* 17:281
14. Chiappe C, Pieraccini D (2005) *J Phys Org Chem* 18:275
15. Wasserscheid P, Hilgers C, Boesmann A. Solvent Innovation Gmbh, EP1182196-A1
16. Holbrey JD, Seddon KR (1999) J Chem Soc-Dalton Trans 2133
17. Forsyth S, Golding J, MacFarlane DR, Forsyth M (2001) *Electrochim Acta* 46:1753
18. MacFarlane DR, Meakin P, Sun J, Amini N, Forsyth M (1999) *J Phys Chem B* 103:4164
19. Goldman JL, McEwen AB (1999) *Electrochem Solid State Lett* 2:501
20. Visser AE, Holbrey JD, Rogers RD (2001) Chem Commun 2484
21. Holbrey JD, Reichert WM, Swatloski RP, Broker GA, Pitner WR, Seddon KR, Rogers RD (2002) *Green Chem* 4:407

22. Brinchi L, Germani R, Savelli G (2003) *Tetrahedron Lett* 44:2027
23. Kitazume T, Tanaka G (2000) *J Fluorine Chem* 106:211
24. Golding J, Forsyth S, MacFarlane DR, Forsyth M, Deacon GB (2002) *Green Chem* 4:223
25. Pringle JM, Golding J, Forsyth CM, Deacon GB, Forsyth M, MacFarlane DR (2002) *J Mater Chem* 12:3475
26. Leveque JM, Luche JL, Petrier C, Roux R, Bonrath W (2002) *Green Chem* 4:357
27. MacFarlane DR, Golding J, Forsyth S, Forsyth M, Deacon GB (2001) Chem Commun 1430
28. MacFarlane DR, Forsyth SA, Golding J, Deacon GB (2002) *Green Chem* 4:444
29. Xu W, Wang LM, Nieman RA, Angell CA (2003) *J Phys Chem B* 107:11749
30. Larsen AS, Holbrey JD, Tham FS, Reed CA (2000) *J Am Chem Soc* 122:7264
31. Fuller J, Carlin RT, Osteryoung RA (1997) *J Electrochem Soc* 144:3881
32. Cammarata L, Kazarian SG, Salter PA, Welton T (2001) *Phys Chem Chem Phys* 3:5192
33. Wilkes JS, Zaworotko MJ (1992) J Chem Soc-Chem Commun 965
34. Helfferich F (1962) Ion Exchange. New York: McGraw-Hill
35. Lall SI, Mancheno D, Castro S, Behaj V, Cohen JI, Engel R (2000) Chem Commun (Cambridge): 2413
36. Mizuta K, Kasahara T, Hashimoto H, Arimoto Y (2006) PCT/JP2006/322693
37. Seddon KR, Stark A, Torres MJ (2000) *Pure Appl Chem* 72:2275
38. Chauvin Y, Olivierbourbigou H (1995) *Chemtech* 25:26
39. de Souza RF, Rech V, Dupont J (2002) *Adv Synth Catal* 344:153
40. Siriwardana AI, Crossley IR, Torriero AAJ, Burgar IM, Dunlop NF, Bond AM, Deacon GB, MacFarlane DR (2008) *J Org Chem* 73:4676
41. Kuhn N, Steimann M, Weyers G (1999) *Zeitschrift Fur Naturforschung Sect B J Chem Sci* 54:427
42. Tommasi I, Sorrentino F (2005) *Tetrahedron Lett* 46:2141
43. Holbrey JD, Reichert WM, Tkatchenko I, Bouajila E, Walter O, Tommasi I, Rogers RD (2003) Chem Commun 28
44. Moulton SE, Minett AI, Murphy R, Ryan KP, McCarthy D, Coleman JN, Blau WJ, Wallace GG (2005) *Carbon* 43:1879
45. Kuhlmann E, Himmler S, Giebelhaus H, Wasserscheid P (2007) *Green Chem* 9:233
46. Modro AM, Modro TA (1989) *J Phys Org Chem* 2:377
47. Burns JA, Butler JC, Moran J, Whitesides GM (1991) *J Org Chem* 56:2648
48. Cassol CC, Ebeling G, Ferrera B, Dupont J (2006) *Adv Synth Catal* 348:243
49. Jodry JJ, Mikami K (2004) *Tetrahedron Lett* 45:4429
50. Himmler S, Hormann S, van Hal R, Schulz PS, Wasserscheid P (2006) *Green Chem* 8:887
51. Yoshizawa M, Xu W, Angell CA (2003) *J Am Chem Soc* 125:15411
52. Yoshizawa M, Belieres JP, Xu W, Angell CA (2003) *Abst Pap Am Chem Soc* 226:U627
53. Ohno H, Yoshizawa M (2002) *Solid State Ionics* 154:303
54. Greaves TL, Drummond CJ (2008) *Chem Rev* 108:206
55. Nuthakki B, Greaves TL, Krodkiewska I, Weerawardena A, Burgar MI, Mulder RJ, Drummond CJ (2007) *Aust J Chem* 60:21
56. MacFarlane DR, Pringle JM, Johansson KM, Forsyth SA, Forsyth M (2006) Chem Commun 1905
57. Johansson KM, Izgorodina EI, Forsyth M, MacFarlane DR, Seddon KR (2008) *Phys Chem Chem Phys* 10:2972
58. Janus E, Goc-Maciejewska I, Lozynski M, Pernak J (2006) *Tetrahedron Lett* 47:4079
59. MacFarlane DR, Pringle JM, Johansson KM, Forsyth SA, Forsyth M (2006) Chem Commun 1905
60. Abbott AP, Capper G, Davies DL, Rasheed R (2004) *Inorg Chem* 43:3447
61. Lin IJB, Vasam CS (2005) *J Organomet Chem* 690:3498
62. Hitchcock PB, Seddon KR, Welton T (1993) J Chem Soc-Dalton Trans 2639
63. Dent AJ, Lees A, Lewis RJ, Welton T (1996) J Chem Soc-Dalton Trans 2787
64. Gao Y, Twamley B, Shreeve JM (2004) *Inorg Chem* 43:3406

65. Kolle P, Dronskowski R (2004) Inorg Chem 43:2803
66. Sun XG, Angell CA (2005) Electrochem Commun 7:261
67. Palgunadi J, Kwon OS, Lee H, Bae JY, Ahn BS, Min NY, Kim HS (2004) Catal Today 98:511
68. Dullius JEL, Suarez PAZ, Einloft S, de Souza RF, Dupont J, Fischer J, De Cian A (1998) Organometallics 17:815
69. Zhao DB, Fei ZF, Scopelliti R, Dyson PJ (2004) Inorg Chem 43:2197
70. Xiao JC, Twamley B, Shreeve JM (2004) Org Lett 6:3845
71. Hasan M, Kozhevnikov IV, Siddiqui MRH, Femoni C, Steiner A, Winterton N (2001) Inorg Chem 40:795
72. Chen J, Burrell AK, Collis GE, Officer DL, Swiegers GF, Too CO, Wallace GG (2002) Electrochim Acta 47:2715
73. Matsumoto K, Tsuda T, Nohira T, Hagiwara R, Ito Y, Tamada O (2002) Acta Crystallogr Sect C Cryst Struct Commun 58:m186
74. Sentman AC, Csihony S, Waymouth RM, Hedrick JL (2005) J Org Chem 70:2391
75. Deetlefs M, Raubenheimer HG, Esterhuysen MW (2002) Catal Today 72:29
76. Dyson PJ, McIndoe JS, Zhao DB (2003) Chem Commun: 508
77. Wasserscheid P, Waffenschmidt H (2000) J Mol Catal A: Chem 164:61
78. Earle MJ, Hakala U, Hardacre C, Karkkainen J, McAuley BJ, Rooney DW, Seddon KR, Thompson JM, Wahala K (2005) Chem Commun: 903
79. Edgar A, Williams GVM, Sagar PKD, Secu M, Schweizer S, Spaeth JM, Hu X, Newman PJ, Macfarlane DR (2003) *J Non-Cryst Solids* 326:489
80. Hitchcock PB, Mohammed TJ, Seddon KR, Zora JA, Hussey CL, Ward EH (1986) *Inorg Chim Acta* 113:L25
81. Nockemann P, Thijs B, Postelmans N, Van Hecke K, Van Meervelt L, Binnemans K (2006) *J Am Chem Soc* 128:13658
82. Lee SG (2006) Chem Commun: 1049
83. Davis JH (2004) *Chem Lett* 33:1072
84. Visser AE, Swatloski RP, Reichert WM, Mayton R, Sheff S, Wierzbicki A, Davis JH, Rogers RD (2002) *Environ Sci Technol* 36:2523
85. Visser AE, Swatloski RP, Reichert WM, Mayton R, Sheff S, Wierzbicki A, Davis JH, Rogers RD (2001) Chem Commun 135
86. Cole AC, Jensen JL, Ntai I, Tran KLT, Weaver KJ, Forbes DC, Davis JH (2002) *J Am Chem Soc* 124:5962
87. Xing HB, Wang T, Zhou ZH, Dai YY (2005) *Ind Eng Chem Res* 44:4147
88. Fukumoto K, Yoshizawa M, Ohno H (2005) *J Am Chem Soc* 127:2398
89. Kim S, Lee JK, Kang SO, Ko J, Yum JH, Fantacci S, De Angelis F, Di Censo D, Nazeeruddin MK, Gratzel M (2006) *J Am Chem Soc* 128:16701
90. Lombardo M, Pasi F, Trombini C, Seddon KR, Pitner WR (2007) *Green Chem* 9:321
91. Kottsieper KW, Stelzer O, Wasserscheid P (2001) *J Mol Catal A Chem* 175:285
92. Brauer DJ, Kottsieper KW, Liek C, Stelzer O, Waffenschmidt H, Wasserscheid P (2001) *J Organomet Chem* 630:177
93. Branco LC, Rosa JN, Ramos JJM, Afonso CAM (2002) *Chem Eur J* 8:3671
94. Ouadi A, Gadenne B, Hesemann P, Moreau JJE, Billard I, Gaillard C, Mekki S, Moutiers G (2006) *Chem Eur J* 12:3074
95. Siyutkin DE, Kucherenko AS, Struchkova MI, Zlotin SG (2008) *Tetrahedron Lett* 49:1212
96. Fraga-Dubreuil J, Bazureau JP (2001) *Tetrahedron Lett* 42:6097
97. Fraga-Dubreuil J, Famelart MH, Bazureau JP (2002) *Org Process Res Dev* 6:374
98. Bates ED, Mayton RD, Ntai I, Davis JH (2002) *J Am Chem Soc* 124:926
99. Rickert PG, Antonio MR, Firestone MA, Kubatko KA, Szreder T, Wishart JF, Dietz ML (2007) Dalton Trans: 529
100. Yoshizawa M, Hirao M, Ito-Akita K, Ohno H (2001) *J Mater Chem* 11:1057
101. Holbrey JD, Turner MB, Reichert WM, Rogers RD (2003) *Green Chem* 5:731
102. Bao WL, Wang ZM, Li YX (2003) *J Org Chem* 68:591

103. Leitner W, Seddon KR, Wasserscheid P (2003) *Green Chem* 5:G28
104. Habermann J, Ponzi S, Ley SV (2005) *Mini-Reviews in Org Chem* 2:125
105. Varma RS, Namboodiri VV (2001) *Pure Appl Chem* 73:1309
106. Varma RS, Namboodiri VV (2001) Chem Commun 643
107. Thanh GV, Pegot B, Loupy A (2004) European Journal of Organic Chemistry 2004:1112
108. Law MC, Wong KY, Chan TH (2002) *Green Chem* 4:328
109. Khadilkar BM, Rebeiro GL (2002) *Org Process Res Dev* 6:826
110. Deetlefs M, Seddon KR (2003) *Green Chem* 5:181
111. Cravotto G, Boffa L, L'Eveque JM, Estager J, Draye M, Bonrath W (2007) *Aust J Chem* 60:946
112. Namboodiri VV, Varma RS (2002) Chem Commun 342
113. Kim YJ, Varma RS (2005) *Tetrahedron Lett* 46:1467
114. Rong H, Li W, Chen ZY, Wu XM (2008) *J Phys Chem B* 112:1451
115. Clare BR, Bayley PM, Best AS, Forsyth M, MacFarlane DR (2008) Chem Commun (Cambridge, UK) 2689
116. Scammells PJ, Scott JL, Singer RD (2005) *Aust J Chem* 58:155
117. Appetecchi GB, Scaccia S, Tizzani C, Alessandrini F, Passerini S (2006) *J Electrochem Soc* 153:A1685
118. Earle MJ, Gordon CM, Plechkova NV, Seddon KR, Weton T (2007) *Anal Chem* 79:758
119. Davis JH Jr, Gordon CM, Hilgers C, Wasserscheid P (2003) In: Wasserscheid P, Welton T (eds) Ionic liquids in synthesis. (Wiley, Weinheim) Chap 2
120. Endres F, Zein El Abedin S, Borissenko N (2006) *Z Phys Chem (Muenchen, Ger.)* 220:1377
121. Nockemann P, Binnemans K, Driesen K (2005) *Chem Phys Lett* 415:131
122. Kreher UP, Rosamilia AE, Raston CL (2004) *Molecules* 9:387
123. Fraser KJ, Izgorodina EI, Forsyth M, Scott JL, MacFarlane DR (2007) Chem Commun 3817
124. Rebelo Luis PN, Canongia Lopes Jose N, Esperanca Jose MSS, Filipe E (2005) *J Phys Chem B* 109:6040
125. Earle MJ, Esperanca JMSS, Gilea MA, Canongia Lopes JN, Rebelo LPN, Magee JW, Seddon KR, Widegren JA (2006) *Nature (London, UK)* 439:831
126. Leal JP, Esperanca JMSS, Da Piedade MEM, Lopes JNC, Rebelo LPN, Seddon KR (2007) *J Phys Chem A* 111:6176
127. Widegren JA, Wang Y-M, Henderson WA, Magee JW (2007) *J Phys Chem B* 111:8959
128. Rudolph P, Fukuda T (1999) *Cryst Res Technol* 34:3
129. Thalladi VR, Weiss H-C, Blaeser D, Boese R, Nangia A, Desiraju GR (1998) *J Am Chem Soc* 120:8702
130. Kirchner MT, Boese R, Billups WE, Norman LR (2004) *J Am Chem Soc* 126:9407
131. Choudhury AR, Winterton N, Steiner A, Cooper AI, Johnson KA (2005) *J Am Chem Soc* 127:16792
132. Choudhury AR, Winterton N, Steiner A, Cooper AI, Johnson KA (2006) *Cryst Eng Commun* 8:742
133. Koenig A, Wasserscheid P (2006) Proceedings of the 13th International Workshop on Industrial Crystallization BIWIC 2006, September 13–15, 2006, Delft, the Netherlands, p 79
134. Burrell AK, Del Sesto RE, Baker SN, McCleskey TM, Baker GA (2007) *Green Chem* 9:449
135. Armarego WLF, Chai CLL (2003) Purification of laboratory chemicals, 5th ed. (Butterworth–Heinemann)
136. Ramnial T, Taylor Stephanie A, Bender Marissa L, Gorodetsky B, Lee Peter TK, Dickie Diane A, McCollum Brett M, Pye Cory C, Walsby Charles J, Clyburne Jason AC (2008) *J Org Chem* 73:801
137. Mendham J et al. (2000) Vogel's textbook of quantitative chemical analysis, 6th edn. Addison Wesley Publishing Co
138. Holbrey JD, Seddon KR, Wareing R (2001) *Green Chem* 3:33

Top Curr Chem (2009) 290: 41–81
DOI: 10.1007/128_2008_43

Published online: 10 July 2009

Ionic Liquid Structure-Induced Effects on Organic Reactions

Annegret Stark

Abstract Understanding the ways in which the constituents of ionic liquids, i.e. the type of cation, its substitution, and the type of anion chosen, interact with reactants is prerequisite to deliberately designing an ionic liquid solvent with optimum performance. Several approaches, including physico-chemical and spectroscopic measurements and computational studies of binary ionic liquid-substrate mixtures have been presented that investigate the strength of interactions.

The qualitative order of the basicity (hydrogen bond acceptor potential) of anions as most prominent force is already reasonably well understood, and reliably determined using, e.g. selective solvatochromic dyes. In certain reactions, the relative order of basicity correlates well with the reactivity of substrates. However, the determination of a relative order for the cations is still in its infancy. Owing to the fact that potential cation-derived interactions may not solely be due to hydrogen bond interactions, but also to ion pair interactions (electron pair donor/acceptor properties), the relative magnitudes of interactions between the anion and cation vary considerably – even in the absence of solutes – depending on the experimental method. In addition, it appears that the basicity of the anion superimposes in many instances on the effects exhibited by the cation and/or the cation's substituent. Hence, understanding the effect of the cation on the activation of substrates is still a challenge.

This chapter aims at summarising the trends observed for binary model systems in experimental and computational investigations, and drawing conclusions about ionic liquid structure-induced effects relevant to organic reactions, in particular nucleophilic substitution reactions.

A. Stark
Institute for Technical Chemistry and Environmental Chemistry,
Friedrich-Schiller University Jena, Lessingstr. 12, 07743, Jena, Germany
e-mail: annegret.stark@uni-jena.de

Keywords Buffer • Esterification • Nucleophilic substitution • Organocatalysis • Structure–property relationship • Water scavenger

Contents

1 Introduction

Solvents play an important role in governing chemical reactions. Not only are they involved in heat and mass transport, but – if chosen sensibly – they can affect an increase of the rate of reaction and selectivity, and a shift of the position of the equilibrium towards the products. Hence, ionic liquids can only reach their full potential as new and alternative solvents if their physico-chemical properties and ways of interactions with solutes are fully understood.

In an ongoing project, we have set out to investigate the nature and extent of interactions exhibited by the ionic liquid constituents on various solutes. In particular, the Fischer-type esterification was chosen as a model reaction as its kinetics and thermodynamic equilibrium were assumed to be sensitive towards small changes in

the solutes' environments. Therefore, the ionic liquid acts first as a solvent (which may not be strictly necessary for liquid reactants), second as a potential water scavenger (if strong interactions between the water liberated and the ionic liquid occur), and third as an organocatalyst (if a site on the substrate is activated by specific ionic liquid–solute interactions, facilitating the productive reaction with a second reactant).

The most intriguing and challenging aspect about ionic liquid research is that many rules and principles, which have been derived from observations made in aqueous or organic solvent chemistry and which a chemist takes as a given, have to be questioned and in many instances cannot be used to explain ionic liquid chemistry. Tobias and Hemminger recently pointed out that 'the existence and widespread applicability of the Hofmeister series suggest an underlying simplicity. Yet, specific ion effects continue to defy all-encompassing theories' [1].

An example is the question of the pH-value of acidic solutes in ionic liquids. From a practical point of view, this issue is extremely difficult to resolve, as pH-electrodes cannot be used in ionic liquids. Furthermore, the pH-value is defined as the negative logarithm of the H_3O^+ activity, but in a dry ionic liquid, water is not present to form this species with dissociated protons. Does this then mean that protons are 'naked', tending to exhibit super-acidic character? The answer to this question lies of course in the solvation properties of the ionic liquid under investigation.

A second example is the question of the polarity of ionic liquids, which has been addressed in various studies to-date. Chemists have developed a rather intuitive understanding of the nature of a solvent, which is often selected by rules-of-thumb such as *similis similibus solvuntur* (like dissolves like), and generalised categories such as 'protic/non-protic' or 'polar/non-polar', which are used to choose a solvent. In general, the potential of solvent optimisation has probably not been fully exploited for any solvent system.

Both examples highlight the importance of understanding ionic liquid – solute interactions to exploit fully the ionic liquids' potential as solvents.

In order to rationalise the effect of small changes in the ionic liquid structure, studying homologous series of ionic liquids is a valuable methodology.

Of course, Fig. 1 only displays a small choice of the proposed 10^{18} [2] ionic liquids, and does not include the third generation, task-specific structures in which further functionalities are introduced in the alkyl substituent, thus adding a fourth dimension. Mixtures of two ionic liquids (i.e. ternary or quaternary systems, depending on whether both anions and/or both cations are different) may exhibit interesting properties deviating from linearity and will further increase the choice. While the plethora of possible ionic liquid variations may be optimistically seen as a chance to find a suitable ionic liquid for any application, others view it as a huge challenge. Setbacks are prone to occur, such as the realisation that tremendous effects are exhibited by impurities in ionic liquids, rendering much of the early data inadequate for interpretation.

This chapter aims at drawing conclusions about ionic liquid structure-induced effects relevant to organic reactions, in particular nucleophilic substitution reactions, to allow predicting which ionic liquid constituents lead to beneficial interactions. This information can be obtained from the combination of physico-chemical data of

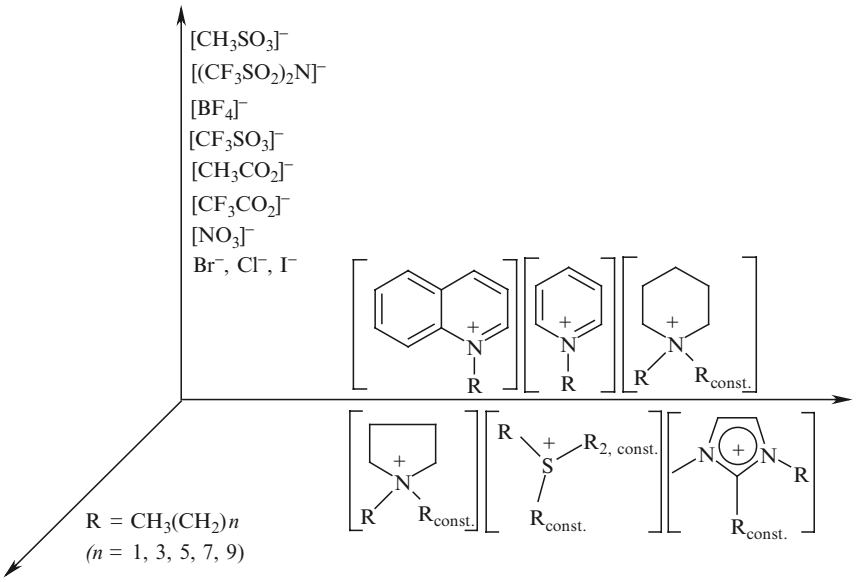

Fig. 1 Three-dimensional representation of the functional variations of some ionic liquids

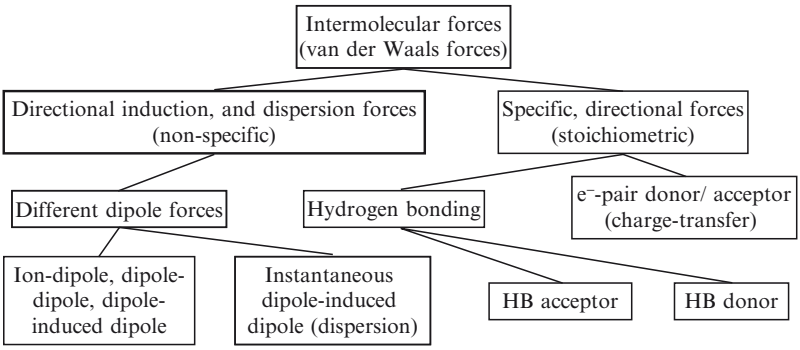

Fig. 2 Categories of solvent–solute interactions according to [4]

pure ionic liquids and their mixtures with solutes, computational studies, as well as from reactions carried out in ionic liquid solutions, the toolbox to deliberately designing [3] ionic liquids.

In this context, interactions between ionic liquids and solutes are understood as intermolecular (and in extension: interionic) solvation forces, which can be categorised according to Reichardt [4] (Fig. 2) as non-specific induction and dispersion (Coulomb) forces, and specific directional stoichiometric forces (hydrogen bond acceptor and donor, electron pair acceptor and donor) [4].

The solvent polarity, which is defined as the overall solvation capability of a liquid derived from all possible, non-specific and specific intermolecular interactions between solute and solvent molecules [4], cannot be represented by a single value encompassing all aspects, but constants such as the refractive index, the dielectric constant, the Hildebrand solubility parameter, the permanent dipole moment, the partition coefficient log*P* [5] or the normalised polarity parameter E_T^N [6] are generally employed to describe the polarity of a medium. The effect of a solvent on the equilibrium position of chemical reactions, e.g. the keto–enol tautomerism, may also be used. However, these constants reflect only on some aspects of many possible interactions of the solvent, and the assignment to specific interactions is difficult if not impossible.

Nevertheless, the possibly most eye-opening conclusion since the advent of ionic liquid research is derived from these unspecific measurement tools: in principle salts, it crystallised that their 'polarities' are in fact not as high as expected, and do not necessarily range at the upper end of the polarity scales, as opposed to molten salts.

2 Ionic Liquid-Inherent Interactions

2.1 Studies Using Solvatochromic Dyes

Very early on, it was attempted to determine the ionic liquid polarity using solvatochromic dyes by UV/Vis-spectroscopy [7–13], and to arrange ionic liquids in polarity scales together with conventional organic solvents. It was found that the comparison to organic solvents was not satisfactorily achieved in this way: for example, using Reichardt's dye, the E_T^{30} value for $[C_4mim][PF_6]$ indicated a polarity similar to ethanol, while pyrene and 1-pyrenecarbaldehyde gave a higher polarity (similar to acetonitrile and dimethyl sulfoxide), and studies with Nile Red indicated a polarity between that of 90 wt% glycerol in water and pure water. These rather large deviations can be assigned to the chemical nature (and hence solvation) of the dyes used, and the purity of the ionic liquid sample, the temperature and recording technique also affect the measurement. Nevertheless, from these studies an anion-dependent basicity scale was established, which has been reproduced (with only slight changes in order) many times with other techniques. Hence, in series of homologues in which the anion is systematically altered, these studies indicate a decrease in basicity with increasing anion size, attributed to a higher charge delocalisation, in the order of $[NO_2]^-$>$[NO_3]^-$>$[BF_4]^-$>$[BTA]^-$>$[PF_6]^-$,[7] and $[CF_3SO_3]^-$>$[BTA]^-$>$[PF_6]^-$ [10].

More recent solvatochromic studies [14–20] employ specialised dyes reflecting specific microscopic molecular interactions. For example, the Abboud–Kamlet–Taft solvent parameters [21–23] α, β and π* give information on hydrogen bond donor and acceptor properties and the polarisability of a compound, respectively. For ionic liquids with $[C_4mim]$-cations, the following order of β- values was estab-

lished: Cl^->Br^->$[OAc]^-$>$[CH_3SO_3]^-$>I^->$[CF_3CO_2]^-$>$[SCN]^-$>$[DCA]^-$>$[CF_3SO_3]^-$>$[BF_4]^-$>$[BTA]^-$ [17]. For $[BF_4]$- and [BTA]-based anions, the α-values for hydrogen bond donation decreases in the order of $[C_4mim]^+$>$[C_4mpyr]^+$>$[C_4dmim]^+$[14].

A normalised hydrogen bond acceptor scale has recently been established by Lungwitz and Spange, who attributed ion pair formation in $[C_4mim]$-based ionic liquids preferentially to the basicity of the anion. An excellent correlation of the ^1H NMR chemical shift of the C-2 proton of the imidazolium cation with the β-value determined using a solvatochromic dye was found. The normalisation of the results was carried out between the least and most hydrogen bond accepting anions of this study, tetraphenylborate and chloride, respectively [17]. The same group extended their approach to the hydrogen bond donating ability α of $[C_4mim]$-based ionic liquids, and found a linear correlation to the β-values of the earlier study [19].

2.2 Studies of the Dielectric Constant

Some measurements of the dielectric constant (relative dielectric permittivity) determining electrostatic interactions have been published recently [24–26], reporting a decreasing dielectric constant with increasing length of the alkyl side chain, and $[CF_3SO_3]^-$>$[BF_4]^-$>$[PF_6]^-$>$[BTA]^-$, and $[C_4mim]^+$~ $[C_4py]^+$~ $[C_4dmim]^+$>$[C_4mpyr]^+$. Quantitatively, the ionic liquids investigated were found to behave as moderately polar solvents such as *n*-pentanol ($\varepsilon = 15.1$), and thus to be less 'polar' than estimated by other methods [27].

2.3 Studies Using ESI–MS

The strength of cation–anion interaction was investigated in detail by the group of Chiappe using electrospray ionisation mass spectrometry (ESI–MS). From the ratios of the aggregates observed in positive- and negative-ion mode, a qualitative strength of interaction with bromide was derived as $[C_2mim]^+$>$[C_4mim]^+$>$[C_1C_2morph]^+$>$[C_6mim]^+$>$[C_8mim]^+$>$[C_1C_4morph]^+$>$[C_4py]^+$>$[C_4mpyr]^+$>$[picol]^+$>$[C_4dmim]^+$>$[N_{4444}]^+$[28]. Several observations made in synthetic studies have been assigned to the strength of cation–anion interactions present in the ionic liquid solvent, which are discussed below [28].

2.4 Studies of the Refractive Index

Although very limited data for the refractive index is available to date, it can be concluded that it increases linearly with increasing alkyl chain for a given cation type, $[C_nmim]^+$<$[C_ndmim]^+$<$[C_npy]^+$ and $[BF_4]^-$<$[BTA]^-$<$[CF_3SO_3]^-$ [29–32].

2.5 Considerations of Gas Phase Acidities

Following the methodology of Crowhurst et al. [14], the basicity of an anion should in general be reciprocal to the acidity of its conjugate acid. Thus, the ionic liquid basicity was correlated to established gas-phase basicities of the anions, calculated as Gibbs free energy change for the gas-phase deprotonation of its conjugate acid ΔG_H [33]. An increasing value of ΔG_H was interpreted as increasing basicity of the anion. The following sequence of ΔG_H values (expressed in kJ mol^{-1}) can thus be established: $[BTA]^-$(1187.8)>$[BF_4]^-$(1204.5)>$[CF_3SO_3]^-$(1224.6)>$[CH_3SO_3]^-$(1308.3) ~ $[CF_3CO_2]^-$ (1304.2).

In summary, it has been demonstrated by various techniques that the anion contributes essentially to the basicity, while the hydrogen bond donor ability is a function of the cation choice. However, each anion influences the relative effects exhibited by its counter-cation (and vice versa) in sometimes unpredictable ways. An example is the lower viscosity of ionic liquids based on $[C_n mim]^+$ compared to $[C_n dmim]^+$, which is counterintuitive as in the former instance, a stronger hydrogen bonding network and hence reduced mobility of the ions would be expected. Possible explanations of this phenomenon are discussed in detail [182]. Besides the number of different types of interactions (e.g. hydrogen bond donor ability, ion pairing etc.) which may be exerted by the cation, the number of cation types is still scarce compared to the large number of anions investigated in series of analogues.

3 Ionic Liquid–Organic Solute Interactions

Only a few approaches to obtain specifically a detailed understanding of ionic liquid–solute interactions have been presented in the literature to date. In many cases, however, knowledge on such interactions can be derived from physico-chemical measurements. Still, it should also be pointed out that many of these studies lack any purity specification of the ionic liquids used, although impurities are well known to affect such measurements [34].

Very little data on the Hildebrand solubility parameters of ionic liquid–solute systems is available to date. A study of eight ionic liquids using viscosity measurements in different solvents indicated polarities similar to allyl alcohol or dimethylsulfoxide [35]. More recent work has shown that the solubility parameters can be reliably estimated from surface tension and density measurements [36]. The equilibrium position of keto–enol tautomers in conjunction with quantitative ^{1}H-NMR-, IR- and UV/Vis-spectroscopy has been studied in ionic liquids [37, 38], where the stabilisation of the enol form is favoured in non-polar solvents in general. Comparison to the relative tautomer ratios obtained in methanol and acetonitrile indicated that even hydrophobic (non-polar) [BTA]-based ionic liquids were more polar than these organic solvents.

3.1 Evidence from Solubility Data

From solubility data, a general understanding of ionic liquid–solute interactions can be derived. Thus, by lengthening the alkyl chain substituent on the cation, the lipophilic character is increased, and the solubility of non-polar substrates increases [39–58]. The effect of the anion on the solubility of a substrate is more difficult to correlate. For example, the solubility of hex-1-ene [43] increases for $[C_4mim]^+$ in the order of $[BF_4]^-<[PF_6]^-<[CF_3SO_3]^-<[CF_3CO_2]^-<[BTA]^-$, while a different order is found for alcohols [54]: $[PF_6]^-<[BF_4]^-<[BTA]^-<[CF_3SO_3]^-<[DCA]^-$. For the CO_2- and CO-solubilities, $[NO_3]^-<[DCA]^-<[BF_4]^- \sim [PF_6]^-<[CF_3SO_3]^-<[BTA]^-<[CTf_3]^-$ [59] and $[BF_4]^-<[PF_6]^-<[SbF_6]^-<[CF_3SO_3]^-<[BTA]^-$ [55] were established, respectively. Similar to the interactions of methanol, CO_2 is solvated by the anions of an ionic liquid ($[C_4mim][BF_4]$ or $[C_4mim][PF_6]$), with the axis of the O=C=O molecule perpendicularly orientated towards the P–F or B–F bonds, as determined by attenuated total reflectance infra-red spectroscopy. The interaction with tetrafluoroborate was stronger than with hexafluorophosphate, indicating that the former anion acts as a stronger Lewis base towards CO_2 [60].

3.2 Evidence from Computational Studies

Pádua et al. [61] observed in all-atom force field molecular simulations of pure $[C_nmim][PF_6]$ and $[C_nmim][BTA]$ aggregation of alkyl chains in non-polar domains if the length of the alkyl side chain $n \leq 4$. Upon lengthening of the chain, the polar domains (anions/cationic head groups) attained a tridimensional network of ionic channels, while the non-polar domains became larger and microphase separation occurred as observed by the swelling of the ionic network. In an extension to ionic liquid–solute mixtures, the same group introduced either *n*-hexane, acetonitrile, methanol or water into $[C_4mim][PF_6]$ in sub-stoichiometric quantities. While water and hexane concentrated in either the polar or non-polar domain, respectively, acetonitrile and methanol exhibit interactions in both domains of the ionic liquid. The selective concentration of water and hexane are reflected on macroscopic scale in the partial solubility of these solutes, while acetonitrile and methanol are soluble over the full molar composition with this ionic liquid. Both methanol and acetonitrile interact strongly with the anion, the former by strong directional hydrogen bonding, the latter in a less directional way, with the methyl group pointing towards the anion. With regard to the interaction with the cation, acetonitrile acts as a stronger hydrogen bond acceptor than methanol. Water exhibits similar interaction patterns as methanol towards the anion, but features stronger hydrogen bond interactions with the cation. According to these studies, the mechanism of the dissolution of the ionic liquid network by incremental addition of a solute such as acetonitrile to the ionic liquid can be described as initial aggregation of the solute in the preferred domain, where it causes a disruption of the ionic

network. Further addition of solute causes the ions to rearrange into aggregates such as micelles or ion clusters in excess solute, before electrolytes are formed [62, 63]. A detailed discussion on micro-heterogeneity is presented in chapter by Prof. M. Gomez 5 of this book.

3.3 Evidence from Gas–Liquid Chromatography

Solvent–solute interactions were studied using the solvation parameter model developed by Abraham [64, 65], which uses a large number of probe molecules exhibiting various solute–solvent interactions due to acidic, basic, electron-donating, electron-withdrawing, and aromatic functional groups. For this purpose, capillary tubing is coated with various ionic liquids, and the retention of the probes on these gas chromatographic columns analysed by multiple linear regression analysis. It was found that the most dominant types of interaction are dipolarity, hydrogen bond basicity and dispersion forces. The dispersion force was very similar for all ionic liquids, but the hydrogen bond basicity depends mostly on the anion of the ionic liquid. The substitution of the imidazolium cation played a crucial role for the interaction with probes containing non-bonding or π-electron systems. If the substituents are capable of inducing a higher electron density at the ring, stronger interactions with such probes were achieved [66].

3.4 Evidence from the Activity Coefficient at Infinite Dilution

Using a similar experimental set-up as for the determination of Abraham's solvation parameters, the activity coefficient of solutes at infinite dilution γ^{∞} can be determined from their retention times using gas–liquid chromatography [12, 67–72]. Alternatively, the diluter technique is applied [67, 73] for which an inert gas transports the solute from the headspace (which is in equilibrium with the ionic liquid matrix) to a GC-column. The continuous decrease of the concentration in the headspace is measured as a function of time, generating an exponential function from which γ^{∞} is calculated.

At present, the systematic compilation and comparison of γ^{∞} from different labs is hampered by uncertainties in the baseline. Although this is also the case for measurements of other solvent systems, this becomes especially obvious when reviewing the data available for ionic liquids, for which in most instances a narrow set of ionic liquids has been investigated with a variety of solutes. Interpolation of the data from different publications to compile the behaviour over a homologous series of ionic liquids is not viable. We have therefore set out [74] to determine the structural effects of the ionic liquids' constituents as functions of the cation, the cation's substituent and the anion, according to the methodology presented in Fig. 1.

3.4.1 Selection of Ionic Liquids and Solutes

Three series of homologues of ionic liquids were derived by alteration of either the type of cation: $[C_n\text{quin}]^+$, $[C_n\text{mim}]^+$, $[C_n\text{py}]^+$, $[C_n\text{mpyr}]^+$, the length of the substitution on the cation: allyl, C_{2-8}= butyl, hexyl, octyl, or the type of the anion: $[\text{BTA}]^-$, $[BF_4]^-$, Cl^-, $[CH_3SO_4]^-$, $[\text{OAc}]^-$ [74].

The activity coefficient at infinite dilution of a solute γ^∞ is related to the relative strength of an intermolecular interaction with the ionic liquid. The choice of the model solutes was based on their Abbout–Kamlet–Taft parameters [4, 75, 76], to exhibit prevailing forces with regard to the hydrogen bond acceptor, donor and polarisability properties. Similar probe molecules have been used in computational studies [62, 63].

Three solutes were investigated in the category of non-specific interactions (Fig. 2): for ion–dipole interactions, acetonitrile was chosen as model solute to shed light on the ability of the ionic liquid to solvate dipolar molecules. The n-electron and π-electron dispersion forces are investigated using *n*-heptane and toluene, respectively. In the category of specific stoichiometric interactions, the hydrogen bond acceptor and donor properties of the ionic liquid are investigated with *n*-propanol (a hydrogen bond donor) and 1,4-dioxane (a hydrogen bond acceptor), respectively. For methodological reasons, the solutes were also selected on the grounds of their boiling points (between 80 and 130 °C), hence allowing for equilibration at elevated temperatures and reducing ionic liquid viscosities while avoiding decomposition of the ionic liquids.

3.4.2 Headspace Gas Chromatography

Headspace gas chromatography (HS-GC) is very useful to determine solvent-induced effects on solutes, because it is sensitive enough to measure small structural variations in the ionic liquid at concentrations in which the ionic liquid is present in excess, thus simulating its application as a solvent.

The activity coefficients are obtained according to the following procedure. From thermostated and equilibrated vials containing a constant volume of ionic liquid and varying amounts of solute, a headspace sample is injected into a gas chromatograph [77]. Due to the negligible volatility of the ionic liquids at the temperatures used in this investigation [78, 79], the peak area A of a solute is related to the partial vapour pressure p of a solute at a given temperature according to

$$A = \text{RF}p. \tag{1}$$

The partial vapour pressure is expressed as [77]

$$p = p^0 xy, \tag{2}$$

where p^0 is the vapour pressure of the solute at a given temperature, interpolated from tabulated data [76], x is the mole fraction of the solute, and γ the activity coefficient of the solute. The response factor RF is a reflection of certain apparatus-inherent

effects, such as the sensitivity of the detector, the split ratio and adsorption/absorption phenomena on the capillary. It is a constant for each solute for fixed apparatus parameters, and is obtained from measurements of the solute in absence of ionic liquid. For the determination of the peak area A, four samples of a solute in a constant amount of ionic liquid are analysed successively, and a linear regression performed on the data obtained.

$$y = bx + a \tag{3}$$

with a= blank value and b= averaged peak area of 1 µ solute in the sample. The gradient b is hence equal to the averaged peak area obtained from 1 µL solute in an ionic liquid matrix.

With

$$y = \frac{b}{RFp^0 x} \tag{4}$$

the activity coefficient is obtained. Since the solute concentration in the sample is low ($x \sim 1/1{,}000$), the activity coefficient γ is in first approximation equivalent to γ^∞. However, as it can be argued that the activity coefficient may show a nonlinear concentration dependency as the solute concentration approaches 0, the activity coefficient obtained from these data is termed 'activity coefficient at pseudo-infinite dilution' $\gamma^{'\infty'}$. Hence, the variation of the peak area A of a solute (at constant RF, equilibrium temperature and mole fraction x) for two samples containing different ionic liquid matrices is related to a change in partial pressure and therefore a change in $\gamma^{'\infty'}$ of the solute, where a low $\gamma^{'\infty'}$ indicates that the ionic liquid's interaction with the solute is high, and thus the solute's 'mobility' reduced. It should be noted that due to the specific temperatures at which the measurements were conducted for each solute, comparisons of $\gamma^{'\infty'}$ of two solutes in a particular ionic liquid are not admissible.

3.4.3 Effect of Possible Ionic Liquid-Inherent Impurities

In a preliminary study, the effect of ionic liquid-inherent impurities on the peak area A (and hence the vapour pressure) of a solute was investigated using the example of toluene in [C_6mim]Cl, to which either water or 1-methylimidazole were deliberately added to simulate the most likely impurities occurring in ionic liquids.

Figure 3 shows that the vapour pressure of toluene from a [C_6mim]Cl matrix increases exponentially at water concentrations >30 mol% (>3.7 wt%), while the effect of 1-methylimidazole is less drastic. Considering the qualities of ionic liquids used in this study (Table 1), the effect of impurities can be regarded negligible, although the degree of interactions between ionic liquid and impurity leading to vapour pressure effects may significantly depend on the nature of the impurity, and the constitution of the ionic liquid itself.

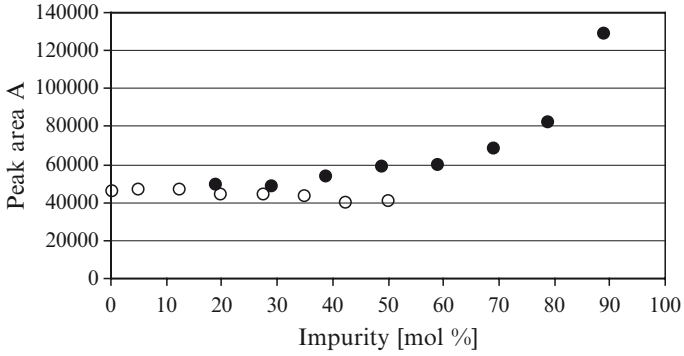

Fig. 3 Effect of the content of the impurities water (*filled circles*) and 1-methylimidazole (*open circles*) on the resulting peak areas (and hence vapour pressure) of 1 µL toluene in [C_6mim]Cl (ionic liquid + impurity = 7.872 mmol) [74]

Table 1 Qualities of ionic liquids investigated by HS–GC

Ionic liquid	Source	Water [wt%]	MIM [wt%][a]	Halide [ppm][b]
[C_6mpyr][BTA]	Merck	0.18	–	<LOD
[C_4mim][BF_4]	Fluka/purum >97%/1248750 40506249	0.14	< LOD	<LOD
[C_4mim]Cl	BASF	8.14	0.77 ± 0.03	–
[C_4mim][CH_3SO_4]	Fluka/purum >97%/1276316 21306310	0.40	<LOD	<LOD
[C_4mim][OAc]	Own synthesis	0.74	<LOD	<LOD
[C_4mim][BTA]	Own synthesis	0.10	<LOD	<LOD
[C_6mim][BTA]	Own synthesis	0.08	<LOD	<LOD
[C_6mim]Cl	Own synthesis	2.00	2.00 ± 0.03	–
[C_8mim][BTA]	Own synthesis	0.17	0.26 ± 0.03	<LOD
[Allylmim][BTA]	Own synthesis	0.38	<LOD	<LOD
[C_6quin][BTA]	Own synthesis	0.15	–	<LOD
[C_6py][BTA]	Own synthesis	0.03	–	<LOD

[a]*LOD* limit of detection: 0.3 wt% for a sample with 6 g/L ionic liquid. Limit of quantification of 1-methylimidazole: 0.09 wt%

[b]Halide titration with 0.1 M Ag(NO_3) expressed as chloride (automated Mettler Toledo titration, redox electrode), limit of detection <200 ppm Cl^- using 1 g of ionic liquid (LOD = limit of detection)

3.4.4 Effect of the Cation Substitution

The influence of the alkyl chain length on the cation was investigated using the example of [$C_n$mim][BTA]. Figure 4 shows that this structural aspect of the ionic liquid has no significant effect on the molecular dipole interactions probed with acetonitrile. The γ^{∞} of *n*-propanol decreases slightly for longer alkyl chains indicating increasing interactions with the ionic liquid. This is also reflected in the solubility

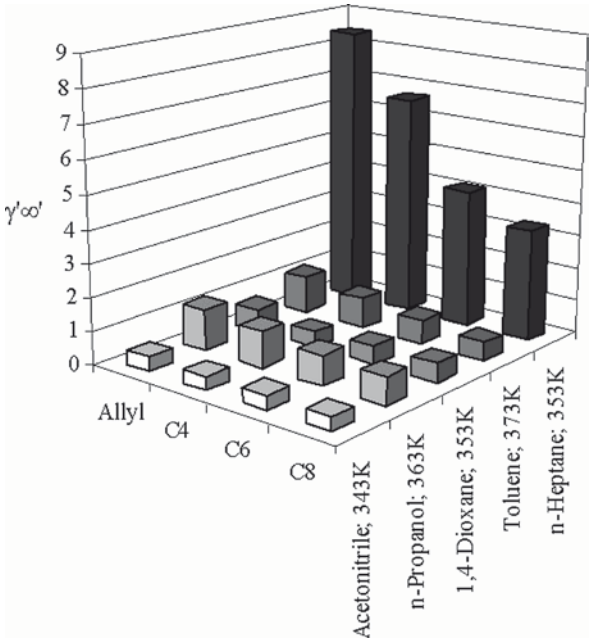

Fig. 4 Effect of the cation substitution of [$C_n$mim][BTA] on the activity coefficient γ^{∞} of the five model solutes [74]

of alcohols or water in ionic liquids with longer alkyl chain substitution, and is most likely not due to increased hydrogen bond interactions, but rather dispersion forces. As expected, the hydrogen bond donor ability of the ionic liquids (probed with 1,4-dioxane) is not significantly affected by the length of the alkyl chain.

However, both model solutes for the π- and n-electron dispersion forces, toluene and *n*-heptane, respectively, show a clear trend. With increasing alkyl chain length, the activity coefficient decreases by factor 2.0 in the case of toluene, and 2.5 in the case of *n*-heptane, indicating stronger interactions in ionic liquids bearing longer alkyl chains.

3.4.5 Effect of the Anion

The influence of the anion on the solvation properties of ionic liquids was investigated with five ionic liquids comprised of the $[C_4mim]^+$ cation, which was combined with various anions ($[OAc]^-$, Cl^-, $[CH_3SO_4]^-$, $[BF_4]^-$ and $[BTA]^-$).

The effect of the nature of the anion on γ^{∞} of the model solutes is displayed in Fig. 5. With regard to the molecular dipole interactions (acetonitrile), both acetate and chloride give higher γ^{∞} than in the polarisable methylsulfate, $[BF_4]^-$ and $[BTA]^-$, where the dipole is better accommodated. The relatively high γ^{∞} of acetonitrile in the acetate-based ionic liquid cannot be explained at present: a lower value would have been expected as acetate should be more polarisable than chloride.

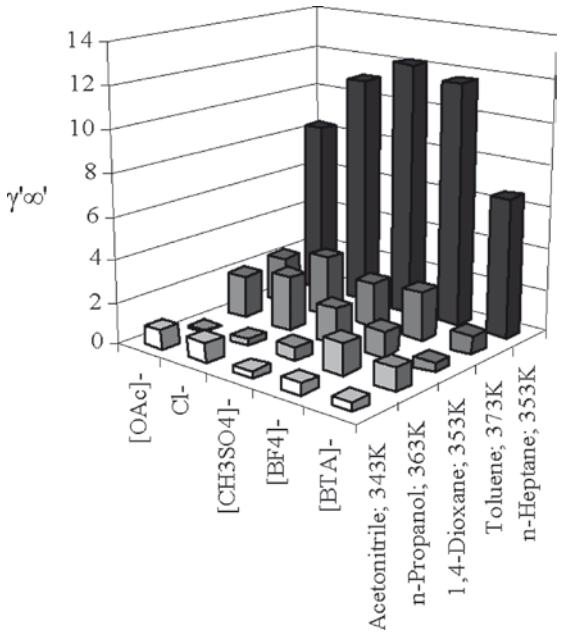

Fig. 5 Effect of the anion on γ^{∞} of the five model solutes in [C_4mim]-based ionic liquids [74]

The choice of the anion on the hydrogen bond acceptor and donor property of the ionic liquid is of central importance. While the γ^{∞} of *n*-propanol decreases in the order of $[BF_4]^-$>$[BTA]^-$>$[CH_3SO_4]^-$>Cl^->$[OAc]^-$ by a factor of 20, the γ^{∞} of 1,4-dioxane decreases according to Cl^->$[OAc]^-$>$[CH_3SO_4]^-$>$[BF_4]^-$>$[BTA]^-$ (for [C_4mim]-based ionic liquids).

For *n*-propanol, the results show that smaller and harder anions are better hydrogen bond acceptors than polarisable and bulky ones, and thus reduce the mobility of *n*-propanol. By the same token, 1,4-dioxane can only interact with the cation's hydrogen atoms if they are not engaged in strong interactions with basic anions, and hence the activity is highest in the chloride-based ionic liquid. While the order of β-values established for the anions [17] is not strictly followed in the *n*-propanol series, it is in fact reflected in detail in the results for 1,4-dioxane.

For the π-electron dispersion forces the choice of the anion also plays a significant role. γ^{∞} for toluene is lowest for the [BTA]-anion, followed by $[OAc]^-$, $[CH_3SO_4]^-$ and $[BF_4]^-$, which feature similar values. The highest γ^{∞} of toluene, and hence the lowest degree of interaction, is found for the chloride-containing ionic liquid.

The picture is less clear for the n-electron dispersion forces investigated with *n*-heptane. While the soft $[BTA]^-$ anion also leads to the lowest γ^{∞}, Cl^-, $[CH_3SO_4]^-$ and $[BF_4]^-$ belong to the group featuring the highest. However, due to the large error (5–9%) for these weak interactions, a differentiated analysis is not possible. Interestingly, however, acetate ranges between these two extremes.

3.4.6 Effect of the Cation

For the investigation of the influence of the cation on the solvation interactions in ionic liquids, [C_6mim][BTA], [C_6py][BTA], [C_6quin][BTA], and [C_6mpyr][BTA] were investigated (Fig. 6).

The effect of the cation on the relative activity of the solutes is low compared to the other structural aspects. Very little influence was found for the model solute acetonitrile, indicating a low degree of variation in the dipole interaction. The lowest γ^{∞} was found for the only non-aromatic cation *N*-hexyl-*N*-methyl-pyrrolidinium, indicating that dipole interactions occur to a slightly larger extent with the aliphatic cation than with those containing π-electron systems. Interestingly, no differences between the chosen cations were found with regard to hydrogen bond donor or acceptor interactions (1,4-dioxane, *n*-propanol). Both π- and n-electron dispersion forces are most prominent for the large *N*-hexylquinolinium cation, and aromatic systems are more prone to interactions than the non-aromatic example.

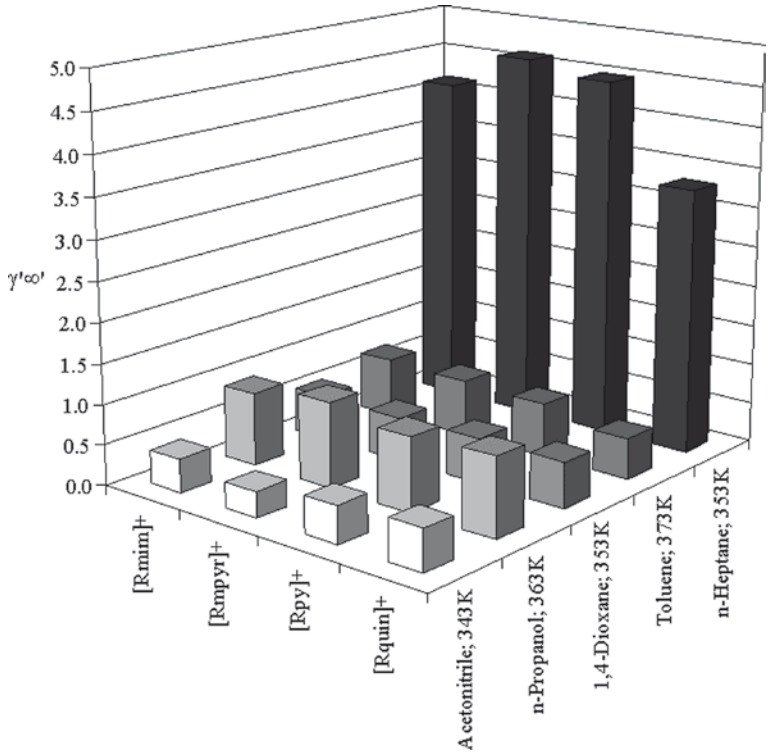

Fig. 6 Effect of the cation on the activity coefficient γ^{∞} of the five model solutes in [BTA]-based ionic liquids, where R = hexyl [74]

3.4.7 Comparison to Activity Coefficient Data from the Literature

Other authors have investigated the activity coefficient at infinite dilution mainly using two techniques: gas–liquid chromatography and the diluter technique. For the comparison of the activity coefficients at infinite dilution with γ^{∞}, literature data was chosen containing γ^{∞} at several temperatures, thus allowing for inter- and extrapolation to the temperatures investigated in this present study. For this procedure, the same equations as those employed by the respective authors were used (Table 2).

In general, the deviation between different methods and groups is expected to be quite high, due to the dependencies on various parameters of the apparatus (e.g. carrier gas flow), the use of literature data (e.g. vapour pressure) for the calculations, and variations in the equations used for the inter- and extrapolation of the activity coefficients. In addition, the above-mentioned deviation of the activity from linearity at concentrations approaching zero may play a role.

The comparison of the values for $[C_4mim][BF_4]$, $[C_4mim][BTA]$, $[C_6mim][BTA]$ and $[C_8mim][BTA]$ shows a good agreement for toluene, *n*-propanol, 1,4-dioxane and acetonitrile, but a large discrepancy for the activity coefficient at infinite dilution for *n*-heptane at 80 °C. Since there are only very weak interactions of *n*-heptane with the ionic liquid, it may be reasoned that the retention time in gas–liquid chromatography of this solute is extremely short, which would lead to a high apparent activity coefficient. The exceptionally low value for 1,4-dioxane in $[C_6mim][BTA]$ reported [83] cannot be explained at present. Interestingly, our results indicate a decrease in activity coefficient for toluene and *n*-propanol when increasing the alkyl chain length on the cation. This agrees with the data obtained by Kato et al.

Table 2 Activity coefficients of the five solutes in $[C_4mim][BF_4]$, $[C_4mim][BTA]$, $[C_6mim][BTA]$ or $[C_8mim][BTA]$ in comparison to literature data (glc – gas–liquid chromatography, diluter–diluter technique)

	$\gamma^{\infty}_{\text{Toluene}}$ 373.15 K	$\gamma^{\infty}_{n\text{-Heptane}}$ 353.15 K	$\gamma^{\infty}_{n\text{-Propanol}}$ 363.15 K	$\gamma^{\infty}_{1,4\text{-Dioxane}}$ 353.15 K	$\gamma^{\infty}_{\text{Acetonitrile}}$ 343.15 K
$[C_4mim][BF_4]$[a]	2.34 ± 0.07	**11.63 ± 0.57**	1.49 ± 0.03	1.23 ± 0.06	0.52 ± 0.01
glc [80]	4.12	93.30	2.00	–	–
glc [81, 82]	3.09	69.16	1.36	1.58	0.77
$[C_4mim][BTA]$[a]	0.92 ± 0.04	**6.65 ± 0.34**	1.10 ± 0.03	0.47 ± 0.04	0.41 ± 0.03
glc [70]	0.84	13.85	1.08	0.53	0.43
$[C_6mim][BTA]$[a]	0.73 ± 0.01	**4.15 ± 0.24**	0.91 ± 0.02	0.56 ± 0.05	0.42 ± 0.01
Diluter [67]	–	9.11	–	–	–
glc [67]	1.16	8.83	1.15	–	–
glc [83]	1.10	8.30	1.20	0.03	0.42
glc [84]	–	8.47	–	–	–
$[C_8mim][BTA]$[a]	0.56 ± 0.02	**3.36 ± 0.29**	0.84 ± 0.04		
Diluter [67]	–	6.07	–		
glc [67]	0.89	6.51	0.96		

[a]This work, activity coefficient at *pseudo*-infinite dilution

[67], while it stands in direct contrast to the trends from gas–liquid chromatographic investigations [70, 71, 83].

Hence, although the quantitative deviations are in general quite high owing to differences in the set-up of the measuring devices as well as differing purities of ionic liquids used, the qualitative comparison of the activity coefficients at pseudo-infinite dilution matches the trends in literature data.

3.4.8 Conclusions

HS-GC has been developed to serve as a sensitive tool to determine even small differences in the solvation properties of ionic liquids using a choice of model solutes featuring specific interactions: molecular ion–dipol interactions, hydrogen bond donor and acceptor interactions, and n- and π-electron dispersion forces can be probed by model solutes such as acetonitrile, 1,4-dioxane, *n*-propanol, *n*-heptane and toluene, respectively. Bearing in mind that no solute exhibits exclusively one specific interaction, the systematic investigation of the effect of the variation of the structural elements of ionic liquids, i.e. choice of cation, cation substitution and anion, lead to the following conclusions.

The ionic liquids investigated display similar solvation properties for the molecular dipoles, and the choice of anion can be singled out as the main tool to tune the solvation by this means. From the combination of the results of this set of ionic liquids, [$C_n$mpyr][CH_3SO_4] is predicted as the ionic liquid most capable to interact with dipoles. On the other hand, [$C_n$quin]Cl would exhibit the least tendencies in this respect.

Likewise, the hydrogen bond donor and acceptor properties of an ionic liquid are governed mainly by the choice of the anion. The strongest interactions with hydrogen bond donating solutes are observed with the nucleophilic anions chloride and acetate, while in [BTA]-based ionic liquids, hydrogen bonding with the anion is lowest.

The n- and π-electron dispersion interactions of a solute with the ionic liquid increase as the length of the aliphatic substituent increases. Furthermore, n-electron dispersion interactions are more prominent for aromatic cations, in particular for the large *N*-hexylquinolinium cation, while no effect of the cation was found with respect to the π-electron dispersion forces. Dispersion interactions become obvious especially if $[BTA]^-$ is chosen as the counter anion. From the results, [C_8quin][BTA] is predicted as the ionic liquid with the strongest n- and π-electron dispersion interactions. In [Allylmpyr][CH_3SO_4] and [Allylmim]Cl such interactions will likely not prevail.

In comparison, the effect of the alkyl chain length on the cation on the solubility of solutes capable to exhibit n- or π-dispersion interactions compares well to the trends found in the study on the activity coefficient at pseudo-infinite dilution γ^{∞}. With respect to the anion effect on the solubility of either hexene [43] or alcohols [54], the trends observed in the solubility data match that from the γ^{∞} study within this narrow set of examples.

Activity coefficients can be used as a predictive tool to design the ionic liquid structure to suit a particular application, as previously demonstrated in the screening for an optimal ionic liquid entrainer [85–89].

Interestingly, a similar headspace set-up is used by the pharmaceutical industry to determine solvent residues from synthesis in the products. Ionic liquids have been advertised as matrices for such measurements. Unlike molecular solvents, chromatograms obtained using ionic liquids do not feature broad solvent peaks, limited temperature range and carry-overs from consecutive injections. Due to their negligibly low vapour pressure, interfering solvent peaks are not generated, lower detection limits achieved, and the application range of headspace gas chromatography extended [90, 91]. However, the results presented above demonstrate that while this technique may prove useful for quality control, impurities exhibiting strong ionic liquid interactions may not be detected, as their vapour pressure may be greatly reduced depending on the choice of ionic liquid matrix.

Future investigations will focus on the influence of amino-, carboxyl-, hydroxy- and nitrile functionalities introduced into the cation substituent.

3.5 Evidence from ^{1}H NMR Spectroscopy

^{1}H NMR spectroscopy has been used to determine the degree of ionic liquid–ethanol interactions by studying the relative change in hydroxyl-shift (relative to its CH_3-resonance: 'OH-shift') in dependence of the ionic liquid's constituents [92]. If shifted downfield, a strong interaction reflecting the hydrogen bond acceptor ability of the ionic liquid anion occurs. In addition, ^{1}H NMR spectra simultaneously allow for the investigation of interactions with the C2-proton of the cation, expressed as the shift relative to its ethyl or butyl CH_3-resonance ('C2-shift'). As opposed to other studies aiming at understanding solvent–solute interactions, these investigations were carried out at a molar ratio ionic liquid: ethanol (1:1) for several practical reasons, such as its positive solvation properties towards most ionic liquids, yielding solutions of low viscosity, even for ionic liquids with melting points above room-temperature, leading to well-resolved ^{1}H NMR spectra in all cases.

The system ethanol–ionic liquid is characterised by different potential interactions (Fig. 7): the anion can act as a hydrogen bond acceptor, either resulting in interactions with the OH-group of ethanol (interaction 1) or with the cation, especially if an imidazolium-based ionic liquid possesses an acidic proton at its C-2 position (interaction 2) [29, 93–103].

Furthermore, the electron pairs of oxygen in ethanol can act as acceptors, leading to possible hydrogen bonds between ethanol and acidic cationic positions (interaction 3) and intermolecular interactions of ethanol (interaction 4). However, in the case of series of homologues of a cation at constant ethanol concentrations, the effects of these interactions are likely similar and were thus disregarded for the interpretation.

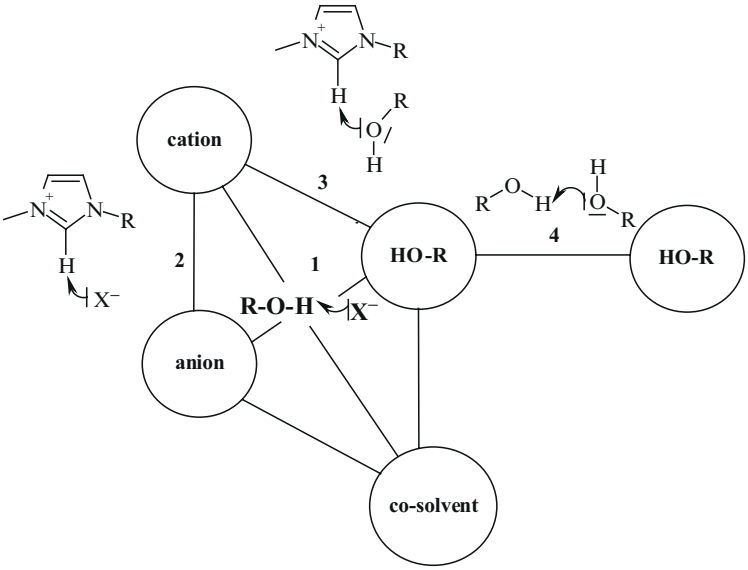

Fig. 7 Possible hydrogen bonding interactions in the solvent–solute system ionic liquid–ethanol

The chemical shift of the ethanol–OH was hence interpreted as the hydrogen bond basicity of ionic liquids, and an overall good correlation with Abboud–Kamlet–Taft β-values of Lungwitz and Spange [17] and γ^{∞} of *n*-propanol [74] was found: $[OAc]^-$>$[HCO_2]^-$>[DEP]$^-$>Cl^->$[CF_3CO_2]^-$>[OTs]$^-$~$[CH_3SO_3]^-$>Br^-> $[EtSO_4]^-$ ~ $[CH_3SO_4]^-$>[SCN]$^-$>[DCA]$^-$>$[CF_3SO_3]^-$>I^->$[BF_4]^-$>[BTA]$^-$, reproducibly for $[C_2mim]^+$ and $[C_4mim]^+$[92].

It is interesting to note that the trends of these three studies match each other, even though the solutes' concentrations in both the β-value and the γ^{∞} study are very low, while ethanol was used in equimolar amounts in the ^{1}H NMR studies. The only deviation to the β-values was observed in the relative position of the halides, which in the solvatochromic study were identified as the most basic anions. Interestingly, the authors [17] have correlated the β-values to the C2–H ^{1}H NMR chemical shift (measured in deuterated dichloromethane), and obtained an excellent linear correlation for all anions. When related to the 'C2-shift', the ethanol NMR data [92], on the other hand, shows separate linear trends for the multi- and monoatomic anions (Fig. 8). The origin of this divergence is presently not understood, but may reflect preferential hydrogen bonding interactions, depending on the physical constitution of the anion.

As in other studies, the determining factor for hydrogen bond basicity was found to be the anion. However, the interaction of a given anion with the solute can be modulated somewhat using different cations. As opposed to the γ^{∞} study [74], that proved to be not sensitive enough to detect changes in the *n*-propanol interactions with the cation, the results obtained by NMR show that ethanol has the strongest

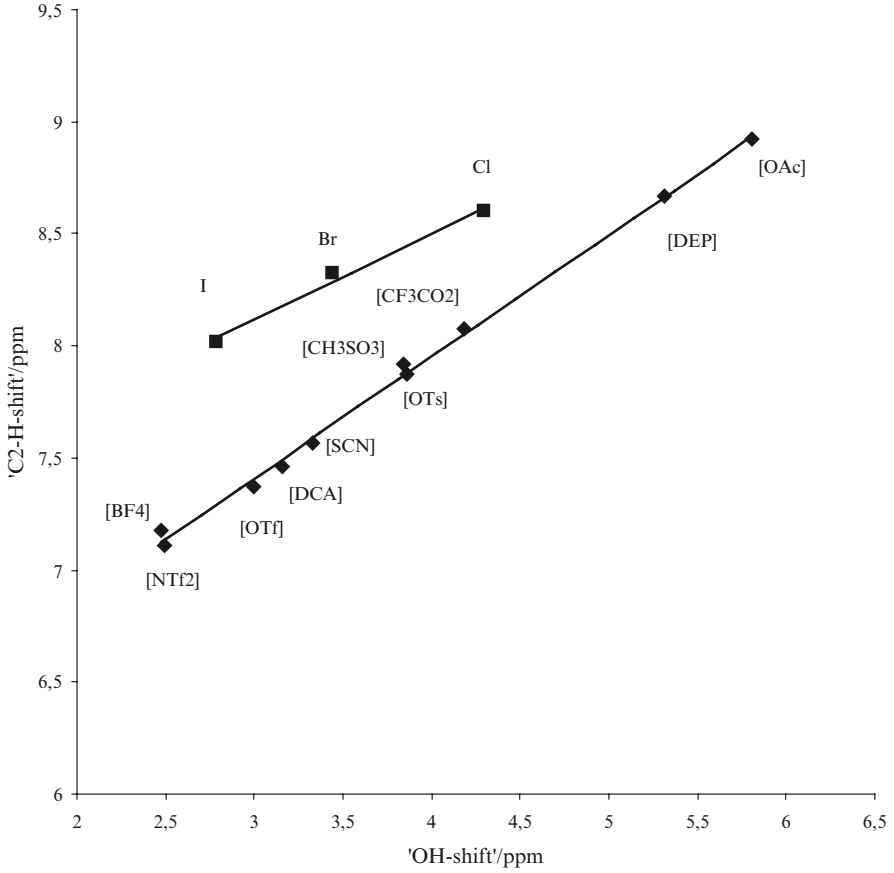

Fig. 8 Correlation between the ^{1}H NMR chemical shift of the ethanol OH-proton ('OH-shift') and the ^{1}H NMR chemical shift of the cationic C2-proton ('C2-H-shift') in equimolar ethanol-[C_2mim]-based ionic liquid mixtures referred to the methyl protons of ethanol and cationic side chain, respectively [92]

interactions with the anion in [$C_n$dmim]-based ionic liquids, which decrease in the order [$C_n$dmim]$^+$>[$C_n$mim]$^+$~ [$C_n$py]$^+$>[$C_n$mpyr]$^+$>trialkylsulfonium>tetraalkylammonium [92]. In other words, in this series of cations, cation–anion interactions would be expected to be strongest in tetraalkylammonium salts, where the anion is less engaged in hydrogen bonding with ethanol. However, this order does not reproduce the anion–cation interaction strength found by ESI–MS [28], nor the order of halide solvation determined by Daguenet and Dyson, as discussed below [104].

3.6 Liquid Clathrate Formation: Excursus

An interesting example is the interaction of benzene with [C_1mim][PF_6], which has been investigated by crystallography, neutron scattering and computational studies.

Many aromatics have a remarkably high solubility in ionic liquids of the 1-alkyl-3-methylimidazolium type, but in most instances phase separation occurs at high concentrations of the substrate. At certain molar rations, however, stable clathrates (inclusion compounds) [105] are formed, in which the cation–anion interactions of the pure ionic liquids are disrupted by the presence of the aromatic compound, leading to a new internal structure, based on associative interactions between the aromatic compound and the salt ions. An energetic equilibrium between the forces driving the crystallisation of the pure salt (e.g. cation–anion association) and the solvation interactions of the ions with the aromatic compound must exist to obtain a stable clathrate. Such liquid clathrates exhibit low viscosities (as compared to the pure ionic liquid), and constant, but not necessarily stoichiometric, compositions [106]. A 1:2 $[C_4mim][PF_6]$ – benzene crystalline inclusion compound has been obtained [106], in which benzene is sandwiched between the aromatic 1,3-dimethylimidazolium cations, while the anions reside in the equatorial regions. This type of interaction is also obtained in computer simulations, impressively highlighting the predictive power of MD studies [107], and was confirmed by conducting Empirical Potential Structure Refinement (EPSR) of neutron scattering data [108, 109]. The existence of such inclusion compounds highlights yet again the importance of understanding the interactions possible in ionic liquids. For example, when reactions involving aromatic compounds are carried out in an ionic liquid, this phenomenon will have a strong impact on the separation of the product from the solvent, and possibly on the reactivity of the aromatic compound as well. Furthermore, it has been shown that ionic liquids may be used to favourably influence the separation of aromatics from aliphatic compounds [88, 106].

In conclusion, the comparison of the experimental methods (HS-GC, ^{1}H NMR) shows that, with regard to the anion's interaction with alcohols, excellent correlation in the relative order of the anions is found [74, 92], which also reflects the trends for anion basicity established using solvatochromic dyes [17]. In contrast, quite diverging information on cation interactions are obtained by HS-GC and ^{1}H NMR, which may be due to a lower sensitivity of HS-GC towards such interactions. Furthermore, the lack of correlation to other cation-dependent studies, e.g. ESI–MS, is still inconclusive [28].

4 Ionic Liquid–Water Interactions

An interesting solute is water. It was recognised quite early that ionic liquids are hygroscopic, and both the absorption rate and capacity are a function of the cation, its substituent and the anion [30, 34, 110]. Although a high absorption rate and capacity is expected for ionic liquids containing anions with strong tendency of forming hydration shells (e.g. halides), it is surprising that even ionic liquids containing anions with relatively low coordination ability (e.g. $[BTA]^-$ or $[PF_6]^-$) can exhibit hygroscopic behaviour. The driving force for this absorption must be related to a change of internal order, leading to a more favourable structure of lower energy.

The influence of water on the diffusion rates of ionic and neutral species in voltametric studies leads to the suggestion that a nanostructure consisting of polar and

non-polar regions is present in ionic liquids. Such an inhomogeneity allows the neutral molecules to reside in less polar regions, whereas ionic species undergo fast diffusion in the more polar ("wet") regions [111].

For [C_4mim]-based ionic liquids, investigations by attenuated total reflectance and transmission infra-red spectroscopy indicate that up to the saturation point, water forms distinct 2:1 complexes in which both protons of water are hydrogen-bonded to two discrete anions, $A^{-}\cdots H–O–H\cdots A^{-}$ (where A^{-} represents anions with relatively low coordination ability such as $[PF_6]^{-}$, $[SbF_6]^{-}$, $[BTA]^{-}$, $[BF_4]^{-}$, $[ClO_4]^{-}$, and $[CF_3SO_3]^{-}$), and areas of clusters or pools of water are not present. However, in ionic liquids based on anions such as nitrate, clusters of water molecules may occur in addition to the above complexes. The enthalpies of the interaction of water with different anions were determined from the spectral shifts. They increase in the following order: $[PF_6]^{-}$ $<[SbF_6]^{-}<[BF_4]^{-}<[BTA]^{-}<[ClO_4]^{-}<[CF_3SO_3]^{-}<[NO_3]^{-}$ [110, 112].

These findings are also reflected in molecular dynamics simulation studies of water with either [C_1mim]Cl or [C_1mim][PF_6] as functions of composition where, at low water concentrations, water molecules are isolated from each other and rather hydrogen bond to the anion than to other water molecules, irrespective of the hydrophilicity of the ionic liquid, and few large clusters of water exist. At higher water concentrations, a percolation network of water molecules is formed, with some isolated water molecules interacting with the anions, and regions containing water clusters. Such a continuous water network changes the mixture and its properties dramatically. For example, it was found that the molecular motion increases as the proportion of water increases [113].

Likewise, in all-atom force field simulation studies, water was found to reside selectively in the polar domain of [$C_n$mim]-based ionic liquids, i.e. in the vicinity of the cation and anion, forming strong hydrogen bonds with both moieties [62, 63].

Intermolecular NMR-spectroscopic Nuclear Overhauser Enhancements of [C_4mim] [BF_4]-water mixtures led to the suggestion that, in addition to anion–water interactions, solvation (hydration) of the cation also occurs [96]. Water replaces the cation–anion hydrogen bonds and also reduces cation–cation associations. Conformational changes in the structure of the butyl chain with respect to the plane of the imidazolium ring were suggested, which were evidenced in various studies in 2003 [114–117].

In summary, since water is capable of exhibiting multiple interactions with the ionic liquid constituents, influences on the properties of the mixture, such as the molecular motion, excess thermodynamic functions [34, 118–121], and water diffusion coefficients [111, 113] can be quite dramatic.

5 Ionic Liquid–Acid Interactions

Maybe one of the most important questions to be answered relates to the degree of dissociation of Brønsted acids and bases in ionic liquids. Acids are ubiquitously used as catalysts to initiate reactions such as the Fischer-type esterification or ether formation from alcohols.

The relative basicity of anions in ionic liquids is directly related to the question of their acid–base properties which cannot be determined by pH measurements due to the non-aqueous nature of these media. However, MacFarlane and Forsyth argue that an acid dissolved in an ionic liquid based on anions which are typically more basic than water, such as acetate, must be more dissociated than when dissolved in water [122].

The determination of a Brønsted acidity scale of various acids in ionic liquids has been evaluated from Hammett acidity functions using UV–visible spectra obtained from the 2,4-dinitroaniline indicator at various acid concentrations [123]. It was found that both trifluoromethanesulfonic acid and HBTA possess a similar level of acidity in [C_4mim][BTA], and addition of water reduces the acidity. Interestingly, the results indicate that HBTA is more acidic in [C_4mim][BF_4] and [C_4dmim][BF_4] than in [C_4mim][BTA], suggesting that the [BF_4]-anion is less solvating towards H^+ than $[BTA]^-$. Unfortunately, the comparison of different acids in the same ionic liquid by this approach is hampered by the relative sensitivity of the indicator, which is not universal to allow for the investigation of both strong and weaker acids under similar conditions [123].

A theoretical ab initio approach to assess the basicity of ionic liquid anions has been presented, based on the proton as a probe 'charge' to determine the charge on the anion. According to the equilibrium

$$A^- + H_3O^+ \rightleftharpoons A\text{–}H + H_2O$$

anions with a low degree of charge delocalisation show higher proton affinity values. The established proton affinity scale [124] (Fig. 9) reflects very well the β-values of anions determined in solvatochromic studies [17], as discussed above.

Ab initio molecular dynamics simulations of the interactions of a HCl molecule in [C_1mim]Cl delivered the formation of a linear $[Cl\text{–}H\text{–}Cl]^-$ species, which may be interpreted as a highly solvated complex of the proton. In extension to this consideration, a reduced activity of the proton results [125, 126].

Possibly one of the earliest accounts in which an ionic liquid structure-induced effect was reported is the reaction of toluene and nitric acid reported by Earle et al. [127], who not only observed an improvement in conversion rate or selectivity, but demonstrated that the reaction type (nitration, halogenation, oxidation) is governed by the choice of the ionic liquid. Thus, the nitration of toluene using 67% nitric acid

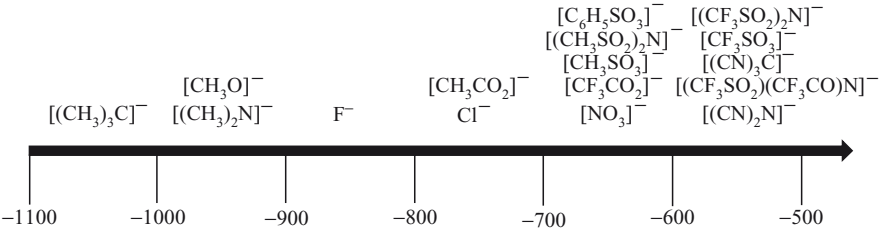

Fig. 9 Proton affinity scale [kJ mol^{-1}] derived from ab initio calculations [124]

gave the three corresponding mono-substituted nitrotoluenes in trifluoromethanesulfonate-based ionic liquids, with di-substitution occurring only after prolonged reaction times.

In contrast, if halide-based ionic liquids were used under similar conditions, halogenated products were isolated. If hydrochloric acid was used in a nitrate-based ionic liquid, halogenated products also resulted. In methanesulfonate-based ionic liquids, nitric acid acts as an oxidising agent rather than a nitrating agent, which is capable of oxidising toluene to benzoic acid. Likewise it was possible to use a nitrate-based ionic liquid with added methanesulfonic acid [127].

Although this study gives only a few anion–acid combinations, the results can be carefully reinterpreted with regard to the activity of protons in ionic liquids and their interplay with mixtures of anions. For example, in the case of the nitration reaction, trifluoromethanesulfonic acid ($pK_a = -13$) is more acidic than nitric acid ($pK_a = -1.5$), and hence according to the general acid–base theory, the corresponding anion of the former is less basic than the latter. Therefore, in the ionic liquid mixture, the proton is active (i.e. not 'quenched') and nitric acid can efficiently undergo the nitration reaction. In analogy, the mixture obtained from adding HNO_3 to a chloride-based ionic liquid is virtually the same as HCl in $[NO_3]$-based ionic liquid: due to the higher basicity of the $[NO_3]$-anion, proton exchange results. The same argument would apply to the oxidation example, thus explaining at least one of the peculiar observations. These observations are predated by a study of the nitration of various aromatic solutes in [BTA]-based ionic liquids [128]. Interestingly, the nitration of 1,3-dialkyl- and 1,2,3-trialkylimidazolium cations had already occurred in mild conditions (25 °C, acetylnitrate as nitrating agent) but was not reported to occur under the harsh conditions used by Earle et al. (reflux, 18 h, 67% HNO_3) [127]. However, using $[C_4C_1pyr][BTA]$ as solvent instead, very good conversions were obtained, and even deactivated aromatics such as bromo- or chlorobenzene were converted, whereas in dichloromethane, no conversion was observed under otherwise similar conditions [128].

In conclusion, few approaches to understand the dissociation of acids in ionic liquids have been undertaken to date. Experimental approaches using indicators provided a narrow set of data, but it may not be possible to establish a single comprehensive scale similar to pK_a values, including many acids, and various ionic liquid compositions.

6 Observations from Synthesis Pointing to Structurally Derived Effects

In many publications, an effect of the ionic liquid solvent on the rate or selectivity of organic and catalytic reactions has been reported [129]. For industrial applications, it has been recognised that process intensification using ionic liquids is in most cases not a question of retrofitting by simply substituting a solvent by an ionic liquid, but further tuning strategies, such as the immobilisation of catalysts

by using ionic ligands as reviewed recently by Šebesta et al. [130] to allow for efficient recycling of the ionic liquid–catalyst system, are required. In addition, and most importantly, the ionic liquid itself exhibits strong effects on the reaction. Beside the viscosity, vapour pressure, density, solubility, etc. which affect mass-transfer properties and the choice and lay-out of the unit operations of a process, the ionic liquid constituents may play a direct role in the reaction mechanism, in what we regard as organocatalytic interactions. One of the most challenging aspects of such organocatalytic interactions is the induction of stereoselectivity, a topic that has only started to be explored in ionic liquids. The efficient use of ionic liquids featuring a chiral centre on either the cation [131–137] or on both moieties [138] to evoke enantiomeric excesses is still in its infancy, but the concept has been proven to work, for example in the enantioselective hydrogenation of a keto-function of the ionic liquid's cation in the presence of a (*R*)-camphorsufonate anion, resulting in up to 80% *ee*. It was postulated that a strong interaction of the enantiomerically pure anion by ion-pairing was responsible for this induction [139].

In the following, some recent observations and theories presented in the literature are discussed in an exemplary fashion to highlight such specific interactions, with emphasis on nucleophilic and condensation reactions.

6.1 Oxidation Reactions

The efficient solvation of water [96, 110, 112, 113] outlined above can be exploited in condensation reactions, in which water formed during the course of the reaction is 'deactivated by absorption', which can improve conversion and/or selectivity. For example, in the catalytic oxidation of an alcohol to the aldehyde [140, 141], water is formed as by-product which can undergo further reaction with the aldehyde to yield unwanted carboxylic acid. In ionic liquids, neither a reduced rate of reaction nor the formation of carboxylic acid is observed, even in the presence of up to 1 equiv. of water. However, at higher concentrations of water (absorption from air or accumulated by-product) the selectivity of aldehyde decreases, and the carboxylic acid is formed instead. Upon vigorous drying of the catalyst-ionic liquid mixture, the selectivity of the system is restored [141].

6.2 Diels–Alder Reactions

Specific anion- and cation-reactant effects have been reported to play a role in Diels–Alder reactions [142–144], in particular for the *endo*-selectivity. Using the model reaction cyclopentadiene and methyl acrylate (Fig. 10, left) in various ionic liquids, the authors [142] demonstrated that the *endo/exo* ratio decreased when the reactions were carried out in $[C_4mim]^+$ homologues in the order of:

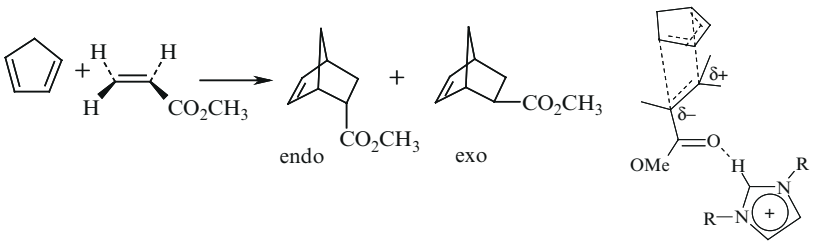

Fig. 10 The Diels–Alder reaction of cyclopentadiene and methyl acrylate (*left*), intermediate complex suggested in the Diels–Alder reaction leading to higher endo-selectivity (*right*) [142]

$$[C1O_4]^- = [PF_6]^- > [BF_4]^- > [CF_3SO_3]^- > [BTA]^- > [CF_3CO_2]^-,$$

thus following approximately the decrease in the order of anion basicity determined in other studies [7, 10]. Mechanistically, this can be explained by arguing that if the anion–cation interaction is weak due to a low basicity of the anion, the cation is capable of interacting with the substrate methyl acrylate to yield an intermediate complex (Fig. 10, right), which in turn results in improved *endo*-selectivities.

This study also highlights the importance of cation choice. If, for example, the hydrogen bond donor ability of the solvent is reduced by substituting the acidic proton in the C-2 position in $[C_4mim][BF_4]$ with a methyl group ($[C_4dmim][BF_4]$), the *endo*-selectivity decreased significantly. Introduction of other hydrogen bond donor sites into the cation (N–H or O–H), on the other hand, increases the *endo*-selectivity [142].

6.3 Acetylation Reactions

Anion-effected organocatalysis has been reported by MacFarlane et al. [145, 146] to be exhibited by dicyanamide- or acetate-based ionic liquids in the acetylation of glucose and other alcohols. As opposed to other protocols, which require an excess of both the activating amine and acetic anhydride, the authors demonstrated that excellent yields can be achieved at moderate temperatures, thus providing a clean, rapid and mild method which may be helpful in ‘cleaning up’ cellulose acetylation in ionic liquids.

6.4 Nucleophilic Substitution

Welton’s group has conducted a huge body of work to elucidate the effect of ionic liquid compositions in nucleophilic reactions.

In first approximation, the Hughes–Ingold approach to predict solvent effects has been shown to be viable for ionic liquids. This approach qualitatively considers electrostatic interactions between ions or dipolar molecules, and states that more 'polar' solvents stabilise charged transition states, leading to increased rates if the charge density of the transition is higher than in the reactants [147, 148].

While this theory holds for ionic liquids in general when compared to organic solvents, it cannot be efficiently used to select the best ionic liquid from a pool of ionic liquids. This has been attributed to the fact that ionic liquids feature very similar π*-values, which determine polarisability/dipolarity.

Predictions based on Abboud–Kamlet–Taft parameters lead to better results, since the anion's basicity (β-value) and the cation's hydrogen bond donor ability (α-value) are assessed separately. For example, in the nucleophilic substitution of methyl-*p*-nitrobenzene sulfonate and a halide (Fig. 11) the hydrogen bond donor ability of the cation should be reduced in order to eliminate strong interactions with the halide. This was impressively demonstrated for the rates of reaction, which decreased according to $[C_4mpyr][BTA] > [C_4dmim][BTA] > [C_4mim][BTA]$ [149, 150].

The effect of the ionic liquid's anion is less simple to determine, and changing orders of nucleophilicity were found for chloride, bromide and iodide depending the choice of the ionic liquid's anion (and cation). Correlation was neither possible with the Abboud–Kamlet–Taft nor Abraham's parameters [151]. From the study of a large range of nucleophiles, including mono-atomic and multi-atomic anions, the authors came to the conclusion that the delicate competition for interaction between the nucleophile and the ionic liquid anion with the cation of the ionic liquid is governed also by the nature of charge distribution according to the concept of hard and soft acids and bases (HSAB) [152]. Hence, due to the overall hard nature the $[C_4mim]^+$ cation (likely due to the acidity of the proton on C-2), ion pairing is preferred with a hard anion, such as chloride.

In an extension of this study, nucleophilic substitution with charge-neutral nucleophiles was studied. In the case of the reaction of amines with methyl-*p*-nitrobenzene sulfonate, highly hydrogen bond accepting anions are capable of increasing the nucleophilicity of the amines, and increase the rate of the reaction, while hydrogen bond donating cations reduce their nucleophilicity [153]. In a similar fashion, the nucleophilic aromatic substitution of *p*-fluorobenzene and *p*-anisidine (Fig. 12) was positively affected by using anions with hydrogen bond acceptor potential. Interestingly, the choice of anions was based on a theory whereby the gas phase acidity of an acid is reciprocally related to the basicity of the corresponding anion [154].

An extreme example of tuning anion nucleophilicity was presented by Chiappe et al., who demonstrated on the example of the nucleophilic dediazoniation that, in

Fig. 11 Nucleophilic substitution of methyl-*p*-nitrobenzene sulfonate and a halide [149, 150]

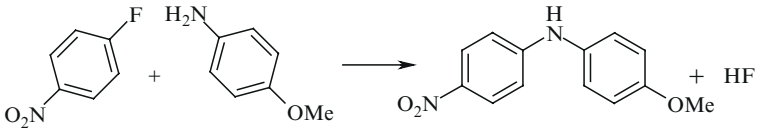

Fig. 12 Nucleophilic aromatic substitution of *p*-fluorobenzene and *p*-anisidine [154]

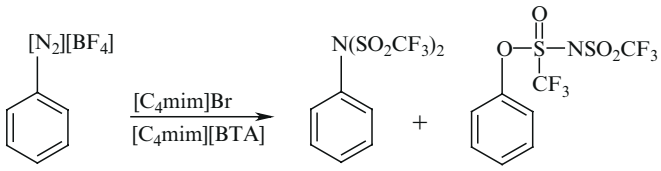

Fig. 13 Dediazoniation in [C_4mim]Br – [C_4mim][BTA] mixtures [155]

certain cases, the apparent nucleophilicity of anions such as $[BTA]^-$ is higher than that of bromide or chloride. Hence, when [PhN_2][BF_4] was treated with a mixture of [C_4mim]Br – [C_4mim][BTA], two unusual BTA-derivatives were detected instead of the expected bromobenzene (Fig. 13). Although at first sight this appears to be surprising as the [BTA]-anion is thought to be 'non-nucleophilic', a closer look at the reaction mechanism reveals that the nucleophilic activity of the bromide is reduced due to strong hydrogen bonding with the ionic liquid cation. The less solvated $[BTA]^-$ is hence capable of approaching the reactive site to substitute the diazo-group.

Similar behaviour was found in mixtures with [C_4mim]Cl, but when the corresponding iodide was investigated, only iodobenzene was found as product, indicating that iodide is the only halide capable of competing with BTA [155].

6.5 *Hydrogenation Reactions*

Daguenet and Dyson [156] have shown in the hydrogenation of styrene to ethylbenzene using [Ru(dppm)(*p*-cymene)Cl]Cl that the reaction mechanism is influenced by the anion of the ionic liquid, and the least coordinating anion ($[BTA]^-$) investigated gave the highest conversions. As for the influence of the cation, the rate increased with decreasing chloride solvation, which was established in a thermodynamic study of the dissociation of a chloride-templated nickel(II) metallacage to be $[N_{5222}]^+ < [C_4mpyr]^+ < [C_4mim]^+ \leq [C_4dmim]^+ < [C_4py]^+$. It was noted that this order, based on reaction enthalpies, does not correlate to the dielectric constant nor E_T^{30} [104]. The authors conclude that higher catalytic activities can be achieved by providing a medium with low chloride solvation, in which the unsolvated chloride is available to enter the catalytic cycle [156].

6.6 Heck and Related Reactions

Very likely, similar effects are responsible for the solvent effects observed in Heck and related reactions [157–159]. For example, Calò et al. demonstrated that the butoxycarbonylation of 4-bromoacetophenone proceeded much less efficiently in $[C_4mim]Br$ than in $[N_{4444}]Br$ (16 and 76% yield, respectively, under otherwise identical conditions), likely due to the reduced availability of the bromide anion in the former system [159].

6.7 Fischer-Type Esterification

Equilibrium reactions, such as the Fischer-type esterification of an alcohol and a carboxylic acid, are an interesting group of reactions to study in ionic liquids, as both kinetic and thermodynamic aspects of the reaction could be solvent dependent.

A relatively large number of reports on esterification reactions has been published, aiming at increasing the yield and demonstrating solvent recycling by using Brønsted acidic ionic liquids giving biphasic mixtures. Four categories of ionic liquids used for Fischer esterifications can be distinguished:

- Brønsted-acidic functionality on the anion, e.g. by using ionic liquids based on $[HSO_4]^-$ or $[H_2PO_4]^-$ [160–167]
- Brønsted-acidic functionality on the cation, e.g. by neutralising amines or phosphines with an equimolar amount of acid [167–170]
- 'Neutralised' betaine-structures, as first described by the group of Davis [160, 161, 163, 166, 171–173]
- Ionic liquids not bearing labile protons, and addition of auxiliary acid [174–176]

In all instances, the reaction reportedly proceeds smoothly and results in good selectivities and yields. Interestingly, until recently [176] comparative studies of ionic liquid constituent effects had not been carried out for esterifications.

In order to understand these interactions, we consider systems containing second generation ionic liquids (i.e. without functionalisation on the cation substituent, no labile protons on either the cation or the anion, and bearing a hydrolytically stable anion).

Evidence of shifting the equilibrium position towards the product has been presented on the example of the esterification of ethanol and acetic acid, catalysed by *p*-toluenesulfonic acid. Although the reaction proceeded slower in $[C_4mim][PF_6]$, the position of the equilibrium was shifted towards the product side, as compared to the solvent-free reaction. The decrease in reaction rate was attributed to the higher viscosity and hence mass-transfer limitations [174].

In a related reaction, i.e. the dehydration of alcohols to yield ethers (Fig. 14), good yields were obtained in $[C_{10}mim][BF_4]$ (>90%), while no conversion was observed in either hexafluorophosphate- or chloride-based ionic liquids [177].

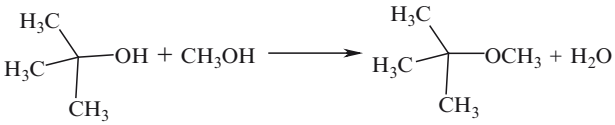

Fig. 14 Dehydration of alcohols to yield esters [177]

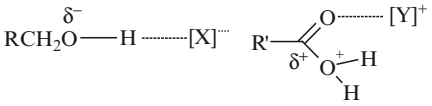

Fig. 15 Possible activating interactions between ionic liquid components and reactants

Both examples indicate that the water scavenging ability of some ionic liquids may influence the thermodynamics of a reaction, although in the light of more recent findings concerning the hydrolysis of hexafluorophosphate and tetrafluoroborate to acidic HF [178], which in turn may act as catalyst, the scope of ionic liquid anions should be extended to verify the results.

In general, the acid-catalysed esterification proceeds by the protonation of the alcohol (ROH) with subsequent proton transfer to the carboxylic acid (R'COOH), rendering the carboxyl carbon electron deficient. Nucleophilic attack of the alcohol is thus facilitated, and water liberated. In an ionic liquid [X][Y], interactions will occur with the solutes, as exemplarily depicted in Fig. 15.

These (or similar) interactions find their antecedents in the literature [74, 92, 142, 153, 179]. The stronger the interaction of the anion with the hydroxyl group of the alcohol, the more activated the alcoholate will be for nucleophilic attack on the carboxyl carbon, which itself can be activated by a Lewis-type complex formed with a Lewis acidic cation. A third beneficial interaction with a basic anion may arise from strong interactions (hydration) with the water formed, which would drive the equilibrium reaction towards the product side [96–112].

To prove our hypothesis on the organocatalytic effects of anions, we chose a series of relatively basic anions, combined with 1-butyl-3-methylimidazolium cations. Surprising results were obtained in the esterification of benzyl alcohol and acetic acid, which not only showed that the yields with any of the ionic liquids investigated are much lower than in the absence of ionic liquid (27% after 5 h; 75–80% after 100 h in equilibrium), but also that in none of the cases equilibrium was reached after 5 h at 100 °C (ROH:R'COOH:ionic liquid = 1:1.5:1). However, slight effects of the nature of the anion were observed, giving decreasing reaction rates in the order $[BTA]^-$>$[CF_3SO_3]^-$>$[CF_3CO_2]^-$>$[CH_3SO_4]^-$>$[CH_3SO_3]^-$>Cl^-. Interestingly, the results correlate exactly with the β-values of Lungwitz and Spange [17], albeit in the reverse order. Similarly, a preliminary study of the effect of the anion on the maximum yield (equilibrium) (Fig. 16) reflects these findings, with higher yields obtained in ionic liquids carrying less basic anions.

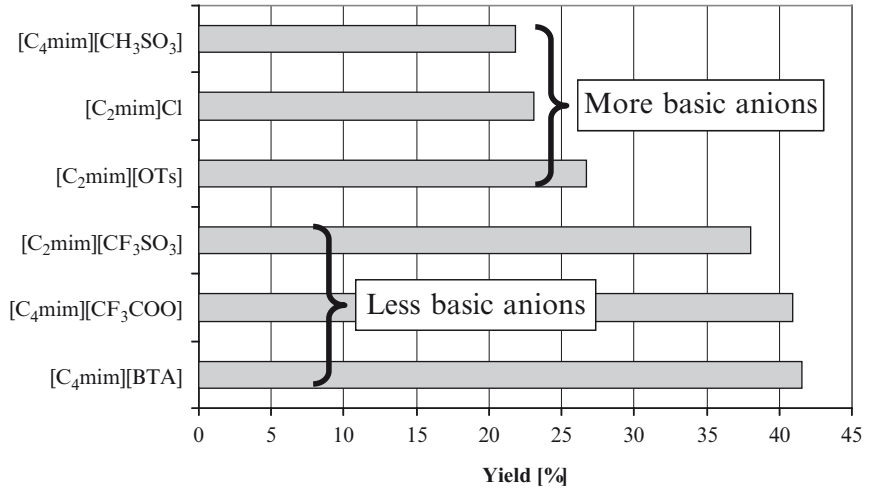

Fig. 16 Dependence of the maximum yield of ester (equilibrium) on ionic liquid anion (ROH:R'COOH:IL = 1:1.5:1, 60 h, 80 °C)

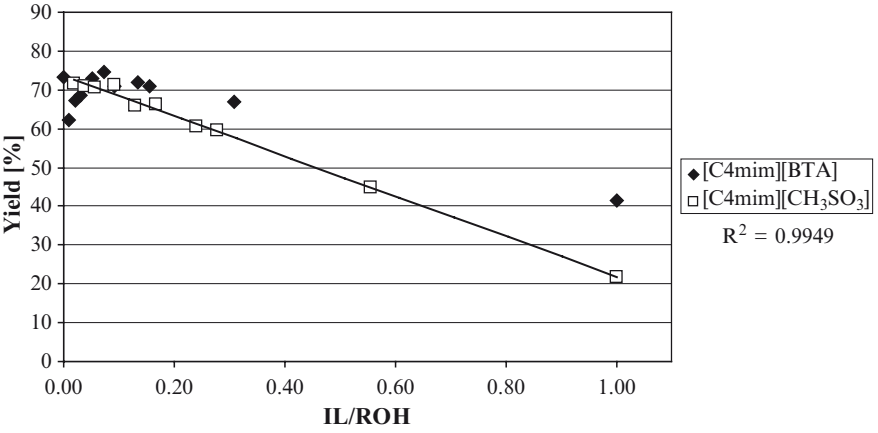

Fig. 17 Dependence of the maximum yield of ester (equilibrium) on the amount of ionic liquid added (ROH:R'COOH = 1:1.5, 60 h, 80 °C)

Hence, the anion affects both the equilibrium position and the rate of reaction. This latter aspect has been previously correlated to the Abboud–Kamlet–Taft parameters of ionic liquids and organic solvents [176], where more basic anions gave lower rates of reaction.

The effect of the ionic liquid concentration on the equilibrium was studied in more detail. Figure 17 clearly shows that the addition of ionic liquid, independent of the basicity of the anion, shifts the position of the equilibrium towards the starting material, contradicting earlier reports [174]. While the deviation from linearity

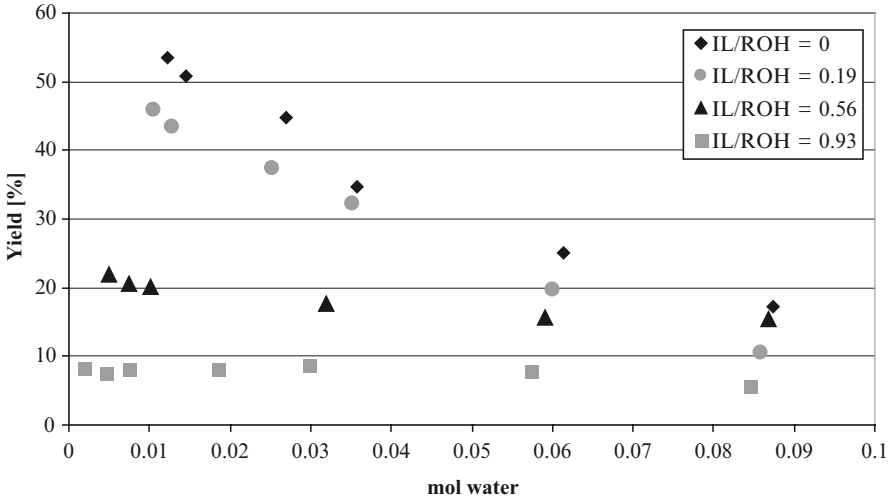

Fig. 18 Dependence of the yield on the amount of water added (ROH:R'COOH = 1:1.5, 24 h, 100 °C,) to $[C_4mim][CH_3SO_3]$

at low $[C_4mim][BTA]$ concentrations is not yet understood, an excellent linear correlation was obtained in the case of $[C_4mim][CH_3SO_3]$, indicating stoichiometric interactions influencing the equilibrium. Again, this effect is more pronounced for the more basic anion $[CH_3SO_3]^-$. In summary, both the equilibrium position and the rate of reaction are adversely affected in the presence of (basic) ionic liquid anions, hence contradicting our initial hypothesis.

With regard to a possible water scavenging effect which would result in a shift of the equilibrium towards the products, studies were conducted in mixtures of ionic liquid and water.

Figure 18 shows that the addition of water to any ($[C_4mim][CH_3SO_3]$ + ROH) mixture suppresses the formation of ester, and increasing amounts of ionic liquid also decreases the yield, irrespective of the ionic liquid/water composition. Due to these superimposing effects, a possible (albeit small) water scavenging effect of this particular anion is difficult to extrapolate, and further studies with different anions are required.

Mechanistic considerations explain the above results: the rate of this autocatalytic reaction is related to the activity of catalytic protons, and protonation occurs at the most basic site. If the ionic liquid anion is more basic than both ROH and R'COOH, the anion acts as a buffer. This has a twofold detrimental effect: first, the proton activity in the solution is greatly reduced, and second, the activating interactions between the anion and the reactants are broken.

If one would opt for the other extreme, i.e. an ionic liquid consisting of a very weakly basic anion such as $[BTA]^-$, hardly any interaction between the reactants and the anion are expected. However, protonation would occur at the alcohol and/or carboxylic acid instead of at the anion, which is beneficial for the reaction (Fig. 19). In fact, the [BTA]-based ionic liquid gives the highest rate, as shown above.

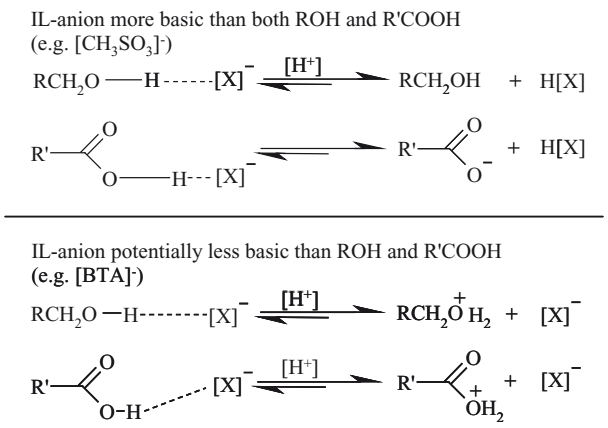

Fig. 19 Schematic considerations of interactions in dependence of the basicity of the ionic liquid anion

Additionally, a basic anion will 'block' electron-deficient sites (e.g. on the carboxylic acid), leading to reduced rates and also equilibrium constants, possibly due to a stabilisation of the intermediate. In comparison to the solvent-less system, such interactions lead to lower reaction efficiency, irrespective of the basicity of the anion. Whether the decrease in reaction rate is also due to a higher viscosity leading to mass-transfer limitations [174] remains to be investigated.

7 Conclusion

In summary, the literature data suggests that the hydrogen bond basicity is still the most reliable parameter to which reaction outcomes can be correlated. The effect of the cation is often not easily predicted, due to a delicate interplay specific to each anion and cation combination in the pure ionic liquid, which exhibits unique interactions when a solute is added.

For reactions, the influence of the ionic liquid's constituents is highly delicate, and the precision of predictions made on the basis of solvent parameters is dependent on the complexity of the reaction under investigation. As in conventional solvents, tuning the interactions governing the strength of the solvation of the reactants and products, and the stabilisation of intermediates and transition states is the key to obtaining good reaction rates. As opposed to conventional solvents, however, these interactions are functions of the nature of both the cation and anion, which not only undergo independent specific interactions with the solutes, but also influence each other's specific interaction. In this sense, ionic liquids are rather binary mixtures than homogeneous, single component solvents.

These anion–cation interactions are governed by several aspects, such as hydrogen bonding and ion pairing. Studies concentrating on the investigation of series of

cation homologues may improve on this situation in the future. A particular interesting aspect in this regard is whether and how the concept of HSAB can be applied to the strength of anion–cation interactions, and how these affect the dissociation of solutes, e.g. acids, in ionic liquid.

8 Experimental

8.1 Activity Coefficient at Pseudo-Infinite Dilution

Chemicals: n-Heptane (≥99%, Sigma), toluene (purum, ≥99.0%, Fluka), acetonitrile (LiChrosolv, Merck), *n*-propanol (≥99%, Aldrich), 1,4-dioxane (purum, ≥99.0%, Fluka), and 1-methylimidazol (puriss., ≥99,0%, Fluka) were used as received.

Ionic liquids: Table 1 displays the source, water and 1-methylimidazole content of the ionic liquids investigated, determined by Karl–Fischer titration and HPLC, respectively [180]. Own syntheses were carried out according to literature methods [29, 181].

Sample preparation and analysis: The ionic liquid (7.872 mmol ± 0.5 mg) was weighed into 20 mL headspace vials, and 1, 2, 3 and 4 µL of the solute was added using a 5 -µL syringe, resulting in a molar ratio x between 0.800×10^{-3} and 9.700×10^{-3}. Each sample was injected at least three times to give a mean value.

Experiments were conducted on a headspace gas chromatograph (86.10, Dani, Italy), equipped with a headspace sampler (HS 40, Perkin Elmer, Germany), and a FID detector (temperature: 240 °C). Samples were equilibrated on a shaker (at 80, 100, 70, 90 and 80 °C for *n*-heptane, toluene, acetonitrile, *n*-propanol and 1,4-dioxane, respectively) for 1 h. The sample was automatically injected (injector temperature: 130 °C) with nitrogen as carrier gas. A Hewlett Packard 25 m × 0.32 mm; HP-1 0.17-µm column was used for 1,4-dioxane, toluene, *n*-heptane and acetonitrile, while a Varian 30 m × 0.25 mm; CP WAX52CB 0.25-µm column was used for *n*-propanol. An isothermal programme was run for 8 min. at 80 °C.

In order to ascertain the linear relationship between the vapour pressure of a solute and the resulting peak area, a series of experiments were conducted on pure toluene as a function of p^0 between 4 and 77 kPa (eight data points) by adjustment of the equilibrium temperature. Statistic evaluation of the linear regression of the data obtained yielded a correlation coefficient of 0.9981, a relative standard deviation of 5.7%, and obeyed linearity according to MANDEL.

8.2 Esterification

Chemicals: Benzyl alcohol (Riedel, ≥95%) and acetic acid (Merck, 100%) were used as received. The purities of the ionic liquids used for esterifcation experiments are listed in Table 3.

experimental procedure: The reactions were carried out in a carousel 6 reactor station (Radleys) in 250-mL flasks equipped with a reflux condenser, and a magnetic follower at 100 °C under inert conditions (dry argon). All ionic liquids were dried prior to use (5 mbar, 80 °C), then benzyl alcohol and acetic acid were added. The relative ratio of benzyl alcohol (2.390 mL, 0.0231 mol, ROH) and acetic acid (1.980 ml, 0.0347 mol, R'COOH) was kept constant at a molar ratio of 1:1.5.

Sampling procedure: After the time indicated, samples (1 mL) were taken, diluted with 5 mL of water and 25 μL octane (internal standard), and extracted with diethylether (2 × 20 mL). The combined ether extracts were washed once with 5 mL water, and then diluted to 25 mL with diethylether. Then 0.250 mL of this solution was further diluted to 1 mL with diethylether, and analysed by GC. Most reactions were carried out twice, with each sample being injected twice. The data points presented are hence average values. Since the selectivity of all reactions performed was 1, conversion equals yield.

Quantitative analysis: Quantitative analyses were conducted on a Hewlett Packard 5890 Series II GS-System (Chrompak HP5, 30 m; 0.25 μm; FID detector) against an external calibration with benzoic acid methyl ester. The column pressure was adjusted to 15 psi, split 75 mL min^{-1}, injected volume 1 μL. Both, the injector and detector temperatures were at 250 °C. The temperature programme consisted of a ramp of 20 °C min^{-1} to 100 °C, 1 °C min^{-1} to 104 °C, followed by 20 °C min^{-1} to 210 °C. With this programme, the retention times are 2.8, 4.2, 10.7 and 1.2 min for benzyl alcohol, benzyl acetate, benzyl ether and octane, respectively. The total error was determined to be ±5%.

Table 3 Batches of ionic liquids, and their analytical specification, used in the esterification

Ionic liquid	Source	Water [wt%]	MIM [wt%][a]	Halide [ppm][b]
$[C_4mim][CH_3SO_3]$	Solvent innovation, 99%, 99/847, 99/961, 99/951	0.29	<LOD	<LOD
$[C_4mim]Cl$	Merck, >98%, EQ4003579638	0.40	0.10 ± 0.03	–
$[C_4mim][CH_3SO_4]$	Fluka/purum >97%/1276316, 21306310	0.98	<LOD	<LOD
$[C_4mim][CF_3SO_3]$	Solvent innovation, >99%, 99 847	0.24	<LOD	<LOD
$[C_4mim][CF_3CO_2]$	Merck,>98%, EQ508558616	0.14	0.13 ± 0.03	<LOD
$[C_4mim][BTA]$	Own synthesis	0.10	<LOD	<LOD

[a]1-Methylimidazole content determined by HPLC, *LOD* limit of detection: 0.03 wt% for a sample with 6 g/L ionic liquid. Limit of quantification of 1-methylimidazole: 0.09 wt%

[b]Halide titration with 0.1 M $Ag(NO_3)$ expressed as chloride (automated Mettler Toledo titration, redox electrode), limit of detection (LOD) <200 ppm Cl using 1 g of ionic liquid

9 Ionic Liquid Nomenclature

$[BTA]^-$	Bis(trifluoromethanesulfonyl)amide
$[C_nC_m morph]^+$	*N,N*-Dialkylmorpholinium
$[C_n dmim]^+$	1-Alkyl-2,3-*dim*ethyl*im*idazolium
$[C_n mim]^+$	1-Alkyl-3-methylimidazolium
$[C_n mpyr]^+$	*N*-Alkyl-*N*-methylpyrrolidinium
$[C_n picol]^+$	*N*-Alkylpicolinium (1-alkyl-4-methylpyridinium)
$[C_n py]^+$	1-Alkylpyridinium
$[C_n quin]^+$	*N*-Alkylquinolinium
$[CTf_3]^-$	Tris(trifluoromethanesulfony)methide
$[DCA]^-$	Dicyanamide
$[DEP]^-$	Diethylphosphate
$[Hmim]^+$	1-*H*-3-Methylimidazolium
$[N_{wxyz}]^+$	Tetraalkylammonium
$[OAc]^-$	Acetate
$[OTs]^-$	*p*-Toluenesulfonate
$[P_{wxyz}]^+$	Tetraalkylphosphonium

n, *m*, *w*, *x*, *y*, *z* = Number of carbons in one of the linear alkyl chains

Acknowledgements I would like to thank Prof. Dr. B. Ondruschka for the support granted at the Institute for Technical Chemistry and Environmental Chemistry of the Friedrich-Schiller University Jena. Furthermore, a big thank you to all members of the Ionic Liquids Group, in particular C. Palik, O. Braun, M. Sellin and M. M. Hoffmann (visiting scientist from SUNY Brockport, USA in 2007/08) for their various contributions. The donation of ionic liquid samples (BASF SE, Merck KGaA, Sigma-Aldrich Chemie GmbH) is greatly appreciated. For financial support, I am indebted to the Friedrich-Schiller University (HWP) and the DFG for funding within the Priority Programme SPP 1191 Ionic Liquids.

References

1. Tobias DJ, Hemminger JC (2008) Science 319:1197–1198
2. Seddon RS (1999) Ionic liquids: designer solvents? In: Boghosian S, Dracopoulos V, Kontoyannis CG, Voyiatzis GA (eds) The International George Papatheodorou Symposium, Institute of Chemical Engineering and High Temperature Chemical Processes, Patras, pp 131–135
3. Freemantle M (1998) Chem Eng News 76(13):32–37
4. Reichardt Ch (2003) Solvents and solvent effects in organic chemistry, 3rd edn. Wiley, Weinheim
5. Abraham MH, Zissimos AM, Huddleston JG, Willauer HD, Rogers RD, Acree WE (2003) Ind Eng Chem Res 42:413–418
6. Dimroth K, Reichardt Ch, Siepmann T, Bohlmann F (1963) Liebigs Ann Chem 661:1–37
7. Carmichael AJ, Seddon KR (2000) J Phys Org Chem 13:591–595
8. Fletcher KA, Storey IA, Hendricks AE, Pandey S, Pandey S (2001) Green Chem 3:210–215
9. Aki SNVK, Brennecke JF, Samanta A (2001) Chem Commun 413–414
10. Muldoon MJ, Gordon GM, Dunkin IR (2001) J Chem Soc Perkin Trans 2433–435
11. Baker SN, Baker GA, Bright FV (2002) Green Chem 4:165–169
12. Poole CF (2004) J Chrom A 1037:49–82
13. Reichardt Ch (2005) Green Chem 7:339–351
14. Crowhurst L, Mawdsley PR, Perez-Arlandis JM, Salter PA, Welton T (2003) Phys Chem Chem Phys 5:2790–2794

15. Oehlke A, Hofmann K, Spange S (2006) New J Chem 30:533–636
16. Fukaya Y, Sugimoto A, Ohno H (2006) Biomacromol 3295–3297
17. Lungwitz R, Spange S (2008) New J Chem 32:392–394
18. Fukaya Y, Hayashi K, Wada M, Ohno H (2008) Green Chem 10:44–46
19. Lungwitz R, Friedrich M, Linert W, Spange S (2008) New J Chem 32:1457–1644
20. Fujisawa T, Fukuda M, Terazima M, Kimura Y (2006) J Phys Chem A 110:6164–6172
21. Kamlet MJ, Taft RW (1976) J Am Chem Soc 98:377–383
22. Taft RW, Kamlet MJ (1976) J Am Chem Soc 98:2886–2894
23. Kamlet MJ, Abboud JL, Taft RW (1977) J Am Chem Soc 99:6027–6038
24. Wakai C, Oleinikova A, Ott M, Weingärtner H (2005) J Phys Chem B 109:17028–17030
25. Weingärtner HZ (2006) Z Phys Chem 220:1395–1405
26. Daguenet C, Dyson PJ, Krossing I, Oleinikova A, Slattery J, Wakai C, Weingärtner H (2006) J Phys Chem B 110:12682–12688
27. Weingärtner H (2008) Angew Chem 120:664–682
28. Bini R, Bortolini O, Chiappe C, Pieraccini D, Siciliano T (2007) J Phys Chem B 111:598–604
29. Bonhôte P, Dias AP, Papageorgiou N, Kalyanasundaram K, Grätzel M (1996) Inorg Chem 35:1168–1178
30. Huddleston JG, Visser AE, Reichert WM, Willauer HD, Broker GA, Rogers RD (2001) Green Chem 3:156–164
31. Deetlefs M, Shara M, Seddon KR (2005) Refractive indices of ionic liquids. In: Rogers RD, Seddon KR (eds) Ionic liquids IIIa: fundamentals, progress, challenges, and opportunities, properties and structure. American Chemical Society, Washington, pp 219–233
32. Deetlefs M, Seddon KR, Shara M (2006) New J Chem 30:317–326
33. Koppel IA, Burk P, Koppel I, Leito I, Sonoda T, Mishima M (2000) J Am Chem Soc 122:5114–5124
34. Seddon KR, Stark A, Torres M-J (2000) Pure Appl Chem 72:2275–2287
35. Lee SH, Lee SB (2005) Chem Commun 3469–3471
36. Jin H, O'Hare B, Dong J, Arzhantsev S, Baker GA, Wishart JF, Benesi AJ, Maroncelli M (2008) J Phys Chem B 112:81–92
37. Earle MJ, Engel BS, Seddon KR (2004) Austr J Chem 57:149–150
38. Angelini G, Chiappe C, De Maria P, Fontana A, Gasparrini F, Pieraccini D, Pierini M, Siani G (2005) J Org Chem 70:8193–8196
39. Wasserscheid P, Keim W (2000) Angew Chem Int Ed 39:3772–3789
40. Brasse CC, Englert U, Salzer A, Waffenschmidt H, Wasserscheid P (2000) Organometallics 19:3818–3823
41. Wasserscheid P, Gordon CM, Hilgers C, Muldoon MJ, Dunkin IR (2001) Chem Commun 1186–1187
42. Blanchard LA, Brennecke JF (2001) Ind Eng Chem Res 40:287–292
43. Favre F, Olivier-Bourbigou H, Commereuc D, Saussine L (2001) Chem Commun 15:1360–1361
44. Anthony JL, Maginn EJ, Brennecke JF (2001) J Phys Chem B 105:10942–10949
45. Swatloski RP, Visser AE, Reichert WM, Broker GA, Farina LM, Holbrey JD, Rogers RD (2002) Green Chem 4:81–87
46. Najdanovic-Visak V, Esperanca JMSS, Rebelo LPN, Nunes da Ponte N, Guedes HJR, Seddon KR, de Souza HC, Szydlowski J (2002) Phys Chem Chem Phys 4:1701–1703
47. Heintz A, Lehmann JK, Wertz C (2003) J Chem Eng Data 48:472–474
48. Wu C-T, Marsh KN, Deev AV, Boxall JA (2003) J Chem Eng Data 48:486–491
49. Najdanovic-Visak V, Esperanca JMSS, Rebelo LPN, da Ponte MN, Guedes HJR, Seddon KR, Szydlowski J (2003) J Phys Chem B 107:12797–12807
50. Heintz A, Lehmann JK, Verevkin SP (2003) Thermodynamic properties of liquid mixtures containing ionic liquids. In: Rogers RD, Seddon KR (eds) Ionic liquids as green solvents: progress and prospects. American Chemical Society, Washington, pp 134–150
51. Domanska U, Marciniak A (2003) J Chem Eng Data 48:451–456
52. Marczak W,Verevkin SP, Heintz A (2003) J Sol Chem 32:519–526

53. Aki SNVK, Mellein BR, Saurer EM, Brennecke JF (2004) J Phys Chem B 108:20355–20365
54. Crosthwaite MJ, Aki SNVK, Maginn EJ, Brennecke FJ (2004) J Phys Chem B 108:5113–5119
55. Ohlin CA, Dyson PJ, Laurenczy G (2004) Chem Commun 1070–1071
56. Kato R, Krummen M, Gmehling J (2004) Fluid Phase Equil 224:47–54
57. Stark A, Ajam M, Green M, Raubenheimer HG, Ranwell A, Ondruschka B (2006) Adv Synth Catal 348:1934–1941
58. Domanska U, Pobudkowska A, Eckert F (2006) Green Chem 8:268–276
59. Cadena C, Anthony JL, Shah JK, Morrow TI, Brennecke KF, Maginn EJ (2004) J Am Chem Soc 26:5300–5308
60. Kazarian SG, Briscoe BJ, Welton T (2000) Chem Commun 20:2047–2048
61. Canongia Lopes JNA, Pádua AAH (2006) J Phys Chem B 110:3330–3335
62. Canongia Lopes JNA, Costa Gomes MF, Pádua AAH (2006) J Phys Chem B 110:16816–16818
63. Pádua AAH, Costa Gomes MF, Canongia Lopes JNA (2007) Acc Chem Res 40:1087–1096
64. Abraham MH (1993) Chem Soc Rev 22:73–83
65. Abraham MH, Acree WE (2006) Green Chem 8:906–915
66. Anderson JL, Ding J, Welton T, Armstrong DW (2002) J Am Chem Soc 124:14247–14254
67. Kato R, Gmehling J (2005) J Chem Thermodyn 37:603–619
68. Kato R, Gmehling J (2004) Fluid Phase Equil 226:37–44
69. Kato R, Gmehling J (2005) Fluid Phase Equil 235:124
70. Heintz A, Casas LM, Nestrerov IA, Emel'yanenko VN, Verevkin SP (2005) J Chem Eng Data 50:1510–1514
71. Heintz A, Verevkin SP (2005) J Chem Eng Data 50:1515–1519
72. Letcher TM, Marciniak A, Marciniak M, Domanska U (2005) J Chem Eng Data 50:1294–1298
73. Krummen M, Gruber D, Gmehling J (2000) Ind Eng Chem Res 93:2114–2123
74. Braun O (2007) Zur Beziehung zwischen Struktur und Lösungsmitteleigenschaften von ionischen Flüssigkeiten mittels Headspace-Gaschromatographie (Regarding the structure-solvent property relationship of ionic liquids investigated by headspace gas chromatography). Dissertation, Institute for Technical Chemistry and Environmental Chemistry, Friedrich-Schiller University Jena, Germany
75. Latscha HP, Schilling G, Klein HA (1990) Chemie – Datensammlung. Springer, Berlin Heidelberg New York
76. Lide DL (2002) Handbook of chemistry and physics. CRC, Boca Raton
77. Hachenberg H, Beringer K (1996) Die Headspace-Gaschromatographie als Analysen- und Meßmethode. Vieweg Verlag, Braunschweig
78. Kosmulski M, Gustafsson J, Rosenholm JB (2004) Thermochim Acta 412:47–53
79. Baranyai KJ, Deacon GB, MacFarlane DR, Pringle JM, Scott JL (2004) Aust J Chem 57:145–147
80. Beste Y, Eggersmann M, Schoenmakers H (2005) Chem Ing Tech 77:1800–1808
81. Selvan MS, McKinley MD, Dubois RH, Atwood JL (2000) J Chem Eng Data 45:841–845
82. Gmehling J, Krummen M (to Carl v. Ossietzky University Oldenburg), DE10154052 Separation of aromatic hydrocarbons from non-aromatic hydrocarbons, comprises using a selective solvent selected from liquid onium salts publication date: 2003-07-10
83. Jork C, Kristen C, Pieraccini D, Stark A, Chiappe C, Beste YA, Arlt W (2005) J Chem Thermodyn 37:537–558
84. Acre A, Rodriguez O, Soto A (2004) J Chem Eng Data 49:514–517
85. Liu F, Jiang Y (2007) J Chrom A 1167:116–119
86. Koch P, Kuesters E (to Novartis Corporate Intellectual Property), WO2004013612 Analytical process 2004-02-12
87. Foco GM, Bottini SB, Quezada N, de la Fuente JC, Peters CJ (2006) J Chem Eng Data 51:1088–1091
88. Zhou Q, Wang LS (2006) J Chem Eng Data 51:1698–1701
89. Zhou Q, Wang LS, Wu JS, Li MY (2007) J Chem Eng Data 52:131–134
90. Heintz A, Verevkin SP, Ondo D (2006) J Chem Eng Data 51:434–437

91. Letcher TM, Marciniak A, Marciniak M, Domanska U (2005) J Chem Thermodyn 37:1327–1331
92. Sellin M, Ondruschka B, Balensiefer T, D'Andola G, Massonne K, Stark A (2008) in preparation
93. Avent AG, Chaloner PA, Cay MP, Seddon KR, Welton T (1994) J Chem Soc Dalton Trans 3405–3413
94. Huang J, Chen P, Sun I, Wang SP (2001) Inorg Chim Acta 320:7–11
95. Headley AD, Jackson NM (2002) J Phys Org Chem 15:52–55
96. Mele A, Tran CD, De Paoli SH (2003) Angew Chem Int Ed 42:4364–4366
97. Lin S, Ding M, Chang C, Lue S (2004) Tetrahedron 60:9441–9446
98. Tubbs JD, Hoffmann MMJ (2004) J Sol Chem 33:379–392
99. Headley AD, Kotti SRSS, Nam J, Li K (2005) J Phys Org Chem 18:1018–1022
100. Consorti CS, Suarez PAZ, De Souza RF, Burrow RA, Farrar DH, Lough AJ, Loh W, Da Silva LHM, Dupont J (2005) J Phys Chem B 109:4341–4349
101. Mele A, Romano G, Giannone M, Ragg E, Fronza G, Raos G, Maron V (2006) Angew Chem Int Ed 45:1123–1126
102. Singh T, Kumar A (2007) J Phys Chem B 111:7843–7851
103. Palomar J, Ferro VR, Gilarranz MA, Rodriguez JJ (2007) J Phys Chem B 111:168–180
104. Daguenet C, Dyson PJ (2007) Inorg Chem 46:403–408
105. Atwood JL, Atwood JD (1976) Non-stoichiometric liquid enclosure compounds ('Liquid Clathrates') In: King B (ed) Inorganic compounds with unusual properties. American Chemical Society, Washintgton, 112–127
106. Holbrey JD, Reichert WM, Nieuwenhuyzen M, Sheppard O, Hardacre C, Rogers RD (2003) Chem Commun 476–477
107. Harper JB, Lynden-Bell RM (2004) Mol Phys 102:85–94
108. Deetlefs M, Hardacre C, Nieuwenhuyzen M, Sheppard O, Soper AK (2005) J Phys Chem B 109:1593–1598
109. Hardacre C, Holbrey JD, Nieuwenhuyzen M, Youngs TGA (2007) Acc Chem Res 40:1146–1155
110. Tran CD, Lacerda SHD, Oliveira D (2003) Appl Spectr 57:152–157
111. Schröder U, Wadhawan JD, Compton RG, Marken F, Suarez PAZ, Consorti C, de Souza RF, Dupont J (2000) New J Chem 24:1009–1015
112. Cammarata L, Kazarian SG, Salter PA, Welton T (2001) Phys Chem Chem Phys 3:5192–5200
113. Hanke CG, Lynden-Bell RM (2003) J Phys Chem B 107:10873–10878
114. Hayashi S, Ozawa R, Hamaguchi H (2003) Chem Lett 32:498–499
115. Saha S, Hayashi S, Kobayashi A, Hamaguchi H (2003) Chem Lett 32:740–741
116. Holbrey JD, Reichert WM, Nieuwenhuyzen M, Johnston S, Seddon KR, Rogers RD (2003) Chem Commun 1636–1637
117. Ozawa R, Hayashi S, Saha S, Kobazashi A, Hamaguchi H (2003) Chem Lett. 32:948–949
118. Rodríguez H, Brennecke JF (2006) J Chem Eng Data 51:2145–2155
119. Gómez E, González B, Domínguez Á, Tojo E, Tojo J (2006) J Chem Eng Data 51:696–701
120. Pires RM, Costa HF, Ferreira AGM, Fonseca IMA (2007) J Chem Eng Data 52:1240–1245
121. Acre A, Soto A, Ortega J, Sabater G (2008) J Chem Eng Data 53:770–775
122. MacFarlane DR, Forsyth SA (2003) Acids and bases in ionic liquids. In: Rogers RD, Seddon KR (eds) Ionic liquids as green solvents: progress and prospects. American Chemical Society, Washington, pp 264–276
123. Thomazeau C, Olivier-Bourbigou H, Magna L, Luts S, Gilbert B (2003) J Am Chem Soc 125:5264–5265
124. Izgorodina EI, Forsyth M, MacFarlane DR (2007) Aust J Chem 60:15–20
125. Del Pópolo MG, Kohanoff J, Lynden-Bell RM (2006) J Phys Chem B 110:8798–8803
126. Del Pópolo MG, Kohanoff J, Lynden-Bell RM, Pinilla C (2006) Acc Chem Res 40:1156–1164
127. Earle MJ, Katdare SP, Seddon KR (2004) Org Lett 6:707–710

128. Lancaster NL, Llopis-Mestre V (2003) Chem Commun 2812–2813
129. Stark A, Seddon KR (2007) Ionic liquids. In: Seidel A (ed) Kirk-Othmer Encyclopaedia of chemical technology, 5th edn. Wiley, Hoboken, pp 836–920
130. Šebesta R, Kmentová I, Toma Š (2008) Green Chem 10:484–496
131. Wasserscheid P, Bösmann A, Bolm C (2002) Chem Commun 200–201
132. Pégot B, Vo-Thanh G, Gori D, Loupy A (2004) Tetrahedron Lett 45:6425–6428
133. Luo S, Mi X, Zhang L, Liu S, Xu H, Cheng J-P (2006) Angew Chem Int Ed 45:3093–3097
134. Earle MJ, McCormac PB, Seddon KR (1999) Green Chem 1:23–25
135. Fukomoto K, Ohno H (2006) Chem Commun 3081–3083
136. Machado MY, Dorta R (2005) Synthesis 2473–2475
137. Gausepohl R, Buskens P, Kleinen J, Bruckmann A, Lehmann CW, Klankermayer J, Leitner W (2006) Angew Chem Int Ed 45:3689–3692
138. Machado MY, Dorta R (2005) Synthesis 2473–2475
139. Schulz PS, Müller N, Bösmann A, Wasserscheid P (2007) Angew Chem Int Ed 46:1293–1295
140. Farmer V, Welton T (2002) Green Chem 4:97–102
141. Seddon KR, Stark A (2002) Green Chem 4:119–123
142. Aggarwal A, Lancaster NL, Sethi AR, Welton T (2002) Green Chem 4:517–520
143. Nobuoka K, Kitaoka S, Kunimitsu K, Iio M, Harran T, Wakisaka A, Ishikawa Y (2005) J Org Chem 70:10106–10108
144. Bartsch RA, Dzyuba SV (2003) Polarity variation of room temperature ionic liquids and its influence on a Diels-Alder reaction. In: Rogers RD, Seddon KR (eds) Ionic liquids as green solvents: progress and prospects. American Chemical Society, Washington, pp 289–299
145. Forsyth SA, MacFarlane DR, Thomson RJ, von Itzstein M (2002) Chem Commun 714–715
146. MacFarlane DR, Pringle MJ, Johansson KM, Forsyth SA, Forsyth M (2006) Chem Commun 1905–1917
147. Ingold CK (1969) Structure and mechanism in organic chemistry, 2nd edn. Cornell University Press, Ithaca
148. Hughes DE, Ingold CK (1935) J Chem Soc 244–251
149. Lancaster NL, Welton T, Young GB (2001) J Chem Soc Perkin Trans 2 2267–2270
150. Lancaster NL, Salter PA, Welton T, Young GB (2002) J Org Chem 67:8855–8861
151. Lancaster LN, Welton T (2004) J Org Chem 69:5986–5992
152. Crowhurst L, Falcone R, Lancaster NL, Llopis-Mestre V, Welton T (2006) J Org Chem 71:8847–8853
153. Crowhurst L, Lancaster NL, Pérez-Arlandis JM, Welton T (2004) J Am Chem Soc 126:11549–11555
154. Newington I, Pérez-Arlandis JM, Welton T (2007) Org Lett 9:5247–5250
155. Bini R, Chiappe C, Marmugi E, Pieraccini D (2006) Chem Commun 897–899
156. Daguenet C, Dyson PJ (2006) Organometallics 25:5811–5816
157. Carmichael AJ, Earle MJ, Holbrey JD, McCormac PB, Seddon KR (1999) Org Lett 7:997–1000
158. Herrmann WA, Böhm VPW (1999) J Organometal Chem 572:141–145
159. Calò V, Giannoccaro P, Nacci A, Monopoli A (2002) J Organometal Chem 645:152–157
160. Fraga-Dubreuil J, Bourahla K, Rahmouni M, Bazureau JP, Hamelin J (2002) Catal Commun 3:185–190
161. Gui JZ, Cong XH, Liu D, Zhang XT, Hu ZD, Sun ZL (2004) Catal Commun 5:473–477
162. Zhang ZF, Wu WZ, Han BX, Jiang T, Wang B, Liu ZM (2005) J Phys Chem B 109:16176–16179
163. Xing HB, Wang T, Zhou ZH, Dai YY (2005) Ind Eng Chem Res 44:4147–4150
164. Ganeshpure PA, Das J (2007) React Kin Catal Lett 92:69–74
165. Naydenov D, Bart H-J (2007) Chem Ing Tech 80:137–143
166. Li X, Eli W (2008) J Mol Catal A Chem 279:159–164
167. Ganeshpure PA, George G, Das J (2008) J Mol Catal A Chem 289:182–186
168. Zhu HP, Yang F, Tang J, He MY (2003) Green Chem 5:38–39
169. Joseph T, Sahoo S, Halligudi SB (2005) J Mol Catal A Chem 234:107–110

170. Zhang HB, Xu F, Zhou XH, Zhang GY, Wang CX (2007) Green Chem 9:1208–1211
171. Cole AC, Jensen JL, Ntai I, Tran KLT, Weaver KJ, Forbes DC, Davis JH (2002) J Am Chem Soc 124:5962–5963
172. Forbes DC, Weaver KJ (2004) J Mol Catal A Chem 214:129–132
173. Fang D, Zhou XL, Ye ZW, Liu ZL (2006) Ind Eng Chem Res 45:7982–7984
174. Jiang T, Chang YH, Zhao GY, Han BX, Yang GY (2004) Synth Commun 34:225–230
175. Izak P, Mateus NMM, Afonso CAM, Crespo JG (2005) Sep Purif Technol 41:141–145
176. Wells TP, Hallett JP, Williams CK, Welton T (2008) J Org Chem 73:5585–5588
177. Shi F, Xiong H, Gu Y, Guo S, Deng Y (2003) Chem Commun 1054–1055
178. Villagrán C, Banks CE, Deetlefs M, Driver G, Pitner WR, Compton RG, Hardacre C (2005) Chloride determination in ionic liquids. In: Rogers RD, Seddon KR (eds) Ionic liquids IIIb: fundamentals, progress, challenges, and opportunities – transformations and processes. American Chemical Society, Washington, pp 244–258
179. Bogel-Lukasik E, Domanska U (2004) Green Chem 6:299–303
180. Stark A, Behrend P, Braun O, Müller A, Ranke J, Ondruschka B, Jastorff B (2008) Green Chem 10:1152–1162
181. Wilkes S, Zaworotko MJ (1992) Chem Commun 965–967
182. Kirchner B (2009) Ionic liquids from theoretical investigations. Top Curr Chem. doi: 10.1007/128_2009_36

Top Curr Chem (2009) 290: 83–126
DOI: 10.1007/128_2008_33

Published online: 30 July 2009

Task Specific Ionic Liquids and Task Specific Onium Salts

Mathieu Pucheault and Michel Vaultier

Abstract Task specific ionic liquids (TSILs), or more generally task specific onium salts (TSOSs), can be defined as an association of a cation and anion, one at least being organic, to which has covalently been attached through a linker a function that confers the assembly a specific task. After presentation of the general concept of TSILs and TSOSs, the different methods of preparation of these compounds are developed. Regarding their applications in chemistry, TSILs and TSOSs can be used as soluble supports for reagents and catalysts in multiphasic reactions, enabling high activity and easy recovery of the supported agent. However, additionally, they can be used as soluble supports for organic synthesis in a similar manner to resins and offer several advantages over traditional methods.

Keywords Supported catalysts • Supported reagents • Supported synthesis • Task specific ionic liquids • Task specific onium salts

Contents

M. Pucheault (✉) and M. Vaultier (✉)
UMR CNRS 6510, 263 Avenue du Général Leclerc, Campus de Beaulieu
Université de Rennes 1, 35042 Rennes Cedex, France
e-mail: michel.vaultier@univ-rennes1.fr
e-mail: mathieu.pucheault@univ-rennes1.fr

Abbreviations

beim	Butylethylimidazolium
bmim	Butylmethylimidazolium
CIL	Chiral ionic liquid
emim	Ethylmethylimidazolium
IL	Ionic liquid
OS	Onium salt
OSSOS	Onium salt supported organic synthesis
RTIL	Room temperature ionic liquid
SILP	Supported ionic liquid phase
SWNT	Single wall nanotube
TSIL	Task specific ionic liquid
TSOS	Task specific onium salt

1 Generalities

1.1 Introduction

Sustainable chemistry unarguably is one of our main endeavors of the twenty first century. Chemists are at the cutting edge in this area, injecting lots of efforts and imagination to reduce dramatically energy, matter costs, wastes and risks. Compared to the reaction itself, purification and isolation steps are far more costly in terms of solvent wastes and energy expenses. Additionally, reagents, including transition metal complexes used as catalysts, can be rather difficult to withdraw extensively from the product, preventing its use for the final product in material science or drug industry. As a result, many strategies have been envisioned in the last decades to facilitate removal of reagents and catalysts, aiming for recycling. Multiphasic systems, based on organoaqueous [1] or perfluoroorganic mixtures, rely on confining reagents and or catalysts in one phase (water or fluorinated solvent) while keeping substrates and products in the organic phase.

Meanwhile, ionic liquids (ILs) recently appeared in the literature as a new class of solvents. They are considered as designer solvents owing to the quasi-infinite numbers of possible cations and anions combination that can be envisioned. Ethylammonium nitrate was first mentioned as being a liquid at room temperature in the early 1910s by Walden [2]. Almost a century later, such compounds have undergone a massive success which has built up only over the last two decades [3–9]. Indeed, they offer several advantages over traditional molecular solvents including negligible vapor pressure, properties modulation, easy access, etc. ILs are the association of a cation and an anion with at least one being organic. They belong to the vast family of onium salts and are simply particular cases having a low melting point which must be below 100 °C.

The demonstration that an ionic liquid could act both as the catalyst and solvent in a reaction was made by Wilkes and his group as early as 1986 [10] when they

reported that ethylmethylimidazolium chloroaluminate could function as an electrophilic catalyst of which the reactivity depends on the ratio $Cl^-/AlCl_3$. These working salts, later called task specific ionic liquids, are water sensitive and subsequent research focused mostly on creating water stable liquid salts [11] with tetrafluoroborate, hexafluorophosphate and bis(trifluoromethylsulfonyl)amide anions. In 1998, Davis reported the synthesis of ionic liquids with structurally rather large complex cations derived from the antifungal drug miconazole [12]. This definitely showed that it was possible to design salts that remain liquid at room temperature while incorporating functional groups in the cation structure. This discovery originated the introduction of the task specific ionic liquid concept in 2000 [13]. Since that time, a wide diversity of TSILs have appeared in the literature. In this review we will only consider TSILs where the ions, mostly cations, bear a covalently tethered functional group. Several excellent reviews dealing with other classes of TSILs like protic ionic liquids [5], ionic liquids with aminoacids carboxylate anions [14], anions functioning as bases [15, 16] or Lewis acids have recently been published and will not be included in this review.

1.2 Definitions and Properties

1.2.1 Task Specific Ionic Liquids and Task Specific Onium Salts

A task specific ionic liquid (TSIL) is defined as an ionic liquid which incorporates a covalently linked reactive functionality. This function confers to the assembly additional properties (chemical, optical, magnetic, physical or biological) which can then be employed to perform a specific task. If the melting points of these salts are above 100 °C they are called task specific onium salts (TSOSs) [17]. The latter constitutes a much larger family of compounds that include TSILs and all associations of cations and anions, regardless of their melting points.

The function can either be linked to the cation, the anion or both through a spacer generally used for minimizing interactions between the reactive part **F** and the ionic moiety (**+/–**). A modulation of the function's reactivity can be expected as a function of the length and structure of the linker (Fig. 1).

As an example, the 5-hydroxypentyltrimethylammonium bistriflimide $[N_{1115OH}][NTf_2]$ can be described as an ionic moiety (trimethylammonium = N_{111}) linked to a reactive function (a hydroxyl group) via a five carbons linker ($=_{5OH}$).

1.2.2 Binary Task Specific Ionic Liquids

In fact, the majority of functionalized onium salts are solids, very viscous or waxy at room temperature, which makes them difficult to use as such. This is even truer for salts bearing complex substituents. Since non-functional room temperature ionic liquids can usually easily dissolve other salts, they can be used as solvents to make low viscosity solutions of high melting point TSOSs, resulting in mixtures

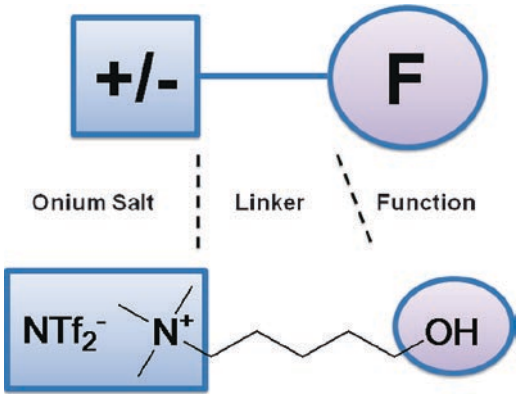

Fig. 1 General structure of a task specific ionic liquid with $[N_{1115OH}][NTf_2]$ as an example

which can be named binary task specific ionic liquids (BTSILs). These BTSILs have physical properties close to the RTILs matrixes properties to which has been added the capacity to behave as a reagent or a catalyst in some reaction or process. The viscosity of the reaction medium can then be adjusted as a function of the concentration of the added functional salt [18].

1.2.3 Properties

The introduction of functional groups on cations and (or) anions of ionic liquids allows for marked changes of the physicochemical properties and imparts a particular reactivity pattern to the ionic liquid. TSILs usually display negligible vapor pressure, a physical property close to analogous non-functionalized ILs. Other physicochemical properties, such as solubility in molecular solvents or thermal stability, and chemical properties, such as complexation ability for example and reactivity, largely depend on the nature of the functional group as well [19].

We believe that the arbitrary 100 °C limit fixed for onium salts to be called ionic liquids introduces unnecessary limitations to what has to be considered as an ionic liquid. The distinction between RTILs including solutions of OSs in RTILs and OSs which melting points are above room temperature is far more relevant and easier to handle. Anyway, TSILs are undeniably TSOSs and as a consequence the onium salts generic terminology will be applied next.

1.3 Synthesis

The synthesis of TSOSs is analogous to non-functionalized ILs. Indeed, the same key steps can be applied depending on the nature of the cation and the anion. Quaternisation of tertiary amines, phosphines and sulfides with a functionalized alkyl halide affords the desired functionalized ammonium, phosphonium and sulfonium halides in usually

good yields. These salts can be further modified by ion metathesis, anion exchange with acids or ion exchange resins. In the following we will focus mainly on the synthesis of TSOSs whose cations are centered on nitrogen (ammonium, pyridinium, imidazolium, etc.) as phosphonium and sulfonium based OSs are more scarcely used than their nitrogen analogs due to their higher melting points or chemical reactivity respectively. Additionally, protonation of alkyl amines by acids with non-coordinating counter anions lead to salts which often meet the OSs criteria. Mainly used as Brönsted acids catalysts, they consequently lose their ionic nature through the acid-base equilibrium during the reaction and don't remain TSOSs [5].

1.3.1 Alcohol Derived OSs

The general approach for the synthesis of alcohol derived ionic liquids relies on a quaternarisation of a tertiary amine (trialkylamine, pyridine or 1-alkylimidazole) using hydroxyalkyl halides such as 3-choropropan-1-ol in acetonitrile [20]. Using an excess of amine, the reaction affords ammonium halides in good yields (>90%). Depending on needs, halides can then be exchanged using acids (HBF_4, HPF_6) or metal salts ($LiNTf_2$) (Fig. 2 and Table 1).

In the case of trimethylammonium cations, products are obtained as solid except for the bistriflimide salts. In contrast, pyridinium and methylimidazolium salts usually have low melting points. In all, physical properties can easily be modulated by modifying the cation, the anion and the linker length [20].

Alternatively, methylsulfate and triflate salts can be obtained using dimethylsulfate and methyltriflate as methylating agents. Methylsulfates are highly soluble in water, and easily perform ion metathesis with an anion such as bistriflimide in that solvent. Additionally, monitoring of quaternarisation and exchange reaction can be easily done by ^1H NMR. This method can also provide an efficient way to prepare halide free TSOS (Fig. 3).

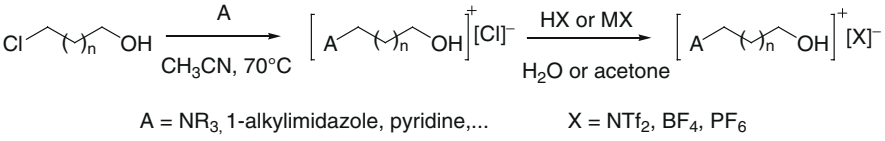

Fig. 2 Synthesis of hydroxyl containing OSs using hydroxyalkyl halides

Table 1 Hydroxyl derived nitrogen based onium salts

A	NMe_3																
n	0			1				2		4		8	1		1		
X	NTf_2	PF_6	BF_4	Cl	NTf_2	PF_6	BF_4	Cl	NTf_2	Cl	NTf_2	Br	Cl	NTf_2	Cl	NTf_2	
Yield (%)	90	83	83	91	94	80	86	92	93	95	93	95	89	98	80	98	

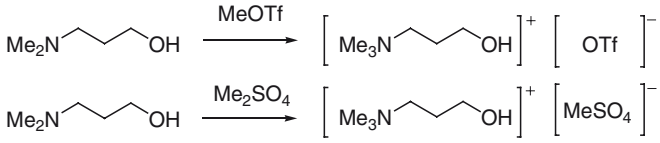

Fig. 3 Synthesis of hydroxyl containing OS by direct quaternatisation of aminoalcohol

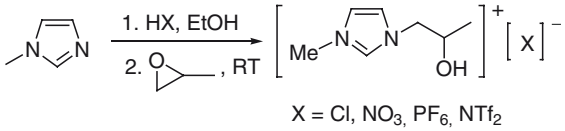

Fig. 4 Synthesis of hydroxyl containing OS by epoxide opening

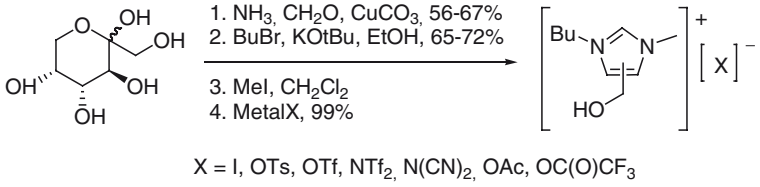

Fig. 5 Synthesis of hydroxyl containing OS from saccharides

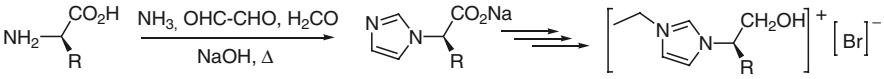

Fig. 6 Synthesis of hydroxyl containing OS from amino acids

Several other methodologies have been employed for the synthesis of hydroxylated TSOSs. Ring opening of propylene oxide by conjugated acid of amine such as methyl imidazole provides 2-hydroxypropylmethylimidazolium salts in excellent yields bearing a counter anion resulting from the acid used for obtaining the methylimidazolium in the first step [21] (Fig. 4).

Additionally, starting from naturally occurring fructose, Dickenson developed a method allowing for preparation of hydroxymethyl-substituted bmim by alkylation of hydoxymethylbutylimidazole prepared following previously reported methods. These products can be obtained in four steps from renewable sources with moderate yields [22] (Fig. 5).

Coming from natural sources as well, some TSOSs can be obtained directly from aminoacids. In this sequence, condensation with ammonia, glyoxal and formaldehyde under basic conditions affords the corresponding imidazole bearing a chiral center in α-position to the nitrogen. An esterification-reduction sequence followed by alkylation of the resulting hydroxyl substituted imidazole leads to the corresponding TSOS [23] (Fig. 6).

One synthesis approach towards γ-hydroxylated ionic liquids is a Michael-type addition of a protonated ammonium salt to a α, *β*-unsaturated carbonyl compound such as methylvinyl ketone yielding an oxobutyl functionalized cation. Intrinsically unstable due to retro-Michael reaction, this OS could however be transformed by a heterogeneous catalyzed hydrogenation reaction yielding a hydroxyl functionalized TSIL [24] (Fig. 7).

Interestingly, Wasserscheid et al. have developed an efficient method to prepare TSOS derived from alkaloids such as ephedrine or amino alcohols such as valinol. In both cases, TSOS were obtained on the kilogram scale using a three step procedure (Leuckart–Wallach reaction followed by alkylation with Me_2SO_4 and anion metathesis) [25] (Fig. 8).

Some water solubility can be conferred to commonly water immiscible hexafluorophosphate salts by appending some oligomers of ethylene glycol to the imidazolium cation [26, 27]. Its miscibility with water could be modulated by using different chain length (Fig. 9).

1.3.2 Halogen Derived OSs

Similarly, halogen derived TSOSs can be prepared from dihalogenoalkanes. Bisammonium salts can then be obtained in addition to the monosubstitution product. When performed in THF under anhydrous conditions, however, intermediate monosalts precipitate out and consequently fail to react with a second amine molecule [20] (Fig. 10).

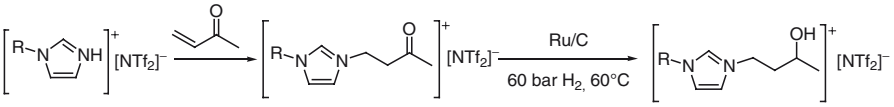

Fig. 7 Synthesis of hydroxyl containing OS by Michael addition-reduction

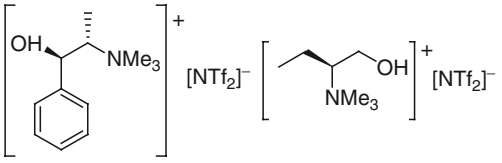

Fig. 8 OSs derived from alkaloids

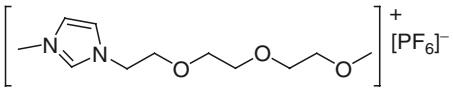

Fig. 9 A water soluble hexafluorophosphate salt

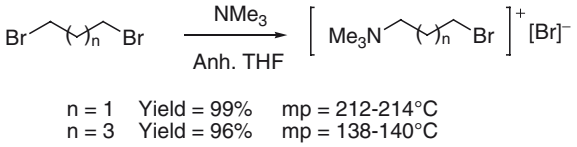

Fig. 10 Synthesis of bromine containing OS using dibromoalkanes

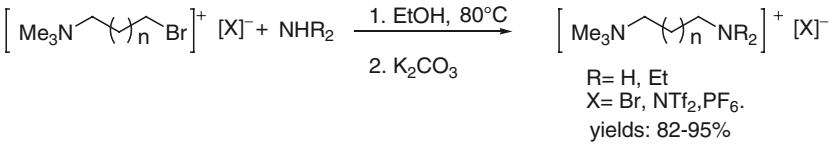

Fig. 11 Synthesis of amino-substituted OSs from halide functionalized salts

Anion metathesis steps are identical to those described above and a large variety of halide derived TSOSs can be obtained this way.

Alternatively, methylation of halogenoalkyldialkylamines with dimethylsulfate efficiently leads to the formation of halogenoalkyldialkylmethylammonium methylsulfates.

1.3.3 Amine Derived OSs

Amine derived TSOSs can be prepared by reaction of ammonia on previously prepared bromide derived onium salts in ethanol followed by deprotonation using potassium carbonate [20]. Another method relies on performing the quaternarisation of the trisubstituted amine by an ammonium-functionalized alkylhalide. Similarly, after reaction, the amine function is obtained by deprotonation using the same base [28]. Secondary and tertiary amines can been prepared from the corresponding halide derivatives by nucleophilic substitution using the relevant amine. Eventually, these amines can further be functionalized. Trisubstituted amines have been used as supported bases and ligand (see Sect. 2) (Fig. 11).

Davis recently reported triflimide salts derived from classical Girard's reagents which are hydrazine derived onium salts [29].

1.3.4 Complex Function Derived OSs

All other TSOS are generally obtained from halogen, alcohol or amine derived onium salts. However, purifications of salt mixtures are often tricky and preparation methods often need to be carefully optimized. In some cases, when compatible with other functional group, quaternarisation can be performed at a later stage in the process.

As examples, classical and efficient ways to obtain in few steps more complex TSOSs with various functions are detailed below. Often used as a quick way to

increase the complexity of a molecule, the ester linkage can be obtained using direct esterification with the corresponding acyl chloride or using coupling agents such as DCC and DMAP. For example, acryloyl chloride reacts smoothly with hydroxyl derived onium salts to afford acrylates in good yields. In this case, potassium carbonate was found to be optimal to trap released HCl [20] (Table 2):

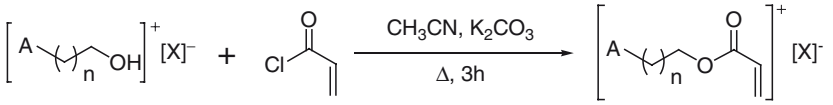

Table 2 Synthesis of OS supported acrylates

A	NMe_3							PBu_3	Pyridine	MeIm	
n	1			2		3	5	2	2	2	1
X	NTf_2	NTf_2	Br	BF_4	PF_6	NTf_2	NTf_2	NTf_2	NTf_2	NTf_2	PF_6
Yield(%)	90	98	98	93	90	77	78	77	80	85	98

For benzoic esters, coupling between the corresponding benzoic acid and the alcohol using DCC and DMAP as coupling agents turned out to be optimal. Dicyclohexylurea formed during reaction as a by-product can be removed after anion metathesis. Following this procedure, supported aryl iodides have been prepared and isolated in good yields under pure form after simple recrystallization (Table 3):

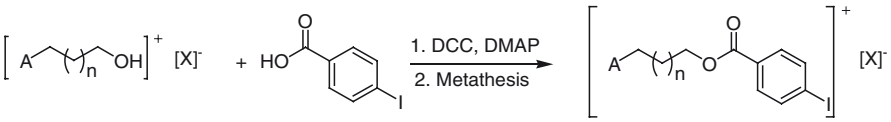

Table 3 Synthesis of OS supported iodobenzoic esters

A	NMe_3		MeIm		NMe_3			
N	0		0		1			4
X	Cl	BF_4	Br	BF_4	Cl	BF_4	NTf_2	BF_4
Yield%	93	90	92	85	95	83	95	87

Similarly, more complex acids can be used [30] and even amino protected amino-acids can be directly attached to an hydroxyl derived onium salt [31] (Fig. 12)

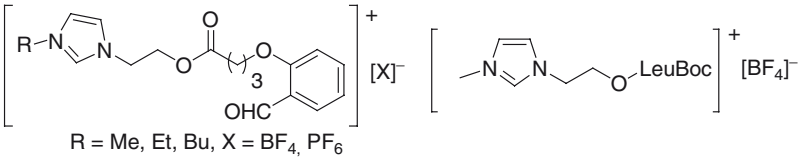

Fig. 12 Supported aldehyde and supported aminoacid prepared from OH derived OS

Finally, ether linkage can also be obtained from the corresponding halides. In that case, classical Williamson alkylation proceeds smoothly and can afford more complex TSOSs bearing benzaldehyde moieties [32] or benzylic alcohol [33] (Fig. 13).

A recent very flexible approach for the preparation of TSOS has been published by Liebscher [34]. It relies on a two step procedure with one so-called "click chemistry" step, which is a regioselective copper catalyzed [3 + 2] Huisgen cycloaddition between an azide and a terminal alkyne, followed by quaternarisation of resulting triazoles. Both reagents can be functionalized prior to cyclisation and furthermore such triazolium synthesis can tolerate a large variety of substituents owing to its chemoselectivity (Fig. 14).

If most work has been done using functionalized cations, anions can also be functionalized for specific applications and historically have probably been developed even before the concept of TSOS has been formally described. For example, *m*-TPPTS and *m*-TPPTC [35] are respectively sulfonate- and carboxylate-derived triphenylphosphine that have long been used as ligands for transition metal catalysis in organoaqueous systems. However, these ligands could also be seen as phosphine derived onium salts with functional anions [36]. Sulfonates are another example; long chain acrylate derived sulfonates [37] have been used as monomers for polymerization, but these molecules can also been described as TSOSs with a functional anion bearing an acrylate moiety conferring a new functionality to the assembly. Examples of functional anions and uses as TSOSs for lubricant of nanoparticle stabilizers have been recently reviewed [19].

Additionally, TSOSs can bear multiple functionalities both on cation and anion, and the function can be identical or different enabling dual use of single molecules. For example, using alkene derived methylimidazolium in combination with nitrile derived trifluoroborate, Dyson's group managed to prepare low melting point (−89 °C) and low viscosity (25 cP at 20 °C) dually functionalized ionic liquids [38]. Alternatively, one ion can be multiply functionalized. Overall, possibilities are almost infinite and strongly due to TSOSs synthesis flexibility.

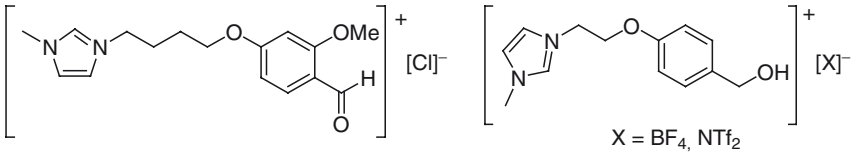

Fig. 13 Aldehyde and benzyl alcohol derived OS with ether linkage

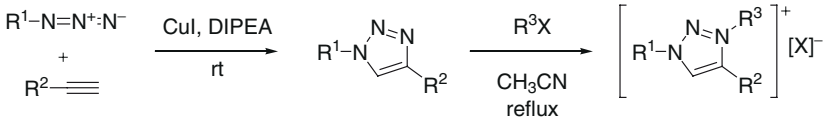

Fig. 14 [3 + 2]Cycloaddition-quaternisation sequence for preparation of triazolium salts

2 Applications

TSOSs can be described as normally functionalized molecules bearing an ionic appendix to which a specific function has been grafted via a linker. The molecule properties are obviously a combination of properties of the onium salt and the function properties. These molecules can be used in many applications but when it comes to chemistry they mainly serve in confining a molecule in the ionic liquid phase. Whether TSOSs are used under pure form or in solution in an RTIL matrix, the general principle remains identical: the goal is using the ionic moiety as an anchor point to facilitate the separation. Using only simple operations such as decantation, precipitation and filtration, final molecules can be easily recovered under analytically pure form.

Starting from this unique general principle, applications appeared to be numerous. TSOSs can be used as trapping agents, supported reagents, lubricants, stabilizers, electrolytes, supported catalysts, phase transfer catalysts, soluble resin analog for supported synthesis and more [39–41]. TSOS's tasks are not limited to chemical functions and one of the first TSOSs actually bears miconazole (antifungal) as a side chain [12].

Finally, TSOSs can also be used directly as solvents, and applications of those for which the appended entity has a chemical effect on the outcome of the reaction will be explained in more detail during the next sections. On the other hand, some are used as sole solvent and have no effects besides traditional solvent effects. This is the case of chiral ionic liquids (CILs) which have been used extensively as chiral solvents in the hope of transferring the chiral information to the reaction product. CILs could eventually be seen as TSILs where the task would be to induce chirality, despite some promising results, detailing all their features would unnecessarily lengthen this review as other authors skillfully already did [42, 43].

TSOSs offer several advantages over traditional immobilization approaches. In short, TSOSs have low molecular weight, highly tunable properties, high thermal and chemical stability; they can be used under pure form or in solution in ILs, in anhydrous molecular solvents or even in pure water at concentrations identical to those classically used in organic synthesis (0.1–1 M). Reactivity for example is highly enhanced compared to solid supports or even soluble polymers as reaction occurs in the whole three-dimensional space in contrast to a 2D-surfacic reactivity (resin, heterogeneous catalysts) or a pseudo diluted solution (PEG) where reactive sites are deeply confined in the polymeric network (Fig. 15).

TSOSs can be used in all different compartiments of reaction conditions: as solvent replacing regular volatile molecular solvents (see other articles), as reagents allowing for easy workup and recovery (supported reagents and catalysts) and finally as substrate (onium salt supported organic synthesis) (Fig. 16).

The general concept of onium salt supported reagents and catalysts is rather similar to all multiphasic systems, where one reagent (catalyst) is retained in one phase whilst substrates and forthcoming products remain in another. In our case, the OSs supported reagents have an almost exclusive affinity for the IL phase, and

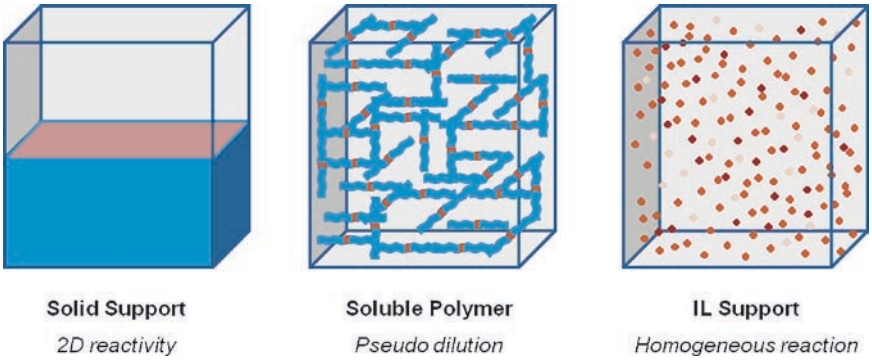

Fig. 15 Comparison between immobilizing techniques

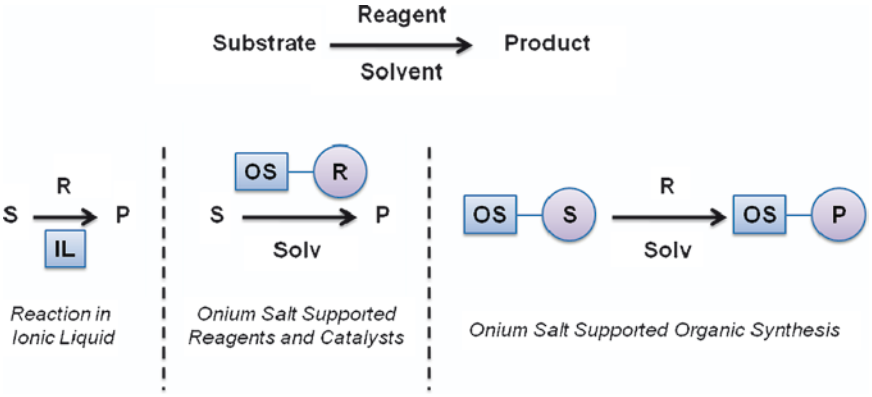

Fig. 16 Different uses of onium salts leading to different concept

none for apolar solvents such as alkanes, toluene or dialkylether. As such, after the reaction, the catalysts (or used reagent) can easily be separated from the organic phase, containing the products. Eventually, this IL phase can be recycled and reused with another batch of reagents.

Another method used for recycling TSOSs consists in using the so-called supported ionic liquid phase (SILP) [44–49]. The general principle is using an OS with a trialkoxysilane moiety that can be grafted covalently to a particle of silica. The particle, now coated with onium salt, has a special affinity for other onium salts, especially ILs. ILs can therefore get immobilized on a solid particle and subsequently be used for immobilizing other reagents (transition metal complexes, proline, etc.). This method has recently been reviewed and employs mostly non-functional ILs, so it won't be explained in more detail [44–49] (Fig. 17).

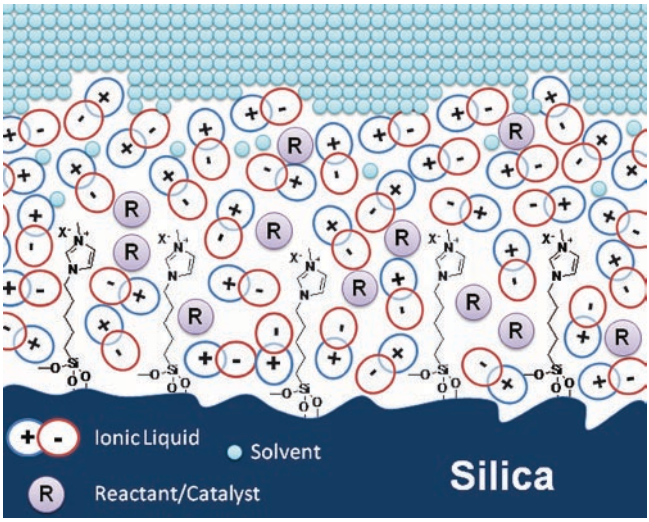

Fig. 17 General concept of supported ionic liquid phase (SILP)

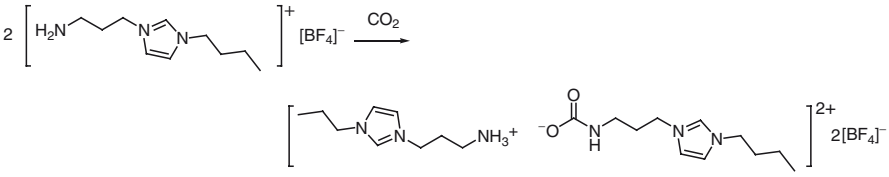

Fig. 18 CO_2 capture using a amine derived onium salt

2.1 Supported Reagents

One of the first applications of TSOSs was reported in 2002. Davis and his team have shown that an amine-derived imidazolium salt can capture carbon dioxide by forming a ammonium carbamate [28]. Primary amine functionalized imidazolium salts have also been used for facilitating CO_2 transport through a supported liquid membrane showing high selectivity and high stability for CH_4/CO_2 separation [50] (Fig. 18).

However, in addition to gas, several TSOSs have been designed to capture other species, in particular heavy metal cations. As water contamination by heavy metal ions appears of much concern, the attractiveness of TSOSs was evaluated towards application in toxic cation extraction. Numerous TSOS have been designed for extracting Hg^{2+}or Cd^{2+}. Indeed, imidazolium cation bearing urea, thiourea or thioether moieties can be used for coordinating with high affinity heavy metal ions. Used in an IL/water system, the metal distribution was increased by several order

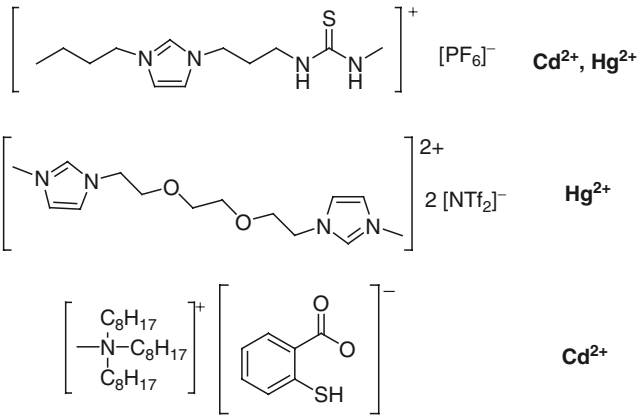

Fig. 19 TSOSs used for complexing heavy metal cations

of magnitude (distribution up to 360) whether they were used as pure compound or in solution in a non-functional matrix such as [bmim][PF_6] [51, 52]. Additionally by appending a diethyleneglycol link between two imidazolium salts it is possible to enhance the Hg(II) uptake in an IL solution [53]. Finally, one of the few TSILs bearing a functional anion (i.e. thiosalicylate) has been shown to bind selectively to Cd^{2+} as compared to other cation commonly contained in natural waters such as Na^+, K^+ or Ca^{2+} [54] (Fig. 19).

Water pollution is not the only problem that can be tackled using TSILs' possibilities. For example, separating actinides and lanthanides from nuclear wastes is one challenging problem and fission products such as $^{137}Cs^+$ or $^{90}Sr^{2+}$ are of great importance as well. Several TSOSs have been designed to induce coordination and extraction selectively of those species in the IL phase. Aza-crown ether fragments for example can be appended on the side arm of an imidazolium salt [55]. Resulting TSOSs as a 0.1 M solution in [bmim][BF_4] can improve the distribution coefficient up to 400. However, due to ionic repulsion between the imidazolium and the metal cation caused by a short linker (three carbons), the coordination is less efficient than when employing aza-crown ethers alone. It is also possible to extract uranyl cations such as UO_2+ from nitric acid solution using phosphorus derived onium salts such as phosphonates, phosphates or phosphoramides [56]. Similarly, aminophenol derived imidazolium salts have been used to extract americium in pure or diluted form. Furthermore, americium could easily be recovered from the IL phase by further treatment with nitric acid [57] (Fig. 20).

Onium salts can also be used to support reagents that would transform a substrate. After reaction the IL phase can be recovered and the reagent regenerated for being reused in another cycle. For example, carboxylic acids have been supported on onium halides. Simply synthesized by quaternarisation of methylimidazole followed by acid hydrolysis, this compound can react with epoxides to afford halohydrines in 76–95% yields [58]. Additionally, an OS supported version of TEMPO has been used in oxidation of alcohol into ketone [59] (Fig. 21).

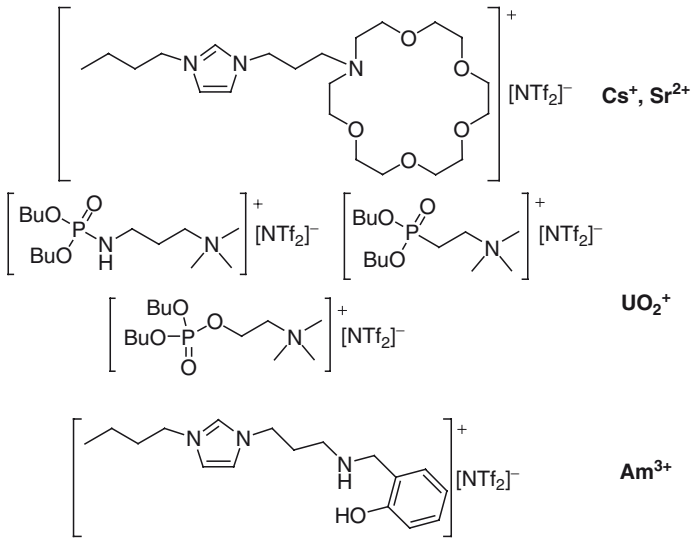

Fig. 20 Different TSOS used for extraction of fission products

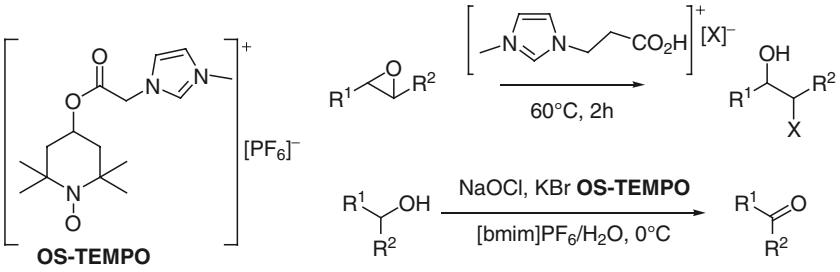

Fig. 21 Supported TEMPO and carboxylic acid used as reagents for oxidation of alcohol and epoxide ring opening respectively

2.2 Supported Catalysts

2.2.1 Acid/Base Catalysts

The onium salt supporting strategy is also applicable to reagents that can be used in substoichiometric quantities and recovered without alteration after reaction, i.e. catalysts. Naturally, the first acids that were tested in this sense were Brönsted acids and bases. The discussion here will therefore be limited to bases and acids covalently appended to an onium salt.

Indeed, a sulfonic acid functionalized onium salt can be prepared in few steps. Probably the best strategy relied on opening the corresponding sultone with the relevant amine. The internal salt could then be acidified using HBF_4 or HPF_6 (Fig. 22).

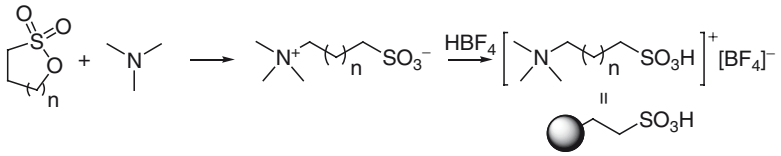

Fig. 22 Synthesis of supported sulfonic acid

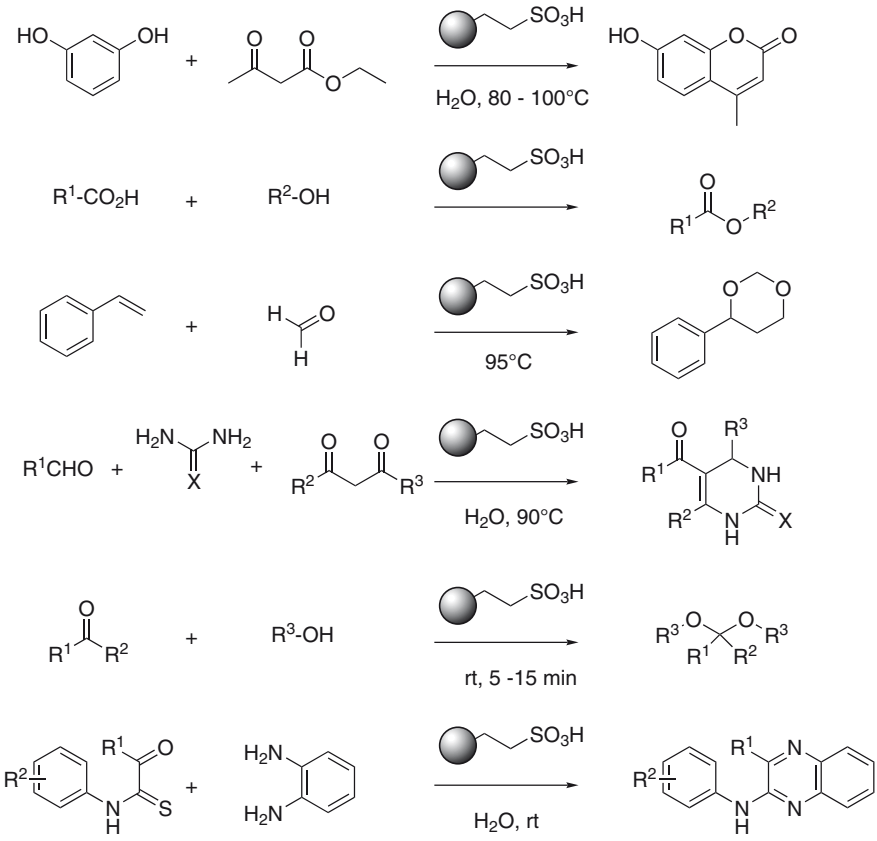

Fig. 23 Various applications for supported sulfonic acid catalysis

It has subsequently been used in a wide diversity of reactions including Pechman reaction in water [60], esterification [61], Prins reaction [62], Biginelli condensation [63], protection of carbonyl compounds [64], or quinoxaline derivatives synthesis [65] (Fig. 23).

Another application of these reagents is the synthesis of porphyrines. By playing on the difference of concentration of both organic and IL phase, reaction occurs smoothly at the interface affording 41% of the tetraarylporphyrine **TArP** with only 8% of the so-called NC tetraarylporphyrine **NC-TArP** (which is similar to the

selectivity obtained with the classical Lindsey's method). Additionally, the TSOS can be recycled up to ten times without any loss in activity [66]. The sulfonyl chloride analog hydrolyzed in situ into the corresponding sulfonic acid could be used to promote Beckmann rearrangement. Using 20% of this compound, it is possible to obtain ε-caprolactam from cyclohexanone by simple extraction with water, owing to the low hydrosolubility of the TSOS [67] (Fig. 24).

Apart from ammonium derived hydroxide, few onium salts have been used as supported bases. However, an analog of Hunig's base was prepared and employed as a catalyst in Knoevenagel condensations [68]. Increase in the linker length was found critical to observe a good activity, as cation effect on amine basicity can be detrimental for short alkyl chains. Finally, using a biphasic liquid–liquid mixture, no significant decrease in activity has been noticed after five cycles (Fig. 25).

2.2.2 Organometallic Catalysts

Hydroformylation of Alk-1-Ene

Of particular importance for industry is the hydroformylation of alk-1-enes and one of the best processes developed so far for C_2–C_5 olefins employs a biphasic system in combination with a hydrosoluble rhodium complex bearing TPPTS as ligand [69–71]. From this statement, Wasserscheid et al. investigated in the early 2000s the possibility of using ILs supported catalysts for this reaction [71–75], owing to the discovery by Chauvin that good linear/branched selectivities could be achieved

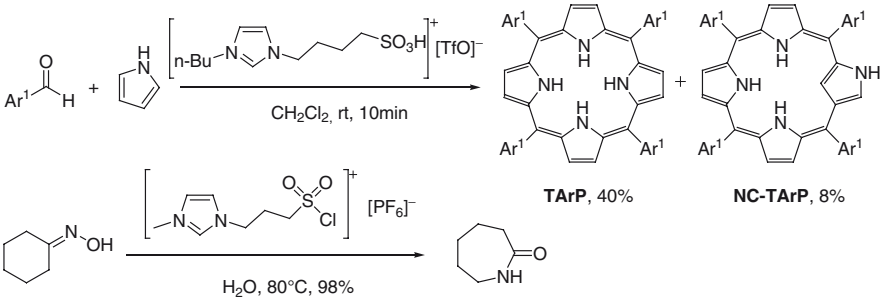

Fig. 24 Porphyrine synthesis and Beckmann rearrangement using sulfonyl containing OS

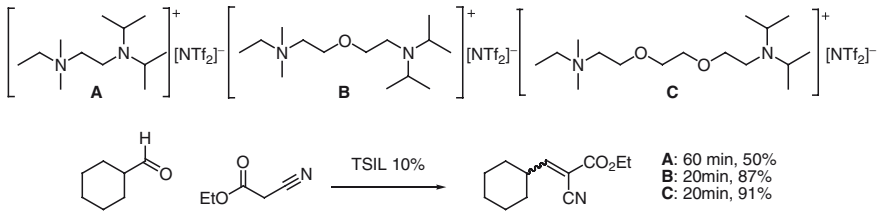

Fig. 25 Supported Hunig's Base used for Knoevenagel condensation

with PPh_3 as ligand using ILs as solvents [76]. For that matter, all the approaches relied on using onium salt derived phosphines, whether they had already been used for other applications or specially designed for hydroformylation.

A cobaltocenium salt (**L1**) bearing two phosphines, analogous to dppf, was used in association with $[Rh(CO)_2acac]$ in $[bmim][PF_6]$ [72]. This complex turned out to be a very active catalyst, enabling high selectivity for the *n*-product with no observable leaching from the IL phase. The onium salt moiety can be directly connected to the phosphorus center (**L2**) [73], showing high activity but poor selectivity. Alternatively, diphosphine (**L3**) with xanthenes backbone or phosphine bearing guanidinium salts showed interesting selectivities [75]. Other active phosphines (**L4**) were easily prepared from vinylimidazole by hydrophosphination followed by quaternarisation of the imidazole assuming the phosphorus atom has been properly protected from alkylation by reaction with sulfur [74]. Using the same approach, hydrophosphination of vinylpyridine followed by quaternarisation using Meerwein Salts provided a pyridinium supported diarylalkylphosphine (**L5**). This phosphine displayed good selectivities but poorer activities [77]. Finally, a bisimidazolium supported analog of xanthphos combined both high selectivity and activity (**L6**) [78] (Fig. 26 and Table 4).

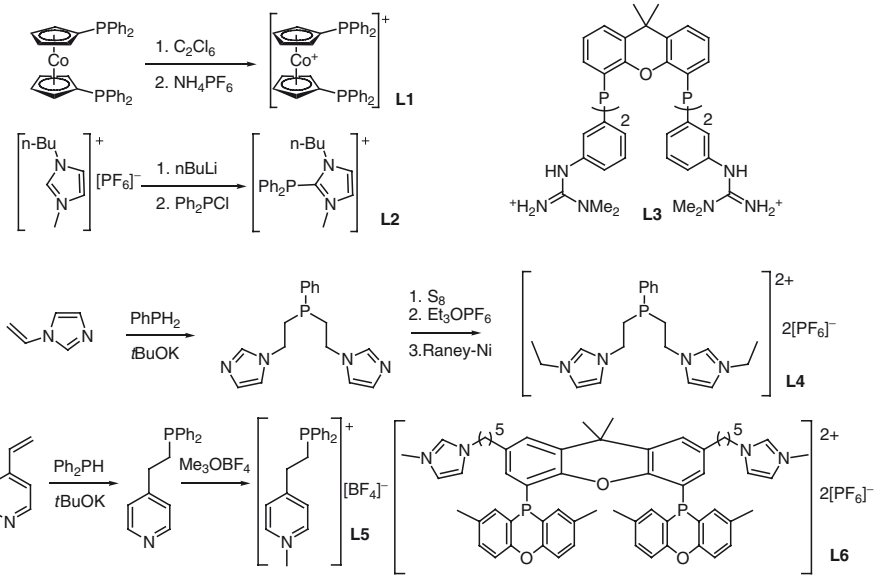

Fig. 26 OS supported ligands used for hydroformylation

Table 4 Selectivity and activity of catalysts in hydroformylation of alk-1-ene

Ligand	L1	L2	L3	L4	L5	L6
TOF (h^{-1})	810	552	52	32	240	317
l/b	16	1.1	21	2.8	2.6	49
References	[72]	[73]	[75]	[74]	[77]	[78]

Palladium Catalyzed Cross Coupling Reaction

Another large field of applications of supported phosphines is unsurprisingly palladium catalysis, highly compatible with ILs as solvents [79], and where most ligands used before 2000 were phosphorus based ligands. Water soluble ligands mimicking triphenylphosphine (anionic such as TPPTS or TPPTC, or cationic such as AmPHOS and GUAPHOS) [1] can eventually be seen as onium salt supported ligands, and be used as such in palladium catalyzed cross coupling reactions [80]. Imidazolium supported phosphonites (**L7**) associated with palladium chloride efficiently catalyzed reactions allowing for easy recovery of the catalyst. The OS supported palladium complex showed a decrease in activity only after the seventh run, which shows moderate leaching of palladium [81]. However, as phosphorus compounds are often prone to oxidation, nitrogen based ligands have become a much more attractive family of molecules for recycling. Imidazole (**L8**) [82], pyrazoyl (**L9**) [83], oxime (**L10** and **L11**) [84, 85] or simply nitrile [86] functionalized Onium Salts were designed, prepared and used in biphasic catalysis. Pyrazolyl-functionalized methylimidazolium (**L8**) were synthesized in a three step sequence, alkylation of the imidazole ring using NaH as a base followed by quaternarisation and ion metathesis [83]. Quasi-symmetrical imidazolium supported imidazole (**L9**) was prepared by successive alkylation of 2,2'-bisimidazole [82]. Oximes can be functionalized either on the aromatic ring (**L10**) [85] or directly on the oxygen of the oxime **L11** [84]. In all cases, the ligand turned out to be really active and could be recycled several times without loss in activity (Fig. 27).

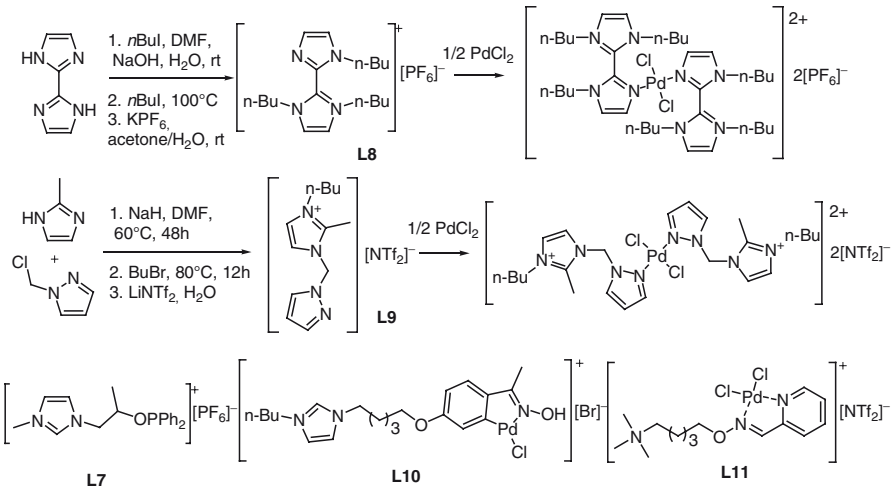

Fig. 27 Ligands and catalysts used for biphasic palladium catalyzed cross coupling

Ruthenium Catalyzed Olefin Metathesis

Olefin metathesis has undoubtedly become one major reaction in organic synthesis and is used in many total syntheses. However, despite its success, this reaction still suffers from requiring higher catalysts loading (1–20%) than other classical transition metal catalyzed reactions (10 ppm for Heck reactions, 0.01% for asymmetric hydrogenation). It is as a consequence of great importance to design a system that would be easily recoverable after reaction. Indeed, since 2003 several groups have been working on supporting (Hoveyda)–Grubbs ruthenium catalysts. An imidazolium supported analog of Hoveyda first generation's **HG 1** catalyst has for example been successfully prepared and used in RCM reactions performed in [bmim][PF_6] without loss of activity after ten cycles, where unsupported version of catalysts showed no activities after the third one. The imidazolium moiety can be grafted directly to the aromatic ring **Ru1** [87, 88] or by the mean of an ether linkage **Ru2** [89]. Analogously, second generation Hoveyda-Grubbs catalyst **HG 2** bearing a carbene ligand instead of the tricyclohexylphosphine have been prepared, one with the alkyl chain linker **Ru3** [90] the other one with the same ether linkage **Ru4** [91] (Fig. 28).

Hydrogenation

On the industrial scale hydrogenation is a transformation of great importance, but, due to the cost of catalysts and eventual chiral ligands, it is still in need of an efficient way to recover the catalysts. The onium salt supported strategy appeared appealing as hydrogenation can be performed with good enantioselectivities in IL solutions. Analogs of ruthenium catalysts developed for hydrogenation of ketones or β-ketoesters were synthesized bearing imidazolium or ammonium salts as side chains. Concerning Noyori's type catalysts prepared from [Ru(*p*-cymene)Cl]$_2$ and *N*-tosyldiphenylenediamine, the onium salts moiety can be attached on either the aromatic ring **Ru5** [92] or directly on the diamine **Ru6** [93]. In both cases, reduction of acetophenone proceeded smoothly providing expected product in high yield and ee. Simple *diam*-BINAP can also be used in association with Genet's precursor [Ru(η_3-2-methylallyl)$_2$(η_2-COD)] to afford a diphosphine ruthenium(II) dihalide **Ru7** [94]. Reduction of ethylacetoacetate using this catalyst afforded expected alcohol with good enantioselectivity albeit lower than under regular optimized conditions. Rhodium catalysts are known to give better selectivity for carbon carbon double bond reduction, especially in the case of dehydroaminoesters for which reduction products are highly desirable aminoacids. An imidazolium supported chiral analog of dppb was prepared and coordinated to a cationic rhodium complex **Rh1**. This catalyst turned out to be really efficient in enamide hydrogenation and used four cycles while keeping high enantioselectivities (>95%) [95]. Finally, palladium catalyst **Pd1** formed by using the same nitrile derived imidazolium as mentioned previously has been used as an IL soluble analog of $PdCl_2(CH_3CN)_2$, commonly used as homogeneous catalyst for hydrogenation of olefins [96]. Starting from cyclo-1,3-hexadiene, cyclohexene was obtained with 97% selectivity and TOF up to 237 h^{-1} (Fig. 29).

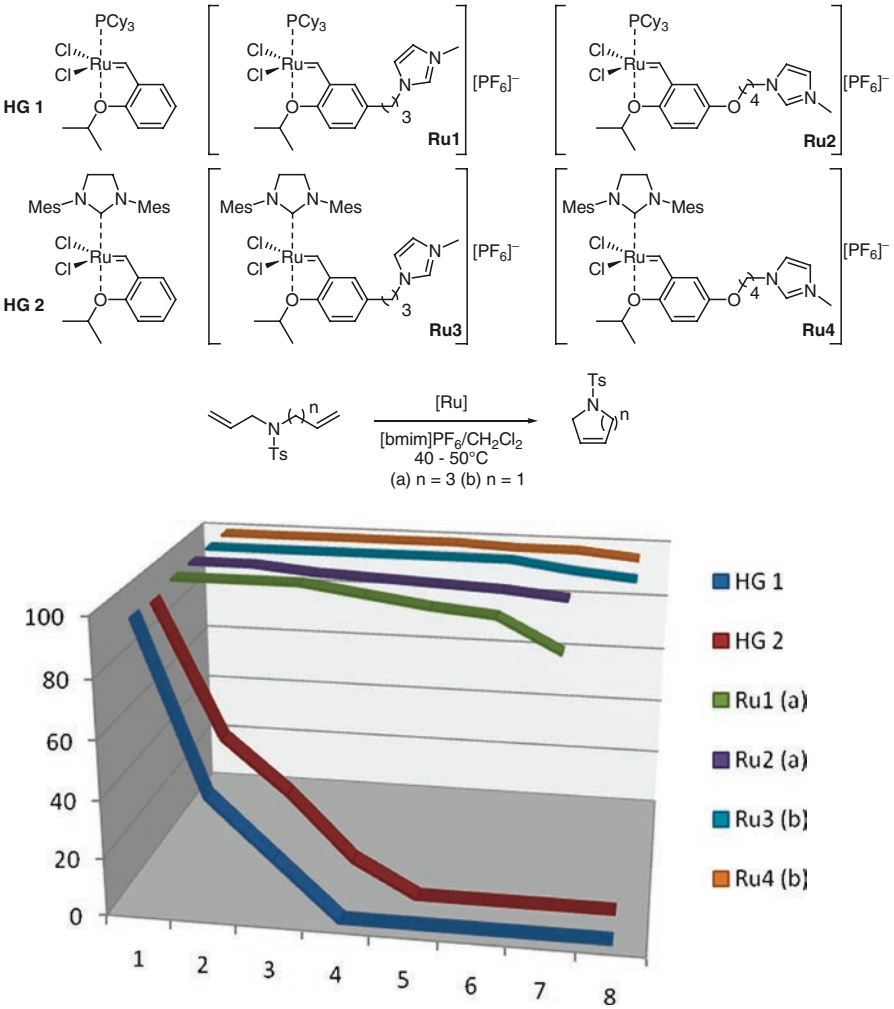

Fig. 28 OS supported Grubbs type catalysts and comparaison in recycling

Copper Catalyzed Reactions

Hardacre and Doherty described the synthesis and use of OSs supported bis(oxazolines) in various copper catalyzed reactions such as Diels–Alder reaction [97] and Mukaiyama–Aldol reactions [98]. Starting from mono methyl substituted box ligand, deprotonation followed by alkylation using an excess of dibromopentane provided the required alkyl halide for quaternarisation. After ion metathesis the imidazolium supported box ligand (**L12**) is isolated in a good 62% overall yield (Fig. 30).

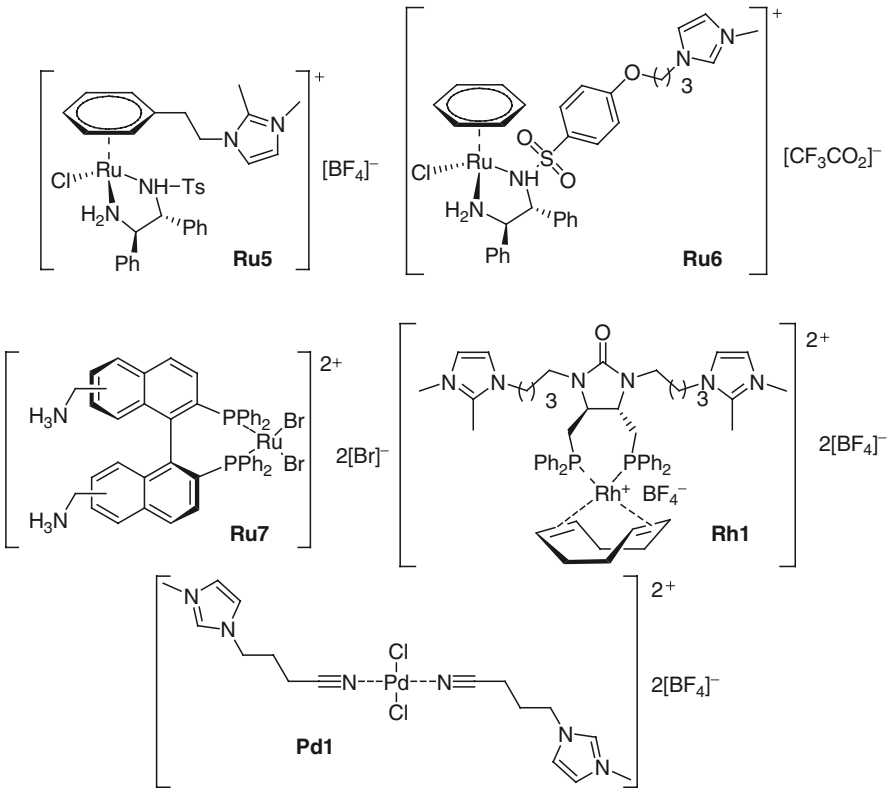

Fig. 29 Ruthenium, rhodium and palladium catalysts used for hydrogenation under biphasic conditions

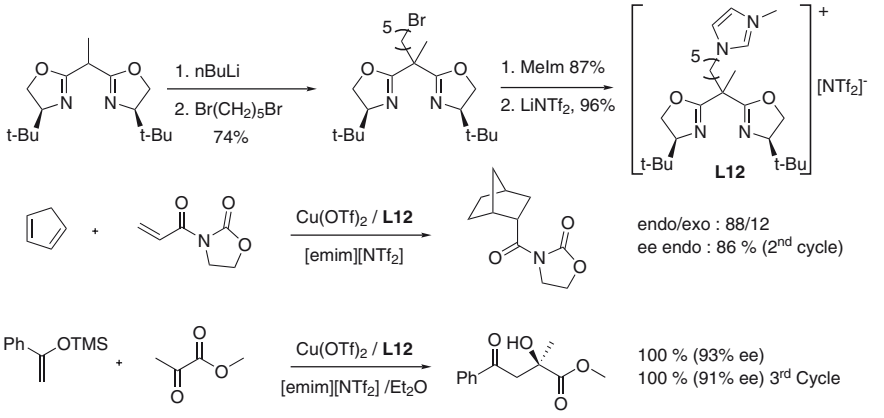

Fig. 30 OS supported box ligand: application to Diels Alder and Mukaiyama aldol reactions

Other ligands have been designed for copper catalyzed reactions. Bipyridines have been used for aerobic TEMPO mediated oxidation of alcohols into ketones. Namely, starting from 6,6'-dimethyl-2,2'-bipyridine, bromination of the methyl group followed by quaternarisation using methylimidazole provided the bisimidazolium salt. Ion metathesis using KPF_6 in acetone afforded the bis(hexafluorophosphate) (**L13**) [99]. Additionally, supported pyridine has been simply prepared by monoalkylation of bipyridine leading to **L14** which has been used as ligand in Ullmann type cross coupling for introducing perfluoroalkyl chain on aromatic rings [100] (Fig. 31).

Vanadyl Salen Complexes

Vanadyl salen complexes can be used to catalyze cyanosilylation of aldehydes. As a consequence, onium salt supported analogs of these active species have been prepared and compared to other method of immobilization. Unsurprisingly, the OS supported version was much more active (TOF 18 h^{-1}) than the solid supported version but afforded the product in lower enantiomeric excesses than the non-supported salen complex, most certainly due to the detrimental presence of chloride anion [101, 102] (Table 5):

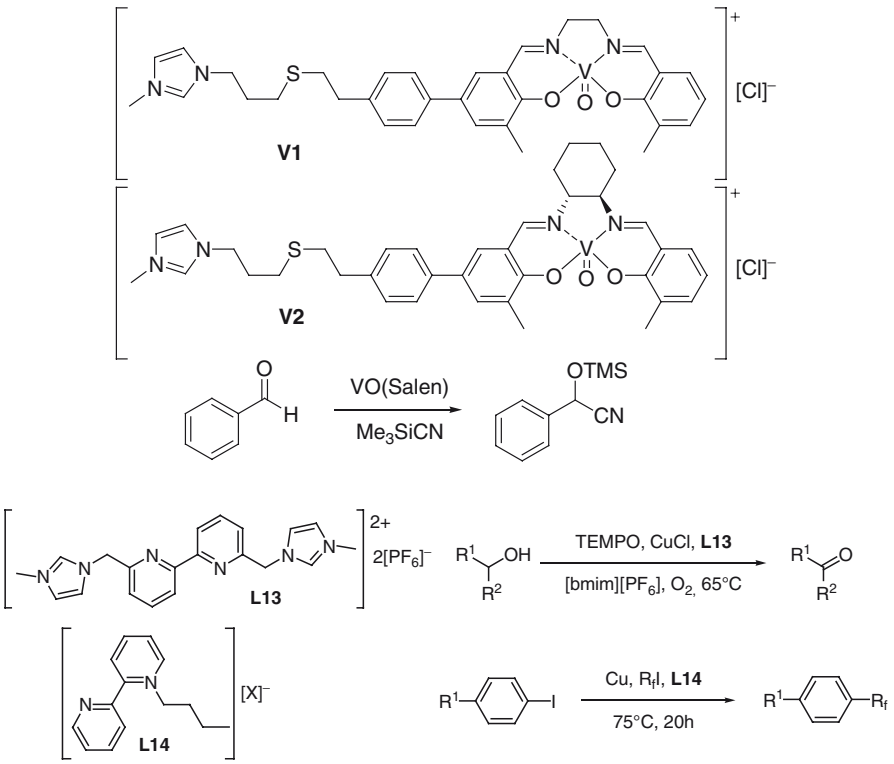

Fig. 31 Pyridine based OS supported ligand for copper catalysis

Table 5 Comparison of catalytic activities of various supporting methods

Catalyst	Conditions	Conv. (%)	TOF (h^{-1})	ee (%)
VOSalen	[beim]PF_6, rt	85	3.5	89
VOSalen on silica	$CHCl_3$, 0 °C	78	2.7	85
VOSalen on SWNT	$CHCl_3$, 0 °C	67	3.1	66
VOSalen on carbon	$CHCl_3$, 0 °C	81	3.7	48
VOSalen on OS (V2)	[beim]PF_6, rt	88	18.3	57

2.2.3 Organocatalysis

Apart from transition metal and acido basic catalysis, the field of organocatalysis has undergone a major development during the last decade due to the discovery of efficient systems [103–107]. As a consequence, several groups went naturally into trying to use supported analogs of the most popular catalysts such as proline. OS supported *N*-hydroxyphthalimide, for example, can be used as a catalyst for oxidation of alcohols in ILs such as [bmim][PF_6] and nitration of alkanes [108]. Proline catalysis has also been widely investigated and many chiral pyrolidines have been prepared, by modifying the carboxylic acid group into an ester [109], an amide [110], a triazole [111], imidazolium [112] or by grafting through the hydroxyl group of naturally occurring hydroxyproline either with short [109] or long [113] alkyl chains. All these catalysts were tested in aldol reaction or nitro Michael and, besides enabling recyclability, gave enantiomeric excesses often lower than regular proline. Finally, an imidazolium supported trialkylamine was used as a catalyst to promote hydrogenation of carbon dioxide into formic acid [114] (Fig. 32).

2.3 Onium Salts as Soluble Supports for Organic Synthesis

2.3.1 Pure TSILs, a New Class of Soluble Supports for Synthesis

Using ILs as support for organic synthesis was envisioned in the early 2000s in Rennes [39]. The general idea at this time was anchoring the substrate to an onium salt in order to facilitate workup by simple washes, decantation and filtration. Indeed, the first experiments were performed using neat TSILs; however, as mentioned previously, viscosity arose as an issue when structures became more complex. Microwave heating was often mandatory to achieve high conversion, even for reactions that could be performed under mild conditions in solution phase. Facing such difficulties, it was necessary to develop new alternatives allowing for broader scope of the concept. As a result, BTSIL [20] and onium salt supported organic synthesis (OSSOS) [18] concepts have been formalized and have extended the use of TSILs to all TSOSs in supported synthesis. (see Sect. 2.3.2 and 2.3.3).

Nonetheless some examples using neat TSIL turned out to be successful, such as the application of the Knoevenagel condensation on supported benzaldehyde [30]. Using piperidine as a catalyst under microwave heating conditions, olefins could be

obtained in the pure form after simple washes. The same aldehyde has been used in other transformations; 1,3-dipolar cycloaddition on the imine obtained by condensation with propylamine under microwave conditions [30] or condensation of thioacids on the same imine leading to thiazolidinone in variable yields [115] (Fig. 33).

It has been shown that supported acrylates could serve as partners in various reactions such as Diels Alder, Heck coupling followed by dihydroxylation of resulting

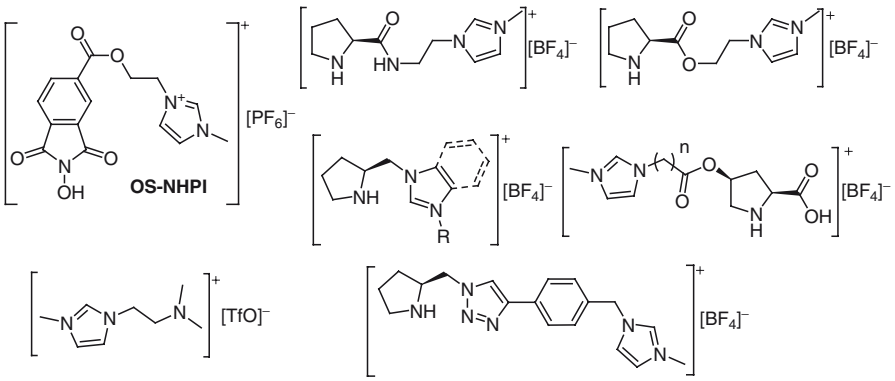

Fig. 32 OS supported organocatalysts: tertiary amine, *N*-hydroxy-phthalimide and chiral pyrolidines

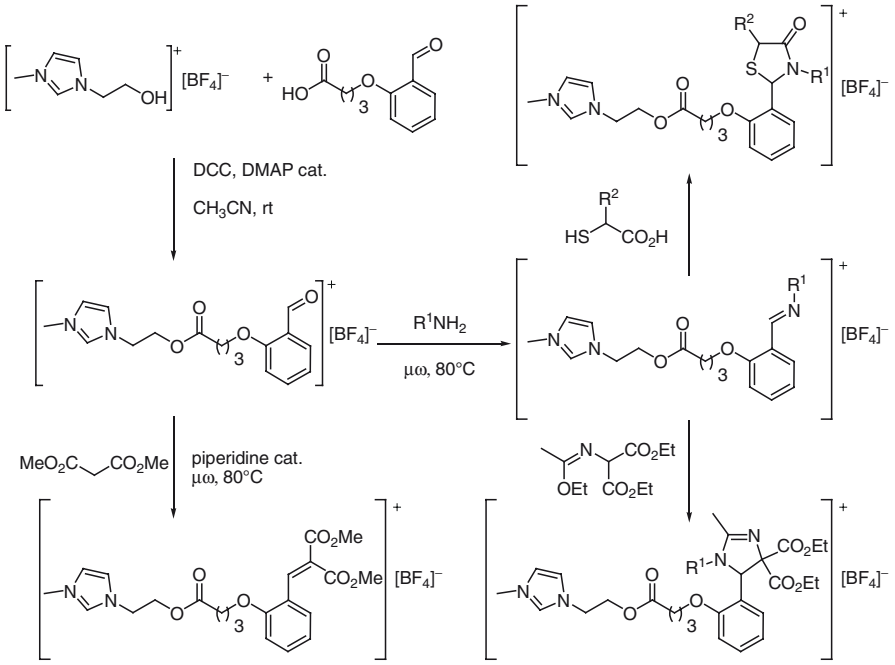

Fig. 33 OS supported synthesis of imidazolidine and Knoevenagel adducts using microwave

cinnamates or Michael addition [33]. Stetter reactions with electron poor aldehydes such as pyridine carboxaldehyde were also successful (Fig. 34).

By using this methodology, other scaffolds can be accessed in a few steps. Aminothiophene can be obtained in a two steps sequence from [mimC_{2OH}][BF_4] using a Gewald condensation as a key step [116, 117]. Nitrile is obtained by coupling the alcohol with cyanoacetic acid. Reaction with elemental sulfur and ketones or aldehydes afforded 2-aminothiophenes in good yields (70–91%). Other heteroaromatics were obtained by condensation of arylidenemalonitrile on supported acetoacetates under microwave conditions [118]. Supported acetoacetate can be obtained by reaction of the alcohol with ethylacetoacetate under microwave conditions or alternatively by reaction of hydroxyalkyltrimethylammonium salts with ketene dimer [119]. Finally, pyranes were released from the IL moiety with sodium ethoxide in ethanol and the resulting IL could be reused in another cycle of synthesis. Using the same acetoacetate in combination with ammonia, a dimedone and an aldehyde, the 4-component reaction affords hydroquinolines which eventually could be oxidized into quinolines by DDQ in CH_2Cl_2 before being cleaved from the support [120] (Fig. 35).

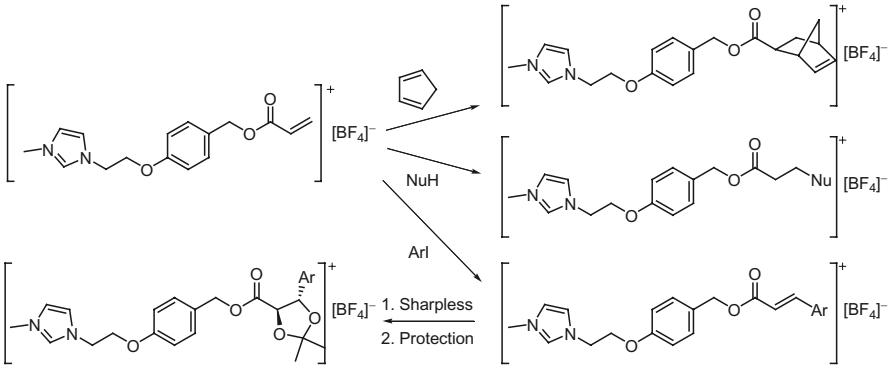

Fig. 34 Various reactions using OS supported acrylates

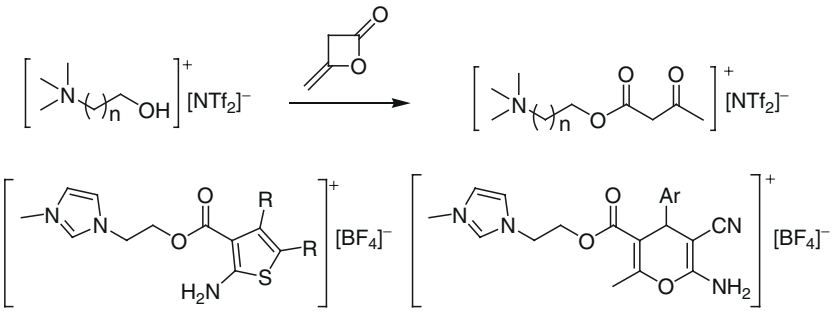

Fig. 35 OS supported synthesis of acetoacetate and heterocycles

2.3.2 Binary Task Specific Ionic Liquids

After proof of concept with various reactions including, Suzuki–Miyaura cross coupling [20], Heck Cross coupling [20], Diels Alder reaction [20], Baylis Hillman reaction [20] and Grieco's 3-MCR [20, 121], the principle was applied to the synthesis of an antithrombotic in a sole solution of [bmim][PF_6] [32] (Fig. 36).

After grafting of protected tyrosine through a reductive amination, the secondary amine was sulfonylated using phenylsulfonyl chloride. Deprotection of allyl group using palladium catalysis, followed by Williamson's alkylation of relevant alkyliodide, yielded the supported analog of tirofiban. After concomitant deprotection of the Boc and cleavage from the support, the tirofiban analog was extracted from the ionic liquid phase ([bmim][PF_6]) with water after neutralizing with triethylamine. Even if overall yield (11%) after five steps was not optimal, it represents the first multi-step synthesis of a bioactive compound using the BTSIL technology. Authors interestingly confirmed the advantages over traditional solid phase synthesis: "*An attractive feature of this ionic phase approach is that reactions can be monitored at all times using common techniques such as HPLC/MS*" [32]. In the same publication, they reported the synthesis of a small library of sulfonamides using the same support and the same sequence of reactions.

Recently, another library was prepared using BTSILs [122]. Starting from 2-hydroxyethylmethylimidazolium chloride ([mimC_{2OH}][Cl]) in solution in [bmim][PF_6], coupling using classical DCC/DMAP conditions with 4-formylbenzoic acid was followed the imine direct formation with various aromatic and aliphatic amines. After simple washing, the [bmim][PF_6] solution of supported imines was treated with a ketene generated in situ from the corresponding acylchloride in the

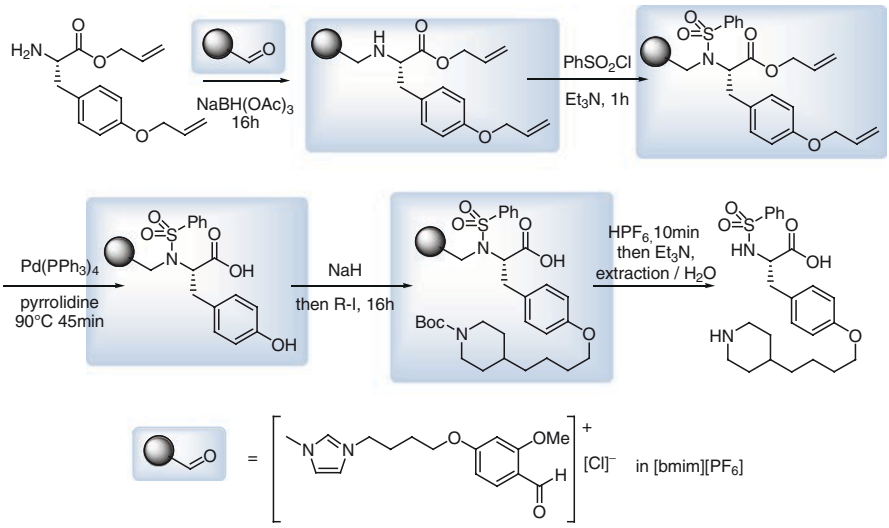

Fig. 36 BTSIL synthesis of an antithrombotic compound using [bmim][PF_6] as sole matrix

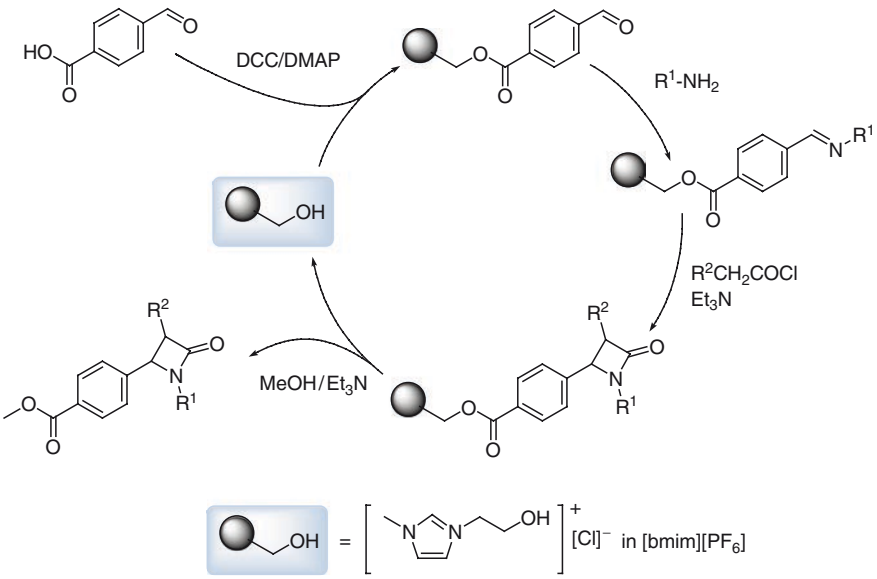

Fig. 37 BTSIL synthesis of β-lactams using a hydroxyl derived imidazolium dissolved in [bmim][PF_6]

presence of triethylamine. A variety of onium salt supported β-lactam was then obtained which could be cleaved using a 4/1 MeOH/Et_3N mixture. 21 methyl esters were subsequently isolated in 78–83% yields with 87–98% purity without any purification using chromatography [122] (Fig. 37).

Undoubtedly, orgametallic catalysis in ionic liquids has undergone a massive development in the last decade owing to the high propensity of ionic liquids to solubilize and stabilize transition metal complexes [6]. Eventually, they would form new complexes such as-heterocyclic carbene-metal species obtained by deprotonation at the 2 position on imidazolium salts [123]. Supporting the catalyst in an ionic liquid phase is one possibility (see above) but using supported olefins or halide could be equally envisioned. Consequently, palladium catalyzed reactions were evaluated in the BTSIL strategy. This coupling reaction is particularly well suited to ionic liquids physicochemical properties as it is favored by using polar solvent or in the presence of ammonium salts [124] which stabilize Pd complexes [125]. In the presence of 1% of [$Pd(OAc)_2$] as a catalyst and potassium carbonate as a base, supported olefin reacts efficiently at 80 °C with iodobenzene to afford OS supported cinnamates. Quantitative conversion were achieved in [tmba][NTf_2] and [emim][NTf_2] after 2 h although only 70% was observed in acetonitrile. Furthermore *E*/*Z* selectivity was highly superior in ionic liquids as only (*E*)-isomer is observed where 12% of the (*Z*)-compound was obtained in CH_3CN. Notably, supported acrylate is much more reactive than the corresponding methyl ester as unsupported acrylate underwent reaction with a poor 26% conversion under the same conditions in acetonitrile [18, 20, 126] (Fig. 38).

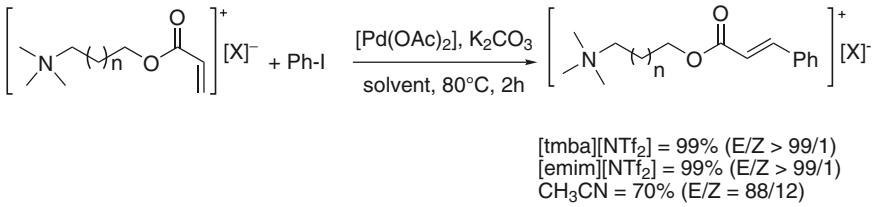

Fig. 38 Heck reaction using the BTSIL strategy

Similarly, OS supported iodide can be used with the same success. For example, using only 100 ppm of $Pd(OAc)_2$ as catalyst, it has been possible to perform the Heck reaction between a supported 4-iodobenzoic ester and *tert*-butylacrylate. All parameters were evaluated in this reaction, and the overall message is that every parameter has a noticeable influence on the outcome of the reaction, including spacer length, nature of the counter anion, nature of the IL matrix, and nature of the base [18, 20]. In all cases, disubstituted olefins could be isolated by transesterification of the benzoate support under basic (NH_3/MeOH) or acidic (HCl/MeOH) conditions.

Additionally, Suzuki–Miyaura cross coupling reactions can be performed on similar supported iodides. Aryl bromides could be employed in this reaction as well. After optimization of conditions, it turned out that a hydroxyl-derived IL was the best solvent for this reaction. Namely, reaction completion was obtained after 12 h at room temperature in $[N_{1113OH}][NTf_2]$ in the presence of 1% $Pd(OAc)_2$ and using potassium carbonate as a base. Under these conditions, less than 1% of homocoupling product is observed and easily eliminated by washing with diethyl ether prior to transesterification with methanol. Overall, biphenyls were isolated under analytically pure form in 90–95% yields [126].

2.3.3 Onium Salt Supported Organic Synthesis, a More General Concept

Generalities

Indeed, BTSILs strategy turned out to be really efficient, especially in terms of kinetics compared to using pure TSILs as supports for synthesis. However, if adding an IL matrix enhanced all physical characteristics of the assembly and allowed for modulation of reactivity, it is rather difficult to separate the synthetic OS supported intermediates from the matrix without releasing them from the support. As a result, the concept of BTSIL was extended to the use of molecular solvents which could be removed after reaction under reduced pressure.

Onium salt supported organic synthesis (OSSOS) is a concept fairly similar to the solid phase supported analog, the only difference being the nature of the anchor point: an onium salt instead of a resin. Namely, a TSOS is put in solution in a molecular solvent; after reaction under standard conditions, the resulting product is

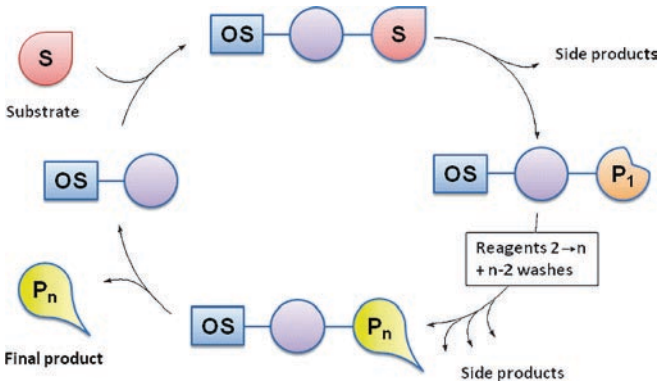

Fig. 39 OSSOS concept

isolated using simple operations such as precipitation (using a non-solvent), decantation, washes and filtration. The isolated TSOS product can then be engaged in a new reaction. Last, the final product is separated from the original support which eventually can be reused in another cycle of reaction (Fig. 39).

This method has numerous advantages over traditional supported organic synthesis. First, due to low molecular weight of the molecule, the loading capacity is superior to 2 mmol g^{-1} and can reach up to 12 mmol g^{-1} for multivalent onium salts. A typical onium salt support in $[N_{1113OH}][NTf_2]$ (M.W. 398) has a loading capacity of 2.5 and 6.5 mmol g^{-1} under the chloride form. For comparison, typical resin hardly reaches 1 mmol g^{-1} and a commonly used MPEG 5,000 has a loading capacity of 0.2 mmol g^{-1}. This low molecular weight is subsequently allowing for working at regular concentration (in the 1 M range) where apparent reaction kinetics are not affected dramatically by supporting the substrate. Indeed, reaction conditions developed for unsupported molecules are often directly applicable without any loss in reactivity. As an example, only few hundred milligrams of compound (1 mmol) can easily be dissolved in 1 mL of acetonitrile, when it is unrealistic hoping achieving such concentration by dissolving 5 g of $MPEG_{5000}$ in 1 mL of solvent (Table 6).

Reaction monitoring is highly facilitated as routine experiments such as ^{1}H NMR, ^{13}C NMR, mass spectrometry, IR spectroscopy, elemental analysis can be performed. This is mainly due to the simplicity of the structure. Unlike polymeric supports where signals from the support often prevent accurate measurement of conversion or side product concentration, trimethylammonium salts have only a limited effect on NMR spectra with a singlet and a multiplet in the 3.0–3.2 ppm region. Additionally onium salt supported products can eventually be analyzed using HPLC and mass spectrometry.

However, in addition to high reactivity and easy monitoring, like all homogeneous methods, the OSSOS strategy affords easy purification of supported products, as simple washes using diethyl ether, water and/or alkanes, withdraw all side products. After final reaction, products can be released from the support and recovered using diethyl ether extraction for example. Additionally, the use of onium salts as

Table 6 Comparison of soluble support loading capacity

A	*n*	X	Molecular weight	Loading capacity (mmol g^{-1})
MeIm	2	Cl	146.5	6.82
MeIm	2	NTf_2	391	2.56
Me_3N	2	Cl	139.5	7.17
Me_3N	2	NTf_2	384	2.60
Me_3N	3	Cl	153.5	6.51
Me_3N	3	BF_4	205	4.87
Me_3N	3	PF_6	263	3.80
Me_3N	4	Cl	167.5	5.97
Me_3N	4	OTf	283	3.53
Me_3N	4	NTf_2	398	2.51
Me_3N	6	Cl	181.5	5.50
Me_3N	6	NTf_2	426	2.34
	–	MPEG 5,000	5,000	0.2

Table 7 Comparison of supported synthesis methods

	Solid (resin)	Soluble polymer (PEG)	Onium salt
Loading	0.1–1 mmol G-1	<0.2 mmol g-1	2–10 mmol g-1
Analysis	HR-MAS NMR, FT-IR	NMR, MS, IR	NMR, SR, IR, HPLC, elemental analysis
Conditions	Heterogeneous (resin swelling)	Homogenous (pseudo dilution)	Homogenous (1 M)
Recycling	Easy	Difficult	Easy
Purification	Filtration, washes	Precipitation, filtration, washes	Filtration, washes
Product recovery	Easy	Difficult	Easy
Automation	Easy	Possible	Possible

soluble supports is much less expensive than traditional resins which are still very expensive (Table 7).

Synthesis of Library

Due to the attractivity of this method several groups have developed onium salt supported versions of classical reactions. For example, starting from hydroxyl derived imidazolium salts, formation of supported acrylates with acryloyl chloride followed by reaction with diene in refluxing toluene afforded Diels Alder adduct in good yields (>65%). After saponification, products are isolated without further purification [127]. Alternatively, starting from carboxylic acid derived imidazolium salts, acyl chloride formation with thionyl chloride in acetonitrile, followed by reaction with 4-aminophenol led to supported *N*-arylamide. Williamson alkylation using NaOH as a base and subsequent cleavage from the onium salt support under acidic condition (HCl/H_2O/AcOH) allowed for isolation of various alkoxy substituted anilines with >98% purity

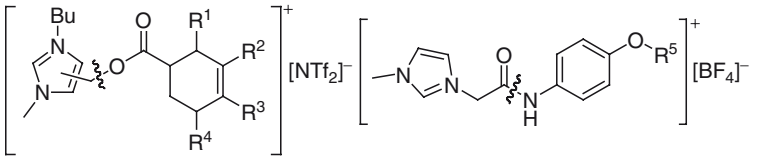

Fig. 40 Libraries of cyclohexenes and aminophenoxides using the OSSOS strategy

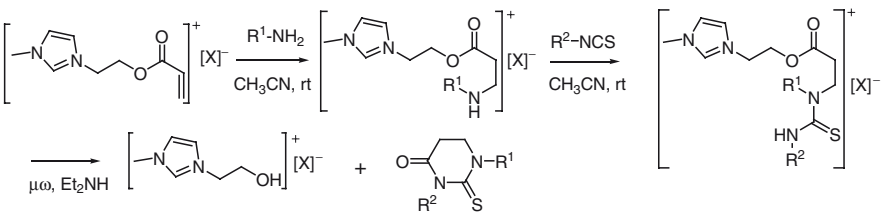

Fig. 41 Thioxotetrahydropyrymidinone synthesis using the OSSOS strategy

[128]. Noteworthy, in both these applications, after washing with diethyl ether or ethyl acetate, no side product or excess reagent could be detected in HPLC (Fig. 40).

Acrylates can also be used in Michael addition with primary amine and, after further reaction with isothiocyanate, supported thioureas are isolated. These can then undergo a cleavage under basic conditions leading to cyclisation and formation of tetrahydrothioxopyrimidinones [129]. Onium salts supported isothiocyanates can also be used with this methodology and lead to the formation of various guanidines [130] (Fig. 41).

As previously mentioned, one advantage of the OSSOS strategy relies on using reactions conditions close to those which have been developed for unsupported molecules. Indeed, concentration belongs to the classical range used in organic synthesis, and no limiting diffusion phenomena are observed in homogeneous phases. Therefore it was interesting to tackle radical reaction as good yields may result from the fine equilibrium between all reaction kinetics. As can be predicted, solid phase supported radical reaction for preparation of small molecules turned out to be unsuccessful as it is rather difficult to reach yields above 30%. This is totally detrimental to any use in a multistep sequence. In 2002 Zard applied his reaction [131] to soluble polymers as supports and found decent conditions for which higher yields can be obtained. In 2007, Vaultier reported that TSOSs were even more efficient supports for this kind of reaction, as addition of supported xanthates to olefins (or xanthates to supported olefin) proceeded smoothly using less stringent conditions [132] (Fig. 42):

Support	Cleavage condition	*n*	DLP	Yield (%)
Wang resin [131]	10% TFA/CH_2Cl_2	10	0.32 eq.	26
Soluble polymer[131]	10% TFA/CH_2Cl_2	3.3	0.4 eq.	54
TSOS [132]	50% DIPEA/MeOH	1.3	0.2 eq.	87

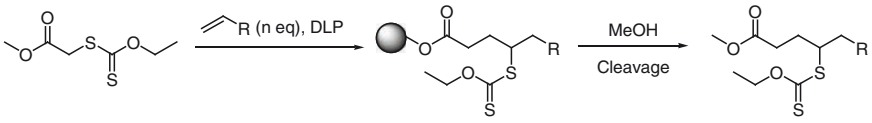

Fig. 42 Zard's reaction in the OSSOS strategy and comparison of immobilisaton methods

Multicomponent Reactions (MCRs)

One of the main applications of organic supported synthesis is to multicomponent reactions. Indeed, by achieving high molecular diversity in a single step, MCRs are perfectly suited for supported synthesis where side products combining several but not all the different reagents can be easily removed from the mixture by filtration. Indeed, supporting MCRs is allowing for using excess of reagents and as a consequence can often afford better yields than those obtained under classical conditions. However, when solid supports are employed, resin swelling frequently appears as an issue since limited access to the reactive site hampers complete conversion.

As a consequence, MCRs have been evaluated using the OSSOS strategy. Grieco's synthesis of tetrahydroquinolines, for example, was evaluated using both OS supported aldehyde and OS supported anilines. In both cases, reaction under acidic conditions in acetonitrile with an olefin afforded the tetrahydroquinolines in good yields. Noteworthy, no purification other than washing with diethyl ether and phase separation were needed to isolate cycloadducts with purity >98% [121]. Interestingly, by simply adjusting the counter anion it was possible to perform the reaction using water as the sole solvent. Indeed, bistriflimides are more hydrophobic than halides and their ammonium or imidazolium salts are mostly soluble in acetonitrile or dichloromethane. In contrast, chlorides are highly prone to solubilize in water and appending an ammonium chloride to any of the partners in Grieco's tetrahydroquinoline synthesis allowed for performing reactions in pure water under homogeneous and mild conditions [133]. It was also found that, by simply changing the acid from TFA to tetrafluoroboric acid, oxidation could be performed in situ and led directly to the formation of quinolines [133]. In all cases, reactions proceeded smoothly at room temperature where, using pure TSIL, the same reaction needed microwave activation [134] (Fig. 43).

Finally, other reactions can be performed directly using water as a solvent. Ugi's four components reaction, for example, provides an expedient access to peptidic scaffolds starting from an isocyanide, an amine, an aldehyde and a carboxylic acid. However, in competition to Ugi's reaction, Passerini ester formation often pollutes the reaction mixture and it is of great interest to perform this type of highly complex transformation in supported versions. Indeed, when an ammonium chloride supported aldehyde, similar to those used in Grieco's multicomponent reactions, are dissolved in water in the presence of an amine, the imine formation occurs within 15 min and isocyanide and acid can subsequently be added to the mixture. After 24 h at room temperature, amides were isolated in high yield with no other purification than washing with diethyl ether [135] (Fig. 44).

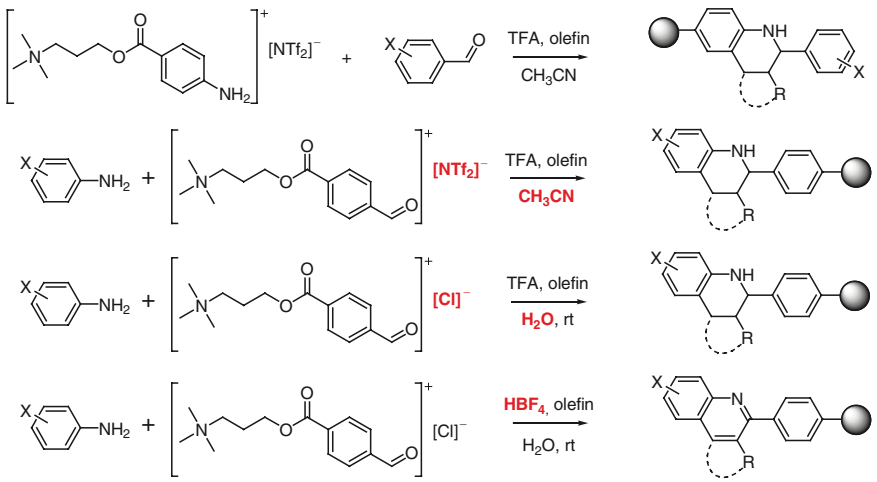

Fig. 43 Grieco's MCR and quinoline synthesis in water using the OSSOS strategy

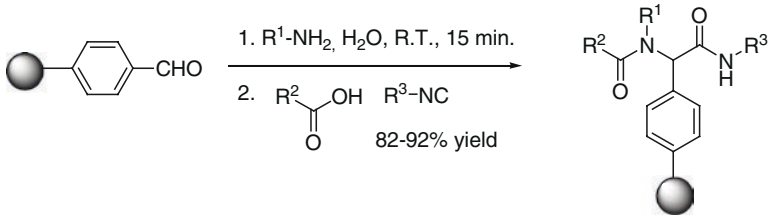

Fig. 44 Ugi's four components reaction using the OSSOS strategy

Transition Metal Catalyzed Reactions

As catalytic reactions turned out to work efficiently using the TSILs and BTSILs strategies, it was natural to evaluate their effectiveness using molecular solvents. Suzuki Miyaura cross coupling for example could be performed in DMF using the same supported iodides and bromides as described previously (see Sect. 2.3.2). Namely, using supported 4-bromobenzoates with a variety of boronic acids in the presence of $Pd(OAc)_2$ led, after 5 h at 80 °C, to a small library of supported biphenyls. DMF evaporation followed by recrystallization of the residue afforded the pure compounds in >90% yields [18]. This reaction has also been shown to be efficient using imidazolium supported iodides [136]. In this case, reaction using cesium fluoride as activating agent in water in combination with $Pd(OAc)_2$ provided the biphenyl adducts in 55–83% yield after transesterification (Fig. 45).

Heck reactions were similarly evaluated towards the same parameters dependence. As such, a library of supported stilbenes has been prepared using a styrene supported on a trimethylammonium tetrafluoroborate in association with a mixture of seven

aryl iodides. After 2 h at 100 °C in DMF, reaction monitoring using HPLC showed that conversion was complete. Washes eliminated unsupported side products and salts; transesterification using MeOH consequently led to the isolation of a mixture of seven stilbenes with excellent purity, especially without remaining starting material (iodides or styrene) [18, 126] (Fig. 46).

Concerning Sonogashira cross coupling, supported alkynes were synthesized by esterification of ammonium supported carboxylic acid with propargylic alcohol using DCC/DMAP conditions. Then, reaction with various aryl iodides in acetonitrile at room temperature using 10 mol% $PdCl_2(PPh_3)_2$, 20% CuI and triethylamine as base led to arylethynes in good yields (77–92%) (Fig. 47).

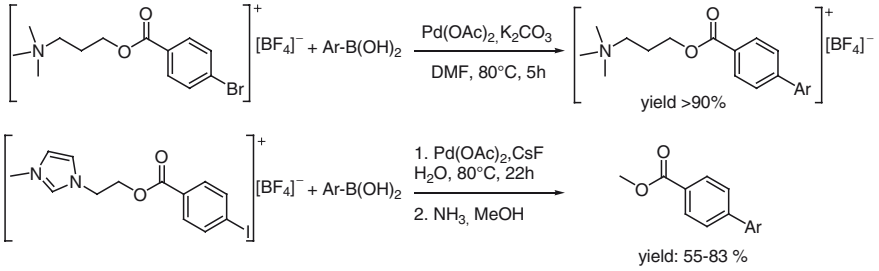

Fig. 45 Suzuki–Miyaura reaction using the OSSOS strategy

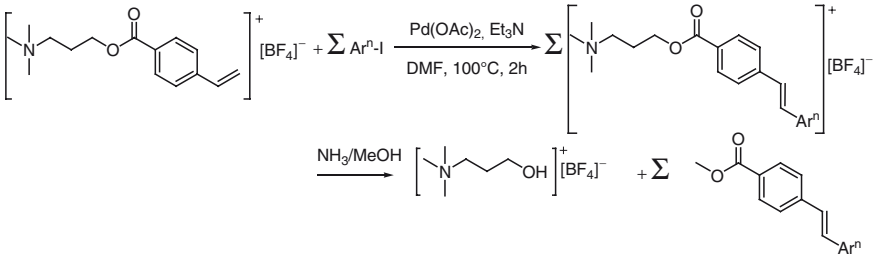

Fig. 46 Heck products library synthesis using the OSSOS strategy

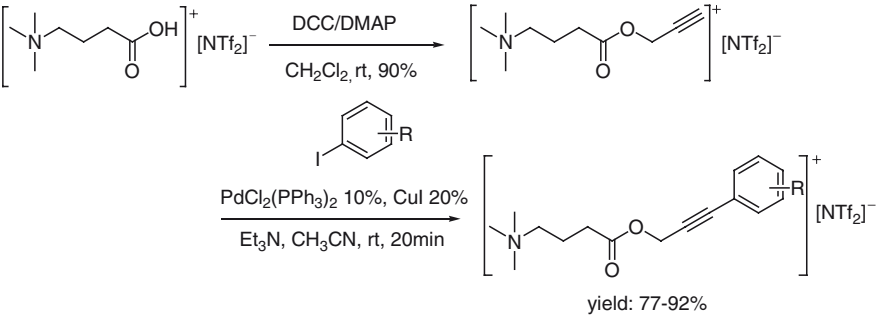

Fig. 47 Sonogashira reaction using the OSSOS strategy

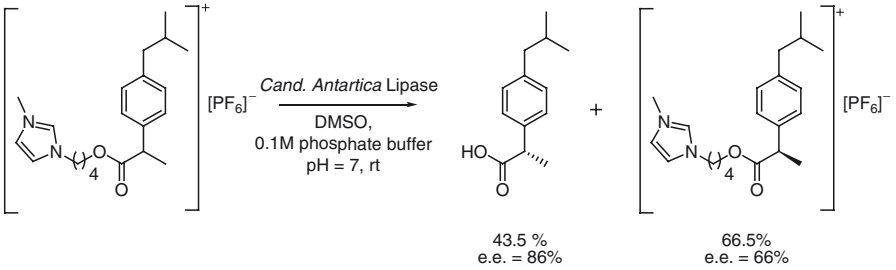

Fig. 48 Enzymatic kinetic resolution of supported esters

On the basis of these three cross coupling reactions, it is probably fair to say that using the OSSOS concept is highly compatible with palladium catalysis but probably not limited to it. For example, a lipase can be used for the kinetic resolution of a racemic ibuprofen ester supported on an imidazolium salt. In a DMSO/phosphate buffer mixture and in the presence of the lipase isolated from *Candida antartica*, the *S*-(+)-supported ibuprofen ester is hydrolyzed selectively (87% ee) in 87% yield. Noticeably, during workup, the support can easily be recovered and reused for another cycle while the other enantiomer can be obtained by hydrolysis using K_2CO_3 [137] (Fig. 48).

Natural Polymer Synthesis

The first publication concerning the solid phase organic synthesis was related to the synthesis of peptides [138], and naturally several groups have been interested by the applications of the OSSOS strategy to the synthesis of natural polymers.

Oligosaccharides for example are of high biological and therapeutical significance. Owing to special properties of the onium salt moiety on which is grafted the monosaccharide, it was possible to improve workup by playing on the relative solubility of each (side) product. Indeed, the imidazolium immobilized sugar is soluble mainly in polar organic solvent such as acetone or methanol but highly insoluble in diethyl ether or hexane like most onium salts. As a consequence, it is fairly easy to remove excess reagents and side products by simply washing and extracting the IL phase using alkanes or diethyl ether. Additionally, reaction kinetics remained similar to those observed in homogeneous classical conditions, enabling the use of lesser reagent excess than with solid or fluorous tagged methods [139]. This method has been applied to the synthesis of oligomannan (a tetrasaccharide) [140] (Fig. 49).

When it comes to peptides several approaches can be envisioned. The first to be published has been related using the Fmoc strategy in both direct and reverse synthesis [141]. Anchoring strategy relied on the esterification of a benzhydril functionalized linker using Fmoc protected amino acids. Supported protected amino acids were obtained as a mixture of chloride and bromide salts which confers

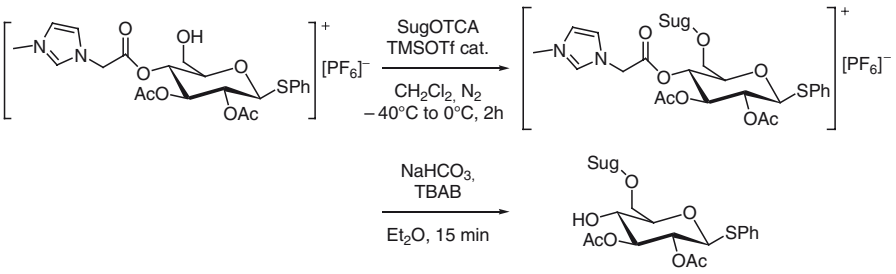

Fig. 49 Oligosaccharrides synthesis using the OSSOS strategy

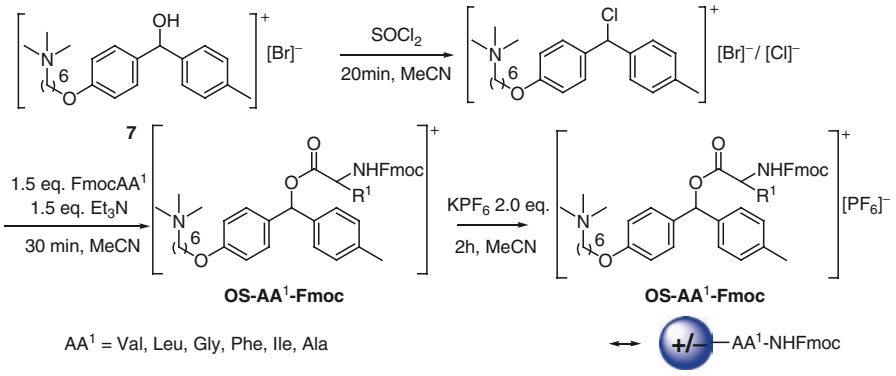

Fig. 50 Onium salt supported amino acid preparation

them non-negligible aqueous solubility incompatible with further aqueous workup. This difficulty was solved by undergoing an ion metathesis with potassium hexafluorophosphate conferring hydrophobic properties to the support (Fig. 50).

Deprotection was cleanly achieved using standard piperidine/MeCN (1/5) solution. Following this procedure, conversions were quasi-quantitative and TSOS loaded with amino acids such as Ala, Gly, Ile, Leu, Phe and Val were obtained in about 85% over four steps. Under the same conditions, coupling of a second Fmoc-protected amino acid (Ala, Gly, Ile, Leu, Val) was high yielding and deprotection led to only 5% diketopiperazine formation which was suitable for pursuing the synthesis. Repetition of the sequence led to the supported tripeptide (Gly, Leu, Val) in good yields (83–98% over two steps). Finally, the peptide was cleaved from the TSOS using a catalytic amount of HPF_6 in refluxing methanol (85% yield for the tripeptide Val-Leu-Ala). For purification, peptide was soluble in water whereas the derivatives from the TSOS were soluble in DCM (Fig. 51).

One advantage of this method over solid phase peptide synthesis is the possibility offered by homogenous conditions to perform convergent supported synthesis. In this case, two peptides, one synthesized by the direct approach and the other synthesized through the reverse strategy, can be coupled to each other as they

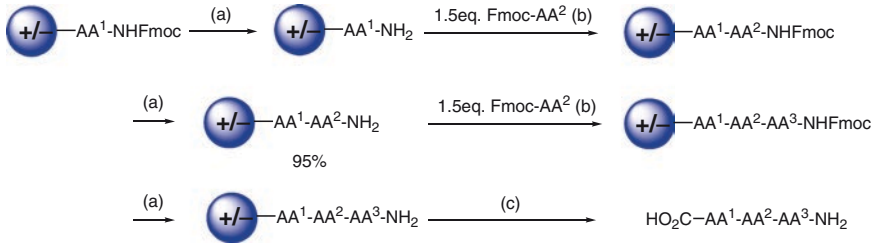

(a) piperidine/MeCN:1/5, RT, 15min (b) DCC / HOBt / TEA MeCN, 30min, RT (c) 0.01eq. HPF_6 aq. MeOH, Δ, 1h.
AA^1 = Val, Leu, Gly, Phe, Ile, Ala; AA^2 = Ala, Gly, Ile, Leu, Val ; AA^3 = Gly, Leu, Val

Fig. 51 Onium salt supported peptide synthesis [141]

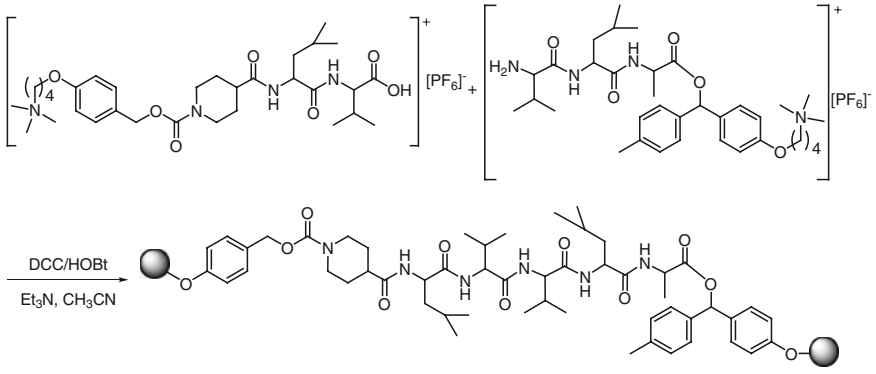

Fig. 52 Convergent onium salt supported peptide synthesis

belong to the same phase. Namely, DCC/HOBt system turned out to lead efficiently to the peptide supported on both ends by an onium salt (Fig. 52).

Other onium salts support can be used for the Fmoc strategy such as phosphonium salts analog to the Wang (R = H) or Sasrin resins (R = OMe) [142]. Alternatively, the Boc strategy has been evaluated in the OSSOS concept. As a proof of concept, Chan showed that a bioactive pentapeptide could be prepared using imidazolium based support bearing a hydroxyl moiety. To avoid diketopiperazine forming, the first coupling was directly performed using a dipeptide in combination with DCC/DMAP in acetonitrile; after sequences of deprotection/loading, the pentapeptide was isolated as a TFA salt in 50% overall yield without any purification step using chromatography [31]. Using the very same strategy, a cyclic peptide, Sansalvamide A, was prepared in 12 steps and 11% overall yield, the limiting steps being loading (70%), cleavage (60%) and cyclisation (51%) [143] (Fig. 53).

Finally, oligonucleotides were synthesized using the same OSSOS strategy [144, 145]. After grafting the first nucleotide using an ester linkage, tri and tetra nucleotides

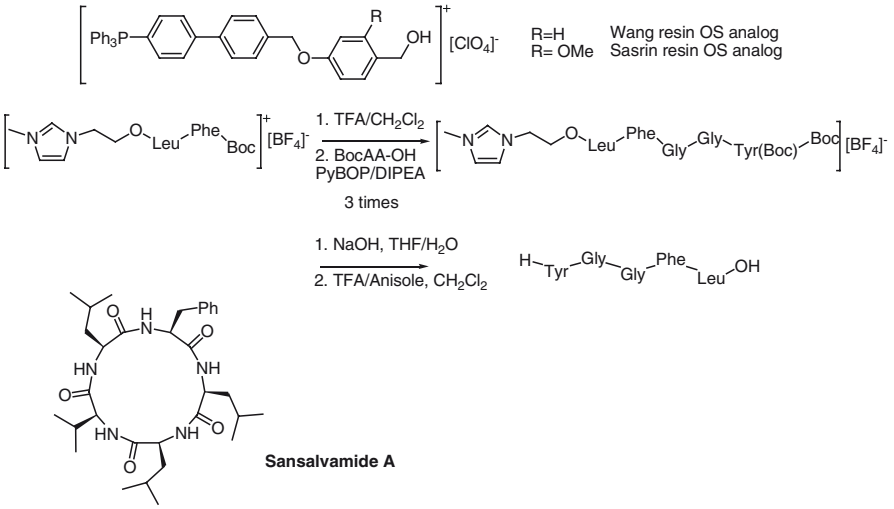

Fig. 53 Boc strategy for onium salt supported peptide synthesis using imidazolium or phosphonium based supports

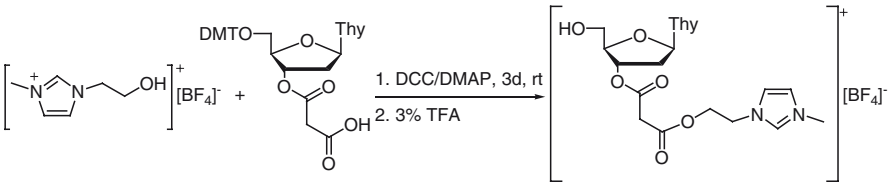

Fig. 54 Oligonucleotide preparation in OSSOS

have been prepared on a 100-μmol scale using coupling with CDI in association with the next nucleotide as a phosphoramidite (Fig. 54).

Applications in Microreactor Area

Exciting applications in the field of e-microreactors have recently appeared. The real-time monitoring of powerful approach combining a droplet-based, open digital microfluidic lab-on-a-chip using task-specific ionic liquids as soluble supports and electrowetting as the fluidic motor to perform solution-phase synthesis has been reported as a new tool for chemical applications [146, 147]. The multicomponent Grieco's reaction was used to validate the concept which should impact many areas, notably combinatorial chemistry, parallel synthesis, optimization of protocols, synthesis of dangerous products, and embedded chemistry on a portable device. This technology opens the way to easy synthesis of minute amounts of compounds without the use of complex, expensive, and bulky robots and allows complete automation of

the process for embedded chemistry in a portable device. It offers several advantages, including simplicity of use, flexibility, and scalability, and appears to be complementary to conventional microfluidic lab-on-a-chip devices usually based on continuous flow in microchannels. A number of challenging issues have been addressed to allow standard macroscale organic chemistry to be transposed directly in these non-classical microreactors. In particular, since standard (i.e. magnetic or mechanical) stirring methods are prohibited in such wall-free microreactors, effective alternatives have been developed to circumvent mass transfer limitations [148]. For this purpose, a fluorogenic version of a 1,2,3-triazoles synthesis by a 1,3-dipolar cycloaddition of azides with acetylenes using TSILS in ionic liquid droplets acting as soft wall-free microreactors was developed to evaluate the efficiency of alternative mixing methods on the reaction kinetics. The real-time monitoring of the reaction was performed by fluorescence measurements. This click chemistry reaction appeared to be a powerful tool to evaluate the efficiency of different mixing activation methods on the reaction progress by comparing the initial reaction velocities. This study provided demonstration that the combination of chaotic advection created by SAW and temperature increase allows for an approach of a kinetic regime similar to that for macroscale standard organic reactions in solution (i.e. magnetically stirred solutions of organic reagents in regular "hard" flasks). It has been demonstrated that the combination of chaotic advection created by surface acoustic waves (SAW) combined with a temperature increase (Marangoni effect) led to the same kinetics regime as in standard macroscale conditions. This opens the route for application of this new generation of lab-on-a-chip to efficient organic synthesis in microscale.

3 Conclusion and Perspective

Ionic liquids have been shown to be "designer solvents" as was stated more than 10 years ago [149]. It is clear from that review and others that the statement should be extended to "designer functional molecules or materials" since so many applications of ionic liquids and onium salts in so many different fields appeared in the literature. Functionalized onium salts, among which task specific ionic liquids are particular cases, are capable molecules, provided a proper design, which can be used for accomplishing a very broad variety of tasks ranging from metal extraction from water solutions to immobilization of catalysts, soluble supports for organic synthesis, separation techniques and material sciences. Almost any functionalization of these salts is possible, therefore opening the way to any kind of task specific materials and molecules. It should be pointed out that imidazolium salts are not the only available salts although they have been the workhorses up to now. Ammonium and phosphonium salts have to be considered as well as other quaternarized heterocycles like pyridinium, pyrazolium, tetrazolium, etc.. Triazolium salts deserve a special mention since they are very efficiently accessible via a Huisgen 1,3 dipolar cycloaddition of azides with acetylenes catalyzed by copper salts as recently shown by Liebscher et al. Numerous developments are predictable in the area of supported

chemistry. It clearly appears that TSILs, and TSOSs are a valuable addition to the arsenal of tools available for supported chemistry and in particular in the field of solution phase chemistry. Several advantages of these new supports have been pointed out in this review including simple synthesis, solution phase reaction conditions, flexibility, diversity of feasible chemistry, stability, high loading, and easy monitoring of reactions. These working salts have brought a wide variety of efficient solutions to the immobilization and recycling of catalysts which should allow for the development of commercial applications. Immobilization of TSILs and TSOSs on solids like silica (SILPs) or zeolites should bring further fascinating developments. Several other fields of chemistry, including combinatorial chemistry, physical organic chemistry, material sciences, process development, fixed bed and flow through reactors to mention but a few are directly connected to the development of this field. A good example of this kind of development in the field of microfluidic has been reported showing that it is a very open and promising area. Although the chemistry of TSILs and TSOSs is still in its infancy, it can be safely stated that, generally speaking, they should have a bright future.

References

1. Cornils B, Herrmann WA (2005) In: Cornils B, Herrmann WA (eds) Aqueous-phase organometallic catalysis, 2nd edn. Wiley, Weinheim, p 1
2. Walden P (1914) Bull. Acad. Sci. St. Petersburg 405:1800
3. Wasserscheid P, Welton T (2007) Ionic liquids in synthesis, 2nd edn. Wiley, New York
4. Dupont J, de Souza RF, Suarez PAZ (2002) Chem Rev 102:3667
5. Greaves TL, Drummond CJ (2008) Chem Rev 108:206
6. Parvulescu VI, Hardacre C (2007) Chem Rev 107:2615
7. Ranke J, Stolte S, Stormann R, Arning J, Jastorff B (2007) Chem Rev 107:2183
8. vanRantwijk F, Sheldon RA (2007) Chem Rev 107:2757
9. Welton T (1999) Chem Rev 99:2071
10. Boon JA, Levisky JA, Pflug JL, Wilkes JS (1986) J Org Chem 51:480
11. Wilkes JS, Zaworotko MJ (1992) J. Chem. Soc., Chem. Commun.: 965
12. Davis JH Jr, Forrester KJ, Merrigan T (1998) Tetrahedron Lett 39:8955
13. Visser AE, Swatloski RP, Reichert WM, Davis Jr. JH Jr, Rogers RD, Mayton R, Sheff S, Wierzbicki A (2001) Chem. Commun.: 135
14. Yue C, Mao A, Wei Y, Lue M (2008) Catal Commun 9:1571
15. Ranu BC, Banerjee S (2005) Org Lett 7:3049
16. Ranu BC, Jana R (2006) Eur. J. Org. Chem.: 3767
17. Davis JH Jr (2004) Chem Lett 33:1072
18. Vaultier M, Gmouh S, Hassine F (09/07/2003) In: CNRS, Rennes 1 U (eds), WO2005005345, p 190
19. Fei Z, Geldbach TJ, Zhao D, Dyson PJ (2006) Chem Eur J 12:2122
20. Vaultier M, Gmouh S (26/09/2002) In: CNRS, Rennes1 U (eds), WO2004029004, p 129
21. Holbrey JD, Turner MB, Reichert WM, Rogers RD (2003) Green Chem 5:731
22. Handy ST, Okello M, Dickenson G (2003) Org Lett 5:2513
23. Bao W, Wang Z, Li Y (2003) J Org Chem 68:591
24. Boesmann A, Schulz PS, Wasserscheid P (2007) Monatsh Chem 138:1159
25. Wasserscheid P, Bosmann A, Bolm C (2002) Chem. Commun.: 200
26. Schrekker HS, Stracke MP, Schrekker CML, Dupont J (2007) Ind Eng Chem Res 46:7389

27. Schrekker HS, Silva DO, Gelesky MA, Stracke MP, Schrekker CML, Goncalves RS, Dupont J (2008) J Braz Chem Soc 19:426
28. Bates ED, Mayton RD, Ntai I, Davis JH (2002) J Am Chem Soc 124:926
29. Soutullo MD, Odom CI, Salter EA, Stenson AC, Sykora RE, Wierzbicki A, Davis JH Jr (2007) J Comb Chem 9:571
30. Fraga-Dubreuil J, Bazureau JP (2001) Tetrahedron Lett 42:6097
31. Miao W, Chan T-H (2005) J Org Chem 70:3251
32. de Kort M, Tuin AW, Kuiper S, Overkleeft HS, van der Marel GA, Buijsman RC (2004) Tetrahedron Lett 45:2171
33. Anjaiah S, Chandrasekhar S, Gree R (2004) Tetrahedron Lett 45:569
34. Hanelt S, Liebscher J (2008) Synlett: 1058
35. Amengual R, Genin E, Michelet V, Savignac M, Genet J-P (2002) Adv Synth Catal 344:393
36. Mehnert CP, Cook RA, Dispenziere NC, Afeworki M (2002) J Am Chem Soc 124:12932
37. Yoshizawa M, Ogihara W, Ohno H (2002) Polym Adv Technol 13:589
38. Zhao D, Fei Z, Ohlin CA, Laurenczy G, Dyson PJ (2004) Chem. Commun.: 2500
39. Vaultier M (2008) Ionic liquids in synthesis, 2nd edn. Wiley, New York
40. Miao W, Chan TH (2006) Acc Chem Res 39:897
41. Lee S-G (2006) Chem. Commun.: 1049
42. Chen X, Li X, Hu A, Wang F (2008) Tetrahedron Asymmetry 19:1
43. Ohno H, Fukumoto K (2007) Acc Chem Res 40:1122
44. Riisager A, Fehrmann R (2008) Ionic liquids in synthesis, (2nd eEdition,)vol 2:, p 527
45. Riisager A, Fehrmann R, Wasserscheid P (2008) Handbook of heterogeneous catalysis, 2nd edn, vol 1, p: 631
46. Burguete MI, Galindo F, Garcia-Verdugo E, Karbass N, Luis SV (2007) Chem. Commun.: 3086
47. Riisager A, Eriksen KM, Wasserscheid P, Fehrmann R (2003) Catal Lett 90:149
48. Riisager A, Flicker S, Haumann M, Wasserscheid P, Fehrmann R (2006) Proc Electrochem Soc 2004 24:630
49. Riisager A, Wasserscheid P, Van Hal R, Fehrmann R (2003) J Catal 219:452
50. Hanioka S, Maruyama T, Sotani T, Teramoto M, Matsuyama H, Nakashima K, Hanaki M, Kubota F, Goto M (2008) J Membr Sci 314:1
51. Visser AE, Swatloski RP, Reichert WM, Mayton R, Sheff S, Wierzbicki A, Davis JH, Rogers RD (2001) Chem. Commun.: 135
52. Visser AE, Swatloski RP, Reichert WM, Mayton R, Sheff S, Wierzbicki A, Davis JH, Rogers RD (2002) Environ Sci Technol 36:2523
53. Holbrey JD, Visser AE, Spear SK, Reichert WM, Swatloski RP, Broker GA, Rogers RD (2003) Green Chem 5:129
54. Kogelnig D, Stojanovic A, Galanski M, Groessl M, Jirsa F, Krachler R, Keppler BK (2008) Tetrahedron Lett 49:2782
55. Luo H, Dai S, Bonnesen PV, Buchanan AC (2006) J Alloys Compd 418:195
56. Ouadi A, Klimchuk O, Gaillard C, Billard I (2007) Green Chem 9:1160
57. Ouadi A, Gadenne B, Hesemann P, Moreau JJE, Billard I, Gaillard C, Mekki S, Moutiers G (2006) Chem Eur J 12:3074
58. Ranu BC, Banerjee S (2005) J Org Chem 70:4517
59. Wu X-E, Ma L, Ding M-X, Gao L-X (2005) Synlett: 607
60. Dong F, Jian C, Kai G, Qunrong S, Zuliang L (2008) Catal Lett 121:255
61. Cole AC, Jensen JL, Ntai I, Tran KLT, Weaver KJ, Forbes DC, Davis JH (2002) J Am Chem Soc 124:5962
62. Wang W, Shao L, Cheng W, Yang J, He M (2007) Catal Commun 9:337
63. Dong F, Luo J, Zhou X, Ye Z, Liu Z (2007) J Mol Catal A Chem 274:208
64. Fang D, Gong K, Shi Q, Liu Z (2007) Catal Commun 8:1463
65. Dong F, Kai G, Fei Z, Zhou X, Liu Z (2007) Catal Commun 9:317
66. Kitaoka S, Nobuoka K, Ishikawa Y (2004) Chem. Commun.: 1902
67. Gui J, Deng Y, Hu Z, Sun Z (2004) Tetrahedron Lett 45:2681

68. Paun C, Barklie J, Goodrich P, Gunaratne HQN, McKeown A, Parvulescu VI, Hardacre C (2007) J Mol Catal A Chem 269:64
69. Cornils B, Kuntz EG (2005) Multiphase homogeneous catalysis 1:148
70. Kuntz EG (1987) Chemtech 17:570
71. Haumann M, Riisager A (2008) Chem Rev 108:1474
72. Brasse CC, Englert U, Salzer A, Waffenschmidt H, Wasserscheid P (2000) Organometallics 19:3818
73. Brauer DJ, Kottsieper KW, Liek C, Stelzer O, Waffenschmidt H, Wasserscheid P (2001) J Organomet Chem 630:177
74. Kottsieper KW, Stelzer O, Wasserscheid P (2001) J Mol Catal A Chem 175:285
75. Wasserscheid P, Waffenschmidt H, Machnitzki P, Kottsieper KW, Stelzer O (2001) Chem. Commun.: 451
76. Chauvin Y, Mussmann L, Olivier H (1996) Angew Chem Int Ed 34:2698
77. Favre F, Olivier-Bourbigou H, Commereuc D, Saussine L (2001) Chem. Commun.: 1360
78. Bronger RPJ, Silva SM, Kamer PCJ, van Leeuwen PWNM (2002) Chem. Commun.: 3044
79. Calò V, Nacci A, Monopoli A (2006) Eur J Org Chem 2006:3791
80. Machnitzki P, Tepper M, Wenz K, Stelzer O, Herdtweck E (2000) J Organomet Chem 602:158
81. Iranpoor N, Firouzabadi H, Azadi R (2007) Eur J Org Chem 2007:2197
82. Xiao JC, Twamley B, Shreeve JM (2004) Org Lett 6:3845
83. Wang R, Piekarski Melissa M, Shreeve Jean'ne M (2006) Org Biomol Chem 4:1878
84. Brochwitz C, Feldhoff A, Kunz U, Vaultier M, Kirschning A (2006) Lett Org Chem 3:442
85. Corma A, Garcia H, Leyva A (2004) Tetrahedron 60:8553
86. Zhao D, Fei Z, Geldbach TJ, Scopelliti R, Dyson PJ (2004) J Am Chem Soc 126:15876
87. Audic N, Clavier H, Mauduit M, Guillemin JC (2003) J Am Chem Soc 125:9248
88. Clavier H, Audic N, Guillemin J-C, Mauduit M (2005) J Organomet Chem 690:3585
89. Yao Q, Zhang Y (2003) Angew Chem Int Ed 42:3395
90. Clavier H, Audic N, Mauduit M, Guillemin J-C (2004) Chem. Commun.: 2282
91. Yao Q, Sheets M (2005) J Organomet Chem 690:3577
92. Geldbach TJ, Dyson PJ (2004) J Am Chem Soc 126:8114
93. Kawasaki I, Tsunoda K, Tsuji T, Yamaguchi T, Shibuta H, Uchida N, Yamashita M, Ohta S (2005) Chem. Commun.: 2134
94. Berthod M, Joerger J-M, Mignani G, Vaultier M, Lemaire M (2004) Tetrahedron Asymmetry 15:2219
95. Lee S-G, Zhang YJ, Piao JY, Yoon H, Song CE, Choi JH, Hong J (2003) Chem. Commun.: 2624
96. Zhao D, Fei Z, Scopelliti R, Dyson PJ (2004) Inorg Chem 43:2197
97. Doherty S, Goodrich P, Hardacre C, Knight JG, Nguyen MT, Pârvulescu VI, Paun C (2007) Adv Synth Catal 349:951
98. Doherty S, Goodrich P, Hardacre C, Parvulescu V, Paun C (2008) Adv Synth Catal 350:295
99. Wu X-E, Ma L, Ding M-X, Gao L-X (2005) Chem Lett 34:312
100. Xiao JC, Ye C, Shreeve JM (2005) Org Lett 7:1963
101. Baleizão C, Gigante B, Garcia H, Corma A (2003) Tetrahedron Lett 44:6813
102. Baleizao C, Gigante B, Garcia H, Corma A (2004) Tetrahedron 60:10461
103. Berkessel A, Groerger H (2005) In: Berkessel A, Groerger (eds) Asymmetric Organocatalysis Wiley , Weinheim , p 1
104. Ley SV (2006) In Christmann M, Bräse S (Ed) Asymmetric Synthesis – The Essentials Wiley-VCH Weinheim: 201
105. Pellissier H (2007) Tetrahedron 63:9267
106. Dalko PI, Moisan L (2001) Angew Chem Int Ed 40:3726
107. Seayad J, List B (2005) Org Biomol Chem 3:719
108. Koguchi S, Kitazume T (2006) Tetrahedron Lett 47:2797
109. Miao W, Chan TH (2006) Adv Synth Catal 348:1711

110. Yang S-D, Wu L-Y, Yan Z-Y, Pan Z-L, Liang Y-M (2007) J Mol Catal A Chem 268:107
111. Wu L-Y, Yan Z-Y, Xie Y-X, Niu Y-N, Liang Y-M (2007) Tetrahedron Asymmetry 18:2086
112. Luo S, Mi X, Zhang L, Liu S, Xu H, Cheng J-P (2007) Tetrahedron 63:1923
113. Siyutkin DE, Kucherenko AS, Struchkova MI, Zlotin SG (2008) Tetrahedron Lett 49:1212
114. Zhang Z, Xie Y, Li W, Hu S, Song J, Jiang T, Han B (2008) Angew Chem Int Ed 47:1127
115. Fraga-Dubreuil J, Bazureau JP (2003) Tetrahedron 59:6121
116. Hu Y, Wei P, Huang H, Han S-Q, Ouyang P-K (2006) Synth Commun 36:1543
117. Hu Y, Wei P, Huang H, Han S-Q, Ouyang P-K (2006) Heterocycles 68:375
118. Yi F, Peng Y, Song G (2005) Tetrahedron Lett 46:3931
119. Dahr D, Vaultier M Unpublished results
120. Legeay JC, Goujon JY, Vanden Eynde JJ, Toupet L, Bazureau JP (2006) J Comb Chem 8:829
121. Hassine F, Gmouh S, Pucheault M, Vaultier M (2007) Monatsh Chem 138:1167
122. Tao X-L, Lei M, Wang Y-G (2007) Tetrahedron Lett 48:5143
123. Xu L, Chen W, Xiao J (2000) Organometallics 19:1123
124. Jeffery T (1985) Tetrahedron Lett 26:2667
125. Reetz MT, Westermann E (2000) Angew Chem Int Ed 39:165
126. Hassine F, Vaultier M Unpublished results
127. Handy ST, Okello M (2003) Tetrahedron Lett 44:8399
128. Peng Y, Yi F, Song G, Zhang Y (2005) Monatsh Chem 136:1751
129. Hakkou H, Vanden Eynde JJ, Hamelin J, Bazureau JP (2004) Tetrahedron 60:3745
130. Hakkou H, Vanden Eynde JJ, Hamelin J, Bazureau JP (2004) Synthesis: 1793
131. Dublanchet A-C, Lusinchi M, Zard SZ (2002) Tetrahedron 58:5715
132. Verron J, Joerger J-M, Pucheault M, Vaultier M (2007) Tetrahedron Lett 48:4055
133. Ouach A, Gmouh S, Pucheault M, Vaultier M (2008) Tetrahedron 64:1962
134. Li M, Sun E, Wen L, Sun J, Li Y, Yang H (2007) J Comb Chem 9:903
135. Ouach A, Pucheault M, Vaultier M (2007) Heterocycles 73:461
136. Miao W, Chan TH (2003) Org Lett 5:5003
137. Naik PU, Nara SJ, Harjani JR, Salunkhe MM (2007) J Mol Catal B Enzym 44:93
138. Merrifield RB (1963) J Am Chem Soc 85:2149
139. Huang J-Y, Lei M, Wang Y-G (2006) Tetrahedron Lett 47:3047
140. Pathak AK, Yerneni CK, Young Z, Pathak V (2008) Org Lett 10:145
141. Vaultier M, Roche C, Gmouh S, Commercon A (16/02/05) In: Aventis pharma SA F, CNRS (eds), WO2008003836, p 67 pp
142. Stazi F, Marcoux D, Poupon J-C, Latassa D, Charette AB (2007) Angew Chem Int Ed 46:5011
143. Chen L, Zheng M, Zhou Y, Liu H, Jiang H (2008) Synth Commun 38:239
144. Donga RA, Hassler M, Chan T-H, Damha MJ (2007) Nucleosides Nucleotides Nucleic Acids 26:1287
145. Donga RA, Khaliq-Uz-Zaman SM, Chan T-H, Damha MJ (2006) J Org Chem 71:7907
146. Marchand G, Vinet F, Delapierre G, Hassine F, Gmouh S, Vaultier M (2006). (CEA, Fr.; CNRS), FR2872715, p 63
147. Dubois P, Marchand G, Fouillet Y, Berthier J, Douki T, Hassine F, Gmouh S, Vaultier M (2006) Anal Chem 78:4909
148. Marchand G, Dubois P, Delattre C, Vinet F, Blanchard-Desce M, Vaultier M (2008) Anal Chem 80:6051
149. Freemantle M (1998) Chem Eng News 72:32

Top Curr Chem (2009) 290: 127–159
DOI: 10.1007/128_2008_34

Published online: 04 April 2009

Heavy Elements in Ionic Liquids

Andreas Taubert

Abstract Heavy elements have in the recent past been studied extensively in the context of ionic liquids (ILs). This is because ILs have initially been thought of as "solve-it-all" problem solvers, from catalysis, to extraction, and inorganic and electrochemistry. In due course, it has been shown that ILs are indeed very versatile solvents and reaction media. As a consequence, many elements have been dissolved in ILs and their properties have been studied in IL solution. The current chapter focuses on the use of ILs for inorganic chemistry, in particular on what heavy elements have been studied in ILs, their properties and applications.

Keywords metals • metal ions • heavy elements • solution • salvation • speciation • solubility • s-elements • p-elements • d-elements • f-elements • complex ions • ionic liquids

Contents

A. Taubert
Institute of Chemistry, University of Potsdam 14476, Golm, Germany
Max-Planck-Institute of Colloids and Interfaces 14476, Golm, Germany
e-mail: ataubert@uni-potsdam.de

1 Introduction

Ionic liquids (ILs) have attracted more and more attention over the last few years. This is due to the fact that they have been promoted as "green" solvents (although more recent data demonstrate that there are issues with this claim). Furthermore, ILs have interesting physical and chemical properties like high electrical conductivity, tunable solubility and miscibility, and a wide range of viscosities. Some ILs are even stable up to a few hundred degrees [1–6].

As a result, organic and, more recently, inorganic chemists have studied ILs for many applications, including catalysis and liquid/liquid extraction, to name two examples [1, 4, 6–9]. Among others, inorganic chemists have recently focused on the synthesis of materials from ILs [10–15]. Many studies show that inorganic and materials chemists can exploit ionic liquids for the synthesis of inorganic materials that are not (or not easily) accessible via conventional synthetic pathways [12, 16–19]. For example, ILs have been used as morphology-modifying templates [13, 20–26]. There have been some early studies on the growth of metal particles in ILs [20, 22, 27–29], but only in recent years have these proof-of-concept studies been backed up with more quantitative investigations [30–34]. The first studies simply used an IL or a mixture of an IL with a conventional solvent as a reaction medium. This empirical approach sometimes gives interesting and useful results, but it lacks a systematic and rational design element, which would be advantageous for targeted materials synthesis [10, 20–22, 28, 29, 35–52]. More recent examples are more advanced [10, 15, 24–26, 31–33, 53–63], but materials synthesis in ILs is still hampered by the fact that a rational design or a deliberate exploitation of specific interactions between IL and growing inorganic is, due to the lack of understanding, not possible.

As a result, there is a clear need to study further not only the formation and properties of inorganic materials from ILs, but also the solubility, structure, and behavior of heavy elements in ILs as such. For example, Kirchner, Binnemans, and coworkers have recently shown that the solubility of metal oxides can be rationalized and treated quantitatively [64]. Their study represents a major step forward in the understanding of the interactions of ILs with inorganics and with the precursors of the respective inorganic. This latter point is also often overlooked when treating growth of inorganics from ILs: in order to understand quantitatively the growth and structure formation of inorganics from ILs one must know the structure and behavior of the precursor and the ILs. Indeed a recent study by Nockemann et al. has shown that in ILs, interesting polynuclear metal complexes that have not been observed in other solvents, form [65]. Furthermore, it has been shown that both the anion and the cation have strong effects on nucleation and growth of inorganic particles [66].

Moreover, the combination of ILs with metallic species (metal-containing ILs) provides access to ILs with interesting magnetic, spectroscopic, or catalytic properties [67–75]. As the properties largely depend on the metal ion, the combination of metal ions with organic cations and also the solubility and behavior of many metallic elements has attracted tremendous attention over the last few years. ILs have been studied as hosts for photochemical and spectroscopic studies. In some cases,

metal-containing ILs can be regarded as new optical materials [71, 76–79]. For example, ILs can in some cases increase the photochemical stability of tetrakis β-diketonate complexes [80]. Moreover, combining materials synthesis with lanthanide chemistry, Lunstroot et al. have synthesized luminescent ionogels by doping a Eu(III) tetrakis(β-diketonate) into an IL confined in mesoporous silica, yielding an interesting macroscopic luminescent material [81]. Finally, ILs have also been reported to provide low energy phonon matrices, which enables highly efficient near-infrared luminescence of Nd(III), Er(III) and Yb(III) [82, 83]. As a result, the combination of metal ions dissolved in ILs with either catalysis or materials chemistry aspects is a challenging field, which strongly relies on a detailed understanding of what happens if a heavy element is present in an IL. The current chapter gives an overview over the different structures, chemistries, properties, and problems that have been reported over the last few years.

2 Structure of Ionic Liquids

The ever increasing interest in ionic liquids stems from their interesting physical properties and the simplicity by which they can be adapted for a specific system. Over the years the number of publications describing different ILs and their use for various applications has rapidly increased. Accordingly, a number of reviews have appeared as well [1–4, 10, 11, 13–15, 71, 84–92].

The structure of ILs has been studied some years now, but still, there are open questions, in particular with respect to what structural (and thereby property) changes occur, as solutes become part of an IL solution. Initially, ILs have been regarded as liquids like classical organic solvents. That is, ILs have been treated as liquids with properties similar to organic solvents, although with higher viscosity and the possibility to transport electrons. Relatively rapidly, however, it has been realized that ILs are in fact very complex substances [85, 93–96]. Nowadays, it is clear that detailed knowledge of IL structures are key to understanding molecular and supramolecular processes occurring in ILs. Identification of the important interactions and parameters will help identifying (and possibly at some point predicting) the key parameters that are needed for a certain application or question.

A variety of experimental techniques have been used to investigate IL structures. Neutron diffraction, X-ray scattering, extended X-ray absorption fine structure (EXAFS) [97–105], and theoretical methods [64, 106–111] are probably the most powerful approaches to quantify IL structure and interactions. For example, X-ray diffraction and absorption studies along with computer simulations have shown that ILs are by no means molecular liquids [64, 89, 94, 112, 113]. Unlike a conventional solvent like hexane or chloroform, ILs contain a large number of internal interfaces and exhibit different degrees of order [89, 114]. ILs can form liquid crystals, extended hydrogen-bonded networks, inclusion compounds, or microphase separated structures, where polar and non-polar regions are separated by a complex interface [86, 89, 114].

Enderby and colleagues were the first to study molten salts. Among others, they showed that molten NaCl has a structure which is mainly dominated by alternating anion and cation interactions, which extend up to three anion–cation pairs. As a result, the molten NaCl is highly structured [115, 116]. Igarashi et al. [117] have examined the liquid structure of a LiF–NaF–KF eutectic mixture. For the ion pairs Li–F, Na–F, and K–F, the nearest neighbor coordination and distances were almost identical to those found in the melts of the individual components.

More recently, Hardacre and colleagues have studied a range of ILs using a variety of techniques. Besides the pure IL structure, these authors were also interested in determining the interaction of solutes with the components of the ILs. They studied a series of 1,3-dimethylimidazolium (Dmim) salts via neutron diffraction [96, 118, 119]. The rationale behind using the symmetric rather than the unsymmetric imidazolium salts (which are typically used in ILs) was to simplify data analysis. Indeed the authors showed that, despite the different melting points, useful information can be extracted from the neutron data.

For example, for Dmim-Cl, strong charge ordering was found [99, 120–124]. Similar to the NaCl example above, they found alternating anion and cation layers in the radial distribution functions. A detailed comparison between the effects of chloride vs other anions showed that, depending on the anion (chloride vs hexafluorophosphate vs bis(trifluoromethyl sulfonyl) imide) (NTf_2)), different cation–cation distances are observed [96, 118]. With increasing anion size the cation–cation distance increases from 5.5 (Cl^-) to 6.3 Å (PF_6^-), and finally to 7.0 Å (NTf_2^-). Along with an increasing cation–cation distance, the anion–cation distance also increases and the charge ordering becomes less pronounced.

In addition to the pure size effects, the NTf_2^- anion is peculiar in that it can adopt either *cis* or *trans* conformation (Fig. 1) [125–131]. While the liquid form of the IL exhibits a distribution of forms (although the *trans* conformer is most pronounced), the crystalline Dmim-NTf_2 seems to exhibit a very large fraction of *trans* conformers.

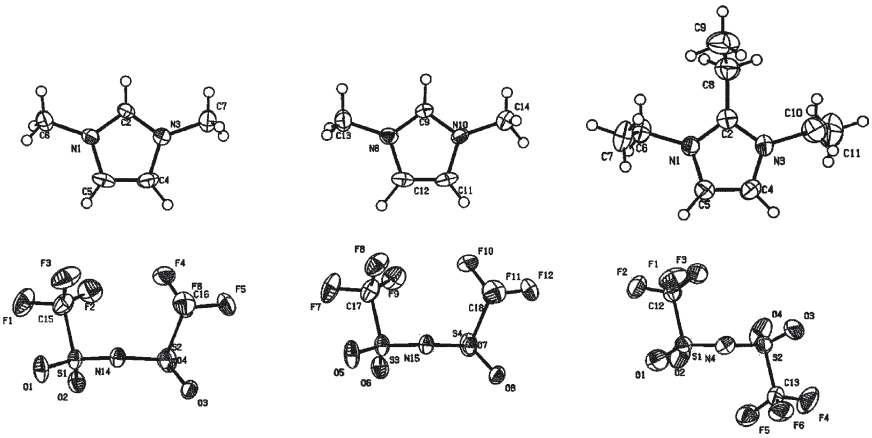

Fig. 1 *Cis* and *trans* geometry of the NTf_2^- anion in 1,3-dimethylimidazolium NTf_2 (*left and center*) and in 1,2,3-triethylimidazolium NTf_2 (*right*). Image adapted from [125]. Image Copyright Royal Society of Chemistry (2004)

The authors speculate that the corresponding crystal structure is just one of several possible polymorphs.

Besides the symmetric Dmim cations, ILs based on other cations have also been studied. Hardacre et al. have studied the structure of 1-methyl-4-cyanopyridinium NTf_2 using neutron scattering and molecular dynamics simulations. They found a significant degree of apparent charge ordering in the liquid state although the more complex shape of the cation led to a more complex structure than the examples discussed above [95].

Hunt et al. have used ab initio methods to study ion pairs in 1-butyl-3-methylimidazolium (Bmim) ILs. The anions were Cl^-, BF_4^-, and NTf_2^-. The authors established relationships between ion-pair association energy and a derived parameter called the "connectivity index". Overall, the results suggest that Bmim-Cl forms a strongly connected and quite highly structured network, which leads to the rather high viscosity observed experimentally. In contrast, Bmim-NTf_2 only forms a rather weak network, where the connectivity and the viscosity are much lower [106].

Given the strong connectivities in many ILs, it can be expected that strong cooperative effects are often observed in ILs. Indeed, several studies have also addressed cooperativity in ILs [110, 111]. Kossman et al. have studied cooperative effects in Dmim-Cl ILs by quantum chemical calculations [109]. Moreover, it has been shown that ILs are not (always) innocent bystanders of a reaction but much rather that ILs can interact in many ways with solutes. These developments have recently been reviewed [132].

As ILs are already rather complex substances with microphase separated structures [89, 114], it is not surprising that ILs also come as liquid crystals, so-called ionic liquid crystals (ILCs) [86, 133–136]. ILCs should not be confused with metallomesogens, which are essentially liquid crystalline metal complexes. Although the first examples of ILCs can also be viewed as metallomesogens, their key difference is that ILCs need not contain metals, just ions, and second, that the metal (if present) in ILCs is not usually present as single metal ion, but rather as a complex metal ion like tetrachlorocuprate, tetrabromozincate, or a similar charged entity. For example, Bowlas et al. have reported ILCs from alkylpyridinium tetrachlorometallates [133]. Similar compounds have subsequently been studied by others [25, 31, 32, 63, 134–137]. Other studies have investigated the structure and behavior of long alkyl chain imidazolium salts with various anions [138–140].

3 Heavy Elements and their Solutions in ILs

It has been pointed out above that ILs have many advantages. However, it is often overlooked that ILs are not suited for every application, for various reasons. For example, the BF_4^- and PF_6^- anions hydrolyze in aqueous solutions and can therefore not be used for long term application involving water. Similarly, Binnemans has pointed out that the solubility of common inorganic ionic compounds like NaCl in the classic imidazolium ionic liquids is very low [71]. This fact – which at first sight is rather surprising – is due to the poor solvating power of ionic liquids containing

only weakly coordinating ions like BF_4^-, PF_6^-, or NTf_2^-. Typically, the solubility of metal salts increases if more coordinating anions, such as chloride or bromide, are present. Indeed, chloroaluminate ionic liquids are good solvents for a range of transition metal salts, including lanthanide and actinide salts [71]. The solubility of metal salts in so-called task-specific ionic liquids (TSILs) can be higher than that in the common types of ionic liquids, because the TSILs can be designed to exhibit excellent metal-salt solubilizing power (Fig. 2) [64, 65, 141–144].

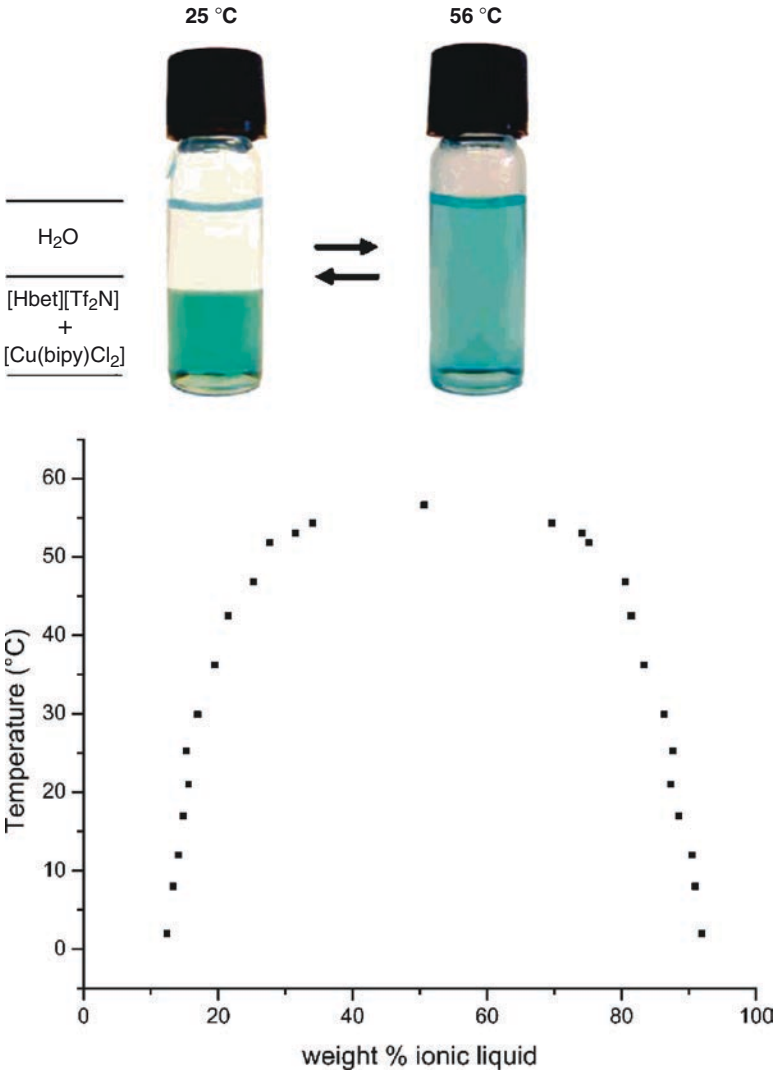

Fig. 2 *Top*: solubilization of $[Cu(bipy)Cl_2]$ by a TSIL and the temperature dependent phase separation. *Bottom*: liquid–liquid equilibrium phase diagram of the binary mixture TSIL-water. Figure adapted from [64]. Image Copyright American Chemical Society (2006). For color image see online version

At this point it is important to realize that (although often neglected) ILs more often than not contain quite significant amounts of water. Knowing that many metal salts have high solubilities in water, it is important to keep in mind that even a few percent of water in an IL will often dramatically change the solubility of an inorganic compound in an IL. It has been pointed out that high solubilities of ionic compounds in hydrophilic ionic liquids can often be attributed to the solubilizing properties of the water present and not to the ionic liquid itself [71]. Indeed Li et al. have recently shown that using water as a cosolvent dramatically affects the outcome of inorganic nanoparticle synthesis from either a pure IL, an IL hydrate, or an IL hydrate with where more water was deliberately added to the reaction mixture [145–147].

On the other hand, coordination complexes or organometallic compounds can be solubilized in ionic liquids, especially hydrophobic or anionic complexes [71, 78]. It has been pointed out earlier that there are tricks to circumvent dissolution problems such as dissolving a metal salt and the IL in an organic solvent followed by solvent evaporation. Furthermore, the viscosity, which is much higher in ILs than in conventional solvents, will dramatically reduce mass transfer, which in turn will lead to a much slower metal salt dissolution [71].

Experimental and computational studies also show differences in solvation depending on whether or not water is present in an IL (Fig. 3) [148, 149]. For example, in dry Bmim-PF_6, Eu(III) is surrounded by PF_6^- anions, whereas in wet Bmim-PF_6, Eu(III) ion is surrounded exclusively by water molecules in the first coordination shell.

Finally, it has to be noted that hydrophobic ionic liquids can take up significant amounts of water, even though they will not mix with water. As a result, the absence, presence, and amount of water in an IL may not be neglected. While in some cases it is sufficient to determine the fraction of water in the IL, other cases are more critical. For example, water has been shown to reduce dramatically the emission yield from lanthanides dissolved in ILs (see also the respective chapter by Mudring, in this volume) [142, 148, 150–153].

In summary, dissolution of heavy elements in ILs is not straightforward. Moreover, for certain questions, consideration of the role of water in the IL is a key requirement, in particular if it comes to optical or spectroscopic properties. Over the last years a rather good understanding of the structure, the chemistry, and the properties of ILs has been established. It is, however, obvious that there is a need to study further the details of solubilization and the resulting structures and properties of the resulting metal/IL mixtures. This is particularly evident in the context of spectroscopy, magnetic ILs, catalysis and materials aspects.

It has been mentioned above that ILs are by no means able to dissolve everything that comes along in a chemist's life. However, it has been found that there are groups of elements that share similarities, mostly along their electron configuration. In the following, the behavior of heavy elements in ILs will therefore be discussed in terms of their position in the periodic table of elements, starting with the s-elements and finishing with the f-elements.

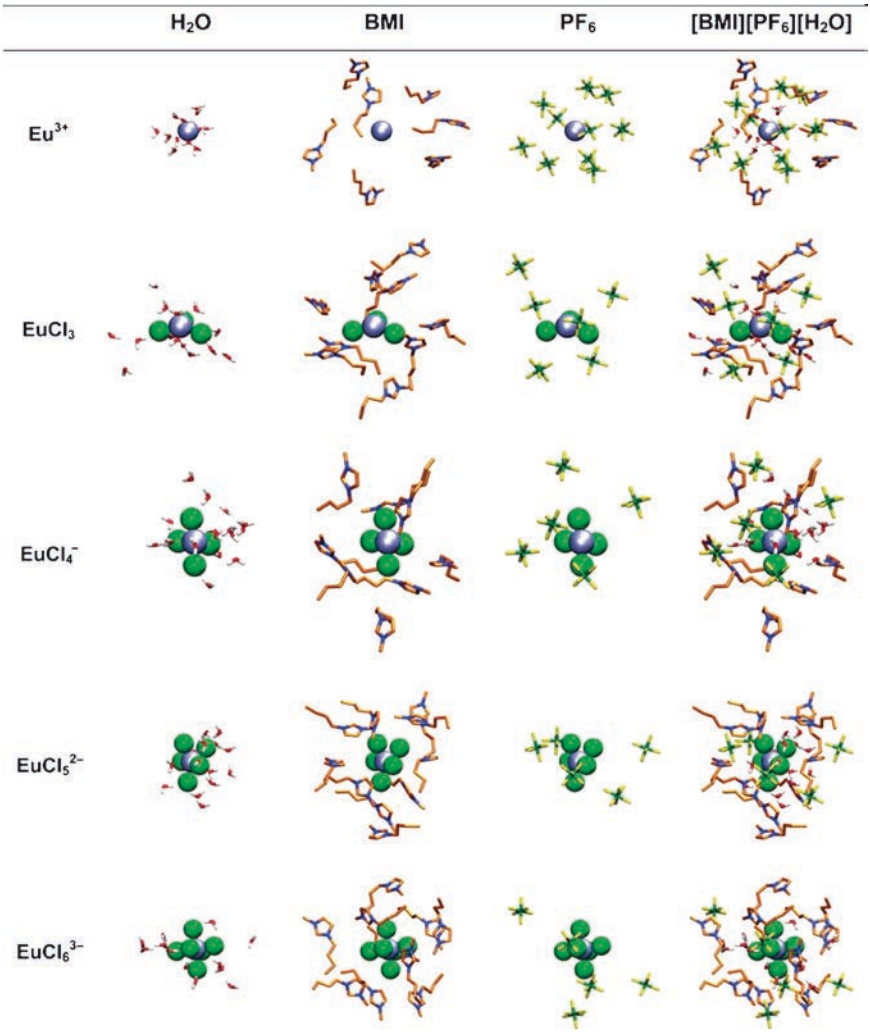

Fig. 3 Behavior of Eu(III) chloro complexes in wet Bmim-PF_6 ILs. The simulated structures clearly show the hydration layer around the central metal ion. The image shows final snapshots of the first shell (within 9 Å) of Eu, showing (*from left to right*) H_2O only, BMI^+ only, PF_6^- only, and the complete wet IL solvent. Eu is *blue* and chloride is *green*, BMI = Bmim. Adapted from [149]. Image Copyright American Chemical Society (2004). For color image see online version

3.1 Alkali and Earth Alkali Elements (s-Block Elements)

ILs containing alkali or earth alkali elements have been rather sparse, but there are a few examples that should be discussed. Because of potential applications in battery technology, the combination of lithium with IL technology has attracted some

attention. Hardwick et al. performed an in-depth Raman spectroscopy study of lithium salts in Emim-NTf_2 [126]. Among others, the authors showed that, while the Li^+ interacts with the IL in the absence of carbonate species, the presence of carbonate additives in the IL leads to disappearance of the IL–Li^+ interaction.

Accordingly, DFT calculations on the same system and a combined Raman/DFT study on *N*-butyl-*N*-methylpyrrolidinium bis(trifluoromethanesulfonyl)imide (Bmp-NTf_2) suggests that two NTf_2^- ions bind to one metal ion. The lithium ion may be four-coordinated through the O atoms of two bidentate NTf_2^- ions [127]. Moreover, the authors showed that around the Li^+ ion, the *cis* conformer is preferred over the *trans*, which is contrary to the bulk structure in the absence of the lithium salt. The *cis* conformer is also preferred in $Li_2(Emim)(NTf_2)_3$ crystals [128]. With increasing temperature the fraction of *cis* conformers also increases [129, 130]. This effect has been ascribed to the fact that the enthalpy of the conformation change from *trans* to *cis* is positive [131].

The same authors show that the fraction of *cis* conformer increases with increasing concentration of the lithium ion: that is, the more NTf_2^- anions there are in proximity of an Li ion, the higher the fraction of *cis* conformers [131]. The results on the Li^+ are in line with an earlier study by Lassegues et al. [154] and with ab initio calculations for the Li^+ NTf_2^- ion pair [155, 156]. Similarly, the *cis* conformer is preferred in $AE(NTf_2)_4^{2-}$ (AE = Ca^{2+}, Sr^{2+}, and Ba^{2+}) crystals (Fig. 4) [157].

Endres et al. have studied the effects of very small amounts of inorganic impurities on the behavior of ILs [158]. Among others, the authors report that when an IL made from 1-butyl-1-methylpyrrolidinium chloride ($Py_{1,4}Cl$) and Li-NTf_2 is not thoroughly washed after the synthesis, instead of being stable throughout the whole

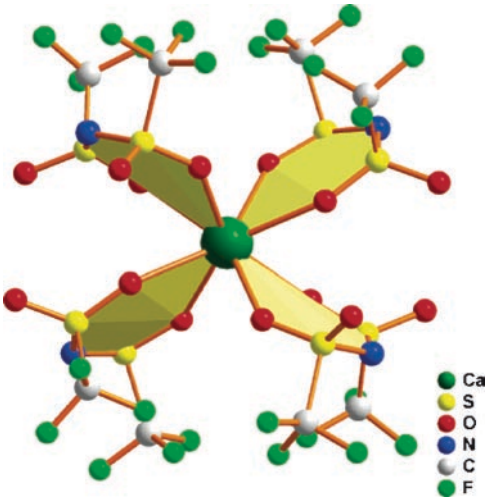

Fig. 4 Coordination of Ca^{2+} by NTf_2^- ligands in $[mppyr]_2[Ca(NTf_2)_4]$. Note the *cis* conformation of the NTf_2 ligands. Image adapted from [157]. Image Copyright American Chemical Society (2006). For color image see online version

experiment, several monolayers of Li are deposited in the cathodic regime. The same study also shows that a spectroscopically ultrapure Emim-NTf_2 may contain traces of Al if treated with Al_2O_3 during purification. The authors suggest that some Al_2O_3 is dissolved in the IL, which can, depending on the exact conditions, either be redeposited as Al_2O_3 or as Al. This paper thus suggests that not only deliberate addition of metal ions but also trace impurities can have a dramatic impact on the outcome of a chemical reaction in ILs. The authors even suggest that "better synthesis routes will be necessary to make ultrapure ILs for fundamental physicochemical studies".

Bazito et al. have reported that ILs based on 1-*N*-butyl-2,3-dimethylimidazolium (Bmmi) and *N*-*n*-butyl-*N*-methylpiperidinium (Bmp) and NTf_2^- as an anion are stable towards metallic Li [159]. Unfortunately, although the ILs did not react with metallic Li, the authors report the formation of metal carbenes. These findings suggest that the acidic proton in ILs can have a dramatic influence on the stability of Li-containing ILs and therefore on their use in Li ion battery technology.

Besides Li, only a few studies with s-elements in ILs have been carried out. Babai et al. have prepared the first homoleptic alkaline earth (AE = Ca, Sr, Ba) AE-NTf_2 complexes from *N*-methyl-*N*-propylpyrrolidinium bis (trifluoromethanesulfonyl) imide (Mmpyr-NTf_2) and the respective alkaline earth bis (trifluoromethanesulfonyl) imide [157]. The Ca and Sr complexes are similar in that in both cases the metal is coordinated to four bidentate (chelate) NTf_2 ions resulting in an isolated (distorted) square antiprismatic $[AE(NTf_2)_4]^{2-}$ complex separated by Mmpyr cations. In the case of the Ba complex, the resulting [mppyr][$Ba(NTf_2)_3$] exhibits a more extended structure. The Ba ions are surrounded by three NTf_2^- (chelating) anions and three further oxygen atoms of the same ligands yielding infinite chains.

Popov et al. have investigated stability constants of alkali complexes in ILs [160]. Stability constants of Na and Cs complexes with 18-crown-6 (18C6) and dibenzo-18-crown-6 (DB18C6) in 1-butyl-4-methylpyridinium tetrafluoroborate (BMP-BF4) were determined via ^{23}Na and ^{133}Cs NMR. The study found a rapid cation exchange between free and complexed ions. Furthermore, only 1:1 complexes were observed. The log *K* values for $[M(18C6)]^+$ were much higher than in aqueous solution, whereas those of DB18C6 complexes were lower. In a similar study, the transfer of Sr into a series of 1-alkyl-3-methylimidazolium-based ILs using dicyclohexano-18-crown-6 (DCH18C6) ligands was shown to depend on the hydrophobicity of the IL cation [161].

A detailed study of the Sr(II)-crown ether complexes formed in 1-methyl-3-pentylimidazolium bis[(trifluoromethyl)sulfonyl]amide has been reported by Jensen et al. [102]. Using X-ray absorption fine structure (XAFS) spectroscopy at the Sr K-edge, they found that the structure around the Sr strongly depends on the dissolution process. The differences in the coordination around the Sr were assigned to differences in the extraction of Sr ions into the IL phase.

Similar to the Sr example, lanthanide extraction into ILs has been reported to yield different structures than when prepared with an organic solvent instead the IL. In ILs, the formation of anionic $Nd(tta)_4^-$ or $Eu(tta)_4^-$ (Htta = 2-thenoyltrifluoroacetone) complexes with no water coordinated to the metal center is preferred. In nonpolar organic solvents, hydrated, neutral complexes, $M(tta)_3(H_2O)_n$ (n = 2 or 3) form [162].

Finally, Rogers et al. have reported a detailed study on the electrochemical oxidation of Bmim-I and AI (A = Li, Na, K, Rb, Cs) in Bmim-NTf_2 (Fig. 5). The two oxidation peaks were assigned to the oxidation of iodide to triiodide and a further oxidation of triiodide to iodine. The slightly smaller diffusion coefficients obtained for the AI salts in comparison to Bmim-I was suspected to arise from AI ion pairs in the IL [163].

3.2 *p-Block Elements*

So far, mostly solutions of heavy elements *dissolved in* ILs have been discussed. The p-block elements are peculiar in the sense that the haloaluminate ILs constitute an important class of ILs. However, unlike the more conventional cases, where the IL is composed of an organic cation and an organic anion or at most a simple inorganic ion like chloride, the haloaluminates are more complex. In aluminate ILs, the Al ion is an integral part of the IL and not, as discussed so far, a simple solute in an independent IL. As a result, both solutions of p-elements in regular ILs and systems like the haloaluminates will have to be discussed here.

$AlCl_3$-*N*-butylpyridinium chloride, $AlCl_3$-1-ethyl-3-methylimidazolium chloride, HCl-1-ethyl-3-methylimidazolium chloride, and $AlCl_3$–LiSCN mixtures have been studied using X-ray and neutron scattering [164–167]. These studies have provided information about the specific interactions between anions and cations within the ILs. Unfortunately, little additional information could be extracted from the data. In particular, no information about the structure of the respective ILs beyond the first coordination sphere could be obtained. Importantly, however, the authors show that in $AlCl_3$-LiSCN, the N and not the S atom of the SCN ion coordinates to the Al ion. This was explained with a hard base/hard acid interaction which can be expected for a Lewis acid compound like $AlCl_3$.

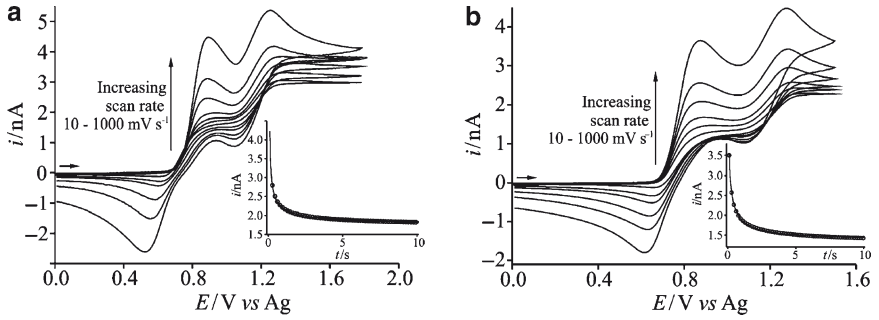

Fig. 5a,b Cyclic voltammetry for the oxidation of KI (**a**) and RbI (**b**) in Bmim-NTf_2. *Inset* to each is the experimental (–) and fitted theoretical (O) chronoamperometric transients recorded for the oxidation of I^-. The potential was stepped from 0.0 to +1.0 V. Image adapted from [163]. Image Copyright American Chemical Society (2008)

Besides X-ray and neutron methods, Al-based ILs were also studied with computational methods. Kirchner et al. have studied the properties of isolated $AlCl_3$ clusters and bulk $AlCl_3$ ILs via static and dynamic electronic structure methods. The data show that different connectivities such as edge and corner connectivity depend on the number of monomeric $AlCl_3$ units in a given structure. Furthermore, the trimer cluster exhibits an interesting ring structure with large cooperative effects relative to the dimer. This study suggests that, in the bulk IL, the most prominent connectivity should be the edge connectivity. Moreover, the authors suggest that the most prominent species in the bulk is the dimer, although other oligomers are also present [108]. Kirchner et al. also performed Car–Parrinello molecular dynamics simulations of the IL imidazolium chloride-$AlCl_3$. Again, the data revealed that the anion in $AlCl_3$-based ILs is most likely more complex (Fig. 6). The predominant species found in the simulations was $Al_4Cl_{13}^-$. The authors explain the formation of these large and rather complex anions by an electron deficiency of the acidic melt [107].

Similarly, chloroindate(III) ILs have been reported. However, so far, mostly their catalytic activity has been studied and no data on their physical properties or structure are available [75]. A related study reports some basic data on another chloroindate IL [168].

Timofte et al. report the synthesis of perfluoroalkoxyaluminate $Al(ORF)_4^-$ (ORF = $OCH(CF_3)_2$ (hfip), $OC(CF_3)_3$ (nftb)) ILs, for which the authors report a low viscosity at 60 °C and high electrochemical stability [169].

In a study on Al electrodeposition from ILs, Liu et al. show that the deposition is not only controlled by the electrochemical conditions chosen for the reaction.

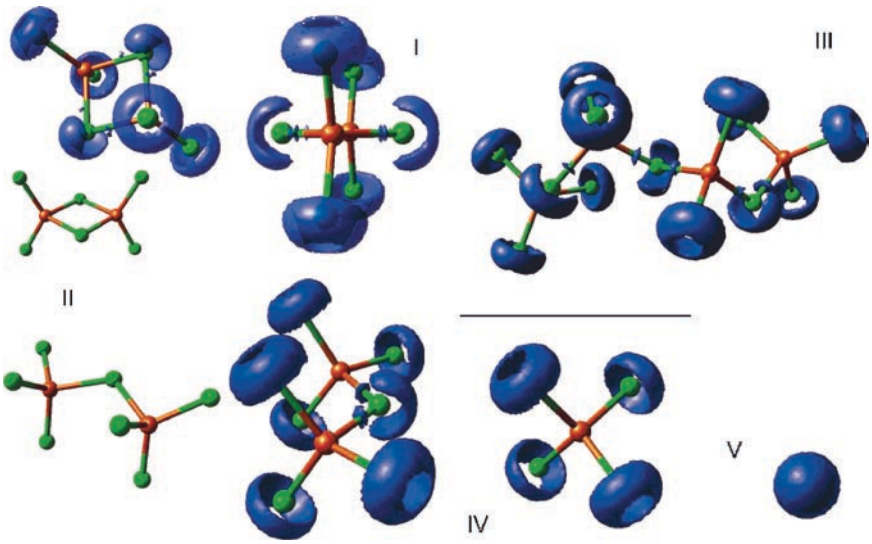

Fig. 6 Electron localization functions obtained from Car-Parinello simulations of $AlCl_3^-$-based ILs. I: Al_2Cl_6. II: $Al_2Cl_7^-$. III: $Al_4Cl_{13}^-$. IV: $AlCl_4^-$. V: Cl^-. Green: Cl; orange: Al. Image adapted from [107]. Image Copyright American Chemical Society (2007). For color image see online version

It is suggested that some IL decomposes, leading to cation decomposition products in solution, which in turn leads to a change of the crystal growth during Al film formation. The resulting films are not microcrystalline anymore, but nanocrystalline [170].

Interestingly, little work has been done on non-metallic p-block elements in ILs. Besides the oxidation of Bmim-I and alkali metal iodides discussed above [163], also the electrochemical reduction of iodine in Bmim-NTf_2 was studied. Similar to the oxidation study, the authors report two reduction peaks. A detailed mechanistic and kinetic analysis was performed and the electrode process was found to be consistent with Butler–Volmer kinetics [171].

Sylvester et al. have studied the electrochemistry of PCl_3 and $POCl_3$ in 1-butyl-1-methylpyrrolidinium bis(trifluoromethylsulfonyl)imide (BMPyr-NTf_2). This is a particularly interesting study, as to the best knowledge of the author there are no comparable studies in conventional solvents. The authors have proposed a reaction mechanism and determined diffusion coefficients. Furthermore, the authors suggest that the reaction is rather complex and that there are intermediate species, which tend to undergo side reactions [172].

Finally, X-ray diffraction has been used to examine the liquid structure of binary ionic liquids of 1,3-dialkylimidazolium fluoride with HF [173, 174]. The solid state and liquid structures are closely related as both contain $[HF_2]^-$ anions. In contrast, Shodai et al. reported that the structure of liquid $[(CH_3)_4N]F^*n$ HF (n = 3–5) has a range of anion structures of the form $[(HF)xF]^-$ (x = 1–3). In this case, structures with x = 4 or 5 were not found in the liquid phase although similar compositions have been found in the solid state [175]. These studies show that even elements that are rarely studied in the IL context like P (other than in PF^-_6 or phosphonium cations) or F could provide access to interesting and potentially useful ILs.

3.3 Transition Metals (d-Elements)

While there has been comparatively little work on s- and p-block elements in ILs, the situation is different for both d- and f-elements. In part the large number of studies devoted to these elements is due to their interesting properties, ranging from magnetic to catalytically active and luminescent species, to just name a few examples. Although there are thus interesting applications of transition metals in ILs, one of the problems is to stabilize the metal ions in the IL or, after for example a catalytic reaction has been performed, to extract both the IL and the catalytically active metal from the reaction mixture. In order to overcome issues with low solubility of some metal salts in ILs, task-specific ILs (TSILs) with a high metal-solubilizing power have been developed [141, 176]. In short, a functional group, which enhances metal salt solubility by coordinating to the metal ion, is attached to an IL building block, mostly the cation.

Nockemann and colleagues have shown that the betainium-based TSIL Hbet-Tf_2N (Hbet = betaine bis-(trifluoromethylsulfonyl)imide) is not only able to dissolve many metal salts; it is also possible to remove the metal by pH change and

thus to establish a reversible system that could be interesting for example in soil remediation (Fig. 2). The crystal chemistry of Hbet-based complexes is quite surprising and strongly depends on the metal cation (Fig. 7) [64, 65]. With Co(II), trimeric units, with Zn(II) and Mn(II) tetramers, with Ni(II) pentamers, and with Ag(I), polymeric species are observed. For Pb(II), oxohydroxo-cluster formation was reported. The authors suggest that the anion plays an important role in structure formation. They suggest that the coordination strength is a key parameter that guides structure formation. Most importantly, it is suggested that weakly coordinating anions like perchlorate or triflate lead to polynuclear complexes [177, 178].

Further examples of metal coordinating ILs were reported by Harjani et al. [179]. They synthesized imidazolium-based TSILs with ethylamine diacetic acid moieties. These molecules readily form 2:1 octahedral complexes with Co(II),

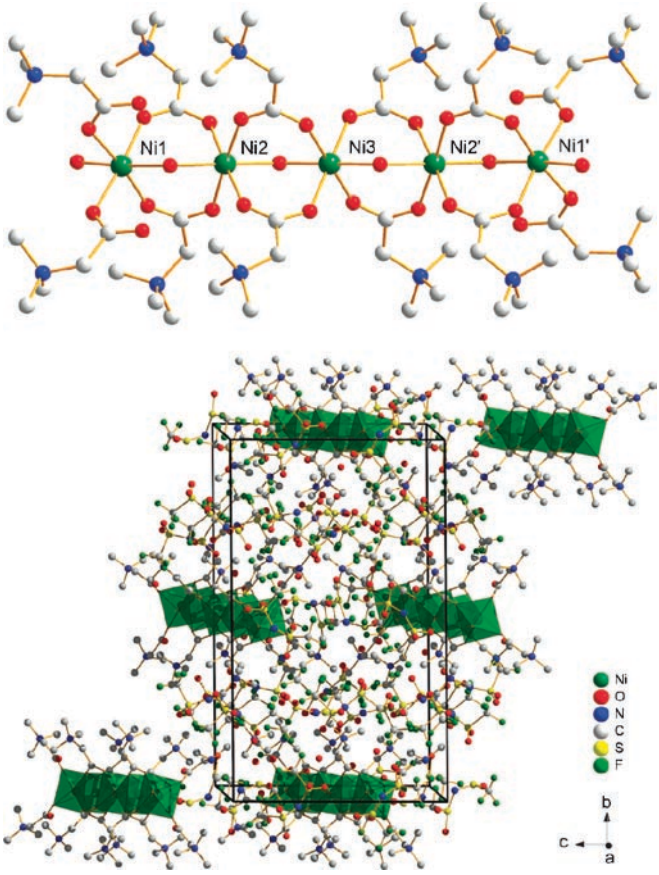

Fig. 7 *Top*: pentameric cationic unit $[Ni_5(bet)_{10}(H_2O)_6]^{10+}$ in the crystal structure of $[Ni_5(bet)_{12}(H_2O)_6][NTf_2]_{10}$. *Bottom*: view of the packing of the molecules along the *a*-axis in the crystal structure of $[Ni_5(bet)_{12}(H_2O)_6][NTf_2]_{10}$. Image adapted from [65]. Image Copyright American Chemical Society (2008). For color image see online version

Ni(II), and Cu(II) in aqueous solution. Similar to Nockemann et al. [64, 65] the authors suggest that the metal ions could be recovered by a pH change.

Another example of dissolving metals in ILs is linking a complex to an IL. Tan et al. synthesized a series of salen Mn(III) complexes functionalized by 1-propylamine-3-methylimidazolium tetrafluoroborate ILs [180]. Iida et al. have reported an interesting set of Ag-based ILs, bis(*N*-2-ethylhexylethylenediamine) silver(I) nitrate, $[Ag(eth\text{-}hex\text{-}en)_2]NO_3$, and bis(*N*-hexylethylenediamine)silver(I) hexafluorophosphate, $[Ag(hex\text{-}en)_2]PF_6$ [181], which are precursors for silver nanoparticles (Fig. 8).

In some cases, chemical functionalization of ILs is not necessary. Using a eutectic melt of choline chloride and urea, Abbott et al. dissolved several metal oxides. In particular, the eutectic melt dissolves Zn and P and leaves Fe and aluminosilicates behind [182]. Abbott et al. have also reported on the behavior of eutectic mixtures of zinc chloride and urea or acetamide [183]. Using FAB-MS it was possible to determine that the resulting ILs are made up of metal-containing anions.

A further example of metal ion extraction with ILs was reported by Papaiconomou et al. [184]. The authors extracted dilute aqueous metal salt solutions with ILs based on 1-octyl-4-methylpyridinium (4Mopyr), 1-methyl-1-octylpyrrolidinium (Mopyrro), or 1-methyl-1-octylpiperidinium (Mopip), and the anions tetrafluoroborate, trifluoromethyl sulfonate, or nonafluorobutyl sulfonate. In particular, the authors report that the octylpyridinium-based ILs are quite specific for Hg(II), while other cations are not extracted. Disulfide-containing ILs selectively extract Hg(II) and Cu(II) and nitrile-functionalized ILs selectively extract Ag(I) and Pd(II). This study clearly shows that a seemingly simple modification of an IL with either disulfide or nitrile groups can lead to very specific changes in performance.

Kumano et al. have studied the transfer of metal ions into *N*,*N*,-diethyl-*N*-methyl-*N*-(2-methoxyethyl) ammonium bis(trifluoromethanesulfonyl)imide by addition of 8-hydroxyquinoline (HQ) to the IL [185]. The addition of HQ to the IL significantly enhances the extraction efficiency of the IL. As a result, up to 5 μmol of Cu, Zn, Cd, and Mn could be recovered with 100 μl of the HQ/IL mixture.

In many cases, dissolution can also be achieved simply by heating MX_2 (M = Fe, Co, Ni, Cu, Zn, Pd, Cd, and others; X = Cl, Br, I) salts with an imidazolium or pyridinium halogenide. In this case, the dissolution of the MX_2 is associated with the formation of a complex anion and the resulting products are of the type MX_4^{2-}(imidazolium or pyridinium)$_2$. Especially the variants with longer alkyl chains often show interesting liquid crystalline behavior [63, 113, 133–138, 140, 186]. Dobbs et al. have shown that similar structures can also be generated using pseudohalogenides like CN^- [26]. It has to be noted, though, that better results are usually obtained if the reaction is not done in the melt but in solution, for example in acetonitrile, at elevated temperatures [134]. More recently, Del Sesto et al. have reported a series of ILs where paramagnetic metal ions like Fe, Co, Mn, or Gd were incorporated (Fig. 9). They suggest that the ILs could be candidates for magnetic or electrochromic switching; furthermore, they report that the tetraalkylphosphonium-based ionic liquids reveal anomalous magnetic behavior [187].

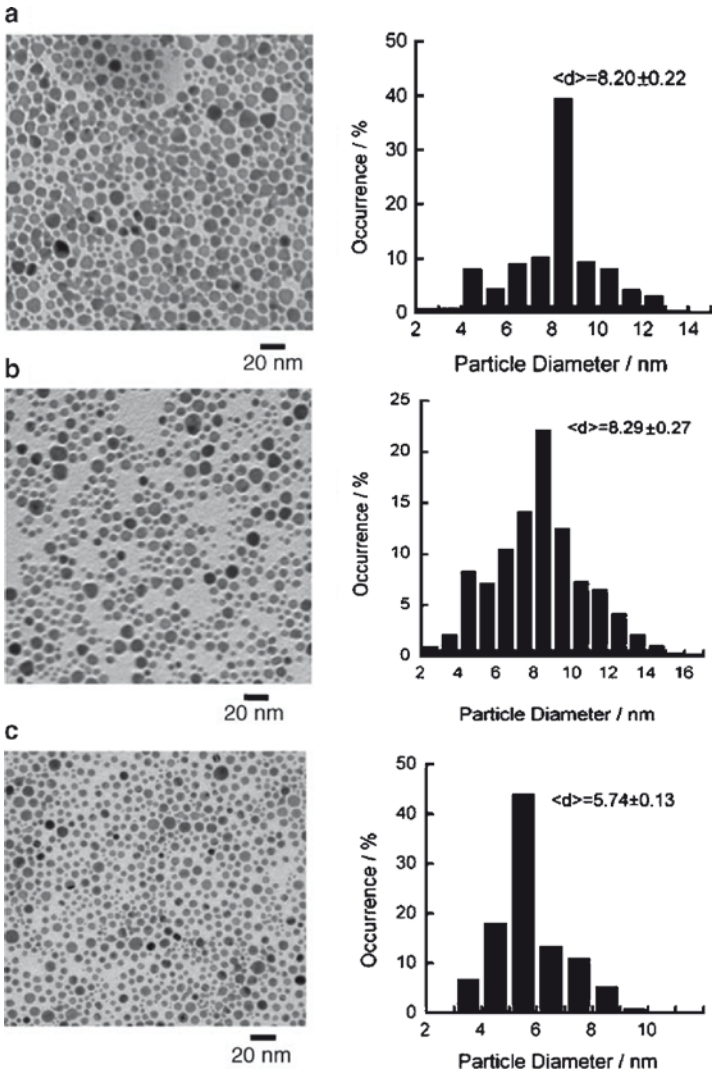

Fig. 8 TEM images and size distribution of Ag(0) nanoparticles obtained by chemical reduction of the Ag-ILs with $NaBH_4$. **a** [Ag(eth-hex-en)$_2$]NO_3*0.3 H_2O liquid. **b** [Ag(eth-hex-en)$_2$]NO_3*5 H_2O. **c** [Ag(eth-hex-en)2]NO_3·0.3 H_2O + eth-hex-en (molar ratio = 1:1). Image adapted from [181]. Image Copyright Wiley-VCH (2008)

Some materials can only be isolated as crystals or their liquid behavior has not been reported. Sun et al. reported on an interesting Bmim-octachlorotricuprate(II). The complex crystal is triclinic with space group P−1, $Z = 2$, with $a = 8.986(1)$, $b = 12.595(1)$, $c = 13.081(1)$ Å, $\alpha = 88.561(9)$, $\beta = 79.743(9)$, $\gamma = 81.724(9)°$ and dc = 1.734. The Cu atoms show square-pyramidal coordination geometry with a

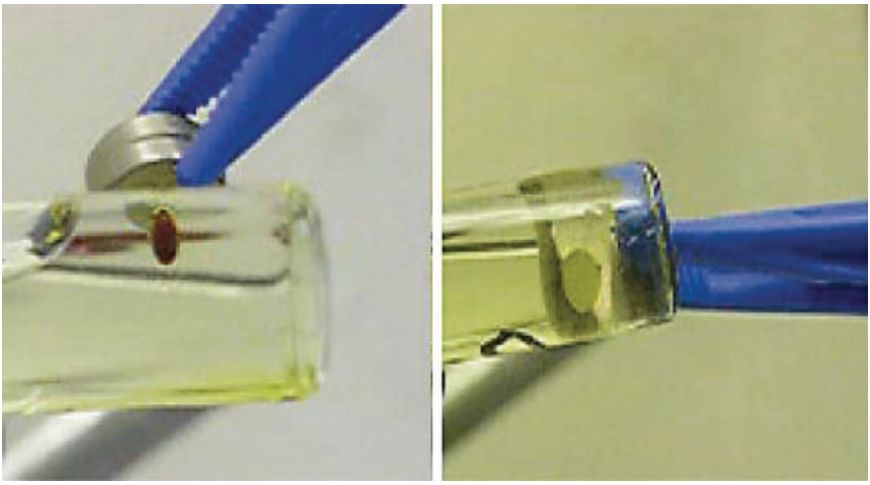

Fig. 9 Behavior of $[C_{10}mim][FeCl_4]$ (*left*) and $[PR_4][FeCl_4]$ (*right*) ionic liquid droplets in water when exposed to a $Nd_2Fe_{14}B$ magnet. Image adapted from [187]. Image Copyright Royal Society of Chemistry (2008). For color image see online version

long bond length Cu–Cl of 2.623–2.676 Å in axial direction [188]. Similarly, ILs can also be used for the growth of more complex structures. Willems et al. have reported the synthesis of $(Emim)_4[(Zr_6Fe)Br_{18}]$ and $(Emim)_4[(Zr_6Be)Br_{18}]$. The two cluster phases are isostructural with the monoclinic space group P21/c, $Z = 2$ [189].

It has been pointed out above that X-ray and neutron techniques are powerful methods to study the structure of ILs. In an early study, Crozier et al. have used EXAFS to in detail study the structure of solid and liquid $[Bu_4N][MnBr_3]$ and $[Bu_4N]_2[MnBr_4]$ between room temperature and 400 K [97]. In the molten state, the authors find Mn–Br bond distances of 2.46 and 2.50 Å for $[Bu_4N][MnBr_3]$ and $[Bu_4N]_2[MnBr_4]$, respectively. In addition, the authors found an approximate coordination number of 3 around the Mn in the liquid state and of 6 in the solid state, showing that in some cases quite drastic differences can occur upon melting.

More recently, several reports on the structure of molten CuBr have appeared. Using EXAFS, the authors have evaluated Cu–Cu, Br–Br, and Cu–Br distances. Overall the data seem to suggest that, unlike in the above example, the liquid and the solid structures are quite similar and are dominated by covalent interactions. Similar results have been found for AgBr [99, 120, 121].

Further EXAFS studies have focused on the relation between molten and solid Rb_2ZnC_{l4} and $ZnCl_2$/RbCl [103, 104]. On melting $ZnCl_2$, Zn is surrounded by tetrahedrally coordinated chlorines and an extended network forms via corner-sharing of chlorines. RbCl in contrast shows disorder in the chloride shell around the rubidium and a much more dynamic structure with strong movements of both the Rb and the Cl. Similar to the liquid crystalline ILs described above [113, 133–138, 140, 186], the $ZnCl_4^{2-}$ unit in Rb_2ZnCl_4 is an isolated unit. In contrast, the coordination

number around the Rb is between 8 and 9. In this case, the liquid and solid state structures are similar, but the authors point out that this does not always have to be the case [103, 104].

It is not surprising, given the wealth of information that can be extracted from EXAFS and related techniques, that in the recent past quite a number of studies on different aspects have appeared [101]. Dent et al. have studied the dissolution of Emim-MCl_4 in EmimCl–$AlCl_3$ binary mixtures (M = Mn, Co, Ni) [98]. The most important finding of this study is probably that, for the first time, it could be shown that IL components may or may not be innocent bystanders in a reaction. In particular, the authors found that with increasing $AlCl_3$ fraction, the coordination changes from MCl_4^{2-} to $[M(AlCl_3)_4]^-$. It was also found that $[Ni[AlCl_4]_3]^-$ species form in catalytically active chlororaluminate melts. Catalyst degradation was found to be due to the formation of tetrachloronickel species or by reduction to metallic nickel. Furthermore, EXAFS revealed the presence of carbene complexes in $NiCl_4^{2-}$-based ionic liquids used for Suzuki coupling [190].

Another important reaction, the Heck reaction catalyzed by palladium salts and complexes, has been studied as well via EXAFS [191]. The authors of the study highlight the importance of correlating structural data with reaction kinetics. Among others the authors showed that in chloride-based ionic liquids the Heck reaction shows poor reactivity until, at some point during the reaction, Pd nanoparticles form, which initiates the reaction. They pointed out that the correlation between the induction period and the nanoparticle formation was strong, and although the metal may not be the active site for the catalysis [91], the presence of Pd(0) is clearly important.

Roeper et al. have studied $NiCl_2$ in aluminium chloride/EmimCl ILs via cyclic voltammetry and EXAFS [192]. Acidic melts exhibit metal stripping peaks, while in basic melts no metal stripping peaks are observed. EXAFS again reveals that the d-element, in this case Ni, is tetrahedrally coordinated by chloride ions in the basic melt. In the acidic melts, the structure is more complicated as the Ni is coordinated by six chloride ions, which, however, are also coordinating to Al ions. In an interesting further study, Mallick et al. report the formation of Cr–Cr metal–metal bonds in $[Bmim]_2[CrCl_3]_3[OMe]_2$ (Fig. 10) [193].

Besides EXAFS and related techniques, electrochemical methods have been used extensively to characterize metals in ILs. Lagunas et al. studied the electrochemistry of the ferricenium/ferrocene couple in Bmim-based ILs [194, 195]. In a similar study, Rogers et al. studied ferrocene and cobaltocenium hexafluorophosphate in a range of common ILs, including phosphonium ILs. The authors report solubilities and diffusion coefficients for a variety of concentrations and suggest that both ferrocene and cobaltocenium hexafluorophosphate are useful and reliable internal standards for use in ILs [196].

Rogers et al. also studied the voltammetry and kinetics of the Ag/Ag^+ system *N*-butyl-*N*-methylpyrrolidinium bis(trifluoromethylsulfonyl)imide (Bmpyrr-NTf_2). AgOTf, $AgNTf_2$, and $AgNO_3$ [197]. In all cases the voltammetry gives rise to a redox couple characteristic of a deposition/stripping process at the Pt electrode surface. In the same study, the authors also investigated the volt-ammetry

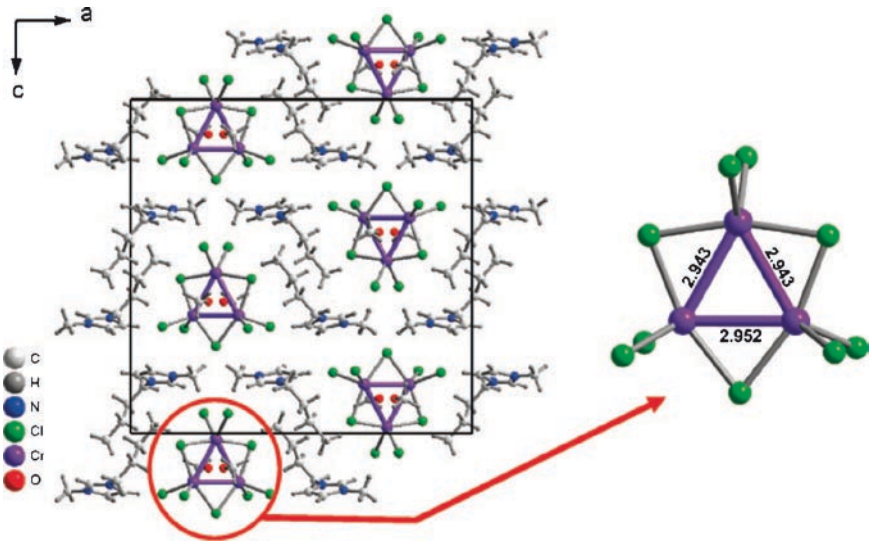

Fig. 10 $[Bmim]_2[CrCl_3]_3[OMe]_2$. View of the crystal structure along *b* (*left*); molecular $[CrCl_3]_3$ unit (*right*). Image adapted from [193]. Image Copyright American Chemical Society (2008). For color image see online version

and kinetics of TMPD/$TMPD^+$ (TMPD = *N*,*N*,*N*′,*N*′-tetramethyl-*p*-phenylenediamine). Given the faster kinetics of the latter system, the authors suggest that it may be better as a reference system in ILs than the Ag/Ag^+ system. Further electrochemical studies involve cyclic voltammetric studies of *trans*-$[Mn(CN)(CO)_2\{P(OPh)_3\}(Ph_2PCH_2PPh_2)]$ [198], and of a podand (PD), 1,3,5-tris(3-((ferrocenylmethyl)amino)pyridiniumyl)-2,4,6-triethylbenzene hexafluorophosphate, $[PD][PF_6]_3$ [199].

Metal containing ILs are also interesting for catalysis [9]. Forbes et al. have used a carboxylate-modified imidazolium IL for solubilizing Rh(II). The resulting Rh(II) dimer is an effective catalyst for the cyclopropanation of styrene using ethyl diazoacetate [200]. Further studies on Rh-catalyzed reactions suggest that *N*-heterocyclic carbenes are involved in hydroformylation reactions in ILs [201]. Dupont et al. reported the two-phase hydrogenation of dienes catalyzed by palladium acetylacetonate dissolved in Bmim-BF_4 [202]. Einloft et al. have reported the dimerization of ethylene to butenes using nickel(II) complexes dissolved in Bmim-$Cl/AlCl_3$ molten salt in the presence of $AlEtCl_2$ and aromatic solvents [203].

Illner et al. have studied in detail the formation kinetics of the active species *cis*-$[Pt^{II}(PPh_3)_2Cl(SnCl_3)]$ and *cis*-$[Pt^{II}(PPh_3)_2(SnCl_3)_2]$ from the hydroformylation catalyst precursor *cis*-$[Pt^{II}(PPh_3)_2Cl_2]$. They prepared several chlorostannate melts consisting of Bmim cations and $[Sn_xCl_y]^{(-y+2x)}$ anions with varying molar fraction of $SnCl_2$. Based on ^1H and ^{119}Sn NMR, the authors suggest that, depending on the concentration of Sn, significant structural changes affecting the catalytic activity occur in the anionic species [204].

On the coordination chemistry side, ligand substitution on metal complexes in ILs has attracted quite some interest. This is mainly due to the fact that both spectroscopic and catalytic properties are strongly governed by the nature of the ligands and the stability of their bond to a metal center. Begel et al. have studied the role of different ILs on ligand substitution reactions on $[Pt(terpy)Cl]^+$ (terpy = 2,2′:6′,2″-terpyridine) with thiourea with stopped-flow techniques. The substitution kinetics show similar trends if compared to conventional solvents with similar polarities. Moreover, much like in conventional solvents, the authors find an associative character of the substitution reaction [205]. These results are essentially supporting an earlier study by Weber et al., who found the same behavior [206].

Illner et al. have studied the substitution kinetics on $[M^{II}(terpy)Cl]^+$ complexes (M = Pt, Pd) in Emim-NTf_2 using stopped-flow techniques [207] and Albrecht et al. have shown that pyridinium salts that are similar to those used in ILs can undergo palladation. The resulting carbenes are, although not technically ILs, catalytically active for Suzuki couplings [208].

Although ILs are widely promoted for their interest in catalysis, Starkey Ott et al. have recently pointed out that ILs, or more accurately, solutions of metal ions or metal nanoparticles in ILs, can exhibit a quite different behavior. These authors have studied a model reaction, acetone hydrogenation, in Bmim-PF_6 [209]. Unlike what is commonly accepted, the authors suggest that the IL is a catalyst poison rather than an advantageous solvent for the hydrogenation. For example, the authors show that the presence of Bmim-PF_6 dramatically reduces the activity of preformed, previously catalytically active, Ir(0) nanoparticles. Interestingly, however, the authors suggest that bulk Ir is the active catalyst in the same reaction. This finding is in line with other reports showing that bulk gold is a very efficient (that is, in some cases better than nanoparticles and other high surface area systems) catalyst for carbon monoxide amination [210].

Besides catalysis, electrochemistry is one of the fields, where solutions of metal ions in ILs are of great importance [18, 19, 170, 211, 212]. Endres and colleagues have studied the electrodeposition of Ti from TiX_4 (X = F, Cl, I) in various NTf_2-based ILs [213]. However, in none of the cases could Ti be deposited, which was partly assigned to the low solubility of $TiCl_2$ and $TiCl_3$ intermediates.

Ionic liquids have also been evaluated for their application in mining. Whitehead et al. report on the leaching of Au, Ag, Cu, and base metals using Bmim-HSO_4 and some derivatives [214, 215]. The authors demonstrate that in many cases the ILs are much more efficient for metal recovery than the classically used acidic solutions both for natural ore and for some model compounds.

Although the authors do not discuss the behavior of the metal in the IL, two further studies are of interest in the context of the topic heavy elements in ILs. Perissi et al. have studied the interaction of ILs with AISI 304 and AISI 1018 steels, which are frequently used in solar energy technology [216]. The study clearly reveals that there are differences in the corrosion behavior of ILs. A similar study on AZ91D alloys shows that with Bmim-NTf_2 the corrosion rate is strongly temperature dependent. While corrosion is very slow at room temperature, it accelerates significantly at higher temperatures [217]. The authors identified two main

processes that are held responsible for the overall corrosion. First, the alloy metals form oxides and fluorides and. second, degradation products of the IL form a carbon-, nitrogen-, and fluorine-rich interlayer on the surface (Fig. 11).

3.4 Lanthanides and Actinides (f-Elements)

3.4.1 Lanthanides

The structure and behavior of lanthanides and actinides in ILs has recently been summarized in detail by Binnemans and the reader is referred to this excellent review for more details [71]. Among others, it has been pointed out that solvation of the metal ions by the IL components is a major issue in f-element coordination chemistry [71, 79, 218, 219]. Understanding the solvation is also a key to understanding f-element extraction processes. Among others, theoretical studies suggest that Ln^{3+} (Ln = La, Eu, Yb) are surrounded by six PF_6^- anions in Bmim-PF_6 and by 11–13 imidazolium ions in the second ionic sphere. The same authors also suggest that free lanthanide cations, that is, cations without a solvation shell, are poorly soluble in Bmim-PF_6 [149, 152, 220–223]. They also report that, while $[LnCl_6]^{3-}$ complexes are unstable in the gas phase, they can be stabilized by solvation in ILs.

In basic $AlCl_3$-EmimCl ILs (that is, chloroaluminate ILs with an excess of chloride ions), calculations predict the existence of different chloro complexes for Eu^{3+} and Eu^{2+} [223]. Similarly, in $AlCl_3$-EmimCl ILs containing some excess of chloride, $[NdCl_6]^{3-}$ species could be identified [224].

Similar to the halometallates described for the d-elements above, lanthanides also exhibit a rich variety of halogen-metal coordination chemistry in ILs.

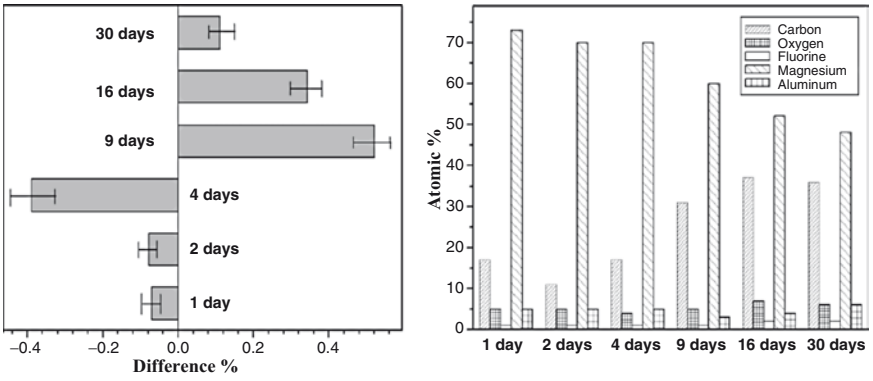

Fig. 11 *Top*: weight changes of AZ91D alloy samples vs immersion time in Bmim-NTf_2. *Bottom*: chemical composition of the sample surface determined via energy dispersive X-ray spectroscopy (EDXS) showing the buildup of a contamination layer. Image adapted from [217]. Image Copyright Wiley-VCH (2007)

Interestingly however, here the fluoride ion is also an important ligand [100, 223, 225–231]. Pellens et al. report the crystal structure of $(C_6H_{11}N_2)_3[EuBr_6]$, a more complex structure where $[EuBr_6]^{3-}$ anions are located at the corners and face-centers of the monoclinic unit cell [232].

Often, however, the halogenide ligands are replaced by other ligands, most prominently IL anions such as triflate [100, 233, 234]. Nockemann et al. have shown that the thiocyanate ion also enables the synthesis of lanthanide ILs (Fig. 12) [67]. These ILs are miscible with hydrophobic ILs like Bmim-NTf_2, but are rapidly hydrolyzed in aqueous solutions.

More common than most anions in ILs, NTf_2 has attracted a tremendous interest, mostly due to its favorable properties like high thermal stability of the resulting ILs. Generally, NTf_2 is considered a non-coordinating anion, but there have been several reports showing that this is, in particular in dry ILs, not always the case. For example, $[La(NTf_2)_3(H_2O)_3]$ crystallizes in the cubic space group P213 with the NTf_2 ligand as a bidentate ligand [235]. Babai and Mudring have shown that in the reaction of

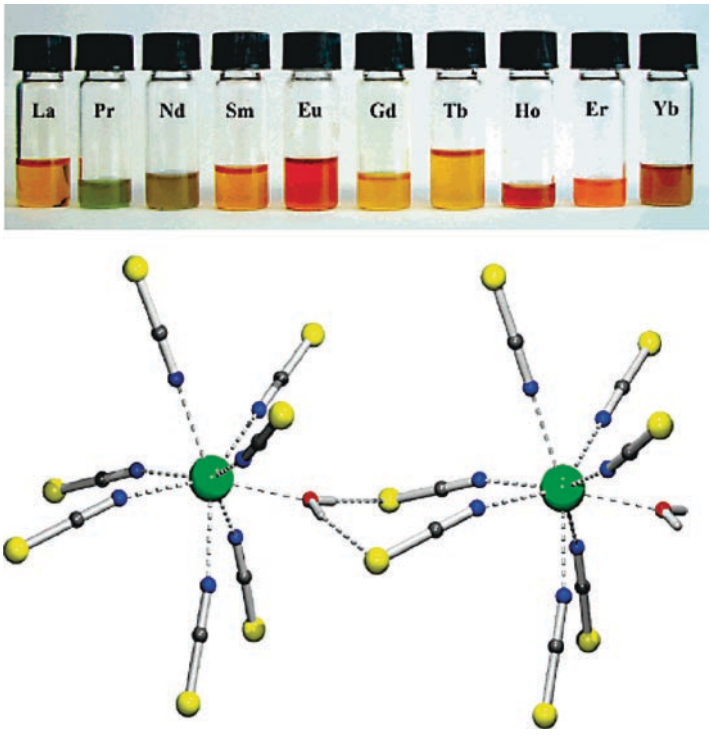

Fig. 12 *Top*: ionic liquids of the type $[Bmim]_4[Ln(NCS)_7(H_2O)]$ with Ln = La, Pr, Nd, Sm, Eu, Gd, Tb, Ho, Er, and Yb. The color is due to the metallate anion. *Bottom*: molecular structure of the anionic unit $[La(NCS)_7(H_2O)]^{4-}$ showing the hydrogen bonding from coordinated water molecules to the isothiocyanate anions. The $[Bmim]^+$ cations were omitted for clarity. Image adapted from [67]. Image copyright American Chemical Society (2006). For color image see online version

PrI_3 with 1-butyl-1-methylpyrrolidinium (Bmpyr) NTf_2, crystals of $[Bmpyr]_4[PrI_6][NTf_2]$ were obtained [233, 236]. The crystal structures of $[Bmpyr]_4[LaI_6][NTf_2]$ and $[Bmpyr]_4[ErI_6][NTf_2]$ were reported later [226]. With divalent ytterbium, NTf_2^- forms the complex $[Mppyr]_2[Yb(NTf_2)_4]$ (Mppyr = 1-methyl-1-propylpyrrolidinium) [233]. A subsequent study describes the crystal structures of $[Bmpyr]_2[Ln(NTf_2)_5]$ (Ln = Nd, Tb) and $[Bmpyr][Ln(NTf_2)_4]$ (Ln = Tm, Lu) [237]. In these compounds, only coordination via the oxygen atoms of the NTf_2^- anion is observed and discrete anionic complexes of the types $[Ln(NTf_2)_5]^{2-}$ and $[Ln(NTf_2)_4]^-$ are built. More recently the same group reported the first homoleptic bis(trifluoromethanesulfonyl) amide complex of yttrium $[Bmim][Y(NTf_2)_4]$ [238]. Further studies with the NTf_2^- anion include studies on the role of alkyl chain lengths on pyrrolidinium ionic liquids on the formation of Sm and Nd complexes [239, 240] and Eu(III) clusters [241].

Several of the above studies point to the conformational flexibility of NTf_2^- anions, which can adopt both *cis* and *trans* conformations; see also the above-mentioned examples of the Li-NTf_2 systems [126, 131, 154–156, 239]. Binnemans has suggested that the conformational flexibility of the NTf_2^- anion is the main culprit for the often poor quality of bis(trifluoromethylsulfonyl)imide complex crystals [71].

Stumpf et al. have shown that the azide ion N_3^- can coordinate to Eu(III) and the actinides Cm(III) and Am(III) in Bmim-NTf_2 using time-resolved fluorescence spectroscopy and EXAFS (Fig. 13) [242]. The complexation of Eu-triflate starts at lower concentration of the azide ion than when the perchlorate ion is used. The authors ascribe this observation to the stronger interaction of the perchlorate ion with the Eu(III) ion than the triflate. Moreover, the authors show that, in the case of the actinides, the complexation is kinetically strongly hindered and that several metal-azide complexes form in Bmim-NTf_2. The same authors have also studied the solvation of $Eu(ClO_4)_3$, $Eu(CF_3SO_3)_3$, $Cm(ClO_4)_3$ and $Am(ClO_4)_3$ in Bmim-NTf_2. They found that the ligands can be arranged according to their relative strengths, which are the same for all elements studied: $ClO_4^- > OTf^- \geq NTf_2^- > H_2O$ [105].

Lopes et al. have reported that ethylammonium nitrate is also a solvent for inorganic salts, as both $LaCl_3$ and Cs_2UCl_6 can be dissolved at 25 °C [243]. Finally, like the tetrahalometallates that have been described for the d-elements [63, 113, 133–138, 140, 186], there are lanthanide ILs containing one or several metals as an integral part [67, 244]. A somewhat exotic example is an IL based on a polyoxometallate $Na_{13}[Ln(TiW_{11}O_{39})_2]^*xH_2O$. ($x$ = 27–44) [244].

3.4.2 Actinides

The coordination chemistry of actinides in ionic liquids has recently been reviewed [71, 92, 245] and will therefore only be discussed briefly. Interestingly, the coordination chemistry of uranium has attracted quite some interest, which may partly be due to the fact that ILs have been studied as an effective alternative for nuclear waste treatment. For example, uranium exhibits a rich coordination chemistry with halogenide anions [246–252] although it has been suggested that the uranyl ion

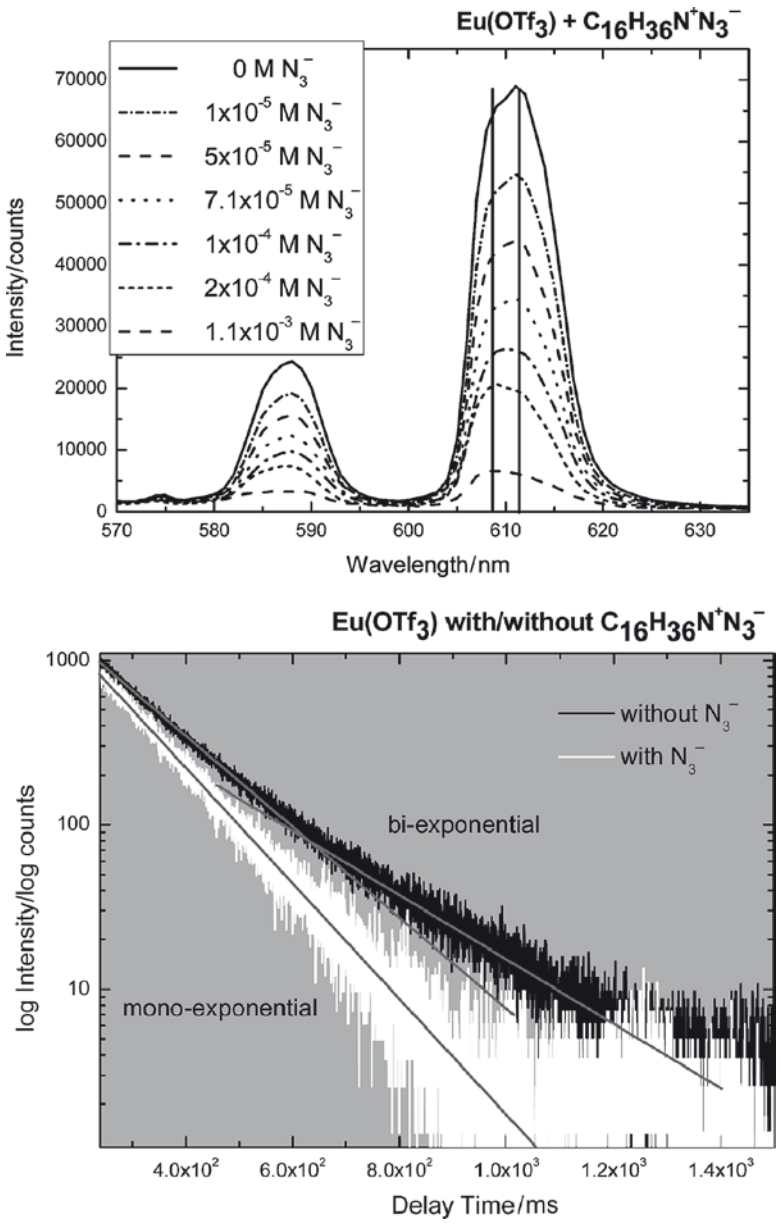

Fig. 13 *Top*: luminescence spectra of 1×10^{-2} M $Eu(OTf)_3$ dissolved in Bmim-NTf_2 at different $C_{16}H_{36}N^+$ N_3^- concentrations. With increasing N_3^- concentration, the luminescence decreases and the shape of the emission signal changes. *Bottom*: luminescence of 1×10^{-2} M $Eu(OTf)_3$ dissolved in Bmim-NTf_2 reveals a biexponential decay behavior. With the addition of 1×10^{-5} M $C_{16}H_{36}N^+$ N_3^- the decay behavior becomes monoexponential. Image adapted from [242]. Image Copyright American Chemical Society (2008)

exists in the dehydrated Bmim nonafluorobutanesulfonate as a naked cation, with no ligands in its equatorial plane [253].

Some of the findings have been supported by computational chemistry [221] Again it was found that the presence of water has dramatic influence of the structures of the resulting complexes. In wet Bmim-PF_6, the uranyl ion forms $[UO_2(H_2O)_5]^{2+}$ complexes are surrounded by eight PF_6^- anions; authors have further observed a strong influence of the presence of water in a few other cases [149, 152, 254].

Schurhammer and Wipff have shown that the solvation of the $[UCl_6]^{3-}$ complexes depends on the oxidation state of the uranium and the nature of the ionic liquid. The first coordination shell of $[UCl_6]^{3-}$ contains only solvent cations. The first solvation shell is surrounded by a second shell that is mainly anionic in nature [255]. Similarly, $[NpCl_6]^{2-}$ and $[PuCl_6]^{2-}$ maintain their structural integrity upon dissolution in Bmim-NTf_2 [256]. Time-resolved laser fluorescence spectroscopy shows that the coordination of Cm(III) in Bmim-NTf_2 is very similar to that of Eu(III) in the same ionic liquid [257]. An interesting new development is the dissolution of U(VI) in a betainium TSIL [258].

Besides the halogenide anions, again the NTf_2^- anion has attracted quite some attention. Gaillard et al. have shown that the NTf_2^- anion, unlike PF_6^- and BF_4^-, does not coordinate to the uranyl ion, at least in wet ILs [259]. Further ligands include nitrate and oxalate [260–263] along with triflate or perchlorate [264].

Cocalia et al. have reported the extraction of Am(III) with dialkylphosphoric or dialkylphosphinic acids from aqueous solution to 1-decyl-3-methylimidazolium bis(trifluoromethanesulfonyl)imide [265]. Their results suggest that the extraction is quite similar to the behavior found for organic solvent systems. Further studies on actinoid extraction using ILs have been reported by Visser et al. [153].

One important point to consider if ILs are to be used in the nuclear fuel cycle is their stability against radiation. Allen et al. have subjected imidazolium ILs to α, β, and γ radiation and studied their stability vs irradiation type and dose [266]. These preliminary results suggest that IL stability is similar to that of benzene, but much higher than that of mixtures of tributylphosphate and kerosine under similar irradiation conditions. That is, imidazolium ILs are rather radiation resistant and no significant decomposition was reported.

Although not directly related to heavy elements in ionic liquids, Krossing and coworkers have investigated the Gibbs free energy of fusion ΔGfus for the phase transition IL(solid) → IL(liquid). Using a set of theoretical tools, including COSMO modeling and quantum chemical calculations, along with experimental methods such as DSC, they showed that ΔGfus is negative, which is expected for liquids. These data thus show that the liquid state is the thermodynamically most favorable at ambient conditions [267-268]. Moreover, the same authors showed that the viscosities, conductivities, and densities of ILs can be predicted based on the molecular volume of the IL components [269]. Finally, the work of Dai and colleagues should also be listed more completely [270-272]. These authors have introduced an interesting silver/olefin complex-based IL, which can, for example, be used in separation processes.

4 Summary and Conclusion

Ionic liquids have been promoted for virtually every application in chemistry and materials science one may think of, but as with many other fields, some will prove more interesting and practical than others. In spite of the large amount of data that has already been assembled, the current chapter shows that there are still many open questions, both on a basic scientific and on an application-related level. This especially applies to the topic of this chapter, heavy elements in ILs. This is mainly due to the sometimes quite complex behavior of metal ions and clusters in an already complex liquid and an even more complex interplay between the two. It is therefore clear that the future will hold surprises, but also that potentially new and unexpected applications will arise.

Note added in the proof

Although not directly related to heavy elements in ionic liquids, Krossing and coworkers have investigated the Gibbs free energy of fusion ΔG_{fus} for the phase transition IL(solid) $\rightarrow$ IL(liquid). Using a set of theoretical tools, including COSMO modeling and quantum chemical calculations, along with experimental methods such as DSC, they showed that ΔG_{fus} is negative, which is expected for liquids. These data thus show that the liquid state is the thermodynamically most favorable at ambient conditions [267–268]. Moreover, the same authors showed that the viscosities, conductivities, and densities of ILs can be predicted based on the moleculer volume of the IL components [269]. Finally, the work of Dai and colleagues should also be listed more completely [270–272]. These authors have introduced an interesting silver/olefin complex-based IL, which can, for example, be used in separation processes.

Acknowledgements I thank the members of my "ionic liquids team" P. Steiner, D. Mumalo-Djokic, Z. Li, A. Uhlmann, A. Hedderich, and R. Göbel for useful comments and their dedication to ILs and the Swiss National Science Foundation, the Fonds der Chemischen Industrie, the Holcim Stiftung Wissen, ERA Chemistry, the MPI of Colloids and Interfaces, and the University of Potsdam for funding.

References

1. Roger RD, Seddon KR Eds, Ionic liquids: industrial applications for green chemistry. American Chemical Society, 2002
2. Roger RD, Seddon KR Eds, Ionic liquids as green solvents: progress and prospects. American Chemical Society, 2003
3. Roger RD, Seddon KR Eds, Ionic liquids IIIA: fundamentals, progress, challenges, and opportunities: properties and structure. American Chemical Society, 2005

4. Wasserscheid, P., Welton, T., Inorg. Chem., 2008, 47 (22), 10758. Ionic liquids in synthesis, 2nd edn. Wiley, Weinheim, 2007
5. MacFarlane DR, Forsyth M, Howlett PC, Pringle JM, Sun J, Annat G, Neil W, Izgorodina EI (2007) Acc Chem Res 40:1165
6. Plechkova NV, Seddon KR (2008) Chem Soc Rev 37:123
7. Wasserscheid P, Keim W (2000) Angew Chem Int Ed 39:3772
8. Welton T (1999) Chem Rev 99:2071
9. Giernoth R (2007) Top Curr Chem 276:1
10. Antonietti M, Kuang D, Smarsly B, Zhou Y (2004) Angew Chem Int Ed 43:4988
11. Reichert WM, Holbrey JD, Vigour KB, Morgan TD, Broker GA, Rogers RD (2006) Chem Commun 4767
12. Taubert A (2005) Acta Chim Slov 52:183
13. Taubert A, Li Z (2007) Dalton Trans 7:723
14. Morris RE (2008) Angew Chem Int Ed 47:443
15. Parnham ER, Morris RE (2007) Acc Chem Res 40:1005
16. Hasan M, Kozhevnikov IV, Rafiq M, Siddiqui H, Femoni C, Steiner A, Winterton N (2001) Inorg Chem 40:795
17. Willems JB, Rohm HW, Geers C, Köckerling M (2007) Inorg Chem 46:6197
18. Zein El Abedin S, Endres F (2006) Chem Phys Chem 7:58
19. El Abedin SZ, Endres F (2007) Acc Chem Res 40:1106
20. Zhou Y, Antonietti M (2003) Adv Mater 15:1452
21. Zhou Y, Antonietti M (2003) Chem Commun: 2564
22. Zhou Y, Antonietti M (2003) J Am Chem Soc 125:14960
23. Zhou Y, Antonietti M (2004) Chem Mater 16:544
24. Nakashima T, Kimizuka N (2003) J Am Chem Soc 125:6386
25. Taubert A (2004) Angew Chem Int Ed 43:5380
26. Dobbs W, Suisse J-M, Douce L, Welter R (2006) Angew Chem Int Ed 45:4179
27. Dupont J, Fonseca GS, Umpierre AP, Fichtner PFP, Teixeira SRJ (2002) Am Chem Soc 124:4228
28. Fonseca GS, Umpierre AP, Fichtner PFP, Teixeira SR, Dupont J (2003) Chem Eur J 9:3263
29. Scheeren CW, Machado G, Dupont J, Fichtner PFP, Ribeiro Texeira S (2003) Inorg Chem 42:4738
30. Scheeren CW, Machado G, Teixeira SR, Morais J, Domingos JB, Dupont J (2006) J Phys Chem B 110:13011
31. Taubert A, Palivan C, Casse O, Gozzo F, Schmitt B (2007) J Phys Chem C 111:4077
32. Taubert A, Steiner P, Mantion A (2005) J Phys Chem B 109:15542
33. Brezesinski T, Erpen C, Iimura K, Smarsly B (2005) Chem Mater 17:1683
34. Taubert A, Uhlmann A, Hedderich A, Kirchhoff K (2008) Inorg. Chem., 2008, 47(22), 10758.
35. Dai S, Ju YH, Gao HJ, Lin JS, Pennycook SJ, Barnes CE (2000) Chem Commun 243
36. Yang L-X, Zhu Y-J, Wang W-W, Tong H, Ruan M-L (2006) J Phys Chem B 110:6609
37. Dupont J, Fonseca GS, Umpierre AP, Fichtner PFP, Teixeira SR (2002) J Am Chem Soc 124:4228
38. Desmukh RR, Rajagopal R, Srinivasan KV (2001) Chem Commun 1544
39. Swatloski RP, Spear SK, Holbrey JD, Rogers RD (2002) J Am Chem Soc 124:4974
40. Rossi LM, Dupont J, Machado G, Fichtner PFP, Radtke C, Baumvol IJR, Teixeira SR (2004) J Braz Chem Soc 15:904
41. Trewyn BG, Whitman CM, Lin VS-Y (2004) Nano Lett 4:2139
42. Yoo K, Choi H, Dionysiou DD (2004) Chem Commun 2000
43. Cassol CC, Umpierrre AP, Machado G, Wolke SI, Dupont J (2005) J Am Chem Soc 127:3298
44. Jiang J, Yu S-H, Yao W-T, Ge H, Zhang G-Z (2005) Chem Mater 17:6094
45. Jiang Y, Zhu Y-J (2005) J Phys Chem B 109:4361
46. Wang Y, Yang H (2005) J Am Chem Soc 127:5316
47. Liu Z, Sun Z, Han B, Zhang J, Huang J, Du J, Miao S (2006) J Nanosci Nanotechol 6:175
48. Gao S, Zhang H, Wang X, Mai W, Peng C, Ge L (2005) Nanotechnology 16:1234

49. Li Z, Liu Z, Zhang J, Han B, Du J, Gao Y, Jiang T (2005) J Phys Chem B 109:14445
50. Li Z, Zhang J, Du J, Gao H, Gao Y, Mu T, Han B (2005) Mater Lett 59:963
51. Li Z, Zhang J, Du J, Han B, Wang J (2005) Coll Surf A 83:19
52. Du J, Liu Z, Li Z, Han B, Huang Y, Zhang J (2005) Microporous Mesoporous Mater 83:145
53. Cooper ER, Andrews CD, Wheatley PS, Webb PB, Wormald P, Morris RE (2004) Nature 430:1012
54. Parnham ER, Morris RE (2006) J Mater Chem 16:3682
55. Parnham ER, Morris RE (2006) Chem Mater 18:4882
56. Parnham ER, Morris RE (2006) J Am Chem Soc 128:2204
57. Parnham ER, Wheatley PS, Morris RE (2006) Chem Commun 380
58. Kaper H, Endres F, Djerdj I, Antonietti M, Smarsly BM, Maier J, Hu Y-S (2007) Small 3:1753
59. Wang T, Kaper H, Antonietti M, Smarsly B (2007) Langmuir 23:1489
60. Farag HK, Endres F (2008) J Mater Chem 18:442
61. Zhu H, Huang J-F, Pan Z, Dai S (2006) Chem Mater 18:4473
62. Lee CK, Vasam CS, Huang TW, Wang HMJ, Yang RY, Lee CS, Lin IJB (2006) Organometallics 25:3768
63. Taubert A, Arbell I, Mecke A, Graf P (2006) Gold Bull 39:205
64. Nockemann P, Thijs B, Pittois S, Thoen J, Glorieux C, van Hecke K, van Meervelt L, Kirchner B, Binnemans K (2006) J Phys Chem B 110:20978
65. Nockemann P, Thijs B, Van Hecke K, Van Meervelt L, Binnemans K (2008) Cryst Growth Design 8:1353
66. Ren L, Meng L, Lu Q, Fei Z, Dyson PJ (2008) J Colloid Interf Sci 323:260
67. Nockemann P, Thijs B, Postelmans N, van Hecke K, van Meervelt L, Binnemans K (2006) J Am Chem Soc 128:13658
68. Yoshida Y, Fujii J, Saito G, Hiramatsu T, Sato N (2006) J Mater Chem 16:724
69. Lin IJB, Vasam CS (2005) J Organomet Chem 690:3498
70. Hasan M, Kozhevnikov IV, Siddiqui MRH, Steiner A, Winterton N (1999) N Inorg Chem 38:5637
71. Binnemans K (2007) Chem Rev 107:2592
72. Liao J-H, Huang W-C (2006) Inorg Chem Commun 9:1227
73. Liao J-H, Wu PC, Huang W-C (2006) Cryst Growth Design 6:1062
74. Mudring A-V, Babai A, Arenz S, Giernoth R, Binnemans K, Driesen K, Nockemann P (2006) J Alloys Compd 418:204
75. Earle MJ, Hakala U, Hardacre C, Karkkainen J, McAuley BJ, Rooney DW, Seddon KR, Thompson JM, Waehaelae K (2005) Chem Commun 903
76. Puntus LN, Schenk KJ, Bünzli J-CG (2005) Eur J Inorg Chem 23:4739
77. Guillet E, Imbert D, Scopelliti R, Bünzli J-CG (2004) Chem Mater 16:4063
78. Binnemans K (2005) Rare-earth beta-diketonates. In: Gschneidner KA Jr, Bünzli J-CG, Pecharsky VK (eds) Handbook on the physics and chemistry of rare earths, Amsterdam, vol 35, p 105
79. Binnemans K, Goerller-Walrand C (2002) Chem Rev 102:2303
80. Nockemann P, Beurer E, Driesen K, Van Deun R, Van Hecke K, Van Meervelt L, Binnemans K (2005) Chem Commun 4354
81. Lunstroot K, Driesen K, Nockemann P, Goerller-Walrand C, Binnemans K, Bellayer S, Le Bideau J, Vioux A (2006) Chem Mater 18:5711
82. Driesen K, Nockemann P, Binnemans K (2004) Chem Phys Lett 395:306
83. Arenz S, Babai A, Binnemans K, Driesen K, Giernoth R, Mudring A-V, Nockemann P (2005) Chem Phys Lett 402:75
84. Silvester DS, Compton RG (2006) Z Phys Chem 220:1247
85. Hardacre C, Holbrey JD, Nieuwenhuyzen M, Youngs TGA (2007) Acc Chem Res 40:1146
86. Binnemans K (2005) Chem Rev 105:4148
87. Endres F, Abedin SZE (2006) Phys Chem Chem Phys 8:2101
88. Harper JB, Kobrak MN (2006) Mini-Rev Org Chem 3:253
89. Dupont J (2004) J Braz Chem Soc 15:341
90. Dupont J, de Souza RF, Suarez PAZ (2002) Chem Rev 102:3667

91. Phan NTS, Van Der Sluys M, Jones CW (2006) Adv Synth Catal 348:609
92. Cocalia VA, Gutowski KE, Rogers RD (2006) Coord Chem Rev 250:755
93. MacFarlane DR, Seddon KR (2007) Aust J Chem 60:3
94. Hardacre C, Holbrey JD, McMath SEJ, Nieuwenhuyzen M (2002) ACS Symp Ser 818:400
95. Hardacre C, Holbrey JD, Mullan CL, Nieuwenhuyzen M, Youngs TGA, Bowron DT (2008) J Phys Chem B 112:8049
96. Hardacre C, McMath SEJ, Nieuwenhuyzen M, Bowron DT, Soper AK (2003) J Phys C 15:S159
97. Crozier ED, Alberding N, Sundheim BR (1983) J Chem Phys 79:943
98. Dent AJ, Seddon KR, Welton T (1990) Chem Commun 315
99. Di Cicco A (1996) J Phys: Condes Matter 8:9341
100. Gaillard C, Billard I, Chaumont A, Mekki S, Ouadi A, Denecke MA, Moutiers G, Wipff G (2005) Inorg Chem 44:8355
101. Hardacre C (2005) Annu Rev Mater Res 35:29
102. Jensen MP, Dzielawa JA, Rickert P, Dietz ML (2002) J Am Chem Soc 124:10664
103. Li HF, Lu KQ, Wu ZH, Dong J (1994) J Phys Condens Matter 6:3629
104. Lu KQ, Li HF, Wu ZH, Dong J, Cheng ZN (1995) Physica B 208:339
105. Stumpf S, Billard I, Gaillard C, Panak PJ, Dardenne K (2008) Radiochim Acta 96:1
106. Hunt PA, Gould IR, Kirchner B (2007) Aust J Chem 60:9
107. Kirchner B, Seitsonen AP (2007) Inorg Chem 46:2751
108. Kirchner B, Seitsonen AP, Hutter J (2006) J Phys Chem B 110:11475
109. Kossmann S, Thar J, Kirchner B, Hunt PA, Welton T (2006) J Chem Phys 124:174506/1
110. Nockemann P, Thijs B, Driesen K, Janssen CR, Van Hecke K, Van Meervelt L, Kossmann S, Kirchner B, Binnemans K (2007) J Phys Chem B 111:5254
111. Zahn S, Uhlig F, Thar J, Spickermann C, Kirchner B (2008) Angew Chem Int Ed 47:3639
112. Carmichael AJ, Hardacre C, Holbrey JD, Nieuwenhuyzen M, Seddon KR (2001) Mol Phys 99:795
113. Hardacre C, Holbrey JD, McCormac PB, McMath SEJ, Nieuwenhuyzen M, Seddon KR (2001) J Mater Chem 11:346
114. Lopes JNAC, Padua AAH (2006) J Phys Chem B 110:3330
115. Edwards FG, Enderby JE, Howe RA, Page DI (1975) J Phys C 8:3483
116. Biggin S, Enderby JE (1982) J Phys C 15:L305
117. Igarashi K, Okamoto Y, Mochinaga J, Ohno H (1998) J Chem Soc Faraday Trans 1 84:4407
118. Hardacre C, Holbrey JD, McMath SEJ, Bowron DT, Soper AK (2003) J Chem Phys 118:273
119. Deetlefs M, Hardacre C, Nieuwenhuyzen M, Padua AAH, Sheppard O, Soper AK (2006) J Phys Chem B 110:12055
120. Di Cicco A, Minicucci M, Filipponi A (1997) Phys Rev Lett 78:460
121. Minicucci M, Di Cicco A (1997) Phys Rev B 56:11456
122. Soper AK (1996) Chem Phys 202:295
123. Soper AK (2000) Chem Phys 258:121
124. Soper AK (2001) Mol Phys 99:1503
125. Holbrey JD, Reichert WM, Rogers RD (2004) Dalton Trans 2267
126. Hardwick LJ, Holzapfel M, Wokaun A, Novak P (2007) J Raman Spectrosc 38:10
127. Umebayashi Y, Mitsugi T, Fukuda S, Fujimori T, Fujii K, Kanzaki R, Takeuchi M, Ishiguro S-I (2007) J Phys Chem B 111:13028
128. Matsumoto K, Hagiwara R, Tamada O (2006) Solid State Sci 8:1103
129. Umebayashi Y, Fujimori T, Sukizaki T, Asada M, Fujii K, Kanzaki R, Ishiguro S (2005) J Phys Chem A 109:8976
130. Fujimori T, Fujii K, Kanzaki R, Chiba K, Yamamoto H, Umebayashi Y, Ishiguro S (2007) J Mol Liq 131/132:216
131. Fujii K, Kanzaki Takamuku T, Fujimori T, Umebayashi Y, Ishiguro S (2006) J Phys Chem B 110:8179
132. Dupont J, Spencer J (2004) Angew Chem Int Ed 43:5296

133. Bowlas CJ, Bruce DW, Seddon KR (1996) Chem Commun 1625
134. Neve F, Francescangeli O, Crispini A, Charmant A (2001) J Chem Mater 13:2032
135. Neve F, Francescangeli O, Crispini A (2002) Inorg Chim Acta 338:51
136. Neve F, Crispini A, Armentano S (1998) Chem Mater 10:1904
137. Neve F, Imperor-Clerc M (2004) Liq Cryst 31:907
138. Downard A, Earle MJ, Hardacre C, McMath SEJ, Nieuwenhuyzen M, Teat S (2004) J Chem Mater 16:43
139. Bradley AE, Hardacre C, Holbrey JD, Johnston S, McMath SEJ, Nieuwenhuyzen M (2002) Chem Mater 14:629
140. Lee CK, Peng HH, Lin IJB (2004) Chem Mater 16:530
141. Visser AE, Swatloski RP, Reichert WM, Mayton R, Sheff S, Wierzbicki A, Davis JH, Rogers RD (2001) Chem Commun 135
142. Visser AE, Swatloski RP, Reichert WM, Mayton R, Sheff S, Wierzbicki A, Davis JH, Rogers RD (2002) Environ Sci Technol 36:2523
143. Davis JH (2004) Chem Lett 33(9):1072
144. Geldbach TJ, Dyson PJ (2004) J Am Chem Soc 126:8114
145. Li Z, Geßner A, Richters JP, Kalden J, Voss T, Kübel C, Taubert A (2008) Adv Mater 20:1279
146. Li Z, Rabu P, Strauch P, Mantion A, Taubert A (2008) Chem Eur J., 14:18409 DOI: 10.1002/chem. 200800106
147. Li Z, Shkilnyy A, Taubert A (2008) Cryst Growth Design, 8(12): 4526 accepted for publication
148. Billard I, Mekki S, Gaillard C, Hesemann P, Moutiers G, Mariet C, Bünzli J-CG (2004) Eur J Inorg Chem 23: 4739
149. Chaumont A, Wipff G (2004) Inorg Chem 43:5891
150. Visser AE, Rogers RD (2003) J Solid State Chem 171:109
151. Visser AE, Swatloski RP, Griffin ST, Hartman DH, Rogers RD (2001) Sep Sci Technol 36:785
152. Chaumont A, Wipff G (2004) Chem Eur J 10:3919
153. Visser AE, Jensen MP, Laszak I, Nash KL, Choppin GR, Rogers RD (2003) Inorg Chem 42:2197
154. Lassegues J, Grondin J, Talaga D (2006) Phys Chem Chem Phys 8:5629
155. Johansson P, Jacobsson P (2001) J Phys Chem A 105:8504
156. Gejji SP, Suresh CH, Babu K, Gadre SR (1999) J Phys Chem A 103:7474
157. Babai A, Mudring A-V (2006) Inorg Chem 45:3249
158. Endres F, Zein El Abedin S, Borissenko N (2006) Z Phys Chem 220:1377
159. Bazito FFC, Kawano Y, Torresi RM (2007) Electrochim Acta 52:6427
160. Popov K, Ronkkomaki H, Hannu-Kuure M, Kuokkanen T, Lajunen M, Vendilo A, Oksman P, Lajunen LHJ (2007) J Inclusion Phenom Macrocycl Chem 59:377
161. Dietz ML, Dzielawa JA, Laszak I, Young BA, Jensen MP (2003) Green Chem 5:682
162. Jensen MP, Neuefeind J, Beitz JV, Skanthakumar S, Soderholm L (2003) J Am Chem Soc 125:15466
163. Rogers EI, Silvester DS, Aldous L, Hardacre C, Compton RG (2008) J Phys Chem C 112:6551
164. Takahashi S, Koura N, Murase M, Ohno H (1986) J Chem Soc Faraday Trans 2 82:49
165. Takahashi S, Suzuya K, Kohara S, Koura N, Curtiss LA, Saboungi M-L (1999) Z Phys Chem 209:209
166. Trouw FR, Price DL (1999) Annu Rev Phys Chem 50:571
167. Lee Y-C, Price DL, Curtiss LA, Ratner MA, Shriver DF (2001) J Chem Phys 114:4591
168. Da Silveira Neto BA, Ebeling G, Goncalves RS, Gozzo FC, Eberlin MN, Dupont J (2004) Synthesis 1155
169. Timofte T, Pitula S, Mudring A-V (2007) Inorg Chem 46:10938
170. Liu QX, El Abedin SZ, Endres F (2008) J Electrochem Soc 155:D357
171. Rogers EI, Streeter I, Aldous L, Hardacre C, Compton RG (2008) J Phys Chem C 112:10976

172. Silvester DS, Aldous L, Lagunas MC, Hardacre C, Compton RG (2006) J Phys Chem B 110:22035
173. Hagiwara R, Matsumoto K, Tsuda T, Ito Y, Kohara S, Suzuya K, Matsumoto H, Miyazaki Y (2002) J Non-Cryst Solids 312/314:414
174. Matsumoto K, Hagiwara R, Ito Y, Kohara S, Suzuya K (2003) Nucl Instr Methods Phys Res B 199:29
175. Shodai Y, Kohara S, Ohishi Y, Inaba M, Tasaka A (2004) J Phys Chem A 108:1127
176. Fei Z, Geldbach TJ, Zhao D, Dyson P (2006) J Chem Eur J:12
177. Silva MR, Paixao JA, Beja AM, da Veiga LA, Martin-Gil J (2002) J Chem Crystallogr 31:167
178. Yang G, Chen HA, Zhou ZY, Chen XM (1999) J Chem Crystallogr 29:309
179. Harjani JR, Friscic T, MacGillivray LR, Singer RD (2006) Inorg Chem 45:10025
180. Tan R, Yin D, Yu N, Jin Y, Zhao H, Yin D (2008) J Catal 255:287
181. Iida M, Baba C, Inoue M, Yoshida H, Taguchi E, Furusho H (2008) Chem Eur J 14:5047
182. Abbott AP, Capper G, Davies DL, Shikotra P (2006) Trans Inst Min Metallurgy C Miner Process Extract Metall 115:15
183. Abbott AP, Barron JC, Ryder KS, Wilson D (2007) Chem Eur J 13:6495
184. Papaiconomou N, Lee J-M, Salminen J, von Stosch M, Prausnitz JM (2008) Ind Eng Chem Res 47:5080
185. Kumano M, Yabutani T, Motonaka J, Mishima Y (2006) Int J Modern Phys B Cond Matter Phys Statist Phys Appl Phys 20:4501
186. Ozawa R, Hayashi S, Saha S, Kobayashi A, Hamaguchi H (2003) Chem Lett 32:948
187. Del Sesto RE, McCleskey TM, Burrell AK, Baker GA, Thompson JD, Scott BL, Wilkes JS, Williams P (2008) Chem Commun 447
188. Sun H, Harms K, Sundermeyer J (2005) Z Kristallogr 220:42
189. Willems JB, Rohm HW, Geers C, Koeckerling M (2007) Inorg Chem 46:6197
190. Zhong C, Sasaki T, Tada M, Iwasawa Y (2006) J Catal 242:357
191. Hamill NA, Hardacre C, McMath SEJ (2002) Green Chem 4:139
192. Roeper DF, Cheek GT, Pandya KI, O'Grady WE (2008) ECS Trans 11:29
193. Mallick B, Kierspel H, Mudring A-V (2008) J Am Chem Soc 130:10068
194. Lagunas MC, Pitner WR, Seddon KR, van den Berg J (2003) Proc Electrochem Soc 2003-12:149
195. Lagunas MC, Pitner WR, van den Berg J-A, Seddon KR (2003) ACS Symp Ser 856 (Ionic Liquids as Green Solvents):421
196. Rogers EI, Silvester DS, Poole DL, Aldous L, Hardacre C, Compton RG (2008) J Phys. Chem C 112:2729
197. Rogers EI, Silvester DS, Jones SEW, Aldous L, Hardacre C, Russell AJ, Davies SG, Compton RG (2007) J Phys Chem C 111:13957
198. Zhang J, Bond AM (2003) Anal Chem 75:6938
199. Zhang J, Bond AM, Belcher WJ, Wallace KJ, Steed JW (2003) J Phys Chem B 107:5777
200. Forbes DC, Patrawala SA, Tran KLT (2006) Organometallics 25:2693
201. Scholten JD, Dupont J (2008) Organometallics 27:4439
202. Dupont J, Suarez PAZ, Umpierre AP, De Souza RFJ (2000) Braz Chem Soc 11:293
203. Einloft S, Kietrich FK, De Souza RF, Dupont J (1996) Polyhedron 15:3257
204. Illner P, Zahl A, Puchta R, van Eikema Hommes N, Wasserscheid P, van Eldik R (2005) J Organomet Chem 690:3567
205. Begel S, Illner P, Kern S, Puchta R, van Eldik R (2008) Inorg Chem 47:7121
206. Weber CF, Puchta R, van Eikema Hommes NJR, Wasserscheid P, van Eldik R (2005) Angew Chem Int Ed 44:6033
207. Illner P, Kern S, Begel S, van Eldik R (2007) Chem Commun 4803
208. Albrecht M, Stoeckli-Evans H (2005) Chem Commun 4705
209. Starkey Ott L, Campbell S, Seddon KR, Finke RG (2007) Inorg Chem 46:10335
210. Zhu B, Angelici RJ (2006) J Am Chem Soc 128:14460
211. Endres F, Zein El Abedin S (2006) Phys Chem Chem Phys 2101

212. Moustafa EM, Zein El Abedin S, Shkurankov A, Zschippang E, Saad AY, Bund A, Endres F (2007) J Phys Chem B 111:4693
213. Endres F, Zein El Abedin S, Saad AY, Moustafa EM, Borissenko N, Price WE, Wallace GG, MacFarlane DR, Newman PJ, Bund A (2008) Phys Chem Chem Phys 10:2189
214. Whitehead JA, Lawrance GA, Owen MP, McCluskey A (2006) Proc Electrochem Soc 2004-24 (Molten Salts XIV):901
215. Whitehead JA, Zhang J, Pereira N, McCluskey A, Lawrance GA (2007) Hydrometallurgy 88:109
216. Perissi I, Bardi U, Caporali S, Fossati A, Lavacchi A (2008) Solar Energy Mater Solar Cells 92:510
217. Caporali S, Ghezzi F, Giorgetti A, Lavacchi A, Tolstogouzov A, Bardi U (2007) Adv Eng Mater 9:185
218. Cossy C, Merbach AE (1988) Pure Appl Chem 60:1785
219. Choppin GR (1995) J Alloys Compd 223:174
220. Chaumont A, Wipff G (2003) Phys Chem Chem Phys 2003:3481
221. Chaumont A, Engler E, Wipff G (2003) Inorg Chem 42:5348
222. Chaumont A, Wipff G (2004) J Phys Chem B 108:3311
223. Chaumont A, Wipff G (2005) Phys Chem Chem Phys 7:1926
224. Lipsztajn M, Osteryoung RA (1985) Inorg Chem 24:716
225. Matsumoto K, Tsuda T, Nohira T, Hagiwara R, Ito Y, Tamada O (2002) Acta Cryst C C58:M185
226. Babai A, Mudring A-V (2006) J Alloys Compd 418:122
227. Branco LC, Rosa JN, Ramos JJM, Afonso CAM (2002) Eur J Inorg Chem 8:3671
228. Tsuda T, Nohira T, Ito Y (2001) Electrochim Acta 46:1891
229. Yadav JS, Reddy BVS, Uma Gayathri K, Prasad AR (2002) Synthesis 4:2357
230. Yadav JS, Reddy BVS, Reddy JSS (2002) J Chem Soc Perkin Trans 1:2390
231. Billard I, Moutiers G, Labet A, Gaillard C, Mariet C, Lützenkirchen K (2003) Inorg Chem 42:1726
232. Pellens M, Thijs B, Van Hecke K, Van Meervelt L, Binnemans K, Nockemann P (2008) Acta Cryst E E64:m945
233. Mudring A-V, Babai A, Arenz S, Giernoth R (2005) Angew Chem Int Ed 44:5485
234. Mehdi H, Bodor A, Lantos D, Horvath IT, De Vos DE, Binnemans K (2007) J Org Chem 72:517
235. Bhatt AI, May I, Volkovich VA, Collison D, Helliwell M, Polovov IB, Lewin RG (2005) Inorg Chem 44:4934
236. Babai A, Mudring A-V (2005) Chem Mater 17:6230
237. Babai A, Mudring A-V (2006) Dalton Trans: 1828
238. Babai A, Mudring A-V (2008) Z Allg Anorg Chem 634:938
239. Babai A, Mudring A-V (2006) Inorg Chem 45:4874
240. Babai A, Mudring A-V (2005) Inorg Chem 44:8168
241. Babai A, Mudring A-V (2006) Z Allg Anorg Chem 632:1956
242. Stumpf S, Billard I, Gaillard C, Panak PJ, Dardenne K (2008) Inorg Chem 47:4618
243. Lopes L, Martinot L, Michaux CJ (1994) Radionucl Nucl Chem 187:99
244. Dai L, Yu SY, Shan YK, He MY (2004) Eur J Inorg Chem 23: 4739
245. Cocalia VA, Visser AE, Rogers RD, Holbrey JD (2008) Solubility and solvation in ionic liquids. In: Wasserscheid P, Welton T (eds) Ionic liquids in synthesis, 2nd ed, vol 1. Wiley, Weinheim, pp 89
246. Heerman L, De Waele R, D'Olieslager W (1985) J Electroanal Chem 193:289
247. Hitchcock PB, Mohammed TJ, Seddon KR, Zora JA, Hussey CL, Ward H (1986) Inorg Chim Acta 113:L25
248. Deetlefs M, Hussey CL, Mohammed TJ, Seddon KR, van den Berg JA, Zora JA (2006) Dalton Trans 2334
249. Nockemann P, Servaes K, Van Deun R, Van Hecke K, Van Meervelt L, Binnemans K, Goerller-Walrand C (2007) Inorg Chem 46:11335

250. Nikitenko SI, Hennig C, Grigoriev MS, Le Naour C, Cannes C, Trubert D, Bosse E, Berthon C, Moisy P (2007) Polyhedron 26:3136
251. Baston GMN, Bradley AE, Gorman T, Hamblett I, Hardacre C, Hatter JE, Healy MJF, Hodgson B, Lewin R, Lovell KV, Newton GWA, Nieuwenhuyzen M, Pitner WR, Rooney DW, Sanders D, Seddon KR, Simms HE, Thied RC (2002) ACS Symp Ser 818:162
252. Bosse E, Den Auwer C, Berthon C, Guilbaud P, Grigoriev MS, Nikitenko S, Le Naour C, Cannes C, Moisy P (2008) Inorg Chem 47:5746
253. Mizuoka K, Ikeda Y (2005) Prog Nucl Energ 47:426
254. Chaumont A, Wipff G (2006) Phys Chem Chem Phys 8:494
255. Schurhammer R, Wipff G (2007) J Phys Chem B 111:4659
256. Nikitenko SI, Moisy P (2006) Inorg Chem 45:1235
257. Stumpf S, Billard I, Panak PJ, Mekki S (2007) Dalton Trans 240
258. Rao CJ, Venkatesan KA, Nagarajan K, Srinivasan TG (2008) Radiochim Acta 96:403
259. Gaillard C, El Azzi A, Billard I, Bolvin H, Hennig C (2005) Inorg Chem 44:852
260. Bradley AE, Hardacre C, Nieuwenhuyzen M, Pitner WR, Sanders D, Seddon KR, Thied RC (2004) Inorg Chem 43:2503
261. Servaes K, Hennig C, Billard I, Gaillard C, Binnemans K, Gorller-Walrand C, Van Deun R (2007) Eur J Inorg Chem 23: 4739
262. Bradley AE, Hardacre C, Nieuwenhuyzen M, Pitner WR, Sanders D, Seddon KR, Thied RC (2004) Inorg Chem 43:2503
263. Bradley AE, Hatter JE, Nieuwenhuyzen M, Pitner WR, Seddon KR, Thied RC (2002) Inorg Chem 41:1692
264. Gaillard C, Chaumont A, Billard I, Hennig C, Ouadi A, Wipff G (2007) Inorg Chem 46:4815
265. Cocalia VA, Holbrey JD, Spear SK, Jensen MP, Rogers RD (2006) Proc Electrochem Soc 2004-24 (Molten Salts XIV):779
266. Allen D, Baston G, Bradley AE, Gorman T, Haile A, Hamblett I, Hatter JE, Healey MJF, Hodgson B, Lewin R, Lovell KV, Newton B, Pitner WR, Rooney DW, Sanders D, Seddon KR, Sims HE, Thied RC (2002) Green Chem 4:152
267. Krossing I, Slattery JM, Daguenet C, Dyson PJ, Oleinikova A, Weingärtner H, J. Am. Chem. Soc, 128 (41), 13427
268. Krossing I, Slattery JM, Daguenet C, Dyson PJ, Oleinikova A, Weingärtner H, J. A. Chem. Soc., 129 (36), 11296.
269. Slattery JM, Daguenet C, Dyson PJ, Schubert TJS, Krossing I, Angew. Chem. Int. Ed., 2007, 46 (28), 5384.
270. Jiang DE, Dai S., J. Phys. Chem. B, 2008, 112 (33): 10202.
271. Huang JF, Luo HM, Liang CD, Jiang JE, Dai S., Ind. Eng. Chem. Res., 2008, 47 (3), 881.
272. Luo H, Dai S., Bonnesen PV, Haverlock TJ, Moyer BA, Buchanan AC, Solvent Extraction and Ion Exchange, 2006, 24 (1): 19.

Top Curr Chem (2009) 290: 161–183
DOI: 10.1007/128_2009_2

Published online: 26 May 2009

Thermodynamics and Micro Heterogeneity of Ionic Liquids

Margarida F. Costa Gomes, J. N. Canongia Lopes, and A. A. H. Padua

Abstract The high degree of organisation in the fluid phase of room-temperature ionic liquids has major consequences on their macroscopic properties, namely on their behaviour as solvents. This nanoscale self-organisation is the result of an interplay between two types of interaction in the liquid phase – Coulomb and van der Waals – that eventually leads to the formation of medium-range structures and the recognition of some ionic liquids as composed of a high-charge density, cohesive network permeated by low-charge density regions.

In this chapter, the structure of the ionic liquids will be explored and some of their consequences to the properties of ionic liquids analyzed.

Keywords Ionic liquids • Force-field • Molecular simulation • Nanosegregation • Solubility

Contents

M.F.C. Gomes (✉) and A.A.H. Padua
Laboratoire Thermodynamique et Interactions Moléculaires, Université Blaise Pascal, Clermont-Ferrand/CNRS, France
e-mail: Margarida.c.gomes@univ-bpclermont.fr

J.N. Canongia Lopes
Centro de Quimica Estrutural, Instituto Superior Técnico, Lisbon, Portugal and Instituto de Tecnologia Quimica e Biologica, Universidade Nova de Lisboa, Oeiras, Portugal

1 Introduction

Among several other remarkable properties, room-temperature ionic liquids possess a high degree of organization in the fluid phase. Many researchers [1, 2] have recognized this feature of ionic liquids as essential, because it has major consequences on their macroscopic properties, namely on their behavior as solvents. Understanding the nature of this self-organization is presently a very active research field that has already brought several major advances.

Some of the initial hypotheses concerning the nature of the liquid structure of room-temperature ionic fluids considered them as a network of cations and anions interacting via electrostatic forces and hydrogen bonds [3]. While H-bonds are certainly relevant when present, not all ionic liquids can establish this kind of interaction (tetraalkylphosphonium cations, for example, do not have H-bond sites). Ionic liquids are one class of molten salts and, inevitably, a substance that is composed solely of anions and cations must possess some kind of short-range organization (called charge ordering [3]) so as to fulfill local electro-neutrality conditions and also to maximize the electrostatic interactions between ions of opposite sign (Fig. 1a). In ionic liquids the surprising feature is that the imposed short-range charge ordering does not lead to long-range ordered structures (crystalline forms) at room temperature. In fact, that is the defining characteristic of this novel and diverse class of compounds.

Recent studies [4–6] provide a more sophisticated view into the structure of ionic liquids, which is totally compatible with charge ordering and with H-bond networks, but involves yet another level of organization at the molecular scale. In this chapter the nature of this self-organization will be explored and some of their consequences to the properties of ionic liquids analyzed.

The difficulty of forming stable crystalline structures in ionic liquids is associated in most cases with the large size, charge delocalization, asymmetrical shape, and flexibility of the ions that compose them. At least one of the ions has to have some of these characteristics that hinder crystallization. Indeed, most of the larger, organic ions have a chemical structure formed by a charged head-group and (one or more) side chains. The latter are most often alkyl chains but there are, of course, almost endless possibilities for variation. The side chains may host functional groups aimed at conferring specific properties to the ionic liquids, a concept known as task-specific ionic liquids [7].

When looking at this kind of molecular architectures, nanosegregation can be regarded as the next logical step in the understanding of the microscopic structure of these liquids: because the ionic liquid must necessarily organize its high-charge density portions into local structures that obey electroneutrality and maximize Coulomb interactions (Figs. 1b, c), it follows that the low-charge density parts of the ions that do not participate in those interactions will tend to be segregated elsewhere. It is this interplay between the two types of interaction, Coulomb and van der Waals, that eventually leads to the formation of medium-range structures and the recognition of some ionic liquids as composed of a high-charge density, cohesive network permeated by low-charge density regions (Fig. 2).

Clearly, there are some similarities between the structural features of ionic liquids and those displayed by some amphiphilic molecules, namely ionic surfactants.

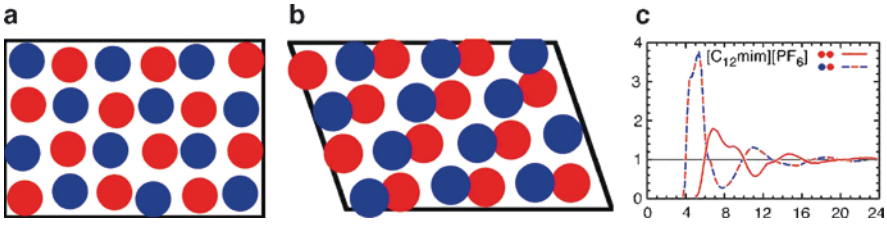

Fig. 1 Diagrams depicting: **a** a layer of a cubic sodium chloride crystal; **b** a monoclinic 1,3-dimethylimidazolium chloride ionic-liquid crystal; **c** two radial distribution functions (RDFs) in liquid 1-dodecyl-3-methylimidazolium hexafluorophosphate. Anions and cations are depicted in *red* and *blue*. In the cases of **b** and **c** the *blue circles* represent the centroid of the imidazolium rings of the cations. The alternating sequences of *red* and *blue circles* in **a** and **b** as well as the two curves in "phase opposition" in **c** clearly indicate the existence and nature of the polar networks in ionic condensed phases

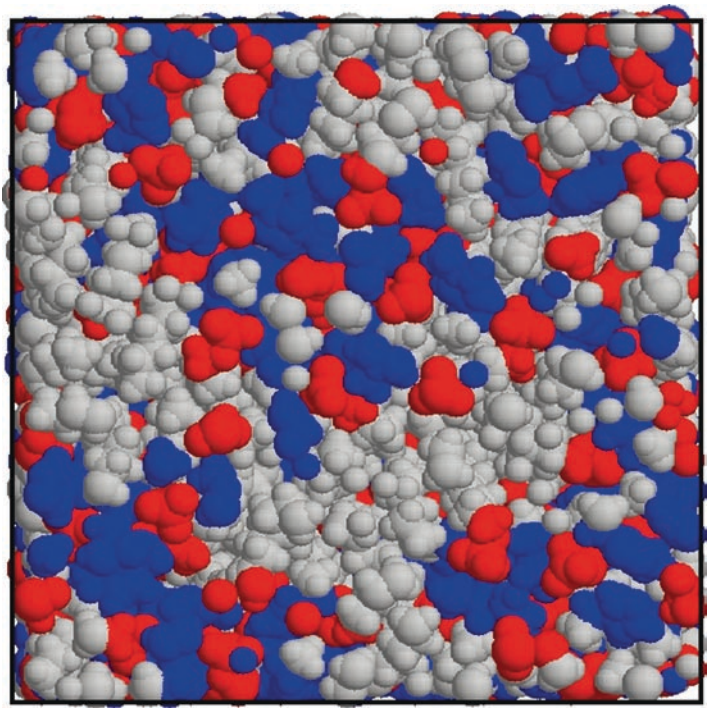

Fig. 2 Slice of a MD simulation box containing the 1-ethyl-3-methylimidazolium octylsulfate ionic liquid. The atoms of the charged parts of the anions and cations are colored as in Fig. 1 (*red* = anion atoms, *blue* = cation atoms) whereas the segregated nonpolar parts (aliphatic tails of the two ions) are colored in *gray*. The interspersing of the *red* and *blue* areas reveals the existence of the polar network. The latter must now allow for the presence of large nonpolar regions (*in gray*)

The amphiphilic ion in these compounds is also a large, organic ion that exhibits a large degree of asymmetry between a high-charge density part (the hydrophilic head-group) and a low-charge density part (the hydrophobic, nonpolar tail). When

dissolved in a dielectric molecular solvent like water these molecules self-aggregate into micelles, vesicles or layered structures, all characterized by nonpolar regions surrounded by a polar domain. If the medium is apolar the inverse counterparts of the above-mentioned structures are formed instead. If the amount of molecular solvent is decreased then lamellar, rod-like, bicontinuous, or liquid–crystal-like structures can also be found. However, and unlike ionic liquids, traditional ionic surfactants are either crystalline or amorphous solids at room temperature, and only exhibit those features when dissolved in a molecular solvent [8].

Not surprisingly, this kind of self-aggregation behavior is also found with suitable ionic liquids in solution [9]. However, one interesting aspect of room-temperature ionic liquids, which is the focus of the present chapter, is that segregation between polar and nonpolar spatial domains can occur in the pure liquid state, a condensed phase composed entirely of ions. The resulting medium-range ordering is more complex than that of "simple" molten salts, composed of smaller, more symmetric ions, in which charge ordering and packing are the factors controlling liquid-phase structure. With many ionic liquids, in addition to these two factors, domain segregation is obtained between high-charge density and low-charge density regions at the nanometer scale, the topology and connectivity of these regions depending on the molecular structure of the ionic liquids.

Because ionic liquids are a new field of research, a comprehensive body of experimental information to which theoretical studies can be anchored is still rather limited. As in other fields, studies using molecular simulation can provide reasonable predictions of properties but in particular they provide insights on how fluids behave at the molecular level. However, in the ionic liquids field, molecular simulation also takes the role of an exploratory tool, leading to new discoveries. Therefore, knowledge about the physical chemistry of ionic liquids is advancing through the interplay between experiment and theory, each providing challenges, guidelines and checks to the other.

2 From Nowhere to Somewhere: A Systematic Force-Field for Ionic Liquids

The first recognition of ionic liquids as nanosegregated structures came from molecular dynamics (MD) studies reported in the sequence of the development of a systematic force-field to model systems containing ionic liquids [4, 5].

At the beginning of the century, the number of models capable of describing the molecular characteristics of ionic liquids was very limited and fragmented – only a few ionic liquids had been studied on an almost case-by-case basis [10–13]. When Canongia Lopes and Padua developed and introduced their own force field [14] (nowadays, the CLAP force-field [14–17] is one of the most widely used force-fields for the molecular simulation of ionic liquids), their main goal was to provide a systematic model that could be generalized to describe entire families of ionic liquids. In order to meet that objective and to take into account the "modular" nature of ionic

liquids, where you can recombine different anions and cations to yield new ionic liquids, three basic specifications were built into the model: internal consistency, transferability and compatibility. The underlying rationale was that, since ionic liquids were a new field of study and these compounds exist in enormous variety, it made more sense to have a more general, though less precise, model instead of a more precise model that would represent just one, specific, ionic liquid.

Ionic liquids share parts of their molecular architectures with molecules that had been parameterized by existing force-field frameworks (AMBER, OPLS, CHARMM, etc.); for example imidazolium rings are present in hystidine, an amino acid. However ionic liquids have one essential difference: they are composed of ions, and although they may be built by the same functional groups, the distributions of electrostatic charge will be specific. In order to represent correctly the structure and interactions of these new compounds, the sets of parameters that determine charge distributions and conformations (at the least) had to be developed for this class of substances.

At the time the CLAP force field was proposed, many of the existing ionic liquid models used to borrow parameters from different, not always compatible, sources. For instance, it was common to see parameterizations of the cation and of the anion using information from different force fields [10, 11, 13]. In the development of the CLAP force-field, in order to respect internal consistency, ab initio calculations were used extensively to provide essential data for the development of an internally consistent force field. This included molecular geometry optimization and the description of electron density using extended basis sets, leading to the evaluation of force field parameters such as torsion energy profiles and electrostatic charges on the interaction centers.

In order to improve transferability, the parameterization of ionic liquids in the CLAP force-field was not meant to be too specific because the objective was to deal with families of similar compounds that could be combined with different counter-ions. Homologous series may be expressed in the cation, such as in alkylmidazoliums, or in the anion, such as alkylsulfates. Force-field parameterization was concentrated on parts of the molecules that were common to an entire family of ions, and strategies were adopted to add specific molecular residues. Moreover, the anions and cations were modeled independently, meaning that an ionic liquid can be assembled from any available cation-anion combination (as illustrated in Fig. 3). This transferability implies different sorts of approximation. For example, it does not account for the possibility of charge–transfer effects between ions, an issue that was thoroughly discussed at different stages of the force-field development and that may not be very significant in condensed phases, where each ion has a large number of neighbors of opposite charge. Also, polarization of electron clouds is not taken into account explicitly, although was included a posteriori through a number of refinement schemes [18, 19]. Inclusion of explicit polarization accelerates the microscopic dynamics obtained with the models, but has little effect on the estimation of equilibrium or structural properties [20].

The CLAP model was built based on the OPLS-AA force field [21] functional form which means that, technically, it is easy to combine any molecule or residue already defined in the OPLS-AA database with the structures developed for ionic

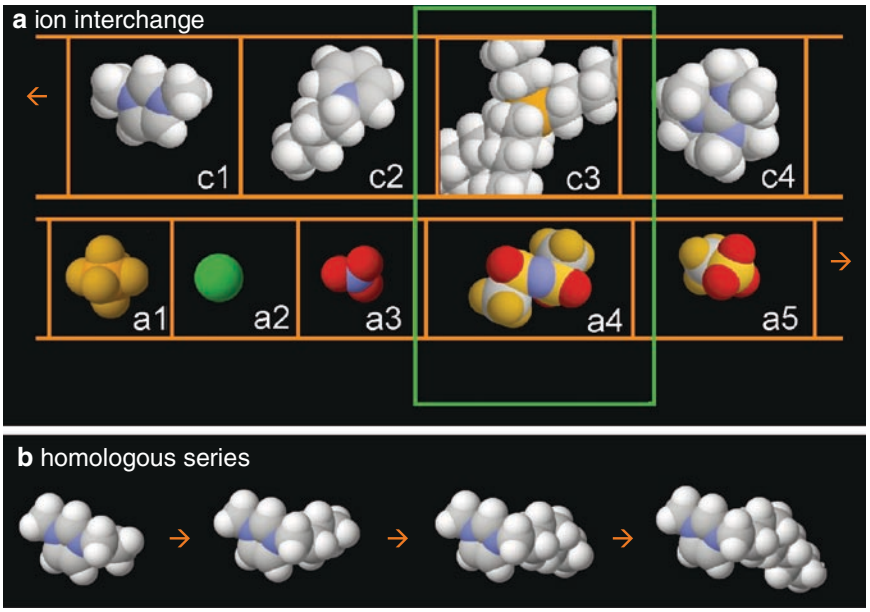

Fig. 3 Schematic representation of the transferability premise developed as a built-in characteristic of the CLAP force-field. **a** c1, c2, c3, and c4 stand for imidazolium- pyridinium-, phosphonium- and guanidinium-based cations, a1 to a5 stand for the hexafluorophosphate, chloride, nitrate, bis-(trifluoromethanesulfonil)imide, and triflate anions. The c3–a4 combination was selected in this case. **b** The possibility to grow an alkyl side chain in, for example, imidazolium-based ionic liquids in order to study an entire homologous series of ionic liquids is illustrated

liquids. Compared to other generalist force fields, special attention was devoted in OPLS-AA to the simulation of liquid-state thermodynamic properties.

While developing the CLAP model, two features became the most significant in terms of the (re)parameterization of the force field: the characterization of the flexibility of the ions (through the parameterization of the corresponding torsions of the dihedral angles) and the atomic point-charge distribution. Basically, the functional form of the potential energy in the CLAP force field consists of nonbonded and bonded interactions. The former are repulsive, dispersive and electrostatic interactions and are given by Lennard-Jones and Coulomb terms, while the latter are related to the covalent-bond stretching, valence-angle bending and dihedral angle torsions (internal rotations and flexions), within a given molecular edifice (see Fig. 4). Because the CLAP is based on the OPLS-AA framework, a large part of the Lennard-Jones, bond and angle parameters could be transferred without major modifications. This is not surprising (or inconsistent) since many ionic liquids are derived from (neutral) molecules that are contained in the OPLS-AA force-field (originally developed for organic residues that are part of biologically relevant molecules like the DNA bases or amino acids). Nevertheless this sort of compatibility leaves out two of the most important features of many of the ions that compose ionic liquids, namely their asymmetrical charge distribution and their

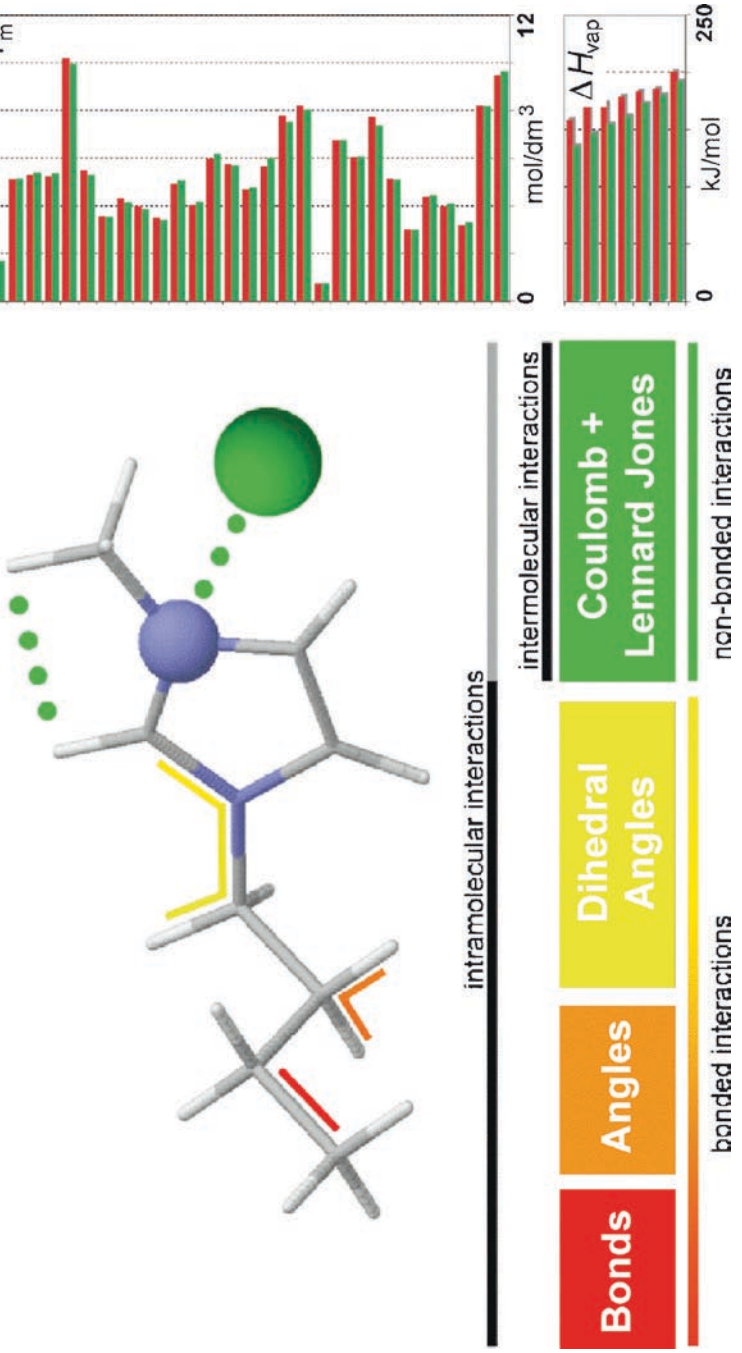

Fig. 4 Schematic representation of the different atom–atom interactions parameterized in the CLAP force field for ionic liquids. The *two bar graphs* summarize the validation of the force field results (*red bars*) against molar density, ρ_m, and molar enthalpy of vaporization, $\Delta H_{m,vap}$, data (*green bars*). The standard deviations between the simulated and experimental sets are $\delta\rho_m = 3\%$ and $\delta\Delta H_{m,vap} = 30\%$

particular conformational flexibility. As was stressed above, these are parameterized by the atomic point charges, responsible for the modeling of the electrostatic field around each ion, and by the parameters associated with the torsions of the dihedral angles, that must reproduce the correct conformational landscape of the ions.

The electrostatic charge distributions and the torsion energy profiles are interrelated because atoms within the same ion (or molecule) also interact through the Lennard-Jones and Coulomb terms (provided they are sufficiently far apart). It is easy to understand that the barrier to internal rotation around a certain bond is affected by the amount of electrostatic or steric repulsion between the atoms attached to those establishing the rotating bond. As such, the parameters representing torsion energy surfaces must be adapted to the sets of atomic charges and Lennard-Jones parameters. Therefore, it is fundamentally incorrect to take parameters for torsion energies from the literature and then calculate electrostatic charge distributions or modify existing terms the nonbonded interactions. If this is done, the model will likely not be able to reproduce conformations in a satisfactory manner. There are several methods to attain this internal consistency between the conformational and intermolecular terms. A stepwise approach was chosen [21, 22] in which the model is built up in such a way that the parameters for a given dihedral angle are invariant for any molecular structure in which a given dihedral term may occur, and without loss of accuracy in representing the conformational features of each particular ion. Other strategies exist in which a set of parameters is obtained for each ion individually, but here generality and transferability are lost [23]. The conformational landscapes in the CLAP fore field reproduce quantum calculations at the MP2 theoretical level using large basis sets, cc-pVTZ(-f) [22].

The Coulomb parameters describing the electrostatic forces acting on each ion are also determined using quantum calculations of the electron density at the MP2 theoretical level and using sufficiently large basis sets (cc-pVTZ(-f)). The point charges placed at the center of mass of each atom of the ion are then calculated from the ab initio electron density using an electrostatic surface potential methodology (CHelpG), in which the values of the atomic charges are optimized to reproduce the electrostatic field generated by the molecule. The most stable conformation obtained by geometry optimization of the isolated ion is generally taken as the reference but, in ions with multiple stable conformers, several ab initio calculations were performed, and an averaging process was implemented to define the charges in each atom. Since one of the objectives of the present force field is the possibility of parameter transfer within families of ionic liquids, the point charges attributed to the various molecular residues were subjected to different degrees of approximation to find general trends that could then be applied along an entire series of analogous ionic liquids, without the need to perform heavy ab initio calculations and parameter fitting procedures for each ion within a family.

The CLAP model has permitted access to the molecular properties of ionic liquids through molecular simulation experiments. Before these results could be fully explored, it was necessary to validate the force field parameters by comparing experimental results to the in silico measurements. Ionic liquids have a nonmeasurable vapor pressure at room temperature conditions or indeed for the larger part of their liquid temperature range. This means that the traditional way to validate a molecular

force field to be used within the framework of statistical mechanics calculations in condensed phases was somehow curtailed at the time the model was introduced. The validation procedure had to rely exclusively on volumetric data available for some selected ionic liquids (Fig. 4). This is not a comfortable situation, since it is better to have at least one property related to the length scale of the ions (volumetric data) and at least one related to the energy scale (such as the heat of vaporization). However, and since the force-field had been built in a systematic way, it was possible to test it against series of homologous ionic liquids by predicting their densities both in the liquid and in the solid states and comparing the results with experimental data (liquid density and X-ray diffraction data).

After the discovery that ionic liquids could be vaporized at moderately high temperature (around 550 K) and reduced pressure (around 500 Pa) [24], new experimental data related to their liquid–vapor equilibrium became available, and it was possible to test the performance of the CLAP force-field against different estimations of the enthalpy of vaporization of 1-alkyl-3-methylimidazolium bis (trifluoromethylsulfonyl) imide ionic liquids. Although the uncertainties both in the simulation and experimental results are still great at this stage due to the extremely difficult nature of the experiments and constraints imposed on the simulation method (bad statistics of the simulation of an isolated ionic pair in the gas phase), it was possible to conclude that for this particular family of ionic liquids the enthalpies of vaporization at room temperature are in the 120–160 kJ mol^{-1} range (with MD over-predicting the experimental results by 15–30%) [25, 26]. It must be stressed that the use of the model is in all cases (density and calorimetric estimations) purely predictive, which means that deviations of a few percentage points in the case of density and a few tens of percentage points in the case of the enthalpies of vaporization are in fact quite reasonable.

3 From Somewhere to Here: Structural Analyses and Nanosegregation in Ionic Liquids

One of the main advantages of using MD simulation is not only to be able to predict physical properties directly from a molecular interaction model, but also to access the structure at a molecular level, something that is quite difficult to achieve experimentally by diffraction techniques in the case of fluid phases. In ionic liquids some of the structural features were expected, like those reflecting local electroneutrality constraints (Fig. 1) and the resulting charge ordering, and were readily probed by different authors. These studies were then refined in order to show the position of a given ion relative to position of the corresponding counterion, with the first studies in the field describing the local structure around anions and cations using structural analysis tools like radial and spatial distribution functions. Somehow the local environment around the alkyl side chains of the ions (at that time the cations) was deemed not so important and was not given much attention. Ironically it was the plotting of the radial distribution functions (RDFs) involving the terminal carbon atoms (C_T) of the long alkyl-side chains of the cations that started the process that led to the recognition of ionic liquids as nanostructured fluids (Fig. 5). What the

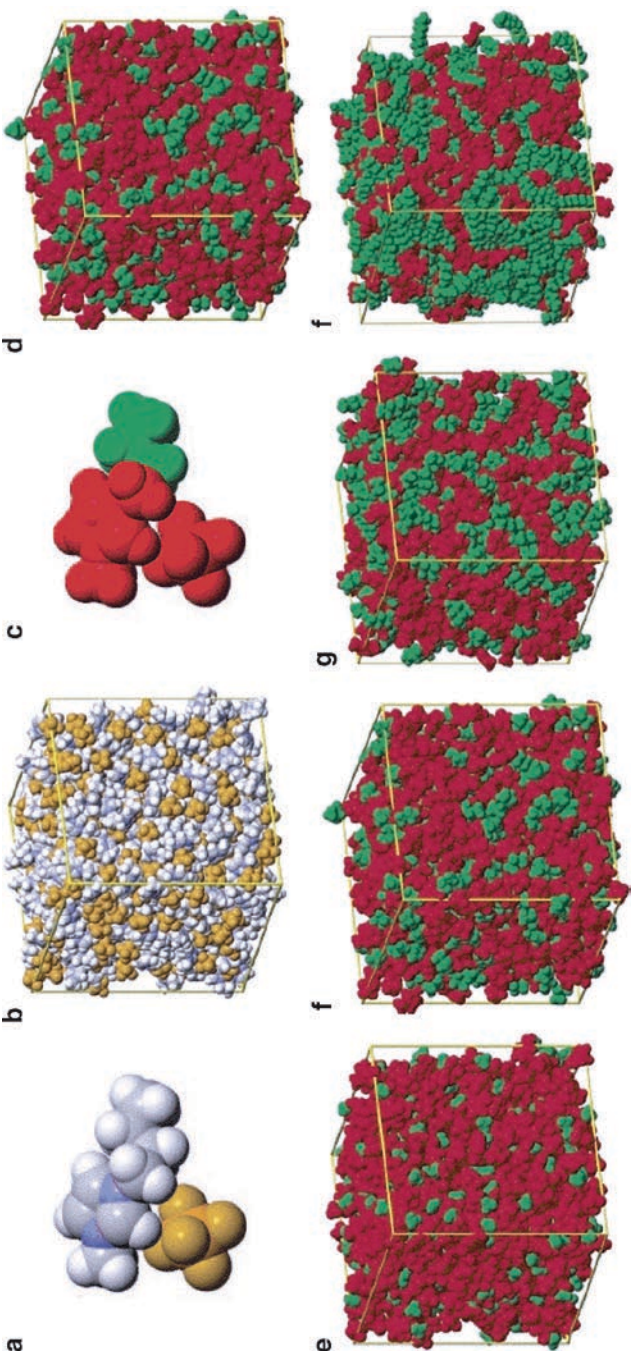

Fig. 5 Color-coding the nanostructural organization of 1-alkyl-3-methylimidazolium hexafluorophosphate ionic liquids. **a,b** One neutral ionic pair (NIP) and one configuration of a MD simulation box containing 500 ions of the 1-butyl-3-methylimidazolium hexafluorophosphate ionic liquid colored according to the CPK convention. **c,d** Application of the *red–green* color scheme to the polar and nonpolar regions of the same ionic liquid. **e,f** Segregation of the two types of region and the transition from disperse to bicontinuous phases in the homologous series 1-ethyl-, 1-butyl-, 1-hexyl, and 1-decyl-3-methylimidazolium hexafluorophosphate ionic liquid

C_T–C_T RDFs shows is that C_T atoms tended to form clusters where the local concentration of those atoms is much larger than the average concentration of C_T in the ionic liquid and that the size of the clusters increase with the length of the alkyl side-chain. This suggested that the alkyl side chains were being segregated from the rest of the ionic liquid and that it was possible to have the formation of nanometer-scale domains, or pockets, in which the alkyl side chains exist in an alkane-like environment. The real breakthrough came when we tried to visualize those domains by color-coding the polar and nonpolar parts of each ion. In those first systems the polar part was painted red and contained the whole anion and the entire cation except the alkyl side chain (from the C_2 atom). The latter was painted green[1] [27].

When the color code was applied to ionic liquids, the segregation suggested by the C_T–C_T RDFs became quite conspicuous. The characteristic length scales of these structural features could then be quantified through calculation of the structure factor of the modeled fluids, yielding domains with sizes in the 1.5–2.5 nm range, depending on the relative sizes of the cation, anion and alkyl side chains of the ions.

Certain pure ionic liquids started to be regarded as nanostructured fluids, with two distinct kinds of spatial domain: one ionic, the other nonpolar. Besides their impact on the properties of pure ionic liquids, these two kinds of domain offer distinct environments to solutes, and therefore the concept of a nanostructured medium offers a novel perspective to interpret the macroscopic properties of ionic liquids, in particular their solvent behavior.

The driving force for the segregation of the nonpolar chains is though to be energetic: they are excluded from the cohesive network of positive and negative charges that is formed by the charged groups of the ions in close contact. The resulting phase is more ordered than if the chains adopted random positions and orientations. If the side-chains are too small, then they do not disrupt the ionic network significantly and, also, they do not possess enough conformational freedom to adopt a low energy configuration through aggregation. If the side-chains are too long, then the ionic liquids will exhibit liquid–crystalline mesophases with anisotropic, long-range ordering. However, in the intermediate case the fluid will still be (long-range) isotropic, with intermediate-range ordering. In all cases, charge ordering will have to be respected, since the energy required for local charge imbalance is too large.

The simulation results just mentioned agreed with other previous molecular simulation studies by Urahata and Ribeiro [28] and by Wang and Voth [5], that also suggested the existence of nanosegregation between polar and nonpolar domains in ionic liquids. Urahata and Ribeiro performed simulation using a united-atom model (in which $–CH_2–$ or $–CH_3$ groups in the alkyl side chains are represented by single

[1] This simple “red and green” color scheme was reused in several publications, including some by other authors. It had been used in previous Monte Carlo simulation studies involving nano-segregated binary mixtures of Lennard-Jones atom, where the colors had been chosen just by numerical order in the RGB system: red is 001 (1 in binary), green is 010 (2 in binary), and they are followed by yellow (011) and blue (100). The fact that red and green are the colors of the Portuguese flag (the nationality of the authors) is merely a coincidence.

sites) and reported signs of intermediate-range order in the form of prepeaks in their calculated structure factors, but did not explore the matter further. Wang and Voth identified segregated domains using a coarse-grained model of ionic liquids, in which interaction sites represent groups of several atoms. The recurrence of similar observations on simulation studies using unrelated molecular models at different scales of representation is a strong indication that the structuring observed is not a result of different artifacts of the models.

Several pieces of indirect experimental evidence can, in hindsight, be related to the presence of nanoscale segregation that, logically, should have an effect on the static and dynamic properties of the systems. It is plausible that nonmonotonous trends are observed in several properties of the ionic liquids when the alkyl side chain is increased in length. This was indeed reported by Tokuda et al. [29] for viscosity, diffusivity and the ration of measured electrical conductivity to that estimated from NMR experiments. This ration is a measure of the ionicity of the liquids, that is, of the ions that are available for charge transport, the remaining supposed to be "locked" in associated form. Tokuda et al. reported results in which, for short side chains, viscosity decreased and ion mobility (diffusivity, conductivity ratio) increased with increasing side-chain length. This is compatible with a less-cohesive medium since the density of charges will diminish as the side chains lengthen. However, for intermediate side chains (butyl) the trends are reversed and now viscosity increases and mobility decreases. This is compatible with the onset of domain segregation as predicted by simulation to happen around butylimidazolium, when the anion is hexafluorophosphate.

Studies of fluorescence of probe molecules [30] in ionic liquids revealed red shifts which are characteristic of organized media with long-lived structures (micelles). The fluorescence of the ionic liquids themselves shows the same signs [31]. This can also be an indication of glassy dynamics.

A curious thermodynamic result is connected to the cohesive energy of an ionic liquid. From calorimetric experiments, performed to determine the heat of vaporization along an homologous family of cations, the increment in enthalpy of vaporization per $–CH_2–$ group was calculated [25] and it closely matches that observed for the *n*-alkanes, suggesting that, in the ionic liquid phase, the alkyl chains exist in an alkane-like environment.

Armstrong [32] showed that stationary phases composed of ionic liquids could be used to separate polar compounds and, unexpectedly, that their resolving power for the series of *n*-alkanes was high, demonstrating the dual nature of the ionic liquids, interacting both with polar and nonpolar compounds.

From that moment ionic liquids started to be regarded as fluids formed by a polar domain with the structure of a tridimensional network of ionic channels (the polar network), and nonpolar domain(s) arranged as a dispersed nanophase in the case of ionic liquids with relatively short alkyl-side chains and as a continuous one for longer side-chains (Fig. 6). In the systems first analyzed (1-alkyl-methylimidazolium hexafluorophosphate ionic liquids), the butyl side-chain marked the onset of the transition from dispersed nonpolar nanodomains to a bicontinuous nanosegregated system. The nanosegregation is also observed in other families of ionic liquids, the presence of nonpolar side chains both in the cation or in the anion being determinant in the structure of the ionic liquid (Fig. 7).

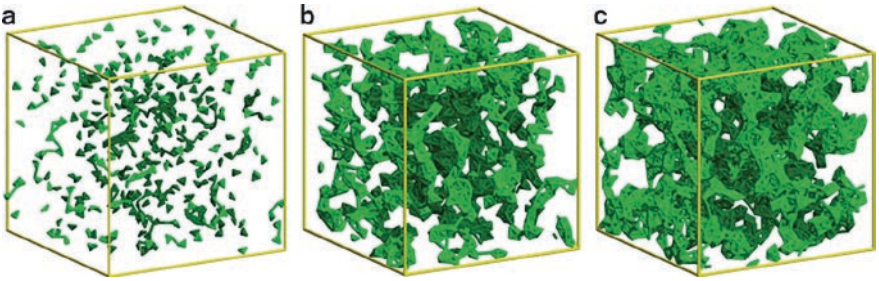

Fig. 6 Continuous tridimensional network of ionic channels: **a** $[C_2C_1Im][PF_6]$; **b** $[C_4C_1Im][PF_6]$; **c** $[C_6C_1Im][PF_6]$

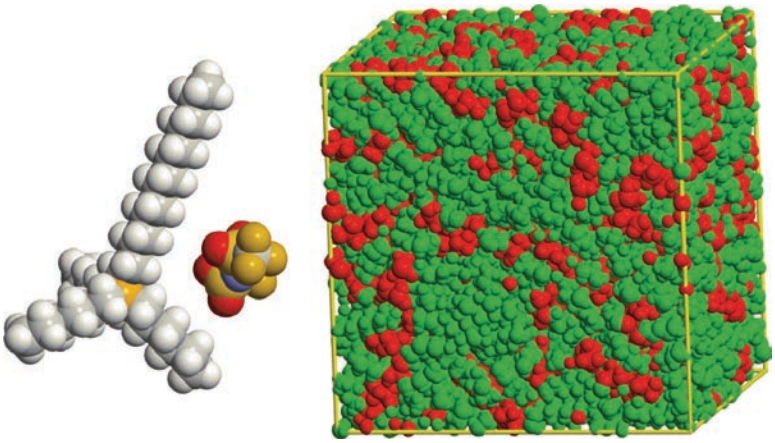

Fig. 7 Color-coding the nanostructural organization of tetra-alkylphosphonium bis (trifluoromethanesulfonyl) imide, $[P(C_6H_{13})_3(C_{14}H_{29})][N(SO_2CF_3)_2]$ ionic liquids. The figures show on the *left* one neutral ionic pair (NIP) of the ionic liquid in CPK colors and, on the *right*, one configuration of a MD simulation box containing 500 ions of the ionic liquid ionic according to the *red–green* convention. The polar (*red*) atoms are all those belonging to the anion, the phosphorus atom and the four carbon atoms attached to it. The large apolar (*green*) segments of the tetra-alkylphosphonium cation (much larger than those of the dialkylimidazolium cations represented in Fig. 5) induce a nanosegregation characterized by a thread-like polar network (in *red*), much "thinner" than the polar networks depicted in Figs. 5e–5h

The direct experimental confirmation of the simulation results only came in 2007 when Triolo et al. [6] reported an X-ray diffraction study showing the existence of nanometer-size structures in pure ionic liquids, with sizes that correlate well with the results of simulations.

The topology and connectivity of the two types of domain is expected to change according the nature of the ions. Relatively small alkyl side chains form discontinuous nonpolar pockets dispersed in a percolating (continuous) ionic network. As the

relative size of the nonpolar groups increases, the nonpolar regions will be of large size and will eventually coalesce to percolate the space, giving rise to a bicontinous system. With even larger side chains there will be disruption of the ionic network with formation of liquid–crystalline phases. Two kinds of percolation transition are therefore expected: one corresponding to the coalescence of the nonpolar domains and the other to the rupture of the ionic network. These transitions may be realized in binary mixtures of an ionic liquid with molecular compounds, in which continuous variation of the relative magnitudes of the two types of domain may be achieved by changes in composition. It is hoped that the simulation results provide a challenge for experimentalists to try to observe such percolation transitions. By comparing different pure ionic liquids with various side-chain lengths only some discrete points can be realized in practice.

4 From Here to There: Conformational Landscapes and Solubility Probes

After asserting the nanostructured nature of ionic liquids, the structural analysis of these fluids continued in two different directions. The first was to check how the built-in flexibility of the isolated ions of the model affect (or are affected by) the nanostructured nature of the ionic liquid, and how that can influence properties like viscosity, electrical conductivity, or diffusion coefficients. It must be stressed that the charges in the CLAP model are fixed to the atomic positions, which means that the most obvious way to probe the relation between the structure of the ionic liquid as a whole in terms of the structure of its individual ions is to investigate the flexibility (conformational landscape) of the latter. The second alternative direction was to probe the structure of ionic liquids not by regarding into the structure of the component ions but by instead using an external probe (for example, a neutral molecular species), solubility experiments with selected solute molecules being the most obvious experimental approach.

The first line of research was pursued by the investigation of the conformational landscapes of different cations (*N*-propyl- and *N*-butyl-*N*-methylpyrrolidinium) and anions (bis(trifluoromethanesulfonyl)amide and bis(fluorosulfonyl)amide), associating data obtained from Raman spectroscopy, molecular dynamics simulations, and ab initio techniques [33]. In the families of ionic liquids studied, different stable isomers were identified and the association of the different approaches adopted (analysis of the three-dimensional potential energy surfaces, the corresponding MD simulations and the Raman spectroscopy data) evidenced the nature of the anion as a flexible, albeit hindered, molecule capable of interchange between conformers in the liquid state (Fig. 8). The liquid phase conformational landscape can be reproduced by ab initio (DFT) calculations on the isolated ions forming the ionic liquid which points to the fact that the ions enjoy enough freedom to adopt the conformations dictated by their internal structure and even interconvert between different conformations in the crystal; due to constraints imposed by the lattice, only one of

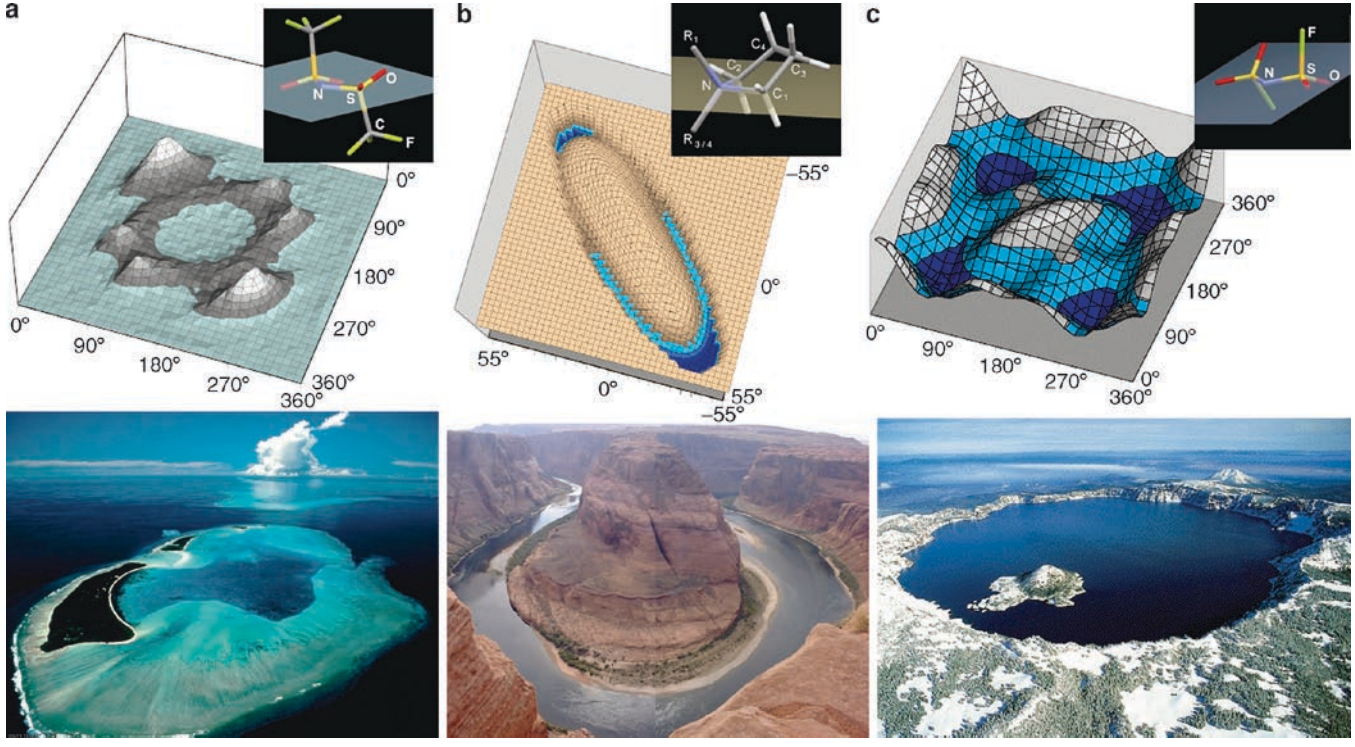

Fig. 8 The conformational landscapes of three flexible ions present in different ionic liquids: **a** bis(trifluorosulfonyl)imide anion; **b***N*,*N*-dialkylpyrrolidinium cation; **c** bis(fluorosulfonyl)imide anion [33]. In **a** the graph shows the distribution of different conformers obtained by rotation of the two interdependent CSNS dihedral angles. The graph resembles a Pacific Ocean atoll. In **b** the graph represents the potential energy surface (PES) of the pyrrolidinium ring pseudorotation. The deep path suggests the steepness of canyon walls. In **c** the graph depicts the PES obtained as a function of the two FSNS angles of the anion. The central high-energy island shows that the interconversion between conformers is only allowed when the two dihedral angles rotate in a concerted way

the possible conformations is usually present. The interplay between the structured nature of ionic liquids and the conformational freedom (flexibility) of its ions can help explain many of the physical and solvation properties of these fluids.

The second line of research started with the simulation of ionic liquid systems where selected molecular solute molecules had been added. The notion that, in ionic liquids, two kinds of spatial domains exist completely modifies the way solvation of molecular solutes can be understood in these media. Different molecular solutes, according to their polarity or tendency to form associative interactions, will not only interact selectively with certain parts of the individual ions but may also be solvated in distinct local environments (Fig. 9) [34, 35]. Nonpolar molecules like *n*-alkanes will be solvated and tend to reside in or near the nonpolar domains. In fact they will be segregated into these domains because they (like the alkyl-side chains of the ionic liquids themselves) are not able to integrate the polar network due to the large cohesive energy between the charged groups. Dipolar solutes, for example acetonitrile, will interact closely with the charged head groups of the ions but will also show affinity for the nonpolar domains through their aliphatic moieties. This makes acetonitrile an excellent solvent for many ionic liquids due the fact that it will be positioned preferentially at the interface between the polar and nonpolar regions of the ionic liquid. Associating solutes, such as alcohols or water, will form powerful hydrogen bonds with the charged parts of the ions and will be solvated in the ionic domain. In this case sometimes the efficiency of those interactions undermines the ability of these molecules to be completely miscible with ionic liquids: if the solute interacts preferentially only with the cation or the anion (and is excluded from the nonpolar domains) then at a certain point the integrity of the polar network can be at risk and the system will phase-separate.

The particular case of mixtures of ionic liquids with aromatic compounds has been studied by different authors and methods [38–41] and has provided several insights on the nature of these mixtures and on the interactions therein.

Although aromatic compounds can have null dipole moments (benzene, naphthalene, etc.) they can have significant quadrupole moments due to the aromatic electron cloud above and below the plane of the rings. A convenient way of assessing the effect of the quadrupole moment of the aromatic compound on the properties of the solutions is by comparing the solvation of benzene, perfluorobenzene, and 1,3,5-trifluorobenzene in ionic liquids, as was done by Harper and Lynden-Bell [41]. In benzene, negatively charged regions exist above and below the ring plane, and a rim of positive charges is found in the ring plane due to the hydrogen atoms. When benzene is solvated in an ionic liquid, cations of the first solvation shell will be found above and below the plane of the ring, with anions of the first solvation shell placed in plane, around the ring. In perfluorobenzene, because of the high electronegativity of fluorine atoms, the sign of the quadrupole is reversed. In this case, the first solvation shell will have anions above and below the ring, and cations in the plane. In 1,3,5-trifluorobenzene the quadrupole moment is strongly attenuated, and the resulting average distribution of ions will reflect the threefold symmetry of the aromatic molecule.

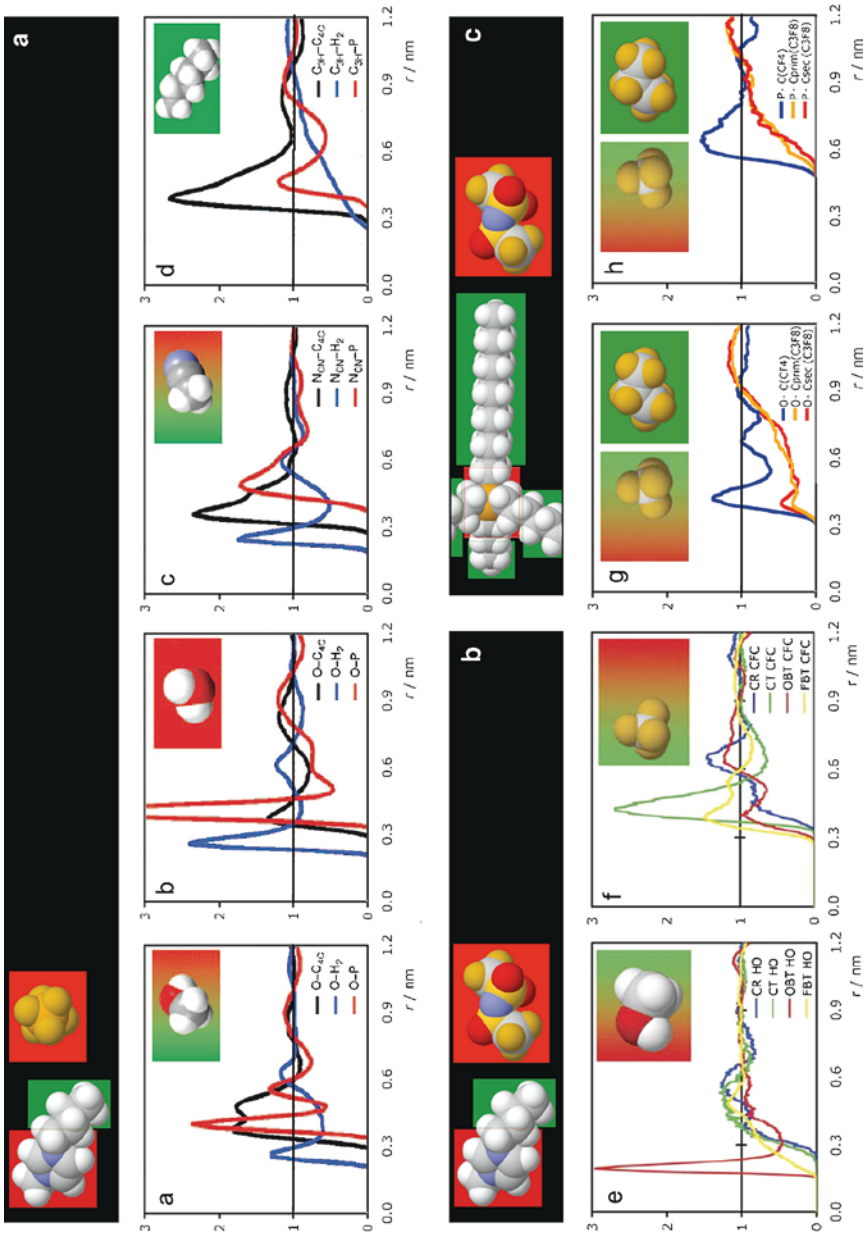

Fig. 9 Pair–pair radial distribution functions of different solutes in different ionic liquid solutions. Solvents: **A** 1-butyl-3-methylimidazolium hexafluorophosphate; **B** 1-butyl-3-methylimidazolium bis(trifluoromethanesulfonyl)imide; **C** tri-hexyl((tetradecyl)phosphonium bis(trifluoromethanesulfonyl)imide. Solutes: **a**,**e** methanol; **b** water; **c** acetonitrile; **d** *n*-hexane; **f**-**h** tetrafluoromethane; **g**,**h** perfluoropropane. The polar and nonpolar regions of the solvent ions **A**–**C** are color-coded using *red* and *green* respectively. The background colors of the *insets* **a**–**h** depict schematically the preference of each solute for the polar (*red*) or nonpolar (*green*) regions [34, 36, 37]

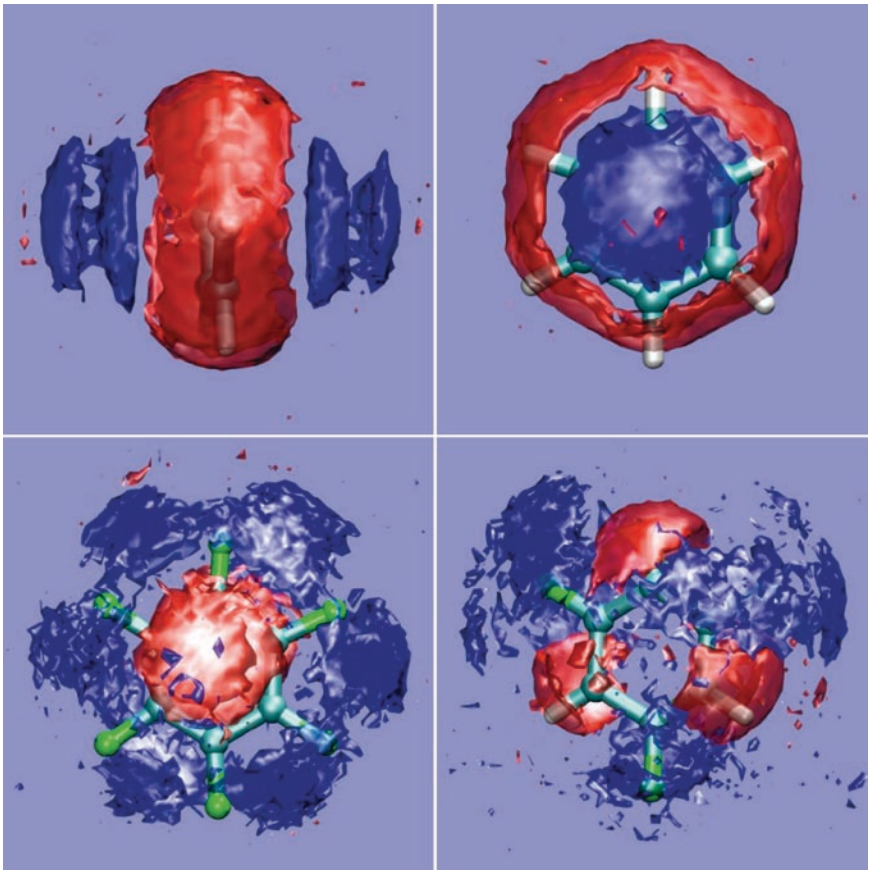

Fig. 10 Spatial distribution functions of atoms of the ionic liquid $[C_2C_1im][tf_2N]$ around a central aromatic molecule. *Blue contour* surfaces enclose regions with a probability of finding C_2 atom of imidazolium ring which is 2.4 times the average density. *Red contour* surfaces enclose regions where the probability of finding O atoms of tf_2N^- anion are 1.8 times the average value in the system. The results were obtained in a liquid-state simulation of 192 ion pairs and 64 aromatic molecules for 1 ns

As seen in Fig. 10, in aromatic hydrocarbons the π-electron-rich regions can interact with cations through so-called cation–π interactions [40]. In mixtures with ionic liquids, the aromatic molecules may be solvated in the nonpolar domains but they may have sufficient affinity for the cationic head-groups to be found among the polar domain as well. When looking at the structure of such mixtures, it is useful to study the local environments of the ions and of the aromatic compound.

Let us take as example mixtures between two closely related ionic liquids and an aromatic molecule: 1-butyl-3-methylimidazolium bis(trifluoromethanesulfonyl) imide $[C_4C_1im][tf_2N]$ and toluene, and between 1-butyl-2,3-dimethylimidazolium bis(trifluoromethanesulfonyl)imide $[C_4C_1C_1im][tf_2N]$ and toluene. Structure and

solvation in these mixtures has been studied by NMR and by molecular dynamics simulation [42]. It is expected that toluene be solvated in the nonpolar domains formed by the alkyl side-chains but, unlike aliphatic hydrocarbons, interactions with the charged regions of the ions will be strong enough so that there will be a significant probability of finding toluene near the imidazolium rings. One interesting point will be to see the effect of methylation of the C_2 carbon of the imidazolium ring upon the distribution of toluene around the cation head-group. Spatial distribution functions are shown in Fig. 11.

The prominent structural features concerning the distribution of anions around the imidazolium ring in $[C_4C_1im][tf_2N]$ are the strong probability of presence of O atoms from the anions near the H_2, H_4, and H_5 atoms of the ring, which can be understood as three H-bonds with eventually different ions. However, there is also a significant probability of presence of anions of the first solvation shell above and below the plane of the imidazolium ring, interacting with the positively charged atoms of the ring but not in a geometric arrangement corresponding to a H-bond. Atoms of toluene are found at larger distances than atoms from the anion around the ring, and are also found near the methyl group attached to N_2.

The situation with $[C_4C_1C_1im][tf_2N]$ presents a number of differences: there is a strongly enhanced presence of toluene near the methyl group in C_2, and no significant presence of anions in that region. Anion O atoms still approach the ring from

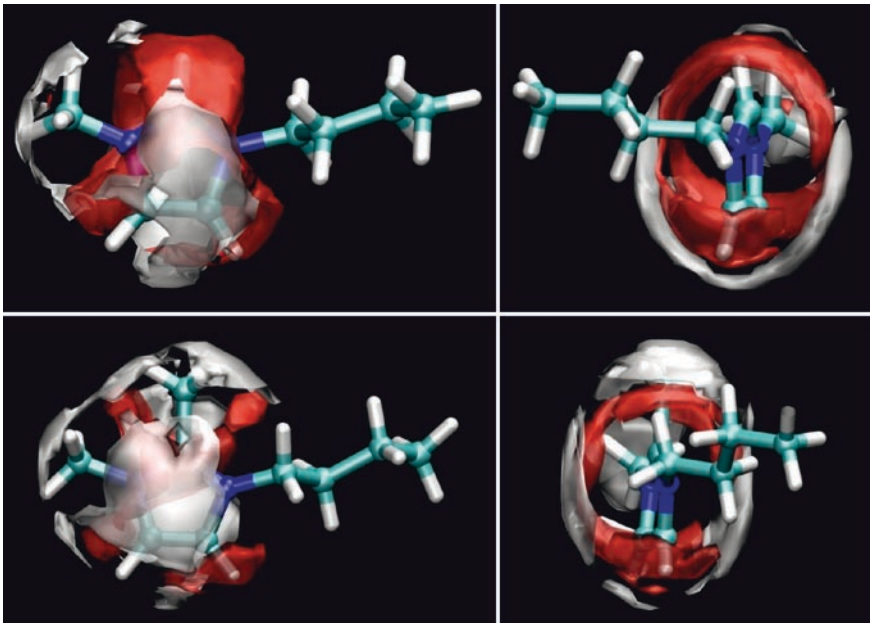

Fig. 11 Spatial distribution functions around the imidazolium rings of the cations of: O atoms from tf_2N^- anions (*red* isosurfaces) and C_1 (ipso) atoms from toluene (*white* isosurfaces). *Top row* $[C_4C_1im][tf_2N]$, *bottom row* $[C_4C_1C_1im][tf_2N]$. Probability density around the butyl side chain is not shown, since it is not easy to plot it in the same referential due to conformational flexibility of the chain

the sides of the methyl group in C_2, near the N_1 and N_3 atoms, and H-bonds are still formed with H_4 and H_5. Therefore, by replacing an acidic H by a methyl group in the imidazolium ring, the environment around the cation in mixtures with toluene changes: the head-group looses one H-bond site and becomes less polar, interacting more with the nonpolar domains and molecules that take part in them.

5 From There to Elsewhere: Future Perspectives

Mixtures of ionic liquids with molecular compounds are complex fluids, with rich structural features that result between the interplay of Coulomb and van der Waals forces, and of energetic and entropic contributions. In fact, the properties of such solutions are not just determined by the energies between molecules; they also depend on configurational aspects resulting both from the particular organization of the molecules constituent of the species in equilibrium and from the conformational changes of each species. This entropic aspect cannot be ignored, as it may even be the predominant factor to explain the properties of these complex fluids. The study of the behavior of solutions containing ionic liquids is a research topic where concepts of classical thermodynamics and macroscopic experimental information can be combined with molecular modeling tools to provide a better understanding of the macroscopic properties of the solutions. This two-way approach brings mutual benefits, since experimental data are still essential to set up the best molecular models that, in turn, can offer detailed microscopic-level insights through the use of atomistic simulation methods.

More than 20 years ago Pitzer and coworkers had already identified such solutions with composition extending continuously from molecular liquids to fused salts as relatively unusual but of considerable interest [43, 44]. Such mixtures were studied over the entire composition range, trying to understand ion association from the dilute electrolyte up to the pure ionic liquid. Because these studies were limited to fused salts, the only fluids totally constituted by ions currently known at the time, the mixtures studied were relatively simple at a molecular level. Ionic liquids form nanometer-scale segregated domains, then the structure of such mixtures will be more complex. Nonpolar liquids will not be very soluble in the ionic liquid: they will be able to dissolve in the nonpolar domains, but will not be able to disrupt interionic contacts. The miscibility limit will probably be determined by how much the nonpolar domains will be allowed to swell against the cohesive force of the ionic network. On the opposite situation, polar molecules that are able to solvate both ions efficiently will lead to ion-pair dissociation, producing total miscibility with the ionic liquids. Intermediate polarity molecules, such as aromatics, will behave in-between those extrema. The different structural regimes along the entire composition range, such as the relative size and connectivity of the domains, the level of ionic association, will have some similarities with our previous analysis in section (above) concerning the structure of pure ionic liquids of varying alkyl side chain length. Percolation transitions are expected, for example when nonpolar

domains coalesce or when the ionic network is disrupted, depending on the nature of both the ionic and of the molecular liquid.

This behavior of the mixtures of ionic liquids with molecular solvents was recently studied, experimentally and by molecular simulation, by Del Popolo et al. [45], for mixtures of $[C_4C_1im][PF_6]$ with naphthalene over the entire composition range. As in the previously discussed mixtures of ionic liquids with aromatics, naphthalene is able to cleave some interionic contacts, but not all of them. With compositions in which the ionic liquid is more dilute, the ionic network subsists in the shape of filaments of continuous cation–anion contacts in a medium composed mostly of the molecular fluid. If dilution is increased, then disjoint ionic clusters, down to ion pairs, will form. Some aromatic compounds are not sufficiently good solvents to the ionic liquids and cannot disrupt the ionic network, leading to an immiscibility gap (as is the case with benzene and toluene, for example, at mole fractions around 0.7–0.8 [46, 47].

These detailed studies of the interactions and structure of mixtures of ionic liquids with aromatic organic compounds have not been yet extended to other families of molecular solutes. In the case of mixtures of ionic liquids with water or acetonitrile, although different experimental data were published with the aim of studying the limit of the low concentration of ionic liquid [48, 49], or the effect on the solubility of a third molecular species [50], no complete picture of the structure of the ionic liquid as a function of concentration has been established (Fig. 12).

Using simple molecules as probes for the structure of the ionic liquids as solvents is especially relevant when the molecules are gaseous at ambient conditions [51]. Solubility is directly proportional to the Gibbs energy of solution, and from its variation with temperature, the enthalpy and entropy of solution can be calculated. When one of the chemical species is a low-pressure gas at the pressure and temperature conditions at which the solution is equilibrated, the solubility can be related directly to the Gibbs energy of solvation, usually defined as the variation of the Gibbs energy when the solute is transferred from an ideal gas at the standard pressure into the infinitely dilute solution [52]. The enthalpy of solvation is then related to the nature of the solute–solvent interactions and the entropy of solvation concerns the structural organization of the solvent molecules surrounding the solute.

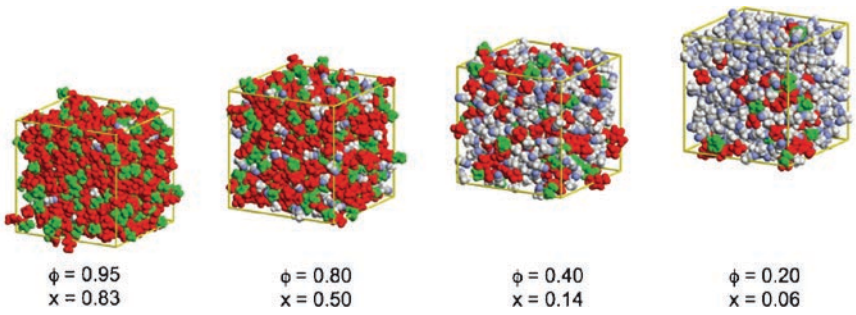

Fig. 12 Molecular dynamics simulation snapshots of mixtures of acetonitrile with $[C_4mim][PF_6]$ with different compositions

The Gibbs energy of solvation is also accessible by models of statistical thermodynamics and can be directly calculated by molecular simulation using realistic intermolecular force fields for both the solvent and the solute. The link between the macroscopic properties and the microscopic interactions can then be established and the molecular mechanisms of solvation can be investigated following adequate and easily implemented in silico experiments.

This idea has been explored to probe the structure of imidazolium based ionic liquids with different alkyl-side chains. For that, the solvation properties of ethane and butane in several 1-alkyl-3-methylimidazolium bis(trifluoromethylsylfonyl) imide ionic liquids were obtained experimentally and interpreted in light of the molecular nanostructure of the ionic liquids which depends on the length of the alkyl chain in the cation [53]. Once the relation between the structure of the ionic liquid and the solvation of gases is understood and the solvation sites are identified [54], it is possible to develop new ionic liquids adequate for different applications. Differences can nevertheless be observed in the solvation of gases belonging to the same homologous series in one ionic liquid depending on the accessibility of the solvation sites in the ionic liquid and on the size of the solute [36].

Ionic liquids have remarkable and promising properties. Their complexity is adapted to the present tools of physical chemistry and thermodynamics and so they provide a challenging terrain of study for scientists and engineers. Measurements and theoretical interpretation of the thermodynamic and physico-chemical properties can advance at equivalent paces providing an interesting interplay and contributing to the rapid advancement of the field and to the development of applications in a growing variety of disciplines including catalysis [55], synthesis, nanomaterial sciences [2] or pharmaceutics [56].

References

1. Dupont J, Suarez PAZ (2006) Phys Chem Chem Phys 8:2441
2. Antonietti M, Kuang D, Smarsly B, Zhou Y (2004) Angew Chem Int Ed 43:4988
3. Hansen J-P, McDonald IR (2006) Theory of simple liquids, 3rd edn. Academic, New York
4. Canongia Lopes JN, Padua AAH (2006) J Phys Chem B 110:3330
5. Wang J, Voth GA (2005) J Am Chem Soc 127:12192
6. Triolo A, Russina O, Bleif H-J, Di Cola E (2007) J Phys Chem B 111:4641
7. Bates ED, Mayton RD, Ntai I, Davis JHJ (2002) J Am Chem Soc 124:926
8. Kumar P, Mittal KL (eds) (1999) Handbook of microemulsion science and technology. Marcel Dekker, New York
9. Gordon CM, Holbrey JD, Kennedy AR, Seddon KR (1998) J Mater Chem 8:2627
10. Shah JK, Brennecke JF, Maginn EJ (2002) Green Chem 4:112
11. Hanke CG, Price SL, Linden-Bell RM (2001) Mol Phys 99:801
12. de Andrade J, Boes ES, Stassen H (2002) J Phys Chem B 106:3546
13. Margulis CJ, Stern HA, Berne BJ (2002) J Phys Chem B 106:12017
14. Canongia Lopes JN, Deschamps J, Padua AAH (2004) J Phys Chem B 108:2038
15. Canongia Lopes JN, Padua AAH (2004) J Phys Chem B 108:16893
16. Canongia Lopes JN, Padua AAH (2006) J Phys Chem B 110:19586
17. Canongia Lopes JN, Padua AAH, Shimizu K (2008) J Phys Chem B 112:5039

18. Borodin O, Smith GD (2006) J Phys Chem B 110:11481
19. Yan TY, Burnham CJ, Del Popolo MG, Voth GA (2004) J Phys Chem B 108:11877
20. Bhargava BL, Balasubramanian S, Klein M (2008) Chem Commun:3339
21. Jorgensen WL, Maxwell DS, Tirado-Rives J (1996) J Am Chem Soc 118:11225
22. Bonifacio RP, Filipe EJM, McCabe C, Costa Gomes MF, Padua AAH (2002) Mol Phys 100:2547
23. Liu ZP, Huang SP, Wang WC (2004) J Phys Chem B 108:12978
24. Earle MJ, Esperança JMSS, Gilea MA, Canongia Lopes JN, Rebelo LPN, Magee JW, Seddon KR, Widegren JA (2006) Nature 439:831
25. Santos LMNBF, Canongia Lopes JN, Coutinho JAP, Esperança JMSS, Gomes LR, Marrucho IM, Rebelo LPN (2007) J Am Chem Soc 129:284
26. Maginn E (2007) J Acc Chem Res 40:1200
27. Canongia Lopes JN (1999) Mol Phys 96:1649
28. Urahata SM, Ribeiro MCC (2004) J Chem Phys 120:1855
29. Tokuda H, Hayamizu K, Kunikazu I, Susan MABH, Watanabe M (2005) J Phys Chem B 109:6103
30. Mandal PK, Sarkar M, Samanta A (2004) J Phys Chem A 108:9048
31. Paul A, Mandal PK, Samanta A (2005) J Phys Chem B 109:9148
32. Anderson JL, Armstrong DW (2003) Anal Chem 75:4851
33. Canongia Lopes JN, Shimizu K, Padua AAH, Umebayashi Y, Fukuda S, Fujii K, Ishiguro S (2008) J Phys Chem B 112:1465
34. Canongia Lopes JN, Costa Gomes MF, Padua AAH (2006) J Phys Chem B 110:16816
35. Padua AAH, Costa Gomes MF, Canongia Lopes JNA (2007) Acc Chem Res 40:1087
36. Pison L, Canongia Lopes JN, Rebelo LPN, Padua AAH, Costa Gomes MF (2008) J Phys Chem B 112:12394
37. Ferreira R, Blesic M, Trindade J, Marrucho IM, Canongia Lopes JN, Rebelo LPN (2008) Green Chem 10:918
38. Lachwa J, Bento I, Duarte MT, Canongia Lopes JN, Rebelo LPN (2006) Chem Commun 2445
39. Deetlefs M, Hardacre C, Nieuwenhuyzen M, Sheppard O, Soper AK (2005) J Phys Chem B 109:1593
40. Hanke CG, Johansson A, Harper JB, Lynden-Bell RM (2003) Chem Phys Lett 374:85
41. Harper JB, Lynden-Bell RM (2004) Mol Phys 102:85
42. Gutel T, Santini CC, Padua AAH, Fenet B, Chauvin Y, Canongia Lopes JN, Bayard F, Costa Gomes MF, Pensado A (2009) J Phys Chem B 113:170
43. Pitzer KS (1980) J Am Chem Soc 102:2902
44. Pitzer KS (1984) J Phys Chem 88:2689
45. Del Popolo MG, Mullan CL, Holbrey JD, Hardacre C, Ballone P (2008) J Am Chem Soc 130:7032
46. Lachwa J, Szydlowski J, Makowska A, Seddon KR, Esperanca JMSS, Guedes HJR, Rebelo LPN (2006) Green Chem 8:262
47. Kato R, Krummen M, Gmehling J (2004) Fluid Phase Equilibria 224:47
48. Malham IB, Letellier P, Turmine M (2006) J Phys Chem B 110:14212
49. Malham IB, Letellier P, Mayaffre A, Turmine M (2007) J Chem Thermodyn 39:1132
50. Hong G, Jacquemin J, Husson P, Costa Gomes MF, Deetlefs M, Nieuwenhuyzen M, Sheppard O, Hardacre C (2006) Ind Eng Chem Res 45:8180
51. Hildebrand JH, Scott RL (1950) The solubility of nonelectrolytes, 3rd edn. Reihnold, New York
52. Costa Gomes MF, Pádua AAH (2005) Pure Appl Chem 77:653
53. Pison L, Pensado A, Padua AAH, Costa Gomes MF (2009) in preparation
54. Deschamps J, Costa Gomes MF, Pádua AAH (2004) Chem Phys Chem 5:1049
55. Parvulescu VI, Hardacre C (2007) Chem Rev 107:2615
56. Rogers RD, Hough WL (2007) Bull Chem Soc Jpn 80:2262

Top Curr Chem (2009) 290: 185–212
DOI: 10.1007/128_2008_32

Published online: 21 May 2009

Thermophysical Properties of Ionic Liquids

David Rooney, Johan Jacquemin, and Ramesh Gardas

Abstract Low melting point salts which are often classified as ionic liquids have received significant attention from research groups and industry for a range of novel applications. Many of these require a thorough knowledge of the thermophysical properties of the pure fluids and their mixtures. Despite this need, the necessary experimental data for many properties is scarce and often inconsistent between the various sources. By using accurate data, predictive physical models can be developed which are highly useful and some would consider essential if ionic liquids are to realize their full potential. This is particularly true if one can use them to design new ionic liquids which maximize key desired attributes. Therefore there is a growing interest in the ability to predict the physical properties and behavior of ionic liquids from simple structural information either by using group contribution methods or directly from computer simulations where recent advances in computational techniques are providing insight into physical processes within these fluids. Given the importance of these properties this review will discuss the recent advances in our understanding, prediction and correlation of selected ionic liquid physical properties.

Keywords Ionic liquid • Group contribution method • QSPR • Correlation

Contents

D. Rooney (✉) and R. Gardas
School of Chemistry and Chemical Engineering, Queen's University Belfast
Belfast, North Ireland
e-mail: d.rooney@qub.ac.uk

J. Jacquemin
Université François Rabelais
Laboratoire PCMB (E.A. 4244), Equipe CIME, Faculté des Sciences et Techniques
parc de Grandmont, 37200, Tours, France

Nomenclature

	Anions
$[NTf_2]^-$	Bis(trifluoromethylsulfonyl)imide
$[OTf]^-$	Trifluoromethanesulphonate
$[C_1SO_4]^-$	Methylsulphate
$[C_2SO_4]^-$	Ethylsulphate
$[PF_6]^-$	Hexafluorophosphate
$[BF_4]^-$	Tetrafluoroborate
$[Methide]^-$	Tris(trifluoromethylsulfonyl)methide
$[DCA]^-$	Dicyanamide
$[FAP]^-$	Tris(perfluoroalkyl)trifluorophosphate
	For cations, *n* represents the carbon number of the alkyl chain, i.e., ethyl = 2, butyl = 4, etc.
$[C_nmim]^+$	1-Alkyl-3-methylimidazolium
$[C_nmpy]^+$	Alkyl-1-methylpyridinium
$[C_nmpyr]^+$	1-Alkyl-1-methylpyrrolidinium
$[P_{66614}]^+$	Trihexyl-(tetradecyl)phosphonium
$[CNpy]^+$	1-Cyanomethylpyridinium
$[CNmpyr]^+$	1-Cyanomethyl-1-methylpyrrolidinium

1 Introduction

Over the last few years there has been a dramatic increase in research relating to the use of ionic liquids as potential replacements for organic solvents in chemical processes [1–4]. More recently specialized areas such as lubricants [5], heat transfer fluids [6] and analytical applications [7] have been investigated. These materials are generally organic salts which have a relatively low melting point when compared to inorganic salts. For example, many are fluid at temperatures below 298 K and these are often described as room temperature ionic liquids (RTILs). However, the term ionic liquid does not exclude those salts which have higher melting points and although this description is associated with salts which melt below 373 K, in reality there is no clear distinction between the term molten salt (often used for high temperature liquids) and the term ionic liquid. The expanding range of applications is not surprising given that approximately 10^{18} anion–cation combinations exist which could generate ionic liquids [8] and thus these liquids could be classified as true designer materials, particularly since many of these designs include in-built functionality. Therefore given the potential range available it is possible for them to have properties suited to a particular application or, if desired, contradict some of

the earlier perceived advantages of dealing with fluids consisting of only ionic species. For example, ionic liquids are generally regarded as having negligible vapor pressure yet recently there have been reports of volatile ionic liquids [9] and the distillation of ionic liquids has been demonstrated [10]. Their biodegradability and toxicity has been questioned yet nutritional or pharmacological ionic liquids are feasible [11]. Similarly while some ionic liquids could be used as flame retardants, others are combustible and energetic ionic liquids are a reality [12].

In each of the potential applications listed above, the ionic liquids often display at least one key advantage over molecular fluids. This may be simply that ionic liquids tend to have much greater liquidus temperature range [13] at atmospheric pressure than common molecular solvents, allowing for greater flexibility in processing conditions, or it could be that the chemistry within an ionic environment is sufficiently different to cause an increase in yield or selectivity. Such chemical effects have been reported for some ionic liquid facilitated reactions [14] although in other cases normal solvent effects can be used to describe the system behavior [15]. For applications such as lubricants, heat transfer fluids, and in general when considering any scale-up or process design, knowledge of thermophysical properties and in particular transport properties is important. The IUPAC ionic liquid database (IL Thermo) [16], which has been operating for approximately 3 years, has collected a significant amount of such data including chemical and physical properties as well as measurement methods, etc. Importantly it also contains information with regard to sample purity and the uncertainty of quoted property values and thus this database serves as an important tool in addressing the need to find reliable physical property data. In particular, experimental data is reported for a large range of properties with density and viscosity being the most widely examined. An additional advantage of such a repository is that it facilitates research into the development of predictive tools to generate group contribution parameters for these important physical properties which overall increases our basic understanding of structure–property relationships of these novel fluids. Currently very few works have systematically studied the qualitative and/or quantitative relationships between the structures of ILs and their fundamental properties [17–21] such as melting point, viscosity, density, surface tension, thermal and electrochemical conductivity, solvent properties and speed of sound. At present, data for many other important physico-chemical properties of ionic liquids are in short supply, or are currently too unreliable to allow for similar structure-property relationship studies. Group contribution models (GCMs) are commonly used as predictive tools by engineers and physical scientists in process design, and many have become an integral part of process simulation software packages, due to their wide applicability, ease of use and relative accuracy. The basic assumptions of GCMs are that the physical properties of a component are dependent on the functional groups which make up its structure and each functional group provides a fixed contribution towards the physical properties, irrespective of the species involved [22]. Herein we will examine a number of key ionic liquid thermophysical properties including those for density, viscosity, heat capacity, surface tension, melting point, and the critical properties and discuss current strategies to model them.

1.1 Liquidus Range

The liquidus range relates to the temperature range where the ionic liquid is in liquid form; in general this is the difference between the melting point and the decomposition temperature. However it could also represent the temperature difference between glass transition point and boiling point, etc. Accurate values for melting points for ionic liquids are scarce as, like in the case of inorganic salts, melting point and glass transition temperatures can be strongly affected by the presence of impurities. For example, reported glass transition temperatures for $[C_4mim][PF_6]$ vary between 196 and 212 K [23, 24]. Van Valkenburg et al. [25] studied the freezing–melting behavior of some ionic liquids when contaminated with water and identified that $[C_2mim][BF_4]$ has two freezing exotherms at 237 and 214 K, respectively. Here they observed that contamination with water substantially extended the lower temperature limit. In this study they also noted that chloride impurities had little effect on the freezing-melting behavior of the studied liquids.

Ngo et al. [26] identified that larger more asymmetric cations tend to yield ionic liquids with lower melting points and the highest melting points are associated with more symmetric cations. It was also shown that branched alkyl chains such as *iso*-propyl displayed higher melting points than those containing straight chains. In general the melting point of an ionic liquid is a function of both the cation and the anion. Figure 1 shows the melting points for the $[C_nmim][BF_4]$ series, where it can be observed that the melting point is initially high and then decreases as the chain length increases, i.e., decreases with increasing asymmetry in agreement with Ngo et al. [26].

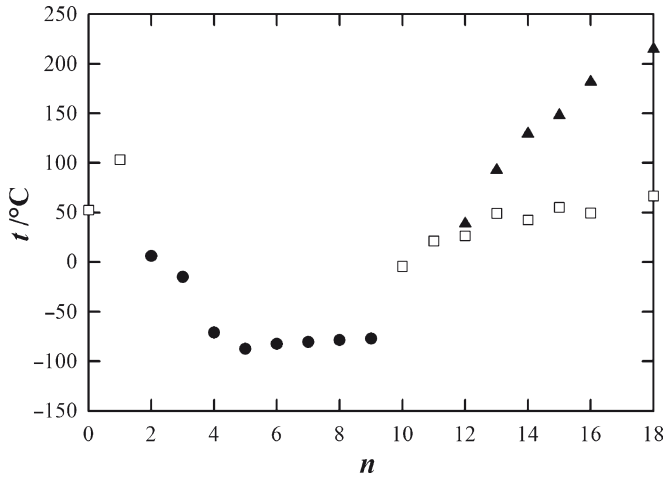

Fig. 1 Phase transition temperature as a function of chain length, *n*, for the $[C_nmim][BF_4]$ series where $n = 0$–16,18 [123]. *open squares*, melting point; *filled circles*, glass transition; *filled triangles*, clearing transition

At chain lengths greater than around nine, the melting point increases again and liquid crystalline regions are observed to form at higher chain lengths; such materials are of interest in areas relating to catalysis and solar cells [27, 28], etc. A similar trend has also been reported for the [$C_n$mim][PF_6] series [29].

In order to investigate ionic liquid structural features which could lead to low melting point salts, Katritzky et al. employed quantitative structure–property relationship (QSPR) methods with reasonable success [8, 17]. In this study, correlations with R^2 values between 0.70 and 0.90 were reported. The premise of this method is that all physical properties of a compound can be directly related to its chemical structure through the use of molecular descriptors. While not all molecular descriptors will be relevant to all properties the correct choice of descriptor can be used to develop a relationship between it and the property under study. Eike et al. [30] used this approach to correlate and predict the melting points of organic salts based on quaternary ammonium and pyridiniun cations and validated the method using the previously reported bromides. For example the correlation represented by (1) gave an R^2 value of 0.79 using five-descriptors for a series of N-pyridinium bromides:

$$T_{\mathrm{m}}/^{\circ}\mathrm{C} = 125.85 + 0.58[D_1] - 2273.22[D_2] - 104.03[D_3] + 254.70[D_4] - 74.37[D_5]. \quad (1)$$

Here, D_1–D_5 are molecular descriptors for the total charge weighted negative surface area, atomic charge weighted fractional negative surface area, bonding information content, relative negative charge and the relative positive charge surface area respectively. Those with negative multipliers, such as the bonding information content (D_3), indicate that the larger the value of the descriptor the lower the melting point; in this case that melting point decreases with increasing asymmetry. By extending the range of molecular descriptors used it is possible to improve the accuracy of the correlation. For example, Carrera and Aires-de Sousa [31] generated regression trees as a method for determining the most significant descriptors and used this for estimating the melting points of a range of pyridinium bromides from their molecular structure. In this study 126 pyridinium cations were analyzed using 1,085 molecular descriptors including those for molecular geometry, charge indices, connectivity between molecules, counts of specific functional groups and atomic weight, etc. Using this approach a reasonably good correlation was obtained between the experimental and calculated values with a reported R^2 = 0.933 and a root-mean-square (rms) error = 12.6 K. Importantly this method was able to estimate the melting point of nine new pyridinium bromides. While this error may seem to be reasonably large, Charton and Charton [32] reported an rms error of 16.4 K for a range of 303 normal and branched substituted alkanes using an 11 term QSPR function. For other data sets Eike et al. [30] found that additional descriptors should be used; for example, tetraalkyl-ammonium bromides and (*n*-hydroxyalkyl)-trialkyl-ammonium bromides necessitated descriptors including the valence-modified connectivity for two bond paths, or three atoms in a row and the complementary information content. Similarly, Trohalaki et al. [33] developed QSPR relationships for the melting points and densities for a range of energetic ionic liquids such as the 1-substituted 4-amino-1,2,4-triazolium bromide and nitrate

salts. A good correlation ($R^2 > 0.85$) with the experimental melting point data was found using the following three parameter equation for the bromide salts:

$$T_m / ^\circ \mathrm{C} = -262.00 - 6.91 \times 10^5 \left[D_6\right] + 47.40 \left[D_7\right] - 136.00 \left[D_8\right]^{-1}, \quad (2)$$

where D_6–D_8 are descriptors for the nucleophilic reactivity index for the amine nitrogen, the area weighted surface charge of the hydrogen-bond acceptor atoms and the energy of the lowest unoccupied molecular orbital. A similar three parameter equation was derived for the nitride salts, in this case using two descriptors for the hydrogen bond donating ability of the cation and the minimum nucleophilic reactivity index for a carbon atom.

Despite the fact that the QSPR approach was successful in each of the above studies, every class of ionic liquid generated its own descriptor function and thus the technique cannot easily be extended to the entire family of potential ionic liquids. More recently, López-Martin et al. [34] treated the cations and anions separately and calculated 1,500 descriptors for each ion, thereby generating 3,000 for each ionic liquid. Importantly this was the first report covering the anion influence on the ionic liquid melting point discussed previously. Here the authors optimized the cation and anion geometries using semi-empirical QM calculations before deriving, ranking by variable importance analysis, and classifying the descriptors into three categories, relating to anion size, anion symmetry and charged surface areas. For the imidazolium based ionic liquids three regions were identified which influence the melting point. These are: the charge-rich region, which is localized on the ring and responsible for ionic interaction; the symmetry-breaking region, which exists in the range of 5.5 until 12 Å; and the hydrophobic region, which increases melting point due to increased Van der Waals forces. These regions are shown schematically in Fig. 2.

Alternative approaches to the study of melting points of ionic liquids include molecular dynamics simulations such as that conducted by Alavi and Thompson [35]. Here simulations of [C_2mim][PF_6] over a wide temperature range, which

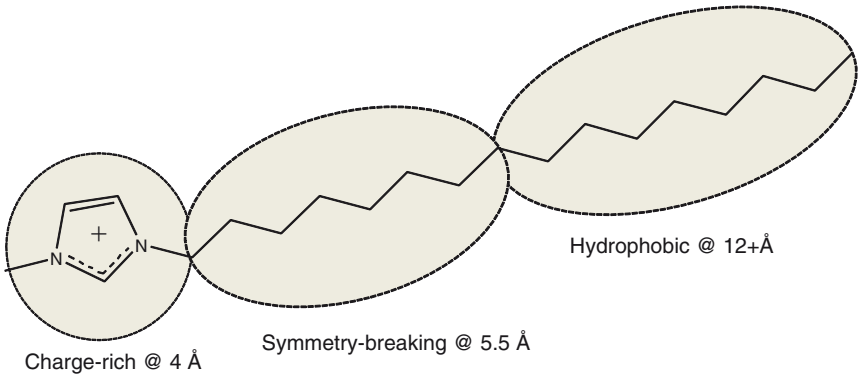

Fig. 2 Structural regions important in determining the melting point of the 1-alkyl imidazolium based cations; adapted from López-Martin et al. [34]

included the known melting point, predicted a value approximately 40 K higher than that given in the literature. Similar atomistic simulations by Jayaraman and Maginn [36] estimated the melting point of the orthorhombic [C_4mim][Cl] at 365 ± 6 K which is some 26 K higher than the literature value.

Krossing et al. [37] assessed the Gibbs free energy of fusion as a predictor of the melting point using a Born–Fajans–Haber cycle which was closed by the lattice and solvation Gibbs energies of the constituent ions in the molten salt. These were calculated using a combination of volume based thermodynamics and quantum chemical calculations for the lattice free energies and the COSMO solvation model and experimental dielectric constants for the free energy of solvation. For the range of 14 different ionic liquids studied, which included a variety of anion and cation combinations, the Gibbs free energy of fusion was found to be negative for all the ionic liquids studied indicating that the liquid state was thermodynamically favorable. It was also shown from this study that it is possible to predict the melting point of an ionic liquid using the dielectric constant.

One of the most publicized advantages of ionic liquids has been their insignificant vapor pressures. On one hand this can reduce fire hazards when employed as solvents in chemical processes or equally it can cause difficulties in the recovery of high boiling point products which would have normally been purified by distillation of the solvent. In reality ionic liquids will exert some degree of vapor pressure although for most aprotic ionic liquids these pressures will be significantly lower than commonly used organic solvents particularly at room temperature. At higher temperatures the ionic liquids may undergo thermal decomposition to a range of undesired products such as water, carbon dioxide and hydrocarbons [38] or could simply revert back to the original components. The latter is generally encountered when using protic ionic liquids such as 1-methylimidazolium chloride ([C_0mim]Cl) generated in the BASIL process [39] which can be reverted back to methylimidazole and hydrochloric acid. Thus all ionic liquids have a maximum operating temperature in order to avoid volatilizing or decomposing of the liquid. The temperature at which this happens represents the other limit of the liquidus range. Table 1 shows the reported liquidus range of a number of different ionic liquids. The onset temperature (T_{onset}) is defined as the intersection of the baseline weight

Table 1 Melting points and thermal decomposition temperatures for a range of selected 1-alkylimidazolium ionic liquids. All temperatures in Kelvin, data taken from Fredlake et al. [123] except for superscript a values which are from Wilkes et al. [25]

Ionic liquid	Melting point (°K)	Glass transition (°K)	T_{onset} (°K)	T_{start} (°K)
[C_4mim]Cl	314	204	537	423
[C_4mim]Br	–	223	546	488
[C_2mim][BF_4]	287[a]	–	718[a]	–
[C_4mim][BF_4]	–	188	634/696[a]	563
[C_4mim][NTf_2]	271	187	695	603
[C_4mim][OTf]	286	–	665	613
[C_4mim][Methide]	–	208	686	633
[C_4mim][DCA]	–	183	573	513

and the tangent of the weight vs temperature curve obtained from TGA analysis as decomposition occurs, while the start temperature (T_{start}) is the temperature at which the decomposition of the sample begins. As such T_{start} is lower than T_{onset}.

For some of the reported ionic liquids in Table 1, the range is significant. For example it is 332 K in the case of $[C_4mim][NTf_2]$, whereas for others this range is relatively small, as in the case of $[C_4mim]Cl$. These examples have used the temperature difference between the melting point and the starting temperature for thermal decomposition (T_{start}). From this it can be observed that even the relatively poor range of $[C_4mim]Cl$ is greater than that of water when operating at atmospheric pressure. The large liquidus range of certain ionic liquids was exploited by Rodríguez et al. [40] in thermometer applications using the ionic liquids tris(2-hydroxyethyl) methylammonium methylsulfate ($[TEMA][C_1SO_4]$) and $[P_{66614}][NTf_2]$.

It can be seen in Table 1 that a significant difference in the T_{onset} values has been reported between groups for $[C_4mim][BF_4]$. Kosmulski et al. [41] observed that the scan rate, mass of the ionic liquid, moisture content and addition of silica all influenced the thermal decomposition. This latter observation agrees with that of Ngo et al. [26] where it was found that the pan construction material was important for certain ionic liquids, most notably the $[PF_6]^-$ salts. It was also observed by Kosmulski et al. [41] that, while the thermal decomposition temperatures are high, slow degradation occurred for a range of $[C_nmim][PF_6]$ ionic liquids at a temperature of 473 K which is more than 100 K lower than the T_{onset} value found. Awada et al. [38] studied the thermal decomposition of a number of ionic liquids and reported that both the chain length and counter ion have an effect on the thermal stability of the imidazolium salts. In this study it was found that $[PF_6]^-$, $[NTf_2]^-$ and $[BF_4]^-$ anions were more thermally stable than the equivalent halide salts and that the stability was inversely proportional to the length of the alkyl chain. It was also shown that the atmosphere has an effect on the thermal stability of the $[BF_4]^-$ and $[PF_6]^-$ salts where both the onset and decomposition temperatures were significantly reduced when run under air as compared to those under an N_2 atmosphere. Kamavaram and Reddy [42] investigated the long term thermal stability of $[C_nmim]Cl$ (n = 4, 6) using isothermal TGA at various temperatures ranging from 423 to 473 K over an extended period under an argon purge. For both liquids it was found that the weight loss was approximately 5% at 423 K increasing to >90% at 473 K over 15 h. The authors fitted the data to a pseudo-first order rate expression and determined the activation energies for the decomposition as 121 and 117 kJ mol^{-1} for n = 4 and 6, respectively. From the above investigations it would appear that it is difficult to predict accurately the thermal decomposition point for ionic liquids as a number of factors can influence the observed temperatures.

Under a combination of high temperatures and low pressures ionic liquids have been shown to evaporate, albeit at very low rates [10]. For example at 573 K and 0.1 mbar the evaporation rate was calculated as 0.12 g h^{-1} for $[C_2mim][NTf_2]$ decreasing to 2.40×10^{-3} g h^{-1} when the alkyl chain length was increased to 16. Similarly $[C_nmim][NTf_2]$ (n = 10, 12) were shown by Rebelo et al. [43] to evaporate at 450 K and a lower pressure of 0.01 mbar. This study was also the first to estimate the critical properties of the ionic liquids using literature correlations based on the

relationship between the critical temperature and the temperature dependence of the surface tension and liquid density. A further generalization that the boiling point is approximately 60% of the critical temperature allowed for a crude estimation of this value. Based on these calculations the estimated boiling points for [$C_n$mim][NTf_2] ionic liquids decreased from around 625 K for $n = 2$ to 479 K when $n = 10$. It was noted in this paper that the vapor pressure at different temperatures is significantly affected by the vaporization enthalpy ($\Delta_{vap}H$) where it was shown, for example, that the vapor pressure drops by one order of magnitude for each 15 K decrease in temperature when using a $\Delta_{vap}H$ of 300 kJ mol^{-1}. Since this initial work a number of groups have investigated the boiling point and $\Delta_{vap}H$ of ionic liquids using a variety of approaches as shown in Table 2.

Zaitsau et al. [44] measured the vapor pressure of a series of [$C_n$mim][NTf_2] ionic liquids using the integral effusion Knudsen method and correlated the $\Delta_{vap}H$ with the molar volumes and the surface tensions of the compounds. What is clear from this study is that the values for $\Delta_{vap}H$ are approximately half that used in Rebelo's initial estimate and further indicated that the Eotvos–Guggenheim correlations which are suitable for molecular solvents do not apply for ionic liquids.

In what is essentially a temperature programmed desorption (TPD) technique, Armstrong et al. [45] evaporated eight imidazolium based ionic liquids using an ultra-high vacuum and analyzed the vapors by line of sight mass spectrometry. Not only was this approach used to determine the $\Delta_{vap}H$ values of the ionic liquids but equally importantly it was able to show that the ionic liquids evaporated as ion pairs. Furthermore an electrostatic model was developed, which in principal related the $\Delta_{vap}H$ to the molar volumes of the ionic liquids which can in turn, as will be shown later, be estimated using group contribution models with reasonable accuracy. The values determined using this technique agree well with those determined by Zaitsau et al. [44] except for the $[BF_4]^-$ and $[PF_6]^-$ salts where contamination of the ionic liquids during the surface tension measurements was suggested as the probable cause for the discrepancy. Verevkin [46] modified the approach of Emel'yaneko et al. [47] which uses a combination of calorimetry and high-level ab initio calculations. Despite the time involved in the combustion and calculation measurements this technique is shown to agree well with that of the TPD results,

Table 2 Estimated values of enthalpies of vaporization ($\Delta_{vap}H_{298}$ in kJ mol^{-1}) for ionic liquids obtained using various methods

Ionic liquid	Surface tension [46]	TPD [47]	Microcalorimetry [48]	TGA[50]	MD calculations [51]
[C_2mim][NTf_2]	136.1	134	132.9	120.6	159
[C_4mim][NTf_2]	134.6	134	137.9	118.5	174
[C_6mim][NTf_2]	141.6	139	142.9	124.1	184
[C_8mim][NTf_2]	149.0	149	147.9	132.3	201
[C_{10}mim][NTf_2]	155.5	–	–	134.0	–
[C_8mim][BF_4]	122.0	162	160.4	–	–
[C_8mim][PF_6]	144.3	169	168.9	–	–

further suggesting that the problems with the $[BF_4]^-$ and $[PF_6]^-$ salts are due to errors in the surface tension measurements. Recently Luo et al. [48] demonstrated an isothermogravimetric technique (TGA) where $\Delta_{vap}H$ is estimated using a combination of the Langmuir and Clausius–Clapeyron expressions using the assumption that the enthalpy of vaporization is independent of temperature. As can be seen in Table 2, the values reported using this technique are lower than those determined using alternative methods although they follow a similar trend to those found using the surface tension technique. Molecular dynamics approaches have also been used to estimate the $\Delta_{vap}H$ of the $[C_n mim][NTf_2]$ ionic liquids, as shown in Table 2, which agree well with literature values [49]. Other purely computational methods include that proposed by Diedenhofen et al. [50] in which the vapor pressures of a range of ionic liquids were estimated using two separate approaches based on the COSMO-RS method and quantum chemical gas phase calculations. It was shown that the $\Delta_{vap}H$ values are predicted with reasonable accuracy using both strategies, indicating that the enthalpic interactions are correctly described in the proposed models. Recently Ludwig [51] reported that a number of thermodynamic properties including vapor pressures, enthalpies of vaporization, boiling points and entropies of vaporization can be predicted from purely theoretical methods using ab initio cluster calculations in combination with statistical thermodynamics. Together these recent papers demonstrate that computational techniques for the determination of these properties have advanced considerably in the last few years.

1.2 Other Critical Properties

Recently, Valderrama and Robles developed and applied the modified Lydersen–Joback–Reid group contribution model for the determination of normal boiling points, acentric factors and critical properties of ionic liquids [52, 53]. Although they were unable to validate this directly, due to the lack of experimental data on ionic liquid boiling points or critical properties, they used the values obtained in a model for the prediction of densities with reasonable accuracy. The developed group contribution model is also highly flexible as the groups are relatively small allowing for an estimation of these properties for a large range of cations and ions.

1.3 Density

A considerable amount of experimental data has been measured for the density as a function of the temperature for a range of imidazolium, pyridinium, ammonium, phosphonium and pyrrolidium based ionic liquids. For pure ILs, the values vary depending on the choice of anion and cation. Typical values range from 1.05 to 1.64 g cm^{-3} at 293 K which decrease with temperature to between 1.01 and 1.57 g cm^{-3} at 363 K. As with molecular solvents the densities are closely related to the molar

mass of the liquid with ILs containing heavy atoms found to be most dense. Figures 3 and 4 show a range of measured densities of dried ionic liquids as a function of temperature at 0.1 MPa where it can be observed that the density is found to be a strong function of anion type and decreases with increasing alkyl chain length.

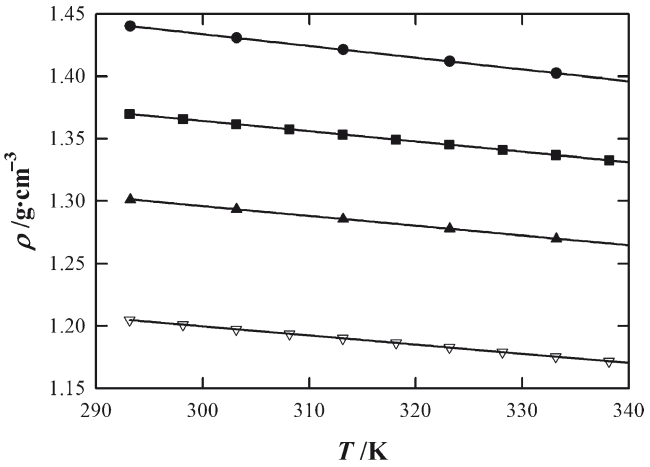

Fig. 3 Effect of the anion on the densities of $[C_4mim]^+$ based ionic liquids: *filled circles*, $[NTf_2]^-$; *filled squares*, $[PF_6]^-$; *filled triangles*, $[OTf]^-$; *inverted open triangles*, $[BF_4]^-$ [61]

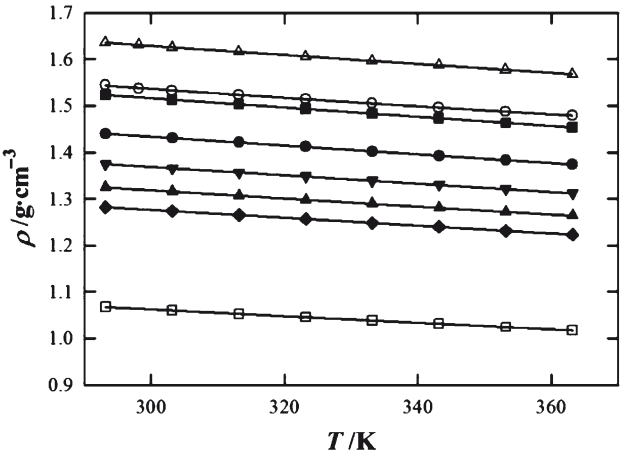

Fig. 4 Effect of the cation on the densities of $[NTf_2]^-$ based ionic liquids: *filled squares*, $[C_2mim]^+$; *filled circles*, $[C_4mim]^+$; *inverted filled triangles*, $[C_6mim]^+$; *filled triangles*, $[C_8mim]^+$; *filled diamonds*, $[C_{10}mim]^+$; *open triangles*, $[CNPy]^+$; *open circles*, $[CNmPyrro]^+$; *open squares*, $[P_{66614}]^+$ [61]

The most widely used method for ionic liquid density measurement is the vibrating-tube densitometer method which relies on a calibration as a function of temperature and pressure using appropriate reference fluids [54, 55]. For many reported ionic liquids this is not routinely performed and corrections for the case of viscous fluids (i.e., >100 mPa s) are often ignored [56–58]. Despite these factors the densities of ionic liquids measured with vibrating tube densitometers have a standard uncertainty to within 0.1%. Alternative methods include the calculation of density through speed of sound measurements [59] or piezometric methods [54]. Both approaches are relatively complex technically but present the advantage of providing extra thermodynamic property data. Pycnometric methods or hydrostatic weighing techniques are also used extensively; however, the use of pycnometers requires a large sample of fluid and extensive volume calibration procedures with a reference fluid to obtain very accurate values of the density.

As with other physical properties impurities can have a significant effect. Jacquemin et al. [60] studied six hydrophobic and hydrophilic ILs including five imidazolium and one ammonium based ionic liquid as a function of temperature up to 393 K and at atmospheric pressure and found that the densities of the water-saturated IL samples were lower when compared with dried samples. This difference was relatively small at around 1–2% for hydrophobic ionic liquids samples containing a mole fraction of water close to 30%. More recently Jacquemin et al. [61] reported experimental densities for a range of selected ionic liquids contaminated by a mass fraction of water (w_w) of 1×10^{-3} at 298.15 K and 0.1 MPa, shown here in Table 3. It can be observed from this data that while the variation on the overall density is small, the change in the calculated molar volume (ΔV_m) is significantly larger given the relative difference in the molecular weights between ionic liquid and water. Here the water mole fraction is given by the x_w value.

Similarly it has been reported that increasing halide (such as chloride and bromide) contamination also tends to decrease the density over a wide range of values [62].

A number of models which can estimate density at atmospheric pressure have recently been reported. For example, Rebelo et al. [63, 64] defined the effective molar volumes of ions at 298.15 K and used the assumption of "ideal behavior" for the determination of the molar volume of ionic liquids. Yang et al. [65] used a theory based on the "interstice model" which correlated the density and the surface tension of the ionic liquid. Group contribution models have been reported by Kim et al. [66, 67] for the calculation of the density and CO_2 gas solubility for 1-alkyl-3-methylimidazolium based ionic liquids as a function of the temperature and CO_2 gas pressure with reasonable accuracy over a 50 K temperature range; however, the

Table 3 Impact of water impurities on the calculated molar volume of ionic liquids

Ionic liquid	ρ g cm^{-3}	V_m (cm^3 mol^{-1})	$10^2 \times x_w$	ΔV_m (%)
[C_2mim][NTf_2]	1.5150	258.29	2.13	−2.0
[C_4mim][NTf_2]	1.4351	292.22	2.27	−2.2
[C_{10}mim][NTf_2]	1.2755	394.77	2.72	−2.6
[P_{66614}][NTf_2]	1.0601	720.70	4.07	−4.0

effect of the anion was not studied. In their work, Ye and Shreeve [68] observed a linear relationship between the density in solid and liquid states of ionic liquids and used a group contribution model for the calculation of the density in solid state coupled with linear regression to estimate the liquid density. Recently, Gardas and Coutinho [69] extended the Ye and Shreeve group contribution method for the estimation of the density over a wide range of temperatures and pressures with a determined uncertainty of 0.6%. As in the original work, the calculation of ionic liquid density was determined from a prior knowledge of their mechanical coefficients thus limiting the general applicability of this methodology. Alternative strategies to the GCM include that of Deetlefs et al. [18] which studied the determination of refractive index, surface tension and density at 298 K for a range of ionic liquids using a parachor function defined by Knotts et al. [70].

Recently Jacquemin et al. [61, 71] extended the concept proposed by Rebelo et al. In this method the effective molar volume of an ionic liquid and hence density can be determined by assuming that the volumes of the ions behave as an "ideal" mixture. This strategy was used to calculate the effective molar volumes of a wide range of ions using a large set of previously reported data as a function of the temperature difference at 0.1 MPa and a reference temperature of 298.15 K using the following equation:

$$V^*_{\text{ion}}\left(\delta T\right) = \sum_{i=0}^{2}\left(C_i \times \delta T^i\right). \tag{3}$$

The coefficients (C_i) were obtained for 44 anions and 102 cations which achieved a high degree of accuracy when using more than 2150 data points. This approach was further extended to include pressure [72] by applying the commonly used Tait equation. In this case the effective molar volumes are estimated using the following equation:

$$V^*_{\alpha}\left(\delta T,\ p,\ G,\ H\right) = \frac{V^*_{\alpha}\left(\delta T,\ p_{\text{ref}}\right)}{1 - G\ln\left(\dfrac{\sum_{i=0}^{2}\left(H_i \cdot \delta T^i\right) + p}{\sum_{i=0}^{2}\left(H_i \cdot \delta T^i\right) + p_{\text{ref}}}\right)}. \tag{4}$$

Here α can represent the cation or anion constituting an IL or an extra -CH_2- group in the alkyl chain length of an 1-alkyl-3-methylimidazolium based ionic liquid and $V^*_{\alpha}\left(\delta T,\ p_{\text{ref}}\right)$ is the effective molar volume obtained using the reference pressure (p_{ref} = 0.1 MPa). The coefficients (G and H_i) were obtained by fitting literature data and, as can be seen in Fig. 5, the approach was successful in estimating the densities over a wide temperature and pressure range yielding 0.36% error for 5,080 experimental data points.

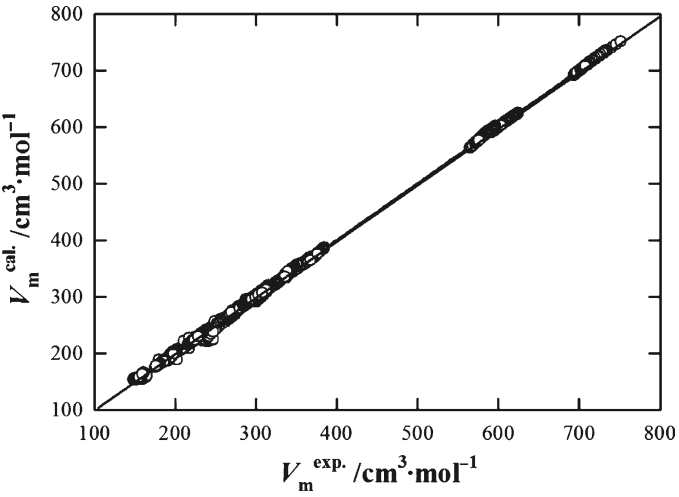

Fig. 5 Predicted vs experimental molar volumes for a range of ionic liquids at varying temperature and pressure using the group contribution method proposed by Jacquemin et al. [72]

1.4 Viscosity

Viscosity relates to the internal friction within the fluid which is caused by intermolecular interactions and is therefore important in all physical processes which involve the movement of the fluid or components dissolved within it. Therefore the design of liquid-liquid extractors, distillation columns, heat-transfer equipment, process piping, reactors, and other units found in various chemical and pharmaceutical industries requires the knowledge of the viscosity of fluids and their mixtures.

Viscosity is arguably the most important physical property when considering any scale-up of ionic liquid applications. In general a low viscosity is desired for solvent applications in order to minimize pumping costs and increase mass transfer rates while higher viscosities may be favorable for other applications such as lubrication or use in supported membrane separation processes. It is known that the viscosity of ionic liquids vary widely depending on the type of cation and anion and are relatively high when compared to those of common organic solvents.

Organic solvents typically have room temperature viscosities ranging from 0.2 to 10 cP [73] whereas ionic liquids display, generally, a broad range of room temperature viscosities, from 10 to 726 cP [74] and significantly higher (Fig. 6). It can be seen in Fig. 6 that the viscosity increases with alkyl chain length of imidazolium cation. For example, in the series of [$C_n$mim][PF_6] with n = 2,4–8, the viscosity at 298.15 K increases monotonously from 172.3 to 677.4 cP. Viscosities for the series of [$C_n$mpy][NTf_2] ionic liquids are slightly higher than those of [$C_n$mim][NTf_2] ionic liquids. The increment with the alkyl chain length of imidazolium cation is more pronounced in case of ionic liquids containing the

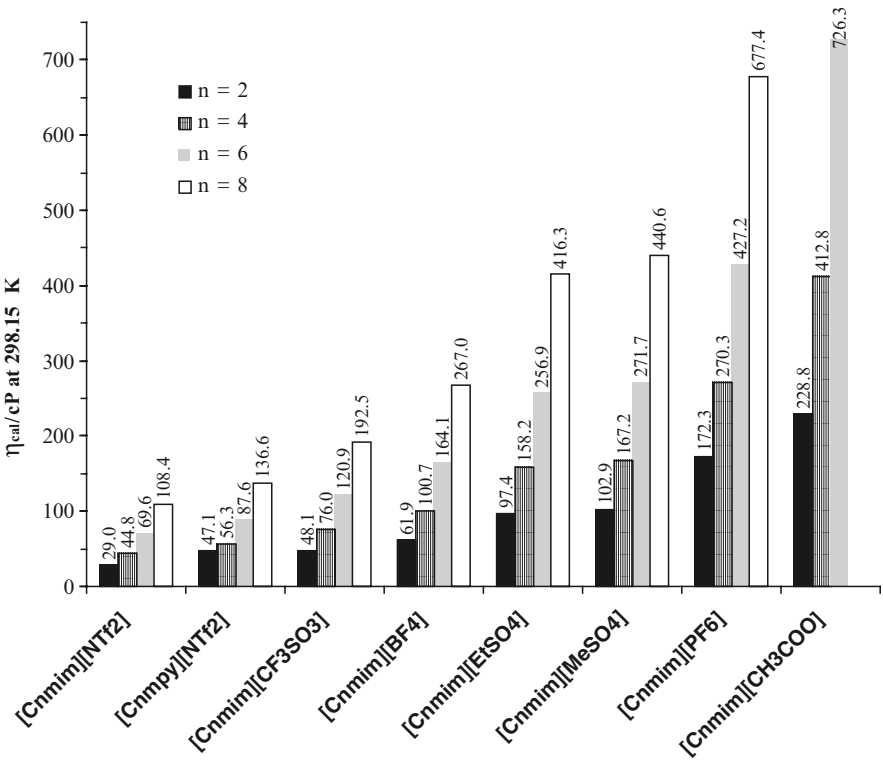

Fig. 6 Viscosity at 298 K of some common ionic liquids as a function of chain length, *n*

Cl^- anion, and seems to decrease with the symmetry of anion, showing the trend $Cl^- > [CH_3COO]^- > [PF_6]^- > [C_1SO_4]^- > [C_2SO_4]^- > [BF_4]^- > [OTf]^- > [NTf_2]^-$. In general ionic liquids having highly symmetric or almost spherical anions are more viscous and viscosity decreases with increasing anion asymmetry. For ionic liquids having a common anion and a similar alkyl chain length on the cation, it is observed that the viscosity increases with cations following the order imidazolium < pyridinium < pyrrolidinium. This is in agreement with the results of Crosthwaite et al. [75] which shows that pyridinium salts are generally more viscous than the equivalent imidazolium salts.

More exhaustive and theoretically based studies are required to rationalize the different trends and care is recommended when comparing or using viscosity data for ionic liquids as differences among the results of several authors may be important since, as it is well known, the presence of small amounts of water or other impurities such as chloride seem to have a remarkable effect on the viscosity [76–81].

These studies show that small changes in the structure of the ionic liquid can produce considerable differences in viscosity. From studies where a series of imidazolium based salts with various alkyl substituents and different anions was characterized in terms of viscosity in order to establish a relationship between

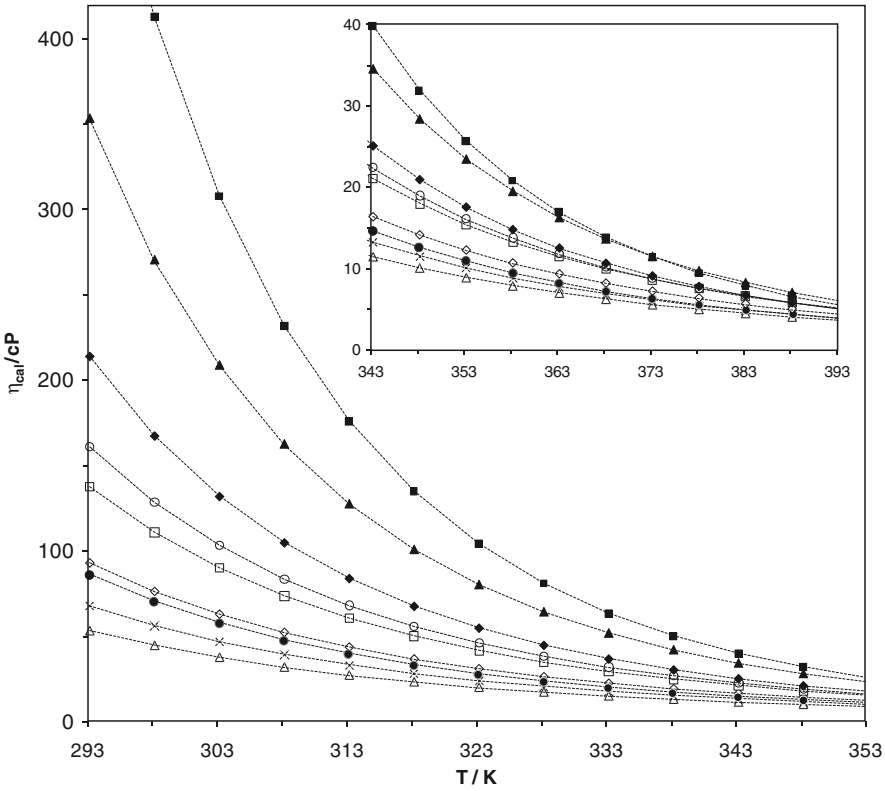

Fig. 7 Viscosities of ionic liquids calculated according to Gardas and Coutinho method [101]. *filled squares*, [C_4mim][CH_3COO]; *filled triangles*, [C_4mim][PF_6]; *filled diamonds*, [C_4mim][C_1SO_4]; *filled circles*, [C_4mpyr][NTf_2]; *open diamonds*, [C_4mim][OTf]; *multiplication signs*, [C_4mpy] [NTf_2]; *open triangles*, [C_4mim][NTf_2]; *open circles*, [C_4mpy] [BF_4]; *open squares*, [C_4mim][BF_4]

chemical structure and physical properties [60, 74, 82–87], it was suggested that the viscosity of ionic liquids is mainly controlled by hydrogen bonding, Van der Waal forces, molecular weight and mobility.

Like many viscous fluids the viscosity can decrease markedly with increasing temperature (Fig. 7). For example, [C_4mim][PF_6] has a viscosity of 270.3 cP at 298 K, which decreases to 80.4 cP at 323 K and 23.5 cP at 353 K.

Viscosity is a difficult property to predict and flexible predictive models will require further experimental data in order to obtain a better understanding of this property. Many prediction methods are available in literature for the viscosity of pure component and their mixtures [88]; most of these are generally based on group contributions (e.g., the Orrick–Erbar method [89], the Sastry–Rao method [90], and the UNIFAC–VISCO method [91]), the corresponding states concept (e.g., Przezdziecki and Sridhar [92], Chatterjee and Vasant [93], Teja and Rice [94, 95],

and Queimada et al. [96, 97]) or the corresponding-states group-contribution (CSGC) method (e.g., Yinghua et al. [98]). Group contribution methods for the estimation of liquid viscosity usually use some variation of temperature dependence proposed by de Guzman [99], known as the Andrade equation [100]. Gardas and Coutinho [101] developed a group contribution method for the viscosity of ionic liquids using an Orrick–Erbar-type approach [102], and for 498 data points of 29 imidazolium, pyridinium, and pyrrolidinium based ionic liquids containing $[PF_6]^-$, $[BF_4]^-$, $[NTf_2]^-$, Cl^-, $[CH_3COO]^-$, $[C_1SO_4]^-$, $[C_2SO_4]^-$, and $[OTf]^-$ anions, observed a maximum deviation of less than 28%. The largest deviations observed in predicted viscosities were mainly due to the discrepancies in viscosity values reported in literature, which may be related to water content, halogen and other impurities present in the samples, or the experimental method adopted. The Orrick–Erbar method [89] requires density data for the prediction of viscosity. To overcome this limitation and to attempt the development of an improved viscosity model with lower deviations in estimated viscosities of ionic liquids, a new correlation model based on the Vogel-Tammann–Fulcher (VTF) equation was recently proposed by Gardas and Coutinho [103]. This model was successful as demonstrated in Fig. 7.

1.5 Surface Tension

The versatility of ILs has driven increasing interest in using them in extraction and multiphasic homogeneous catalytic reactions [104] where one phase is chosen to dissolve the catalyst and be immiscible with the second phase which contains the reactant and products. Such processes occur at the interface between the IL and the overlying aqueous or organic phase, and are dependent on the access of the material to the surface and the transfer of material across the interface. A clearer understanding of the mechanisms behind these processes requires a more detailed examination of the surface properties of the ionic liquids.

Surface tension is an important property in the study of physics and chemistry at free surfaces as it affects the transfer rates of vapor absorption at the vapor–liquid interface. Such data are of importance to scientists, engineers, and practitioners in many fields such as chemical process and reactor engineering, flow and transport in porous media, materials selection and engineering, biomedical and biochemical engineering, electronic and electrical engineering, etc. The surface of a liquid is not only interesting for the fundamental aspects but also for its relevance in environmental problems, biological phenomena, and industrial applications.

Experimental data for surface tensions of ionic liquids is very scarce and currently limited to imidazolium based ionic liquids. Typical values for surface tension are shown in Fig. 8 which shows that these ionic liquids have a lower surface tension than water (71.97 mN m^{-1} at 298 K) but higher than many organics.

For the ILs having similar anion, the surface tension decreases with an increase in alkyl chain length of imidazolium cation and as is observed with organic solvents decreases with increasing temperature.

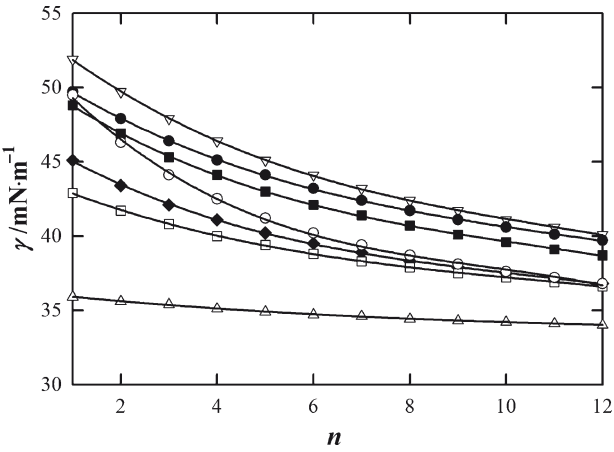

Fig. 8 Surface tension at 298 K as a function of chain length, *n*, for a series of imidazolium based ionic liquids constituted with the following anion: *inverted open triangles*, $[C_1SO_4]^-$; *filled circles*, $[C_2SO_4]^-$; *filled squares*, $[PF_6]^-$; *open circles*, $[CH_3COO]^-$; *filled diamonds*, $[BF_4]^-$; *open squares*, $[OTf]^-$; *open triangles*, $[NTf_2]^-$

When developing ionic liquids for a given purpose, if experimentally measured surface tension data are not available, theoretical or empirical methods must be used to establish if the surface tensions are within acceptable limiting values defined in the design specifications. For this purpose prediction methods for surface tension of ionic liquids are required.

Recently, Deetlefs et al. [18] attempted to predict the surface tension of ionic liquids using parachors and available densities. More recently Gardas and Coutinho [105] have shown that the QSPR correlation of Knotts et al. [106] can be extended to ionic liquids for the estimation of surface tension. By applying this technique it was possible to obtain good predictions for 361 literature data points for 38 imidazolium based ionic liquids containing $[BF_4]^-$, $[PF_6]^-$, $[NTf_2]^-$, $[OTf]^-$, $[C_1SO_4]^-$, $[C_2SO_4]^-$, Cl^-, I^-, $[I_3]^-$, $[AlCl_4]^-$, $[FeCl_4]^-$, $[GaCl_4]^-$ and $[InCl_4]^-$ as anions; the overall mean percentage deviation was 5.75% with a maximum deviation less than 16%. The deviations obtained were surprising since the QSPR correlation for the parachors was developed for neutral compounds and not for salts; it was thus developed without taking Coulombic interactions into account.

1.6 Specific Heat Capacity

Heat capacity represents the relationship between energy and temperature for a specified quantity of material. In general this value relates to the kinetic energy stored within the vibrations of the molecule of interest and can be correlated to such. For example, Strechan et al. [107] reported a predictive method for determining heat capacities

of six different ionic liquids by correlating this property with the intramolecular vibrational contribution where they reported a relative deviation of 0.9%.

The fact that these fluids are ionic should not have a significant effect on the specific heat capacity of ionic liquids and indeed reported values are in line with those one would expect for organic molecules. For example the heat capacity for chlorobenzene is 152.1 J mol^{-1} K^{-1} or 1.36 kJ kg^{-1} K^{-1} when written in terms of weight, is similar to that reported for [C_2mim][NTf_2], i.e., 525 J mol^{-1} K^{-1} or 1.34 kJ kg^{-1} K^{-1}. When written in a molar basis the heat capacities of ionic liquids are generally higher than typical organic solvents which is expected given their relatively large molecular weights, for example, at 298 K the heat capacities of water, ethanol, nitromethane, benzene are between 75 and 292 J mol^{-1} K^{-1} [108, 109].

Figure 9 shows an example of a number of ionic liquid heat capacities as a function of temperature. Here it is observed that an approximately linear relationship is obtained and a secondary relationship between the chain length of the [$C_n$mim][NTf_2] ionic liquids and heat capacity is also apparent. From the results of Ge et al. [110], each additional "-CH_2-" group increases the heat capacity by approximately 35 J mol^{-1} K^{-1} at 298 K which is similar to the observations made by Holbrey et al. [111] Archer et al. [112] and Paulechka et al. [113] who reported incremental increases in C_p of 40, 30 and 31 J mol^{-1} K^{-1}, respectively. Ge et al. [110] also reported measurements on the influence of impurities on the heat capacity where it was found that the heat capacity was lowered with increasing water or chloride and that this followed a linear relationship. Overall it was reported that for small chloride or water mass fraction contents, i.e., up to 1×10^{-3}, a decrease in the heat capacity of ≈ 0.15% or ≈ 1.3% on average when compared with the halide free or dried IL respectively was observed.

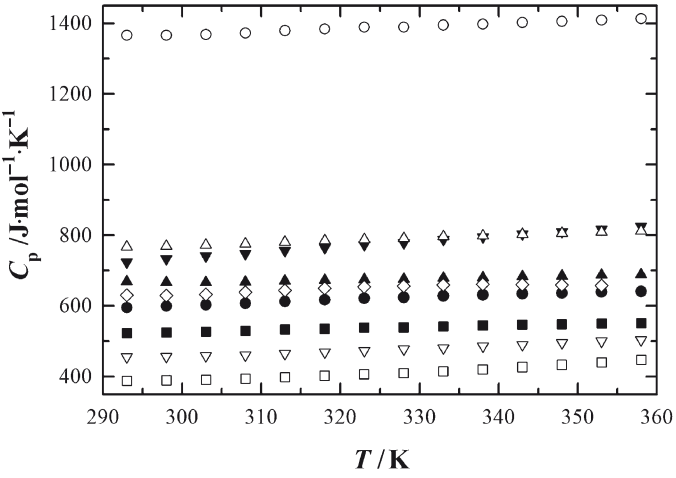

Fig. 9 Heat capacities of ionic liquids as a function of temperature. *filled squares*, [C_2mim][NTf_2]; *filled circles*, [C_4mim][NTf_2]; *filled triangles*, [C_6mim][NTf_2]; *inverted filled triangles*, [C_8mim][NTf_2]; *open circles*, [P_{66614}][NTf_2]; *open diamonds*, [C_4mPyrr][NTf_2]; *open triangles*, [C_4mPyrr][FAP]; *inverted open triangles*, [C_4mim][OTf]; *open squares*, [C_2mim][$EtSO_4$] [110]

As expected, the larger the molecular weight of the ionic liquid, the larger the heat capacity. For example the heat capacity of $[P_{66614}][NTf_2]$ has been reported as 1,366 J mol^{-1} K^{-1}, compared with 525 J mol^{-1} K^{-1} for $[C_2mim][NTf_2]$ at 298 K. Similarly the choice of anion significantly changes the heat capacity for example $[C_4mim][OTf] < [C_4mim][NTf_2]$ and $[C_4mpyr][NTf_2] < [C_4mpyr][FAP]$ demonstrating again that the heat capacity increases with anion size. As found for other properties, such as density and viscosity [60], the anion type has a greater impact than the cation on the heat capacity.

Furthermore, Ge et al. [110] reported an extension to the Joback [114] and Benson [115] group contribution method, a model often used for the estimation of organic materials, by developing new contributions for the "-SO_2-", "P" and "B" groups which are commonly found in these liquids. This was tested against the heat capacities for a range of ionic liquids including measured values determined using a heat flux differential scanning calorimeter technique as described by Diedrichs and Gmehling [116]. As stated above, the Joback method is widely used to predict the ideal gas heat capacities of molecular compounds through application of following equation:

$$C_p^o(T) = \left[\sum_{i=1}^{k} n_i A_{Cpi} - 37.93\right] + \left[\sum_{i=1}^{k} n_i B_{Cpi} + 0.210\right] T + \left[\sum_{i=1}^{k} n_i C_{Cpi} - 3.91\times10^{-4}\right] T^2 + \left[\sum_{i=1}^{k} n_i D_{Cpi} - 2.06\times10^{-7}\right] T^3, \quad (5)$$

where A_{Cpk}, B_{Cpk}, C_{Cpk} and D_{Cpk} are group contribution parameters, n_i is the number of groups of type i in the molecule and T is the temperature in K. However, in order for Ge et al. [110] to apply this equation to ionic liquids, the principle of corresponding states (6) was required [115]:

$$\frac{C_p^r}{R} = \frac{C_p - C_p^o}{R} = 1.586 + \frac{0.49}{1-T_r} + \omega\left[4.2775 + \frac{6.3\left(1-T_r\right)^{\frac{1}{8}}}{T_r} + \frac{0.4355}{1-T_r}\right]. \quad (6)$$

Equation (6) requires knowledge of the critical properties of the ionic liquids which have been discussed previously thereby making this approach more complex than other potential techniques. However despite the number of equations used a relative absolute deviation of 2.9% was observed when testing the model against 961 data points from 53 different ionic liquids reported. Overall this is highly versatile approach given the range of ionic liquids which can be generated using the groups available.

An alternative approach to that of Ge et al. [110] was adopted by Gardas and Coutinho [117]. In this study 2,396 data points for 19 ILs consisting of combinations of imidazolium, pyridinium and pyrrolidinium cations with a range of anions including $[PF_6]^-$, $[BF_4]^-$, $[NTf_2]^-$, Br^-, and $[OTf]^-$ anions, over a wide temperature range from 196.36 to 663.10 K was modeled using the method proposed by

Ruzicka and Domalski [118, 119]. The group contribution equation used in this study was

$$C_{\mathrm{pL}} = R\left[\sum_{i=1}^{k} n_i a_i + \sum_{i=1}^{k} n_i b_i \left(\frac{T}{100}\right) + \sum_{i=1}^{k} n_i d_i \left(\frac{T}{100}\right)^2\right], \tag{7}$$

where R is the gas constant, 8.31 J mol^{-1} K^{-1}, and T is the absolute temperature. Again n_i represents the number of groups of type i, k the total number of different groups. The parameters a_i, b_i, and d_i were reported for three cations, six anions as well as the -CH_2-, -CH_3 and dimethyl ammonium groups. Overall, a mean percent deviation of 0.36% and a maximum deviation of < 2.5% was reported. Therefore this approach gives a slightly higher accuracy than that proposed by Ge et al. [110] although the range of ionic liquids which can be generated from the groups is significantly lower.

1.7 Thermal Conductivity

At present there are limited data available on the thermal conductivities of ionic liquids. Of those which have been reported, two main methods have been used for the measurement of this property, namely the transient hot wire method and the transient grating technique. In the former the measurements are made by heating a probe (containing a heating element and a thermoresistor) within the sample while simultaneously monitoring the temperature change of the probe. The latter technique does not directly measure the thermal conductivity but instead estimates this value from the measured thermal diffusivity and previously reported values for heat capacity and density. This difference in methods can lead to significant differences in the calculated thermal conductivities. For example, Frez et al. [120] calculated a value for the thermal conductivity of [C_4mim][BF_4] which was 15% lower when using the transient gradient approach than that reported by Van Valkenburg et al. [25] where the transient hot wire was used. It is expected that, as the transient grating technique requires additional properties, this method is more prone to errors and thus the transient hot wire method appears to be more accurate.

Reported values for ionic liquids using this technique indicate that ionic liquid thermal conductivities are similar to those of commonly used organic solvents. For example, Tomida et al. [121] determined the thermal conductivity for a series of [$C_n$mim][PF_6] salts and reported values for [C_4mim][PF_6] which compared well with those of benzene, 0.145 and 0.16 W m^{-1}·K^{-1}, respectively. In their study they also concluded that the thermal conductivity was not a strong function of temperature, pressure or chain length.

Ge et al. [122] used a similar technique for the measurement of 11 ionic liquids over the temperature range 293–353 K. In this study the thermal conductivities were found to be between 0.1 and 0.2 W m^{-1} K^{-1}. Here a slight negative and linear relationship with temperature was observed. Similar to that reported by Tomida et al. [121], there

was no significant effect on the thermal conductivity by varying the alkyl chain length, *n*, of the [$C_n$mim] cation family. From these studies it appears that, while the chain length of a particular cation series does not appear to alter significantly the thermal conductivity, the choice of both cation and anion do have an effect. For example, when using the same [NTf_2]$^-$ anion at 298 K the thermal conductivity of [P_{66614}]$^+$> [C_4mim]$^+$> [C_4mpyr]$^+$, 0.144, 0.128 and 0.125 W m^{-1} K^{-1}, respectively. Whereas while keeping the cation as [C_4mim]$^+$ the thermal conductivity of [OTf]$^-$ ≈[PF_6]$^-$ > [NTf_2]$^-$, 0.146, 0.145 and 0.128 W m^{-1} K^{-1}, respectively. The fact that the [P_{66614}]$^+$ ionic liquids have similar thermal conductivities to those of the 1-alkyl-3-methylimidazolium based liquids highlights that this property is independent of viscosity. These studies also indicate that the highest thermal conductivity is associated with [C_2mim][C_2SO_4], 0.181 W m^{-1} K^{-1} at 298 K, while the lowest is the [C_4mpyr][FAP] liquid, 0.106 W m^{-1} K^{-1} at 298 K.

Ge et al. [122] also investigated the impact of both water and halide impurities where it was found that, in the case of small quantities, i.e., up to a mass fraction of 0.01 for water and 0.05 for halide (chloride), no significant effect on thermal conductivity was observed. Above this the thermal conductivity of the mixture could be modeled using the Jamieson correlation:

$$\lambda_m = w_1\lambda_1 + w_2\lambda_2 - \alpha(\lambda_2 - \lambda_1)\left(1 - w_2^{0.5}\right)w_2, \qquad \lambda_2 > \lambda_1, \tag{8}$$

where w_1 and w_2 are mass fractions and the adjustable parameter α varied depending on the system and impurity chosen. For example, values of 0.42, 0.70 and 1.39 were obtained for the binary mixtures [C_4mim][OTf]+water, [C_2mim][C_2SO_4]+water and [C_6mim][NTf_2] + [C_6mim]Cl, respectively.

The use of thermal conductivity, heat capacity and rheological properties for [C_4mim][NTf_2] was also shown by Chen et al. [123] to correlate with Shah's equation for forced convective heat transfer in the laminar flow regime, indicating that knowledge of these parameters can successfully be used to model heat transfer behavior of ionic liquid systems at the larger scale.

1.8 Conclusions

The topic of ionic liquids has grown significantly over the last number of years with the vast majority of this research focusing on their use as solvents for a wide range of chemical reactions. However none of these reactions would ever be industrially exploited without some knowledge of the physical properties of these materials. In an effort to address this problem the ionic liquid thermodynamic property database (IL Thermo) was developed and has grown considerably over recent years to contain a variety of important physical properties such as densities, viscosities, etc. This database shows that ionic liquids can have a wide range of properties depending on the choice of anion and cation. Many of these are intuitively what one would expect. For example, ionic liquids containing heavy inorganic anions will be denser

than those containing lighter organic anions. However, other properties such as melting points and viscosity are more difficult to predict from simple structural information. This review has focused on a number of key ionic liquid properties including those that define the liquid range, density, viscosity and surface tension as well as the main thermal properties of heat capacity and thermal conductivity. In each of these we have attempted to provide typical values as well as show the important factors which influence the observed trends. We have also discussed techniques by several groups which can be used to estimate these properties from simple structural information including methods such as group contributions, molecular descriptors and molecular dynamics approaches. Over the coming years as new data becomes available our understanding of the relationship between ionic liquid formulation and its physical properties will increase allowing us to design ionic liquids which maximize key desired attributes for any desired application.

References

1. Wasserscheid P, Welton T (2003) Ionic liquids in synthesis. Wiley-VCH Verlag, Weinheim
2. Pârvulescu VI, Hardacre C (2007) Catalysis in ionic liquids. Chem Rev 107:2615–2665
3. Silvester DS, Compton RG (2006) Electrochemistry in room temperature ionic liquids: a review and some possible applications. Z Phys Chem 220:1247–1274
4. Harper JB, Kobrak MN (2006) Understanding organic processes in ionic liquids: achievements so far and challenges remaining. Mini-Rev Org Chem 3:253–269
5. Qu J, Truhan JJ, Dai S et al. (2006) Ionic liquids with ammonium cations as lubricants or additives. Tribol Let 22:207–214
6. Holbrey JD (2007) Heat capacities of common ionic liquids – potential applications as thermal fluids? Chim Oggi – Chem Today 25:24–26.
7. Liu JF, Jonsson JA, Jiang GB (2005) Application of ionic liquids in analytical chemistry. TracTrends Anal Chem 24:20–27
8. Katritzky AR, Jain R, Lomaka A et al. (2002) Correlation of the melting points of potential ionic liquids (imidazolium bromides and benzimidazolium bromides) using the CODESSA program. J Chem Inf Comp Sci 42:225–231
9. Widegren JA, Wang YM, Henderson WA et al. (2007) Relative volatilities of ionic liquids by vacuum distillation of mixtures. J Phys Chem B 111:8959–8964
10. Earle MJ, Esperanca JMSS, Gilea MA et al. (2006) The distillation and volatility of ionic liquids. Nature 439:831–834
11. Hough WL, Smiglak M, Rodriguez H et al. (2007) The third evolution of ionic liquids: active pharmaceutical ingredients. New J Chem 31:1429–1436
12. Xue H, Twamley B, Shreeve JM (2005) Energetic salts of substituted 1,2,4-triazolium and tetrazolium 3,5-dinitro-1,2,4-triazolates. J Mat Chem 15:3459–3465
13. Fredlake CP, Crosthwaite JM, Hert DG et al. (2004) Thermophysical properties of imidazolium-based ionic liquids. J Chem Eng Data 49:954–964
14. Earle MJ, Katdare SP, Seddon KR (2004) Paradigm confirmed: the first use of ionic liquids to dramatically influence the outcome of chemical reactions. Org Let 6:707–710
15. Crowhurst L, Falcone R, Lancaster NL et al. (2006) Using Kamlet–Taft solvent descriptors to explain the reactivity of anionic nucleophiles in ionic liquids. J Org Chem 71:8847–8853
16. Dong Q, Muzny CD, Kazakov A et al. (2007) ILThermo: a free-access web database for thermodynamic properties of ionic liquids. J Chem Eng Data 52:1151–1159
17. Katritzky AR, Lomaka A, Petrukhin R et al. (2002) QSPR correlation of the melting point for pyridinium bromides, potential ionic liquids. J Chem Inf Comp Sci 42:71–74

18. Deetlefs M, Seddon KR, Shara M (2006) Predicting physical properties of ionic liquids. Phys Chem Chem Phys 8:642–649
19. Zhang SJ, Sun N, He XZ et al. (2006) Physical properties of ionic liquids: database and evaluation. J Phys Chem Ref Data 35:1475–1517
20. Tochigi K, Yamamoto H (2007) Estimation of ionic conductivity and viscosity of ionic liquids using a QSPR model. J Phys Chem C 111:15989–15994
21. Matsuda H, Yamamoto H, Kurihara K et al. (2007) Computer-aided reverse design for ionic liquids by QSPR using descriptors of group contribution type for ionic conductivities. Fluid Phase Equilib 261:434–443
22. Chopey NP (2004) Handbook of chemical engineering calculations. McGraw-Hill, New York
23. Dzyuba SV, Bartsch RA (2002) Influence of structural variations in 1-alkyl(aralkyl)-3-methylimidazolium hexafluorophosphates and bis(trifluorormethyl-sulfonyl)imides on physical properties of the ionic liquids. Chem Phys Chem 3:161–166
24. Suarez PAZ, Einloft S, Dullius JEL et al. (1998) Synthesis and physical-chemical properties of ionic liquids based on 1-*n*-butyl-3-methylimidazolium cation. J Chim Phys-Chim Biol 95:1626–1639
25. Van Valkenburg ME, Vaughn RL, Williams M et al. (2005) Thermochemistry of ionic liquid heat-transfer fluids. Thermochim Acta 425:181–188
26. Ngo HL, LeCompte K, Hargens L et al. (2000) Thermal properties of imidazolium ionic liquids. Thermochim Acta 357:97–102
28. Yamanaka N, Kawano R, Kubo W et al. (2007) Dye-sensitized TiO_2 solar cells using imidazolium-type ionic liquid crystal systems as effective electrolytes. J Phys Chem B 111:4763–4769
29. Gordon CM, Holbrey JD, Kennedy AR et al. (1998) Ionic liquid crystals: hexafluorophosphate salts. J Mat Chem 8:2627–2636
30. Eike DM, Brennecke JF, Maginn EJ (2003) Predicting melting points of quaternary ammonium ionic liquids. Green Chem 5:323–328
31. Carrera G, Aires-de-Sousa J (2005) Estimation of melting points of pyridinium bromide ionic liquids with decision trees and neural networks. Green Chem 7:20–27
32. Charton, M, Charton B (1994) Quantitative description of structural effects on melting-points of substituted alkanes. J Phys Org Chem 7:196–206
33. Trohalaki S, Pachter R, Drake GW et al. (2005) Quantitative structure-property relationships for melting points and densities of ionic liquids. Energ Fuels 19:279–284
34. López-Martin I, Burello E, Davey PN et al. (2007) Anion and cation effects on imidazolium salt melting points: a descriptor modelling study. Chem Phys Chem 8:690–695
35. Alavi S, Thompson DL (2005) Molecular dynamics studies of melting and some liquid-state properties of 1-ethyl-3-methylimidazolium hexafluorophosphate [emim][PF_6]. J Chem Phys 122:154704–154712
36. Jayaraman S, Maginn EJ (2007) Computing the melting point and thermodynamic stabilty of the orthorhombic and monoclinic crystalline polymorphs of the ionic liquid 1-*n*-butyl-3-methylimidazolium chloride. J Chem Phys 127:214504
37. Krossing I, Slattery JM, Daguenet C et al. (2006) Why are ionic liquids liquid? A simple explanation based on lattice and solvation energies. J Am Chem Soc 128:13427–13434
38. Awada WH, Gilman JW, Nyden M et al. (2004) Thermal degradation studies of alkylimidazolium salts and their application in nanocomposites. Thermochim Acta 409:3–11
39. Freemantle M (2003) BASF'S smart ionic liquid. Chem Eng News 81:9
40. Rodríguez H, Williams M, Wilkes JS et al. (2008) Ionic liquids for liquid-in-glass thermometers. Green Chem 10:501–507
41. Kosmulski M, Gustafsson, Rosenholm JB (2004) Thermal stability of low temperature ionic liquids revisited. Thermochim Acta 412:47–53
42. Kamavaram V, Reddy RG (2008) Thermal stabilities of di-alkylimidazolium chloride ionic liquids. Int J Therm Sci 47:773–777
43. Rebelo LPN, Canongia Lopes J, Esperança J et al. (2005) On the critical temperature, normal boiling point, and vapour pressure of ionic liquids. J Phys Chem B 109:6040–6043

44. Zaitsau DH, Kabo GJ, Strechan AA et al. (2006) Experimental vapour pressures of 1-alkyl-3-methylimidazolium bis(trifluoromethyl-sulfonyl)imides and a correlation scheme for estimation of vapourization enthalpies of ionic liquids. J Phys Chem A 110:7303–7306
45. Armstrong JP, Hurst C, Jones RG et al. (2007) Vapourisation of ionic liquids. Phys Chem Chem Phys 9:982–990
46. Verevkin SP (2008) Predicting enthalpy of vaporization of ionic liquids: a simple rule for a complex property. Angew Chem Int Ed 47:5071–5074
47. Emel'yanenko VN, Verevkin SP, Heintz A (2008) Ionic liquids. Combination of combustion calorimetry with high-level quantum chemical calculations for deriving vaporization enthalpies. J Phys Chem B 112:8095–8098
48. Luo H, Baker GA, Dai S (2008) Isothermogravimetric determination of the enthalpies of vaporization of 1-alkyl-3-methylimidazolium ionic liquids. J Phys Chem B 112:10077–10081
49. Santos L, Canongia Lopes J, Coutinho J et al. (2007) Ionic liquids: first direct determination of their cohesive energy. J Am Chem Soc 129:284–285
50. Diedenhofen M, Klamt A, Marsh K et al. (2007) Prediction of the vapor pressure and vaporization enthalpy of 1-*n*-alkyl-3-methylimidazolium-bis-(trifluoromethanesulfonyl) amide ionic liquids. Phys Chem Chem Phys 9:4653–4656
51. Ludwig R (2008) Thermodynamic properties of ionic liquids – a cluster approach. Phys Chem Chem Phys 10:4333–4339
52. Valderrama JO, Robles PA (2007) Critical properties, normal boiling temperatures and acentric factors fifty ionic liquids. Ind Eng Chem Res 46:1338–1344
53. Valderrama JO, Sanga WW, Lazzús JA (2008) Critical properties, normal boiling temperature, and acentric factor of another 200 ionic liquids. Ind Eng Chem Res 47:1318–1330
54. Wagner W, Kleinrahm R, Losch HW et al. (2003) Density. Hydrostatic balance densimeters with magnetic suspension couplings. Bellows volumetry. Absolute density standards. In situ density measurements. In: Goodwin ARH, Marsh KN, Wakeham WA eds) Experimental thermodynamics, vol VI: measurement of the thermodynamic properties of single phases, IUPAC. Elsevier, Amsterdam
55. Kratky O, Leopold H, Stabinger HZ (1969) Density determination of liquids and gases to an accuracy of 10^{-6} g/cm^3, with a sample volume of only 0.6 cm3. Z Angew Phys 27:273–277
56. Kandil ME, Harris KR, Goodwin ARH et al. (2006) Measurement of the viscosity and density of a reference fluid, with nominal viscosity at T = 298 K and p = 0.1 MPa of 29 mPa s, at temperatures between 273 and 423 K and pressures below 275 MPa. J Chem Eng Data 51:2185–2196
57. Dávila MJ, Aparicio S, Alcalde R et al. (2007) On the properties of 1-butyl-3-methylimidazolium octylsulfate ionic liquid. Green Chem 9:221–232
58. Sanmamed YA, González-Salgado D, Troncoso J et al. (2007) Viscosity-induced errors in the density determination of room temperature ionic liquids using vibrating tube densitometry. Fluid Phase Equilib 252:96–102
59. Goodwin ARH, Trusler JPM (2003) Speed of sound. Measurements of the speed of sound. Thermodynamic properties from the speed of sound. In: Goodwin ARH, Marsh KN, Wakeham WA eds) Experimental thermodynamics, vol VI: measurement of the thermodynamic properties of single phases, IUPAC. Elsevier, Amsterdam
60. Jacquemin J, Husson P, Padua AAH et al. (2006) Density and viscosity of several pure and water-saturated ionic liquids. Green Chem 8:172–180
61. Jacquemin J, Ge R, Nancarrow P et al. (2008) Prediction of ionic liquid properties. I. Volumetric properties as a function of temperature at 0.1 MPa. J Chem Eng Data 53:716–726
62. Troncoso J, Cerdeirina CA, Sanmamed YA et al. (2006) Thermodynamic properties of imidazolium-based ionic liquids: densities, heat capacities, and enthalpies of fusion of [bmim][PF_6] and [bmim][NTf_2]. J Chem Eng Data 51:1856–1859
63. Rebelo LPN, Najdanovic-Visak V, Gomes de Azevedo R et al. (2005) Phase behaviour and thermodynamic properties of ionic liquids, ionic liquid mixtures, and ionic liquid solutions. In: Rogers, RD, Seddon KR eds) Ionic liquids IIIA: fundamentals, progress, challenges, and

opportunities-properties and structure. ACS Symposium Series 901. American Chemical Society, Washington
64. Esperança J, Guedes HJR, Blesic M et al. (2006) Densities and derived thermodynamic properties of ionic liquids. 3. Phosphonium-based ionic liquids over an extended pressure range. J Chem Eng Data 51:237–242
65. Yang J, Lu X, Gui J et al. (2004) A new theory for ionic liquids – the interstice model part 1. The density and surface tension of ionic liquid EMISE. Green Chem 6:541–543
66. Kim YS, Choi WY, Jang JH et al. (2005) Solubility measurement and prediction of carbon dioxide in ionic liquids. Fluid Phase Equilib 256:439–445
67. Kim YS, Jang JH, Lim DB et al. (2007) Solubility of mixed gases containing carbon dioxide in ionic liquids: measurements and predictions. Fluid Phase Equilib 228:70–74
68. Ye C, Shreeve JM (2007) Rapid and accurate estimation of densities of room-temperature ionic liquids and salts. J Phys Chem A 111:1456–1461
69. Gardas RL, Coutinho JAP (2008) Extension of the Ye and Shreeve group contribution method for density estimation of ionic liquids in a wide range of temperatures and pressures. Fluid Phase Equilib 263:26–32
70. Knotts TA, Wilding WV, Oscarson JL et al. (2001) Use of the DIPPR database for development of QSPR correlations: surface tension. J Chem Eng Data 46:1007–1012
71. Jacquemin J, Husson P, Mayer V et al. (2007) High-pressure volumetric properties of imidazolium-based ionic liquids – effect of the anion. J Chem Eng Data 52:2204–2211
72. Jacquemin J, Nancarrow P, Rooney DW et al. (2008) Prediction of ionic liquid properties. II. Volumetric properties as a function of temperature and pressure. J Chem Eng Data 53:2133–2143
73. Riddick JA, Bunger WB, Sakano TK (1986) Organic solvents, physical properties and method of purification, 4th ed. Wiley, New York
74. Bonhote P, Dias AP, Papageorgiou N et al. (1996) Hydrophobic, highly conductive ambient-temperature molten salts. Inorg Chem 35:1168–1178
75. Crosthwaite JM, Muldoon MJ, Dixon JK et al. (2005) Phase transition and decomposition temperatures, heat capacities and viscosities of pyridinium ionic liquids. J Chem Thermodyn 37:559–568
76. Seddon KR, Stark A, Torres MJ (2000) Influence of chloride, water, and organic solvents on the physical properties of ionic liquids. Pure Appl Chem 72:2275–2287
77. Chauvin Y, Olivier-Bourbigou H (1995) Nonaqueous ionic liquids as reaction solvents. Chem Tech 25:26–30
78. Baker SN, Baker GA, Bright FV (2002) Temperature-dependent microscopic solvent properties of 'dry' and 'wet' 1-butyl-3-methylimidazolium hexafluorophosphate: correlation with ET(30) and Kamlet-Taft polarity scales. Green Chem 4:165–169
79. Widegren JA, Laesecke A, Magee JW (2005) The effect of dissolved water on the viscosities of hydrophobic room-temperature ionic liquids. Chem Commun 12:1610–1612
80. Silvester DS, Compton RG (2006) Electrochemistry in room temperature ionic liquids: a review and some possible applications. Z Phys Chem 220:1247–1274
81. Saha S, Hamaguchi HO (2006) Effect of water on the molecular structure and arrangement of nitrile-functionalized ionic liquids. J Phys Chem B 110:2777–2781
82. Tokuda H, Hayamizu K, Ishii K et al. (2004) Physicochemical properties and structures of room temperature ionic liquids. 1. Variation of anionic species. J Phys Chem B 108:16593–16600
83. Tokuda H, Hayamizu K, Ishii K et al. (2005) Physicochemical properties and structures of room temperature ionic liquids. 2. Variation of alkyl chain length in imidazolium cation. J Phys Chem B 109:6103–6110
84. Tokuda H, Ishii K, Susan MABH et al. (2006) Physicochemical properties and structures of room-temperature ionic liquids. 3. Variation of cationic structures. J Phys Chem B 110:2833–2839
85. Tokuda H, Tsuzuki S, Susan MABH et al. (2006) How ionic are room-temperature ionic liquids? An indicator of the physicochemical properties. J Phys Chem B 110:19593–19600
86. Harris KR, Woolf LA, Kanakubo M (2005) Temperature and pressure dependence of the viscosity of the ionic liquid 1-butyl-3-methylimidazolium hexafluorophosphate. J Chem Eng Data 50:1777–1782

87. Harris KR, Kanakubo M, Woolf LA (2007) Temperature and pressure dependence of the viscosity of the ionic liquids 1-hexyl-3-methylimidazolium hexafluorophosphate and 1-butyl-3-methylimidazolium bis(trifluoromethylsulfonyl)imide. J Chem Eng Data 52:1080–1085
88. Millat J, Dymond JH, Nieto de Castro CA (1996) Transport properties of fluids. their correlation, prediction and estimation. Cambridge University Press. Cambridge, UK
89. Orrick C, Erbar EJH (1973) Estimation of viscosity for organic liquids. Proposition Report, Oklahoma State University, Stillwater
90. Sastri SRS, Rao KK (2000) A new method for predicting saturated liquid viscosity at temperatures above the normal boiling point. Fluid Phase Equilib 175:311–323
91. Gastonbonhomme Y, Petrino P, Chevalier JL (1994) UNIFAC visco group-contribution method for predicting kinematic viscosity – extension and temperature-dependence. Chem Eng Sci 49:1799–1806
92. Przezdziecki JW, Sridhar T (1985) Prediction of liquid viscosities. AIChE J 31:333–338
93. Chatterjee A, Vasant AK (1982) Estimation of viscosity of organic liquids. Chem Ind 11:375–376
94. Teja AS, Rice P (1981) Generalized corresponding states method for the viscosities of liquid-mixtures. Ind Eng Chem Fund 20:77–81
95. Teja AS, Rice P (1981) The measurement and prediction of the viscosities of some binary-liquid mixtures containing normal-hexane. Chem Eng Sci 36:7–10
96. Queimada AJ, Marrucho IM, Coutinho JAP et al. (2005) Viscosity and liquid density of asymmetric *n*-alkane mixtures: measurement and modeling. Int J Thermophys 26:47–61
97. Queimada AJ, Rolo LI, Caço AI et al. (2006) Prediction of viscosities and surface tensions of fuels using a new corresponding states model. Fuel 85:874–877
98. Yinghua L, Peisheng M, Ping L (2002) Estimation of liquid viscosity of pure compounds at different temperatures by a corresponding-states group-contribution method. Fluid Phase Equilib 198:123–130
99. de Guzman J (1913) Relation between fluidity and heat fusion. An Soc Esp Fis Quim 11:353–362
100. Andrade ENDC (1930) The viscosity of liquids. Nature 125:309–310
101. Gardas RL, Coutinho JAP (2008) A group contribution method for viscosity estimation of ionic liquids. Fluid Phase Equilib 266:195–201
102. Reid RC, Prausnitz JM, Sherwood TK (1987) The properties of gases and liquids, 4th edn. McGraw-Hill, New York
103. Gardas RL, Coutinho JAP (2009) Group contribution methods for the prediction of thermophysical and transport properties of ionic liquids AIChE J. (in press) DOI: 10.1002/aic.11737
104. Leclercq L, Suisse L, Agbossou-Niedercorn F (2008) Biphasic hydroformylation in ionic liquids: interaction between phosphane ligands and imidazolium triflate, toward an asymmetric process. Chem Commun 3:311–313
105. Gardas RL, Coutinho JAP (2008) Applying a QSPR correlation to the prediction of surface tensions of ionic liquids. Fluid Phase Equilib 265:57–65
106. Knotts TA, Wilding WV, Oscarson JL et al. (2001) Use of the DIPPR database for development of QSPR correlations: surface tension. J Chem Eng Data 46:1007–1012
107. Strechan AA, Paulechka YU, Blokhin AV et al. (2008) Low-temperature heat capacity of hydrophilic ionic liquids [BMIM][CF_3COO] and [BMIM][CH_3COO] and a correlation scheme for estimation of heat capacity of ionic liquids. J Chem Thermodyn 40:632–639
108. García-Miaja G, Troncoso J, Romaní L (2007) Density and heat capacity as a function of temperature for binary mixtures of 1-butyl-3-methylpyridinium tetrafluoroborate + water, + ethanol, and + nitromethane. J Chem Eng Data 52:2261–2265
109. Graziano G (2005) On the hydration heat capacity change of benzene. Biophys Chem 116:137–144
110. Ge R, Hardacre C, Jacquemin J et al. (2008) Heat capacities of ionic liquids as a function of temperature at 0.1 MPa – measurement and prediction. J Chem Eng Data 53:2148–2153
111. Holbrey JD, Reichert WM, Reddy RG et al. (2003) Heat capacities of ionic liquids and their applications as thermal fluids. In: Rogers RD, Seddon KR eds) Ionic liquids as green solvents: progress and prospects. ACS Symposium Series. ACS, Washington DC

112. Archer DG, Widegren JA, Kirklin DR et al. (2005) Enthalpy of solution of 1-octyl-3-methylimidazolium tetrafluoroborate in water and in aqueous sodium fluoride. J Chem Eng Data 50:1484–1491
113. Paulechka YU, Blokhin AV, Kabo GJ et al. (2007) Thermodynamic properties and polymorphism of 1-alkyl-3-methylimidazolium bis(triflamides). J Chem Thermodyn 39:866–877
114. Joback KG (1984) A unified approach to physical property estimation using multivariant statistical techniques. MSc thesis in chemical Engineering. Massachusetts Institute of Technology, Cambrdige.
115. Poling BE, Prausnitz JM, O'Connell JP (2001) The properties of gases and liquids. McGraw-Hill, New York
116. Diedrichs A, Gmehling J (2006) Measurement of heat capacities of ionic liquids by differential scanning calorimetry. Fluid Phase Equilib 244:68–77
117. Gardas RL, Coutinho JAP (2008) A group contribution method for heat capacity estimation of ionic liquids. Ind Eng Chem Res 47:5751–5757
118. Ruzicka V, Domalski ES (1993) Estimation of the heat-capacities of organic liquids as a function of temperature using group additivity. 1. Hydrocarbon compounds. J Phys Chem Ref Data 22:597–618
119. Ruzicka V, Domalski ES (1993) Estimation of the heat-capacities of organic liquids as a function of temperature using group additivity. 2. Compounds of carbon, hydrogen, halogens, nitrogen, oxygen, and sulfur. J Phys Chem Ref Data 22:619–657
120. Frez C, Diebold GJ, Tran C et al. (2006) Determination of thermal diffusivities, thermal conductivities, and sound speeds of room temperature ionic liquids by the transient grating technique. J Chem Eng Data 51:1250–1255
121. Tomida D, Kenmochi S, Tsukada T et al. (2007) Thermal conductivities of [bmim][PF_6], [hmim][PF_6], and [omim][PF_6] from 294 to 335 K at pressures up to 20 MPa. Int J Thermophys 28:1147–1160
122. Ge R, Hardacre C, Nancarrow P et al. (2007) Thermal conductivities of ionic liquids over the temperature range from 293 K to 353 K. J Chem Eng Data 52:1819–1823
123. Chen H, He Y, Zhu J et al. (2008) Rheological and heat transfer behaviour of the ionic liquid, [C_4mim][NTf_2]. Int J Heat Fluid Flow 29 (2008) 149–155

Top Curr Chem (2009) 290: 213–262
DOI: 10.1007/128_2008_36

Published online: 30 July 2009

Ionic Liquids from Theoretical Investigations

Barbara Kirchner

Abstract Theoretical investigations of ionic liquids are reviewed. Three main categories are discussed, i.e., static quantum chemical calculations (electronic structure methods), traditional molecular dynamics simulations and *first-principles* molecular dynamics simulations. Simple models are reviewed in brief.

Keywords All-atom • Basis sets • Continuum models • Coulombic interaction • Dispersion • Dispersion effects • Downscaling of charges • Electronic structure methods • Fully-flexible • Polarizable models • Reduced charges • Simulation time • Structure • Transferability • United atom

Contents

B. Kirchner
Wilhelm-Ostwald Institute for Physical and Theoretical Chemistry, University of Leipzig, Linnéstr. 2, D-04103, Leipzig, Germany
e-mail: bkirchner@uni-leipzig.de

Abbreviations

σ	Hard-sphere diameter
ε_0	Dielectric permittivity
μA	Chemical potential of substance A
ΔE	Energy difference, adiabatic interaction energy
$\Delta E_{\text{diss}}^{\text{cp}}$	Dissociation energy counterpoise corrected, adiabatic interaction energy counterpoise corrected
ΔE_{diss}	Dissociation energy, adiabatic interaction energy
ΔG_{solv}	Solvation free energies
Δh_{vap}	Molar enthalpy of vaporization
μi	Dipole moment
$[BF_4]^-$	Tetrafluoroborate
$[C_n\,C_n\text{im}]^+$	1-Alkyl-3-alkyl imidazolium
$[C_n\text{mim}]^+$	1-Alkyl-3-methyl imidazolium
$[DCA]^-$	Dicyanamide
$[DMFH]^+$	*N*,*N*′-Dimethylformamide cation
$[EtSO_4]^-$	Ethylsulfate
$[FeCl_4]^-$	Tetrachloroferrate
$[FS(O_2)_2N]^-$	Bis(fluorosulfonyl)imide
$[L]^-$	Lactate
$[MeSO_4]^-$	Methylsulfate
$[N_{abcd}]^+$	Ammonium with *a*–*d* different alkyl-chains
$[NO_3]^-$	Nitrate
$[NTf_2]^- = [TFSI]^-$	Bis(trifluoromethylsulfonyl)imide
$[P_{14}]^+$	*N*-Butyl-*N*-methyl-pyrrolidinium
$[PF_6]^-$	Hexafluorophosphate
$[PSPy]^+$	*N*-Propane sulfonic acid pyridinium
$[pTSA]^-$	*p*-Toluenesulfonic acid anion
$[SCN]^-$	Thiocyanite
$[TfO]^- = [CF_3SO_3]^-$	Triflate, trifluoromethanesulfonate
$[TMG]^+$	1,1,3,3-Tetramethylguanidinium
< >	Ensemble average
AIMD	Ab initio molecular dynamics; molecular dynamics with electronic structure calculations on the fly; see also FPMD and [1]
AMI	Semiempirical model; see [2]

CNDO	Complete neglect of differential overlap; semiempirical method; see [2]
DFT	Density functional theory; static quantum chemical method using functionals of the electronic density to account for electron correlation; see [2]
e	Electronic charge
FPMD	*First-principles* molecular dynamics; see AIMD
$\hat{H}$	Hamilton operator
H	Solvent interaction energy of a hybrid molecule
HF	Hartree–Fock; static quantum chemical method neglecting electron correlation per definition; see [2]
IL	Ionic liquid
MC	Monte-Carlo (simulations); see [3]
MD	Molecular dynamics (simulations); dynamical description based on classical mechanics; see [4]
MP2	Second-order Moller–Plesset perturbation theory; correlated static quantum chemical method; see [2]
NEMD	Non-equilibrium molecular dynamics
NPA	Natural population analysis
NPT	NPT ensemble: isothermal–isobaric ensemble; constant particle (N), pressure (P), and temperature (T) simulation
PES	Potential energy surface
PIL	Protic ionic liquids
PM3	Semiempirical method; see [2]
QC	Quantum chemical
QM/MM	Hybrid quantum-mechanical/molecular-mechanical calculations
QSAR	Quantitative structure activity relationships
RDF	Radial distribution functions, these functions reflect the structure of a liquid
u	Molar internal energy

1 Introduction

Ionic liquids (ILs) are an interesting new class of solvents for both industry and academia. From an academic point of view, these liquids are appealing mainly because they are tunable solvents. It is possible to adjust them to a given problem with many properties and contradicting behaviors that we are only now beginning to understand fully. In the several reviews that have appeared on the subject, interesting facts about the physical properties of ILs keep emerging [5–8]. For example, it has been observed that in more hydrophobic ILs the excess chemical potential of water increases by only a small amount, whereas a much larger change would have been expected [9]. Furthermore, it has been found that in imidazolium-based ILs the replacement of the most acidic hydrogen with a methyl group and thus the reduction of a hydrogen bond leads to an increase in viscosity [10]. Although these substances are salts, ILs are liquid below 100 °C. Finding an explanation for their properties and contradicting behaviors is in many cases still a matter of debate. Much insight can be expected from theoretical investigations, because these studies

allow an understanding on the microscopic level, which in a best-case scenario is likely to complement the experimental findings in illuminating ways.

Very early theoretical work on ILs was derived initially from the topic of molten salts which will not be covered here. Theoretical treatment of ILs mainly started in the group of Lynden-Bell [9, 11], and also in the group of Maginn [12, 13] and others [14, 15] at the end of the 1990s and in the early days of the new millennium.

A review of molecular dynamics (MD) simulations and imidazolium-based ILs covering the literature up to 2005 was written by Hunt [16]. In 2007, Maginn published an excellent account of chemical research article discussing atomistic simulations of the thermodynamic and transport properties of ILs [17]. In the same journal the Lynden-Bell group published an outstanding overview of the challenging simulations of ILs, their solutions, and surfaces [18]. Furthermore, Bhargava et al. presented an excellent review article about modeling room temperature ILs [19]. Furthermore, a review of structural studies on alkyl-imidazolium-based ILs containing fluoro-anions was presented by Matsumoto and Hagiwara [20].

Available methods and problems: Describing the liquid phase – especially of complicated liquids such as ILs – is still a nontrivial task [21]. Whereas gas phase properties of such substances might be accessible by making use of quantum chemical (QC) methods (i.e., electronic structure methods, see [2, 22]), involving one single molecule or ion pair in an isolated and static picture, most properties of the liquid state are not effectively captured by single molecule approaches of this sort, simply because of the neglect of temperature and environment as well as of the dynamics.

Sometimes simple models derived from continuum theory promise better results, but MD or Monte-Carlo (MC) simulations are still the preferable approaches for condensed-matter investigations [3, 4]. These methods were developed in the early 1950s [3, 4]. They include a model-inherent dynamical description in the case of MD, and large samples can be accounted for. These methods allow working scientists to treat more than one molecule and make use of so-called periodic boundary conditions which mimic images around the central cell in such a way that problems due to surface effects can be overcome.

Nevertheless, these methods are mostly applied with fixed charges (even if these are chosen in a sophisticated way) and with pairwise additivity approximation as well as with the neglect of nuclear quantum effects. Suggestions for polarizable models appeared in literature mainly for water [23]. The quality of potential parameterization varies from system to system and from quantity to quantity, raising the question of transferability. Spontaneous events like reactions cannot appear in simulations unless the event is included in the parameterization. Despite these problems, it is possible to reproduce important quantities as structural, thermodynamic and transport properties with traditional MD (MC) mainly due to the condition of the nanosecond time scale and the large system size in which the simulation takes place [24].

Developments in *first-principles* simulations (FPMD) such as the Car–Parrinello (CPMD) method were the most important theoretical progress made in the last century [25]. The reason for this is that the *first-principles* simulations approach is a combination of molecular-dynamics simulations with electronic structure calculations on the fly. In the Car–Parrinello simulation method the expensive QC part is

tackled by applying an extended Lagrangian technique. A two-component quantum mechanical/classical problem is mapped onto a two-component purely classical problem, while constraints make sure that the requirements of quantum mechanics are met. In principle, Car–Parrinello as well as Born–Oppenheimer dynamics can be combined with every electronic structure ansatz. Due to the lack of computer time these methods mostly work with density-functional theory (DFT) models. Other post-Hartree–Fock methods are not used frequently. This need for large amounts of computer time when applying the method reflects one of the major drawbacks of FPMD nowadays. Quantities that are reliably determined only on a large simulation time scale like transport properties are mostly out of the range of present FPMD simulations with trajectory lengths of 10–50 ps.

Outline: This review concentrates on work which mainly treats ILs from theoretical considerations and not from an experimental point of view. If calculations play only a supportive role in them, articles may have been neglected on principle. We also refrain from an introduction to methodological aspects and rather refer the reader to good textbooks on the subjects. The review is organized as follows: Static QC calculations are discussed in detail in the next section including Hartree–Fock, density functional theory (Sect. 2.2) and correlated (i.e., more sophisticated) methods (Sect. 2.4) as well as semiempirical methods (Sect. 2.1). We start with these kinds of small system calculations because they can be considered as a basis for the other calculations, i.e., an insight into the intermolecular forces is obtained.

We then present the most important theoretical treatment for ILs, namely traditional MD simulations in Sect. 3. Here, we also report on some recent aspects of force-field development in the framework of ILs (Sect. 3.1.1) and discuss the newly applied strategy of charge-downscaling. The problem of a reduced hydrogen bond resulting in higher viscosities is also presented in Sect. 3.2. The following section, Sect. 4, gives a detailed evaluation of *first-principles* simulations, also known as ab initio simulations, which are applied to ILs and their problems. Simple models to predict thermodynamic data are examined in Sect. 5. Finally, Sect. 6 gives a brief discussion and conclusions.

2 Static QC Methods

Apart from the neglect of temperature, environment and large system size, it is important for a particular problem to chose the appropriate electronic structure method and basis set. The basis sets for all atoms represent the wavefunction of a system and the methods are usually applied in a single determinant ansatz. However, especially in approaching or departing ionic systems, it is not obvious that this single-determinant ansatz is valid in each case; see [22, 26]. If dispersion effects might play a role, special care should be taken when Hartree–Fock or density functional theory is applied [27]. This problem is discussed in depth at the end of Sect. 2.4. Using one of the most employed methods that treats correlation properly, namely second-order Moller–Plesset perturbation (MP2) theory, the right basis set should be chosen. Good praxis always tests the accuracy of the method

and basis set by calculating the smallest example with a "better" method or a "larger" basis set. Please note that a more expensive method need not necessarily result in a better outcome which is also true for the basis set, please see [2] for further instructions. For example, it was found that the more expensive B3LYP functional provides worse results than applying for example BP, PBE or BLYP functionals in combination with the TZVPP basis set [28].

2.1 Semiempirical Methods

In order to study hydrogen bonding between cation and anion, Meng et al. analyzed the structure and energetics of $[C_4mim][PF_6]$ with semiempirical AM1 and PM3 calculations as well as with Hartree–Fock, second-order MP2 theory and density functional theory applying small Pople basis sets [15]. The authors determined energies along the proton transfer coordinate and found in general an inharmonic behavior rather than a double minimum potential [15].

Complete neglect of differential overlap calculations on imidazolium based cations and subsequent molecular descriptor analysis, for example surface areas, were carried out by Studzińska et al. in order to study the hydrophobicity of ILs [29].

2.2 Hartree–Fock, Density Functional and Perturbation Theory

Density functional theory is the most widely applied method in order to study small components of ILs such as ions or pairs by means of static QC calculations for reasons of low computational costs. In this part of the review we also include these articles that contain correlated methods such as second-order MP2 theory and coupled cluster calculations if the calculations are provided only for the purpose of comparison, but are not the main workhorse to obtain the data.

2.2.1 Imidazolium Based ILs

$[C_4mim][Cl]$ ion pairs were studied with the aid of charge densities, natural bond orbitals (NBO), and delocalized molecular orbitals using B3LYP and MP2/6–31++G(*d*,*p*) combinations [30]. The electronic structure of the $[C_4mim]^+$ cation was observed to be described best by a $C_4{=}C_5$ double bond at the rear (see also Fig. 1), and a delocalized three-center $4e^-$ component across the front (N_1–C_2–N_3) of the imidazolium ring; delocalization between these regions was observed to be significant [30]. It was furthermore found that hydrogen-bond formation might be driven by Coulombic stabilization, which compensated for an associated destabilization of the electronic part of the system. Interactions were dominated by a large positive charge at C_2 and the formation of π-electron density above and below the ring [30].

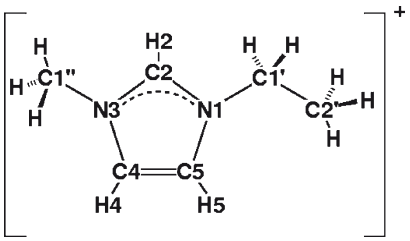

Fig. 1 Lewis structure of the $[C_2mim]^+$ cation in order to illustrate the applied labeling of the imidazolium ring. The H2 hydrogen atom is bonded to the C2 carbon atom of the ring. Note that this structure is constructed after the suggestion for the $[C_4mim]^+$ cation of Hunt et al. [30]

Hartree–Fock and DFT (B3LYP) calculations were carried out in order to investigate the $[C_2min]^+$ cation, the anions $[BF_4]^-$ and $[PF_6]^-$, and the combined ion pairs with the 6–31+G(*d*,*p*) basis set [31]. The optimized $[C_2mim][BF_4]$ and $[C_2mim][PF_6]$ ion pair conformers appeared such that the anions were located outside the imidazolium ring plane between the ethyl group and the methyl group. The interaction energy (ΔE^{cp}_{diss}) for $[C_2mim][PF_6]$ amounted −328.8 kJ mol^{-1} (B3LYP) and −326.6 kJ mol^{-1} (Hartree–Fock) and for $[C_2mim][BF_4]$ −353.5 kJ mol^{-1} (B3LYP) and −350.5 kJ mol^{-1} (Hartree–Fock) [31].

Hunt et al. examined a large number of ion pair structures with B3LYP and the 6–31++G(*d*,*p*) basis set in order to determine whether such calculations are offering insight into the physical properties of the liquid state, particularly viscosity and melting points [32]. The cation $[C_4mim]^+$ was combined with a range of anions ($[Cl]^-$ (ΔE_{diss} = −375.6 kJ mol^{-1}), $[BF_4]^-$ (ΔE_{diss} = −345.0 kJ mol^{-1}), and $[NTf_2]^-$ (ΔE_{diss} = −315.3 kJ mol^{-1})). These were chosen because of the range of viscosities exhibited by the corresponding ILs. A relationship between ion pair association energy, a derived "connectivity index," and the diversity of structures with viscosity and melting point was established. The calculations indicated that ions in $[C_4mim][Cl]$ form a strong, highly connected and regular array, thus rationalizing the high viscosity and melting point. In contrast, the ion pairs of $[C_4mim][NTf_2]$ showed a weakly interacting, highly disordered, and low connectivity network consistent with the low viscosity and melting point. $[C_4mim][BF_4]$ was observed to lie in between these two extremes [32].

IR-, Raman or mass spectroscopic studies: Köddermann et al. carried out FTIR measurements and DFT calculations with the B3LYP functional and a 6–31+G* basis set for $[C_2mim][NTf_2]$ [33]. By analyzing the ΔE^{cp}_{diss} energies, a preference for ion pairs H-bonded via C2 (see Fig. 1) was observed. Normal modes and harmonic vibrational frequencies were calculated for all structures. The reported harmonic frequencies were scaled with a factor of 0.96 [33]. Ion pair formation was observed in the neat IL, rising with temperature.

Dhumal studied $[C_1mim][NTf_2]$ with Hartree–Fock and DFT methods [34]. Different conformers were studied and molecular interactions in the vibrational spectra were discussed. Direction of the normal vibration frequency shifts for the ion pairs relative to those in the free anion and cations were explained by electron density differences coupled to the molecular electron density topography [34].

The difference in viscosities for the IL consisting of the $[C_2mim]^+$ cation and either the bis(trifluoromethane-sulfonyl)imide anion ($[CF_3S(O_2)_2N]^-$: 33 mPa s) or

the bis(fluorosulfonyl)imide ($[FS(O_2)_2N]^-$: 18 mPa s) anion has prompted Fujii et al. to measure and calculate their Raman spectra [35]. The authors applied the B3LYP functional in combination with different Pople basis sets [35].

One of these ILs ($[C_2mim][NTf_2]$) was also investigated with the aid of calculated and experimental Raman spectroscopy [36]. The authors aimed at a better understanding of the $[C_2mim]^+$ and $[NTf_2]^-$ conformational isomerism as a function of temperature. Characteristic Raman lines of the planar and nonplanar $[C_2mim]^+$ conformers were identified using $[C_2mim][Br]$ as a reference [36]. The $[NTf_2]^-$ anion conformer of C_2 symmetry was observed to be more stable than the *cis* (C_1) conformer by 4.5 ± 0.2 kJ mol^{-1} in accordance with [37]. At room temperature, the authors found populations for *trans* (C_2) anions and for nonplanar cations of 75 ± 2% and of 87 ± 4%, respectively. Fast cooling resulted in quenching of a metastable glassy phase composed of mainly C_2 anions conformers and planar cation conformers, whereas slow cooling gave a crystalline phase composed of C_1 anion conformers and of nonplanar cation conformers [36].

The Raman spectra of different $[C_4mim][C_l]$ ion pair conformers differed considerably when recorded at room temperature and ambient pressure, which prompted Chang et al. to carry out DFT calculations and measurements applying pressure [38]. B3LYP/6–31+G* calculations with a scaling factor for the calculated frequencies of 0.955 indicated that the methyl and butyl C–H groups are suitable proton donor sites.

Chiu et al. found in a mass spectrometric analysis of electrospray current primarily $X^{\pm}[C_2mim][NTf_2]_n$ ions (X = $[C_2mim]$ or $[NTf_2]$) with n = 0, 1, and 2 [39]. Minor trace ions were also observed. DFT calculations (B3LYP/6–31++G(*d*,*p*)) indicated that the n = 1 ions have thermal energies near or above the dissociation limit at the temperatures of these experiments. The $[C_2mim]^0$ radical, formed by the addition of an electron to $[C_2mim]^+$, showed significant deviation from the planar structure. A Löwdin population analysis of $[C_2mim]^0$ inferred that the unpaired electron is primarily centered on C_3. The authors also found that it is energetically more favorable by 35 kJ mol^{-1} to add a second cation, rather than another anion, to the $[C_2mim][NTf_2]$ ion pair [39].

Thermodynamic properties: Thermodynamic properties of $[C_4mim][PF_6]$ in the ideal gas state were calculated from molecular and spectral data [40]. The geometries of the cation, the anion, and the ion pair were optimized with the HF/6–31G* combination. Subsequently the authors carried out MP2 single point calculations with the 6–31G* basis set. The calculated thermodynamic quantities of the ideal gas state $S°$, C_p, and –(G°–H°(0)/T) were 657.4, 297.0, and 480.3 JK^{-1} mol^{-1} at 298 K and 843.1, 424.4, and 252.8 JK^{-1} mol^{-1} at 500 K. The calculated vapor pressure obtained by combining a published value of the cohesive energy density, measured heat capacities, and thermodynamic properties in the ideal gas state was found to be 10^{-10} Pa. Thus the authors found a value that is much smaller than the lower detection limit for effusion measurements [40].

The molar enthalpy of formation of $[C_4mim][DCA]$ was determined to be 206.2 ± 2.5 kJ mol^{-1} with combustion calorimetry [27]. The molar enthalpy of vaporization of $[C_4mim][DCA]$ (157.2 ± 1.1 kJ mol^{-1}) was obtained from the temperature dependence of the vapor pressure measured using the transpiration method. The

reliability of this method was tested at the $[C_4mim][NTf_2]$ IL measured by the effusion technique. The first experimental determination of the gaseous enthalpy of formation of the IL $[C_4mim][DCA]$, 363.4 ± 2.7 kJ mol^{-1}, from thermochemical measurements (combustion and transpiration) was carried out [27]. The enthalpy of formation in the gaseous phase of $[C_4mim][DCA]$ was calculated applying the G3MP2 model. This newly developed approach was estimated to allow the determination of thermodynamic properties which are not available so far.

2.2.2 Other ILs

N,*N*′-Dimethylformamide $[DMFH][NO_3]$ ion pairs were optimized with the 6–31G* Pople basis set and the B3LYP hybrid functional [41]. Subsequently, energies with the 6–311++G** basis set were obtained. The enol form of the $[DMFH]^+$ cation was observed to form three stable conformers with the anion, while the cation of the keto form is unstable and the proton transfer occurs to form three kinds of neutral molecule pairs [41]. Moreover, the neutral pairs were more stable than the ion pairs, and the ion pairs tended to tautomerize to neutral pairs without barriers, which was interpreted as decomposition of the ILs [41].

DFT fails to treat dispersion or van der Waals effects properly; for example this method was observed to produce unreliable geometries for hydrogen-bonded species [28, 42]. These findings prompted Johansson et al. to carry out geometry optimizations and vibrational frequency calculations with MP2 and the 6–31+G(*d*,*p*) basis set for *N*-methylpyrrolidine–acetic acid mixtures [42]. Improved electronic energies were obtained by applying a triple-ζ quality basis set 6–311+G(3*df*,2*p*). The authors investigated counterpoise corrected binding energies (ΔE^{cp}_{diss}). Proton affinity energies of the acetate and dimer acetate anion, $(AcO)_2H^-$, were treated with the MP2/aug-cc-pVTZ combination. Corrections for the zero-point vibrational energies were computed using scaled MP2/6–31+G(*d*,*p*) frequencies. The potential energy surface (PES) of the N–H stretch in the complex of two acetic acid molecules and the *N*-methylpyrrolidine base was calculated with B3LYP/6–31+G(*d*). Subsequently, energies were obtained with the MP2/6–31+G(*d*,*p*) combination [42]. The authors described the fluidity and conductivity as a function of composition in these mixtures. The 1:1 acid–base mixture was found to form an IL with a low degree of ionicity. Thus the authors recommended to characterize such liquids rather as poorly dissociated mixtures of acid and base [42]. The composition consisting of 3 mol acetic acid and 1 mol *N*-methylpyrrolidine was shown to form the highest ionicity mixture due to the presence of oligomeric anionic species $[(AcO)_xH_{x-1}]^-$ stabilized by hydrogen bonds. These oligomeric species were found to be the origin for the higher degree of ionicity than that of the 1:1 mixture [42].

Conformational analysis of the *N*-butyl-*N*-methyl-pyrrolidinium $[P_{14}]^+$ ion as found in the ion pair with $[NTf_2]^-$ and $[Br]^-$ were carried out by means of DFT calculations and Raman spectroscopy. This article also contains a very valuable overview over pyrrolidinium studies from theoretical calculations [43]. The authors found various types of stable conformations with respect to the pyrrolidinium ring

and *N*-butyl group. The DFT calculations indicated that conformers with the *N*-butyl group at equatorial and axial positions are relatively stable and that the former constitutes the global minimum. By comparing observed and calculated Raman spectra the calculations revealed that the $[P_{14}]^+$ ion is present mainly as the axial-envelope conformer in $[P_{14}][Br]$, while the equatorial- and axial-envelope conformers are present in equilibrium in $[P_{14}][NTf_2]$ IL [43].

Nockemann et al. applied density functional theory with the functionals BP and B3LYP and the TZVP basis set for isolated complexes of choline saccharinate and choline acesulfamate [44]. Furthermore, MP2 with TZVPP was employed. Counterpoise corrected interaction energies (ΔE^{cp}_{diss}) as well as atomic charges with multicenter corrections from the shared electron population analysis were considered and a natural population analysis was carried out [44]. Two types of hydrogen bonding were observed for choline saccharinate; see Fig. 2 for anion Lewis structures. In one type of ion pairs, the hydroxyl group of the choline cation was found to be hydrogen-bonded with the nitrogen atom of the saccharinate anion, but in other conformers the hydroxyl group was detected to be hydrogen-bonded to the carbonyl oxygen of the saccharinate anion. The percentage of the occupation of the non-Lewis orbitals in saccharinate and acesulfamate (Fig. 2) was considered, and it was observed that the negative charges are more delocalized in the saccharinate anion than in the acesulfamate anion due to the presence of the phenyl ring in the saccharinate anion. In the acesulfamate anion, the negative charge was found to be largely localized on the nitrogen atom. Therefore, preferential hydrogen bonding occurs only between the hydroxyl group of choline and the nitrogen atom of acesulfamate. Calculated dipole moments for the choline saccharinate and choline acesulfamate ion pairs were very large, ranging from 8 to 23 Debye. These high values were explained with the strong charge separation in the ion pairs. The authors warned that the interaction energies were calculated for ion pairs in the gas phase and that the interaction energies in the liquid phase and in the solid phase are different. The differences in interaction energies calculated for the experimental molecular geometries (as obtained from the crystal structures) and for the gas-phase optimized structures indicated that solvent effects are playing an important role [44].

In order to deepen the understanding of cation–anion interaction in ILs, Yu and Zhang investigated the structure and interionic interaction of 1,1,3,3-tetramethylguanidinium lactate ([TMG][L]) ion pairs [45]. The objective of their study were stable configurations, hydrogen bonding, frontier molecular orbitals, electron density, ion interaction energy and charge transfer [45]. Using B3LYP and MP2 with the 6–31G* basis set, a charge-localized character of [TMG][L] was detected. The interaction energy was observed to be about 65.3–109.3 kJ mol^{-1} higher than that of $[C_4mim]$-based ILs. It was also found that the frontier molecular orbitals of $[L]^-$ and of $[TMG]^+$ can effectively interact and charges are transferred between cation and anion.

Brønsted acidities of sulfonic acid-functionalized ILs with pyridinium cations were investigated with HF/6–31(*d*,*p*) [46]. The Brønsted acidities were found to be dependent on the anions following the order $[PSPy][BF_4]$>$[PSPy][HSO_4]$>[PSPy][pTSA]>$[PSPy][H_2PO_4]$. Minimum-energy geometries revealed that the anions

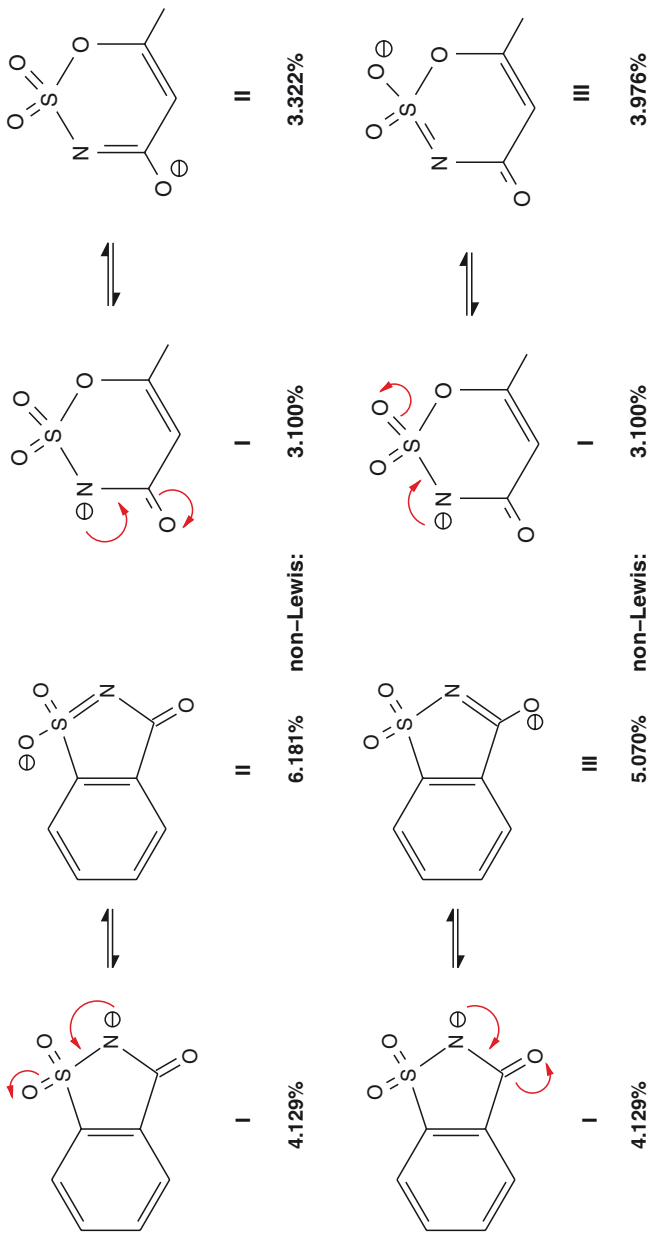

Fig. 2. *Left*: Lewis structures for the saccharinate anion. *Right*: Lewis structures for the acesulfamate anion. The percent values give the percentage of the occupation of the nonLewis orbitals. A small nonLewis occupancy indicates a more localized charge in the molecule. Figure adapted from [44]. Image Copyright American Chemical Society 2007

strongly interact with the sulfonic acid proton. The authors inferred that, in addition to the alkyl sulfonic acid group, the anion is likely to serve as available acid sites. Hence the acidities and catalytic activities of ILs depend on the kind of anions [46].

2.2.3 Solute–Solvent and Solvent–Solvent Intermolecular Forces

The interaction of a CO_2 molecule with different anions commonly used in room temperature ILs was studied under isolated conditions [47]. Minimum energy structures obtained using DFT based calculations (BP with plane waves) suggested the dominance of Lewis acid–base interactions between the species. In the optimized configurations, the authors found the CO_2 molecule to adopt a nonlinear geometry [47]. The extent of the consequent split in the CO_2 bending mode calculated from a Hessian analysis agreed qualitatively with vibrational spectroscopic results. In the case of halides, the interaction strength was observed to decrease with increasing size of the anion. In complexes containing multinuclear anions, CO_2 preferred the location near the position in which its carbon atom can interact with two electronegative atoms of the anion. This location and orientation was found to be the minimum energy conformations for all the polyatomic anions studied [47].

Gong et al. applied DFT (B3LYP and B3PW91) together with MP2 and in combination with the 6–311++G** basis set in order to obtain geometries and vibrational frequencies for $(HF)_n$ (n = 1–6) with the imidazolium cation [48]. NBO analysis and nucleus-independent chemical shifts analyses were carried out in order to study the aromaticity [48].

The interaction between water molecules and imidazolium-based ILs with the anions $[Cl]^-$, $[Br]^-$, $[BF_4]^-$, and $[PF_6]^-$ was investigated with B3LYP and MP2 and the 6–31G* and 6–31++G** basis sets [49]. The predicted geometries and interaction energies implied that the water molecules interact with the anions to form X…W (X = $[Cl]^-$ or $[Br]^-$, W = H_2O), 2X…2W, $[BF_4]^-$…W, and W…$[BF_4]^-$…W complexes. For DFT the hydrophobic $[PF_6]^-$ anion did not form a stable complex with the water molecules. Further indications that the cation and ion pairs could also form a strong interaction with the water molecules were found. The $[C_2mim]^+$ cation was used as model. Wang et al. found that the strengths of the interactions follow the trend anion-W>cation-W>ion pair-W [49].

To investigate the interactions between water molecules and amino acid-based ILs, QC calculations were performed on a [HGly][BF_4] (Gly, glycine) ion pair and one water molecule [50]. Geometry optimizations were carried out with B3LYP/6–31+G(*d*,2*p*), B3LYP/6–311++G** and MP2/6–311++G**. The frequencies of each optimized molecule were analyzed with the first two methods. Interaction energies $\Delta E_{\text{diss}}^{\text{cp}}$ between the ion pair and water were calculated. It was found that, comparing with imidazolium-based ILs, the present amino acid-based IL was more hydrophilic, because the $[HGly]^+$ cation is also hydrophilic [50].

Transition metal complexes: Weber et al. demonstrated the usual behavior and innocence of the selected IL ([C_4mim][NTf_2]) in ligand-substitution reactions of Pt(II) complexes [51]. The apparent insensitivity of the IL towards polarity changes

in going to the transition state was ascribed to its tendency to form well-structured cation–anion aggregates. As a result of the apparent absence of solvent reorganization due to changes in electrostriction in this medium, the observed activation volume was correlated with intrinsic volume changes that resulted from changes in bond lengths and bond angles on going to the transition state [51].

2.3 Beyond Single Ions Pairs: Clusters

In order to gain deeper insight into the behavior of these ILs, Koßmann et al. [52] constructed higher clusters from [C_1mim][Cl] monomer units and carried out DFT (BP86) and MP2 calculations with TZVP and larger basis sets. In the dimer elements the monomer units were incorporated in a very relaxed way, which led to the conclusion that the monomer units are thus able to establish virtually ideal arrangements in the condensed phase. Ring structure motifs exhibited highly reduced dipole moments as compared to the analogous chain elements in accordance with polarity measurements that found polarities comparable to alcohols [53]. Furthermore a comparison to radial pair distribution functions showed similar C–H …Cl distances than the one established in the cyclic structure. These structures yielded similar energies per monomer unit as the most stable monomer [52]. The Cl…H distance of the chloride to the most acidic proton in a systematic constructed chain was found to increase with an increasing number of monomer units. The value for the average bond was found to grow asymptotically to 218.9 pm which was again comparable to radial pair distribution functions. The dipole moment showed almost linear increase and the dipole moment per monomer unit reached the asymptotic value of 16.3 D. The charges on the chloride atoms were observed to decrease with an increasing chain length to a value around −0.8*e*. This observed behavior is interesting in the light of recent force field development, where the charges on the ions were downscaled; see [54] and Sect. 3.1.1. The authors also calculated binding energies considering monomer ion pairs and ions. The energies were found to grow linearly with an increasing number of units. Considering the ion binding energy per unit an increasing stability for the dimer was observed. While the dimer and the trimer were found to be less stable than the monomer, from the tetramer on the aggregates showed comparable stability to the monomer unit [52].

Ludwig carried out static calculations of larger clusters [C_1mim][SCN] [55]. The author considered clusters up to 16 ion pairs for calculating structures and energetics and clusters up to four ion pairs for calculating thermodynamic properties including frequency analysis [55]. Optimized geometries and harmonic vibrational frequencies for a variety of cluster species were obtained from Hartree–Fock calculations in combination with a 3–21G basis set. Subsequently, Ludwig derived partition functions in order to calculate thermodynamic properties. The author found that if large enough clusters (n = 6, 8, 10) are considered, enthalpies of vaporization and boiling points can be predicted which are close to measured values. Interestingly, Ludwig had to apply a structure that is not the global minimum as

gas-phase reference. Ludwig warned that the main problem of applying static QC method would be that the structure of the ion pair representing the gas phase is not exactly known. Predicted enthalpies of vaporization varied between 120 and 140 kJ mol^{-1} and boiling points between 880 and 940 K. Possible uncertainties for the enthalpies of vaporization were found to be of the order of 50 kJ mol^{-1} which is close to the differences obtained for various experimental methods and obtained for different force fields used in MD simulations. Ludwig estimated that the quality of the ab initio method and the basis set is a less serious problem because the interactions between cations and anions are described on the same theoretical footing for the gas phase as they are for the bulk phase of the IL [55].

2.4 Sophisticated Methods and the in-Plane-Above-Plane Problem

The performance of several general gradient approximation, meta general gradient approximation, and hybrid functionals was tested against MP2 [28]. Two dispersion-corrected approaches (addition of van der Waals forces by a $1/r^6$ term and employing a dispersion-corrected atom-center dispersion pseudopotential) were studied [28]. For the $[C_4mim]^+$ cation neglecting dispersion, different trends for structural stabilities were observed. The two applied correction schemes for DFT improved the results tremendously. Investigating several $[C_4mim][DCA]$ ion pairs showed a mean absolute deviation from the MP2 interaction energy of 35.7 kJ mol^{-1} for HF and up to 33.2 kJ mol^{-1} for the DFT methods. The dispersion-corrected methods reduced the mean absolute deviation to less than 10 kJ mol^{-1}. Comparing adducts of the investigated ion pair with Diels–Alder educts (cyclopentadiene and methylacrylate) led to similar energetic differences as for the ion pairs. Furthermore, large deviations in geometries for the intermolecular distances were found for the HF approach (mean absolute deviation: 190 pm) and DFT (mean absolute deviation up to 178 pm), while for the dispersion-corrected methods the mean absolute deviation was less than 50 pm. Furthermore for Hartree–Fock and all uncorrected functionals it was found that the most stable $[C_4mim][DCA]$ structure is one where the anion lies in front of the C2–H2 position in plane with the imidazolium ring instead of the MP2 favored structure (by −10.7 kJ mol^{-1}) where the anion is located above the imidazolium ring. This structure is by 3.7 kJ mol^{-1} less stable for HF and by 4.3 kJ mol^{-1} less stable for B3LYP [28]. Thus, depending on the methodology either the in-plane imidazolium ion pair or the above-plane imidazolium ion pair is favored. In contrast to the failure of HF and usual DFT, the corrected DFT methods showed the same trends as MP2 and should therefore be applied in calculations of IL systems.

Nine ion pairs were studied by MP2/6–311G** calculations [56]. The interaction energies of the $[C_2mim]^+$ ion pairs followed the trend $[CF_3CO_2]^-$>$[BF_4]^-$>$[CF_3SO_3]^-$>$[(CF_3SO_2)_2N]^-$≈$[PF_6]^-$ (−375.7, −356.5, −345.6, −329.7 and −328.0 kJ mol^{-1}) [56]. The interaction energies of $[BF_4]^-$ ion pairs with $[C_2mim]^+$, ethylpyridinium, *N*-ethyl-*N*,*N*,*N*-trimethylammonium, and *N*-ethyl-*N*-methylpyrrolidinium were not very different (−356.5, −346.4, −354.0 and −353.1 kJ mol^{-1}). Comparison with the

Table 1 Interaction energies ΔE_{diss}^{cp} for $[C_2mim][BF_4]$ in kJ mol^{-1}. Please note that the aug-cc-pVDZ contains 398 basis functions and the aug-cc-pVTZ contains 851 basis functions for this system [56]

Basis set	HF	MP2	MP3	CCSD	CCSD(T)
6–311G*	−356.9	−366.1	−366.5	−366.5	−368.2
6–311G**	−354.8	−362.3	−362.3	−363.6	−365.3
aug-cc-pVDZ	−352.3	−369.4	–	–	–
aug-cc-pVTZ	−351.0	−372.0	–	–	–

experimental ionic conductivities showed that the magnitude and directionality of the ion pair interaction energy plays a crucial role in determining the ionic dissociation/association dynamics. The electrostatic interaction was found to be the major source of attraction between ions. The induction contribution was observed to be small but not negligible. The hydrogen bonding with the C2–H2 of the imidazolium cation was estimated to be nonessential for the attraction in the ion pair. Obtained counterpoise corrected interaction energies ΔE_{diss}^{cp} are listed in Table 1. The MP3, CCSD, and CCSD(T) interaction energies shown in Table 1 are not very different from the MP2 interaction energies.

Conformational energies for the butyl group of $[C_4mim]^+$ were calculated with ab initio methods [57]. Estimated relative energies for different rotamers of the $[C_4mim]^+$ cation with the CCSD(T)/cc-pVTZ combination were observed to be up to 2.1 kJ mol^{-1}. The close contact of a $[Cl]^-$ anion to the C2–H2 increased the relative stability of one rotamer. The effects of the $[Cl]^-$ anion close to the C4–H4 and C5–H5 are small [57].

Symmetry-adapted perturbation theory based on CCSD electronic structure calculations was applied by Zahn et al. in combination with the aug-cc-pVDZ-basis set for different structures of the $[C_1mim][Cl]$ ion pair. The starting geometries were calculated using the MP2 approach and the aug-cc-pVTZ-basis set. PESs were obtained increasing the distance between cation and anion. Zahn et al. could show the importance of dispersion and induction interactions for this imidazolium-based IL in contrast to [Na][Cl] [58]. The results indicated that care has to be taken when Hartree–Fock or DFT is applied regarding the incorrect description of dispersion interactions for these methods. On the other hand, the importance of induction effects asks for polarizable force fields if not for *first-principles* simulations. For [Na][Cl] the authors could show that dispersion interactions do not play a role at all. Considering that the repulsive region of a potential is related to the melting point, while the attractive region is associated with the boiling point, a flat repulsive region corresponds to a lower melting point than a steep curve would [58]. It could be shown that such a flattening of the repulsive region is induced in ILs by dispersion and induction forces. Furthermore, the study of $[C_1mim][Cl]$ showed that the equilibrium distance is not exclusively determined by the most important attractive force, namely, the electrostatic interaction. It was found, instead, to be shifted to smaller distances, implying that the ions interact in the repulsive potential region in terms of the electrostatic forces only. Because the individual contributions did not add up in an optimal fashion, a shallow potential curve was obtained for the IL in contrast to that of [Na][Cl] [58].

Hunt and Gold examined multiple stable conformers of [C_4mim][Cl]. The most stable conformers were found to be almost degenerate and (a) to form a chloride H-bonding to the C2–H2 position or (b) to lie above the imidazolium plane [59]. Hunt and Gold applied the HF, DFT(B3LYP, PBE1PBE), and MP2 (frozen core) methods using 3–21G, 3–21G(*d*) and 6–31++G(*d*,*p*) basis sets. Furthermore, single point energy calculations on optimized structures were carried out with the MP2/6–31++G(*d*,*p*) combination and with coupled cluster theory [22] in combination with the Dunning basis sets cc-pVDZ and aug-cc-pVDZ. The authors observed that changing the basis set has a significant effect on the MP2 calculations: Although the relative energy ordering between the conformers was retained, the cc-VDZ basis set would appear to overestimate the energy of one of the top-conformers by 15 kJ mol^{-1}. Applying CCSD and CCSD(T) with the cc-pVDZ basis set did not improve the situation. Using an aug-cc-pVDZ basis set in combination with the MP2 method stabilized this top-conformer. The CCSD(T) calculations indicated that this top-conformer is slightly (<1 kJ mol^{-1}) more stable than the front conformer. The results of Hunt and Gold indicated that correlation and basis set effects are important for the top conformer which was the reason why the authors suggested that the MP2/631++G(*d*,*p*) method is a better medium-cost choice than the B3LYP method [59].

3 MD Simulations

Within this Sect. 3 we mainly consider atomistic simulations. Coarse grained simulations or numerical integration methods are briefly summarized in the model section (Sect. 5). As reported in our introduction, Maginn has presented a very interesting article about atomistic simulations [17]. Maginn emphasizes that atomistic simulations have emerged in recent years as an important compliment to experiment. Macroscopic properties of ILs can thereby be linked to their underlying chemical structure [17]. The authors warn that the ability to obtain reliable thermodynamic and transport properties from a simulation depends both on the quality of the force field and on the use of a proper simulation method. Properties such as densities and heat capacities are already within the scope of standard techniques. The next step would consist of more advanced simulation methods allowing solid–liquid and vapor–liquid phase equilibria to be determined. Maginn furthermore warned that transport properties can also be computed, but the notoriously slow dynamics of many IL systems demands that great care must be taken to ensure that the simulations are accurate [17].

3.1 Imidazolium Based ILs

3.1.1 Force Field Developments and Validation

Early models: Intermolecular potentials suitable for MD or MC simulations were developed for $[C_1mim]^+$ and $[C_2mim]^+$ ions [11]. The predicted crystal structures

satisfactorily compared with experimental crystal structures for $[Cl]^-$ and $[PF_6]^-$. This required that the dominant electrostatic interactions were modeled by either an accurate distributed multipole description or a simplified atomic point charge model. Using united atoms in place of methyl or methylene groups on the side chains resulted in less satisfactory crystal structures. Liquid $[C_1mim][Cl]$ and $[C_1mim][PF_6]$ were simulated using the explicit atom and united atom potentials [11]. The local structure showed a strong preference for the $[Cl]^-$ to be located in certain regions around the cation, and a similar, but less strong localization of the larger $[PF_6]^-$. Significant differences in density and diffusion rates were found when the explicit atom model was replaced by the cheaper united atom model, showing that the latter potential is significantly poorer for modeling both the static solid and dynamic liquid simulations.

In 2002, Morrow and Maginn presented an all-atom force field for $[C_4mim][PF_6]$ using a combination of DFT calculations (B3LYP/6–311+G*) and CHARMM 22 parameter values [13]. MD simulations were carried out in the isothermal–isobaric ensemble at three different temperatures. The calculated properties contained infrared frequencies, molar volumes, volume expansivities, isothermal compressibilities, self-diffusivities, cation–anion exchange rates, rotational dynamics, and radial distribution functions. These thermodynamic properties were found to be in good agreement with available experimental values [13].

In 2004, Canogia Lopes et al. introduced a new force field for $[C_nC_nim]^+$ cations. The model was based on the OPLS-AA/AMBER parameters. In order to obtain several terms in the force field that had not been defined in the literature, ab initio calculations were performed [60]. These included torsion energy profiles and distributions of atomic charges. Validation was carried out by comparing simulated and experimental data on 14 different salts.

Charge downscaling and altering Lennard–Jones parameters: Working specifically with reduced electrostatics started around 1994 when Mueller–Plathe found in a study of salt-polymer mixtures that this affects the mobility [61]. Reducing the dielectric constant led to the desired and increased mobility of the ions, see [61] and quotations therein.

Bhargava and Balasubramanian transferred this concept onto ILs [54]. In earlier investigations [62, 63] Bhargava and Balasubramanian showed that the model potentials of imidazolium based ILs were unable to reproduce accurately the cation–anion hydrogen bond. Therefore a refined fully-flexible all-atom potential for $[C_4mim][PF_6]$ that predicts the density of the liquid at different temperatures between 300 and 500 K within 1.4% of the experimental value was presented [54]. The model contained reduced charges (0.8), because unit positive and negative charges on the cation and the anion predicted slower diffusion of the ions compared to experiment. The calculated diffusion coefficients of ions and the surface tension of the liquid with their model agreed well with experiment [54]. Furthermore, 256 and 2,048 ion pairs of $[C_4mim][PF6]$ were simulated [64] at 200 K in the canonical ensemble using the fully flexible all-atomistic model in order to study the IL structure of [54]. The calculated peak positions and intensities agreed very well with the experimental ones [64].

Schröder and Steinhauser elucidated the consequences of different charge sets on the structure and dynamics of [C_2mim][DCA] [65]. The structural features seemed to be more or less independent of the partial charge set, pointing to a dominance of shape forces as modeled by Lennard–Jones parameters. This was observed in the radial distribution and orientational correlation functions. The role of electrostatic forces becomes imperative when studying dynamical properties. Significant deviations between different charge sets were observed. Overall, the dynamics seemed to be governed by viscosity. The authors mentioned that all dynamical parameters presented convert from one charge set to another by viscosity scaling.

A systematic study of charge scaling was provided in 2008 by Youngs and Hardacre [66]. The authors could show that charges of ±1 lead to over-structuring as well as to a reduced mobility. These changes are for the diffusion coefficients of the magnitude of multiple orders [66]. Scaled charges result in faster anion diffusion than cation diffusion in the case of [C_1mim][Cl] [66].

Other improvements or force field models: In a seminal article Lynden-Bell et al. carried out two case studies in order to analyze the local structure in liquids and how it responds to changes in the intermolecular potential [67]. The authors used realistic next to unrealistic potentials in order to determine the sensitivity of local liquid structure to potential parameters. The first part dealt with two families of modified water models. In the "hybrid" family, the hydrogen bond strength was reduced, but the geometry was kept constant; in the second family, the molecular geometry was changed by reducing the bond angle, keeping a constant molecular dipole moment [67]. Subsequently, the local structure was measured by radial distribution functions, three-dimensional probability distribution functions and three-body angular correlations. The second case study applied the above discussed concepts to [C_1mim][Cl]. In addition, the effect of reducing the hydrogen bonding potential of the cations while maintaining their charge was examined [67].

Denesyuk and Weeks introduced a simplified version of local molecular field theory to treat Coulomb interactions by splitting into short-range and long-range parts in simulations of ILs [68]. The long-ranged parts were taken into account through a self-consistently determined effective external field. The simulation results for thermodynamic and structural properties of uniform ionic mixtures were found to agree well with results of Ewald simulations of the full ionic system. Furthermore, the authors stressed that simulations using short-ranged truncations of the Coulomb interactions alone did not satisfy the exact condition of complete screening of the fixed ion, but this condition was recovered when the effective field was taken into account [68].

Bagno et al. investigated the diffusion of [C_4mim][BF_4] [69]. MD simulations were carried out employing a classical, nonpolarizable force field. Shortcomings of the simulations were found to be a strong underestimation of diffusion coefficients which was traced to artefacts in the simulation and deficiencies in nonpolarizable force fields [69]. Such deficiencies were also discussed by Bhargava and Balasubramanian [70]. The comparison of traditional MD simulations with Car–Parrinello which was carried out by Bhargava and Balasubramanian [70] is reviewed in Sect. 4.1.

A united-atom model for [C_4mim][PF_6] and [C_4mim][NO_3] was developed in the framework of the GROMOS96 force field [71]. The equilibrium properties in the 298–363 K temperature range were validated against known experimental properties, namely, density, self-diffusion, shear viscosity, and isothermal compressibility [71]. The properties obtained from the MD simulations agreed with experimental data and showed the same temperature dependence.

AIMD data were used to improve the classical description of [C_1mim][Cl] by applying the force matching approach [72]. A self-consistent optimization method for the generation of classical potentials of general functional form was presented and applied. A force field that better reproduces the observed *first-principles* forces was obtained [72].

The third force field parameter set developed within the spirit of the OPLS-AA model and thus oriented toward the calculation of equilibrium thermodynamic and structural properties was presented [73]. The parameter sets concerned the cations alkylimidazolium, tetraalkylphosphonium, and *N*-alkylpyridinium, and the anions $[Cl]^-$, $[Br]^-$, and the $[DCA]^-$. Validation of the force field consisted of comparison with experimental crystal structure and liquid density data [73]. The fourth parameterization of a force field was published only recently. The ions modeled were the 1,2,3-trialkylimidazolium and alkoxycarbonyl imidazolium cations and alkylsulfate and alkylsulfonate anions [74].

Although many approximations are made in classical MD simulations Kelkar and Maginn found that their simulation results for ILs allow the neglect of a polarizable force field for obtaining accurate thermodynamic and transport properties [75].

3.1.2 Simulation of Thermodynamic Properties

Prado and Freitas carried out a 5-ns NPT MD simulation to investigate thermodynamical and structural properties of [C_4mim][BF_4] [76]. All force field parameters were taken from the OPLS-AA except charges and geometries. The partial charges and geometry parameters were obtained with the MP2 method and with the 6–31G(*d*) basis set. Charges were computed using the ChelpG procedure [77]. This same method and basis set was employed to calculate energies for cation–anion interactions at several configurations to validate the force field parameters [76]. The density obtained of 1.178 g cm^{-3} agreed well with the experimental value of 1.17 g cm^{-3}. The calculated heat of vaporization (413 kJ mol^{-1}) was found to be larger than those usually observed for molecular liquids, in accordance with the very low vapor pressure observed for ILs. In comparison to the anion, the cation self-diffusion constant was observed to be larger despite the fact that it is heavier and bigger [76]. This is now a well-known fact and it was also pointed out by others; see for example [62, 63]. Compared to the values observed for molecular liquids, the self-diffusion constants obtained for cation and anions were about three orders of magnitude smaller [76].

Jayaraman and Maginn calculated two crystal polymorphs of [C_4mim][Cl] using a thermodynamic integration-based atomistic simulation method [78]. The computed

melting point of the orthorhombic phase was found to range from 365 to 369 K, depending on the classical force field [60, 79]. The experimental value ranges from 337 to 339 K. The simulation procedure used to perform the melting point calculations was an extension of the so-called pseudosupercritical path sampling procedure [78]. The computed enthalpy of fusion was observed to range from 19 to 29 kJ mol^{-1}, compared to the experimental values of 18.5–21.5 kJ mol^{-1}. Only one [79] of the two force fields evaluated yielded a stable monoclinic phase, despite the fact that both applied force fields gave accurate liquid state densities [60, 79]. The computed melting point of the monoclinic polymorph was found to be 373 K (exp.: 318–340 K). The computed enthalpy of fusion was 23 kJ mol^{-1} (exp.: 9.3–14.5 kJ mol^{-1}). The simulations predicted that the monoclinic form is more stable than the orthorhombic form at low temperature, in agreement with one set of experiments but in conflict with another [78]. The difference in free energy between the two polymorphs was found to be very small, due to the fact that a single *trans-gauche* conformational difference in an alkyl sidechain distinguishes the two structures. The authors explained that constructing simple classical force fields that are accurate enough to definitively predict which polymorph is most stable is a difficult task. A liquid phase analysis of the dihedral angles probability distribution in the alkyl chain indicated that less than half of the dihedral angles were in the *gauche–trans* conformation that is adopted in the orthorhombic crystal. The low melting point and glass forming tendency of this IL was inferred to be due to the energy barrier for conversion of the remaining dihedral angles into the *gauche–trans* state [78].

Heat of vaporization: Applying classical simulations of $[C_n mim][NTf_2]$, Kelkar and Maginn calculated enthalpies of vaporization [80]. The molar enthalpy of vaporization, Δh_{vap}, was calculated by the authors as

$$\Delta h_{vap}(T,P) = < h_{gas}(T) > - < h_{liq}(T,P) > \tag{1}$$

where $<h_{gas}(T)>$ and $<h_{liq}(T)>$ are the ensemble average molar enthalpies of an ideal gas and neat liquid, respectively, at temperature T and pressure P. Lowercase symbols refer to molar (intensive) energies, whereas uppercase symbols refer to total (extensive) energies. These molar enthalpies are given by

$$< h_{gas}(T) > = < u_{gas}(T) > - RT, \tag{2}$$

$$< h_{liq}(T,P) > = < u_{liq}(T,P) > - Pv, \tag{3}$$

where u is the molar internal energy, R is the universal gas constant, P and v are the pressure and molar volume of the liquid phase, and the gas was assumed to be ideal. The value of the pressure–volume work was negligible for the liquid when compared to the internal energies, and hence was ignored. The ideal gas internal energy was calculated by simulating a noninteracting cluster and ensemble averaging the internal energy [80]. It can be easily recognized that Eqs. (2) and (3) lead to an equation depending of the internal energies only, which is how the authors obtained this quantity. The authors deduced from their results that the enthalpy of vaporization

is lowest for neutral ion pairs. The enthalpy of vaporization increased by about 40 kJ mol^{-1} with the addition of each ion pair to the vaporizing cluster. Nonneutral clusters are not expected to make up a significant fraction of volatile species. The enthalpy of vaporization increased slightly as the cation alkyl chain length increases and as temperature decreased [80].

Köddermann et al. calculated the heats of vaporization for imidazolium-based ILs $[C_n mim][NTf_2]$ with $n = 1, 2, 4, 6, 8$ by means of MD simulations [81]. The authors applied a force field which they had developed recently. Within this force field the authors reduced the Lennard–Jones parameters in order to reproduce experimental diffusion coefficients [81]. The refined force field also led to absolute values of heats of vaporization as well as their increase with the chain length of the imidazolium cation such that this quantities were described correctly. The overall heats of vaporization were split in several contributions and discussed in detail. The authors observed that with increasing alkyl chain length, the Coulomb contribution to the heat of vaporization remained constant at around 80 kJ mol^{-1}, whereas the van der Waals interaction increased continuously. The calculated grow of about 4.7 kJ mol^{-1} per CH_2-group of the van der Waals contribution in the IL exactly matched the increase in the heats of vaporization for *n*-alcohols and *n*-alkanes, respectively. The results support the importance of van der Waals interactions even in systems completely composed of ions [81].

3.1.3 Simulation of Transport Properties

The simulation of transport properties like the viscosity is especially a delicate task, because these properties need to be calculated on a very long time scale [17]. In addition to this, typical organic solvents exhibit viscosities ranging from 0.2 to 10 cP while ILs can have variations in room temperature viscosities that span several orders of magnitude [75]. Kelkar and Maginn explain [75] that next to variations due to different force fields, "it may also be that the accuracy of a viscosity calculation depends on how the calculation is carried out" [75]. IL viscosity calculations that relied on equilibrium MD simulations tended to overestimate the viscosity of which most relied on the integration of autocorrelation functions in either momentum or stress. The problem with these formally correct methods would lie in notoriously difficult integrals to compute numerically. The initial decay of the stress–stress time correlation function would be rapid, but after this it would decay very slowly, oscillating about zero for a long time [75]. Kelkar and Maginn further explained that these long time fluctuations are often of the same size as the random noise in the stress tensor. The authors warned that, due to the dynamic behavior of ILs, this long time behavior must be accurately integrated to get a reliable viscosity [75].

Transport properties and solvation dynamics of model $[C_n C_n im][Cl]$ melts at 425 K were investigated by Bhargava and Balasubramanian [62, 63]. The authors found self-diffusion constants of $D_+ = 0.31 \times 10^{-10} m^2 s^{-1}$ for the cation and $D_- = 0.22 \times 10^{-10} m^2 s^{-1}$ for the anion; thus the cation diffuses faster in accordance with experimental findings [62, 63].

Equilibrium MD simulations of self-diffusion coefficients, shear viscosity, and electrical conductivity for [$C_n$mim][Cl] at different temperatures were carried out [82] The Green–Kubo relations were employed to evaluate the transport coefficients. Compared to experiment, the model underestimated the conductivity and self-diffusion, whereas the viscosity was over-predicted. These discrepancies were explained on the basis of the rigidity and lack of polarizability of the model [82]. Despite this, the experimental trends with temperature were remarkably well reproduced. The simulations reproduced remarkably well the slope of the Walden plots obtained from experimental data and confirmed that temperature does not alter appreciably the extent of ion pairing [82].

Reverse nonequilibrium MD (NEMD) and equilibrium MD simulations were carried out by Zhao et al. to compute the shear viscosity of the pure IL system [C_4mim][PF_6] at 300 K [83]. The two methods (NEMD and MD) yielded consistent results comparable to experiments. The calculated viscosity was below the experimental value by 25–40% depending on which experiment was used as reference. This result was a vast improvement over some previous force fields, which typically overestimated the viscosities of ILs by more than one order of magnitude [83].

3.1.4 Simulation of Orientational, Dielectric, and Other Properties

Reorientational time correlation functions $C_l(t)(\equiv<P_l[cos\theta(t)]>)$ for a diatomic solute in [C_2mim][PF_6] were analyzed via MD computer simulations [84]. <…> denotes an equilibrium ensemble average, P_l the lth order Legendre polynomial, and θ the angle between the solute orientation at time t and its initial direction. The results indicated a heterogeneous dynamics. For a small nondipolar solute, C_l was observed to be well-described as stretched exponential functions in wide time ranges. After rapid initial relaxation, $C_2(t)$ decayed more slowly than $C_1(t)$ which is a striking feature [84]. Due to this the correlation time associated with the former was considerably longer than that with the latter. This was ascribed to solvent structural fluctuations, which allowed large-amplitude solute rotations. As the solute size grew, relaxation of $C_l(t)$ approached exponential decay [84].

Three different ILs were investigated via atomistic MD simulations using the force field of Lopes and Padua [73]. $[C_2mim]^+$ was studied with three different anions $[Cl]^-$, $[BF_4]^-$, and $[NTf_2]^-$ [85]. It was found that the preferred positions of the anions change of the $[Cl]^-$ from being close to the imidazolium hydrogens to being above and below the imidazolium rings. Lifetimes of hydrogen bonds were calculated and found to be of the same order of magnitude as those of pure liquid water and of some small primary alcohols [85]. Three kinds of short-range cation–cation orderings were studied, among which the offset stacking dominated in all of the investigated ILs. The offset stacking became weaker from [C_2mim][Cl] to [C_2mim][BF_4] to [C_2mim][NTf_2]. Further investigation of the dynamical behavior revealed that cations in [C_2mim][NTf_2] exhibit a slower tumbling motion compared with those in [C_2mim][Cl] and [C_2mim][BF_4]. Pure diffusive behavior was observed after 1.5 ns for all three systems at temperatures 90 K above the corresponding melting temperatures [85].

MD simulations of [C_4mim][I], [C_4mim][BF_4], and [C_4mim][PF_6] were carried out over a time period of more than 100 ns [86]. The angular correlation functions revealed interesting insights into the local structure. A collective network of ILs was characterized by the Kirkwood factor [86]. The short-range behavior of this factor was observed to predict the water miscibility of the ILs. The long-range limit was below unity which demonstrated the strongly coupled nature of the IL networks. In addition, this factor related the orientational structure and the dielectric properties of the ILs. The static dielectric constant $\varepsilon(\omega = 0)$ was observed to be 8.9–9.5 [86].

The aim of this study was the analysis of the rotational motion and the viscosity of [C_4mim][BF_4] [87]. By comparing single-particle and collective motion, it was found that the Madden–Kivelson relation is fairly fulfilled in long-term simulation studies of about 100 ns, i.e., the collective reorientation can be predicted by the corresponding single-particle property and the static dipolar correlation factor [87]. Simulated reorientation was in accordance with hydrodynamic theories yielding hydrodynamic radii comparable to van der Waals radii. While the static dielectric constant agreed with dielectric reflectance experiment, the hydrodynamic radii derived from the experiments were much lower as a consequence of enhanced rotational motion [87].

The complex ionic network of $[C_4mim]^+$ combined with the trifluoroacetate anion was simulated over a time period of 100 ns [88]. The influence of the shape anisotropy and charge distribution of both ions on the local "molecular" and global "collective" structure and dynamics was analyzed. The distance-dependent coefficients of the orientational probability function were found to be an excellent way to interpret local structure. Dynamics at the molecular level was characterized by the time correlation function of the center-of-mass corrected molecular dipole moment. Upon uniting the set of molecular dipoles to a single collective rotational dipole moment, dynamics on a global level was studied. Breaking down into subsets of cations and anions, respective self terms as well as the prominent cross term could be extracted. This breaking down also enabled the authors to carry out a detailed peak assignment in dielectric spectra [88].

The same authors presented an MD study of the molecular dipole moment and a net charge for $[C_4mim]^+$ combined with $[BF_4]^-$, $[DCA]^-$ and the trifluoromethylacetate [89]. In contrast to a solution of simple ions in a (non)polar solvent, rotational and translational effects were found to play a role. The theoretical framework necessary to compute the conductivity spectrum and its low frequency limit of ILs was newly developed. Merging these computed conductivity spectra with previous simulation results on the dielectric spectra resulted in the spectrum of the generalized dielectric constant [89]. It was calculated for the three ILs over six orders of magnitude in frequency ranging from 10 MHz to 50 THz [89].

3.2 The Viscosity-Hydrogen-Bond-Reduction Problem

This particular controversial behavior was reviewed by Cammarata et al. in an experimental study of IL–water mixtures [10]. In imidazolium-based ILs ([$C_n$mim])

substitution of the acidic hydrogen (C2–H2, see Fig. 1) with a methyl group results in the reduction of one possible hydrogen bond donor. The elimination of this hydrogen bond interaction could be expected to lead to a reduction in melting point and a decrease in viscosity, because the ions should now interact more loosely; however the opposite was observed experimentally [10, 90]. Because of this controversy, only a few studies have appeared in the literature so far.

Hunt investigated several ion pair conformers of [$C_n$mim][Cl] with static QC methods and hypothesized that the effects due to a loss in hydrogen bonding would be counterbalanced by those due to a gain in entropy [91]. A possible explanation was introduced by the amount of disorder in the system, which can be reduced in two ways: elimination of ion pair conformers, which are stable for [C_4mim][Cl] but not [C_4C_1mim][Cl], and an increase in the rotational barrier of the butyl chain, which limits free rotation and facilitates alkyl chain association. The reduction in entropy would lead to greater ordering within the liquid, raising the melting point and increasing viscosity. These deductions were based on static B3LYP/6–31++G(*d*,*p*) calculations [91].

Zahn et al. carried out static QC calculations and MD simulations in order to determine the difference between the two imidazolium-based IL types [92]. A single energy path curve was calculated with changing C_1–C_2–N_1–C_5 dihedral angle; see Fig. 1 for labels of [C_1C_1mim][Cl] and of [C_1mim][Cl] and see Fig. 3 left for the single energy path. The energy barrier for the change from one side of the imidazolium ring to the other ($X_B \rightarrow X_B$, see Fig. 3 and figure caption for explanation) was found to be below 10 kJ mol^{-1} for the lower melting [C_1mim][Cl], while it was increased above 40 kJ mol^{-1} for [C_1C_1mim][Cl]. Other pathways where the anion changes the sides of the imidazolium plane with an energy barrier below 10 kJ mol^{-1}

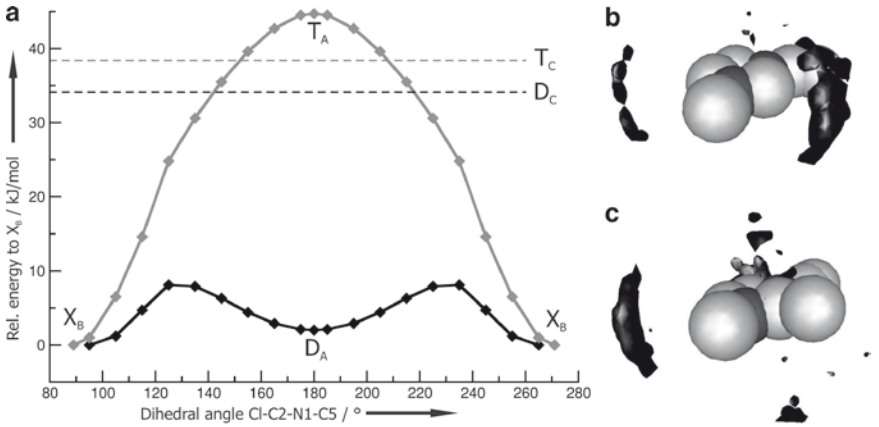

Fig. 3 *Left*: Single energy path for the side change of the $[Cl]^-$. *Right*: Spatial distribution function around the imidazolium. *D*: [C_1mim][Cl] conformers; *T*: [C_1C_1mim][Cl] conformers; D_A: chloride in front of the H_2; T_A: chloride anion in front of the additional methyl group. X_B structures with the chloride above respectively below the imidazolium ring. D_C and T_C: hydrogen bonded via the rear protons. Reproduced after [92]

were excluded for [C_1C_1mim][Cl], because the anion must always pass the minimum structures which are at least 35 kJ mol^{-1} less stable (T_C, D_C) than the D_A minimum of [C_1mim][Cl]. As a result, the anion might be caught in a potential surface bucket at the top side of the imidazolium ring in [C_1C_1mim][Cl]. In contrast, the anion in the lower melting [C_1mim][Cl] was expected to change the position easily relative to the imidazolium plane [92]. MD simulations were carried out on the systems [C_2mim][Cl] and [C_2C_1mim][Cl]. In agreement with the static QC calculations a more localized anion position of [C_2C_1mim][Cl] above and below the imidazolium plane at the [C_2C_1mim]$^+$ cation was observed in the spatial distribution functions; see Fig. 3 right side. However, the top position with a dihedral angle Cl–C2–N1–C5 of approximately 90° was found to be less often populated than expected from the static calculations. The reason for this was explained by the fact that this position was occupied by an adjacent cation. Regardless of these complications, the anion of [C_2mim][Cl] was found to be more delocalized than the one of [C_2C_1mim][Cl] at 15 times the corresponding average density [92].

3.3 Mixtures of ILs with Other Substances

3.3.1 Mixtures with Other Solvents

Vibrational energy relaxation dynamics of a diatomic solute in [C_2mim][PF_6] were studied via MD and NEMD techniques. The time scale for this relaxation was found to decrease markedly with the increasing solute dipole moment [93]. A detailed analysis of NEMD results showed that, for a dipolar solute, dissipation of an excess solute vibrational energy occurred almost exclusively via Lennard–Jones interactions between the solute and solvent, while an oscillatory energy exchange between the two was mainly controlled by their electrostatic interactions [93]. Comparison with water and acetonitrile showed that overall characteristics of vibrational energy relaxation in the IL was similar to those in acetonitrile, while relaxation in water was much faster than in the two former. It was also found that the Landau–Teller theory predictions for the time scale of this dynamics obtained by equilibrium simulations were in reasonable agreement with the NEMD results [93].

Jeong et al. investigated the effects of solute polarizability on solvation and solute transport in [C_2mim][PF_6] [94]. Therefore, the authors placed one solute in 112 ion pairs interacting via a Lennard–Jones potential with each other in MD simulations. A valence-bond description was employed to account for the instantaneous adjustment of the solute electronic charge distribution to the fluctuating solvent environment [94]. It was found that the ultrafast inertial component of solvation dynamics became slower with increasing solute polarizability which seemed to be reasonable. Moreover, its contribution to overall solvent relaxation was reduced with increasing polarizability, especially in the case of nonequilibrium solvation dynamics [94]. Overall, the inclusion of the solute electronic polarizability in the simulations improved the agreement of the simulations with time-dependent Stokes

shift measurements. The authors also recommended that further studies of different ILs are conducted with their techniques in order to clarify the ongoing controversies surrounding solvation dynamics, in particular, uniphasic vs biphasic relaxation behavior [94].

External perturbations on ILs were studied by Hu and Margulis [95]. The authors investigated three related problems. First the response of the [C_6mim][Cl] to different external perturbations was studied, second the calculation of its shear viscosity was carried out, and third the validity range of linear response theory for these types of systems was investigated [95]. Therefore the authors derived a set of equations linking bulk hydrodynamic predictions with microscopic simulations which were supposed to be valid when linear response theory is applicable [95]. Their study of up to 8,232 ion pairs showed that even for systems with a very large box length the viscosities computed from perturbation frequencies have not reached the bulk hydrodynamic limit. This was in contrast to the case of other solvents such as water [95]. The authors comprehensively investigated how the IL relaxed upon weak external perturbations at different wavenumbers in order to be able to calculate the desired property. They also studied the steady-state flow created by external shear acceleration fields. The short time behavior of instantaneous velocity profiles was compared with the results of linear response theory. The short time response appeared to match the prediction from linear response theory, while the long time response deviated as the external field became stronger. From their study, the range on which a perturbation can be considered "weak" in the linear response sense could be established. The relaxation of initial velocity profiles was also examined and correlated to the decay of the transverse-current autocorrelation function. Even though none of their calculations reached the bulk hydrodynamic limit, the authors were able to make predictions for the shear viscosity of the bulk system at different temperatures which qualitatively agreed with experimental data [95].

3.4 Water

In 2003, Hanke and Lynden-Bell carried out MD simulations of IL–water mixtures [96]. The behavior of [C_1mim][Cl] and the hydrophobic [C_1mim][PF_6] ILs was compared. Differences in the signs of both the excess volumes and the enthalpies of mixing were found. In both liquids, water molecules tended to be isolated from each other in mixtures with more ions than water molecules. When the molar proportion of water molecules reached 75%, a percolating network of waters was found as well as some isolated molecules and small clusters. In all cases, molecular motion became faster as the proportion of water increased [96].

Chevrot et al. reported MD simulations of the interface between water and the partly hygroscopic IL [C_4mim][PF_6] comparing different force field models for water and two IL models where the ions were charged ±1 and ±0.9 [97]. For the IL–humidity better agreement was found with experiment when the reduced charges were applied. The authors also studied demixing and found the phases to

separate very slowly (≈20 ns) compared to chloroform–water mixtures (≤1 ns) [97]. The difficulty in computationally and experimentally equilibrating water–IL mixtures was attributed to the slow dynamics and microheterogeneity of the IL and to the different states of water in the IL phase [97].

MD simulations of $[C_6mim][PF_6]$ and water mixtures were carried out [98]. The authors found water to be closely associated with the anions and that its presence enhances both the translational and rotational dynamics of the IL. The mean square displacement and rotational correlation functions reflected that the diffusive regime was achieved faster when water was present in the IL or the observed decay of correlations was faster when water was present, respectively [98]. From this the authors deduced that the experimentally observed decrease in viscosity is a consequence of the faster translational and rotational dynamics caused by the presence of water [98]. In agreement with experiments, the authors found that the fluorescence spectra of Coumarin-153 is red-shifted because of the presence of water [98].

This fact that small amounts of impurities alter the viscosities of ILs tremendously prompted Kelkar and Maginn to carry out MD simulations in order to examine the dependence of the viscosity of $[C_2mim][NTf_2]$ on temperature and water content [75]. A NEMD procedure was employed together with a fixed charge force field [75]. The simulations quantitatively captured the temperature dependence of the viscosity as well as the drop in viscosity that occurs with increasing water content. Furthermore, mixture viscosity models were applied in order to show that the relative drop in viscosity with water content was less than expected from an ideal system [75]. Because of the preferential water–anions association and the formation of water clusters, the excess molar volume was found to be negative. A possible interpretation considered dissolved water as less effective at lowering the viscosity of these mixtures when compared to a solute obeying ideal mixing behavior. Importantly, the authors found that application of NEMD simulations allows diffusive behavior to be observed on the time scale of the simulations, and standard NEMD resulted in subdiffusive behavior even over 2 ns of simulation time [75].

Nanostructural organization in mixtures of $[C_8mim][NO_3]$ and water was studied [99]. The calculated static partial structure factors showed that with different water contents, polar networks, water networks, and micelles possessed an approximately invariant characteristic length at around 20 Å. Furthermore, the calculations indicated the disruption of the polar network as the amount of water increased by the intruding water, while the structural organization of the water network and the micelle exhibited a turnover. At the turnover point, the most ordered micelle (cation–cation) structure and water (water–anion–water) network were formed. Thereafter, the structural organization abated drastically, and only loose micelle structure existed due to the dominant water–water interactions. The turnover of structural organization agreed with the sharpest peak in the experimentally obtained structure factor in aqueous solutions of similar ILs [99]. The liquid-like associated aggregates were attributed due to the planar symmetry and strong basicity of $[NO_3]^-$ [99].

MD simulations of the aqueous interface and the hydrophobic IL ($[C_4mim][NTf_2]$) were carried out [100]. Different liquid models, the Ewald vs the reaction field treatments of the long-range electrostatics, and different starting conditions

were compared. Randomly mixed liquids separated much more slowly (20–40 ns) than classical water–oil mixtures (≤1 ns). The final state of water in the IL depended on the protocol and was related to IL heterogeneities and viscosity [100]. Water mainly fluctuated in hydrophilic basins, separated by more hydrophobic domains, in the form of monomers and dimers in the weakly humid IL phase, and as higher aggregates when the IL phase was more humid. There was more water in the IL than IL in water, to different extents, depending on the model.

The collective structure of aqueous IL solutions was studied by means of MD simulations [101]. Various concentrations of $[C_4mim][BF_4]$ and TIP3P water were simulated at the very same size of the simulation box. For the analysis, the ternary system cation/anion/water was subdivided into binary networks. The local structure of each of these six networks and the mutual orientation of the network constituting partners were studied. Furthermore, the collective structure of the whole samples was characterized by the contribution of each species to the static dielectric constant $\varepsilon(\omega = 0)$ and to the Kirkwood factor [101].

Excess chemical potentials: As early as 2002 Lynden-Bell et al. published an investigation about the chemical potential of water and organic solutes in $[C_1mim][Cl]$ [9]. The authors stated: "… the chemical potential is the most important thermodynamic property of a solute in solution because it determines the solubility and chemical reactivity of a solute." Within this seminal article the authors determined the excess chemical potential (μ_A^{XS}) by means of theoretical methods. The excess chemical potentials μ_A of a series of molecules dissolved in the IL $[C_1mim][Cl]$ were calculated by a sequence of transformations [9]. It is defined by

$$\mu_A - \mu_A^{\text{ideal}} + \mu_A^{XS} \tag{4}$$

where μ_A^{ideal} is the ideal gas chemical potential of substance A at the same number density as in solution. In order to calculate directly the excess chemical potential the Widom particle insertion method was applied [3]. By the method of thermodynamic integration the chemical potential could be determined:

$$\mu_A - \mu_B = \int_0^1 \left\langle \frac{\partial H(\lambda)}{\partial \lambda} \right\rangle_\lambda d\lambda. \tag{5}$$

where $H(\lambda)$ is the solvent interaction energy of a hybrid molecule which is identical to molecule A when $\lambda = 0$ and to molecule B when $\lambda = 1$. Lynden-Bell et al. mostly applied a linear coupling:

$$H(\lambda) = (1 - \lambda)H_A + \lambda H_B. \tag{6}$$

The solute molecules were chosen as water, methanol (MeOH), dimethyl ether, acetone and propane. Because the transformation from a hydroxyl group to an *O*-methyl group does not behave smoothly, extra care had to be taken. Lynden-Bell et al. introduced an additional site in order to stabilize the transformation [9]. For water and methanol large negative values of the excess chemical potential (−29 kJ

mol^{-1} and −14 kJ mol^{-1} respectively) were calculated; the polar molecules dimethyl ether and acetone showed positive values of about 7 kJ mol^{-1} while the value for propane is 26 kJ mol^{-1}. For the transformation from water to MeOH two processes were found: first the growth of an uncharged Lennard–Jones site near the hydroxyl group, pushing the chloride ion away and thus breaking off the water–anion hydrogen bond, and second the final transformation to MeOH. Thus, hydrogen bonding to the anion plays an important part in the stabilization of water [9].

3.4.1 Polymer Mixtures

MD simulations were performed for polymer electrolyte models in which the salt consisted of $[C_n mim]^+$ cations and the polymer was polyethylene oxide (PEO). A systematic investigation of IL concentration, temperature, and the 1-alkyl-chain length effects on resulting equilibrium structure was provided [102]. It was shown that the IL was dispersed in the polymeric matrix. However, ionic pairs remained in the polymer electrolyte. Imidazolium cations were coordinated by both the anions and the oxygen atoms of PEO chains. Conformational changes on PEO chains upon addition of the IL were identified. The equilibrium structure of simulated systems was also analyzed in reciprocal space by using the static structure factor which displayed a low wave–vector peak, indicating that spatial correlation in an extended-range order prevails in the IL polymer electrolytes [102]. In a subsequent article on the same system the cation diffusion coefficient was found to be higher than those of anion and oxygen atoms of PEO chains [103]. The calculated ionic mobility in the $[C_4mim]^+$ mixture was higher than in the $[C_1mim]^+$ mixture [103]. For this purpose Costa and Ribeiro applied united atom models. Polarization effects were not considered by the authors [103]. Costa et al. investigated polymer electrolytes based on poly(ethylene glycol) dimethyl ether and the IL $[C_4mim][PF_6]$ by different techniques [104]. The coordination of the IL by the polymer was found to occur mainly in the amorphous phase [104].

3.4.2 ILs and Surfaces or Interfaces

The question of IL surface structures was investigated by Sloutskin et al. [105]. Comparing the $[C_4mim][PF_6]$ simulations of Balasubramanian and those by Lynden-Bell with experiment considerable deviations were found. Next to the importance of quantum effects, the authors discussed the possibility of polarizable effects missing in the simulations which might be responsible for the differences between experiment and calculations [105].

The influence of ion size asymmetry on the properties of IL–vapor interfaces was investigated using soft primitive model MD simulations [106]. The ion size asymmetry resulted in charge separation at the liquid–vapor interface and therefore in a local violation of the electroneutrality condition [106].

MD simulations for the liquid–vacuum interface of $[C_2mim][NO_3]$ were performed for both electronically polarizable and nonpolarizable PES [107].

The simulations with both models demonstrated the existence of an inhomogeneous interfacial structure normal to the surface layer. In the outmost surface layer, the cation is likely to lie on the surface with the imidazolium ring parallel to the interface, while there is a second region with enhanced density from that in the bulk where the cation tended to be perpendicular to the surface. It was found that the cation is likely to be segregated at the IL surface for the polarizable model, while for the nonpolarizable model, the anion was found to be more likely exhibiting such behavior. The surface tension obtained from the polarizable model was much smaller (>28%) than that obtained from the nonpolarizable model, in better agreement with extrapolated experiments [107].

Liquid/vacuum surfaces of $[C_4mim][PF_6]$, $[C_4mim][BF_4]$, and $[C_4mim][Cl]$ were investigated with the aid of MD simulations at various temperatures [108]. A structure with the top monolayer containing oriented cations and anions was found. The butyl side chains tended to face the vacuum and the methyl side chains the liquid. However, as the butyl chains were not densely packed, both anions and rings were visible from the vacuum phase. The effects of temperature and the anion on the degree of cation orientation was small, but the potential drop from the vacuum to the interior of the liquid was greater for liquids with smaller anions. Lynden-Bell and coworkers compared the simulation results with a range of experimental observations and suggested that neutron reflection from samples with protiated butyl groups would be a sensitive probe of the structure [108].

In a simulation of 34,284 atoms in a periodic box employing a nonpolarizable force field, Liu et al. studied the IL $[C_4mim][NO_3]$/rutile (110) interface. Anions were found to segregate and tightly bind on the surface. The orientation of the cations was modulated by the absorbed anions [109].

MD studies on the solvation of sodium chloride in $[C_4mim][NTf_2]$ were performed by Sieffert and Wipff [110]. Dissociation of a single [Na][Cl] ion pair in ILs and in conventional solvents, [Na][Cl] condensation in the IL, and solvation of [Na][Cl] microcrystals were investigated. Characteristics of the solid/IL interface was analyzed. The single ion pair preferred to be associated rather than dissociated. In a concentrated [Na][Cl] solution the ions spontaneously associated. Simulations of $Na_{13}Cl^-_{14}$ and $Na_{14}Cl^+_{13}$ microcrystals in the IL showed that both remain associated [110]. The crystal surface was solvated by the less polar IL components rather than by the polar ones. In the first IL layer the ions were ordered rather parallel to the surface, whereas in the second layer they were more perpendicular. The solvation of the crystal seemed to be rather apolar due to the mismatch between the IL and the crystal ions [110].

The interaction of an IL ($[C_1mim][Cl]$) with an external field, i.e., an IL confined between electrified walls, was investigated by the Lynden-Bell group [111]. The potential between the ions and the walls was modeled by a Lennard–Jones type potential and additional forces on each charged site in z-direction were obtained by $F_{i,z} = \frac{q_i \sigma}{\varepsilon_0}$ with q_i being the charge on that site, σ being the surface charge density and with ε_0 the vacuum permittivity [111]. After a sudden release of the applied electric field the authors determined a fast (0.2 ps) and a slow (8 ps) relaxation

process. This relaxation was dominated by the anion rather than by the cation and ionic diffusion was not involved in this process [111].

A model for an electro-active interface in which a metallic electrode is maintained at a preset electrical potential was introduced into MD simulations [112]. In the model, variable charges with magnitudes adjusted on-the-fly were applied. It included polarization of the electrode by the electrolyte. The model was applied to electrochemical cells as a pair of parallel planar electrodes separated by the electrolyte using a two-dimensional Ewald summation. The interfacial structure in two ILs, consisting of binary mixtures of molten salts chosen to exemplify the influences of dissimilar cation size and charge, were examined. The stronger coordination of the smaller and more highly charged cations by the anions prevented them from approaching the negatively charged electrode closely [112]. Marcus free energy curves to model the electrochemical interface with an IL was examined [113] with a model in the spirit of [112]. Pronounced oscillations in the mean electrical potential seen in molten salt systems in the double-layer region were not reflected in the reaction free energy for the electron transfer event. The reorganization energy depended markedly on the distance of the redox ion from the electrode surface because of image charge effects.

The structure and properties of the interfaces between $[C_1mim][Cl]$ and different Lennard–Jones fluids as well as water was examined by MD simulations and compared to the IL–vapor interface [114]. Thermodynamically stable interfaces and diffusing interfaces were studied. The density profiles of different species through the interface were presented. Cations and water molecules near the former type of interface were aligned relative to the surface, but no orientational preference was found near or in the broad diffusing interface. The IL showed a negative electrostatic potential relative to vapor or the Lennard–Jones fluid, but was more positive than pure water [114]. Furthermore, Lynden-Bell studied for a model system of charged spherical ions in $[C_1mim][Cl]$, $[C_1mim][PF_6]$, and acetonitrile the applicability of Marcus theory to electrochemical half-cell redox processes in these liquids [115]. The free energy curves for solvent fluctuations were found to be approximately parabolic and the Marcus solvent reorganization free energies and activation free energies were determined for six possible redox processes in each solvent. The striking similarities between the different types of solvent were attributed to the essentially long-range nature of the relevant interactions and the effectiveness of the screening of the ion potential [115].

Simulation studies of a spherical ion with various charges dissolved in two imidazolium ILs and in acetonitrile were compared [116]. The average vertical ionization potentials as a function of the charge on the ion were found to be similar for all three systems. The Landau free energies of each system as a function of the vertical ionization potential were close to being parabolic. The similarities of solvent reorganization energies and activation free energies were interpreted in terms of continuum models [116]. Very different dynamics for both liquids were inferred, because in the former case screening occurred by reorientation of molecules and in the latter case it occurred by translation of ions [116].

3.4.3 Heavy Element Compounds in ILs

Gaillard et al. presented a joint spectroscopic MD simulation study of the uranyl coordination in a series of imidazolium as well as ammonium based ILs [117]. The first coordination sphere of the uranyl cation in ILs resulted from the competition between its initially bound counterions, the IL anions, and other anions (e.g., present as impurities or added to the solution) [117].

MD simulations of halide anions $[X]^-$ and their inclusion complexes $[X]^- \subset [L^{4+}]$ with a macrotricyclic tetrahedral host built from four quaternary ammonium sites dissolved in $[C_4mim][PF_6]$ were carried out [118]. In the dry IL the uncomplexed halides were surrounded by four to five $[C_4mim]^+$ cations which bond via hydrogen bonding to facial coordination. The first solvation shell of $[Cl]^-$, $[Br]^-$, and $[I]^-$ comprised of three to four cations next to four H_2O molecules for the humid system. The solvation of the $[L^{4+}]$ host and of its $[X]^- \grave{I} [L^{4+}]$ complex mainly involved anions in the dry IL, and additional H_2O molecules in the humid IL. Free energy perturbation calculations predicted that in the dry liquid $[F]^-$ is preferred over $[Cl]^-$, $[Br]^-$ and $[I]^-$ in contrast to the aqueous solution where $[L^{4+}]$ was selective for $[Cl]^-$. In the humid liquid no $[F]^-/[Cl]^-$ discrimination was observed, showing the importance of small amounts of water on the complexation selectivity [118].

MD simulations of biphasic systems involved in the rhodium-catalyzed hydroformylation of 1-hexene dissolved in $[C_4mim][PF_6]$ were carried out [119]. The neat $[C_4mim][PF_6]$ interface with hexene was oriented perpendicular, i.e., the butyl chains pointed towards the organic phase, whereas hexene molecules tended to be somewhat parallel to the interface. The interface with heptanal was twice as broad due to attractions and due to the solvent molecules disorder at the interface. No IL ions solubilized in the organic phase, whereas approximately two to three hexene or heptanal molecules diffused into the IL phase [119]. The presence of the CO and H_2 gases did not modify the nature of the hexene/IL interface. In the IL phase a few CO monomers were present. The phase separation of randomly mixed IL/hexene liquids with the $[RhH(CO)L_3]$ precatalyst as a solute was explored. The phases separated much more slowly than in the case of classical liquids, and the neutral complex with PPh_3 ligands solubilized in the hexene phase, displaying loose dynamical contacts with the IL interface. This was in contrast to the −9 charged $[RhH(CO)(TPPTS)_3]^{9-}$ complex that was located immobilized on the IL side of the interface and was mainly solvated by $[C_4mim]^+$ cations [119].

The solvation of $[UO_2(NO_3)(CMPO)]^+$ and $[UO_2(NO_3)_2(CMPO)_2]$ complexes (CMPO = octyl(phenyl)-*N*,*N*-diisobutylmethylcarbamoyl phosphine oxide) dissolved in $[C_4mim][PF_6]$ was investigated with the aid of MD simulations [120]. For the $[UO_2(NO_3)(CMPO)]^+$ complex the monodentate vs bidentate coordination modes of CMPO were compared and the first solvation shell of uranyl was found to be completed by one to three $[PF_6]^-$ anions in the dry IL and by two to three water molecules in the humid IL, leading to a total coordination number close to five. The energy analysis showed that interactions with the IL stabilize the $[UO_2(NO_3)_{bi}(CMPO)_{mono}]^+$ form (with bidentate nitrate and monodentate CMPO) in the dry IL and the $[UO_2(NO_3)_{mono}(CMPO)_{mono}]^+$ form (with monodentate nitrate and CMPO)

in the humid IL. The extracted compound characterized by EXAFS was thus proposed to be a $[UO_2(NO_3)_{mono}(CMPO)_{mono}(H_2O)_3]^+$ species [120].

MD studies of UCl_6^-, UCl_6^{2-}, and UCl_6^{3-} complexes dissolved in $[C_4mim][NTf_2]$ and $[N_{1444}][NTf_2]$ were carried out [121]. Two electrostatic models, i.e., an ionic model with −1 charged halides vs quantum mechanically derived charges, yielded similar solvation features. The first complex solvation shell was positively charged and was build by solely cations in the case of UCl_6^{3-} and by a mixture of cations and anions in the case of UCl_6^-. UCl_6^{3-} was exclusively coordinated to cations interacting via their CH aromatic protons or their N–Me group, respectively. At the UCl_6^- complex, the cations interacted via the less polar moieties (butyl chain) and the anions displayed nonspecific interactions. According to an energy analysis UCl_6^{3-} interacted more attractively with the $[C_4mim][NTf_2]$ liquid than with $[N_{1444}][NTf_2]$, while UCl_6^- did not show any preference, suggesting a significant solvation effect of the redox properties of uranium [121]. The effect of IL humidity was investigated by simulating the three complexes in 1:8 water/IL mixtures. In contrast to the case of naked ions (e.g., lanthanide^{3+}, UO_2^{2+}, alkali, or halides), water showed little influence on the solvation of the UCl_6^{n-} complexes in the two simulated ILs [121].

3.4.4 Bio- or Organic Molecules and ILs

Binary mixtures of benzene, 1,3,5-trifluorobenzene and hexafluorobenzene with $[C_1mim][PF_6]$ were modeled with MD simulations [122]. The local ordering of the ions at an aromatic molecule was found to depend on the quadrupole moment of the aromatic species and to remain qualitatively the same on varying the mole fraction of the aromatic species. Interaction energies showed the most significant interactions to be between the aromatic molecule and the ions located at its equator [122].

MD simulations of β-glucose in $[C_1mim][Cl]$ were carried out. Both single molecule and 1:5 glucose:IL (16.7 wt%) solutions were studied. The hydrogen bonding between sugar and solvent was examined [123]. The primary solvation shell around the perimeter of the glucose ring consisted predominantly of chloride anions (coordination number 4) which hydrogen bonded to the hydroxyl groups. A small presence of the cation was also found, with the association occurring through the weakly acidic hydrogen at the 2-position of the imidazolium ring interacting with the oxygen atoms of the sugar secondary hydroxyls. In relation to the cation, the glucose molecules occupied positions above and below the plane of the imidazolium ring. Even at high glucose concentrations, no significant change in the anion–cation interactions and overall liquid structure of the IL was found, indicating that the glucose is readily accommodated by the solvent at this concentration [123].

An MD study of an enzyme, the serine protease cutinase from *Fusarium solani* pisi, in $[C_4mim][PF_6]$ and $[C_4mim][NO_3]$ was presented. The authors observed an enzyme structure that is dependent on the amount of water present in the IL [124]. They showed that the enzyme is preferentially stabilized in $[C_4mim][PF_6]$ at 5–10 wt% (weight of water over protein) water content at 298 K. $[C_4mim][PF_6]$ rendered a more native-like enzyme structure at the same water content of 5–10 wt% as

found for hexane. The system displayed a similar bell-shape-like dependence with the water content in the IL media. $[C_4mim][PF_6]$ was shown to increase significantly the protein thermostability at high temperatures, especially at low hydration. The analysis indicated that the enzyme is less stabilized in $[C_4mim][NO_3]$ relative to $[C_4mim][PF_6]$ at 298 K and 343 K. This was attributed to the strong affinity of the $[NO_3]^-$ anion toward the protein main chain. It was found that the ILs strip off most of the water from the enzyme surface in a degree similar to that found for polar organic solvents such as acetonitrile, and that the remaining waters at the enzyme surface are organized in many small clusters [124].

3.4.5 Gas Dissolution and Liquid–Vapor Interface in ILs

Huang et al. mentioned that when supercritical CO_2 is dissolved in an IL, its partial molar volume is much smaller than that observed in most other solvents [125]. In their article they explored in atomistic detail the peculiar volumetric behavior experimentally observed when supercritical CO_2 is dissolved in $[C_4mim][PF_6]$. The authors found that the liquid structure of $[C_4mim][PF_6]$ in the presence of CO_2 was nearly identical to that in the neat IL. In agreement with experiments, it was observed that partial miscibilities of one fluid into the other are very unsymmetrical, CO_2 being highly soluble in the IL phase while the IL is highly insoluble in the CO_2 phase. These results were analyzed in terms of the size and shape of spontaneously forming cavities in the IL phase. It was proposed that CO_2 occupies extremely well-defined locations in the IL. Although their accurate prediction of cavity sizes in the neat IL indicated that these cavities are small compared to the van der Waals radius of a single carbon or oxygen atom, CO_2 appears to occupy a space that was for the most part a priori empty [125].

An all-atom force field was developed using a combination of DFT calculations and OPLS force field parameter values for the 1,1,3,3-tetramethyl-guanidium lactate (cation) lactic acid (anion) ILs, because this kind of IL shows very good solubility of SO_2 and CO_2. It was found that CO_2 primarily associates with the anion while SO_2 associates with both the cation and the anion [126].

The effect of adding SO_2 on the structure and dynamics of $[C_4mim][Br]$ was investigated by low-frequency Raman spectroscopy and MD simulations [127]. The long-range structure of neat $[C_4mim][Br]$ was found to be disrupted resulting in a liquid with relatively low viscosity and high conductivity, but strong correlation of ionic motion persisted in the $[C_4mim][Br]$–SO_2 mixture due to ionic pairing. Raman spectra within the $5<w<200$ cm^{-1} range at low temperature revealed the short time dynamics, which was consistent with the vibrational density of states calculated by MD simulations [127].

The structure of the $[C_1mim][Cl]$ gas–liquid surface was studied using atomistic simulation [128]. A region of enhanced density immediately below the interface in which the cations were oriented with their planes perpendicular to the surface and their dipoles in the surface plane was observed [128]. A negligible segregation of cations and anions was also found. The temperature dependence of the surface

tension was predicted to be anomalously low or to be reversed in sign. The vapor–liquid interfaces between mixtures of water and [C_1mim][Cl] showed similar regions of enhanced density and preferential orientation of the cations. Water molecules also showed preferential orientation in the interface region and were preferentially adsorbed on the vapor side of the interface. The surface tension decreased with increase in the mole fraction of water [128].

The structure of the planar liquid–vapor interface [C_4mim][PF_6] was examined by MD simulations [129]. Layering of the ions at the interface was observed as oscillations in the corresponding number density profiles. These oscillations were diminished in amplitude in the electron density profile, due to a near cancellation in the contributions from the anions and the cations. The butyl chains were observed to be preferentially oriented along the interface normal, thus imparting a hydrophobic character. In the densest region of the interface, the imidazolium ring plane was found to lie parallel to the surface normal [129].

3.4.6 Reactions in ILs

The S_N1 reaction for 2-chloro-2-methylpropane in [C_2mim][PF_6] was studied via MD simulations [130]. By employing a two-state valence-bond description for electronic structure variations of the reaction complex, the free energy curve relevant to its S_N1 ionization in [C_2mim][PF_6] was computed via thermodynamic integration and compared with those in water and in acetonitrile. It was found that the detailed reaction mechanism differs among the three solvents. The dissociation of 2-chloro-2-methylpropane in [C_2mim][PF_6] was observed to be a stepwise process consisting of the formation of a solvent-separated ion pair and ensuing dissociation [130], while that in acetonitrile appeared to proceed without any stable reaction intermediates. The S_N1 pathway in water on the other hand was characterized by the formation of a contact ion pair, followed by dissociation to free ions. The activation free energy in water was much lower than that in [C_2mim][PF_6] and acetonitrile. Between the two latter solvents, the barrier height was lower in [C_2mim][PF_6] than in acetonitrile, indicating that the S_N1 reactivity of 2-chloro-2-methylpropane would be higher in [C_2mim][PF_6] than in acetonitrile [130].

Reaction free energetics and dynamics of unimolecular electron-transfer processes in [C_2mim][PF_6] and in acetonitrile were studied using MD simulations [131]. The diabatic curves were found to vary with the solute charge distribution. The Marcus free energy relationship held reasonably well, provided that the reorganization free energy averaged between the reactant and product states was employed. The effective polarity was higher for [C_2mim][PF_6] than for acetonitrile. Thus, activation barriers for charge separation and recombination reactions were, respectively, lower and higher in [C_2mim][PF_6] than in acetonitrile. Even though overall solvent relaxation dynamics in [C_2mim][PF_6] were considerably slower than those in acetonitrile, the deviation of the rate constant from the transition state theory predictions is found to be small for both solvents [131].

3.5 Other ILs

MD simulations on triazolium-based ILs including 1,2,4-triazolium, 1,2,3-triazolium, 4-amino-1,2,4-triazolium, and 1-methyl-4-amino-1,2,4-triazolium cations combined with [NO_3^-] and the perchlorate anion were reported [79]. A force field was developed using a mixture of ab initio calculations and parameter fitting at the example of 1H-1,2,4-triazole. Heat capacities, cohesive energy densities, gravimetric densities/molar volumes as a function of temperature and pressure, self-diffusivities, rotational time constants, and various pair correlation functions were calculated. For the solid phase, heat capacities and lattice parameters were computed. The agreement with the experimental crystal structures was good [79]. Compared to imidazolium-based ILs the triazolium-based ILs were observed to possess smaller molar volumes, higher cohesive energy densities, and larger specific heat capacities. They also tended to be less compressible, showed a higher gravimetric density, and exhibited faster rotational dynamics but similar translational dynamics [79].

A quaternary ammonium salt with an ether side chain (*N*-ethyl-*N*,*N*-dimethyl-*N*-(2-methoxyethyl)ammonium with [$NTf_2]^-$) was investigated applying united atom MD simulations by Siqueira and Ribeiro [132]. Charges for the force fields were obtained from MP2 calculations using a 6–311+G^* basis set. In line with experiment the authors found that this particular system should be classified as a poor IL. The authors were able to deduce that the presence of large sized ions is the reason for a low melting point in ILs [132].

MD simulations were performed on an energetic IL, 1-hydroxyethyl-4-amino-1,2,4-triazolium nitrate. The generalized amber force field was used, and an electronically polarizable model was further developed [133]. With simulated annealing technique from a liquid state at 475 K down to a glassy state at 175 K, the MD simulations identified a glass-transition temperature region at around 250–275 K. The self-intermediate scattering functions showed vanishing boson peaks in the supercooled region, indicating that the IL may be a fragile glass former. A complex hydrogen bond network was revealed by the calculation of partial radial distribution functions. When compared to the similarly sized [C_2mim][NO_3] a hydrogen bond network resulting in the poorer packing efficiency of ions was observed, which is responsible for the lower melting/glass-transition point. The structural properties of the liquid/vacuum interface shows that there is vanishing layering at the interface, in accordance with the poor ion packing. The effects of electronic polarization on the self-diffusion, viscosity, and surface tension of the IL were found to be significant, in agreement with [C_2mim][NO_3] [133].

MD simulations were carried out on *N*-methyl-*N*-propylpyrrolidinium bis (trifluoromethanesulfonyl) imide [mppy][NTf_2] from 303 to 393 K calculating the density, ion self-diffusion coefficients, conductivity, and viscosity [134]. The time-dependent shear modulus of the IL was calculated and compared to that for non-ILs. On average each [mppy]$^+$ cation was found to be coordinated by four [NTf_2] anions. The angular distributions of anion–cation–anion and cation–anion–cation exhibited a maximum at 80–90° and a second maximum at 180°. Correlation of ion motion was found to lower ionic conductivity by approximately one-third from the

expected value. Rotational motions of the cation and anion were anisotropic, with the degree of anisotropy increasing with decreasing temperature. Electrostatic interactions were responsible for slowing down the dynamics of the IL by more than an order of magnitude and a dramatic decrease of the time-dependent shear modulus [134].

The conformational landscapes of two ILs build from [NTf_2] and from *N*-propyl- and *N*-butyl-*N*-methylpyrrolidinium were investigated from Raman spectroscopy, MD, and ab initio techniques [135]. For [NTf_2] the three-dimensional PES and the corresponding MD simulations confirmed the existence of two stable isomers (see also [37, 36]). The anion was calculated to be flexible, albeit hindered, but capable of interconversion between conformers in the liquid state, a result also confirmed by the Raman data. In the case of the *N*,*N*-dialkylpyrrolidinium cations, the PES showed a much more limited conformational behavior of the pyrrolidinium ring [135].

3.6 Monte-Carlo

Shah et al. carried out a Monte-Carlo simulation in the isothermal–isobaric (NPT) ensemble of [C_4mim][PF_6] [12]. The authors calculated the molar volume, cohesive energy density, isothermal compressibility, cubic expansion coefficient, and liquid structure as a function of temperature and pressure. A united atom force field was developed using a combination of ab initio calculations and literature parameter values were also developed. Calculated molar volumes were within 5% of experimental values, and a reasonable agreement was obtained between calculated and experimental values of the isothermal compressibility and cubic expansion coefficient. $[PF_6]^-$ anions were found to cluster preferentially in two favorable regions near the cation, namely around the C2 carbon atom, both below and above the plane of the imidazole ring [12].

Bresme and Alejandre investigated the formation of cavities in ILs in the vicinity of the liquid binodal curve by means of MC simulations with a restricted primitive model [136]. The restricted primitive model consisted of an equimolar mixture of charged hard spheres (α, β) of which half were positively charged ($Z_\alpha = 1$) and half negatively ($Z_\beta = -1$):

$$U_{\alpha B} = \begin{cases} \infty & \text{if } r < \alpha \\ \dfrac{Z_a Z_\beta e^2}{4\pi\varepsilon_0 r} & \text{if } r \geq \sigma \end{cases} \tag{7}$$

with ε_0 being the dielectric permittivity, e the electron charge, and σ the hard-sphere diameter. The authors found that cavities of sizes 0.1–1 nm emerge, the larger cavities being favored by the Coulombic forces [136]. The mean cavity size grew with the square root of the temperature. Furthermore, the authors computed the reversible work needed to create a cavity in the IL and estimated the surface tension

of the IL–vapor interface. The accuracy of theoretical approaches based on the scaled particle theory and Ornstein–Zernike equation to estimate the cavity work of formation in ILs was discussed. It was found that both simulations and integral equations predict density depletion with increasing cavity size, suggesting the existence of surface drying in ILs.

The solubility of water and carbon dioxide in $[C_6mim][NTf_2]$ was computed using atomistic MC simulations [137]. A newly developed biasing algorithm was applied to enable the computation of complete isotherms and a recently introduced pairwise damped electrostatic potential calculation procedure was employed. The computed isotherms, Henry's law constants, and partial molar enthalpies of absorption were all in quantitative agreement with available experimental data. The simulations predicted that the excess molar volume of CO_2/IL mixtures would be large and negative. Analysis of IL conformations showed that CO_2 did not perturb the underlying liquid structure until very high CO_2 concentrations were reached. At the highest CO_2 concentrations, the alkyl chain on the cation stretched out slightly, and the distance between cation and anion centers of mass increased by about 100 pm. Water/IL mixtures have excess molar volumes that are also negative but much smaller in magnitude than those for the case of CO_2.

4 First-Principles Simulations

4.1 Imidazolium Based ILs

A CPMD simulations study of $[C_1mim][Cl]$ was carried out by Bhargava and Balasubramanian in 2006 [70]. It was found that the apparently good agreement between the pair correlation functions from classical MD and FPMD masks subtle, but crucial, differences. The radial pair distribution functions between the most acidic proton (H2, see Fig. 1) and the chloride anion were extremely different in location and width of the peaks [70]. Furthermore, Bhargava and Balasubramanian found differences between FPMD and MD in the spatial distribution of chloride ions around the cation; see Fig. 4 [70]. The data were explained in terms of the formation of a hydrogen bond between the acidic hydrogen on the imidazolium ring and the chloride ion. The authors even repeated the traditional MD simulations with only 32 ion pairs in order to exclude size effects. A strong interaction between the π electron clouds of neighboring imidazolium rings enabled the ring planes to be aligned nearly parallel to each other. The cation–anion hydrogen bond present in the melt was observed as a red shift in the C–H stretching frequency [70].

Ab initio MD (AIMD) simulations on $[C_1mim][Cl]$ were carried out by Del Pópolo et al. [138]. The local structure around the cation showed significant differences compared to both the classical calculations and the neutron results. In particular, and unlike the gas-phase ion pair, chloride ions tended to be located near a ring C–H proton in a position suggesting hydrogen bonding. For their DFT

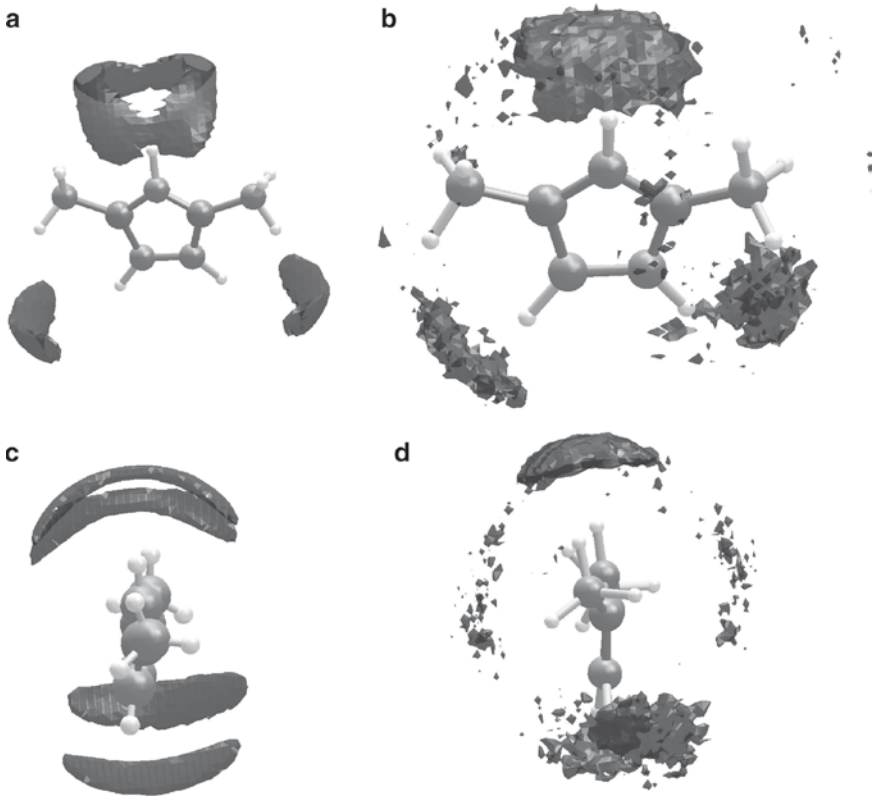

Fig. 4 Spatial distribution functions from FPMD and classical MD reproduced after [70]. *Left*: Traditional MD simulations; *Right*: Results of the CPMD simulations. It can be recognized that while the CPMD indicate hydrogen bonding at H_2, the traditional MD lacks certain conformers with H_2 hydrogen bonding. Figure adapted from [70]. Image Copyright Elsevier

calculation the "on top" conformer actually turned out to be lower in energy [138]. In other static QC calculations the opposite was observed (see for example [28]) which might be due to the different basis sets applied. The AIMD results were used to suggest ways in which the classical potentials may be improved [138]. Subsequently, the Lynden-Bell group carried out a Wannier center analysis of this IL in order to determine the local electrostatic properties of ions in this IL [139]. Being aware that multipoles higher than the monopole are origin dependent, the authors always calculated the geometric center of the particular ion as the origin in order to determine the dipole moment. For the cation $[C_1mim]^+$ an average net polarization of 0.7 D was obtained. The fluctuation of the cation was determined to be geometric and electrostatic, while the fluctuations of the anion dipole moment with the anion being spherical was only due to electrostatic fluctuations [139]. Therefore it could be concluded that most properties might be captured by a force-field

with fixed but modified charges. However, for a quantitative analysis the authors propose FPMD simulations [139].

AIMD of a single HCl molecule in [C_1mim][Cl] showed that the acidic proton exists as a symmetric, linear ClHCl-species [140]. The proton-transfer process was investigated by applying a force along the antisymmetric stretch coordinate until the molecule broke. Changes in the free energy and local solvation structure during this process were investigated. In the reaction mechanism identified, a free chloride approached the proton from the side. As the original ClHCl distorted and the incoming chloride formed a new bond to the proton, one of the original chlorine atoms was expelled and a new linear molecule was formed [140].

Several computational protocols for the prediction of the NMR spectrum of a molecular ion in an IL were tested [141]. Therefore, the proton NMR chemical shifts of the [C_2mim]$^+$ cation in [C_2mim][Cl] were computed. Environmental effects on the imidazolium ring proton chemical shifts were quite significant and had to be taken into account explicitly [141]. Calculations performed on the isolated imidazolium cation as well as on the [C_2mim][Cl] ion pair largely failed to reproduce the correct spacing between proton signals. In contrast, calculations performed on clusters extracted from the trajectory of a CPMD simulation yielded very good results [141].

CPMD simulations were applied for [C_4mim][I] at 300 K [142]. The anion exhibited a strong interaction with any three C–Hs of the imidazolium ring. The imidazolium ring underwent bending such that the two nitrogen atoms held the same distance to the anion. The electron donating butyl group was observed to contribute to the electronic polarization in addition to geometrical "out-of-plane" polarization of the ring. This resulted in ring bending along the axis constructed by the two nitrogen atoms. The average bending angle depended largely on the alkyl chain length and slightly on the anion type. Redistribution of electron density over the ring caused by the electron donating alkyl group provided additional independent evidence to the instability of the lattice structure, hence the low melting point of the IL. Simulated viscosity and diffusion coefficients were in agreement with the experiments.

4.2 Mixtures with ILs

4.2.1 Water ILs Mixtures: Solvent-Enhanced Ion Pairs

A single [C_2mim][Cl] ion pair dissolved in 60 water molecules was simulated with the aid of CPMD [143]. A preference of the in-plane chloride coordination with respect to the cation ring plane as compared to the energetic slightly more demanding on top coordination was found in agreement with Del Pópolo et al. [138]. Evaluation of the different radial distribution functions demonstrated that the structure of the hydration shell around the ion pair differed significantly from bulk water and that no true ion pair dissociation in terms of completely autonomous solvation shells took place on the timescale of the simulation. In addition, dipole moment

distributions of the solvent in distinct solvation shells around different functional parts of the ion pair were calculated from maximally localized Wannier functions [143]. The analysis of these distributions gave evidence for a depolarization of water molecules close to the hydrophobic parts of the cation as well as close to the anion. Examination of the angular distribution of different angles in turn showed a linear coordination of chloride accompanied by a tangential orientation of water molecules around the hydrophobic groups, being a typical feature of hydrophobic hydration. Based on these orientational aspects, a structural model for the preference of ion pair association was proposed, namely a solvent-enhanced ion pair model, which justified the associating behavior of solvated ions in terms of an energetically favorable interface between the solvation shells of the anion and the hydrophobic parts of the cation [143].

4.2.2 Other Mixtures

CPMD simulations were carried out for imidazolium chloride/$AlCl_3$ by inserting one pair of [C_2mim]Cl into liquid $AlCl_3$, forming an acidic mixture [144]. Two different starting conditions were studied. For both simulations, large anions within the equilibrium phase were found: In both trajectories at longer simulation time, the anion size converged to four monomer units, i.e., to $Al_4Cl_{13}^-$. The cluster size fluctuations indicated that Grotthus diffusion must play a role. One possible mechanism of such a reaction changing the anionic species was discussed. This process involved many steps of chlorine rattling, bond breaking, and bond forming. With the aid of the electron localization function, a probable rationale for the formation of larger anions was determined: Large anionic species were formed simply to account for the "lack of electrons" present in the acidic melt [144].

[C_4mim][PF_6] and its mixture with CO_2 were studied using CPMD [145]. Results from these simulations and empirical potential MD were compared and were found to differ in some respects. With a strong resemblance to the crystal, the CPMD neat liquid exhibited many cation–anion hydrogen bonds, a feature that was almost absent in the MD results. The anions were observed to be strongly polarized in the condensed phase. The addition of CO_2 increased the probability of this hydrogen bond formation. CO_2 molecules in the vicinity of the ions of [C_4mim][PF_6] exhibited larger deviations from linearity in their instantaneous conformations. The polar environment of the liquid induced a dipole moment in CO_2, lifting the degeneracy of its bending mode. The calculated splitting in the vibrational mode compared well to infrared spectroscopic data. The solvation of CO_2 in [C_4mim][PF_6] was primarily facilitated by the anion, as observed from the radial and spatial distribution functions. CO_2 molecules were found to be aligned tangential to the $[PF_6]^-$ spheres with their most probable location being the octahedral voids of the anion [145].

AIMD studies were used for simulating a [C_4mim][PF_6] and supercritical CO_2 mixture [146]. Partial radial distribution functions RDFs for different sites were computed to see the organization of the CO_2 molecules around the IL. Several

partial RDFs around the carbon atom of CO_2 molecule were compared. These data revealed that the CO_2 has specific interactions with a carbon atom present in the imidazolium ring. The CO_2 was also found to be very well organized around the terminal carbon atom of the butyl chain. The partial RDFs for the oxygen atoms around oxygen and carbon atoms of the CO_2 implied that there is very good organization of CO_2 molecules around themselves even in the $[C_4mim][PF_6]$–CO_2 mixture [146]. The instantaneous quadrupole moment tensor was calculated for the anion and the cation. The ensemble average of diagonal components of the quadrupole moment tensor of the cation had finite values, whereas the off-diagonal components of the cation and both the diagonal and off-diagonal components of the anion had the value of zero with a large standard deviation. The CPMD studies performed on CO_2 clusters revealed the greater tendency of the clusters with more CO_2 units to deviate from the linear geometry [146].

CPMD simulations of a $[C_2mim][F]$-hydrogen fluoride mixture were undertaken by Bhargava and Balasubramanian [147]. The calculated structure factor was found to be in good agreement with X-ray scattering data. The solution consisted of $[C_2mim]$ cations and polyfluoride anions of the kind $F(HF)_n^-$. With increasing n, the length of the H–F covalent bond in the polyfluoride species was found to decrease, with a concomitant blue shift in the frequency of its stretching mode. Evidence for the presence of a hydrogen bond between the acidic ring hydrogen of the cation and the fluoride ion was presented.

4.3 QM/MM Calculations

The dependence of ^1H and ^{13}C NMR chemical shifts of $[C_4mim]^+$-based ILs with the anion $[BF_4]^-$ and $[MeSO_4]^-$ was investigated experimentally and computationally [148]. Clusters extracted from the simulation runs were used to calculate ^1H and ^{13}C chemical shifts by means of QM/MM methods with various partition schemes [148]. The H2 of the imidazolium ring (see Fig. 1) was the most sensitive proton to the counteranion; its chemical shift was strongly dependent on subtle details of the arrangement of the two closest anions. It was shown that a correct spacing of signals can be attained by including the two anions closest to C2 and H2 (see Fig. 1) in the QM layer [148].

The nucleophilic substitution reactions of halides toward the aliphatic carbon of methyl *p*-nitrobenzenesulfonate dissolved in $[C_4mim][PF_6]$ was investigated using QM/MM simulations by Arantes and Ribeiro [149]. This reaction was chosen because it is well studied in ILs. It is known to possess a slower reaction rate in the IL than in dichloromethane which is due to the solvation of the halide anion. However, this observation does not necessarily apply to different ILs. A calibrated semiempirical Hamiltonian was parameterized for the reaction in gas phase. In the condensed phase, free energy profiles were obtained for the reaction applying standard force fields; for details see [149]. During the reaction extensive hydrogen bonding between the imidazolium and the nucleophile or the leaving group was detected.

5 Models

5.1 Models to Predict or Explain Melting Points

A simple but quantitative explanation for the relatively low melting temperatures of ILs was presented by Krossing and coworkers [150]. The basic concept was to assess the Gibbs free energy of fusion for the process IL(s)→IL(l), which related to the melting point of the IL. This was done using a suitable Born–Fajans–Haber cycle that was closed by the lattice (i.e., IL(s)→IL(g)) Gibbs energy and the solvation (i.e., IL(g)→IL(l)) Gibbs energies of the constituent ions in the molten salt. Lattice free energies were estimated using a combination of volume based thermodynamics and QC calculations. Free energies of solvation of each ion in the bulk molten salt were calculated using a continuum solvation model and the experimental dielectric constants [150]. Under standard ambient conditions the Gibbs free energy of fusion was found to be negative for all the ILs studied, as expected for liquid samples. Thus, these ILs are liquid under standard ambient conditions, because the liquid state is thermodynamically favorable, due to the large size and conformational flexibility of the ions involved, which led to small lattice enthalpies and large entropy changes that favor melting. A comparison of the predicted vs experimental melting points for nine of the ILs (excluding those where no melting transition was observed and two outliers that were not well described by the model) gave a standard error of the estimate at 8 °C [150].

Markusson et al. investigated protic ILs (PILs) based on alkylamines. The aim of the work was to determine the parameters that dominate liquid range and conductivity [151]. Almost linear relations of experimental melting temperature with calculated anion volume was found, whereas the dependence of melting temperatures with increasing cation volume showed a minimum for relatively short side chain lengths [151]. The authors found that the melting temperature of PILs could be estimated by the same approach as proposed for aprotic ILs by Krossing et al. [150], which was attributed to a bad description of the PIL lattice energy. However, the PIL melting temperature was largely determined by the size of its ions. The PILs generally had higher melting temperatures the larger their anion size. If the density, volume, and ΔG_{solv} (solvation free energies) of the ions were known, it was possible to choose the beginning of the working temperature range. ΔE (energy difference for transferring the proton) was important for the decomposition temperature and for the ionicity of the PIL and thus for their conductivity [151].

In their investigation of the *N*-ethyl-*N*,*N*-dimethyl-*N*-(2-methoxyethyl) ammonium bis(trifluoromethanesulfonyl)-imide IL Siqueira and Ribeiro [132] noted an interplay between structure and thermodynamics, because the average Coulombic energy of this IL was smaller than that of the archetypical molten salt [Na][Cl]. This was related to the anion–cation distance which was for the IL larger than for [Na][Cl]. It was concluded that the presence of ions of large size was the reason for a low melting point in ILs. However, melting temperature or glass transition temperature increased again for ILs containing too large cations, because of the addition

of van der Waals interactions which gave rise to negative contributions to the average potential energy [132].

5.2 Models to Describe Free Energy and Other Thermodynamic Data

Nonatomistic simulations: A model to perform coarse grained MD simulations of the [$C_n$mim][PF_6] was developed by Bhargava et al. [152]. Large scale simulations of ILs with butyl, heptyl, and decyl side chains were carried out. Calculated structure factors demonstrated intermediate range ordering in these liquids. The spatial correlations between anions were shown to dominate the neutron or X-ray scattering at low wave vectors. ILs with long side chains exhibited a bicontinuous morphology, one region consisting of polar moieties and the other of nonpolar, alkyl tails. Further discussions can be found in [19].

A polymer-like model based on Flory-Huggins theory including different sizes of ions was applied in order to study the effect of ionic size on the solubility. It was found that the size effect can be characterized by introducing effective volumes and that with larger effective volume better solvent power is achieved as expressed by Henry's law constant [153].

The prediction of molar volumes and densities of several ILs was investigated using a group contribution model as a function of temperature between 273 and 423 K at atmospheric pressure [154]. It was observed that the calculation of molar volumes or densities could be performed using the ideal behavior of the molar volumes of mixtures of ILs. This model is based on the observations of Canongia Lopes et al. [60] which showed that this ideal behavior is independent of the temperature and allows the molar volume of a given IL to be calculated by the sum of the effective molar volume of the component ions. Using this assumption, the effective molar volumes of ions constituting more than 220 different ILs were calculated as a function of the temperature at 0.1 MPa using more than 2,150 data points. These calculated results were employed to build up a group contribution model for the calculation of IL molar volumes and densities with an estimated repeatability and uncertainty of 0.36% and 0.48%, respectively [154].

Prediction models for ionic conductivity and viscosity of ILs using quantitative structure property relationships coupled with the descriptors of group contribution type were introduced [155]. The polynomial expansion model based on the type of cation, length of side chain, and type of anion was applied to the expression of IL properties. Parameters of these polynomial expansion models were determined by means of a genetic algorithm. The reverse design of ILs was also tested [155].

Eutectic mixtures of quaternary ammonium salts with Lewis or Brønsted acids were described as ILs [156]. The conductivity, viscosity, density, and surface tension of a number of glycolic mixtures with choline chloride were measured over the mole fraction range 0–0.33. The data were fitted to hole theory. It was proposed that the composition at which the measured conductivity matched the theoretical value

was the point at which hole mobility becomes the dominant mechanism for charge mobility [156].

5.3 Continuum Model Theory in Order to Predict Macroscopic Data

In order to study the mutual solubilities of hydrophobic but also hygroscopic imidazolium-, pyridinium-, pyrrolidinium-, and piperidinium-based ILs in combination with the anions bis-(trifluoromethylsulfonyl)imide, hexafluorophosphate, and tricyanomethane with water, UV spectroscopic measurements were carried out at temperatures between 288.15 and 318.15 K. Continuum model calculations were used to support these measurements of the Gibbs energy, enthalpy, and entropy. It was found that the hydrophobic tendency increases from imidazolium to pyridinium to pyrrolidinium to piperidinium and with increasing alkyl chain length within the same cation-varying anion ion pair [157].

Palomar et al. have carried out continuum model calculations on B3LYP/6–31++G** optimized geometries of the following cations: $[C_n\text{mim}]^+$ with n = 1, 2, 4, 6, 8 and the following anions: $[Cl]^-$, $[BF_4]^-$, $[FeCl_4]^-$, $[PF_6]^-$, $[NTf_2]^-$, $[MeSO_4]^-$, $[EtSO_4]^-$, $[TfO]^-$ in order to estimate density and molar volume [158]. A satisfactory prediction of the data is found with the exception of the ion pairs containing $[PF_6]^-$ and $[BF_4]^-$ anions.

5.4 Models to Describe Other Data

A mathematical model was designed to extract electrode kinetic data for the deposition of Ag^+ from solution and the stripping of silver from silver on the electrode from experimental data [159]. The results suggested that the TMPD|$TMPD^{+\bullet}$(TMPD = *N*,*N*,*N*′,*N*′-tetramethyl-*p*-phenylenediamine) system is more suitable than the Ag|Ag^+ system as a redox couple for use in reference electrodes for ILs [159].

5.5 Characterizing ILs

As stated by Siqueira and Ribeiro [132], "The Walden rule, that is, the inverse relation between η and Λ, where Λ is the specific conductivity, allows for a further classification as good or poor IL, provided that Λ is respectively above or below than expected for a given η. It has been claimed that good ILs or at least those systems that follow the ideal Walden rule prediction should have an "ideal" quasilattice structure and then diminished correlation of ionic motions and high conductivity. Furthermore, such an ideal ionic structure would imply larger energy for releasing

ion pairs into the gas phase, that is, low vapor pressure, which is one of the most important properties that makes ILs such interesting solvents in green chemistry."

A theoretical method to estimate the molar volume was applied to a series of ILs. The variation of experimentally-measured ε and π^* values with molar volume were explored [160]. Both variables are found to vary with molar volume. An anomaly in the behavior of π^* that offers insight on the nanoscale inhomogeneity of ILs was observed. An important outcome of this work is a simple scheme for the estimation of the relative polarities of ILs; while not quantitatively accurate, the scheme permits prediction of the change in solvent polarity on ionic substitution or derivatization [160].

Several mean-field theories describing the liquid–vapor equilibrium of simple, polar, and ionic model fluids, namely, the restricted primitive model of ionic fluids, a fluid composed of dipolar hard spheres, the Yukawa fluid and the square-well fluid were analyzed [161]. The latter two allow for a systematic study of the influence of the interaction range on both the absolute magnitude of the slope of the diameter and of the relative contribution that each source of liquid–vapor asymmetry makes. In addition, the strength of the Yang–Yang ratio for each model fluid was estimated. Results for a number of different theories for each fluid were presented. The results indicated a system governed by long-range interactions. The dipolar fluid seemed to be intermediate between simple and ionic fluids [161].

The phase diagrams of IL solutions ($[C_n mim][BF_4]$) with various alcohols were analyzed by means of a novel function, which presumes Ising behavior and the applicability of the rectilinear diameter rule [162]. Estimates of the critical point data were in good agreement with that determined independently by the equal volume criteria. Two different types of corresponding state analysis were carried out. First, the critical data were expressed in terms of the dimensionless variables of the model system of equal sized hard spheres in a dielectric continuum. The corresponding critical composition was above the figure predicted. The reduced critical temperature increased linearly with the dielectric constant of the solvent. This correlation, which includes higher alcohols and water, indicated a continuous change from phase transitions determined by Coulomb interactions to those driven by solvophobic forces. Second, the thermodynamic corresponding states analysis, where the reduced variables are given by differences to the critical point, reduced by the critical data, revealed corresponding state behavior for all solutions investigated [162].

6 Conclusion

Imidazolium-based ILs are the most frequently studied ILs, not just experimentally, but also with regard to theoretical calculations. Although most of the theoretical studies are based on traditional MD simulations, several calculations are carried out by applying static QC methods. The focus of these studies lies on (1) the importance of different conformers discussed with energetic criteria as well as spectroscopic data comparable to experimental results, (2) generating input for MD simulations, especially calculations of charges, and (3) method evaluations. MD

simulations are important not only because of the molecular level insight they provide but also because some otherwise unavailable properties relevant to further experiments can be investigated. It is important to recognize that, despite the benefits of MD simulations, special care has to be taken how the simulation parameters are chosen. This is especially striking with regard to the recent discussion on charge-downscaling. FPMD are not carried out so often for the reasons of high computational costs and the short simulation times connected to this problem. However, structural insights won from these kind of simulations have proven to be very useful. In summary, there is ample evidence that our current theory is not only able to complement experiment and reveal some properties that are so far not accessible; it has also been proven to be able to provide elegant explanations for many contradicting behaviors of the ILs considered.

Acknowledgment This work was supported by the DFG, in particular by the ERA Chemistry Program and by the SPP-1191 Program. Computer time from the RZ Leipzig, the HLRS Stuttgart and NIC Jülich is gratefully acknowledged. I would furthermore like to thank the following individuals for helpful suggestions and discussions: Christian Spickermann and Dietmar Dath.

References

1. Thar J, Reckien W, Kirchner B (2007) Atomistic approaches in modern biology. Topics in Current Chemistry, vol 268. Springer, Berlin Heidelberg New York, pp 133–171
2. Jensen F (2007) Introduction to computational chemistry. Wiley, Chichester
3. Frenkel D, Smit B (2002) Understanding molecular simulations. Academic, San Diego
4. Allen MP, Tildesley DJ (1987) Computer simulations of liquids. Claredon, Oxford
5. Cocalia VA, Gutowski KE, Rogers RD (2006) Coord Chem Rev 150:755–764
6. Welton T (1999) Chem Rev 99:2071–2083
7. Welton T (2004) Coord Chem Rev 248:2459–2477
8. Wilkes JS (2002) Green Chem 4:73–80
9. Lynden-Bell RM, Atamas NA, Vasilyuk A, Hanke CG (2002) Mol Phys 100:3225–3229
10. Cammarata L, Kazarian SG, Salter PA, Welton T (2001) Phys Chem Chem Phys 3: 5192–5200
11. Price SL, Hanke CG, Lynden-Bell RM (2001) Mol Phys 99:801–809
12. Shah JK, Brennecke JF, Maginn EJ (2002) Green Chem 4:112–118
13. Morrow TI, Maginn EJ (2002) J Phys Chem B 106:12161–12164
14. de Andrade J, Boes ES, Strassen H (2002) J Phys Chem B 106:3546–3548
15. Meng Z, Dölle A, Carper WR (2002) J Mol Struct 585:119–128
16. Hunt PA (2006) Mol Simul 32:1–10
17. Maginn EJ (2007) Acc Chem Res 40:1200–1207
18. Lynden-Bell RM, Del Pápolo MG, Youngs TGA, Kohanoff J, Hanke CG, Harper JB, Pinilla CC (2007) Acc Chem Res 40:1138–1145
19. Bhargava BL, Balasubramanian S, Klein ML (2008) Chem Commun 29:3339–3351
20. Matsumoto K, Hagiwara R (2006) J Fluorine Chem 128:317–331
21. Kirchner B (2007) Phys Rep 1–3:1–111
22. Szabo A, Ostlund NS (1996) Modern quantum chemistry. Dover, NY, USA
23. Halgren TA, Damm W (2001) Curr Opin Biol 11:236–242
24. Huber H, Dyson AJ, Kirchner B (1999) Chem Soc Rev 28:121–133
25. Car R, Parrinello M (1985) Phys Rev Lett 55:2471–2474

26. Peyerimhoff SD (2003) Interactions in molecules, 1st edn. Wiley, Weinheim
27. Emel'yanenko VN, Verevkin SP, Heintz A (2007) J Am Chem Soc 129:3930–3937
28. Zahn S, Kirchner B (2008) J Phys Chem A 112:8430–8435
29. Studzińska S, Stepnowskib P, Buszewski B (2007) QSAR Comb Sci 26:963–972
30. Hunt PA, Kirchner B, Welton T (2006) Chem Eur J 12:6762–6775
31. Lü R, Cao Z, Shen G (2007) J Natur Gas Chem 16:428–436
32. Hunt PA, Gould IR, Kirchner B (2007) Aust J Chem 60:9–14
33. Köddermann T, Wertz C, Heintz A, Ludwig R (2006) Chem Phys Chem 7:1944–1949
34. Dhumal NR (2007) Chem Phys 342:245–252
35. Fujii K, Seki S, Fukuda S, Kanzaki R, Toshiyuki Takamuku YU, Ishiguro S (2007) J Phys Chem B 111:12829–12833
36. Lasségues JC, Grondin J, Holomb R, Johansson P (2007) J Raman Spectrosc 38:551–558
37. Nockemann P, Thijs B, Pittois S, Thoen J, Glorieux C, Van Hecke K, Van Meervelt L, Kirchner B, Binnemans K (2006) J Phys Chem B 110:20978–20992
38. Chang H-C, Jiang J-C, Su J-C, Chang C-Y, Lin SH (2007) J Phys Chem A 111:9201–9206
39. Chiu Y-H, Gaeta G, Levandier D, Dressler R, Boatz J (2007) Int J Mass Spectrom 265:146–158
40. Paulechka YU, Kabo GJ, Blokhin A, Magee OAVJW, Frenkel M (2003) J Chem Eng Data 48:457–462
41. Zhang L, Li H, Wang Y, Hu X (2007) J Phys Chem B 111:11016–11020
42. Johansson KM, Izgorodina EI, Forsyth M, MacFarlane DR, Seddon KR (2008) Phys Chem Chem Phys 10:2972–2978
43. Fujimori T, Fujii K, Kanzaki R, Chiba K, Yamamoto H, Umebayashi Y, Ishiguro S (2007) J Mol Liq 131/132:216–224
44. Nockemann P, Thijs B, Driesen K, Van Hecke CJK, Van Meervelt L, Kossmann S, Kirchner B, Binnemans K (2007) J Phys Chem B 111:5254–5263
45. Yu G, Zhang S (2007) J Fluid Phase Equilib 255:86–92
46. Xing H, Wang T, Zhou Z, Dai Y (2007) J Mol Cat A 264:53–59
47. Bhargava BL, Balasubramanian S (2007) Chem Phys Lett 444:242–246
48. Gong L, Guo W, Xiong J, Li R, Wu X, Li W (2006) Chem Phys Lett 425:167–178
49. Wang Y, Li H, Han S (2006) J Phys Chem B 110:24646–24651
50. Li W, Qi C, Wu X, Rong H, Gong L (2008) J Mol Struct 855:34–39
51. Weber CF, Puchta R, van Eikema Hommes NJR, Wasserscheid P, van Eldik R (2005) Angew Chem Int Ed Engl 44:6033–6038
52. Kossmann S, Thar J, Kirchner B, Hunt PA, Welton T (2006) J Chem Phys 124:174506
53. Weingärtner H (2008) Angew Chem Int Ed Engl 47:654–670
54. Bhargava BL, Balasubramanian S (2007) J Chem Phys 127:114510
55. Ludwig R (2008) Phys Chem Chem Phys 10:4333–4339
56. Tsuzuki S, Tokuda H, Hayamizu K, Watanabe M (2005) J Phys Chem B 109:16474–16481
57. Tsuzuki S, Arai AA, Nishikawa K (2008) J Phys Chem B 112:7739–7747
58. Zahn S, Uhlig F, Thar J, Spickermann C, Kirchner B (2008) Angew Chem Int Ed Engl 47:3639–3641
59. Hunt PA, Gould IR (2006) J Phys Chem A 110:2269–2282
60. Canongia-Lopes JN, Deschamps J, Pádua AAH (2004) J Phys Chem B 108:2038–2047
61. Müller-Plathe F, van Gunsteren WF (1995) J Phys Chem 103:4756–4756
62. Bhargava BL, Balasubramanian S (2005) J Chem Phys 123:144505
63. Bhargava BL, Balasubramanian S (2006) J Chem Phys 125:219901
64. Bhargava BL, Klein ML, Balasubramanian S (2008) Chem Phys Chem 9:67–70
65. Schröder C, Steinhauser O (2008) J Chem Phys 128:224503
66. Youngs TGA, Hardacre C (2008) Chem Phys Chem 9:1548–1558
67. Lynden-Bell RM, Youngs TGA (2006) Mol Sim 32:1025–1033
68. Denesyuk NA, Weeks JD (2008) J Chem Phys 128:124109
69. Bagno A, D'Amico F, Saielli G (2007) J Mol Liq 131/132:17–23
70. Bhargava BL, Balasubramanian S (2006) Chem Phys Lett 417:486–491

71. Micaelo NM, Baptista AM, Soares CM (2006) J Phys Chem B 110:14444–14451
72. Youngs TGA, Del Pápolo MG, Kohanoff J (2006) J Phys Chem B 110:5697–5707
73. Canongia-Lopes JN, Pádua AAH (2006) J Phys Chem B 110:19586–19592
74. Canongia-Lopes JN, Pádua AAH, Shimizu K (2008) J Phys Chem B 112:5039–5046
75. Kelkar MS, Maginn EJ (2007) J Phys Chem B 111:4867–4876
76. Prado CER, Freitas LCGF (2007) J Mol Struct 847:93–100
77. Brenneman CM, Wiberg KB (1990) J Comp Chem 11:361
78. Jayaraman S, Maginn EJ (2007) J Chem Phys 127:214504
79. Cadena C, Maginn EJ (2006) J Phys Chem B 110:18026–18039
80. Kelkar MS, Maginn EJ (2007) J Phys Chem B 111:9424–9427
81. Köddermann T, Paschek D, Ludwig R (2008) Chem Phys Chem 9:549–555
82. Rey-Castro C, Vega LF (2006) J Phys Chem B 110:14426–14435
83. Zhao W, Balasubramanian FLS, Müller-Plathe F (2008) J Phys Chem B 112:8129–8133
84. Shim Y, Jeong D, Choi MY, Kim HJ (2006) J Chem Phys 125:061102
85. Qiao B, Krekeler C, Berger R, Delle Site L, Holm C (2008) J Phys Chem B 112:1743–1751
86. Schröder C, Rudas T, Steinhauser O (2006) J Chem Phys 125:244506
87. Schröder C, Wakai C, Weingärtner H, Steinhauser O (2007) J Chem Phys 126:084511
88. Schröder C, Rudas T, Neumayr G, Gansterer W, Steinhauser O (2007) J Chem Phys 127: 044505
89. Schröder C, Haberler M, Steinhauser O (2008) J Chem Phys 128:134501
90. Wasserscheid E, Welton T (2003) Ionic liquids in synthesis. Wiley, Weinheim
91. Hunt PA (2007) J Phys Chem B 111:4844–4853
92. Zahn S, Bruns G, Thar J, Kirchner B (2008) Phys Chem Chem Phys, 10: 6921–6924
93. Shim Y, Jeong D, Choi MY, Kim HJ (2006) J Chem Phys 125:024507
94. Jeong D, Shim Y, Choi MY, Kim HJ (2007) J Phys Chem B 111:4920–4925
95. Hu Z, Margulis CJ (2007) J Phys Chem B 111:4705–4714
96. Hanke CG, Lynden-Bell RM (2003) J Phys Chem B 107:10873–10878
97. Chevrot G, Schurhammer R, Wipff G (2006) Phys Chem Chem Phys 8:4166–4174
98. Annapureddy HVR, Hu Z, Xia J, Margulis CJ (2008) J Phys Chem B 112:1770–1776
99. Jiang W, Wang Y, Voth GA (2007) J Phys Chem B 111:4812–4818
100. Sieffert N, Wipff G (2006) J Phys Chem B 110:13076–13085
101. Schröder C, Rudas T, Neumayr G, Benkner S, Steinhauser O (2007) J Chem Phys 127:234503
102. Costa LT, Ribeiro MCC (2006) J Chem Phys 124:184902
103. Costa LT, Ribeiro MCC (2007) J Chem Phys 127:164901
104. Costa LT, Lavall RL, Borges RS, Rieumont J, Silva GG, Ribeiro MC (2007) Electrochim Acta 53:1568–1574
105. Sloutskin E, Lynden-Bell RM, Balasubramanian S, Deutsch M (2006) J Chem Phys 125:174715
106. Bresme F, González-Melchor M, Alejandre J (2005) J Phys Condens Matter 17:S3301–S3307
107. Yan T, Li S, Jiang W, Gao X, Xiang B, Voth GA (2006) J Phys Chem B 110:1800–1806
108. Lynden-Bell RM, Del Pópolo MG (2006) Phys Chem Chem Phys 8:949–954
109. Liu L, Li S, Cao Z, Peng Y, Li G, Yan T, Gao X-P (2007) J Phys Chem C 111: 12161–12164
110. Sieffert N, Wipff G (2007) J Phys Chem B 111:7253–7266
111. Pinilla C, Del Pópolo MG, Kohanoff J, Lynden-Bell RM (2007) J Phys Chem B 111: 4877–4884
112. Reed SK, Lanning OJ, Madden PA (2007) J Chem Phys 126:084704
113. Reed SK, Madden PA, Papadopoulos A (2008) J Chem Phys 128:124701
114. Lynden-Bell RM, Kohanoff J, Del Pópolo MG (2005) Faraday Discuss 129:57–67
115. Lynden-Bell RM (2007) J Phys Chem B 111:10800–10806
116. Lynden-Bell RM (2007) Electrochem Commun 9:1857–1861
117. Gaillard C, Chaumont A, Billard I, Hennig C, Ouadi A, Wipff G (2007) Inorg Chem 46: 4815–4826
118. Chaumont A, Wipff G (2006) New J Chem 30:537–545

119. Sieffert N, Wipff G (2007) J Phys Chem B 111:4951–4962
120. Chaumont A, Wipff G (2006) Phys Chem Chem Phys 8:494–502
121. Schurhammer R, Wipff G (2007) J Phys Chem B 111:4659–4668
122. Harper JB, Lynden-Bell RM (2004) Mol Phys 102:85–94
123. Youngs TGA, Hardacre C, Holbrey JD (2007) J Phys Chem B 111:13765–13774
124. Micaelo NM, Soares CM (2008) J Phys Chem B 112:2566–2572
125. Huang X, Margulis CJ, Li Y, Berne BJ (2005) J Am Chem Soc 127:17842–17851
126. Wang Y, Pan H, Li H, Wang C (2007) J Phys Chem B 111:10461–10467
127. Siqueira LJA, Ando RA, Bazito FFC, Torresi RM, Santos PS, Ribeiro MCC (2008) J Phys Chem B 112:6430–6435
128. Lynden-Bell RM (2003) Mol Phys 101:2625–2633
129. Bhargava BL, Balasubramanian S (2006) J Am Chem Soc 128:10073–10078
130. Shim Y, Kim HJ (2008) J Phys Chem B 112:2637–2643
131. Shim Y, Kim HJ (2007) J Phys Chem B 111:4510–4519
132. Siqueira LJA, Ribeiro MCC (2007) J Phys Chem B 111:11776–11785
133. Jiang W, Yan T, Wang Y, Voth GA (2008) J Phys Chem B 112:3121–3131
134. Borodin O, Smith GD (2006) J Phys Chem B 110:11481–11490
135. Canongia-Lopes JN, Shimizu K, Pádua AAH, Umebayashi Y, Fukuda S, Fujii K, Ishiguro S (2008) J Phys Chem B 112:1465–1472
136. Bresme F, Alejandre J (2003) J Chem Phys 118:4134–4139
137. Shi W, Maginn EJ (2008) J Phys Chem B 112:2045–2055
138. Del Pápoloand RM, Lynden-Bell MG, Kohanoff J (2005) J Phys Chem B 109:5895–5902
139. Resende Prado CE, Del Pápolo MG, Youngs TGA, Kohanoff J, Lynden-Bell RM (2006) Mol Phys 194:2477–2483
140. Del Pápolo MG, Kohanoff J, Lynden-Bell RM (2006) J Phys Chem B 110:8798–8803
141. Bagno A, D'Amico F, Saielli G (2007) Chem Phys Chem 8:873–881
142. Ghatee MH, Ansari Y (2007) J Chem Phys 126:154502
143. Spickermann C, Thar J, Lehmann SBC, Zahn S, Hunger J, Buchner R, Hunt PA, Welton T, Kirchner B (2008) J Chem Phys 129:104505
144. Kirchner B, Seitsonen AP (2007) Inorg Chem 47:2751–2754
145. Bhargava BL, Balasubramanian S (2007) J Phys Chem B 111:4477–4487
146. Bhargava BL, Balasubramanian S (2008) Bull Mater Sci 31:327–334
147. Bhargava BL, Balasubramanian S (2008) J Phys Chem B 112:7566–7573
148. Bagno A, D'Amico F, Saielli G (2006) J Phys Chem B 110:23004–23006
149. Arantesa GM, Ribeiro MCC (2008) J Chem Phys 128:114503
150. Krossing I, Slattery JM, Daguenet C, Dyson PJ, Oleinikova A, Weigärtner H (2006) J Am Chem Soc 128:13427–13434
151. Markusson H, Belieres J, Johansson P, Angell CA, Jacobsson P (2007) J Phys Chem A 111:8717–8723
152. Bhargava BL, Devane R, Klein ML, Balasubramanian S (2007) Soft Matter 3:1395–1400
153. Lou P, Kang S, Ko KC, Lee JY (2007) J Phys Chem B 111:13047–13051
154. Jacquemin J, Ge R, Nancarrow P, Rooney DW, Costa Gomes MF, Padua AAH, Hardacre C (2008) J Chem Eng Data 53:716–726
155. Matsuda H, Yamamotob H, Kurihara K, Tochigi K (2007) J Fluid Phase Equilib 261:434–443
156. Abbott AP, Harris RC, Ryder KS (2007) J Phys Chem B 111:4910–4913
157. Freire MG, Neves CMSS, Carvalho PJ, Fernandes AM, Gardas RL, Marrucho IM, Santos LMNBF, Coutinho JAP (2007) J Phys Chem B 111:13082–13089
158. Palomar J, Ferro VR, Torrecilla JS, Rodriguez F (2007) Ind Eng Chem Res C 46:6041–6048
159. Rogers EI, Silvester DS, Jones SEW, Aldous L, Hardacre C, Russell AJ, Davies SG, Compton RG (2007) J Phys Chem C 111:13957–13966
160. Kobrak MN (2008) Green Chem 10:80–86
161. Weiss VC, Schröer W (2008) J Stat Mech P04020
162. Schröer W (2006) J Mol Liq 125:164–173

Top Curr Chem (2009) 290: 263–283
DOI: 10.1007/128_2008_37

Published online: 10 July 2009

NMR Spectroscopy in Ionic Liquds

Ralf Giernoth

Abstract Today, NMR spectroscopy is the most important analytical tool for synthetically working chemists. This review describes the development of NMR spectroscopic methods for use in ionic liquid media and the state-of-the art in terms of routine analytics as well as modern advanced techniques.

Keywords Dynamics • Interactions • Ionic Liquids • NMR Spectroscopy • Structure

Contents

Abbreviations

bdmim 1-Butyl-2,3-dimethylimidazolium
bmim 1-Butyl-3-methylimidazolium
DOSY Diffusion-ordered spectroscopy

R. Giernoth
University of Cologne, Chemistry Department, Greinstr. 4, D-50939, Köln Germany
e-mail: Ralf.Giernoth@uni-koeln.de

emim	1-Ethyl-3-methylimidazolium
IL	Ionic liquid
mnim	1-Methyl-3-nonylimidazolium
MTO	Methyltrioxorhenium
NOE	Nuclear Overhauser effect/enhancement
omim	1-Octyl-3-methylimidazolium
PSE	Pulsed field gradient spin-echo
PSTE	Pulsed field gradient stimulated echo
ROE	Rotating-frame NOE
RTIL	Room-temperature ionic liquid
Tf_2N	Bis(trifluoromethylsulfonyl)amide
TSIL	Task-specific ionic liquid

1 Introduction

The modern world of chemical synthesis is unthinkable without NMR spectroscopy. Especially in organic synthesis, the information content of a combination of various NMR techniques is tremendeous and unmatched by any other spectroscopic method. Thus, since ionic liquids ("ILs" for short) are predominantly used as solvents these days, the application of magnetic resonance spectroscopy to ionic solvents has become very important. None the less, the unique properties of this modern solvent class has put quite some challenge to researchers trying to apply NMR for ILs. In this review, I will describe the development of NMR in "modern" (i.e. air- and moisture-stable, predominantly imidazolium-based) ILs of the last 8 years historically from an experimental perspective. If you are looking for a more substrate-specific point of view or are interested in the "early" developments with chloroaluminate ILs, you are kindly asked to refer to the recent literature [1].

1.1 NMR and Salt-Containing Samples

NMR spectroscopy, while containing a high information-density, is quite an unsensitive method. Therefore, the main challenge is to obtain well-resolved spectra of high signal-to-noise ratio. Apart from sample concentration, the signal intensity depends mainly on the linewidth. Linewidth, in turn, depends mainly on relaxation.

Relaxation is a complex phenomenon, depending on many factors [2], such as dipole–dipole relaxation, chemical shift anisotropy, spin-rotation relaxation, quadrupolar relaxation etc. Examples for "macroscopic" factors are sample and magnetic field homogenity and the viscosity of the NMR solvent. When running NMR experiments on ionic liquids, we have to deal with three main challenges:

1. Viscosity. Many ILs are highly viscous, especially in pure form. For these samples, strong relaxation leads to relatively broad signals. Apart from lowering the viscosity, e.g., by raising the sample temperature, not much can be done about this.
2. In most cases, the IL under investigation is not available in deuterated form. This of course limits the applicability of proton NMR. One (expensive) solution to this problem can be the synthesis of a deuterated version of the particular IL ([3] and references therein). Other solutions to this problem will be discussed in Sect. 5.
3. NMR spectroscopy with salt-containing samples results in broad lines. Now ILs are most certainly the "upper limit" with respect to "salt-containing samples". In addition to line-width related problems, the NMR radiation may be partially absorbed, causing heating of the sample and substantially longer pulse lengths [4]. These kinds of problems may be overcome by using a specially designed cryo-probe in combination with an ellipsoid tube geometry [5], but to the best of my kowledge this setup has not yet been used for NMR in ionic liquid samples.

Taking these points into consideration, it is obvious why for so long many people believed in the myth that NMR in ILs is a quite difficult task. But with careful adjustment of spectrometer parameters and a little time at hand, routine NMR spectroscopy is possible with modern NMR spectrometers, even without any specialized equipment [4].

2 Structure

Among the most important topics that are frequently addressed via NMR spectroscopy are questions about the *structure* of a chemical compound. Thus, it is not surprizing that the liquid-phase structure of many common ILs has been investigated using NMR techniques.

2.1 Structure of Neat Ionic Liquids

One of the very first "thorough" structural investigations was published in the year 2000 by the group of Dupont [6]. They investigated a neat IL with an anion that has not become too common over the years: [bmim]BPh_4. Since the crystal structure of this IL was dominated by C–H–π interactions between the cations and the anions, the question arose whether this motif would transpose to the liquid phase structure as well. By applying ^{1}H NOESY NMR and measuring ^{13}C T_1 relaxation data, they could find almost identical modes of interaction in the liquid phase as compared to the crystal structure. The authors therefore assumed "floating aggregates" via

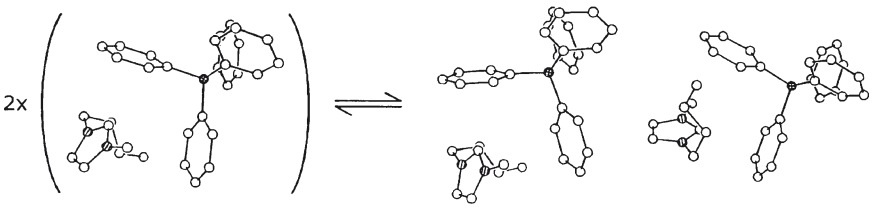

Fig. 1 Formation of contact ion pair aggregates [6]. Copyright Wiley. Reproduced with permission

hydrogen bonds in neat solution (Fig. 1). Addition of two different organic solvents – DMSO and $CDCl_3$ – was also studied, and the NMR spectra in these two solvents differed significantly. Consequently, it was concluded that the DMSO solution contained mainly solvent-separated ion-pairs while the formation of contact ion pairs took place in $CDCl_3$. (The interaction of ILs with organic solvents and other "impurities" is discussed much more in detail in Sect. 2.4.)

It is remarkable that this – more or less – first publication on this topic already contained the main questions and ideas that are still in the focus of many investigations: supramolecular structure of the ionic liquid phase, ion-pairing and the interaction of ILs with solute (or solvent) molecules. The same group continued their investigations and subsequently focussed on a larger variety of imidazolium salts with different weakly-coordinating anions (BF^-_4, PF^-_6, and BPh^-_4) [7]. They were able to demonstrate that each cation was surrounded by at least three anions (and vice versa) and by this fashion hydrogen-bound "supermolecules" were present in the liquid state. Therefore, one could honestly speak of ILs as "nanostructured materials".

Lin et al. have studied variations in the chemical shifts for a variety of methylimidazolium salts with different alkyl chain substituents and Br^-, BF^-_4, and BF^-_6 anions [8]. They observed a high sensitivity in chemical shift (depending, among other factors, predominantly on the alkyl chain length) for the 2-proton in the imidazolium ring. The effect was most pronounced for the bromide salts. Additionally, they observed unexpected H/D exchange for the 2-proton. Today, these results can be interpreted as H-bonding effects, and of course the acidity of H2 comes to no surprise ([3,9] and references therein).

The change in chemical shift for different imidazolium ILs has been investigated by Lyčka et al. using ^{15}N NMR spectroscopy [10]. They found that the length of the alkyl chain has a much larger effect on the ^{15}N chemical shifts than the choice of anion. Since for unsymmetrically substituted ILs individual signals for the two nitrogen nuclei could be observed, a small asymmetry in the nitrogen charge distribution of the aromatic ring was proposed. The group of Blümel, on the other hand, found very similar electronic surroundings for the two nitrogen atoms when applying ^{14}N NMR spectroscopy [11]. Although they also were able to distinguish between the two signals, these showed very similar half-widths. This also proved that the counteranions did not interact preferentially with one of the nitrogen atoms.

In the same publication, the Blümel group also explored the structure of imidazolium ILs that have been immobilized on silica [11]. By applying ^{1}H and ^{13}C HRMAS NMR it could be demonstrated that the imidazolium moiety stays largely intact. Likewise, Le Bideau et al. used ^{1}H MAS NMR to investigate the structural properties of [bmim]BF_4 being confined in monolithic silica ionogels [12]. Much to surprise, the IL showed only slightly slower dynamics compared with neat liquid [bmim]BF_4; the IL's liquid-like properties seemed to be preserved in the confined state.

To gain more structural insight into neat ILs, H,H-NOESY NMR has been deployed for the determination of H–H distances in the liquid state by Carper [13]. For short mixing times (below 50 ms) the NOESY-distances were in good agreement with theoretical results. Longer mixing times (> 50 ms) resulted in unrealistically short H–H distances due to substantial spin diffusion. In the following, Mele et al. also investigated cation–cation interactions and distances with the help of (gradient-selected) NOESY experiments [14] (Fig. 2). They compared [bmim]BF_4 with [bdmim]BF_4 and were able to correlate their NMR data with X-ray cristallographic data. Here, it needs to be noted that even in the liquid state significant interaction of the butyl chains with the polar domains could be detected. The latter two publications clearly show that neat ionic liquids are supramolecularly ordered in a fashion that mimicks the solid state structures.

Probably inspired by these results, the Ludwig group has looked into the question of how much IR and NMR data actually can tell us about the real-world properties of ILs [15]. By comparing vibrational frequencies, NMR chemical shifts and quadrupole coupling constants together with DFT calculations, they concluded that these spectroscopic data contained a very similar type of electronic pertubation.

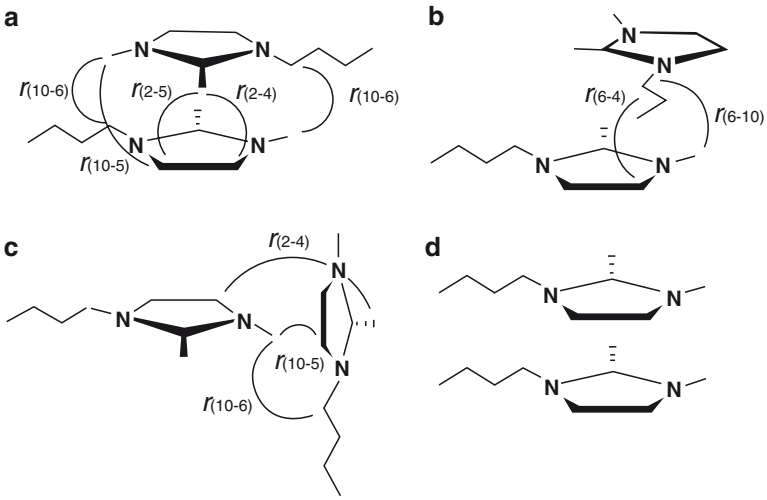

Fig. 2 Aggregation motives of $[bmim]^+$ and $[bdmim]^+$ in solution [14]. Copyright Wiley. Reproduced with permission

Therefore, spectroscopic investigations do really contain substantial information on hydrogen bonding, ion-pair formation as well as the acidity if ring protons in imidazolium ILs and are suitable for developing structure–dynamics relations.

Recently, Moyna and coworkers investigated hydrogen bonding in [bmim]Cl applying $^{35/37}$Cl NMR and deuterium isotope effects [16]. With this setup, they were able to identify interionic Cl-H bonds and differentiate between them according to their different strength. This is the first time that the combination of chlorine NMR and isotope effects has been used to study hydrogen bonding interactions – a method that might have a lot of potential for the exploration of interactions in and with ILs.

2.2 Reorientational Dynamics

A variety of publications are dealing with T_1 relaxation measurements in combination with NOE experiments to investigate the reorientational dynamics of ionic liquids in solution (and sometimes also in the solid state) [17–22]. The data can then be interpreted concerning inter-ionic interactions and phase transitions.

The first publication of this type has been published by Dölle, Carper and coworkers in 2003 [17]. The group examined the reorientational dynamics of [bmim]PF_6 and evaluated the results via mathematical fits and comparison to modelling results. They found strong H2…F bonds via quantum-mechanical calculations of ion-pairs and were able to confirm these findings also for the liquid phase. From these results, they assumed that these H-bonds may lead to even higher aggregates with a kind of layer structure. The combination of the hydrogen bonds with strong Coulombic interactions, so they claim, might be the most prominent reason for the relatively high viscosities of many ILs. An almost identical study (from an NMR point of view) of the same group has been published one year later [18] and a follow-up focussing on [mnim]PF_6 in 2005 [19], without any significant new findings, and again by Carper for [emim]$BuSO_4$ in 2006 [20].

Very recently, the general method has been applied to *N,N*-diethyl-*N*-methyl-*N*-(2-methoxyethyl) ammonium bis(trifluoromethylsulfonyl)amide by Hayamizu and coworkers [21], who also included ^{1}H, ^{19}F and ^{7}Li T_1 relaxation as well as diffusion studies. Imanari et al. finally focussed on [bmim]Br for the detection of phase transitions [22] and were able to trace a liquid state as well as super-cooled liquid and a coagulated state. With their data they could also determine the activation energy for rapid reorientational motions.

2.3 Diffusion

To address the question of hydrogen bonding and ion-pairing in ionic liquids, an obvious approach is to study the self-diffusion coefficients of the individual ions.

This can convieniently be achieved by applying diffusion-ordered NMR spectroscopy (DOSY) [23, 24].

There are principally two basic pulse sequences for measuring molecular diffusion (Fig. 3). In the pulsed field gradient spin-echo (PSE) sequence, magnetization during the diffusion period is *transverse* and therefore dictated by T_2 relaxation. In the pulsed field gradient stimulated echo (PSTE) sequence, magnetization is *longitudinal* during diffusion and thus dictated by (the much slower) T_1 relaxation. Since T_2 relaxation increases with molecular size ([2], p. 369), the PSE sequence can easily become unsuitable for use in ionic liquids, leading to an error of up to 20% [25]. Therefore, the PSTE sequence should always be preferred. This fact has to be taken into account when assessing early publications in this field.

In 2001, Sun and Wang were probably the first to report on diffusion coefficients of [emim]BF_4 measured by NMR [26]. They observed temperature-dependent diffusion radii: below 330 K they found a diffusion radius of 2.79 Å while it was 1.90 Å above 335 K. The authors concluded that ion pairing must take place at lower temperatures while at elevated temperature individual ions are predominantly present.

The Watanabe group focussed on the BF_4^- and Tf_2N^- salts of [emim] and [bpy] [27]. For the BF_4^- salts they reported equal diffusion rates for both cation and anion. Surprizingly, the Tf_2N^- salts showed much higher diffusion coefficients for the cations, which led the authors to proposing some kind of "ionic association" for the anions. Hayamizu et al. studied mixtures of [emim]BF_4 and $LiBF_4$ and measured the self-diffusion coefficients by ^1H, ^7Li and ^{19}F NMR [28]. They also claimed "associated structures" within these ILs since, albeit being larger in molecular size, the $[emim]^+$

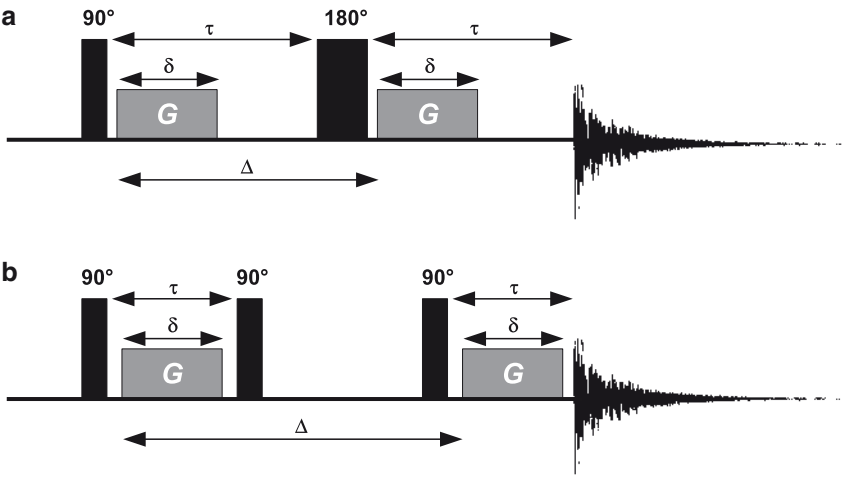

Fig. 3 Pulse sequences for diffusion-ordered NMR spectroscopy (DOSY). **a** The PSE sequence. **b** The PSTE sequence [2]

cation diffused faster than BF_4^-. Therefore, the anion cannot diffuse as a single ion. Interestingly, Li^+, being by far the smallest species in solution, diffused the slowest of all. The authors concluded by proposing $Li^+BF_4^-$ ion complexes diffusing together. The same findings and conclusions have been reported by Passerini for the mixture of [mppyr]Tf_2N with $LiTf_2N$ [29] and by Hayamizu for two other ILs [21].

Watanabe and coworkers also studied a variety of [bmim] ILs with different fluorinated anions and again found the cation always diffusing faster than the anion [30]. By listing the ratios of the molar conductivities versus the conductivities calculated from the NMR self-diffusion coefficients $\Lambda_{imp}/\Lambda_{NMR}$, they were able to propose a "useful parameter to characterize various properties" of ILs with different anions, such as quantitative information on how much individual ions contribute to ionic conduction.

Trimethylsilyl-substituted imidazolium-ILs show very low viscosities, and therefore Chung et al. have studied these via T_1 measurements and diffusion NMR [31]. The low viscosities resulted in narrower NMR signals as well as higher diffusion coefficients, while the authors reported similar diffusion coefficients for both anion and cation in this case. Since at lower temperatures a decoupling of anionic and cationic motion could be measured, ion-pairing effects were proposed.

In 2003, Watanabe reported the development of proton-conducting Brønsted acid–base ILs [32]. With the help of the PSE pulse sequence they could demonstrate fast proton-exchange processes between protonated imidazolium cations and imidazole. Recently, Judeinstein also published two papers on the investigation of proton-conducting ILs, here based on amines and perfluorinated acids [33,34]. With a combination of diffusion NMR and varios NMR correlation methods, interionic spatial correlations have been obtained. Additionally, three different types of ion association were found for three different ILs: (a) mostly associated ion-pairs, (b) dissociated ions and (c) fully dissociated protons (Fig. 4).

Finally, two more specialized publications: The group of Zeidler has developed a modified high-pressure probe in which they were able to measure pressure-dependent self-diffusion coefficients of [bmim]BF_4 (neat and in methanol) [35]. Kanakubo and coworkers have compared the self-diffusion coefficients of pure and 97% pure [bmim]PF_6 [36] and found large differences between the two samples

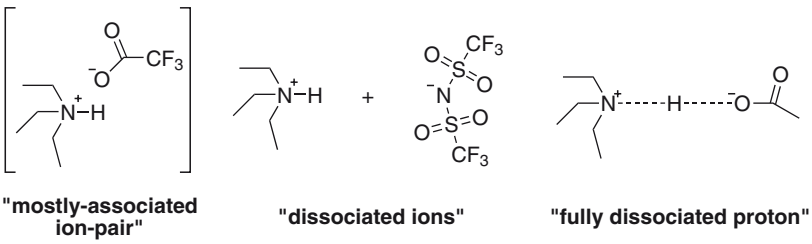

Fig. 4 Three different types of ion association, as described in [34]s

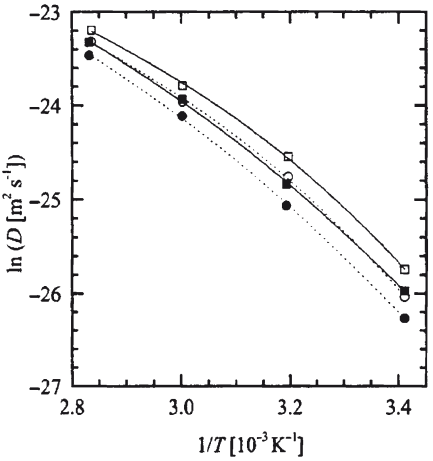

Fig. 5 Arrhenius plots of the diffusion coefficients of the cations (*squares*) and anions (*circles*) of a pure (*closed*) and a 97% pure (*open*) sample of [bmim]PF_6 [36]. Reproduced with permission

(Fig. 5). Although the reasons for this effect were not perfectly clear, they concluded that small amounts of impurities do have a significant effect on transport phenomena in ionic liquids.

2.4 Interaction with Co-Solvents and Impurities

Headley and Jackson were the first to study systematically the chemical shifts of [bmim]BF_4 and [bmim]PF_6 in nine different organic solvents [37]. They found the ring-protons of the PF_6^- salt to be more sensitive to solvation than the ones of the BF_4^- salts. Additionally, the interaction of the 2-proton in the imidazolium ring with the anion was more intimate than with the 4- and 5-proton. They concluded that the smaller BF_4^- anion resulted in a more intimate (ion-pair) interaction with the cation and thus this salt was less sensitive to solvation effects.

Mele was the first to study C–H … O and C–H … F interactions in [bmim]BF_4 with added trace amounts of water using NOE and ROE NMR spectroscopy [38]. Via $^1H\{^{19}F\}$ NOE difference spectra, the group was able to detect cation/cation and water/cation contacts. By this, tight ion pairs were found for the neat IL while increasing water content changed the IL structure substantially by building up a network of H_2O-mediated hydrogen bonds.

Tubbs and Hoffmann [39] looked at [emim]Tf_2N in mixed solvent systems of $CDCl_3$, CCl_4 and C_3D_6O (Fig. 6). They measured proton T_1 relaxation times and thus could monitor ion-pair formation as a function of the dielectric constant of the solvent, the temperature and the IL concentration. They found freely dissolved ions on one end of the scale and ion-pair aggregates with a remarkably long life-time on the other. The interaction of [bmim]BF_4, $–PF_6$ and $–Tf_2N$ with methanol and

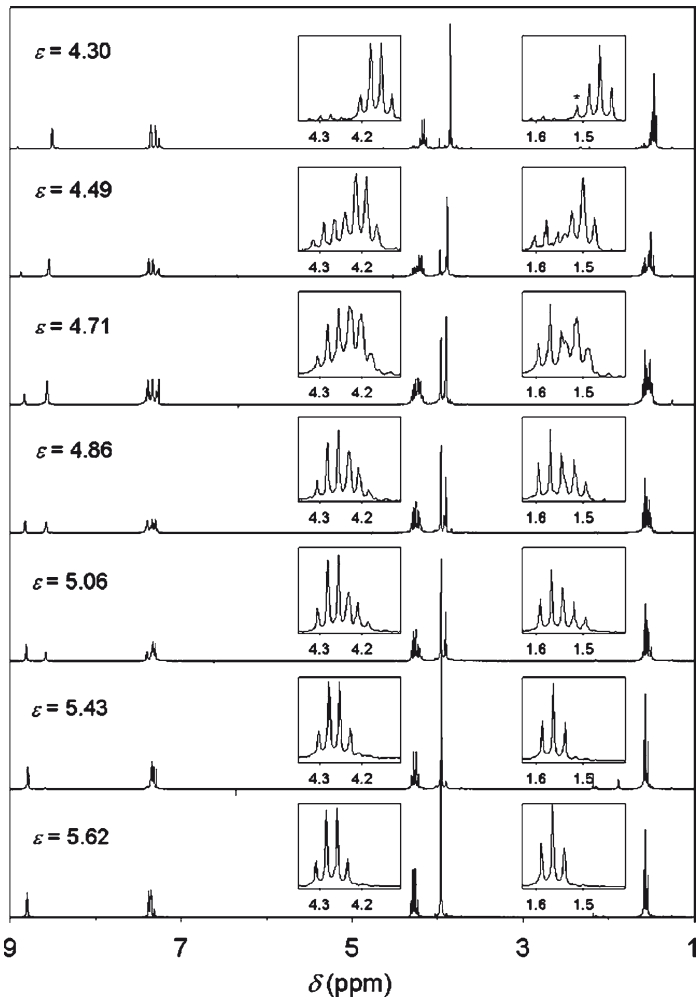

Fig. 6 [emim]Tf_2N in mixed solvents of varying dielectric ε [39]. Reproduced with permission

dichloromethane has been studied with the help of $^{1}H,^{19}F$-HOESY NMR by Pregosin and co-workers [40]. Again, methanol as a polar solvent resulted in separation of the ions while CD_2Cl_2 led to strong ion contacts even at high dilution (Fig. 7). Ion-pairing has subsequently been studied using PSE diffusion NMR.

For the mixture of [bmim]Br and D_2O, anomalous dynamics were found utilizing diffuson NMR as well as ^{1}H and ^{81}Br NMR relaxation measurements [41]. The addition of water here also was found to lead to a network of hydrogen bonding and very dilute samples behaved "in a special manner" (whatever that may mean). The strength of solvation for D_2O and C_6D_6 mixtures with [bmim]Cl and -PF_6 was investigated via the rotational correlation time (cf. Sect. 2.2) [42]. Water rotated two times slower in the Cl-IL as compared with the PF_6-IL while no difference in

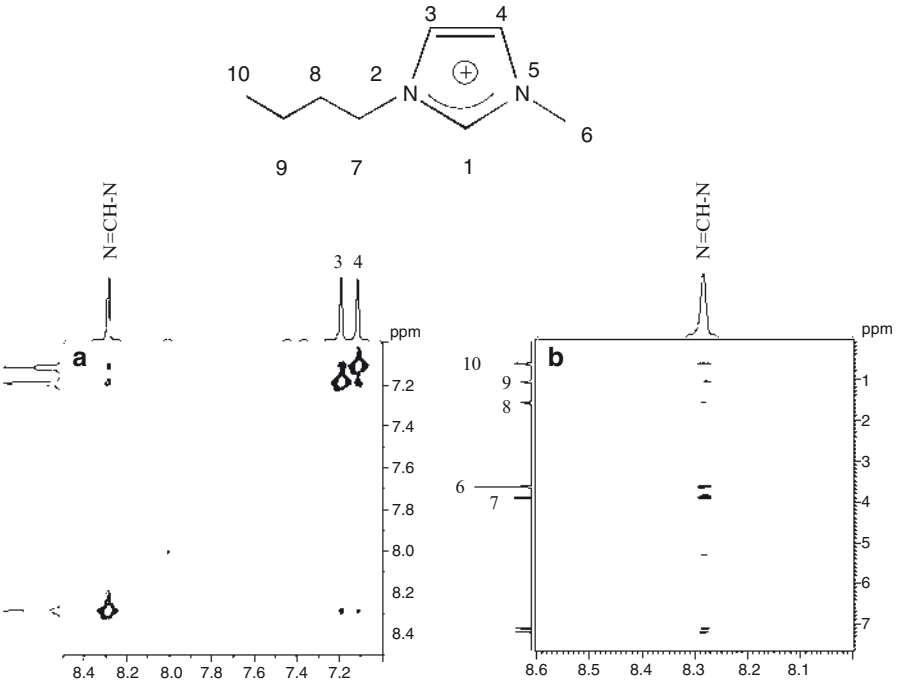

Fig. 7 H,H-NOESY NMR spectrum of neat [bmim]Tf_2N [40]. The –N=C**H**–N–proton shows contact to all other protons, demonstration interionic interactions. Reproduced with permission

rotational dynamics has been found for benzene. There was strong Coulombic solvent–solute attraction in [bmim]Cl, thus the slowdown of the water molecules was attributed predominantly to Coulombic interactions, not to viscosity. Investigation of the interactions between [bmim]Cl with water and DMSO by another group [43] gave basically again the same results again – completely solvated ions at low concentrations in water and ion clusters in DMSO even below 10 wt%.

The Zhao group [44] prepared aqueous solutions of five different methylimidazolium bromide ILs and studied aggregation via proton and deuterium NMR, H,H-NOESY, and proton T_1 relaxation time measurements. From these data they were able to determine the corresponding critical aggregation concentrations which decreased with increasing alkyl chain lengths. The aggregation *numbers*, on the other hand, *increased* with chain length. Since the imidazolium rings were found to be exposed to the water phase, they proposed a liquid-phase structure (Fig. 8).

On the more exotic side, the group of Stalcup investigated interactions between halophenoles and [emim]BF_4 and tetraethylammonium-BF_4, respectively [45]. NMR spectroscopy was used to distuinguish between hydrogen bonding and π-stacking effects. Thiophene interaction with three different ILs was studied via multinuclear NMR spectroscopy by Su and Zhang [46]. They found a 4:1 π-stacking ratio for the system thiophene/[bmim]PF_6, 2:1 for [bmim]BF_4 and 1:1 for

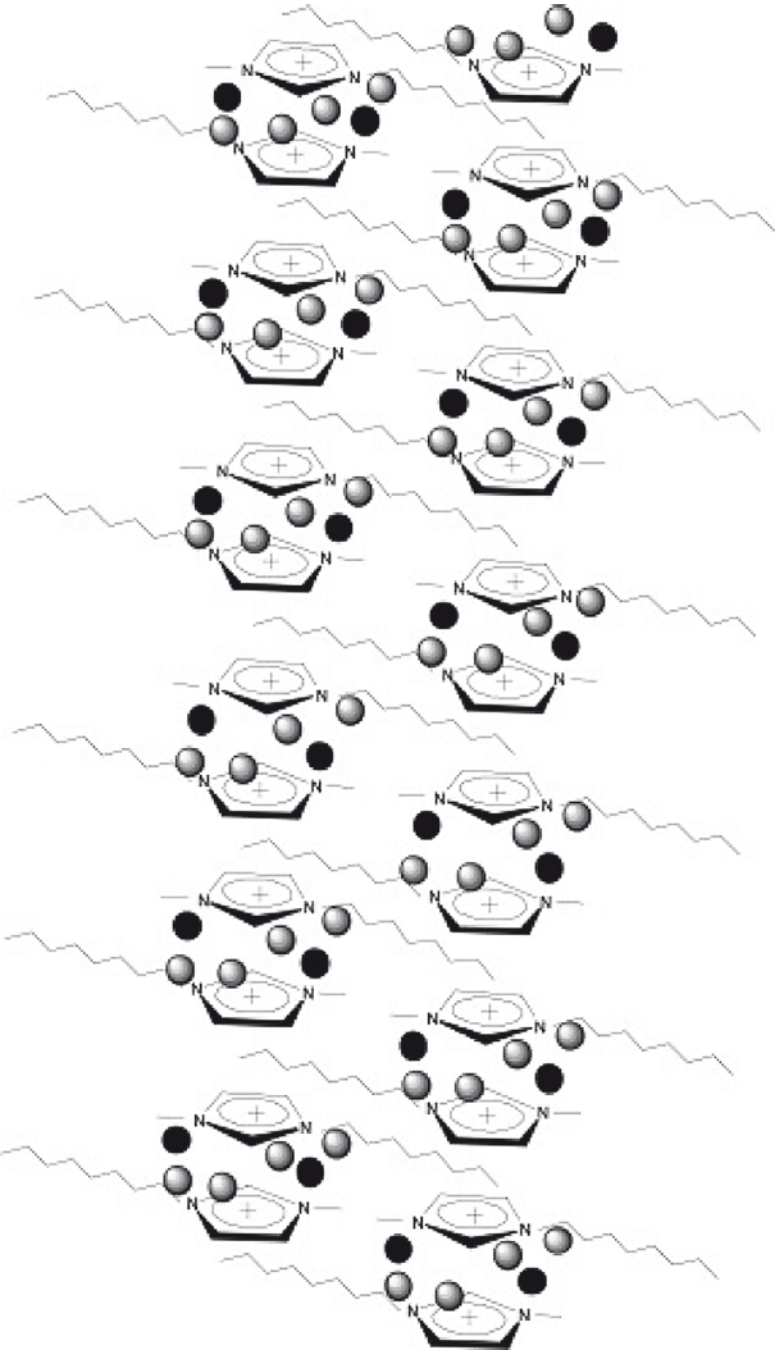

Fig. 8 Liquid-phase structure of [omim]Br in H_2O as proposed by Zhao and co-workers. *Black balls* = Br^-; *gray balls* = D_2O. Reprinted with permission from [44]. Copyright 2008 American Chemical Society

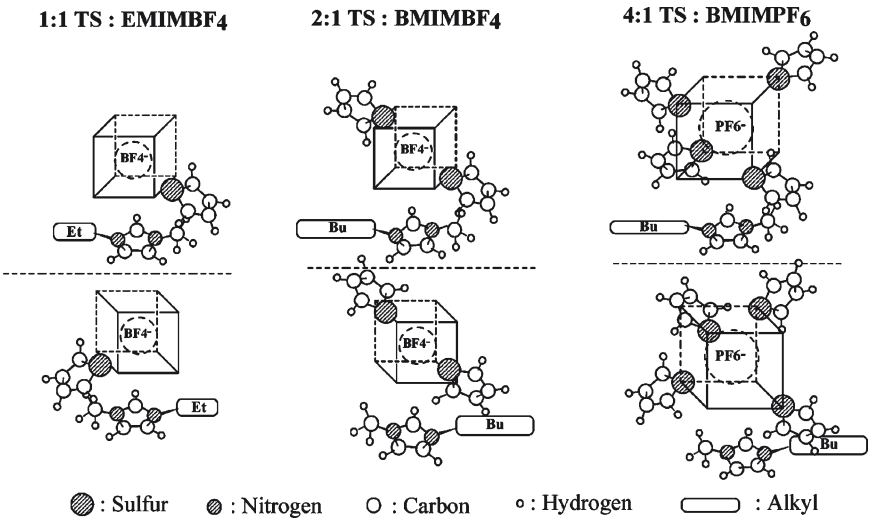

Fig. 9 Proposed structures for thiophene interaction with three different ILs. Reprinted with permission from [46]. Copyright 2004 American Chemical Society

[emim]BF_4 (Fig. 9). Riisager and Wasserscheid [47] used proton NMR in combination with IR spectroscopy to study thermomorphic phase separations of various IL/organic solvent systems. They were able to study miscibility, critical solution temperatures and structural changes in the liquid phase.

3 Interaction of Gases with Ionic Liquids

For two reasons, the interaction of ionic liquids with gas molecules is under constant investigation: First, it is surprising to note that some gases like CO_2 dissolve very readily in many common ILs while others (H_2, O_2,…) do not [48]. Second, from a technical point of view ILs are interesting solvents for typical industrial applications like hydrations, hydroformylations and so on.

None the less, there is a remarkably little number of publications dealing with NMR spectroscopy of gases in ILs. Dyson et al. [49] have used high-pressure NMR to determine the solubility of H_2 in 11 different ILs. Much to surprise, in contrast to earlier successful reports of hydrogenation reactions in ionic liquids, the H_2 solubility was much lower than expected. Subsequently, together with Laurenczy, they did the same for carbon monoxide in 37 (!) different ILs utilizing high-pressure ^{13}C NMR spectroscopy [50]. Here also, solubility was generally very poor, but like in the H_2 case, the rate of a hydroformylation reaction surprisingly did not correlate with CO solubility. Finally in 2008, the same groups again joined forces to determine the change in viscosity of [bmim]Tf_2N and [bmim]PF_6 under CO_2 pressure [51].

4 Chiral Ionic Liquids

A logical development in IL chemistry is the development of chiral ionic liquids [52–55]. Surprisingly, only two major publications are actually dealing with the application of chiral ILs for NMR purposes. The first stems from the Wasserscheid group and focuses on the synthesis of chiral ILs from the chiral pool [56]. For application purposes, the group was asking about chiral recognition via diastereomeric interactions of racemic substrates with chiral ILs. And in fact, a racemic mixture of Mosher's acid sodium salt added to one of the ILs resulted in a split of one of the ^{19}F NMR signals (Fig. 10). In the same year, Saigo and coworkers synthesized a planarchiral cyclophane-type IL cation in combination with a camphorsulfonate anion [57]. Since the anion was enantiopure, the racemic cation resulted in a diastereomeric cation/anion mixture which could be visualized via proton NMR spectroscopy.

These two examples demonstrate quite nicely the potential of chiral ionic liquids as auxiliaries for chiral recognition purposes, especially in combination with routine NMR spectroscopy.

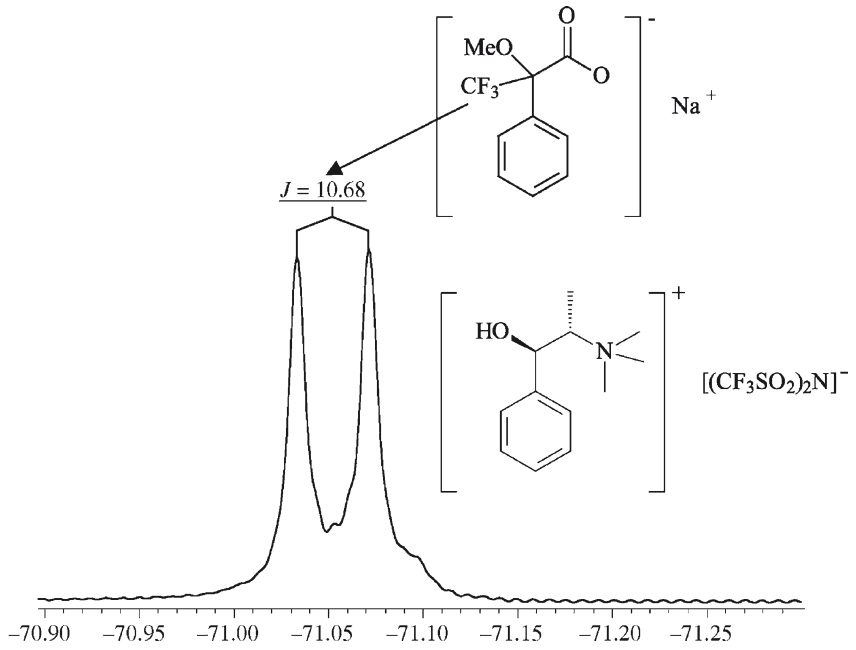

Fig. 10 ^{19}F NMR spectrum of a racemic mixture of Mosher's acid sodium salt in an enantiopure ionic liquid [56]. Reproduced by permission of The Royal Society of Chemistry

5 Reaction Monitoring

Obviously, having common NMR spectroscopical techniques routinely at hand, not only the ionic liquids themselves are interesting targets for in situ spectroscopic investigations. Since ILs are frequently used as solvents for chemical transformations, reactions in these media as well as the formation and the stability of transition metal complexes are studied (Fig. 11)

Pioneers in the field of "real" in situ reaction monitoring in ILs were Abu-Omar and co-workers [58,59], recording time-resolved NMR spectra of reactions under investigation. The obvious problem of high signal intensities in the proton channel for non-deuterated IL solvents was tackled by monitoring via the deuterium NMR channel. To this end, they needed to use (partially) deuterated starting materials. Monitoring several different types of reactions, they could demonstrate that no solvent suppression is needed this way. My own group has re-evaluated some of their results and has come to the conclusion that the need for deuterated samples, although feasible, is still quite a restraint. Our solution to the "solvent suppression problem" was the application of diffusion NMR to differentiate between solvent and solute [60]. This way, "dosy-edited" NMR spectra ideally only contained signals stemming from the solute molecules (Fig. 12). Unfortunately, because of intrinsic limitations of the DOSY experiment, the method only rendered good results for relatively small solute molecules. Therefore, if fully deuterated ILs are needed for exhaustive reaction monitoring, we have also developed an effective and transition-metal free synthetic pathway [3].

The very first NMR investigation of elementary reactions involving transition metals was published by the group of Kollár [61, 62]. Focussing on the mechanisms of complex formation of platinum diphosphine complexes in [bmim]PF_6, the authors found reactions being very similar to the ones in conventional solvents. They also observed a nowadays well-known effect, namely the partial decomposition of PF_6^- in the presence of water.

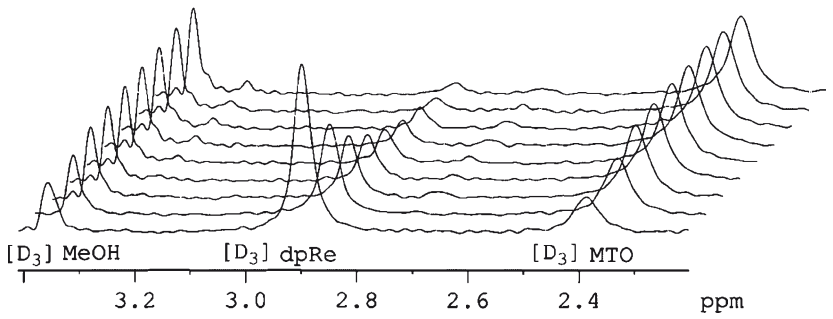

Fig. 11 ^{2}H NMR reaction monitoring: MTO-mediated epoxidation of 2-fluorostyrene in [emim]BF_4 [58]. Copyright Wiley. Reproduced with permission

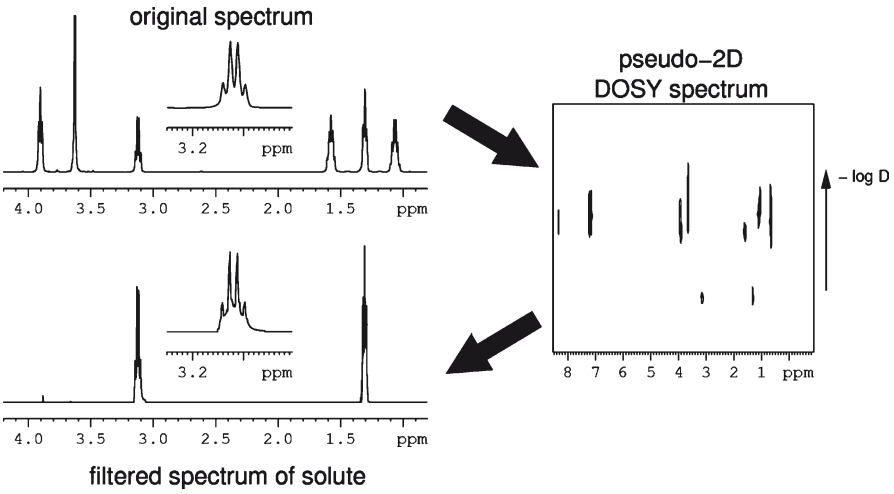

Fig. 12 Solvent-suppression via DOSY NMR [60]. Copyright Wiley. Reproduced with permission

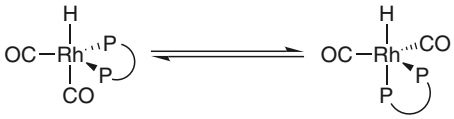

Fig. 13 Dynamic equilibrium of a rhodium complex observed by NMR in [bmim]PF_6 [63]

Dupont and van Leeuwen studied hydroformylation reactions in [bmim]PF_6 [63] and observed the formation of catalytically active rhodium species in operando (Fig. 13). The same class of reaction has been studied again by Dupont, this time in the IL [bmim]Tf_2N [64]. Here, they reported H/D exchange in the 2-position of the imidazolium ring of the IL, especially in the presence of a base – a finding that has been reported earlier already ([3,9], and references therein). The involvement of *N*-heterocyclic carbene species was discussed but not proven.

Alkene hydrogenation with transition metal carbonyl clusters in ILs has been studied using high-pressure NMR by Dyson and Laurenczy [65]. The clusters showed increased stability in the IL and reactions were up to 3.6-fold faster than in conventional solvents.

Yonker and Linehan used the "simple" salt $[(CH_3)_4N]F{\cdot}4\ H_2O$ as a model for more complex ILs [66]. After addition of methanol and CO_2 under pressure, they saw formation of methylcarbonate and fluoromethane. The results are relevant to "real" processes since their reaction conditions equal those used for extractions with supercritical CO_2 on industrial scale. The reaction of CO_2 with epoxides in tetrahaloindate(III) ILs, studied by Varma [67], showed the IL being a highly active catalyst for which hydrogen bonding played an important role.

Iridium(0) nanoclusters reacted with imidazolium-based ILs under formation of imidazolylidenes [68]. The authors believed this reaction to be the reason for the high stability of nanoclusters in ILs. ^{2}H NMR spectroscopy revealed incorporation of deuterium into all three positions at the imidazolium ring but only little deuterium incorporation into the alkyl chain.

Poletti et al. followed a glycosylation reaction in different ILs with the help of low-temperature NMR [69]. In a follow-up paper [70], they analyzed and monitored various organic solutes and corresponding reactions via ^{1}H and ^{13}C HRMAS NMR of liquid sample (Fig. 14). By this they demonstrated the usefulness of HRMAS NMR for IL samples without the need for high solute concentrations.

The kinetics of the complexation reaction of LiI with a cryptand in an imidazolium-Tf_2N IL and one with a functionalized ammonium cation has been studied by Shirai and Ikeda [71]. Here, they found no difference in kinetics for the two ILs, ruling out strong cation participation in the mechanism.

Ghosh et al. characterized polyaniline/IL composites with the help of NMR [72] and found no reactivity between the two components. Similar findings have been reported by Pringle et al. [73], who synthesized polypyrrole in an phosphonium-based IL. ^{31}P, ^{19}F, and ^{13}C solid state NMR revealed incorporation of the IL during film growth which could easily be eliminated from the polymer via oxidation.

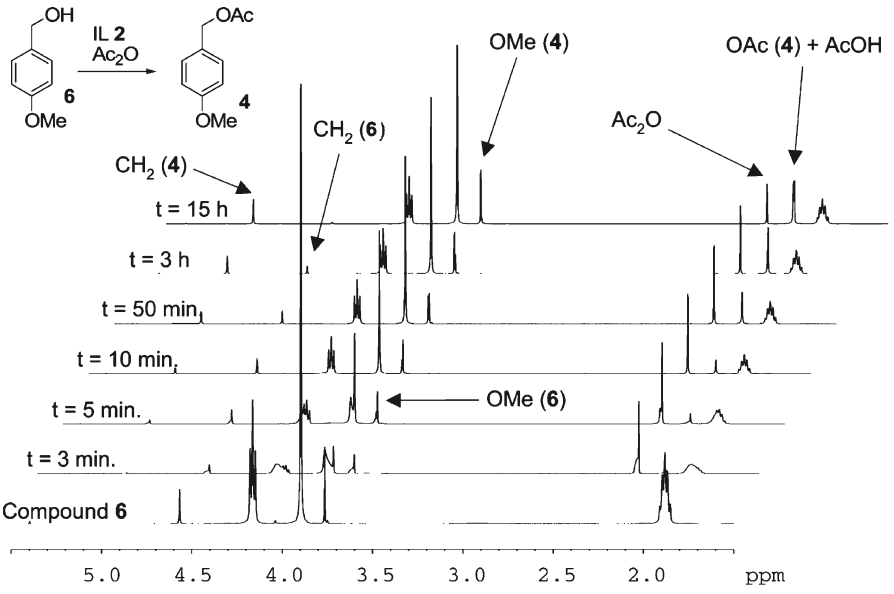

Fig. 14 Monitoring of an acetylation reaction in a methylimidazolium-PF_6 IL via time-dependent ^{1}H HRMAS NMR spectroscopy [70]. Reproduced by permission of The Royal Society of Chemistry

6 Biomass

Ionic liquids are a promising alternative for the processing of biomass, cellulose processing for the production of paper and biomass-to-liquid processes for the development of future energy source technologies being only two prominent examples [74–76]. Interestingly, the very first patent on dissolution and processing of cellulose with the help of ionic liquids [77] has already been issued as early as 1934!

Moyna and Rogers have studied cellulose being dissolved in [bmim]Cl with the help of ^{13}C NMR [78] (Fig. 15). As the main result, the cellulose oligomers are dissolved in the IL as they are in H_2O, which demonstrated again the potential of this technology. The authors claim that NMR spectroscopy can help explaining

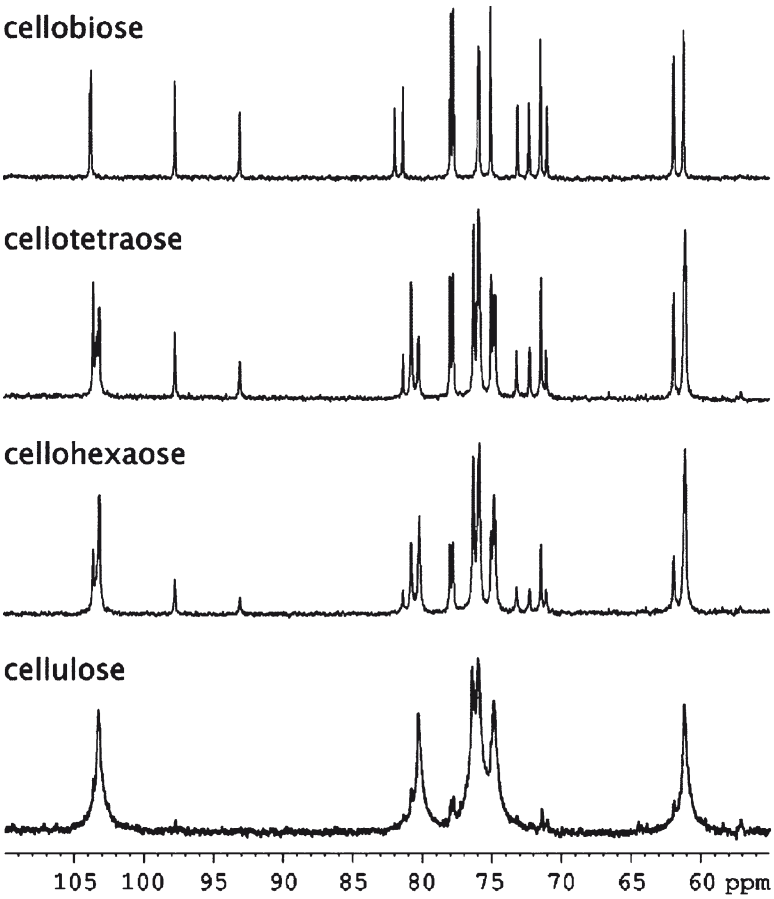

Fig. 15 ^{13}C NMR spectra of various cellulose oligomers in [bmim]Cl/DMSO-d_6 [78]. Reproduced by permission of The Royal Society of Chemistry

cellulose solvation at the atomic level. In a subsequent project, they measured ^{13}C and $^{35/37}Cl$ T_1 relaxation [79]. By this, they could show that solvation involves hydrogen bonding between the hydroxyl protons of the cellulose and the IL cloride anions in a 1:1 fashion.

Obviously inspired by these projects, Moyna et al, [80] investigated the dissolution of banana pulp in [bmim]Cl via ^{13}C NMR spectroscopy. They found substantial variations in the carbohydrate composition for different samples which could potentially be used for the analysis of fruit ripening.

Very recently, the same group extended their studies on the solvation of carbohydrates in various methylimidazolium-ILs [81] by means of T_1 relaxation measurements and PSTE diffusion NMR. For the cation, they found only very small changes in relaxation as a function of carbohydrate concentration, while anions showed a strong effect. From these findings, they concluded that the interactions of the carbohydrates with the anions were nonspecific but actually governing the whole process. No change in solvation mechanism could be found with regard to the anions.

7 Conclusion

Considering the many different applications of NMR spectroscopy in ionic liquids, it has become clear that this method is ready for the whole range of studies related to ionic liquid chemistry. These days, NMR in ILs is not exotic anymore but a routine technique for everyday chemistry. Virtually all standard and advanced NMR experiments can be run in ionic liquids very much like in “ordinary” conventional solvents.

References

1. Bankmann D, Giernoth R (2007) Progr Nucl Magn Res Spectr 51:63
2. Claridge TDW (1999) High-Resolution NMR techniques in organic chemistry Elsevier, Oxford
3. Giernoth R, Bankmann D (2008) Eur J Org Chem 2881
4. Giernoth R, Bankmann D, Schloerer N (2005) Green Chem 7:279
5. Voehler MW, Collier G, Young JK, Stone MP, Germann MW (2006) J Magn Res 183:102
6. Dupont J, Suarez PAZ, De Souza RF, Burrow RA, Kintzinger JP (2000) Chem Eur J 6:2377
7. Consorti CS, Suarez PAZ, De Souza RF, Burrow RA, Farrar DH, Lough AJ, Loh W, da Silva LHM, Dupont J (2005) J Phys Chem B 109:4341
8. Lin ST, Ding MF, Chang CW, Lue SS (2004) Tetrahedron 60:9441
9. Giernoth R, Bankmann D (2006) Tetrahedron Lett 47:4293
10. Lyčka A, Doleček R, Simonek P, Macháček V (2006) Magn Reson Chem 44:521
11. Brenna S, Posset T, Furrer J, Blümel J (2006) Chem Eur J 12:2880
12. Le Bideau J, Gaveau P, Bellayer S, Neouze MA, Vioux A (2007) Phys Chem Chem Phys 9:5419
13. Heimer NE, Del Sesto RE, Carper WR (2004) Magn Reson Chem 42:71

14. Mele A, Romanò G, Giannone M, Ragg E, Fronza G, Raos G, Marcon V (2006) Angew Chem Int Ed 45:1123
15. Wulf A, Fumino K, Michalik D, Ludwig R (2007) ChemPhysChem 8:2265
16. Remsing RC, Wildin JL, Rapp AL, Moyna G (2007) J Phys Chem B 111:11619
17. Antony JH, Mertens D, Dölle A, Wasserscheid P, Carper WR (2003) ChemPhysChem 4:588
18. Carper WR, Wahlbeck PG, Antony JH, Mertens D, Dölle A, Wasserscheid P (2004) Anal Bioanal Chem 378:1548
19. Antony JH, Dölle A, Mertens D, Wasserscheid P, Carper WR, Wahlbeck PG (2005) J Phys Chem A 109:6676
20. Heimer NE, Wilkes JS, Wahlbeck PG, Carper WR (2006) J Phys Chem A 110:868
21. Hayamizu K, Tsuzuki S, Seki S, Ohno Y, Miyashiro H, Kobayashi Y (2008) J Phys Chem B 112:1189
22. Imanari M, Nakakoshi M, Seki H, Nishikawa K (2008) Chem Phys Lett 459:89
23. Johnson CS (1999) Progr Nucl Magnet Res Spectr 34:203
24. Cohen Y, Avram L, Frish L (2005) Angew Chem Int Ed 44:520
25. Annat G, MacFarlane DR, Forsyth M (2007) J Phys Chem B 111:9018
26. Huang JF, Chen PY, Sun IW, Wang SP (2001) Inorg Chim Acta 320:7
27. Noda A, Hayamizu K, Watanabe M (2001) J Phys Chem B 105:4603
28. Hayamizu K, Aihara Y, Nakagawa H, Nukuda T, Price WS (2004) J Phys Chem B 108:19527
29. Nicotera I, Oliviero C, Henderson WA, Appetecchi GB, Passerini S (2005) J Phys Chem B 109:22814
30. Tokuda H, Hayamizu K, Ishii K, Susan MABH, Watanabe M (2004) J Phys Chem B 108:16593
31. Chung SH, Lopato R, Greenbaum SG, Shirota H, Castner J Edward W, Wishart JF (2007) J Phys Chem B 111:4885
32. Noda A, Susan MABH, Kudo K, Mitsushima S, Hayamizu K, Watanabe M (2003) J Phys Chem B 107:4024
33. Iojoiu C, Judeinstein P, Sanchez JY (2007) Electrochim Acta 53:1395
34. Judeinstein P, Iojoiu C, Sanchez JY, Ancian B (2008) J Phys Chem B 112:3680
35. Palmer G, Richter J, Zeidler MD (2004) Z Naturforsch A Phys Sci 59:59
36. Umecky T, Kanakubo M, Ikushima Y (2005) Fluid Phase Equilib 228/229:329
37. Headley AD, Jackson NM (2002) J Phys Org Chem 15:52
38. Mele A, Tran CD, De Paoli Lacerda SH (2003) Angew Chem, Int Ed 42:4364
39. Tubbs JD, Hoffmann MM (2004) J Solution Chem 33:381
40. Nama D, Kumar PGA, Pregosin PS, Geldbach TJ, Dyson PJ (2006) Inorg Chim Acta 359:1907
41. Nakakoshi M, Ishihara S, Utsumi H, Seki H, Koga Y, Nishikawa K (2006) Chem Phys Lett 427:87
42. Yasaka Y, Wakai C, Matubayasi N, Nakahara M (2007) J Chem Phys 127:104506/1
43. Remsing RC, Liu Z, Sergeyev I, Moyna G (2008) J Phys Chem B 112:7363
44. Zhao Y, Gao S, Wang J, Tang J (2008) J Phys Chem B 112:2031
45. Cabovska B, Kreishman GP, Wassell DF, Stalcup AM (2003) J Chromatogr, A 1007:179
46. Su BM, Zhang S, Zhang ZC (2004) J Phys Chem B 108:19510
47. Riisager A, Fehrmann R, Berg RW, van Hal R, Wasserscheid P (2005) Phys Chem Chem Phys 7:3052
48. Anderson JL, Anthony JL, Brennecke JF, Maginn EJ (2008) Ionic liquids in synthesis, In Gas solubilities in ionic liquids, Vol. 1. Wiley New York 103–129
49. Dyson PJ, Laurenczy G, Ohlin CA, Vallance J, Welton T (2003) Chem Commun 2418
50. Ohlin CA, Dyson PJ, Gabor L (2004) Chem Commun 1070
51. Laurenczy G, Dyson PJ (2008) Z Naturforsch, B Chem Sci 63 :681
52. Winkel A, Reddy PVG, Wilhelm R (2008) Synthesis 999
53. Chen X, Li X, Hu A, Wang F (2008) Tetrahedron Asymmetry 19: 1
54. Baudequin C, Bregeon D, Levillain J, Guillen F, Plaquevent JC, Gaumont AC (2005) Tetrahedron Asymmetry 16:3921
55. Ding J, Armstrong DW (2005) Chirality 17:281
56. Wasserscheid P, Bösmann A, Bolm C (2002) Chem Commun 200

57. Ishida Y, Miyauchi H, Saigo K (2002) Chem Commun 2240
58. Owens GS, Durazo A, Abu-Omar MM (2002) Chem Eur J 8: 3053
59. Durazo A, Abu-Omar MM (2002) Chem Commun 66
60. Giernoth R, Bankmann D (2005) Eur J Org Chem 4529
61. Rangits G, Petocz G, Berente Z, Kollár L (2003) Inorg Chim Acta 353:301
62. Rangits G, Berente Z, Kégl T, Kollár L (2005) J Coord Chem 58:869
63. Silva SM, Bronger RPJ, Freixa Z, Dupont J, van Leeuwen PWNM (2003) New J Chem 27:1294
64. Scholten JD, Dupont J (2008) Organometallics 27:4439
65. Zhao D, Dyson PJ, Laurenczy G, McIndoe JS (2004) J Mol Catal A: Chem 214:19
66. Yonker CR, Linehan JC (2004) J Supercrit Fluids 29:257
67. Kim YJ, Varma RS (2005) J Org Chem 70:7882
68. Ott LS, Cline ML, Deetlefs M, Seddon KR, Finke RG (2005) J Am Chem Soc 127:5758
69. Rencurosi A, Lay L, Russo G, Caneva E, Poletti L (2006) Carbohydrate Research 341:903
70. Rencurosi A, Lay L, Russo G, Prosperi D, Poletti L, Caneva E (2007) Green Chem 9:216
71. Shirai A, Ikeda Y (2008) Chem Lett 37:552
72. Ghosh S, Fadeev A, Norris I, Mattes B, Espe M (2004) Polym Prepr 45:304
73. Pringle JM, MacFarlane DR, Forsyth M (2005) Synth Met 155:684
74. Olah GA, Goeppert A, Prakash GKS (2006) Beyond Oil and Gas: The Methanol Economy. Wiley, Weinheim
75. Sheldon RA, Arends I, Hanefeld U (2007) Green Chemistry and Catalysis. Wiley, Weinheim
76. van Steen E, Claeys M (2008) Chem Eng Technol 31:655
77. Graenacher C (1934). Cellulose solution. US Pat. 1943176
78. Moulthrop JS, Swatloski RP, Moyna G, Rogers RD (2005) Chem Commun 1557
79. Remsing RC, Swatloski RP, Rogers RD, Moyna G (2006) Chem Commun 1271
80. Fort DA, Swatloski RP, Moyna P, Rogers RD, Moyna G (2006) Chem Commun 714
81. Remsing RC, Hernandez G, Swatloski RP, Massefski WW, Rogers RD, Moyna G (2008) J Phys Chem B 112:11071

Top Curr Chem (2009) 290: 285–310
DOI: 10.1007/128_2008_45

Published online: 21 July 2009

Optical Spectroscopy and Ionic Liquids

Anja-Verena Mudring

Abstract Ionic liquids have shown to be excellent solvents for optical investigation of solutes. Transition metal complexes as well as *f*-element compounds have been studied in ionic liquids. Not only are neat and clean ionic liquids transparent in the NIR and visible region, but the absence of anions with low frequency oscillators such as C–H, N–H and O–H have been found to be favourable when it comes to photoluminescence and future applications can be envisioned. Of fundamental interest is the study of the absorption spectra of organic dyes dissolved in an ionic liquid as the many physicochemical parameters such as the dipolarity and polarizability of the ionic liquid and its hydrogen bond ability can be determined.

Keywords Acidity • Ionic liquids • Luminescence • Optical Spectroscopy

Contents

A.-V. Mudring
Ruhr-Universität Bochum, Anorganische Chemie I – Festkörperchemie und Materialien,
44780 Bochum, Germany
e-mail: Anja.Mudring@ruhr-uni-bochum.de

Abbreviations Acac: Acetylacetone; BES: 2-[*N*,*N*-Bis(2-hydroxyethyl) amino]ethanesulfonate; BPh_4: Tetraphenylborate; C_2NH_3: Ethylammonium; C_2,C_2NH_2: Diethylammonium; C_2mim: 1-Ethyl-3-methyl imidazolium; C_3NH_3: Propylammonium; $C_3C_3NH_2$: Dipropylammonium; C_3,C_3,C_3NH: Tris(propyl) ammonium; i-C_3NH_3: Isopropylammonium; i-C_4NH_3: Isobutylammonium; C_4NH_3: Butylammonium; C_4mim: 1-Butyl-3-methyl imidazolium; C_6mim: 1-Hexyl-3-methyl imidazolium; C_8mim: 1-Octyl-3-methyl imidazolium; C_4mmim: 1-Butyl-2,3-dimethyl imidazolium; C_8mmim: 1-Octyl-2,3-dimethyl imidazolium; C_4py: *N*-Butyl-pyridinium; C_8py: *N*-Octyl-pyridinium; 4-C_1C_3py: 1-Propyl-4-methylpyridinium; 4-C_1C_4py: 1-Butyl-4-methylpyridinium; 2-C_1C_8py: 1-Octyl-2-methylpyridinium; 3-C_1C_8py: 1-Octyl-3-methylpyridinium; 4-C_1C_8py: 1-Octyl-4-methylpyridinium; C_4mpyr: *N*-Methyl-*N*-butylpyrrolidinium; 1-C_1C_4mim: 1-Methyl-3-butylimidazolium; 1-C_1C_8mim: 1-Methyl-3-octylimidazolium; 2-C_1C_4mim: 2-Methyl-3-butylimidazolium; 4-C_1C_4 mim: 3-Butyl-4-methyl imidazolium; CHES: 2-(Cyclohexylamino)-ethanesulfonate; $HO(CH_2)_2$mim: *N*-Hydroxyethyl imidazolium; MOPSO: 2-Hydroxy-3-(4-morpholino)propanesulfonate; $N_{3,3,3,3}$: Tetrapropylammonium; $N_{4,4,4,4}$: Tetrabutylammonium; $N_{5,5,5,5}$: Tetrapentylammonium; $N_{6,6,6,6}$: Tetrahexylammonium; OAc: Acetate; OAc_F: Trifluoroacetate; Pf_2N: Bis(pentafluoroethanesulfonyl)amide; Tf_2N: Bis(trifluoromethanesulfonyl)amide; tmen: *N*,*N*,*N*′,*N*′-Tetramethylethylenediamine; ε: Dielectric constant; μ: Dipole moment;

1 Introduction

The aim of this chapter is to give an overview of how and where ionic liquids have been and are used in optical spectroscopy. Optical properties of prominent ionic liquids themselves will be presented and then their application as solvents for UV–Vis and luminescence spectroscopy will be discussed. However, special care has to be taken to ensure that the ionic liquids used are optically pure. As the optical determination of ionic liquid acidity is one of the most important applications of optical spectroscopy in and of ionic liquids, a whole chapter has been dedicated to this topic. To limit the length of this overview neither mixtures of ionic liquids nor mixtures of ionic liquids with other solvents are discussed. Available literature published until fall of 2008 has been taken into account.

2 Optically Pure Ionic Liquids – Synthesis and Purification of Ionic Liquids

An ionic liquid has to meet some prerequisites to be used for optical spectroscopy. This circumstance has been paid attention to in the literature [1]. First of all, the ionic liquid must be optically pure. This puts high demands on the synthesis. To start

with, it is advisable to use clean starting materials. If solvents are used, they should be dried and distilled prior to use. Also, working under inert gas conditions helps to prevent the formation of undesired (and sometimes highly coloured) oxidation side products. In addition, during synthesis high temperatures and especially overheating of the reaction mixture should be avoided as this usually gives rise to a yellowish to brown tan of the reaction product. Especially the reaction of an amine/phosphine etc. with an alkyl halide (Scheme 1), which is often the first step in the synthesis of an ionic liquid, is fairly exothermic. It is easier to control the temperature if only smaller amounts of the desired ionic liquid are synthesized.

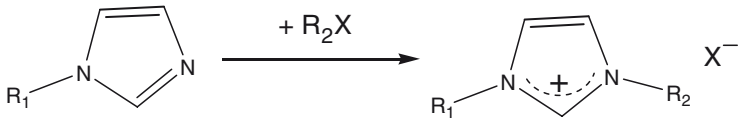

Scheme 1 Quarternisation of an alkylimidazol with an alkyl halide (R_2X)

Even the lowest amounts of organic side products from this reaction lead to intense colourations. Most times their concentration is beyond the detection limit of, for example, vibrational spectroscopy or NMR techniques, and their identity is often unclear. The most efficient way to get rid of these impurities is by stirring the ionic liquids with activated charcoal and subsequently passing the reaction product through a column of (acidic) alumina [2]. In the case of iodide salts attention should be paid to their light sensitive character.

The second typical step in the synthesis of ionic liquids involves the exchange of the halide anion with the desired counter anion of the final ionic liquid. This can be achieved by reaction of the initially obtained halide (Scheme 2) with the silver salt of the respective anion. The silver halide precipitates as a solid. As the silver salts are quite expensive, nowadays lithium salts are generally preferred in this reaction step.

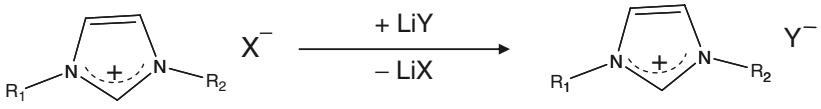

Scheme 2 Anion exchange reaction

However, both the silver and the lithium halide have a non-negligible solubility in most ionic liquids. Although this does not lead to any noticeable colouration of the ionic liquid the "invisible" (except for iodides) halide impurities can exert a crucial influence on the optical spectra. As quite strongly coordinating anions (at least when compared to most anions used for ionic liquids) they will interact strongly with solutes. For example, they will coordinate to transition metal cations and consequently change the ligand field splitting and thus the optical spectra.

This circumstance was noted by several groups when trying to establish an empirical donor strength scale for ionic liquids [3]. This is without considering the influence halide impurities may have on reactions carried out in these liquids! Furthermore, it has been shown that impurities in ionic liquids may lead to decreased photostabilities [4]. All these examples make clear that the ionic liquid must be freed even from colourless impurities if reliable and reproducible optical spectra are to be obtained. In order to reduce the amount of remaining dissolved silver or lithium halide, generally the crude reaction product is washed until the amount of halide is below detection ($AgNO_3$ test or better ion chromatography).

For similar reasons organic solvents used during the last synthesis step such as methanol, dichloromethane and water have to be removed. Water can not only enter the ligand sphere of metal cations as a strong ligand in ionic liquids but also lead to degradation of the ionic liquid itself by hydrolysis. It is well known that water leads to the decomposition of tetrafluoroborate and hexafluorophosphate ionic liquids; fluoride or hydrogen fluoride is released in this reaction.

Some detailed overviews that describe synthesis and purification of ionic liquids have appeared [5].

3 Optical Properties of Neat Ionic Liquids

Most of the commonly used ionic liquids (if pure) are semi-transparent in the UV (at least from 300 nm on) and completely transparent in the visible region of light [6–9]. By far the most ionic liquids are currently based on the imidazolium cation. Because of this the optical properties of imidazolium ionic liquids have been studied quite well. Absorption studies show imidazolium ionic liquids to have a strong absorption below 250 nm. However, the absorption tail reaches – with an appreciable absorbance in the visible region of light – well beyond 400 nm [10]. UV light induces π–π^* transitions in the imidazolium ring [11]. The fluorescence behaviour of such imidazolium based ionic liquids depends strongly on the excitation wavelength [10]. For example, when $[C_4mim][BF_4]$ is excited with light of a wavelength below 340 nm the maximum of the emission is found at 365 nm with a shoulder centred at 425 nm but stretching beyond 500 nm. Upon irradiation of $[C_4mim][BF_4]$ with light of a larger wavelength (up to 420 nm) the second maximum of fluorescence shifts towards larger wavelengths. For $[C_2mim][BF_4]$ and solutions of $[C_4mim]$Cl in acetonitrile a similar two component emission is observed where the maximum of the second emission wavelength is also dependent on the excitation wavelength. Commonly the decay constants for the most intense transition are a few hundred picoseconds, whereas the weaker component has a lifetime in the nanoseconds regime. It is thought that the second emission maximum found at larger wavelengths is due to the excitation of different structures of associated species present in the liquid state [12]. As the excitation wavelength is changed a slightly different associated species is excited and subsequently emits. This red-edge effect (REE) [13, 14], as it is called, points to the formation of structural heterogeneities in ionic liquids.

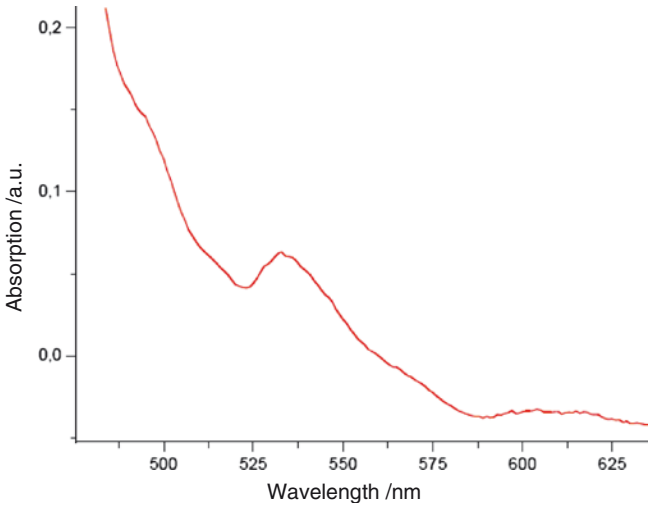

Fig. 1 UV–Vis absorption spectrum of $[C_4mim][FeCl_4]$

Generally the REE occurs when a ground state heterogeneity exists and the excited state relaxation is slow [15]. In the case of ionic liquids their generally high viscosities and short fluorescence lifetimes favour this effect.

Other ionic liquids that show electronic transitions in the visible region of light are based on transition metals and lanthanides. For example, the magnetic ionic liquid $[C_4mim][FeCl_4]$ shows an intense yellow–brownish colour which comes from the intra-configurational *d*-transition Fe^{3+} in a tetrahedral ligand field (Fig. 1) [16].

The europium based ionic liquids $[C_4mpyr]_2[Eu(Tf_2N)_5]$, $[C_3mim][Eu(Tf_2N)_4]$ and $[C_4mim][Eu(Tf_2N)_4]$ show an extremely pale violet colour which is characteristic for trivalent europium [17]. Generally for lanthanide based ionic liquids no intense colour would be expected as the intra-configurational *f–f* transitions are strongly forbidden. However, for magnetic and luminescent dysprosium ionic liquids with a composition of $[C_4mim]_{3-x}[Dy(SCN)_{8-x}(H_2O)_x]$ intense orange–yellow colours are observed which most probably come from charge transfer transitions [18].

4 UV–Vis Absorption Spectroscopy of Solutes in Ionic Liquids

UV–Vis absorption spectroscopy can been used to establish the coordination environment of metal cations in ionic liquids. This is generally done by a comparison of the absorption spectra of the system under investigation with spectra of the metal cations in well-established coordination environments. For example, the formation of chloro complexes of Np(IV) and Pu(IV) in $[C_4mim][Tf_2N]$ and $[C_4mim][Tf_2N]$/$[C_4mim]Cl$ mixtures has been studied [19]. Upon dissolution of $[C_4mim]_2[AnCl_6]$ (An=Np, Pu) in $[C_4mim][Tf_2N]$ the hexachloro complex remains intact. Addition of

$[C_4mim]Cl$ to this solution leads to the formation of higher chloro complexes. Similarly, the UV–Vis absorption spectra of uranyl bis(trifluoromethanesulfonyl) amide, uranylperchlorate, uranylnitrate and uranylacetate as well as of an 18-crown-6 complex have been studied in the ionic liquids $[C_4mpyr][Tf_2N]$, $[C_4mim][Tf_2N]$, $[C_6mim][Tf_2N]$, $[C_6mim]Br$ and $[C_6mim]Cl$ with the aim to investigate the coordination and ligand sphere of the uranyl cation [20]. In was found that the spectra in the presence of chloride, nitrate and acetate are comparable to those in acetone and acetonitrile. The bis(trifluoromethanesulfonyl) amine of the ionic liquid has apparently no influence on the optical spectra of the uranyl anion and, in consequence, was thought to be non-coordinating when stronger competing ligands such as halide are present. In case of wet ionic liquids water was found in the coordination sphere of uranium(VI).

Judging from UV–Vis spectroscopy, Eu^{2+} has a remarkably high stability in $[C_4mim][PF_6]$ and the complexation of Eu^{2+} with 15-crown-5 has been studied in this solvent [21]. Indeed, ionic liquids are useful to stabilize the divalent oxidation state of lanthanides which has been shown by the synthesis and structural characterization of $[C_4mpyr]_2[Eu(Tf_2N)_5]$ [22].

UV–Vis spectrophotometry has also been helpful to study the kinetics of olefin oxidation with hydrogenperoxide using methyltrioxorhenium (MTO) in the ionic liquids $[C_2mim][BF_4]$, $[C_4mim][BF_4]$, $[C_4mim][NO_3]$ and $[C_4py][BF_4]$ [23].

By far the most UV–Vis studies in ionic liquids have been undertaken with the goal of determining solvent polarity by solvatochromic shift of dissolved dyes. Because of the high importance, section 6 of this overview will be dedicated to this topic.

5 Luminescence Spectroscopy in Ionic Liquids

Lanthanide based ionic liquids have been found to be strongly luminescent. $[C_3mim][Eu(Tf_2N)_4]$, $[C_4mim][Eu(Tf_2N)_4]$, and $[C_4mpyr]_2[Eu(Tf_2N)_5]$ represent the first *f*-element ionic liquids that do not need any stabilization of the liquid state by neutral co-ligands and, in addition, are highly luminescent. All the above-mentioned Eu(III) ionic liquids show lifetimes of about 2 ms in the liquid state together with a small line width and high colour purity of emission [17] (Fig. 2).

The room temperature ionic liquids $[C_6mim]_{5-x}[Dy(SCN)_{8-x}(H_2O)_x]$ (x = 0–2) also show excellent photophysical properties with long luminescence decay times and high colour purities. However, the luminescence lifetimes depend on the number of water molecules in the coordination sphere of the trivalent lanthanide ion. The Dy ($^4F_{9/2}$) lifetime of $[C_6mim]_3[Dy(SCN)_6(H_2O)_2]$ at room temperature is 23.8 μs. For $[C_6mim]_4[Dy(SCN)_7(H_2O)]$ the respective lifetime is 40.34 μs. As expected, the anhydrous compound $[C_6mim]_5[Dy(SCN)_8]$ shows the largest lifetime of the excited state with 48.4 μs. Additionally, these dysprosium ionic liquids show a strong response to externally applied magnetic fields and are far superior to the known transition metal ionic liquids because of the extremely high effective moment of $Dy^{(III)}$. In consequence, they represent the first examples of room temperature ionic liquids that combine magnetic and luminescent properties (Fig. 3).

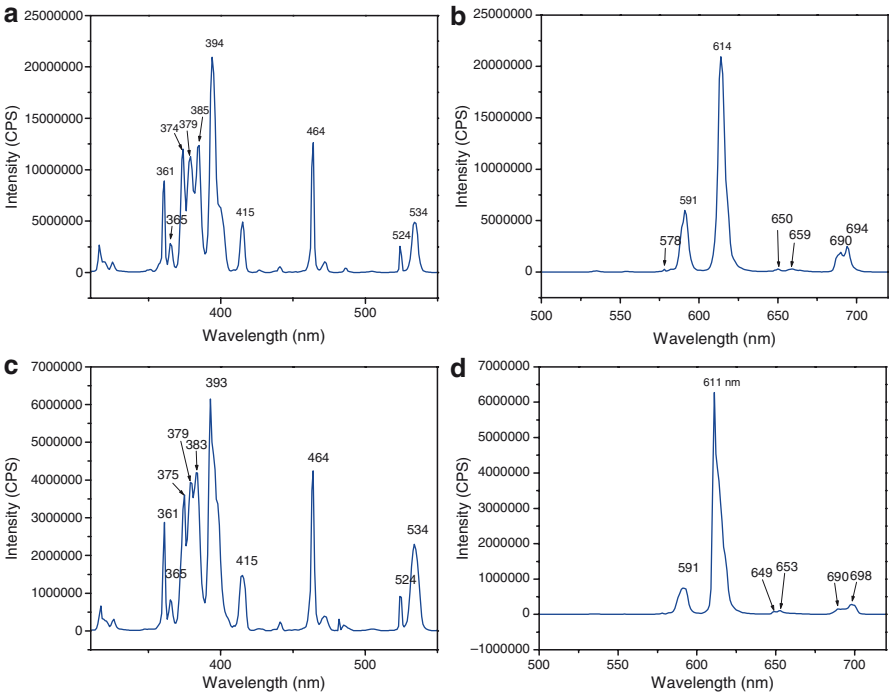

Fig. 2a–d Excitation (**a**,**c**) and emission (**b**,**d**) spectra of solid (**a**,**b**) and liquid (**c**,**d**) $[C_4mim][Eu(Tf_2N)_4]$ at room temperature

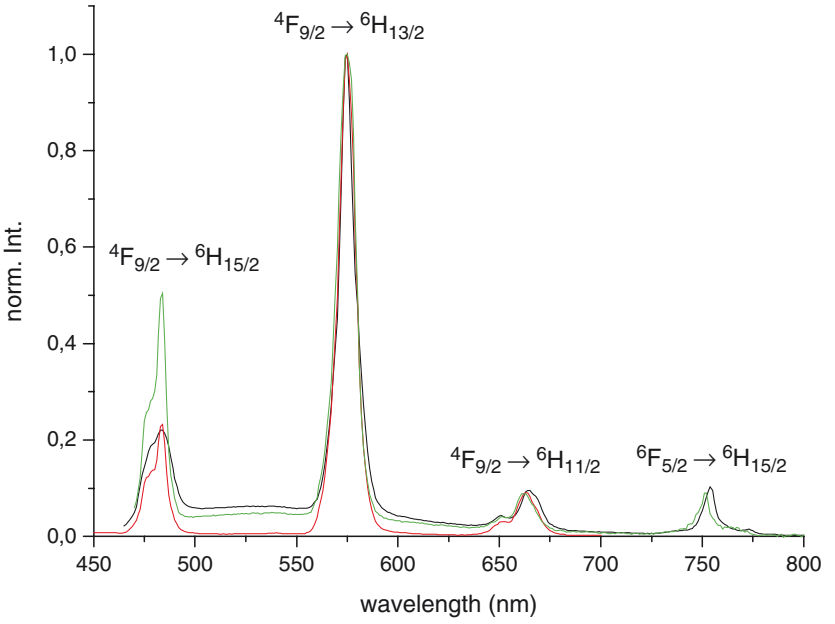

Fig. 3 Emission spectra with transition assignment of $[C_6mim]_3[Dy(SCN)_6(H_2O)_2]$ (*light grey*), $[C_6mim]_4[Dy(SCN)_7(H_2O)]$ (*dark grey*) and $[C_6mim]_5[Dy(SCN)_8]$ (*black*) at room temperature under excitation with λ_{ex} = 453 nm

Similarly, the optical properties of $[C_4mpyr]_2[Pr(Tf_2N)_5]$ which has a melting point just above 100 °C as well as of solutions of $Pr(Tf_2N)_3$ and PrI_3 in $[C_4mpyr][Tf_2N]$ have been studied by luminescence spectroscopy [25]. All of the liquid state spectra show an astonishingly well resolution and strong emission from the ^3P_J (J = 0,1) levels. From the luminescence spectra it can be concluded that in a solution of PrI_3 in $[C_4mpyr][Tf_2N]$ the iodide anion gets completely removed from the ligand sphere of Pr(III) and a bis(trifluoromethanesulfonyl)amide complex anion is formed. This finding is also backed by single crystals X-ray structure analysis.

The dissolution and solvation of Eu(III) in $[C_4mim][Tf_2N]$ has also been studied by luminescence spectroscopy. The excitation and emission spectra together with the decay constants of emission have been evaluated to investigate how water and other anions such as triflate and chloride change the photophysical properties of the emissive lanthanide centre [26]. The interaction of Eu^{3+} with halide has been investigated in the ionic liquids $[C_4mim]X$ (X = $[BF^-$, PF_6^-, OTf^-, $Tf_2N^-]$ [27]. Similarly the luminescence of terbium monodipicolinate dissolved in ethyl ammonium nitrate has been studied [28]. The luminescence lifetime, the luminescence rise time, and the absorption spectrum of terbium monodipicolinate in EAN are measured. The emission and excitation spectra of anhydrous NdI_3, DyI_3 and TbI_3 in the ionic liquid $[C_{12}mim][Tf_2N]$ are reported. It was found that this ionic liquid is an excellent medium in which to study the optical properties of lanthanides and for Dy(III) an exceptionally high lifetime was measured. However, as soon as water (from the atmosphere) was allowed to enter the system the lifetime became dramatically reduced [29]. The near-infrared emitting lanthanide ions Nd(III) and Er(III), are showing in this ionic liquid lifetimes of 15.3 and 10.4 μs, respectively [30]. The quantum yield for Nd(III) has been determined to be 1.5%. It is thought that if water enters the coordination sphere of the oxophilic lanthanide, efficient vibronic coupling leads to high radiationless decay rates. In the case of NIR emitting lanthanides, only a few O–H vibrations have to be excited to bridge the comparatively small energy gap between the excited and the ground state of the lanthanide ion. In consequence, radiationless decay is highly likely.

Improved photophysical properties such as a high quantum yield and enhanced photostability are observed for a solution of 1-hexyl-3-methylimidazolium tetrakis(2-thenoyltrifluoro-acetonate)europate(III) in $[C_6mim][Tf_2N]$ [31]. A europium based luminescent ionogel was synthesized with good performance by first doping an ionic liquid ($C_6mim][Tf_2N]$) with the strongly emissive 1-hexyl-3-methylimidazolium tetrakis(naphthoyltrifluoroacetonate)europate(III) and subsequent immobilization within a silica network. The future aim is the manufacturing of electroluminescent devices [32].

Optical temperature sensor (opt(r)odes) based on the viscosity-dependent intramolecular excimer formation of 1,3bi(1-pyrenyl)propane in $[C_4mypr][Tf_2N]$ have been developed [33]. The relative intensity of the excimer emission was found to gain in intensity with higher temperature. This has been attributed to the generally low viscosity of the ionic liquid. The working temperature of this luminescence thermometer is between 25°C and about 150°C.

Ionic liquid crystals are ionic liquids that also exhibit liquid crystalline properties. It is possible to detect the phase transition of such compounds by doping them with Eu^{3+} and monitoring the temperature dependent photophysical properties of the trivalent lanthanide ion. For the system $[C_{12}mim]Cl/Eu(NO_3)_3$ it was shown that the relative transition probabilities to the different ligand-field sub-levels change when phase transitions occur. In contrast, lifetimes and overall transition intensities to the $^7F_2$ and $^7F_4$ levels vary monotonously with temperature [34]. Furthermore the emission colour of room temperature ionic liquid crystals like $[C_{12}mim]Cl$ can be tuned by doping with various Eu(III) salts and choosing different excitation wavelengths [35]. Enhanced NIR luminescence for Nd(III), Er(III) and Yb(III) was detected when the lanthanide ions were doped as their thenoyltrifluoroacetylacetonato salts into $[C_{12}mim]Cl$ [36]. Aside from luminescence spectra and lifetime measurements, the energy transfer processes of hydrous trivalent lanthanide chloride with 1,10 phenanthroline and 2,2′-bipyridine have been studied in $[C_{12}mim]Cl$ [37].

Investigation of luminescent nanoparticles in ionic liquids is an emerging field. For example, water soluble CdTe nanocrystals have been extracted into an ionic liquid where they showed enhanced photoluminescence [38]. Thiocholine bromide passivated CdTe particles could be incorporated into a polymer matrix. First the nanoparticles were extracted into the ionic liquid 1-(3-acryloyloxypropyl)-3-methylimidazolium bis(trifluoromethanesulfonyl)amide where they already showed improved photoluminescence. Then the ionic liquid got cross polymerised with diethyleneglycol methacrylate finally to obtain a highly luminescent polymer [39]. Highly luminescent Ce(III) and Tb(III) doped $LaPO_4$ nanocrystals have been obtained via a microwave synthesis route in mixtures of $[N_{1,4,4,4}][Tf_2N]$ with a co-solvent such as, for example, ethanol [40]. The particles are characterized by a comparatively small size distribution (9–12 nm) and excellent quantum yields. By re-dispersing the particles in ethanol, transparent luminescent layers could be ink-jet printed on polymer substrates [41]. Well shaped YF_3, EuF_3 and TbF_3 as well as Eu- and Tb-doped YF_3 nanocrystals have been prepared from solutions of their acetylacetonates, nitrates or acetates in ethanol or ethylene glycol/$[C_4mim][BF_4]$ mixtures [42].

In many cases the use of ionic liquids for spectroscopic purposes has been superior to conventional organic solvents and water [30, 43].

6 Solvatochromic Determination of Ionic Liquid Solvent Polarity

6.1 Introduction

One of the many advantages that ionic liquids are able to offer over conventional organic solvents (and water) is the tuneability of the solvent properties thorough the choice of the cation/anion combination. It is estimated that roughly 10^{18} ionic liquids are accessible [44]. An important physicochemical solvent property is its polarity.

Solvent polarity determines the solubility of substances and is also able to influence the outcome of chemical reactions, the position of chemical equilibria, reaction rates and much more [45, 46]. It has been well established that the rate of a reaction that goes through a charge separated transition state (as in case of S_N2 nucleophilic substitutions) is increased in more polar the solvents. This circumstance has been rationalized in the Hughes-Ingold rules [47–51]. Often continuum properties such as the dielectric constant, refractive index (optical polarizability) and dipole moment are seen as a measure for the solvation power. However, this can be misleading. For example, perchloric acid does not dissociate in anhydrous sulphuric acid with a dielectric constant ε of 85 but is dissociated in acetic anhydride with ε = 7; anhydrous HCN (ε = 125) turns out to be a bad solvent for most salts but pyridine (ε = 12) a good one [52]. It was initially thought that a highly polar medium like ionic liquids would easily dissolve other salts. It has been realized that ordinary metal salts have sometimes an astonishingly low solubility in many ionic liquids – although one would think that similar dissolves similar. But solvent–solute interactions take place on a molecular level and a variety of different solvent–solute interactions have to be taken into account. According to Reichardt solvent–solute interactions can be divided into specific and non-specific interactions [46]. Non-specific interactions are instantaneous/induced dipole forces (dispersion or London forces), dipole/induced dipole forces (induction or Debye forces), dipole/dipole forces (orientation or Keesom forces) and ion/dipole forces (Coulomb forces). Specific interactions include hydrogen bond donor and/or hydrogen bond acceptor interactions, electron pair donor/electron pair acceptor or charge-transfer interactions, solvophobic interactions (which can become important only in highly structured solvents).

According to IUPAC the definition solvents polarity "is the overall solvation capability (or solvation power) for (1) educts and products, which influences chemical equilibrium, (2) reactants and activated complexes ("transition states"), which determines reaction rates, and (3) ions or molecules in their ground and first excited state, which is responsible for light absorptions in the various wavelength regions. This overall solvation capability depends on the action of all, non-specific and specific, intermolecular solute–solvent interactions, excluding such interactions leading to definite chemical alterations of the ions or molecules of the solute" [53].

Several methods have been applied to determine the solvent power of ionic liquids determined by solvation polarity and nucleophilicity (donor power). A common approach for determining the solvent polarity and setting up an empirical scale is to evaluate the UV–Vis spectra of optical probes such as solvatochromic dyes or transition metal complexes in the solvents under investigation [53]. The absorption or emission bands of the probe show a strong shift in their optical spectra according to the polarity of the solvent in which they are dissolved [54–57].

6.2 Fluorescent Organic Dye Probes

Generally fluorescent dyes as probes for testing the solvent polarity have the advantage that they are quite sensitive and just a minimal amount of dye needs to be dissolved

in the probed medium. This is of importance as the solubility of many dyes in ionic liquids turns out to be quite scarce.

Pyrene (Scheme 3, left) is a widely used neutral fluorescence dye [58]. The pyrene solvent polarity scale based upon pyrene is set up on the relative emission intensities of two transitions. The first corresponds to the intensity of the π^* ($\nu = 0$) $\rightarrow \pi$ ($\nu = 0$) transition and the second one to the intensity of the π^* ($\nu = 0$) $\rightarrow \pi$ ($\nu = 1$). The solvatochromic effect arises from the vibronic coupling between the weakly allowed pyrene first electronically singlet state and the strongly allowed second electronic singlet state [59]. The basicity of commonly used imidazolium ionic liquids determined by this probe was found to be larger than methanol and comes close to that of acetonitrile. However, it has been suggested that the results using pyrene as a solvatochromic probe strongly depend on the experimental conditions and the results have to be read with caution [60].

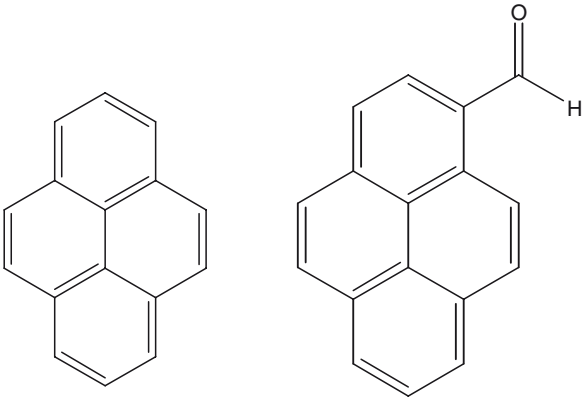

Scheme 3 Pyrene (*left*) and pyrenecarbaldehyde (*right*)

The fluorescence of pyrene shows a redshift with increasing polarity, if $\varepsilon > 10$ [61]. For [C_2mim][Tf_2N] the emission maximum was found at 431 nm, indicating a $\varepsilon < 10$ [62]. Investigations for [C_4mim][PF_6] show an emission maximum of pyrene between those of acetonitrile and ethanol [63]. Similarly, investigation of the polarity of some imidazolium- and pyridinium- ionic liquids with the fluorescent dyes 4-aminophtalimide and 4-(*N*,*N*-dimethylamino)phthalimide indicated that their polarity is strongly cation dependent and lies in the region of methanol and acetonitrile [64].

In 1-pyrenecarbaldehyde (Scheme 3, right) two excitations are possible, (n, π^*) and (π,π^*). In solvents of low polarity the n–π^* transition is important. The n–π^* fluorescence is generally observed as a highly structured signal of low intensity [65]. As the solvent polarity increases the π–π^* transition becomes lower in energy compared to the n–π^* transition because of solvent relaxation effects during the lifetime of the excited state. The n–π^* transition is then observed as a broad, moderately intense fluorescence.

Another popular fluorescent dye used to probe solvent polarity is dansylamide (5-*N*,*N*-dimethylamino-1-naphthalenesulfonylamide, Scheme 4). Its emission shows a large bathochromic shift in polar compared to non-polar solvents. As for the above-mentioned dyes, the Stoke's shift is not only dependent on the interaction of the ground state of dansylamide with the respective solvent but also of the solvent–solute interaction of the excited state of dansylamide. The difference between the absorption maximum and the emission maximum correlates well with the dipolarity/polarizability of the solvent [66]. For $[C_4mim][PF_6]$ the maximum of the emission band of dansylamide is found to lie between that of ethanol and an ethyleneglycol/water mixture; the Stoke's shift is similar to that of acetonitrile [63].

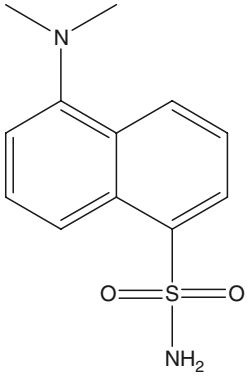

Scheme 4 Dansylamide

The Nile Red dye (Scheme 5) is amongst the dyes that give the larges solvatochromic shift depending on the polarity of the solvent in which it is dissolved [67]. When dissolved in solvents of increasing polarity, the wavelength of its absorption as well as excitation and emission maxima shifts to larger wavelength (bathochromic shift) (Table 1).

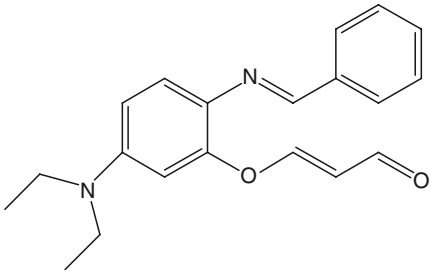

Scheme 5 Nile Red

Nile Red has the advantage over many other used dyes (for example Reichardt's dye, see below) that it is extremely stable in acidic media and shows no loss of molar absorption in the presence of acids [67]. With Nile Red dye the polarity of a

Table 1 Wavelengths of maximum absorption (ν_{max}), and molar transition energies (E_{NR}) for Nile Red dissolved in imidazolium ionic liquids [68]

	λ_{max} nm^{-1}	E_{NR} kJ^{-1} mol^{-1}	E_{NR} $kcal^{-1}$ mol^{-1}
$[C_4mim][NO_2]$	556.0	215.1(1)	51.4
$[C_4mim][NO_3]$	555.7	215.3(1)	51.4
$[C_4mim][BF_4]$	550.8	217.2(1)	51.9
$[C_4mim][PF_6]$	547.5	218.5(1)	52.2
$[C_4mim][Tf_2N]$	548.7	218.0(1)	52.1
$[C_4mim][BF_4]$	550.8	217.2(1)	51.9
$[C_6mim][BF_4]$	551.9	216.8(1)	51.8
$[C_8mim][BF_4]$	549.5	217.7(1)	52.0
$[C_{10}mim][BF_4]$	545.7	219.2(1)	52.4
$[C_4mim][PF_6]$	547.5	218.5(1)	52.2
$[C_6mim][PF_6]$	551.7	216.8(1)	51.8
$[C_8mim][PF_6]$	549.8	217.6(1)	52.0
$[C_4mim][NO_3]$	555.7	215.3(1)	51.4
$[C_6mim][NO_3]$	552.9	216.3(1)	51.7
$[C_8mim][NO_3]$	550.1	217.4(1)	51.9

series of *n*-alkyl substituted imidazolium ionic liquids with various counter anions has been investigated ($[C_nmim][NO_2]$, -$[NO_3]$, -$[BF_4]$,-$[PF_6]$,-$[Tf_2N]$, $n = 4, 6, 8, 10$) [68]. The polarity of these ionic liquids are found to be in the middle to upper half of the polarity table set initially up by Deye et al. [67] and the values are comparable to those of lower alcohols such as methanol, ethanol, butan-1-ol. However, no conclusive picture of the cation/anion dependency of the solvent polarity could be drawn. For the $[C_4mim]^+$ ionic liquids the solvent polarity decreased in the series $NO_2^- > NO_3^- > BF_4^- > Tf_2N^- > PF_6^-$. For investigated nitrate ionic liquids the solvent polarity decreases with increasing alkyl chain length. In contrast, for $[BF_4]^-$ and $[PF_6]^-$ based ionic liquids the solvent polarity rises from $[C_4mim]^+$ to $[C_6mim]^+$ but drops from $[C_6mim]^+$. Investigations on the solvent polarity of $[C_4mim][PF_6]$ positions it between ethanol and water [63]. However, this study shows some discrepancies to that of Carmichael and Seddon [68].

Time resolved studies on dye molecules can help to elucidate the solvation dynamics and can give information on the time constants of diffusion of the ionic components of an RTIL [69–75]. Time resolved fluorescence studies show the diffusional motion of the dissolved solutes [76]. Luminescence quenching of fluorescent transition metal dyes by oxygen has been used in case of so-called core-shell soft-sphere ionic liquids [77] to monitor the oxygen permeability of these ILs [78].

6.3 UV–Vis Absorbing Organic Dye Probes

The most prominent dye to measure solvent polarity empirically is 2,6-diphenyl-4-(2,4,6-triphenylpyridinium-1-yl)phenolate, also called Reichardt's dye (Scheme 6). Like Nile Red it shows an extraordinary dependence of its absorption on the solvent

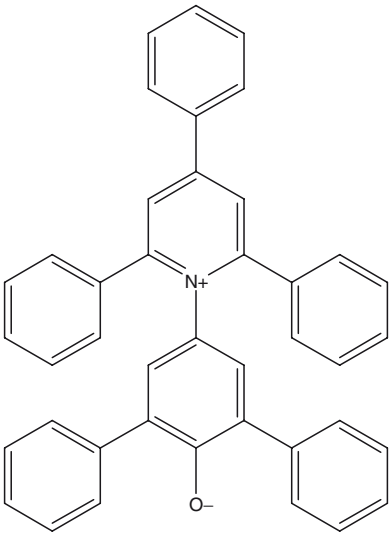

Scheme 6 Reichardt's standard betain dye no. 30 (2,6-diphenyl-4-(2,4,6-triphenylpyridinium-1-yl) phenolate)

in which it is dissolved. However, its absorption not only shows a strong dependency of solvent polarity but is also sensitive to solution temperature, external pressure as well as the nature and concentration of salts added to the solution. Because of strong hydrogen bonding to the phenolate oxygen the dye is also sensitive to even traces of water in ionic liquids [79].

As the dye possesses a large dipole moment it is well suited to monitor permanent dipole/dipole as well as permanent dipole/induced dipole interactions with the solvent. The extended π-electron system of Reichardt's dye is prone to dispersion forces. In addition, the phenolate group represents an electron pair donor centre and can get involved in hydrogen bonding as well as in Lewis acid–base interactions.

The absorption observed in the UV–Vis spectrum comes from the π–π^* transition. The solvatochromism arises from unequal solvation of the highly polar zwitterionic ground state with a dipole moment of $\mu = 15$ D compared to the less polar dipolar first excited state with a dipole moment of $\mu = 6$ D. The more polar the solvent the better the solvatisation of the more polar ground state and the less the polar excited state. In consequence a strong bathochromic shift is observed in solvents of rising polarity. Unfortunately, Reichardt's dye has a low solubility in non-polar solvents. This limitation can be overcome by substitution with five *tert*-butyl groups in the 4-positions of the five outer phenyl rings. Fortunately, a linear correlation between the optical values for both dyes is observed and the obtainable polarity scale extends over a wide range [80].

The limitation of most organic dyes like Reichardt's dye is that one can not directly probe for hydrogen-bond donor or electron pair acceptor properties.

It has been tried to overcome this drawback by the use of multi-parameter correlation equations. One approach involves the Gutmann donor number (DN) [81]. By this the absorption maximum (ν_{max}) observed for a dye in a certain liquid can be calculated from the absorption maximum of the dye in a reference medium ($\nu_{max,0}$) according to [82–85]

$$\nu_{max} = \nu_{max,\,o} + \alpha\, E_T\,(30) + \beta\ \mathrm{DN}. \tag{1}$$

According to Kamlet and Taft [86] for protic solvents the charge transition energy can be correlated with the hydrogen bond donor strength. The transition energy $E_T(30)$ can be calculated from the position of the absorption maximum of Reichardt's standard dye at 25 °C and 1 bar according to

$$E_T\,(30)/\mathrm{kcal\ mol}^{-1} = h\nu_{max} N_A = 28591/(\lambda_{max}/\mathrm{nm}). \tag{2}$$

Often these values get normalized to give the dimensionless E_N^T values, where $E_N^T = 0.0$ for tetramethylsilane (TMS) and $E_N^T = 1.0$ for water:

$$E_T^N = [E_T(30)(\mathrm{solvent}) - E_T\,(30)(\mathrm{TMS})/E_T(\mathrm{water}) - E_T(\mathrm{TMS})] = (E_T(30) - 30.7)/32.4. \tag{3}$$

Kamlet, Abboud and Taft developed a three-parameter linear solvation energy relationship

$$\nu_{max} = \nu_{max,\,0} + s\pi^* + \alpha a + \beta b. \tag{4}$$ [87–94]

The factors σ, α and β are solvent-independent factors. The three values π*, α and β can be obtained from UV–Vis absorption spectroscopy, the π* value from the $\pi \rightarrow \pi^*$ absorption of 4-nitroanisole or *N*,*N*-dimethyl-4-nitroaniline, the α and β values from pairs of homomorphic compounds like 4-nitroanisole and Reichardt's dye as well as 4-nitroaniline and *N*,*N*-diethyl-4-nitroaniline. While π* reports the effect of the dipolarity and polarizability of the solvent, α appears to be largely controlled by the cation of the ionic liquid and like β is dependent on the hydrogen bond basicity of the solvent and is dominated by the nature of the anion.

Often the Kamlet-Taft parameter π* is determined by measuring the wavelength of the absorption maximum ν_{max} of *N*,*N*-diethyl-4-nitroaniline in the respective solvent (Tables 2–5):

$$\pi^* = (\nu_{max}/10^{-3}\mathrm{cm}^{-1} - 27{,}520/10^{-3}\mathrm{cm}^{-1})/-3.182 \tag{5}$$

With π* and $E_T(30)$ known, the Kamlet-Taft parameter α can be easily calculated according to

$$\alpha = (E_T(30) - 14.6\ (\pi^* - 0.23) - 30.31)/16.5 \tag{6}$$

The β parameter can be obtained by determining the relative difference in solvatochromism of 4-nitroaniline and *N*,*N*-diethyl-4-nitroaniline:

$$\beta = (1.035\ \nu_{max,\ N\text{-}N\text{-diethyl-4-nitroaniline}} - \nu_{max,\ 4\text{-}\ nitroaniline} + 2.64)/2.8. \tag{7}$$

Other dyes that have been used to determine solvent polarities of ionic liquids are, for example, a combination of Michler's ketone (MK: 4,4′-bis(dimethylamino)benzophenone)

Table 2 Kamlet-Taft Parameters obtained using Reichardt's dye, *N,N*-diethyl-4-nitroaniline as well as 4-nitroaniline

Solvent	α	β	π*	E_T^N
$[C_2NH_3][NO_3]$ [96]				0.904
$[C_2NH_3][NO_3]$ [97, 98]	1.10	0.46	1.12	0.954
$[C_2,C_2NH_2][NO_3]$ [99]				1.074
$[C_3NH_3][NO_3]$ [97, 98]				0.923
$[C_3,C_3,C_3NH][NO_3]$ [97, 98]				0.803
$[C_4mim][NO_3]$ [100]				0.651
$[C_4mim][NO_3]$ [101]				0.661
$[C_4mim]Cl$ [102]				0.614
$[C_6mim]Cl$ [102]				0.562
$[C_8mim]Cl$ [102]				0.549
$[C_4NH_3][SCN]$ [97, 98]				0.948
$[i\text{-}C_4NH_3][SCN]$ [97, 98]				0.954
$[C_3,C_3NH_2][SCN]$ [97, 98]				1.006
$[HO(CH_2)_2mim][Tf_2N]$ [103]				0.929
$[CH_3O(CH_2)_2mim][Tf_2N]$ [103]				0.722
$[C_2mim][Tf_2N]$ [6, 104]				0.676
$[C_2mim][Tf_2N]$ [105]				0.690
$[C_3mim][Tf_2N]$ [103]				0.654
$[C_4mim][Tf_2N]$ [104, 106]				0.596
$[C_4mim][Tf_2N]$ [3, 107, 108]				0.642
$[C_4mim][Tf_2N]$ [3]	0.617	0.243	0.984	0.644
$[C_4mim][Tf_2N]$ [105]				0.645
$[C_4mim][Tf_2N]$ [95, 109]	0.61	0.24	0.98	
$[C_6mim][Tf_2N]$ [105]				0.654
$[C_8mim][Tf_2N]$ [3, 108]				0.629
$[C_8mim][Tf_2N]$ [107]				0.630
$[C_{10}mim][Tf_2N]$ [103]				0.627
$[C_4mpyr][Tf_2N]$ [110]	0.427	0.252	0.954	0.544
$[C_4mpyr][Tf_2N]$ [95, 109]	0.42	0.25	0.95	
$[C_4m_2mim][Tf_2N]$ [3]	0.381	0.239	1.010	0.541
$[2\text{-}C_1C_4mim][Tf_2N]$ [107]				0.552
$[2\text{-}C_1C_8mim][Tf_2N]$ [107]				0.525
$[1,2\text{-}C_1C_4mim][Tf_2N]$ [95]				0.552
$[1,2\text{-}C_1C_4mim][Tf_2N]$ [105]				0.546
$[1,2\text{-}C_1C_8mim][Tf_2N]$ [95]				0.525
[2-Methoxyethyl-mim][Tf_2N] [103]				0.722
[2-hydroxyethyl-mim][Tf_2N] [103]				0.929
[Benzyl-mim][Tf_2N] [103]				0.670
$[4\text{-}C_1C_4mim][Tf_2N]$ [111]	0.51	0.29	0.98	0.588
$[C_4py][Tf_2N]$ [105]				0.648
$[C_8py][Tf_2N]$ [111]	0.51	0.28	0.99	0.588
$[2\text{-}C_1C_8py][Tf_2N]$ [111]	0.48	0.35	0.95	0.554
$[3\text{-}C_1C_8py][Tf_2N]$ [111]	0.50	0.33	0.97	0.576
$[4\text{-}C_1\ C_8py][Tf_2N]$ [111]	0.50	0.33	0.97	0.576
$[C_{10}mim][Pf_2N]$ [107]				0.685
$[C_{10}mim][Pf_2N]$ [107]				0.574
$[C_2mim][BF_4]$ [110]				0.710
$[C_3mim][BF_4]$ [110]				0.691
$[C_4mim][BF_4]$ [3]	0.627	0.376	1.047	0.670

(continued)

Table 2 (continued)

Solvent	α	β	π*	E_T^N
[C_4mim][BF_4] [3, 107, 108]				0.673
[C_4mim][BF_4] [110]				0.680
[C_4mim][BF_4] [102]				0.738
[*i*-C_4mim][BF_4] [110]				0.679
[2-C_1C_4mim][BF_4] [112]				0.543
[1-C_1C_4mim][BF_4] [95]				0.576
[1-C_1C_8mim][BF_4] [3]				0.543
[C_4m_2mim][BF_4]	0.402	0.363	1.083	0.576
[C_6mim][BF_4] [102]				0.707
[C_8mim][BF_4] [102]				0.670
[C_3py][BF_4] [110]				0.661
[C_4py][BF_4] [110]				0.639
[4-C_1 C_3py][BF_4] [110]				0.670
[4-C_1 C_4py][BF_4] [110]				0.630
[2-Methoxyethyl][BF_4] [110]				0.698
[C_4mim][PF_6] [113]				0.565
[C_4mim] [PF_6] [3]	0.634	0.207	1.032	0.669
[C_4mim][PF_6] [3, 6, 7, 104, 107, 108, 114]				0.667
[C_4mim][PF_6] [106, 115, 116]				0.670
[C_4mim][PF_6] [63, 95]				0.673
[C_4mim][PF_6] [105]				0.676
[C_4mim][PF_6] [110]				0.679
[C_4mim][PF_6] [107]				0.685
[C_6mim][PF_6] [102]				0.657
[C_8mim][PF_6] [102]				0.596
[C_8mim][PF_6] [107]				0.629
[C_8mim][PF_6] [3, 107, 108]				0.633
[C_8mim][PF_6] [114]				0.636
[C_4mim][SbF_6] [95]	0.639	0.146	1.039	0.673
[C_4mim][OTf] [3]	0.625	0.464	1.006	0.656
[C_4mim][OTf] [3, 107, 108]				0.667
[C_4mim][OTf] [107]				0.685
[C_4mpyr][OTf] [95, 109]	0.40	0.46	1.02	
[C_4mim][OAc_F] [107]				0.602
[C_4mim][OAc_F] [115]				0.630
[C_4mim][OAc] [115]				0.571
[C_4mim][ClO_4] [117]				0.571
[$N_{6,6,6,6}$][H_5C_6–CO_2] [99]				0.407
[$N_{6,6,6,6}$][H_5C_6–CO_2] [80]				0.420
[C_2,C_2NH_2][Me_2N–CO_2] [118]				0.818
[$N_{3,3,3,3}$][CHES] [98]				0.624
[$N_{4,4,4,4}$][CHES] [98]				0.617
[$N_{5,5,5,5}$][CHES] [98]				0.580
[$N_{3,3,3,3}$][MOPSO] [98]				0.457
[$N_{3,3,3,3}$][MOPSO] [98]				0.488
[C_5, C_5, C_5, C_5N][MOPSO] [98]				0.512
[$N_{3,3,3,3}$N][BES] [98]				0.565
[$N_{4,4,4,4}$][BES] [98]				0.528
[$N_{5,5,5,5}$][BES] [98]				0.565
[C_2mim][DCA] [105]				0.648

Table 3 β Kamlet-Taft parameter obtained with 3-(4-amino-3-methyl-phenyl)-7-pheyl-benzo[1,2-*b*:4,5-*b*′]-difuran-2,6-dione as a probe and π* with 4-*tert*-butyl-2-(dicyanomethylene)-5-[4-(diethylamino)benzylidene]Δ^3-thiazoline (two evaluation methods, for details see [119])

Solvent	β	π*	E_T^N
[C_6mim][BF_4]	0.61	0.95	0.90
[C_6mim]Br	0.90	1.09	0.96
[C_6mim]Cl	0.97	1.06	0.91
[C_6mim][PF_6]	0.50	0.93	0.91
[C_6mim][OTf]	0.60	0.92	0.86
[C_4mim][SCN]	0.71	1.06	0.99
[C_4mim][$MeOSO_3$]	0.75	1.06	0.97

Table 4 Kamlet-Taft Parameters obtained Michler's ketone and tetracyanoethane [94]

Solvent	α	β	π*	E_T^N
[C_2mim][Tf_2N]	0.705	0.233	0.98	15.44
[C_4mim][Tf_2N]	0.635	0.248	0.971	15.97
[C_4mim][PF_6]	0.654	0.246	1.051	15.96
[C_6mim][Tf_2N]	0.650	0.259	0.971	15.62
[C_4py][Tf_2N]	0.539	0.214	1.009	15.45

Table 5 Kamlet-Taft Parameters obtained using Reichardt's dye and the spirocompounds depicted in Scheme 11 [112]

Solvent	α	β	π*	E_T(30)
[C_4mim][OAc]	0.43	1.05	1.04	50.5
[C_4mim][propionate]	0.48	1.16	0.94	49.1
[C_4mim][butyrate]	0.51	1.23	0.92	49.3
[C_4mim][glycolate]	0.44	0.87	1.12	50.5
[C_4mim]$_2$[maleate]	0.41	1.00	1.10	49.8
[C_4mim]$_2$[succinate]	0.39	1.08	1.09	49.4
[C_4mim]$_2$[maleate]	0.34	1.02	1.11	48.8
[C_4mim][H–maleate]	0.38	0.71	1.03	48.6
[C_4mim][H–succinate]	0.36	0.82	1.07	48.2
[C_4mim][H–maleate]	0.32	0.62	1.08	47.6
[HO–C_3mim][OAc]	0.51	0.99	1.08	51.1
[HO–C_3mim][Tf_2N]	0.91	0.24	1.06	56.8
[HO–C_2mim][Tf_2N]	1.14	0.28	1.08	60.8

and tetracyanoethene (TCNE) (Scheme 7) [94]. The special feature of Michler's ketone and tetracyanoethene is that in non-protic solvents an electron-donor–acceptor complex is formed, whose absorption shifts according to the solvent polarity. However, in protic solvents the carbonyl oxygen atom of Michler's ketone attacks one of the nucleophilic carbon atoms of TCNE and an oxenium zwitterion (also called *n*-complex) is formed (Scheme 7). It was found that MK and TCNE form in ionic liquids of low β values (<0.7) of the electron-donor–acceptor complex.

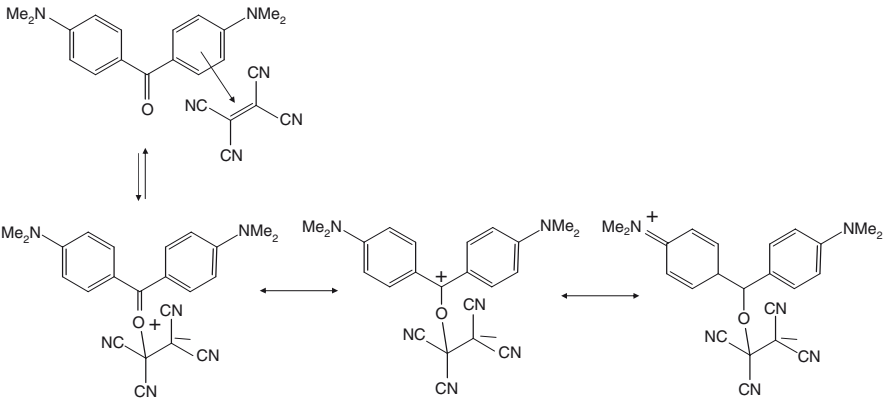

Scheme 7 Possible interactions of Michler's ketone with tetracyanoethene

It was possible to correlate the observed absorption maxima with the Kamlet-Taft values π* and β according to

$$\nu_{max}\,.10^3/cm^{-1} = 16.605 + 3.018\beta - 2.351\pi^* + 1.043\alpha. \quad (8)$$

In most ionic liquids investigated in this study the electron-donor–acceptor complex slowly transformed into the corresponding radical pair ($MK^{+\cdot}$ $TNCE^{-\cdot}$). The hydrogen bond acidity of the ionic liquids under investigation, even in the case of imidazolium ionic liquids, were not high enough to give the *n*-complex.

As dyes well suited to determine the β Kamlet Taft parameter, the compounds 3-(4-amino-3-methyl-phenyl)-7-pheyl-benzo[1,2-*b*:4,5-*b*′]-difuran-2,6-dione (Scheme 8) have been suggested. 4-*tert*-Butyl-2-(dicyanomethylene)-5-[4-(diethylamino)benzylidene]Δ^3-thiazoline should be good to determine the π* parameter [119].

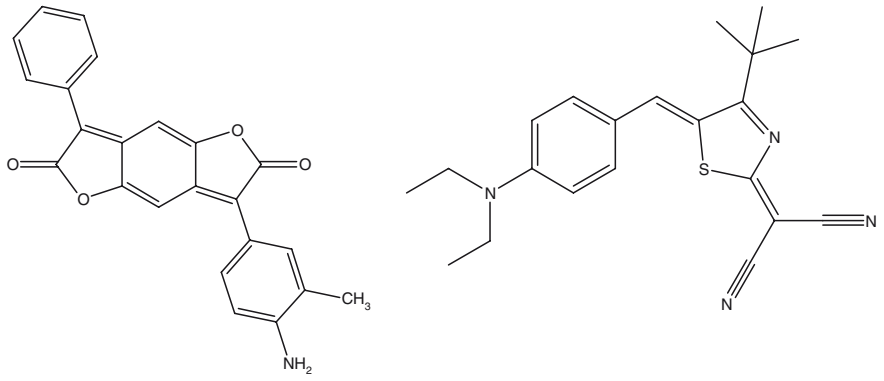

Scheme 8 3-(4-Amino-3-methyl-phenyl)-7-phenyl-benzo[1,2-*b*:4,5-*b*′]-difuran-2,6-dione (*left*) and 4-*tert*-butyl-2-(dicyanomethylene)-5-[4-(diethylamino)benzylidene]Δ^3-thiazoline (*right*)

To obtain the β value from the absorption maximum of 3-(4-amino-3-methyl-phenyl)-7-pheyl-benzo[1,2-*b*:4,5-*b*′]-difuran-2,6-dione the following correlation can be used [120]:

$$\beta = 3.84 - 0.20\,\nu_{max}10^{-3}/\mathrm{cm}^{-1}. \quad (9)$$

According to this the hydrogen bond donor ability of ionic liquid anions increases along the series

$$PF_6^- < CF_3SO_3^- \sim BF_4^- < SCN^- < MeOSO_3 < Br^- < I^-.$$

The π* parameter can be derived from measurements of the absorption maximum of 4-*tert*-butyl-2-(dicyanomethylene)-5-[4-(diethylamino)benzylidene]Δ^3-thiazoline in the respective ionic liquid according to

$$\nu_{max}10^3/\mathrm{cm}^{-1} = 17.5710 - 1.8544\pi^*. \quad (10)$$

Recently, several amino-acid-functionalised solvatochromic probes (Scheme 9) have been suggested and also applied for ionic liquids [121]. The probes are characterized by a push–pull aromatic π-electron system and the amino acid moieties are especially prone to hydrogen bond donor/acceptor interactions.

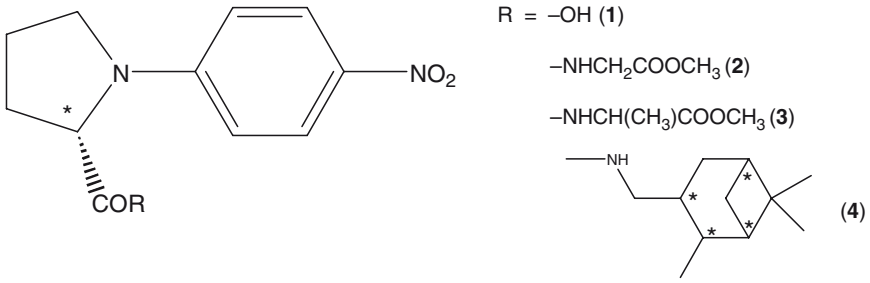

Scheme 9 Amino-acid-functionalised solvatochromic probes

The observed absorption maxima for the compounds **1**–**4** shown in Scheme 9 could be related to the Kamlet-Taft parameters as follows:

$$\text{for } \mathbf{1}: \nu_{max}10^3/\mathrm{cm}^{-1} = 28.061 - 0.879\alpha - 1.198\beta - 2.232\pi^*, \quad (11)$$

$$\text{for } \mathbf{2}: \nu_{max}10^3/\mathrm{cm}^{-1} = 28.932 - 0.373\alpha - 1.036\beta - 3.155\pi^*, \quad (12)$$

$$\text{for } \mathbf{3}: \nu_{max}10^3/\mathrm{cm}^{-1} = 28.886 - 0.408\alpha - 1.143\beta - 3.123\pi^*, \quad (13)$$

$$\text{for } \mathbf{4}: \nu_{max}10^3/\mathrm{cm}^{-1} = 28.785 - 0.394\alpha - 1.073\beta - 3.097\pi^*. \quad (14)$$

Another set of photochromic dyes that got developed to be used when Reichardt's dye fails (for example in acidic media or for fluorinated ILs) are the spiro compounds depicted in Scheme 10.

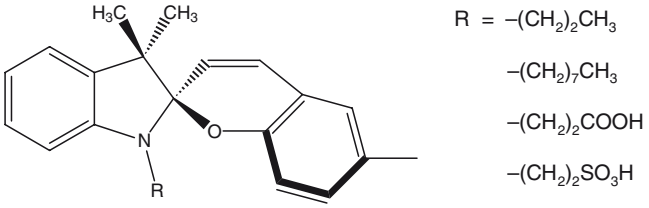

Scheme 10 Photochromic spiro compounds

Upon irradiation with UV light the colourless spiro compounds transform into their highly collared merocyanine forms (Scheme 11). The colour of the merocyanine form is highly dependent on the solvent polarity and an E_{SP} scale was defined similar to the $E_T(30)$ scale:

$$E_{SP}/\text{kcal mol}^{-1} = h\,c\,\nu_{max}\,N_A = 28591/\lambda_{max/nm}. \quad (15)$$

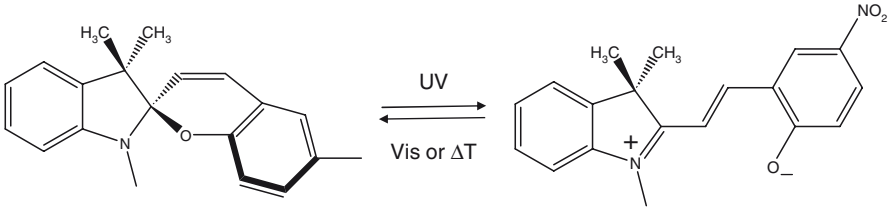

Scheme 11 Spiro-merocyanine transition

However, the spiropyrane compounds are not useful to determine the polarity of ionic liquids with strong hydrogen-bond acceptors as complexes form that exhibit no solvato/photochromism.

$E_T(30)$ or E_N^T, respectively, indeed seems to be especially sensitive to the hydrogen bond donor ability of the cation of the ionic liquid [95, 109]. A compilation of $E_T(30)/E_N^T$ values (Table 2 ff.) shows most common ionic liquids to have a polarity that is expected for typical dipolar hydrogen bonding or dipolar non-hydrogen bonding solvents [122]. Primary, secondary, and tertiary alkyl ammonium salts like ethylammonium nitrate, dimethylammonium dimethylcarbamate and tri-*n*-butylammonium nitrate show a polarity of typical dipolar hydrogen bonding solvents, similar to alcohols. Tetraalkylammonium and phosphonium salts show a polarity of typical dipolar non-hydrogen bonding donor solvents like dimethylformamide (DMF). Imidazolium based ionic liquids fall into two major groups. The polarity of 1-methyl-3-alkylimdazolium ionic liquids is similar to that of short-chain primary and secondary alcohols and secondary amides like *N*-methylformamide. 1-Alkyl and 1,4 dialkylpyridinium salts behave similarly. The 1-methyl-3-alkylimdazolium ionic liquids generally have a higher polarity than the similar 1,2-dimethyl-3-alkylimidazolium salts. An increase of the alkyl substituent causes a decrease in the E value while changing the anion has little effect. However, for 1-(2-methoxyethyl)-1-methylpyrrolidinium salts a strong anion dependency is observed [115].

Studies of the solvent polarity of $[C_4mim]^+$, $[C_8mim]^+$, $[C_4mmim]^+$ and $[C_8mmim]^+$ ionic liquids with $[BF_4]^-$, $[PF_6]^-$, $[OTf]^-$ and $[Tf_2N]^-$ showed the 1,3 dialkyl substituted imidazolium salts to have a polarity comparable to those of short chain length primary alcohols whereas the 1,2,3-trisubstituted compounds have noticeably lower polarities which can be compared to those of secondary alcohols. The C_4 salts generally exhibited a larger polarity than the C_8 ones. The cationic effects are pronouncedly larger than the anionic effect. From this it was concluded that the strongest interaction occurs between the phenoxide group of the dye with the hydrogen of the IL cation.

A comparative study of probing the polarity of $[C_4mim][PF_6]$ with various dyes such as Reichardt's betain dye (Scheme 5), pyrene, dansylamide, Nile Red and 1-pyrenecarbaldehyde has been undertaken [63]. Using Reichardt's dye as the probe a value like ethanol is measured.

$[C_4mim][PF_6]$ hydrogen bonding abilities are similar to that of short chain alcohols, hydrogen bond donor abilities similar to water and acetonitrile but dipolarity/polarizability are substantially higher than for lower chain alcohols but similar to those of water and DMSO [123].

Traces of polar impurities as well as water can change solvent polarity considerably [122]. It is feared that small traces of water will have a strong impact on α parameter determination with Reichardt's dye [124]. The influence of water on the solvatochromic shift of Reichardt's dye in $[C_4mim][PF_6]$ has been investigated. The more water that is added the shorter the wavelength of the absorption maximum [104]. This had been made use of in determining water content of samples.

In general, it can be stated that imidazolium ionic liquids have α values, and hence a hydrogen bond acceptor ability, that are similar or even lower than those of aniline. The β value which describes the hydrogen bond donor ability or basicity is comparable or lower than that of acetonitrile. The polarities of pyridinium ionic liquids are lower than those of imidazolium ionic liquids. The β values are dominated by the anion. Carboxylate based RTILs have higher β values but slightly lower α values. The π* value which describes the dipolarity/polarizability is higher than for most conventional organic solvents but spans only a tiny range. The polarities of ionic liquids decrease with rising temperature [123, 125].

6.4 Cationic Coordination Compounds as Probes for Ionic Liquid Nucleophilicity

The square planar coordination compounds $[Cu(acac)(tmen)][ClO_4]$ and $[Cu(acac)(tmen)][BPh_4]$ have been used to probe the nucleophilicity and hence the donor power of ionic liquids. The cationic complex shows a good correlation between the donor number (DN) of a solvent and the absorption maximum of the lowest *d*–*d*-transition in the absorption spectrum [104]. It has also been used to determine the donor numbers of anions in solutions [126]. Studies of the solvent polarity of $[C_4mim]^+$, $[C_8mim]^+$, $[C_4mmim]^+$ and $[C_8mim]^+$ ionic liquids with $[PF_6]^-$, $[OTf]^-$ and

$[Tf_2N]^-$ showed no IL cation dependence of the *d–d*- transition of the Cu(II) cation. The $[PF_6]^-$ salts showed the lowest absorption maxima, followed by Tf_2N^- and OTf^-, indicating an increasing donor strength in the order

$$[PF_6]^- < [Tf_2N]^- < [OTf]^-.$$

It was soon realized that solvent polarity is complex as many different interactions are involved such as hydrogen bonding, π-interactions and van-der-Waals forces. A set of different probes is required to draw a conclusive picture and gives full credit to the complexity of ionic liquids with the many different types of interaction which are important, and research in this field clearly has to be continued.

References

1. Nockemann P, Binnemans K, Driesen K (2005) *Chem Phys Lett* 415:131
2. Cammarata L, Kazarian SG, Salter PA, Welton T (2001) *Phys Chem Chem Phys* 3:5192
3. Mouldoon MJ, Gordon ChM, Dunkin IR (2001) *J Chem Soc Perkin Trans* 2:433
4. Billard I, Moutiers G, Labet A, El Azzi A, Gillard C, Mariet C, Lützenkirchen K (2003) *Inorg Chem* 42:1726
5. Gordon ChM, Muldoon MJ (2008) Synthesis and purification of ionic liquids. In Wasserscheid P, Welton (eds) Ionic liquids in synthesis T, 2nd edn. Wiley, Weinheim
6. Fletcher KA, Baker SN, Baker GA, Pandey S (2003) *New J Chem* 27:1706
7. Mouldon MJ, McLean AJ, Gordon CM, Dunkin IR (2001) Chem Commun 2364
8. Huddleston JG, Willauer HD, Swatlowski RP, Visser A, Rogers RD (1998) Chem Commun 1765
9. Lancaster NL, Salter PA, Welton T, Young GB (2002) *J Org Chem* 67:8855
10. Paul A, Mandal PK, Samanta A (2005) *J Phys Chem B* 109:9148
11. Getsis A, Mudring A-V (2008) *Cryst Res Technol* 43:1187
12. Paul A, Mandal PK, Samanta A (2005) *Chem Phys Lett* 402:375
13. Chattopadhyay A, Mukherjee S (1993) *Biochemistry* 32:3804
14. Chattopadhyay A, Mukherjee S (1999) *J Phys Chem B* 103:8180
15. Chemchenko AP (2002) *Luminescence* 17:19
16. Hayashi S, Hamaguchi H (2004) *Chem Lett* 33:1590
17. Tang S, Babai A, Mudring A (2008) *Angew Chem Int Ed* 47:7631
18. Mallick B, Balke B, Felser C, Mudring A-V (2008) *Angew Chem Int Ed* 47:7635
19. Nikitenko SI, Moisy P (2006) *Inorg Chem* 45:1235
20. Nockemann P, Servaes K, Van Deun R, Van Hecke K, Van Meervelt L, Binnemans K, Görller-Walrand C (2007) *Inorg Chem* 46:11335
21. Billard I, Moutiers G, Labet A, El Azzi A, Gillard C, Mariet C, Lützenkirchen K (2003) *Inorg Chem* 42:1726
22. Mudring A-V, Babai A, Arenz S, Giernoth R (2005) *Angew Chem Int Ed* 44:5485
23. Owens GS, Durazo A, Abu-Omar MM (2002) *Chem Eur J* 8:3053
24. Mallick B (2006) Diplomarbeit, Universität zu Köln
25. Babai A, Mudring A-V (2005) *Chem Mater* 17:6230
26. Billard I, Mekki S, Gaillard C, Hesemann P, Moutiers G, Mariet C, Labet A, Bünzli J-C (2004) Eur J Inorg Chem:1190
27. Gaillard C, Billard I, Chaumont A, Mekki S, Ouadi A, Denecke MA, Moutiers G, Wipff G (2005) *Inorg Chem* 44:8355
28. Rosen DL (2006) *Appl Spectrosc* 60:1453

29. Mudring A-V, Babai A, Arenz S, Giernoth R, Binnemans K, Driesen K, Nockemann P (2006) *J Alloys Compd* 418:204
30. Arenz S, Babai A, Binnemans K, Driesen K, Giernoth R, Mudring A-V, Nockemann P (2005) *Chem Phys Lett* 402:75
31. Nockemann P, Breuer E, Driesen K, Van Deun R, Van Hecke K, Van Meervelt L, Binnemans K (2004) Chem Commun 4354
32. Lunstroot K, Driesen K, Nockemann P, Görller-Walrand C, Binnemans K, Bellayer S, Le Bideau J, Vioux A (2006) *Chem Mater* 18:5711
33. Baker GA, Baker SN, McCleskey TM (2003) Chem Commun 2932
34. Kocher J, Gumy F, Chauvin A-S, Bünzli J-CG (2007) *J Mater Chem* 17:654
35. Guillet E, Imbert D, Scopelliti R, Bünzli J-CG (2004) *Chem Mater* 16:4063
36. Puntus LN, Schenk KJ, Bünzli J-CG (2005) Eur J Inorg Chem 4739
37. Puntus LN, Zhuravlev KP, Pekareva IS, Lyssenko KA, Zolin VF (2008) *Opt Mater* 30:806
38. Nakashima T, Kwai T (2005) Chem Commun 1643
39. Nakashima T, Sakakibara T, Kawai T (2005) *Chem Lett* 34:1410
40. Bühler G, Feldmann C (2006) *Angew Chem Int Ed* 45:4864
41. Zharkouskaya A, Feldmann C, Trampert K, Heering W, Lemmer U (2008) Eur J Inorg Chem 873
42. Nunez NO, Ocana M (2007) *Nanotechnology* 18:455606
43. Driesen K, Nockemann P, Binnemans K (2004) *Chem Phys Lett* 395:306
44. Seddon KR (1999) In: Boghosian S, Dracopoulos V, Kontoyannis CG, Voyiatzis GA (eds) The International George Papatheodorou Symposium: Proceedings. Institute of Chemical Engineering and High Temperature Chemical Processes, Patras, pp 131–135
45. Reichardt C (2004) *Pure Appl Chem* 76:1903
46. Reichardt C (1988) Solvents and solvent effects in organic chemistry, 2nd edn. Wiley, Weinheim
47. Ingold CK (1969) Structure and mechanism in organic chemistry. Bell, London
48. Hughes ED, Ingold CJ (1953) J Chem Soc 244
49. Hughes ED (1941) *Trans Faraday Soc* 37:603
50. Hughes ED, Ingold CK (1941) *Trans Faraday Soc* 37:657
51. Cooper KA, Dhar ML, Hughes ED, Ingold CK, MacNulty BJ, Woolf LI (1948) J Chem Soc 2043
52. Gutmann V (1968) Coordination chemistry in non-aqueous solution. Springer, Berlin Heidelberg New York
53. Müller P (1994) *Pure Appl Chem* 66:1077
54. Reichardt C (1992) *Chem Soc Rev* 21:147
55. Reichardt C (1994) *Chem Rev* 94:2319
56. Buncel E, Rajagopal S (1990) *Acc Chem Res* 23:226
57. Marcus Y (1993) *Chem Soc Rev* 22:409
58. Dong DC, Winiik MA (1984) *Can J Chem* 62:2560
59. Karpovich DS, Blanchard GJ (1995) *J Phys Chem* 99:3951
60. Street KW Jr, Acree WE Jr (1986) *Analyst* 111:1197
61. Kalyanasundraram K, Thomas JK (1977) *J Phys Chem* 81:2176
62. Bonhote P, Dias A-P, Papageorgiou N, Kalyanasundaram K, Grätzel M (1996) *Inorg Chem* 35:1168
63. Fletcher K, Storey IA, Hendricks AE, Pandey S, Pandey S (2001) *Green Chem* 3:210
64. Aki SNVK, Brennecke JF, Samanta A (2001) Chem Commun 413
65. Bredereck K, Forster Th, Oenstein HG (1960) In: Kallman HP, Spruch GM (eds) Luminescence of inorganic and organic materials. Wiley, New York
66. Lakowicz JR (1999) Principles of fluorescence spectroscopy, 2nd edn. Kluwer, chap. 6 New York
67. Deye JF, Berger TA, Anderson AG (1990) *Anal Chem* 62:615
68. Carmichael AJ, Seddon KR (2000) *J Phys Org Chem* 13:591
69. Karmakar R, Samanta A (2002) *J Phys Chem A* 106:6670
70. Karmakar R, Samanta A (2003) *J Phys Chem A* 107:7340
71. Karmakar R, Samanta A (2002) *J Phys Chem A* 106:4447

72. Saha S, Mandal PK, Samanta A (2004) *Phys Chem Chem Phys* 6:3106
73. Ingram JA, Moog RS, Ito N, Biswas R, Maroncelli M (2003) *J Phys Chem B* 107:5926
74. Chakrabarty D, Hazra P, Chakraborty A, Seth D, Sarkar N (2003) *Chem Phys Lett* 107:5926
75. Chowdhury PK, Halder M, Sanders L, Calhoun T, Anderson JL, Armstrong DW, Song X, Petrich JW (2004) *J Phys Chem B* 108:10245
76. Karmakar R, Samanta A (2003) *Chem Phys Lett* 376:638
77. Bourlinos AB, Raman K, Herrera R, Zhang Q, Archer LA, Gianellis EP (2004) *J Am Chem Soc* 126:15358
78. Han B-H, Winnik MA, Bourlinos AB, Giannelis EP (2005) *Chem Mater* 15:4001
79. Sarkar A, Pandey S (2006) *J Chem Eng Data* 51:2051
80. Reichardt C, Harbusch-Görnert E (1983) Liebigs Ann Chem 721
81. Gutmann V (1978) The donor-acceptor approach to molecular interactions. Plenum, New York
82. Krygowski TM, Fawcett WR (1975) *J Am Chem Soc* 97:2143
83. Krygowski TM, Fawcett WR (1975) *Aust J Chem* 28:2115
84. Fawcett WR (1993) *J Phys Chem* 97:9540
85. Fawcett WR (2004) Liquids, solutions, and interfaces – from classical macroscopic descriptions to modern microscopic details. Oxford University Press, Oxford, chap 9, p 191ff
86. Taft RW, Kamlet MJ (1976) *J Am Chem Soc* 98:2886
87. Kamlet MJ, Abboud J-LM, Taft RW (1977) *J Am Chem Soc* 99:6027
88. Abboud J-LM, Kamlet MJ, Taft RW (1981) *Prog Phys Chem Org Chem* 13:485
89. Kamlet MJ, Abboud J-L, Abraham MH, Taft RW (1983) *J Org Chem* 48:2977
90. Taft RW, Abboud J-L, Kamlet ML, Abraham MH (1985) *J Solution Chem* 14:153
91. Laurence C, Nicolet P, Dalati MT, Abboud J-LM, Notario R (1994) *J Chem Phys* 98:5807
92. Marcus Y (1998) The properties of solvents. Wiley, Chichester
93. Abboud J-L, Notario R (1999) *Pure Appl Chem* 71:645
94. Chiappe C, Pieraccini D (2006) *J Phys Chem A* 110:4937
95. Crowhurst L, Mawdsley PR, Peresz-Arlandis JM, Salter PA, Welton T (2003) *Phys Chem Chem Phys* 5:2790
96. Herfort I-M, Schneider H (1991) *Liebigs Ann Chem*:27
97. Shetty P, Youngberg PJ, Kersten BR, Poole CF (1987) *J Chromatogr* 411:61
98. Poole SK, Shetty PH, Poole CF (1989) *Anal Chim Acta* 218:241
99. Harrod WB, Penta NJ (1990) *J Phys Org Chem* 3:534
100. Kaar JL, Jesionowski AM, Berberich JA, Moulton R, Russel AJ (2003) *J Am Chem Soc* 125:4125
101. Aki SNVK, Brennecke JF, Samanta A (2001) *J Chem Soc Chem Commun* 413
102. Huddleston JG, Broker G, Willauer H, Rogers RD (2002) In: Rogers RD, Seddon K (eds) Ionic liquids – industrial applications for green chemistry. American Chemical Society, Washington DC
103. Dzyuba SV, Bartsch RA (2002) *Tetrahedron Lett* 43:4657
104. Fletcher KA, Pandey S (2002) Proc Electrochem Soc 19:224
105. Chiappe C (2005) In Reichardt Ch (ed) Green Chem 7:339
106. Fletcher KA, Pandey S (2003) *J Phys Chem B* 107:7340
107. Koel M (2005) *Proc Estonian Acad Sci Chem* 54:3
108. Bartsch RA, Dzyuba SV (2003) Ionic liquids as green solvents – progress and prospects. American Chemical Society, Washington
109. Crowhurst L, Falcone R, Lancaster NL, Llopis-Mestre V, Welton T (2006) *J Org Chem* 71:8847
110. Park S, Kazlauskaus RJ (2001) *J Org Chem* 66:8395
111. Lee J-M, Ruckes S, Prausnitz JM (2008) *J Phys Chem B* 112:1473
112. Wu Y, Sasaki T, Kazushi K, Seo T, Sakurai K (2008) *J Phys Chem B* 112:7530
113. Karmakar R, Samata A (2002) *J Phys Chem A* 106:4447
114. Wasserscheid P, Gordon CM, Hilgers C, Muldoon MJ, Dunkin IR (2001) *J Chem Soc Chem Commun* 1186

115. Kaar JL, Jensionowskim JA, Berberich AM, Moulton R, Russel AJ (2003) *J Am Chem Soc* 124:4125
116. Fletcher KA, Pandey S (2002) *Appl Spectrosc* 56:1498
117. Welton T (2003) In: Wasserscheid P, Welton T (eds) Ionic liquids in synthesis. Wiley, Weinheim
118. Schroth W, Schädler H-D, Andersch J (1989) *Z Chem* 29:56
119. Spange S, Rens R, Zimmermann Y, Seifert A, Roth I, Anders S, Hofmann K (2003) *New J Chem* 27:520
120. Oehkle A, Hofmann K, Spange S (2006) *New J Chem* 30:533
121. Schreiter K, Spange S (2008) *J Phys Org Chem* 21:242
122. Reichardt Ch (2005) *Green Chem* 7:339
123. Baker SN, Baker GA, Bright FV (2001) *Green Chem* 3:210
124. Linert W, Jameson RF (1993) *J Chem Soc Perkin Trans* 2:1415
125. Lee J-M, Ruckes S, Prausnitz JM (2008) *J Phys Chem B* 112:1473
126. Linert W, Jameson RF, Taha A (1993) J Chem Soc Dalton Trans 3181

Top Curr Chem (2009) 290: 311–339
DOI: 10.1007/128_2008_35

Published online: 21 May 2009

Ionic Liquids in Biomass Processing

Suzie Su Yin Tan and Douglas R. MacFarlane

Abstract Ionic liquids have been studied for their special solvent properties in a wide range of processes, including reactions involving carbohydrates such as cellulose and glucose. Biomass is a widely available and renewable resource that is likely to become an economically viable source of starting materials for chemical and fuel production, especially with the price of petroleum set to increase as supplies are diminished. Biopolymers such as cellulose, hemicellulose and lignin may be converted to useful products, either by direct functionalisation of the polymers or depolymerisation to monomers, followed by microbial or chemical conversion to useful chemicals. Major barriers to the effective conversion of biomass currently include the high crystallinity of cellulose, high reactivity of carbohydrates and lignin, insolubility of cellulose in conventional solvents, as well as heterogeneity in the native lignocellulosic materials and in lignin itself. This combination of factors often results in highly heterogeneous depolymerisation products, which make efficient separation difficult. Thus the extraction, depolymerisation and conversion of biopolymers will require novel reaction systems in order to be both economically attractive and environmentally benign. The solubility of biopolymers in ionic liquids is a major advantage of their use, allowing homogeneous reaction conditions, and this has stimulated a growing research effort in this field. This review examines current research involving the use of ionic liquids in biomass reactions, with perspectives on how it relates to green chemistry, economic viability, and conventional biomass processes.

Keywords Biomass, Cellulose, Hemicellulose, Ionic liquids, Lignin

S.S.Y. Tan (✉) and D.R. MacFarlane
School of Chemistry, Monash University, Clayton Campus, Wellington Road,
Clayton, VIC 3800, Australia
suzie.tan@sci.monash.edu.au

Contents

Abbreviations

[Amim]	1-Allyl-3-methylimidazolium
[C_2mim]	1-Ethyl-3-methylimidazolium
[C_4mim]	1-Butyl-3-methylimidazolium
[DBU]	1,8-Diazabicyclo 5.4.0 undec-7-enium
[dca]	Dicyanamide
[BF_4]	Tetrafluoroborate
[PF_6]	Hexafluorophosphate

1 Introduction

The world is currently undergoing major change due to global warming, rapid development in countries such as China and India, and a human population which is continuously increasing to unprecedented levels. As a result, increasing pressure has been placed on resources such as fuels, food, raw materials, water, and the natural

environment [1–5]. Since the industrial revolution, economic growth has been the main incentive of most countries, underpinned by advances in the chemical industries. Although environmental concerns have come behind profitability and convenience, pollution such as carbon dioxide emissions is beginning to be attributed a monetary cost, due to the growing reality of climate change. The European Union has had an emissions trading scheme since 2005 [6], the Australian government recently released a framework for a carbon emissions trading scheme due to commence in August 2010 [7], while many other countries including Japan, Canada and New Zealand have set targets to reduce emissions [8].

However, according to climate scientists, the world may soon be approaching greenhouse gas levels dangerously close to "tipping points", beyond which nothing can be done to reverse an accelerated warming [9–15]. The predicted effects of this would be a massive rise in sea levels, extreme weather conditions and widespread extinction of animal and plant species [16].

The realisation that chemical pollution from industry is having a profound effect on the environment of the planet has led to a movement to use chemical knowledge and advances to mitigate these negative effects. According to Anastas et al. [17], green technologies will help to address some of the world's most pressing environmental issues, including "global climate change, sustainable energy production, food production and the associated agricultural practices, depletion of non-renewable resources, and the dissipation of toxic and hazardous materials in the environment". One of the aims of green chemistry is the prevention of waste [18], which includes waste released to air, water and land. Another aspect is that energy requirements should be recognised for their environmental and economic impacts, and should be minimised; thus synthetic methods should be conducted at ambient temperature and pressure where possible [18]. Most relevant to biomass processing is the principle that a raw material or feedstock should be renewable rather than depleting wherever technically and economically practicable [18].

For all of these reasons, there has been a rapid intensification of efforts in recent years to develop processes that will allow us to utilise a variety of plant materials, biomass, as a source of chemicals and liquid fuels. Ionic liquids have been widely investigated as solvents for these processes because of some of the unique properties that they possess. The goal of this overview therefore, is to survey and discuss recent developments in the use of ionic liquids in this extremely important field of biomass processing.

2 Biomass as a Source of Chemicals and Fuels

2.1 Lignocellulose

Lignocellulosic biomass refers to plant-derived material such as bagasse, corn stover, wheat straw, rice straw, wood chips and switch grass. It is an abundant and renewable resource which is also potentially carbon-neutral and potentially economically viable if appropriate processing methods can be developed to extract and

separate the various valuable components. Depletion of petroleum supplies combined with global warming caused by burning fossil fuels has resulted in widespread efforts to use biomass as an alternative chemical feedstock for fuels and other commodity chemicals [19–21].

Despite the variety of sources, all lignocellulosic material is composed primarily of cellulose, hemicellulose and lignin [22]. Agricultural wastes such as bagasse, corn stover and wheat straw are thus a relatively cheap source of these three biopolymers. The major challenge to using lignocellulosic biomass as a feedstock is the development of cost-effective methods to separate, refine and transform it into chemicals and fuels [20].

The production of multiple products is generally seen as necessary to increase the economic viability of biomass conversion. This is encapsulated in the concept of a "biorefinery", which according to the National Renewable Energy Laboratory (NREL) is "a facility that integrates conversion processes and equipment to produce fuels, power and chemicals from biomass" [23]. Examples of chemicals that can be produced from biomass include ethanol, methanol, furfural, paper, lignin, vanillin, lactic acid, dimethylsulfoxide and xylitol. In many cases, using biomass as a feedstock for chemical production requires an initial step to separate or fractionate the three main components into usable fractions [20, 22]. This also maximises the usage of the different biomass components.

2.2 The Carbon Economy

The world currently derives most of its energy from fossil fuels such as petroleum, natural gas and coal, which are finite resources, and produce CO_2 upon burning. The burning of plant material, or fuels derived from plant material, also produces CO_2 but this is offset by the fact that carbon contained in plant material is formed by photosynthesis, which involves taking up CO_2 from the atmosphere, and occurs in a much shorter time frame than the millions of years required to produce fossil fuels. Currently, the world's most widely used biofuel is ethanol, which is produced through fermentation of sugars from corn syrup in the US, sugar cane juice or molasses in Brazil and wheat starch or sugar cane molasses in Australia. The question of whether biofuel use is beneficial for reducing greenhouse gases is compounded by factors such as fossil fuels being used in the production of biofuels, N_2O released during farming of biofuel crops [24], CO_2 released during the fermentation process, and rainforest that may have been cleared to grow crops for biofuels [25, 26]. From both an environmental and economic point of view, it is thus important to consider the carbon economy, monetary cost and environmental impact of not just the beginning and end-products, but also the processes which go into making the end-products.

2.3 Cellulose

Cellulose is a polymer composed of glucose units linked by β-1,4-glycosidic bonds (Fig. 1). Its linear structure is strengthened by hydrogen bonding and van der Waal's forces between chains, resulting in a crystalline structure [27].

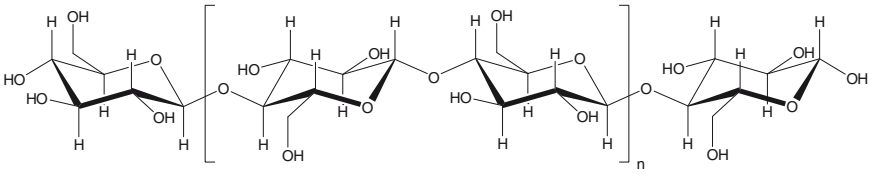

Fig. 1 Cellulose

Due to its high crystallinity, cellulose is much more resistant to depolymerisation than hemicellulose or lignin. Glucose from the hydrolysis of cellulose is a potential substrate for fermentation to produce a large variety of chemicals including ethanol, lactic acid, succinic acid, furmaric acid, malic acid, itaconic acid, citric acid, 3-hydroxypropanoic acid, 1,3-propanediol, glycerol, lysine, glutamic acid, penicillin, ascorbic acid and riboflavin [28–30]. Glucose can also be chemically converted to 5-hydroxymethylfurfural, levulinic acid, gluconic acid, glucaric acid, 2,5-furan dicarboxylic acid and sorbitol [28, 29].

2.4 Hemicellulose

Hemicellulose refers to the non-cellulosic polysaccharides that exist within plant cell walls (Fig. 2). It is an amorphous polymer consisting of xylose, arabinose, glucose, galactose and mannose, all of which are highly substituted with acetic acid [31]. The structure of hemicellulose varies depending on plant species, but a large component is usually xylan, with smaller amounts of glucomannan, galactan, glucan, xyloglucan, arabinan, arabinogalactan and glucuronomannan [27]. Xylose from the hydrolysis of hemicellulose is currently used to produce furfural and xylitol. Other useful intermediate products from xylose are levulinic acid, dithioacetal, xylal, hydroxy-xylal esters and pyrazole or imidazole *N*-heterocycles [29].

2.5 Lignin

Lignin is a high molecular weight branched polymer based on phenylpropane units, with carbon–carbon and ether linkages. The three main building blocks of lignin are guaiacylpropane, syringylpropane and *p*-hydroxyphenylpropane (Fig. 3), which are present in varying amounts depending on plant source [33]. Lignin is potentially a renewable source of aromatic compounds if an economic means of extracting and depolymerising it can be developed. The presence of lignin within lignocellulose is a major barrier to enzymatic hydrolysis of cellulose by cellulases [21, 34, 35], and the degradation of lignin during depolymerisation processes also forms phenolic compounds which inhibit fermentation [36, 37]. Hence the presence of lignin diminishes the value of lignocellulosic materials as sources of chemicals.

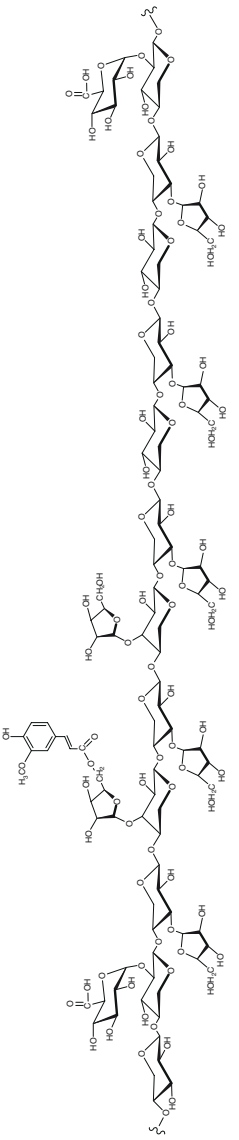

Fig. 2 Hemicellulose (xylan backbone with arabinose, glucuronic acid and feruloyl groups) [32]

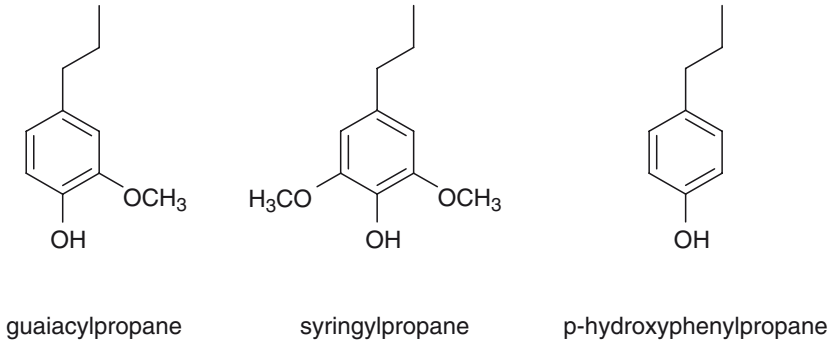

Fig. 3 Building blocks of lignin

Due to its structural heterogeneity and extensive carbon–carbon cross-linking (Fig. 4), lignin is the most recalcitrant of the three lignocellulosic components [22].

The chemical structure of extracted lignin depends on the process used for its extraction, and also determines which applications it can be used in. Both kraft lignin and lignosulfonates from the sulfite process contain sulfur. Most of the lignin extracted by the kraft process is burned to produce energy. Current applications for water-insoluble kraft lignin in polymers include as fillers in thermoplastics, coreactants for thermoplastics, and coreactants in thermosetting phenolic, epoxy and polyurethane resins [38]. Water-soluble lignosulfonates are used as dispersants, emulsifiers and surfactants in a wide range of applications [39]. Low molecular weight products of lignin include vanillin and dimethylsulfoxide [33].

3 Biomass Conversion Processes

3.1 Thermochemical Processes

The oldest method of using biomass to create energy is direct combustion, which has been used for thousands of years. Other thermochemical techniques which can be used for the production of chemicals from biomass usually involve depolymerisation at elevated temperatures and pressures. Among these are gasification, pyrolysis, liquefaction and acid hydrolysis.

Gasification, which involves heating a carbon containing substrate (coal, petroleum, biomass or municipal waste) to 500–1, 100 ºC at 1–10 bar under controlled oxygen conditions, produces a mixture of CO and H_2 (with smaller amounts of CO_2, CH_4 and N_2), which may be catalytically converted into hydrocarbons (via Fischer Tropsch), methanol or hydrogen [31, 41]. A major advantage of gasification

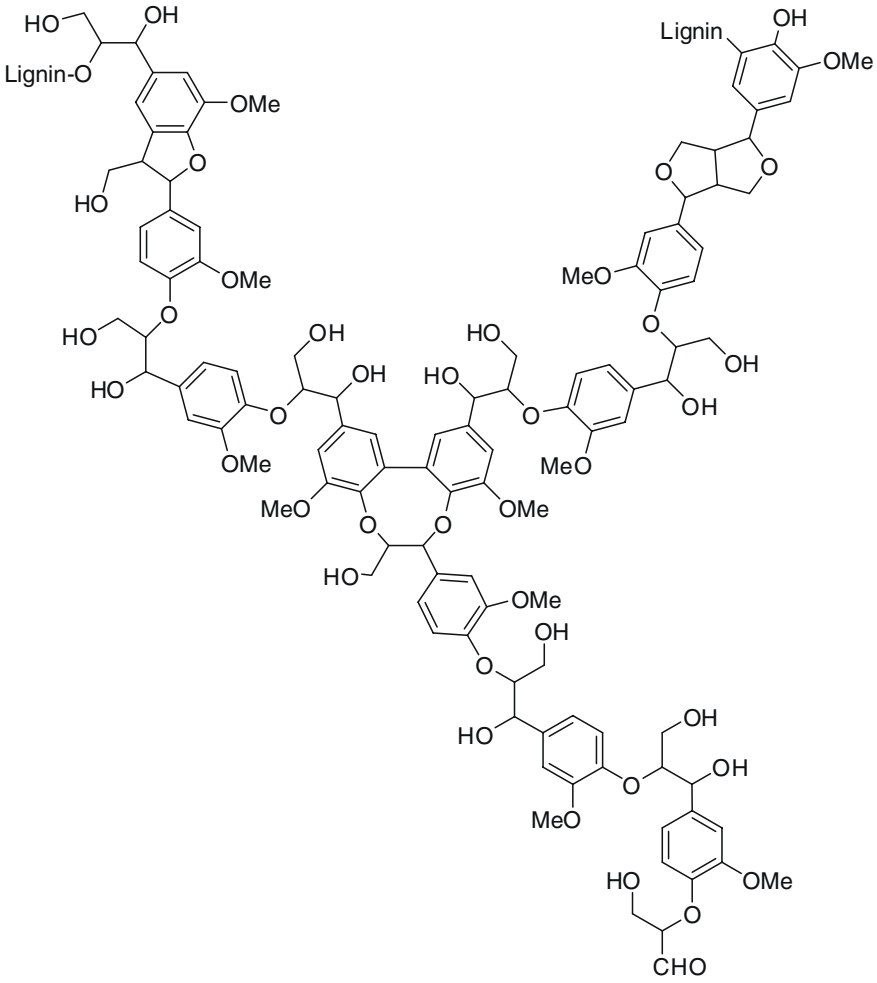

Fig. 4 Proposed structure of softwood lignin showing the functional groups thought to be present [40]

over the hydrolysis of cellulose and hemicellulose to fermentable sugars is that gasification also converts the lignin component.

Pyrolysis and liquefaction of biomass can be used to produce bio-oils, which are mixtures containing up to 400 compounds including acids, alcohols, aldehydes, esters, ketones and aromatic compounds [31, 42]. Bio-oils can be used as boiler fuel or in chemical production. Pyrolysis occurs at 375–525 °C and 1–5 bar in the absence of oxygen. Liquefaction occurs at 250–325 °C and 50–200 bar [31].

Depolymerisation of cellulose to glucose for fermentation has traditionally been achieved via dilute acid hydrolysis using sulfuric acid, with commercial plants

operating since the 1930s [43]. Reaction temperatures vary up to 230 °C for short reaction times. However, this method is now largely unpopular and is used only as a pretreatment for enzymatic hydrolysis [44]. The inherent problem with dilute acid hydrolysis is the decomposition of sugars at the high temperatures required, especially since the activation energy for sugar decomposition is lower than that for hydrolysis of cellulose [44].

The Biofine process produces levulinic acid, furfural and formic acid from lignocellulose in a two-step process using dilute sulfuric acid as a catalyst [45]. The first step depolymerises the polysaccharides and converts the resulting 6-carbon sugars into hydroxymethylfurfural by a dehydration reaction at 210–220 °C and 25 bar. The second step converts hydroxymethylfurfural to the products at 190–200 °C and 14 bar (Scheme 1).

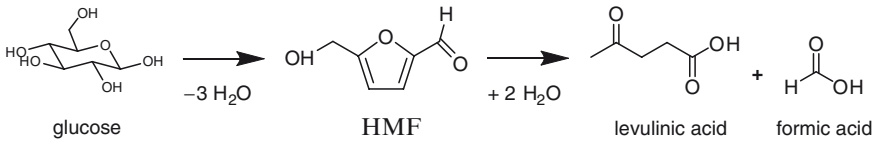

Scheme 1 Glucose decomposition reactions

3.2 Lignin Extraction Processes

Traditional methods of extracting lignin from lignocellulose are industrial processes for the production of papermaking pulp from wood chip and other fibres. These methods consist of the widely used kraft process as well as the sulfite, soda, and organosolv processes. In almost all cases except organic acid pulping, the process requires high pressures and therefore capital intensive plant. The kraft process, which accounts for 80% of chemical pulping [27], consists of treating wood chips or other lignocellulosic material with aqueous sodium hydroxide and sodium sulfide at temperatures around 165 °C and pressures around 0.7 MPa [46]. The high temperature (and therefore high pressure) processing is required in part because the glass transition temperature of lignin is around 150 °C. The main disadvantages associated with the kraft process are pollution and odour problems, high water use and the fact that it is only economical at a capacity of 1,000 tons of pulp per day or more [47].

Newer methods of fractionating biomass using phosphoric acid [48] or acetic acid and formic acid [49] under mild conditions have also been reported, but corrosiveness of the acids would be a major drawback, and the processes have not yet been fully proven in terms of energy usage, solvent recovery, etc.

Hydrotropic pulping, which was patented by McKee in 1943 [50–52], involves the use of sodium xylenesulfonate (30–40%) in aqueous solution at temperatures between 150 and 180 °C and pressures between 0.4 and 1.4 MPa. As with the traditional pulping methods, the initial step in hydrotropic pulping involves hydrolytic

fragmentation of the lignin, followed by solubilisation of the lignin fragments. After reaction at high pressure, the lignin dissolved in hydrotropic solution is precipitated by dilution with water. Hydrotropic agents for lignin typically contain both polar and non-polar groups which enable them to solubilise the lignin via formation of both strong ion-dipole bonds with water as well as interacting strongly with the lignin through, for example, π–π interactions [53]. It has also been suggested that they form micelles that envelop the lignin fragments [54].

3.3 Enzymatic Processes

Enzymes are proteins produced by living organisms for catalysing specific reactions, such as breaking down a polymer or synthesising a chemical. Enzymatic processes are likely to be an essential part of the production of chemicals from biomass due to their potential for high specificity [55].

The use of cellulases for biomass conversion has undergone a large amount of research and improvement over the last 20 years [56]. Cellulases are enzymes which are able to depolymerise cellulose to glucose at much higher yields than acid hydrolysis. However, the kinetics of cellulase-catalysed hydrolysis is slow due to several factors, mainly the high crystallinity of cellulose and the presence of lignin and hemicellulose [21, 57]. Currently, the most efficient reaction mode for the use of cellulases in ethanol production is simultaneous saccharification and fermentation (SSF), which involves cellulose hydrolysis by cellulases with simultaneous fermentation of sugars by yeast. This prevents sugars from accumulating and inhibiting the end product [58]. The high cost of cellulases is still a major hurdle for industrial application [59].

Microbial fermentations involving yeast, bacteria or fungi have the potential to produce fuels and platform chemicals, which may be too complicated, too expensive or impossible to be synthesized chemically [28, 29, 55]. Most fermentations require sugars such as glucose, fructose and sucrose as substrates. Gasification products, CO and H_2, can also be used as substrates for fermentation by mesophilic microorganisms to give short-chain fatty acids or alcohols, including ethanol [60, 61].

4 Ionic Liquids in Biomass Conversion Processes

4.1 Ionic Liquids as Green Solvents

4.1.1 Properties

Characteristics which contribute to the low melting points of ionic liquids are large cations and anions with low symmetry and delocalised charge [62], often featuring an aromatic or cyclic structure and long alkyl chains. Many ionic liquids have negligible vapour pressure [63], and are non-flammable [64, 65]. They can also be

designed to have high thermal stability [66], high conductivity [67] and low toxicity [68, 69]. However, the fallacy of attributing these characteristics to the class of ionic liquids as a whole has been demonstrated by the existence of many ionic liquids which do not have these properties [70]. For example, ionic liquids have been found to be distillable under reduced pressure [71–74], while some have been found to be combustible under certain conditions [64, 65], and ionic liquids displaying low conductivity are thought to participate in ion-pairing or ion aggregation [75].

An important property of an ionic liquid in terms of its applications in biomass processing is its thermal stability, which is usually measured by thermogravimetric analysis. Nucleophilicity of the anion has been found to have an effect on the thermal stability of many ionic liquids due the role of the anion in the degradation of the cation [76]. Quaternary ammonium, imidazolium, phosphonium and pyrrolidinium cations degrade at lower temperatures in the presence of highly nucleophilic anions such as halides due to Hoffman elimination and reverse Menschutkin reactions [76–79].

Hydrophobicity or hydrophilicity is also an important property, which can be controlled by selecting an appropriate cation and anion combination. Longer alkyl chains on the cation have been found to result in increased hydrophobicity [80, 81]. Hydrophobicity also depends on the identity of the anion. For example, ionic liquids containing fluorinated anions such as tetrafluoroborate and hexafluorophosphate are considerably more hydrophobic than the halide salts of the same cation. Ionic liquids containing the bis(trifluoromethanesulfonyl)amide anion [NTf_2] are extremely hydrophobic whereas their non-fluorinated analogues are sometimes completely miscible with water [82]. The immiscibility of the ionic liquid with water or other solvents may be useful for phase separations, but it also has implications on the "greenness" of the ionic liquid in the event of accidental release into the environment [80].

4.1.2 Advantages as Solvents

The property of ionic liquids which has led to them being classed as "green solvents" is that most of them have very low vapour pressure at ambient temperatures and hence do not emit volatile organic compounds (VOCs) [83–85]. Their non-volatility also allows the recovery of products by distillation.

Increased reactivity has been observed in reactions where the ionic liquid acts as an acid or base catalyst [86, 87]. Lewis acidic ionic liquids containing the chloroaluminate anions $AlCl_4^-$ and $Al_2Cl_7^-$ have been successfully used as acid catalysts in a range of reactions including Friedel-Crafts [88–90], dimerisation, cracking and isomerisation reactions [89]. Besides the chloroaluminates, ionic liquids with higher stability in the presence of water have also been used as acid catalysts [91, 92]. The basic ionic liquid [C_4mim][OH] has been used as a base catalyst in organic reactions including the Markovnikov addition of *N*-heterocycles to vinyl esters [93], Knoevenagel condensation of aliphatic and aromatic carbonyl compounds [94], and Michael addition and alkylation of active methylene compounds [95].

The hydrophobicity or hydrophilicity of an ionic liquid can be used to create two or more discrete phases in the presence of other solvents, allowing multiphasic

reaction [96, 97]. This can be extremely useful for the recovery of catalyst, as well as extraction of product into a separate phase.

Many ionic liquids have a wide liquid range, up to 400 °C in some cases [98]. This allows great kinetic control of processes and may be useful for temperature dependent separation techniques such as precipitation or crystallisation [99].

4.1.3 Industrial Application Issues

Although ionic liquids are often cited as "green solvents" due to their ability to reduce atmospheric pollution there are many other issues such as toxicity, cost, corrosiveness, recyclability, auxiliary solvents and final disposal, which would influence their actual application in industry [96]. Besides being effective in the desired reaction, solvents, in general, should be easily separable from the product, and easily recycled for further use. Cleaning up ionic liquids for recycle will require different methods due to their low volatility. Toxicity testing [100–102] and lifecycle analysis [103–105] provide valuable and necessary information on the impact of the ionic liquid. In spite of these issues, more and more ionic liquids are being applied in industrial processes, where they afford significant benefits in terms of efficiency, economics and reducing environmental impact [106–110]. The BASIL process, which was the first industrial ionic liquid process to be publicised, involves the use of 1-methylimidazole to remove HCl by the formation of 1-*H*-3-methylimidazolium chloride as a separate phase, concurrently giving a large increase in reaction rate and yield due to 1-methylimidazole acting as a base catalyst [108–110]. The Difasol process for dimerisation of alkenes in chloroaluminate ionic liquid takes advantage of biphasic operation, and features better dimer selectivity, better catalyst use, higher yield and smaller reactor size [82, 110–112].

4.2 Dissolution of Biopolymers in Ionic Liquids

4.2.1 Dissolution of Carbohydrates in Ionic Liquids

Ionic liquids have been used to dissolve a range of carbohydrates, including glucose, cellulose, sucrose, lactose, amylose, agarose, α-cyclodextrin and β-cyclodextrin [86, 113–118]. Based on work conducted in our own laboratory, dicyanamide ionic liquids [C_2mim][dca] and [C_4mim][dca] were found to dissolve glucose to greater than 10 wt% at room temperature [99, 113]. Disaccharides (e.g. sucrose) and trisaccharides (e.g. raffinose) were also soluble, but to lower concentrations than glucose. The high ability of dicyanamide ionic liquids in dissolving glucose is attributed to the donor solvent properties caused by the Lewis basicity of the dicyanamide anion [99]. Ionic liquids with the acetate anion were also found to be effective in glucose solvation [86]. An investigation of carbohydrate solubility in ionic liquids for the purpose of enzyme-catalysed transformations showed that

[C_4mim][dca] dissolved glucose to 211 and 405 g L^{-1} at 40 and 75 °C, respectively, and sucrose to 195 and 282 g L^{-1} at 25 and 60 °C, respectively [116].

Interestingly, ionic liquids containing an ether group in the side chain of the imidazolium cation were found to be effective in dissolving carbohydrates including glucose, α-cyclodextrin, amylose and agarose [114]. Glucose dissolved to 450 mg mL^{-1} and α-cyclodextrin to 350 mg mL^{-1} with heating in the ether-containing imidazolium bromide ionic liquids, where the solvating ability was attributed to the ether group [114].

According to a molecular dynamics simulation, solvation of glucose in 1,3-dimethylimidazolium chloride involves mainly interaction between the anion and glucose, whereas the cation only weakly interacts with the sugar [119]. Chloride ions, which hydrogen bond to the hydroxyl groups of glucose, were said to form a primary solvation shell around the perimeter of the glucose ring. Only a small presence of the cation was found, with the association occurring due to the weakly acidic hydrogen at the 2-position of the imidazolium ring interacting with the oxygen atoms of the secondary sugar hydroxyls.

Cellulose has been found to dissolve in a range of ionic liquids, the most well-known being 1-butyl-3-methylimidazolium chloride ([C_4mim][Cl]) [117, 118]. Other ionic liquids used in cellulose dissolution include 1-allyl-3-methylimidazolium chloride [120, 121], 1-ethyl-3-methylimidazolium acetate [122, 123], 1-ethyl-3-methylimidazolium methylphosphate [124] and 1,3-dialkylimidazolium formates [125]. The dissolution of cellulose in [C_4mim][Cl] is attributed to disruption of hydrogen bonding and coordination of chloride ions to the hydroxyl groups of cellulose [126]. Cellulose can be dissolved in [C_4mim][Cl] up to a concentration of 10 wt% at 100 °C and up to 25 wt% with microwave heating [118]. Low moisture is required, typically below 1%, as water interferes by coordinating to the chloride ions. Separation is easily achieved by the addition of water or other solvents (methanol, ethanol, acetone, dichloromethane, chloroform, etc.) which causes cellulose to precipitate in relatively pure form.

4.2.2 Dissolution of Wood in Ionic Liquids

Dissolution of wood using [C_4mim][Cl] has also been reported [127–129]. Based on the same mechanism of cellulose dissolution, the dissolution of wood also requires the virtual absence of water, which necessitates extensive drying of the wood, small particle size, drying of the ionic liquid, and reaction under an inert atmosphere. Long dissolution times are usually required unless microwave heating is used.

4.2.3 Dissolution of Lignin in Ionic Liquids

A study on lignin solubility in ionic liquids has shown that up to 20 wt% kraft wood lignin can be dissolved in 1,3-dimethylimidazolium methylsulfate, 1-butyl-3-methylimidazolium methylsulfate and 1-hexyl-3-methylimidazolium

trifluoromethanesulfonate [130]. In one of their patents, BASF reports the dissolution of lignin, cellulose and wood in a range of ionic liquids containing 1,8-diazabicyclo[5.4.0]undec-7-enium or [DBU] as the cation and anions including chloride, formate, methanesulfonate, acetate, tosylate, trifluoroacetate, saccharinate, hydrogensulfonate, lactate, thiocyanate and trifluoromethanesulfamate [131].

4.2.4 Dissolution of Other Biopolymers in Ionic Liquids

Ionic liquids have also been used to dissolve other biologically occurring polymers. Wool keratin, an unbranched polymer of amino acids, has been reported to dissolve in [C_4mim][Cl] up to a concentration of 11 wt% at 130 °C. Chitin has been dissolved in [C_4mim][Ac] up to 6 wt% at 110 °C [132]. Proctor and Gamble has a patent on ionic liquids for the dissolution of biopolymers including chitin, chitosan, elastin, collagen, keratin and polyhydroxyalkanoate [133].

4.3 Advantages of Ionic Liquids in Biomass Conversion Processes

One of the main advantages of ionic liquids in biomass processing is their non-volatility (in many cases), which allows reaction at ambient pressure. This is quite significant as pressurised equipment forms a major part of the capital cost of a delignification plant. For example, the kraft process is only economical at large plant size due to capital cost of equipment [47]. In the case of agricultural wastes it would be better to have smaller processing plants situated within a region of supply due to the relatively high cost of transporting the low-density material. Thus the use of ionic liquids would be a low capital cost alternative that is more likely to be cost-effective at smaller throughput.

Ionic liquids are able to dissolve carbohydrates to high concentrations as mentioned in the previous section. The use of ionic liquids in cellulose dissolution and functionalisation is particularly significant considering the problems associated with conventional processes such as the cupramonium and xanthate processes [117, 118, 120, 134–136]. Lignin is soluble in ionic liquids, as discussed in Sect. 4.2.

The inherent basicity or acidity of various ionic liquids allows them to perform as combined solvents and catalysts, with no requirement for additional expensive transition metal catalysts [86, 99, 113]. If a non-ionic liquid catalyst is used, immobilisation of the catalyst in an ionic liquid phase would potentially allow easy separation of the product and recycling of the catalyst.

4.4 Application Issues

The challenges of using an ionic liquid in a biomass process are general to using an ionic liquid in any process, i.e. designing an effective ionic liquid with low toxicity,

thermal stability and efficient separation of products and co-solvents, recycling of ionic liquid, etc. An added difficulty, which is common to biomass conversion in general, is the high reactivity and heterogeneity of biomass, which results in the formation of a great variety of decomposition products from cellulose, hemicellulose and lignin. The high degree of oxygenation of carbohydrate substrates causes them to undergo dehydration reactions under thermal cracking conditions [137]. Although the non-volatility of ionic liquids allows distillation of reaction products, this may not be feasible in the case of temperature-sensitive and highly reactive biomass products.

4.5 Base-Catalysed Reactions

Ionic liquids containing the dicyanamide anion were shown to be excellent solvents and base catalysts for the *O*-acetylation of glucose and other alcohols [86, 99, 113]. Glucose was acetylated in [C_4mim][dca] with no added catalyst at room temperature, giving 89% yield after 12 min [113]. An even higher yield of 98% was obtained at 50 °C after 6 min (Scheme 2).

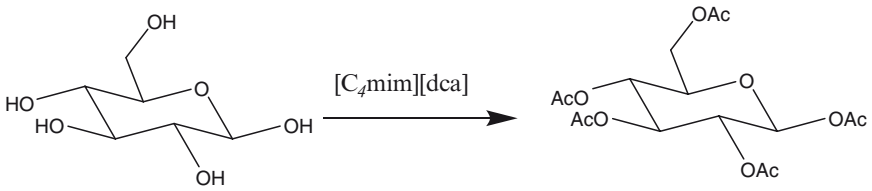

Scheme 2 *O*-acetylation of glucose in [C_4mim][dca]

4.6 Acid-Catalysed Reactions

A study on HCl-catalysed hydrolysis of lignocellulose in [C_4mim][Cl] reported yields of total reducing sugars of up to 81% [138]. Notably, the lignocellulosic materials used were ground to 40 mesh (420 μm) and dried at 90 °C under vacuum for 3 days prior to hydrolysis in order to facilitate dissolution into the ionic liquid. The method used for measuring total reducing sugars was a non-standard spectrophotometric method, as the sugars had not been separated from other components including lignin and ionic liquid. BASF holds a patent which covers a range of ionic liquid cations and anions for acid-catalysed hydrolysis of cellulosic materials [139].

A method for depolymerisation of cellulose in [C_2mim][Cl] using solid acid catalysts produced cellulose oligomers in high yield, which are readily precipitated by the addition of water [209]. The advantage of this method was that it avoided

producing water-soluble molecules such as monosaccharides and dehydration products, which are difficult to separate from the ionic liquid. The catalyst was a sulfonated resin which is inexpensive and has a high selectivity for producing cellulose oligomers.

Acid-catalysed depolymerisation of cellulose and hemicellulose in pine wood using [C_2mim][Cl] produces a range of water-soluble products such as monosaccharides, oligosaccharides, furfural and hydroxymethylfurfural, with 97% conversion of cellulose after 2 hours at 120 °C [210]. Maximum yields of 11% monosaccharides, 3% hydroxymethylfurfural and 0.5% furfural were reported, however, separation of products was acknowledged to be a major problem for practical application, considering the polarity of both the products and the ionic liquid.

4.7 Metal-Catalysed Reactions

5-Hydroxymethylfurfural (HMF), a promising intermediate for chemical production [140], can be produced from glucose (Scheme 1) and fructose by dehydration. Conversion of fructose to HMF using 1-*H*-3-methylimidazolium chloride as both catalyst and solvent was reported to result in 92% yield after only 45 min [141]. The conversion of the more abundant substrate, glucose, often results in poor selectivity, but it was successfully converted with 70% yield using a chromium(II) chloride catalyst in [C_2mim][Cl] [142, 143]. The patented method includes monosaccharides, disaccharides and polysaccharides as substrates [143].

Using a method similar to the immobilised catalyst-ionic liquid systems of Chauvin, Olivier–Bourbigou and Wasserscheid, a team at NREL attempted to create a chemical process to acetylate sugars using vanadium(IV) compounds vanadyl(IV) acetate and VO(salen) as Lewis acid catalysts immobilised in ionic liquids [C_4mim][Cl] and [C_4mim][PF_6] [137]. However, yields seemed to be limited by the by-product acetic acid, and there were difficulties in extracting the product, which did not phase separate as desired and had to be extracted using organic solvents such as chloroform. This caused problems due to the extraction of catalyst into the organic phase, but successful immobilisation and recycling of a less effective and less stable dichlorovanadium(IV) complex was achieved. The same group at NREL also attempted to acetylate the lignin model compound, veratryl alcohol using the same catalyst, vanadium(IV) acetate in [C_4mim][PF_6] [137]. Although the acetylation did not occur, a surprising result was the formation of tricycloveratrylene, possibly due to the formation of a benzyl cation.

4.8 Enzyme-Catalysed Reactions

Although water is the natural medium for enzymes, organic solvents are widely used to improve the solubility of hydrophobic reactants or products, and to shift

equilibria away from hydrolysis to synthesis [144]. The advantage of ionic liquids in this application is their non-volatility and, in some cases, their ability to enhance the stability, activity and stereoselectivity of enzymes [145–148]. The lipase *Candida antarctica* has been used to catalyse alcoholysis, ammoniolysis, and perhydrolysis reactions in ionic liquids [C_4mim][BF_4] and [C_4mim][PF_6] with reaction rates comparable with or better than rates observed in organic media [149]. Using ionic liquids to carry out enzymatic reactions of carbohydrates could have an additional benefit considering the low solubility of carbohydrates in organic solvents.

Lipase-catalysed esterification of sucrose in [C_4mim][dca] with decanoic acid was reported but not much information was given on conversions [116]. Enzymatic acylation of levoglucosan, an anhydro-sugar produced by pyrolysis of biomass, using *Candida antarctica* lipase in 1-methoxyethyl-3-methylimidazolium dicyanamide, gave 61% yield after 5 days at 50–60 °C [150].

The use of cellulases in ionic liquids has been investigated; however, one study showed that cellulase from *Trichoderma reesei* was inactivated by ionic liquids such as [C_4mim][Cl] due to unfolding caused by the high ionic strength of ionic liquids [151]. Successful enzymatic saccharification of cellulose was demonstrated using [C_2mim] diethylphosphate, which seemed to work best at an IL:water ratio of 1:4, giving a 55% yield of glucose after 24 h [152]. Two subsequent patents by BASF involve the use of ionic liquids containing polyatomic anions for enzyme-catalysed hydrolysis of cellulose to glucose [153, 154].

Enzymes which oxidise lignin, including laccases and lignin peroxidases, help to break lignin down by catalysing the cleavage of ether bonds and carbon–carbon bonds in alkyl or aryl groups [155], but have been found to be non-specific in terms of product distribution [22]. Studies on the catalytic activity of lignin-oxidising enzymes in aqueous solutions containing ionic liquids have recently been reported, showing that addition of specific amounts of ionic liquid has the ability to increase catalytic activity compared to reaction in pure water [156–158].

4.9 Cellulose Modification

A broader exploitation of cellulose solubility in ionic liquids lies in modification of cellulose into more useful forms. Cellulose acetate is currently the most useful derivative of cellulose, with uses in photographic film, as a synthetic fibre and as a component of adhesives. Acetylation of cellulose has been carried out effectively in 1-allyl-3-methylimidazolium chloride [Amim][Cl], [C_4mim][Cl], [C_2mim][Cl], 1-butyl-2,3-dimethylimidazolium chloride [C_4dmim][Cl] and 1-allyl-2,3-dimethylimidazolium bromide [Admim][Br] [136, 159–162]. The first report of cellulose acetylation in an ionic liquid involved a one-step reaction in [Amim][Cl] without catalyst, yielding cellulose acetate with a controllable degree of substitution [136]. Yields of cellulose acetate of up to 86% have been obtained via reaction in [C_4mim][Cl] at 80 °C for 2 h [160].

More recently, Eastman Chemical Company published three patents involving the use of ionic liquids containing carboxylate anions for cellulose acetylation [163–165]. Ionic liquids with carboxylate anions resulted in faster acetylation of cellulose at lower temperatures relative to the rate in ionic liquids with the same cation and a chloride anion. Transition metals such as zinc were found to be good catalysts for the acetylation of cellulose in ionic liquids [164].

Ionic liquids have also been used as solvents in other cellulose derivatisation reactions including etherification [166], carboxymethylation [160], phthalation [167, 168], sulfation [169], sulfonation [169], carbanilation [159, 162], silylation [170], succinylation [171], tritylation [172] and tosylation [173].

The formation of cellulose composites containing analytical reagents, magnetite, polyacrylonitrile or enzymes has been found to be possible by dissolution of cellulose and the additional species in an ionic liquid, followed by precipitation using an anti-solvent [174–180]. This opens up a diverse new range of applications for cellulose composite materials, including structural, sensing, separations and catalysis applications. Composite materials have also been produced from the dissolution of cellulose in a polymerisable ionic liquid consisting of an imidazolium cation with styrene-like side chain [181].

4.10 Cellulose Pretreatment

One of the barriers to cellulose hydrolysis by cellulases is the high crystallinity of cellulose in its native form. The regeneration of cellulose after dissolution in ionic liquids results in cellulose of amorphous form. Microcrystalline cellulose was found to be hydrolysed 50–90 times faster by cellulases following regeneration after dissolution in [C_4mim][Cl] or [Amim][Cl] [182], which indicates that dissolution of cellulose in an ionic liquid may be useful as a pretreatment method.

4.11 Thermochemical Depolymerisation

Pyrolysis of cellulose using dicationic imidazolium chloride or bromide was reported to produce anhydrosugars including levoglucosenone at 180 °C [183] (Scheme 3). Although the isolated yield of levoglucosenone was low, the dicationic ionic liquids showed higher thermal stability than [C_4mim][Cl] under the same pyrolysis conditions. A recent patent describes pyrolysis of lignocellulose in ionic liquids [184]. The patent covers the use of a range of ionic liquids, including [Amim][Cl], in partially dissolving lignocellulose for anaerobic reaction at 150–300 °C to give various products including pyrolysis oil, levoglucosenone, levulonic acid, levulinic acid, hydroxymethylfurfural, furfural or 2-methylfurfural. The products were isolated in three main forms – a distillate fraction, a tar fraction and a char fraction. The advantage of using ionic liquids in this application was said to be the

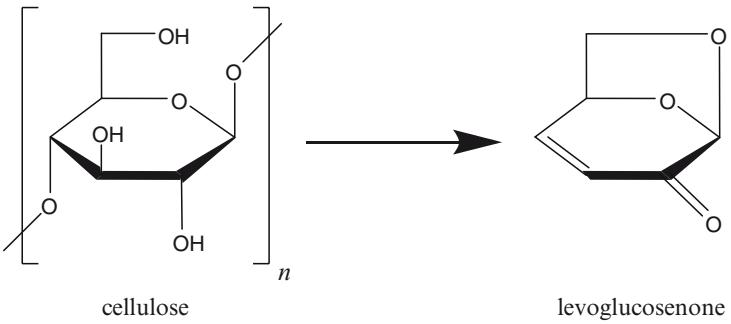

Scheme 3 Production of levoglucosenone from cellulose by pyrolysis

substantial swelling and partial dissolution of lignocellulose in ionic liquids under mild conditions, allowing more homogeneous reaction.

Degradation of dissolved cellulose in ionic liquids including [C_4mim][Cl] with the aid of nucleophiles such as 2,4-dinitrophenylhydrazine has been patented by BASF [185], where the aim was to decrease the degree of polymerisation of cellulose. A different BASF patent describes degradation of cellulose by dissolution and heating in ionic liquids such as [C_4mim] hydrogensulfate, with the optional presence of water [186].

A patent on the production of dihydroxymethylfuran for use as a biofuel describes the hydrolysis and dehydration of carbohydrates such as sugar, cellulose or starch, followed by hydrogenation in an ionic liquid such as [C_4mim][Cl] [187]. Another patent describes microwave-assisted cracking of biomass dissolved in an ionic liquid such as [C_4mim][Cl] to produce bio-oil which can be used as fuel [188]. After microwave reaction for 5–30 min, the bio-oil is separated from the ionic liquid via supercritical CO_2 at 40 °C and 13.8 MPa. Other patents which describe the production of biofuels from biomass using ionic liquids have also appeared, where the ionic liquid performs various purposes as a solvent, catalyst, heat transfer fluid or agent for reducing the crystallinity of cellulose [189, 190].

4.12 Fractionation of Lignocellulose

Based on the effectiveness of sodium xylenesulfonate as a pulping agent, a range of ionic liquids containing the xylenesulfonate anion were designed in our laboratories for lignin extraction [192]. The use of sodium xylenesulfonate in hydrotropic pulping, an aqueous high-pressure process, is described in Sect. 3.2. A commercial grade of xylenesulfonate was used to synthesise the ionic liquids, containing a mixture of alkylbenzenesulfonates [ABS] with xylenesulfonate as the main anion. The most effective in this application has been 1-ethyl-3-methylimidazolium alkylbenzenesulfonate [C_2mim][ABS], which is capable of over 93% extraction of lignin from bagasse [211]. Extraction of lignin via xylenesulfonate ionic liquids occurs at atmospheric pressure, thus obviating the need for expensive pressurised equipment.

A patent on dissolution of lignocellulosic materials in ionic liquids mentions delignification as one of the aims [129]. It describes dissolution of wood in [C_4mim][Cl], with optional microwave heating. Precipitation of the dissolved cellulose via addition of an anti-solvent is mentioned but no details are given on the purity or yields of cellulose produced, how lignin is removed from the ionic liquid or whether the lignin remains dissolved when cellulose is precipitated. A pulping system based on solutions containing 84% [C_4mim][Cl] with 16% DMSO-d_6 has been found to partially dissolve wood shavings, including cellulose and lignin components [127]. Cellulose precipitated from the [C_4mim][Cl]/DMSO-d_6 solution was shown to be to be relatively free of lignin or hemicellulose.

A patent on biomass fractionation using ionic liquids describes extraction of cellulose from lignocellulose by dissolution in [C_4mim][Cl], followed by addition of a caustic solution to precipitate cellulose while solubilising lignin and hemicellulose [191]. One of the main advantages of the process was the partial phase separation between the ionic liquid and the aqueous caustic phase, which enabled easier recycling of the ionic liquid.

5 Ionic Liquids and Separations in Biomass Processing

Separating processes in general play an important role in almost every chemical industry. Often, separation constitutes 60–80% of the total processing cost of a chemical plant [20]. The most common separating process, distillation, is usually very energy intensive and, in some cases, may not give complete separation due to the formation of azeotropes. Using an ionic liquid as a solvent in any process invariably requires a separating step to remove the products. The commercialised ionic liquid processes, BASIL and Difasol, both exploit the unusual phase behaviour of ionic liquids to obtain easy separation of immiscible species by decantation. If a co-solvent or anti-solvent is used, its removal is sometimes necessary for the recycling of the ionic liquid. Separation of compounds (extracted material, reaction products, co-solvent, anti-solvent, etc.) from an ionic liquid can be achieved by a number of methods as summarised with examples in Table 1. The importance of efficient separation of products and auxiliary solvents to the economic viability of an ionic liquid process makes it a prerequisite for industrial application. These interrelated issues of product extraction and ionic liquid recycling should be considered in the design of the ionic liquid.

5.1 Phase Separation

The most desirable separation method in most cases is phase separation, which can be achieved via tuning of the hydrophobicity or hydrophilicity of the ionic liquid to effect immiscibility with the species for extraction. Phase separation may also be

Table 1 Overview of ionic liquid separations

Method	Requirements	Example	Advantages	Limitations
Phase separation	Immiscibility of ionic liquid with product/extract, immobilisation of catalyst in ionic liquid phase	BASIL [108, 109, 193–195], Difasol [82, 111, 112]	Easy removal, low energy requirement	Loss of catalyst to product phase if not well immobilised, contamination of product
Precipitation using anti-solvent	Miscibility of anti-solvent with IL, low solubility of extract in anti-solvent	Cellulose precipitation from [C_4mim][Cl] by addition of water [117, 118]	Easy removal, control of product form	Removal of anti-solvent required for recycling of ionic liquid
Distillation of non-IL component (product or co-solvent, etc.)	Volatility of non-IL component	Separation of lignocellulose pyrolysis products [184]	Unlikely to have IL contamination in product	High energy use, possible instability of ionic liquid or product at high temperature
Liquid/liquid extraction	Solubility of product/extract in extracting solvent	Extraction of organic compounds [196], metal ions [197]	Low energy requirement	Further separations required, phase partitioning, possible use of VOC
Supercritical CO_2	Solubility of product/extract in supercritical CO_2	Hydroformylation [198, 199], hydrogenation [200]	Increased selectivity	High pressure, operational safety, CO_2 emission
Distillation of ionic liquid	Volatile ionic liquid, non-volatile product, thermal stability of product	Macrocyclic compounds and monoarylidene ketones from DIMCARB [72, 73]	Ready recycling of ionic liquid	High energy use, possible incomplete removal of ionic liquid

obtained by pH-induced ionisation to alter the partitioning of the solutes to remove them from the ionic liquid phase [201]. Temperature-induced separations occur in so-called thermomorphic systems, where a single homogeneous phase exists at reaction temperature, but upon cooling separates into an ionic liquid catalyst phase and product phase at ambient temperature [202].

The addition of potassium phosphate to an aqueous solution of [C_4mim][Cl] was reported to result in a phase separation to give an upper ionic liquid rich phase and a lower potassium phosphate rich phase, with both phases being aqueous [203]. This separation, termed a "salting out effect", demonstrated the possibility of partially separating an ionic liquid from an aqueous solution by adding a different species with water-structuring ability. The water-structuring (or kosmotropic) salt increases the dielectric constant of the aqueous phase, forcing the low dielectric [C_4mim] cations into a separate phase with concurrent movement of chloride ions. Although this was proposed as a useful method for ionic liquid recovery, phase partitioning of the different species may not result in a sufficiently effective separation for practical application, especially considering the toxicity of many ionic liquids. The use of sucrose as water-structuring species for separation of hydrophilic ionic liquids has also been reported as moderately effective, with a maximum recovery of 74% of [C_2mim][BF_4] [204].

5.2 Supercritical Carbon Dioxide

The extraction of a non-volatile organic compound from an ionic liquid using supercritical CO_2 was first demonstrated by Brennecke and co-workers [205]. Supercritical CO_2 ($scCO_2$) was used to extract naphthalene from [C_2mim][PF_6] giving 94–96% recovery, with no detectable ionic liquid in the extracted phase. Efficient extraction of an organic compound from an ionic liquid using $scCO_2$ is enabled by the solubility of $scCO_2$ in ionic liquids, and the insolubility of ionic liquids in $scCO_2$.

5.3 Distillation of Ionic Liquids

Two general classes of ionic liquids which are easily distilled are protic ionic liquids (PILs) formed by reaction between a volatile acid and base [86], and dialkylammonium carbamate salts such as dimethylammonium dimethylcarbonate (DIMCARB) [72, 73, 206]. An example of a distillable PIL is methylpyrrolidinium acetate formed from the exchange of a proton between acetic acid and methylpyrrolidine [86]. DIMCARB, a low-cost ionic liquid produced by mixing CO_2 with dimethylamine, has been used as a reaction medium for the synthesis of monoarylidene and macrocyclic compounds, where in each case, the product was separated by distillation of the ionic liquid [72, 73, 206].

5.4 Entrainers in Extractive Distillation

Of particular interest from a biorefinery perspective is the use of ionic liquids as entrainers for the extractive distillation of azeotropic mixtures, including ethanol/water, which has been patented by BASF [207]. Ionic liquids have a strong affinity for water and break azeotropes by dramatically increasing the relative volatility of ethanol to water. Using an ionic liquid as an entrainer results in lower costs for separation and recycling of the entrainer due to lower energy consumption and fewer distillation columns [109, 110]. A recent study suggests that [C_2mim] acetate may be highly effective [208].

6 Conclusions

Ionic liquids have only just begun to be investigated for biomass related processes within the last 10 years, yet there are already many exciting examples of how they can be applied in this area. They have been used in cellulose functionalisation, thermochemical depolymerisation, enzymatic depolymerisation, extraction of biomass components, and biomass pretreatment processes. In a growing number of cases, ionic liquid processes have been patented, which suggests future commercial value.

A major highlight is the solubility of cellulose in ionic liquids, which allows functionalisation to give materials suitable for a diverse range of applications, including novel applications such as materials for sensors and specialised composites. Their use as entrainers in extractive distillation is also very promising.

Ionic liquids have many advantages as reaction media, with the most widely cited advantage being their negligible vapour pressure (under normal conditions), which makes them attractive as green solvents. However, to be genuinely green, they would have to be recycled efficiently and possess low toxicity. Efficient recycling requires facile separation of products and auxiliary solvents, which may be attainable by tuning specific properties of the ionic liquid, such as hydrophobicity, or through the use of auxiliary solvents such as supercritical CO_2. Overall, ionic liquids have unique advantages for biomass processing in terms of phase separation, solvating ability, catalytic ability, and general versatility, which not only makes them a fascinating area for research, but also likely to be used in an increasing number of applications.

Acknowledgements The Australian Sugar Research and Development Corporation and the Centre for Green Chemistry at Monash University are gratefully acknowledged for their financial support.

References

1. Daily G, Dasgupta P, Bolin B, Crosson P, Du Guerny J, Ehrlich P, Folke C, Jansson AM, Jansson B-O, Kautsky N, Kinzig A, Levin S, Maler K-G, Pinstrup-Andersen P, Siniscalco D, Walker B (1998) Science 281:1291

2. Hoegh-Guldberg O, Mumby PJ, Hooten AJ, Steneck RS, Greenfield P, Gomez E, Harvell CD, Sale PF, Edwards AJ, Caldeira K, Knowlton N, Eakin CM, Iglesias-Prieto R, Muthiga N, Bradbury RH, Dubi A, Hatziolos ME (2007) Science 318:1737
3. Okkerse C, van Bekkum H (1999) Green Chem 1:107
4. Shannon MA, Bohn PW, Elimelech M, Georgiadis JG, Marinas BJ, Mayes AM (2008) Nature 452:301
5. Vorosmarty CJ, Green P, Salisbury J, Lammers RB (2000) Science 289:284
6. Emission Trading Scheme (EU ETS), European Commission (2008) http://ec.europa.eu/environment/climat/emission.htm
7. Department of Climate Change, Australian Government (2008) Carbon Pollution Reduction Scheme Green Paper, Department of Climate Change, Australian Government, http://www.climatechange.gov.au/greenpaper/index.html
8. Kyoto Protocol to the United Nations Framework Convention on Climate Change: Annex B (1997) http://unfccc.int/kyoto_protocol/items/2830.php
9. Foley JA (2005) Science 310:627
10. Ham B (2007) Science 318:1396
11. Hansen J (2007) How can we avert dangerous climate change? Los Alamos National Laboratory, Preprint Archive, Physics, http://arxiv.org/abs/0706.3720
12. Hansen J, Sato M, Ruedy R, Kharecha P, Lacis A, Miller R, Nazarenko L, Lo K, Schmidt GA, Russell G, Aleinov I, Bauer S, Baum E, Cairns B, Canuto V, Chandler M, Cheng Y, Cohen A, Del Genio A, Faluvegi G, Fleming E, Friend A, Hall T, Jackman C, Jonas J, Kelley M, Kiang NY, Koch D, Labow G, Lerner J, Menon S, Novakov T, Oinas V, Perlwitz J, Perlwitz J, Rind D, Romanou A, Schmunk R, Shindell D, Stone P, Sun S, Streets D, Tausnev N, Thresher D, Unger N, Yao M, Zhang S (2007) Atmos Chem Phys 7:2287
13. Kerr RA (2008) Science 319:153
14. Spratt D, Sutton P (2008) Climate code red. Scribe Publications, Melbourne
15. Walker G (2006) Nature 441:802
16. Flannery T (2005) The weather makers: the history and future impact of climate change. The Text Publishing Company, Melbourne
17. Anastas PT, Lankey RL (2002) In: Lankey RL, Anastas PT (eds) Advancing sustainability through green chemistry and engineering. ACS Symp Ser 823:1
18. Anastas PT (1998) Green chemistry, theory and practice. Oxford University Press, Oxford
19. Clark JH (2007) J Chem Technol Biotechnol 82:603
20. Ragauskas AJ, Williams CK, Davison BH, Britovsek G, Cairney J, Eckert CA, Frederick WJ Jr, Hallett JP, Leak DJ, Liotta CL, Mielenz JR, Murphy R, Templer R, Tschaplinski T (2006) Science 311:484
21. Zhang YHP (2008) J Ind Microbiol Biotechnol 35:367
22. Chang MCY (2007) Curr Opin Chem Biol 11:677
23. National Renewable Energy Laboratory (2008) What is a biorefinery? National Renewable Energy Laboratory, http://www.nrel.gov/biomass/biorefinery.html
24. Crutzen PJ, Mosier AR, Smith KA, Winiwarter W (2008) Atmos Chem Phys 8:389
25. Ebeling J, Yasue M (2008) Philos Trans R Soc B 363:1917
26. Searchinger T, Heimlich R, Houghton RA, Dong F, Elobeid A, Fabiosa J, Tokgoz S, Hayes D, Yu T-H (2008) Science 319:1238
27. (2001) Kirk–Othmer encyclopedia of chemical technology. Wiley, New York
28. Werpy T, Peterson G (2004) Top value added chemicals from biomass, volume 1 – results of screening for potential candidates from sugars and synthesis gas. U.S. Department of Energy
29. Lichtenthaler FW (2007) In: Tundo P (ed) Methods and reagents for green chemistry. Wiley, New Jersey, p 23
30. Carole TM, Pellegrino J, Paster MD (2004) Appl Biochem Biotechnol 113/116:871
31. Huber GW, Iborra S, Corma A (2006) Chem Rev 106:4044
32. Buchanan BB, Gruissem W, Jones RL (2000) Biochemistry and molecular biology of plants. American Society of Plant Biologists, Rockville, MD

33. Brunow G (2006) In: Kamm B, Gruber PR, Kamm M (eds) Biorefineries – industrial processes and products, vol 2. Wiley, Weinheim, p 151
34. Berlin A, Balakshin M, Gilkes N, Kadla J, Maximenko V, Kubo S, Saddler J (2006) J Biotechnol 125:198
35. Pan X, Xie D, Gilkes N, Gregg DJ, Saddler JN (2005) Appl Biochem Biotechnol 121/124:1069
36. Huang H-J, Ramaswamy S, Tschirner UW, Ramarao BV (2008) Sep Purif Technol 62:1
37. Palmqvist E, Hahn-Hagerdal B (2000) Bioresour Technol 74:25
38. Thielemans W, Can E, Morye SS, Wool RP (2002) J Appl Polym Sci 83:323
39. Pye EK (2006) In: Kamm B, Gruber PR, Kamm M (eds) Biorefineries – industrial processes and products, vol 2. Wiley, Weinheim, p 165
40. Brunow G, Kilpelainen I, Sipila J, Syrjanen K, Karhunen P, Setala H, Rummakko P (1998) In: Lewis NG, Sarkanen S (eds) Lignin and lignan biosynthesis. ACS Symp Ser 697:131
41. Navarro RM, Pena MA, Fierro JLG (2007) Chem Rev 107:3952
42. Elliott DC, Beckman D, Bridgwater AV, Diebold JP, Gevert SB, Solantausta Y (1991) Energ Fuels 5:399
43. Faith WL (1945) J Ind Eng Chem 37:9
44. Lee YY, Iyer P, Torget RW (1999) Adv Biochem Eng Biotechnol 65:93
45. Hayes DJ, Fitzpatrick S, Hayes MHB, Ross JRH (2006) In: Kamm B, Gruber PR, Kamm M (eds) Biorefineries – industrial processes and products, vol 1. Wiley, Weinheim, p 139
46. Smook GA (2002) Handbook for pulp & paper technologists. Angus Wilde Publications, Vancouver
47. Wegener G (1992) Ind Crops Prod 1:113
48. Zhang Y-HP, Ding S-Y, Mielenz JR, Cui J-B, Elander RT, Laser M, Himmel ME, McMillan JR, Lynd LR (2007) Biotechnol Bioeng 97:214
49. Delmas M (2008) Chem Eng Technol 31:792
50. McKee RH (1943) US Patent 2 308 564
51. McKee RH (1954) Pulp Paper Mag Can 55:64
52. McKee RH (1960) Paper Ind 42:255
53. Procter AR (1971) Pulp Paper Mag Can 72:67
54. Bland DE (1976) Research Review – Australia, Commonwealth Scientific and Industrial Research Organization, Division of Chemical Technology, p 27
55. Shanmugam KT, Ingram LO (2008) J Mol Microbiol Biotechnol 15:8
56. Zhang PYH, Himmel ME, Mielenz JR (2006) Biotechnol Adv 24:452
57. Himmel ME, Ding S-Y, Johnson DK, Adney WS, Nimlos MR, Brady JW, Foust TD (2007) Science 315:804
58. Lee S (2007) In: Lee S, Speight JG, Loyalka SK (eds) Handbook of alternative fuel technologies. Taylor & Francis Group, Boca Raton, p 343
59. Yang S-T (2007) In: Yang S-T (ed) Bioprocessing for value-added products from renewable resources: new technologies and applications. Elsevier BV, Oxford, p 1
60. Henstra AM, Sipma J, Rinzema A, Stams AJM (2007) Curr Opin Biotechnol 18:200
61. Brown RC (2006) In: Kamm B, Gruber PR, Kamm M (eds) Biorefineries – industrial processes and products, vol 1. Wiley, Weinheim, p 227
62. Wasserscheid P, Keim W (2000) Angew Chem Int Ed 39:3772
63. Holbrey JD, Rogers RD (2008) In: Wasserscheid P, Welton T (eds) Ionic liquids in synthesis, 2nd edn, vol 1. Wiley, Weinheim, p 57
64. Fox DM, Gilman JW, Morgan AB, Shields JR, Maupin PH, Lyon RE, De Long HC, Trulove PC (2008) Ind Eng Chem Res 47:6327
65. Smiglak M, Reichert WM, Holbrey JD, Wilkes JS, Sun L, Thrasher JS, Kirichenko K, Singh S, Katritzky AR, Rogers RD (2006) Chem Comm 2554
66. Boesmann A, Schulz PS, Wasserscheid P (2007) Monatsh Chem 138:1159
67. Bonhote P, Dias A-P, Armand M, Papageorgiou N, Kalyanasundaram K, Graetzel M (1996) Inorg Chem 35:1168

68. Carter EB, Culver SL, Fox PA, Goode RD, Ntai I, Tickell MD, Traylor RK, Hoffman NW, Davis JH Jr (2004) Chem Comm 630
69. Nockemann P, Thijs B, Driesen K, Janssen CR, Van Hecke K, Van Meervelt L, Kossmann S, Kirchner B, Binnemans K (2007) J Phys Chem B 111:5254
70. MacFarlane DR, Seddon KR (2007) Aust J Chem 60:3
71. Earle MJ, Esperanca JMSS, Gilea MA, Canongia Lopes JN, Rebelo LPN, Magee JW, Seddon KR, Widegren JA (2006) Nature 439:831
72. Kreher UP, Rosamilia AE, Raston CL (2004) Molecules 9:387
73. Rosamilia AE, Strauss CR, Scott JL (2007) Pure Appl Chem 79:1869
74. Wasserscheid P (2006) Nature 439:797
75. Fraser KJ, Izgorodina EI, Forsyth M, Scott JL, MacFarlane DR (2007) Chem Comm 3817
76. Scammells PJ, Scott JL, Singer RD (2005) Aust J Chem 58:155
77. Baranyai KJ, Deacon GB, MacFarlane DR, Pringle JM, Scott JL (2004) Aust J Chem 57:145
78. Glenn AG, Jones PB (2004) Tetrahedron Lett 45:6967
79. Ngo HL, LeCompte K, Hargens L, McEwen AB (2000) Thermochim Acta 357/358:97
80. Freire MG, Neves CMSS, Carvalho PJ, Gardas RL, Fernandes AM, Marrucho IM, Santos LMNBF, Coutinho JAP (2007) J Phys Chem B 111:13082
81. Huddleston JG, Visser AE, Reichert WM, Willauer HD, Broker GA, Rogers RD (2001) Green Chem 3:156
82. Olivier-Bourbigou H, Vallee C (2005) In: Cornils B, Herrmann WA, Horvath IT, Leitner W, Mecking S, Olivier-Bourbigou H, Vogt D (eds) Multiphase homogeneous catalysis, vol 2. Wiley, Weinheim, p 413
83. Earle MJ, Seddon KR (2000) Pure Appl Chem 72:1391
84. Rogers RD, Seddon Kenneth R (2003) Science 302:792
85. Seddon KR (1997) J Chem Technol Biotechnol 68:351
86. MacFarlane DR, Pringle JM, Johansson KM, Forsyth SA, Forsyth M (2006) Chem Comm 1905
87. Sheldon R (2001) Chem Comm 2399
88. Boon JA, Levisky JA, Pflug JL, Wilkes JS (1986) J Org Chem 51:480
89. Earle M (2008) In: Wasserscheid P, Welton T (eds) Ionic liquids in synthesis, 2nd edn, vol 1. Wiley, Weinheim, p 292
90. Earle MJ, Seddon KR, Adams CJ, Roberts G (1998) Chem Comm 2097
91. Sahoo S, Joseph T, Halligudi SB (2006) J Mol Cat A Chem 244:179
92. Yin D, Li C, Li B, Tao L, Yin D (2005) Adv Synth Catal 347:137
93. Xu J-M, Liu B-K, Wu W-B, Qian C, Wu Q, Lin X-F (2006) J Org Chem 71:3991
94. Ranu BC, Jana R (2006) Eur J Org Chem 3767
95. Ranu BC, Banerjee S, Jana R (2006) Tetrahedron 63:776
96. Wasserscheid P (2003) In: Rogers RD, Seddon Kenneth R, Volkov S (eds) NATO science series, II: mathematics, physics and chemistry, vol 92. Kluwer, Dordrecht, p 29
97. Wasserscheid P, Hilgers C, Gordon CM, Muldoon MJ, Dunkin IR (2001) Chem Comm 1186
98. Holbrey JD, Seddon KR (1999) J Chem Soc Dalton Trans 2133
99. Forsyth S (2003) Novel organic salts, novel organic salts. PhD Thesis, Monash University
100. Jastorff B, Stoermann R, Ranke J, Moelter K, Stock F, Oberheitmann B, Hoffmann W, Hoffmann J, Nuechter M, Ondruschka B, Filser J (2003) Green Chem 5:136
101. Docherty KM, Hebbeler SZ, Kulpa CF Jr (2006) Green Chem 8:560
102. Frade RFM, Matias A, Branco LC, Afonso CAM, Duarte CMM (2007) Green Chem 9:873
103. Ranke J, Stolte S, Stoermann R, Arning J, Jastorff B (2007) Chem Rev 107:2183
104. Kralisch D, Reinhardt D, Kreisel G (2007) Green Chem 9:1308
105. Kralisch D, Stark A, Koersten S, Kreisel G, Ondruschka B (2005) Green Chem 7:301
106. Holbrey JD (2004) Chim Oggi 22:35
107. Holbrey JD, Seddon Kenneth R (1999) Clean Prod Proc 1:223
108. Maase M (2005) In: Cornils B, Herrmann WA, Horvath IT, Leitner W, Mecking S, Olivier-Bourbigou H, Vogt D (eds) Multiphase homogeneous catalysis, vol 2. Wiley, Weinheim, p 560

109. Maase M (2008) In: Wasserscheid P, Welton T (eds) Ionic liquids in synthesis, 2nd edn, vol 2. Wiley, Weinheim, p 663
110. Plechkova NV, Seddon KR (2008) Chem Soc Rev 37:123
111. Olivier-Bourbigou H, Favre F (2008) In: Wasserscheid P, Welton T (eds) Ionic liquids in synthesis, 2nd edn, vol 2. Wiley, Weinheim, p 464
112. Olivier-Bourbigou H, Hugues F (2003) In: Rogers RD, Seddon Kenneth R, Volkov S (eds) NATO science series, II: mathematics, physics and chemistry, vol 92, p 67
113. Forsyth SA, MacFarlane DR, Thomson RJ, von Itzstein M (2002) Chem Comm 714
114. Kimizuka N, Nakashima T (2001) Langmuir 17:6759
115. Kimizuka N, Nakashima T (2002) Foundation for Scientific Technology Promotion, Japan, JP Patent 2002/003478
116. Liu Q, Janssen MHA, van Rantwijk F, Sheldon RA (2005) Green Chem 7:39
117. Swatloski RP, Rogers RD, Holbrey JD (2003) University of Alabama, USA, WO Patent 03/029329
118. Swatloski RP, Spear SK, Holbrey JD, Rogers RD (2002) J Am Chem Soc 124:4974
119. Youngs TGA, Hardacre C, Holbrey JD (2007) J Phys Chem B 111:13765
120. Zhang H, Wu J, Zhang J, He J (2005) Macromolecules 38:8272
121. Ren Q, Wu J, Zhang J, He JS (2003) Acta Polym Sin 3:448
122. Zhang J, Ren Q, He J (2004) Inst. of Chemistry, Chinese Academy of Sciences, Peop. Rep. China, CN Patent 1491974
123. Hermanutz F, Gaehr F, Uerdingen E, Meister F, Kosan B (2008) Macromol Symp 262:23
124. Fukaya Y, Hayashi K, Wada M, Ohno H (2008) Green Chem 10:44
125. Fukaya Y, Sugimoto A, Ohno H (2006) Biomacromolecules 7:3295
126. Remsing RC, Swatloski RP, Rogers RD, Moyna G (2006) Chem Comm 1271
127. Fort DA, Remsing RC, Swatloski RP, Moyna P, Moyna G, Rogers RD (2007) Green Chem 9:63
128. Kilpelainen I, Xie H, King A, Granstrom M, Heikkinen S, Argyropoulos DS (2007) J Agric Food Chem 55:9142
129. Myllymaeki V, Aksela R (2005) Kemira Oyj, Finland, WO Patent 2005/017001
130. Pu YQ, Jiang N, Ragauskas AJ (2007) J Wood Chem Technol 27:23
131. D'Andola G, Szarvas L, Massonne K, Stegmann V (2008) BASF, Germany, WO Patent 2008/043837
132. Wu Y, Sasaki T, Irie S, Sakurai K (2008) Polymer 49:2321
133. Hecht SE, Niehoff RL, Narasimhan K, Neal CW, Forshey PA, Phan DV, Brooker ADM, Combs KH (2006) Procter & Gamble, USA, WO Patent 2006/116126
134. Zhu S, Wu Y, Chen Q, Yu Z, Wang C, Jin S, Ding Y, Wu G (2006) Green Chem 8:325
135. Heinze T, Liebert T (2001) Prog Polym Sci 26:1689
136. Wu J, Zhang J, Zhang H, He J, Ren Q, Guo M (2004) Biomacromolecules 5:266
137. Moens L, Khan N (2003) In: Rogers RD, Seddon Kenneth R, Volkov S (eds) NATO science series, II: mathematics, physics and chemistry, vol 92. Kluwer, Dordrecht, p 157
138. Li C, Wang Q, Zhao ZK (2008) Green Chem 10:177
139. Massonne K, D'Andola G, Stegmann V, Mormann W, Wezstein M, Leng W (2007) BASF, Germany, WO Patent 2007/101811
140. Lewkowski J (2001) ARKIVOC [online computer file – http://www.arkat-usa.org/], vol 2, p 17
141. Moreau C, Finiels A, Vanoye L (2006) J Mol Cat A Chem 253:153
142. Zhao H, Holladay JE, Brown H, Zhang ZC (2007) Science 316:1597
143. Zhao H, Holladay JE, Zhang ZC (2008) Batelle Memorial Institute, US Patent 2008/033187
144. Van Rantwijk F, Sheldon RA (2007) Chem Rev 107:2757
145. Cantone S, Hanefeld U, Basso A (2007) Green Chem 9:954
146. Kaar JL, Jesionowski AM, Berberich JA, Moulton R, Russell AJ (2003) J Am Chem Soc 125:4125
147. Kaftzik N, Neumann S, Kula M-R, Kragl U (2003) ACS Symp Ser 856:206
148. Kim M-J, Choi MY, Lee JK, Ahn Y (2003) J Mol Catal B: Enzym 26:115
149. Madeira Lau R, van Rantwijk F, Seddon KR, Sheldon RA (2000) Org Lett 2:4189

150. Galletti P, Moretti F, Samori C, Tagliavini E (2007) Green Chem 9:987
151. Turner MB, Spear SK, Huddleston JG, Holbrey JD, Rogers RD (2003) Green Chem 5:443
152. Kamiya N, Matsushita Y, Hanaki M, Nakashima K, Narita M, Goto M, Takahashi H (2008) Biotechnol Lett 30:1037
153. Balensiefer T (2008) BASF, Germany, WO Patent 2008/090156
154. Balensiefer T, Brodersen J, D'Andola G, Massonne K, Freyer S, Stegmann V (2008) BASF, Germany, WO Patent 2008/090155
155. Kuhad RC, Kuhar S, Kapoor M, Sharma KK, Singh A (2007) In: Kuhad RC, Singh A (eds) Lignocellulose biotechnology: future prospects. Anshan, Tunbridge Wells, p 3
156. Kumar A, Jain N, Chauhan SMS (2007) Synlett 411
157. Shipovskov S, Gunaratne HQN, Seddon KR, Stephens G (2008) Green Chem 10:806
158. Zhou G-P, Zhang Y, Huang X-R, Shi C-H, Liu W-F, Li Y-Z, Qu Y-B, Gao P-J (2008) Colloids Surf B 66:146
159. Barthel S, Heinze T (2006) Green Chem 8:301
160. Heinze T, Schwikal K, Barthel S (2005) Macromol Biosci 5:520
161. Cao Y, Wu J, Meng T, Zhang J, He J, Li H, Zhang Y (2007) Carbohydr Polym 69:665
162. Schlufter K, Schmauder H-P, Dorn S, Heinze T (2006) Macromol Rapid Commun 27:1670
163. Buchanan CM, Buchanan NL (2008) Eastman Chemical Co., USA, WO Patent 2008/100569
164. Buchanan CM, Buchanan NL (2008) Eastman Chemical Co., USA, WO Patent 2008/100577
165. Buchanan CM, Buchanan NL, Hembre RT, Lambert JL (2008) Eastman Chemical Co., USA, WO Patent 2008/100566
166. Myllymaeki V, Aksela R (2005) Kemira Oyj, Finland, WO Patent 2005/054298
167. Liu CF, Sun RC, Zhang AP, Ren JL (2007) Carbohydr Polym 68:17
168. Liu C-F, Sun R-C, Zhang A-P, Qin M-H, Ren J-L, Wang X-A (2007) J Agric Food Chem 55:2399
169. Scheibel JJ, Kenneally CJ, Menkhaus JA, Seddon KR, Chwala P (2007) Procter and Gamble, USA, US Patent 2007/225190
170. Massonne K, Stegmann V, D'Andola G, Mormann W, Wezstein M, Leng W (2007) BASF, Germany; Universitaet Siegen, WO Patent 2007/147813
171. Liu CF, Sun RC, Zhang AP, Ren JL, Wang XA, Qin MH, Chao ZN, Luo W (2007) Carbohydr Res 342:919
172. Erdmenger T, Haensch C, Hoogenboom R, Schubert US (2007) Macromol Biosci 7:440
173. Granstroem M, Kavakka J, King A, Majoinen J, Maekelae V, Helaja J, Hia S, Virtanen T, Maunu S-L, Argyropoulos DS, Kilpelaeinen Iet al. (2008) Cellulose 15:481
174. Holbrey JD, Chen J, Turner MB, Swatloski RP, Spear SK, Rogers RD (2005) In: Brazel CS, Rogers RD (eds) Ionic liquids in polymer systems. ACS Symp Ser 913:71
175. Holbrey JD, Swatloski RP, Chen J, Daly D, Rogers RD (2005) University of Alabama, USA, WO Patent 2005/098546
176. Poplin JH, Swatloski RP, Holbrey JD, Spear SK, Metlen A, Gratzel M, Nazeeruddin MK, Rogers RD (2007) Chem Comm 2025
177. Sun N, Swatloski RP, Maxim ML, Rahman M, Harland AG, Haque A, Spear SK, Daly DT, Rogers RD (2008) J Mater Chem 18:283
178. Swatloski RP, Holbrey JD, Weston JL, Rogers RD (2006) Chimica Oggi 24:31
179. Turner MB, Spear SK, Holbrey JD, Daly DT, Rogers RD (2005) Biomacromolecules 6:2497
180. Egorov VM, Smirnova SV, Formanovsky AA, Pletnev IV, Zolotov YA (2007) Anal Bioanal Chem 387:2263
181. Kadokawa J-I, Murakami M-A, Kaneko Y (2008) Compos Sci Technol 68:493
182. Dadi AP, Schall CA, Varanasi S (2007) Appl Biochem Biotechnol 137/140:407
183. Sheldrake GN, Schleck D (2007) Green Chem 9:1044
184. Argyropoulos D (2008) North Carolina State University, USA, US Patent 2008/0185112
185. Massonne K, D'Andola G, Stegmann V, Mormann W, Wezstein M, Leng W (2007) BASF, Germany, WO Patent 2007/101813

186. Massonne K, D'Andola G, Stegmann V, Mormann W, Wezstein M, Leng W, Freyer S (2007) BASF, Germany, WO Patent 2007/101812
187. Correia P (2008) WO Patent 2008/053284
188. Guo X, Zheng Y, Zhou B (2008) Shanghai University, Peop. Rep. China, CN Patent 101235312
189. Gurin MH (2007) US Patent 2007/161095
190. Ji J, Yu F, Ai N, Ji D, Xu Z, Yu Y (2007) Zhejiang University of Technology, Peop. Rep. China, CN Patent 101085924
191. Edye LA, Doherty WOS (2008) Queensland University of Technology, Australia, WO Patent 2008/095252
192. Upfal J, MacFarlane DR, Forsyth SA (2005) Viridian Chemicals, Australia, WO Patent 2005/017252
193. Maase M, Huttenloch O (2005) BASF, Germany, WO Patent 2005/061416
194. Maase M, Massonne K, Halbritter K, Noe R, Bartsch M, Siegel W, Stegmann V, Flores M, Huttenloch O, Becker M (2003) BASF, Germany, WO Patent 2003/062171
195. Volland M, Seitz V, Maase M, Flores M, Papp R, Massonne K, Stegmann V, Halbritter K, Noe R, Bartsch M, Siegel W, Becker M, Huttenloch O (2003) BASF, Germany, WO Patent 2003/062251
196. Huddleston JG, Willauer Heather D, Swatloski Richard P, Visser AE, Rogers RD (1998) Chem Comm 1765
197. Visser AE, Swatloski RP, Reichert WM, Davis JH Jr, Rogers RD, Mayton R, Sheff S, Wierzbicki A (2001) Chem Comm 135
198. Webb PB, Kunene TE, Cole-Hamilton DJ (2005) Green Chem 7:373
199. Webb PB, Sellin MF, Kunene TE, Williamson S, Slawin AMZ, Cole-Hamilton DJ (2003) J Am Chem Soc 125:15577
200. Jessop PG, Stanley RR, Brown RA, Eckert CA, Liotta CL, Ngo TT, Pollet P (2003) Green Chem 5:123
201. Visser AE, Swatloski RP, Rogers RD (2000) Green Chem 2:1
202. Riisager A, Fehrmann R, Berg RW, van Hal R, Wasserscheid P (2005) Phys Chem Chem Phys 7:3052
203. Gutowski KE, Broker GA, Willauer HD, Huddleston JG, Swatloski RP, Holbrey JD, Rogers RD (2003) J Am Chem Soc 125:6632
204. Wu B, Zhang YM, Wang HP (2008) J Chem Eng Data 53:983
205. Blanchard LA, Hancu D, Beckman EJ, Brennecke JF (1999) Nature 399:28
206. Kreher UP, Rosamilia AE, Raston CL, Scott JL, Strauss CR (2003) Org Lett 5:3107
207. Beste YA, Schoenmakers H, Arlt W, Seiler M, Jork C (2005) BASF, Germany, WO Patent 2005/016484
208. Ge Y, Zhang L, Yuan X, Geng W, Ji J (2008) J Chem Thermodyn 40:1248
209. Rinaldi R, Palkovits R, Schuth F (2008) Angew Chem Int Ed 47:8047
210. Sievers C, Valenzuela-Olarte MB, Marzialetti T, Musin I, Agrawal PK, Jones CW (2009) Ind Eng Chem Res 48:1277
211. Tan SSY, MacFarlane DR, Upfal J, Edye LA, Doherty WOS, Patti AF, Pringle JM, Scott JL (2009) Green chem 11:339

Index